UNIVERSITY OF SOUTHAMPTON
FACULTY OF ENGINEERING AND THE ENVIRONMENT
ENERGY AND CLIMATE CHANGE RESEARCH GROUP

Project Appraisal under Uncertain Futures:

An assessment of Real Options Analysis and Flood Management

By

Myung Jin Kim

Thesis submitted for the degree of Doctor of Philosophy

December 2019

UNIVERSITY OF SOUTHAMPTON

UNIVERSITY OF SOUTHAMPTON

ABSTRACT

FACULTY OF ENGINEERING AND THE ENVIRONMENT

Doctor of Philosophy

Project Appraisal under Uncertain Futures:
An assessment of Real Options Analysis and Flood Management

Climate change is a major concern as it is likely to cause significant human and environmental impacts. However, the uncertainty of the magnitude of climate change impedes adaptation. Recent decision-making approaches tend to employ flexible options or strategies that enable us to observe and learn over time and hence make more informed decisions in the future. This thesis focuses on real-options-approaches as an method or tool to assess flexible adaptation options or strategies in the context of coastal flooding and sea-level rise. An integrated framework for real options analysis of climate change adaptation decisions has been developed, considering the key processes for coastal flood risk management.

The resulting methodology has been applied to an illustrative case study site (Lymington, UK south coast), which has a long history of coastal flooding and adaptation, and sea-level rise must be considered in future decisions. However, due to the uncertainty of future sea-level rise and socio-economic change, the scale and/or timing of adaptation measures are a key question in adaptation planning. The different adaptation pathways of upgrading coastal defences in single or multiple stage(s) are assessed within the integrated framework. Flood simulations and monetisation of flood damages are conducted to quantify the performance of the selected adaptation pathways against the risk and uncertainty of coastal flooding due to sea-level rise.

This analysis makes three main contributions. Firstly, we identify a maximum option value and an optimal investment time for an adaptation option under a given environmental condition. Secondly, we find that the timing of optimum investment can be linked to a threshold value of sea-level rise, independent of the rates of the sea-level rise. Thus, it can be used as an indicator of the optimal investment time to achieve the maximum option value by observations. Lastly, this thesis provides a method to compare single stage investments and multiple stage investments in one metric performance. Hence, the application of the integrated framework enables us to understand how to maximise/optimise the performance (i.e. option value) of single adaptation options or pathways with flexibility, allowing uncertain conditions of sea-level rise and socio-economic change.

The analysis complements previous real option analysis in climate change adaptation with a focus on quantification of adaptation options in economy efficiency. The real-options-based approach developed in this thesis can be applied to any case where irreversible adaptation measures are being planned against climate change induced events. This framework helps to understand when and how to implement the adaptation options efficiently, providing sufficient services to protect Lymington under uncertain conditions.

Table of contents

Appendices

List of Tables

List of Figures

Declaration of authorship

I, Myung-Jin Kim declare that the thesis entitled **'Project Appraisal under Uncertain Futures: An assessment of Real Options Analysis and Flood Management'** and the work presented in the thesis are both my own, and have been generated by me as the result of my own original research.

I confirm that:

- This work was done wholly or mainly while in candidature for a research degree at this University;
- Where any part of this thesis has previously been submitted for a degree or any other qualification at this University or any other institution, this has been clearly stated;
- Where I have consulted the published work of others, this is always clearly attributed;
- Where I have quoted from the work of others, the source is always given.
- With the exception of such quotations, this thesis is entirely my own work;
- I have acknowledged all main sources of help;
- Where the thesis is based on work done by myself jointly with others, I have made clear exactly what was done by others and what I have contributed myself;
- Parts of this work have been published as:

Published Journal Article:

Kim, M.J.; Nicholls, R.J.; Preston, J.M.; De Almeida, G.A., An assessment of the optimum timing of coastal flood adaptation given sea-level rise using real options analysis. *Journal of Flood Risk Management,* 2018

Conference Proceedings:

Kim, M.J.; Nicholls, R.J.; Preston, J.M.; De Almeida, G.A.: Real options analysis in climate change adaptation decisions under uncertainty: *In adaptation future 2016. Tools and approaches to assess disaster reduction strategies,* Rotterdam, Netherlands, 2016.

In preparation (September, 2019):

Kim, M.J.; Nicholls, R.J.; Preston, J.M.; De Almeida, G.A., The optimisation of investment time and its option value under deep uncertainty in climate change adaptation

Kim, M.J.; Nicholls, R.J.; Preston, J.M.; De Almeida, G.A., Evaluation of flexibility in projects of adaptation for climate change considering uncertainty

Dated: 5th December 2019

Acknowledgements

First of all, I would like to express the most gratitude to my supervisors: The first supervisor Prof. Robert J. Nicholls, the second supervisor Prof. John M. Preston and the third supervisor Dr. Gustavo De Almeida. They have led me for the five years of the doctoral degree course, giving me knowledge, instructions, motivations and encouragements to continue my research.

Prof. Robert J. Nicholls has made contributions to most part of this thesis. In particular, he has given me great inspirations on climate change, sea-level rise and coastal flooding in this thesis. His teaching on how to write the papers and thesis was very helpful. Prof. John M. Preston has given me valuable comments and advices on economic analysis. He also provided useful literature and papers for me to improve this research. Dr. Gustavo De Almeida has supervised the flood risk analysis, in particular, the flood modelling. I could not have managed to apply LISFLOOD-FP without his aids and instructions. He also gave me useful ideas on how to derive formulas for optimal investment time which are also important findings in this thesis.

I would like to express my gratitude to Prof. Richard Dawson (University of Newcastle) and Dr. Derek Clarke (University of Southampton) for their dedications to my viva on this thesis. Their advices and comments during the viva helped improve this thesis.

It took almost five years to complete this research. As real options analysis was rarely used in climate change areas when I started my research, it was very difficult to establish proper methods or methodologies for this study. Nevertheless, many other colleagues in Energy and Climate Change Research Group gave their cheerful cooperation and advices.

Special thanks to Dr. Matthew Wadey for providing useful data and information on coastal flood risk analysis in Lymington and the Solent. His previous research was very helpful in completing my thesis.

Dr. Abiy Kebede also gave cheerful comments and heartfelt words for me. His passions and efforts towards his Ph.D completion was a great motivation to me.

Dr. Esme Flegg is a really good company who started the Ph.D. course with me. She helped me adapt to life in Southampton smoothly.

I would like to express sincere thanks to my colleagues: Dr. Sally Brown, Ms. Susan Hanson, Dr. Attila Lazar and Dr. Andres Payo Garcia. They also provided valuable comments on the method of my research so that I could improve the quality and results of my research before I presented it at the conference of Adaptation Futures 2016 (held in Rotterdam, Netherlands).

All other colleagues in our research group are also helpful in conducting this study.

Thanks to Dr. Amy Welch, Dr. Jiayi Fang, Ms. Sien van der Plank and Mr. Alejandro Pinto. I hope all of you complete Ph.D successfully.

I would like to express great gratitude to Dr. Yong-Min Jung who taught me how to use Origin programme. Thanks to his help, I could conduct data analysis for my research. It also helps improve the result and display of data analysis in the thesis.

I would also like to extend my thanks to other South Korean friends: Dr. Min-Chul Shin, Dr. Jae-Sun Kim, Mr. Jun-Dong Lee, Dr. Won-Man Oh, Mr. Jong-Jun Song, Mr. Yong-Jun Kim, Mr. Sang-Hwa Lee, Mr. Tae-Il Kwon, Mr. Ho-Gun Kim, Mr. Hong-Suk Kim and Dr Woo- Min Jung.

They helped my life in Southampton in one or another way.

Special thanks to Pastor Hyun-in Moon. He inspired me to keep and strengthen my religious belief as Christianity while I was studying in Southampton. I wish God's blessing be always with his family.

I also would like to express great appreciation to my father and mother and father-in-law and mother-in-law for their patience and dedications. They always prayed for me to keep continuing my study without any problem. I could feel their heart to me while I was studying in UK.

Lastly, my wife, Mrs. Innes Lee. She deserves all I have made for the last six years. Without her dedications and encouragements, I could not have completed my study in UK and South Korea. She cheered me at all times whenever I was happy or depressed. Her dedications, patience and endurance make this thesis mature without any lacking. Many thanks to Innes.

I am thankful to God my father. I believe his plan and guidance have led me so far. I hope to keep continuing my journey with him. I dedicate this thesis to God in heaven.

Abbreviations

AR5	The Fifth Assessment Report of the Intergovernmental Panel on Climate Change
CBA	Cost-Benefit Analysis
CDF	Cumulative Distribution Function
DEM	Digital Elevation Model
EA	Environment Agency (UK)
EAB	Expected Annual Benefit
EAD	Expected Annual Damage
ESWL	Extreme Still Water Level
FCERM-AG	Flood and Coastal Erosion Risk Management Appraisal Guidance
FRM	Flood Risk Management
FRA	Flood Risk Assesesment
HTL	Hold The Line
GIS	Geographic Information System
IPCC	Intergovernmental Panel on Climate Change
mAOD	metre Above Odnance Datum
MR	Managed Realignment
MSLR	Mean Sea-Level Rise
NAI	No Active Intervention
NPV	Net Present Value
OIT	Optimal Investment Time
PDF	Probabilty Density Function
RCP	Representative Concentration Pathway
RDM	Robust Decision Making
ROA	Real Options Analysis
ROV	Real Option Value
RSLR	Realtive Sea Level Rise
SLR	Sea Level Rise
SWL	Still Water Level
UKCP09	UK Climate Prediction 2009

Definitions/Glossaries

Adaptation pathways (or paths) a strategical approach designed to enable decision-makers to choose diverse decisions or paths at decision points in response to the future states (i.e. sea-level rise). Thus, the adaptation pathway is comprised of sequences of adaptation measures and decision nodes. All the adaptation measures in sequence are well-connected to address future risk within the narratives of future scenarios. This approach is called adaptive management, dynamic approach or managed adaptation.

Adaptive management approaches or strategies that adjust or modify adaptation measures or pathways in response to future climate change (Hallegatte, 2009). This approach is frequently referred to as adaptation pathways approaches or dynamic approaches.

American Style option a financial option which is the right but not obligation to sell stocks at a specific price or to buy stocks at a specific price. This type of option can be exercised at any time before the expiry date. On the contrary, European Style option can be exercised only at the expiry date.

Bellman's equation an equation to describe a decision problem at a certain time in terms of the current states resulting from the previous actions taken and the remaining decisions. For example, a deferrable option offers option holders a choice either to wait, or implement, at a given time. Thus, the remaining choices constitute an optimal policy with respect to the sub-problem starting at the state that results from the initial actions (Bellman, 1957). Bellman's equation provides a method to calculate a continuation value and a termination value for a given year

Binominal lattice approach a numerical method for the valuation of flexible options under two states of futures. Two future states are assumed with the corresponding probabilities of the future states at any decision point. Thus, two choices are available for decision-makers. If multiple decision points are made, various decision paths can be made to describe the complex future states.

Black Scholes model an option evaluation model for financial instruments such as call or put options under the uncertainty of the price of the underlying assets (Black and Scholes, 1973; Cooper, 1999; Park, 2002). This option pricing model is commonly used in evaluating financial options (call or put options) such as stocks.

Breaching is a failure mechanism in which seawater enters floodplains behind the collapsed coastal defence.

Brownian motion describes the random movement of particles in fluid due to their collisions with other atoms or molecules. The Brownian motion is used to represent the deterministic and random motion of uncertain variables in engineering, physics, economics or mathematic issues.

Brownian SLR defines the Brownian motion of sea-level rise.

Coastal defence Man-made structure (usually concrete or masonry) that is built along shoreline to block erosion or prevent flooding or resist erosion. Where necessary, different geometries (e.g. vertical or sloping are distinguished).

Continuation value refers to an option value at a given year when the option is deferred to the next year. This value is estimated by discounting an expected value in the next year by discount factor.

DEFRA UK Government Department (Department of Environment, Food and Rural Affairs) that address policies or issues for the environment, reginal or urban development.

Discount rate an indicative value to represent a social preference of time (Tol, 2003; Hunt and Tailor, 2009). It is socially-agreed value by compromising the values of the future and the present (ibid.). If the present value is more important than the future value, a high discount rate is chosen for option evaluations. Otherwise, a low discount rate is selected.

Drift parameter determines the deterministic motion of variables in Brownian motion. This parameter represents the expectation or mean of motion of variables in the next year.

Environment Agency a non-departmental public body, established in 1995 and sponsored by the United Kingdom government's Department for Environment, Food and Rural Affairs, with responsibilities relating to the protection and enhancement of the environment (including flood risk assessment or management) in England and Wales.

European style option a financial option that can be exercised at the expiry date. Refer to American style option

Expected utility theorem an economic or gamble theory, introduced by Daniel Bernoulli in 1738, which states that subjective values associated with individual's choices that have uncertain outcomes are the statistical expectation of individual's valuations of the outcomes.

Extreme still water level means the elevation of seawater surface in extreme storm surge events (McMillian et al., 2011). This is a consequence of combination of astronomical tides and meteorologically generated skew surges. Probabilities or return period water levels are used to represent the risk of extreme still water levels.

Failure mode any mechanisms or flood dynamics that allow defence or defence system to provide a flood pathway (potentially progressing to flooding).

Flood Risk refers to risk due to flooding which is quantified by the sum of products of the monetised flood damages and the corresponding probabilities of occurrence of the flood damages. Flood risk is represented by expected annual damage (EAD) in this thesis.

Flood risk management is referred to as processes that assess and manage the risk of flooding from all flood mechanisms, identify adaptation measures and provides advice on actions to be taken before and during a flooding.

mAOD stands for metre Above Ordnance Datum, which is height from a vertical datum used by an ordnance survey as the basis for deriving altitude on maps. Usually mean sea level (MSL) is used for the vertical datum

Monte-Carlo simulations Computational algorithms that rely on repeated random sampling to obtain numerical results. The use of the Monte-Carlo simulations is found in physical, economic and mathematical problems due to advances in computational power. These approaches are very useful when other analytical approaches are not impossible to provide solutions. These random-sampling approaches are used for optimisation, numerical integration and the generation of probability distribution.

Multi-Decision criteria approach an approach that evaluates multiple conflicting criteria in decision-marking. Conflicting criteria such as environment, cultures, societal unity are typical in evaluating options: cost or price is usually incommensurable with such conflicting criteria.

Net present value a measurement of profit which is evaluated by subtracting the present values of all the streams of costs from all the streams of benefits during the life of a project. Generally, the metric of the net present value (NPV) is used to assess a project made on a now-or-never basis in cost-benefit analysis. In this thesis, the net present value defines the option value of a project implemented now (i.e. NPV_{now}).

Overflowing refers to a coastal defence failure mechanism that allows a high level of seawater to flow over the crest of coastal defence. Due to a great amount of seawater inflows, the low-lying coastal areas behind coastal defence will be significantly inundated.

Overtopping refers to a coastal defence failure mechanism that allows wave run-up to pass over the crest of coastal defence. The wave overtopping volumes rely on a freeboard which is a difference between the seawater level and the crest level of coastal defence.

Premium additional costs to be paid for incorporating flexibility of future growth in adaptation options (in this thesis, coastal defence)

Real options the right, but not the obligation, to undertake certain business or project initiatives, such as deferring, abandoning, expanding, or contracting a capital investment project. These types of options were vigorously used in finance sectors. This concept has been extended to decision-making on real-life issues under uncertainty. Thus, it is referred to as 'real' as it references projects involving a tangible asset instead of a financial instrument.

Real option value the option value of a project including flexibility (e.g. wait or future growth). This value comprises a net present value (NPV) and a real option premium added to the option. The real option premium is attributable to the flexibility. This value is a maximum net present value that can be achieved by using flexibility. In this thesis, NPV_{opt} denotes the real option value.

Return period a recursive period within which a certain amount of natural event may occur again in a statistical sense. Inversely, it indicates a probability that a certain amount of natural event occurs in a year. For example, a 1-in-200 year return period flood event has a 1/200 chance of its occurrence in a year.

Risk A possibility of an area of interest being damaged or harmed from all the possible events. Risk is statistically defined as the sum of all the damages times the corresponding probabilities. For the risk to be known, the probabilities of occurrence of flood damages should be estimated.

Robust Decision making an approach or analytical framework that pursues the robustness of potential options to all the plausible or considered futures rather than an optimal response to a single most-likely future (Lempert et al., 2007; Hall et al., 2012). This approach invented by Lempert et al. (2007) provides a decision framework in which experts and decision-makers evaluate the performance of candidate options against all the plausible futures.

Root mean square error (RMSE) Statistical measure that indicates the accuracy of measured data of a varying quantity. In the case of LIDAR data, this is calculated by taking a square root of the average set of squared differences between modelled elevations and observed elevations.

Shoreline Management Plan (SMP) A broad-scale assessment of the risk associated with coastal processes. Shoreline Management Plan (SMP) describes a strategy to manage coastlines against flood and/or erosion (DEFRA, 2006; NFDC, 2010). This management plans set out the next 20, 50 and 100-year policy to assist decision-making on flooding from sea and the coastal erosion. Four different shoreline management policies are present in SMP: (1) No active intervention (NAI) (2) Hold the line (HTL); (3) Managed Realignment (MR); and (4) Advance the line (ATL)

Stochastic differential equation a differential equation that models various phenomena (e.g. temperature), states (e.g. probability) or values (e.g. option value) with respect to uncertain variables following a stochastic process. For the existence of a stochastic differential equation, the uncertain variable must follow Brownian motion.

Storm surges A rise above normal water level on the open coast commonly associated with low pressure weather systems, wind stress forcing and orientation of the water body relative to storm path. It is sometimes known as the residual, or surge component of a water level.

Termination value refers to an option value at a given year when the option is implemented.

Uncertainty refers to a state of incomplete knowledge and understanding of what we pursue. Uncertainty concerns futures, physical dynamics, data, models and all the relevant issues.

Variance parameter refers to change in the stochastic process over any finite interval of time. The variance parameter of Brownian motion indicates how far the value in the next year can deviate from the most expected value from the perspective of the present. As the effects of the variance on variables are cumulated over the long-term period, uncertainty becomes large and deep at the end of the stochastic process. Thus, the uncertainty of Brownian motion increases with time.

1. Introduction

1. 1 Background of the research

Climate change is a major concern for human beings as it has the potential to cause significant damages to people and the environment (Nicholls et al., 2014; IPCC, 2014). Appropriate actions or measures against the risk of climate change need to be taken in a timely manner (Ranger et al., 2013). If not, the potential risk of climate change that has currently been observed around our environment will be a significant threat in our world. Recently, climate change induced events seem to become more frequent and extreme worldwide. For example, daily temperature in Seoul (South Korea) has reached the highest (39.4 ℃) on record with this anomaly observed during 31 consecutive days nationwide in 2018 summer. For Japan, Kansai International Airport near Osaka was submerged under seawater due to high waves and storm surges caused by a powerful Typhoon Jebi (the 4th Sept, 2018). The image of runways being under seawater was very shocking, as it is the third busiest airport in Japan in passenger number. Most media reported that the highest temperature and the extreme storms might be caused by climate change.

In literature on climate change, adaptation is defined as adjustment to changes in natural or human environment (Smit and Pilifosova, 2003: p.879). It is a context-specific process that involves 'all activities in natural or human systems in response to actual or expected climatic stimuli or their effects, which moderates harm or exploits beneficial opportunities'. To prepare our systems or societies against such extreme climatic events, adaptation actions need to be taken timely and cost-effectively. However, due to uncertainty in climate change, adaptation is very challenging to those involved (King et al., 2015:p.18-27).

Climate change adaptations involve diverse stakeholders in decision-making processes (Adger et al., 2009). For example, the concern of risk analysts may be an extent to which they protect what they value, or a way in which they manage risk or uncertainty from natural events (Nicholls et al., 2016). Economists or policy makers may be concerned about the economic efficiency or cost-effectiveness of adaptation actions taken against climate change in policy contexts (Stern, 2007). On the other hand, the public may be more concerned about whether their lives and assets are safe against such risks. Therefore, the implementation of adaptation actions or measures necessarily requires a complicated process to understand and

communicate risk and uncertainty in the contexts of climate change adaptation (Adger et al., 2009).

A variety of ideas and approaches have been introduced to reduce the risk or uncertainty in regard to climate change adaptations (Hallegatte et al., 2012). There are a number of approaches used for climate change decisions and, of particular relevance here, flood risk management (hereafter, termed FRM). For example, multi-decision criteria analysis (MCDA), robust decision making (RDM), adaptive management (AD) and many other approaches are currently employed to address uncertainty issues from climate change adaptation (Hall and Solomatine, 2008; Haasnoot et al., 2013; Ranger et al., 2013). All of these methods aim to make well-fitted decisions to the context of sites and the types of risks and uncertainties. However, there are still limited applications of these approaches to climate change issues to date, because climate change is a long-term event including the uncertainty of the future (Tol, 2003; Ranger et al., 2013; Nicholls et al., 2015). In this regard, decisions on climate change adaptation may differ depending on the view of decision-makers towards the future and the contexts of climate change adaptation.

This study is consistent with other research focusing on managing risk and uncertainty in climate change adaptation, in particular, coastal flooding. However, this thesis places more emphasis on the flexibility of wait (or time), by which we might reduce uncertainty in climate change adaptation. A number of studies have been found in resolving uncertainty with time in adaptation decisions. Dutch Delta Programme (Netherlands), Thames Estuaries 2100 (UK) and New York city (US) are appropriate examples of managing risk and uncertainty by using flexibility under the well-developed narratives of climate change scenarios (Hallegatte, 2009; Reeder et al., 2009; Haasnoot et al., 2013; Ranger et al., 2013; Nicholls et al., 2015). However, in-depth analysis into investment timing could lead to more informed adaptation decisions. In other words, investing now gives us safety, but maybe we over-invest and act too quickly. In contrast, waiting allows us to observe and learn the future, and hence make more informed decisions, but may expose us to more risks if we do not act quickly enough. However, there is little explanation on these issues in the previous studies.

This research aims to develop a new method to assess and value coastal adaptation options under flood risk and the uncertainty of climate change with an opportunity to adjust the investment time over the time horizon. For flexible options, this thesis examines single deferrable adaptation options and multiple-stage adaptation options, respectively. Lymington

(UK) is selected as a case study site which has experienced several coastal floods over the last few decades and this coastal village is still susceptible to sea-level rise. In this regard, this research is considered to be relevant to decision-makers and flood risk analysts involved in adaptation decisions in Lymington as well as other areas at the growing risk of coastal flooding due to sea-level rise. In addition, the approach developed in this thesis can give decision-makers or flood risk analysts an important insight or instruction on how to plan or implement adaptation options with flexibility under the uncertainty of climate change.

1. 2 Necessity and timeliness of the research

In most climate change policies, salient problems and issues are associated with uncertainty in the magnitude and occurrence of extreme events (e.g. temperature, rainfalls, droughts or sea-level rise) (Stern, 2007; Hall and Solomatine, 2008; Haasnoot et al., 2013; King et al., 2015). Traditionally, uncertainty was considered as 'unknown risk' when no information would be available to describe its magnitude and probability (Knight, 1919). Thus, decisions under uncertainty were made upon risk analyst's assumptions (i.e. scenarios) to ensure either possible losses were minimised or possible gains were maximised (Hall and Solomaitne, 2008; Van der Pol et al., 2016). Although uncertainty will not be fully resolved, most government guidelines on FRM require the comprehensive understanding of uncertainty before major planning or investment decisions (USWRC, 1983; EA, 2010; MLTM, 2016).

Decision-making on investment in climate change adaptation is undertaken under diverse and plausible climate change scenarios based on scientific understanding and knowledge (Hall and Solomatine, 2008; Nicholls et al., 2014). It is well recognised that adaptation decisions are partly subject to risk analysts' perception and preference to risk aversion (Willow et al., 2003; Hall and Solomatine, 2008). For instance, risk analysts may choose the worst-case scenario to avoid any losses from the risk of coastal flooding under which the possible investment options must be costly. On the contrary, others may prefer the most likely scenario to balance investment cost with reduction in flood risk. Thus, the success of its decision is subject to how risk analysts view the future.

In this regard, ways to treat risk and uncertainty have a significant effect on option evaluation (Tol, 2003; Stern, 2007; Weitzman, 2009; Eijgenraam et al., 2014; Hinkel et al., 2015). Especially when we adopt cost-benefit analysis (CBA) for option evaluation in FRM, the

effect of uncertainty on option evaluation is more apparent. The uncertainty of future scenarios (Tol, 2003; Ranger et al., 2013), experts' views towards risk (Weitzman, 2009; Hinkel et al., 2015) and incommensurability of conflicting values such as environment and culture (Adger et al., 2009; O'Brien, 2009) interact with each other in a complicated way, leading to variations in the result of CBA. Though such issues in CBA have been well recognized by many experts (Stern, 2007; Hunt and Taylor, 2009; Ranger et al., 2013; Van der Pol et al., 2016), CBA is still considered as a mainstay of option evaluation (Maddison, 1996; Tol, 2003; Boardman, 2008).

On the other hand, some approaches deal with uncertainty by finding a 'robust option', which performs relatively well against all the assumed futures (Lempert et al., 2006; Hall et al., 2010). These approaches are characterised by assessing the potential adaptation options under the possible future states assumed by analysts or decision-makers. Thus, they are aimed to assess the robustness of candidate options against the uncertainty of the futures in order to minimise possible regrets or losses (Ranger et al., 2013; Van der Pol et al., 2016). However, additional expenditure for a robust option to cover the various future scenarios may be over-investment or less efficient adaptation, if the realised scenarios are beyond the analysts' assumptions.

In order to resolve such problems with the irreversibility of the investment decision, flexible options that can be adjusted in response to the future states are recently adopted in designs of infrastructure such as coastal defence, dam and water channel as well as any other adaptation measures (Hallegatte, 2009; Haasnoot et al., 2013, Ranger et al., 2013; Woodward et al., 2014). Traditionally, investment decisions are made on a now-or-never basis (Dixit and Pindyck, 1994; Nefuville, 2003; Dobes, 2010). The investment might be either accepted or rejected at the outset by evaluating its utility or performance only with currently available information.

Real option analysis improves such traditional investment decisions by providing a choice available later in the future for decision-makers. It is recognised as an assessment approach to value adjustable options comprising the flexibility of wait, growth, shrinking or/and abandonment (Dixit and Pindyck, 1994; Park, 2002; Linquiti and Vonortas, 2012: Woodward et al., 2014). At the beginning, the uses of real options analysis are mostly found for project appraisals such as R&D, entry into a new market, manufacturing, construction contract or the

building of new factories. Now, it is widely used to a variety of engineering or physical issues by adapting techniques developed from financial sectors to real-life issues.

This thesis starts by focusing on an idea from real options analysis that 'the flexibility of time added on an traditional option is an important element to address uncertainties coming from the future' because it allows us to observe and learn about the future so that we can make more informed decisions as we learn (Dixit and Pindyck, 1994). Adaptive management (AM) - also known as adaptation pathways, dynamic adaptive planning or managed adaptive - and real options approach (ROA) adopt this idea to resolve uncertainties from the futures (Hallegatte, 2009; Ranger et al., 2013, Woodward et al., 2014; Nicholls et al., 2015; Van der Pol et al., 2016; Hino and Hall, 2017). However, a core difference between two approaches is the quantification of flexible adaptation strategies under the future uncertainty of climate change. Both approaches in climate change adaptations are unclear on how the adaptive options have been quantified in terms of economy efficiency as the investment timing is not fully examined in implementing adaptation measures.

Hence, this thesis focuses on quantifying flexible/adaptive strategies with the investment time to vary during a planning horizon so that the investment timing of flexible strategies will be thoroughly addressed under the various future states of sea-level rise and socio-economic development. In the literature on real options analysis, flexible options or strategies are defined as any measures that can be adjusted/modified in the future such as waiting, abandoning, switching, contracting or growing (Dobes, 2010; Linquiti and Vonortas, 2012; Woodward et al., 2014). To introduce the concepts of real options into climate change adaptations, this thesis has to focus on developing a new approach to integrate currently available frameworks for flood risk management such as economic analysis (e.g. cost-benefit analysis, discount rate), climate change scenarios (e.g. IPCC data), risk estimation methods as well as a real options based method. Therefore, the approach developed in the thesis is believed to aid the previous studies with regard to the use of flexibility.

1. 3 Aim and objectives of research

The aim of this research is to develop and apply an integrated approach for evaluation of flexible/adaptive strategies in flood-prone areas against the uncertainty of future flood risk. The newly developed approach enables this thesis to compare various adaptation options including flexibility under uncertain conditions (e.g. climate change or socio-economic change) in a quantitative way. The aim is addressed by considering three research questions which encapsulate the objectives of the thesis. These research questions reflect the steps in applying the framework of real options analysis in climate change adaptation and, thus, help define the potential roles of the real options analysis. The issues and subsequent research questions are as follows.

(1) Implication of the results of real options analysis in climate change adaptation
What do the quantitative values of flexible/adaptive options or strategies have to do with making the adaptation decisions under the uncertainty of climate change?

(2) Ways to use flexibility under the uncertainty of climate change
How can we adapt or optimise the flexible strategies against the uncertainty of future states (i.e. sea-level rise scenarios or socio-economic scenarios) with the quantified values of the flexible strategies?

(3) The effect of real options analysis on reduction in uncertainty
Has the uncertainty been reduced by the flexible strategies and the relevant approach to assess them, or how has it affected the resultant decisions under the uncertainty of the futures?

This thesis also focuses on integrating all the key processes and data that are required in the current FRM while addressing the aim and objectives. Thus, the outcomes from this approach can inform practice in adaptation planning, decision-making, risk analyses and creating public policy in the context of coastal flooding and climate change.

The steps to achieve the aim and objectives are as follows:

- **To develop an integrated method** which comprises the uncertainty modelling of climate change scenarios (in this case, sea-level rise) and socio-economic scenarios (e.g. the number of properties or populations), the setup of flexible/adaptive options,

flood simulations, the monetization of flood risks and, consequently, option evaluations. Thus, all the processes need to be well connected so as to provide a consistent analytical tool to estimate adaptation strategies under the modelled uncertainties.

- **To apply the method via a case study of flood management.** Lymington and its environs (including Pennington and Milford-on-Sea), in the west of the Solent (UK) is selected as a case study site as it is susceptible to coastal flooding and sea-level rise. Adaptation plans to upgrade coastal defenses against sea-level rise are currently available for the Lymington study, providing key information from a FRM perspective (NFCD, 2010; Nicholls et al., 2014). Additional flexibilities (i.e. waiting or dividing) are hypothetically added to the potential upgrade scheme of coastal defenses. This enables the identification of the possible roles of the real-option-based approach in the contexts of coastal flooding under the uncertainty of the futures.

- **To assess the transferability of the framework or method from the experience of the case study application.** This assesses the sensitivity of the results to various factors, including (1) discount rate (r), (2) investment cost (I), (3) the size of coastal defense (S), (4) the type of flexible/adaptive strategies (T), (5) climate change scenarios (C), (6) socio-economic scenarios (SE), etc. The sensitivity test on the flexible/adaptive strategies indicates how each factor has an effect on the results, as well as which factor is more critical in option evaluation.

- **To assess the flexible/adaptive strategies** in terms of risk management, economic efficiency, post-actions (i.e. monitoring), applicability and other relevant factors. The assessment enables this thesis to compare the real-options-based approach to other approaches that have previously been used for decision-making under the uncertainty of climate change. Therefore, the possible roles of the approaches developed in the thesis will be reassessed for further application in climate change adaptation issues.

1. 4 Novelty of the study

This thesis has some distinct points in comparison to previous studies on real options analysis. The key aspects are as follows.

(1) **This thesis has integrated the key processes and data for flood risk analysis and real options analysis.** The adaptation options with flexibility have been quantitatively evaluated in an analytical framework. This integrated method enables us to investigate the effects of the future uncertainty on the value of flexible adaptation options.

(2) **This thesis evaluates two types of real options (i.e. a single deferrable adaptation option and a multiple-stage adaptation option).** Firstly, in terms of an option-to-wait case, the analysis enables us to see how option value changes according to investment time and when it is best implemented. Allowing the investment time to continuously vary, we can estimate all the option values of a deferrable adaptation option in regard to time under the uncertainty of sea-level rise scenarios and socio-economic scenarios.

(3) **Secondly, the analysis of the option-to-grow case also allows us to quantify multiple stage adaptation options under uncertainty in economic terms.** For an option-to-grow case, we can divide a single deferrable investment into multiple sequential investments. As the size of an adaptation option and the number of steps to upgrade the adaptation option change the overall cost, the option-to-grow case requires a more complicated process than the option-to-wait case.

(4) **The evaluation of real options including flexibility has been conducted in both stochastic and deterministic cases.** In the deterministic case, we use mean sea-level rise (MSLR) for option evaluations**,** whereas, in the stochastic case, we have described the uncertainty of sea-level rise by Brownian motion, which is commonly used to depict uncertain variables (e.g. the price of stocks) in physical, engineering or financial analysis. The Brownian motion enables us to describe the deterministic and random evolution of sea-level rise in a numerical way (Dixit and Pindyck, 1994).

Thus, the characteristics of real options have been throughly investigated both in the stochastic and deterministic cases of sea-level rise.

(5) **This research seeks to incorporate the uncertainty of sea-level rise from UKCP 09, as it is, into the analytical framework of flexible strategies.** To evaluate or quantify flexible adaptation options or strategies, the previous studies needed to estimate the probabilities of occurrence of future states (i.e. sea-level rise). Instead of analysing the future states and their own probabilities, this thesis has assessed an adaptation option under individual future scenarios. This approach, to some extent, helps eliminate subjective views on how the future states of sea-level rise will be.

1. 5 Structure of the thesis

The thesis is structured as follows. The logical flow of all the chapters mentioned is illustrated in Figure 1.1.

Chapter 2 provides the understanding of the basic principle and features of real options analysis with reviews on the relevant literature. The current challenges and issues in climate change adaptation have been also reviewed from the perspective of FRM. This enables us to highlight the advantages of real options analysis in comparison with the existing approaches that have been introduced to deal with uncertainty in climate change adaptation or adaptation planning.

Chapter 3 introduces the case study area (Lymington, Milford-on-Sea and Pennington) which experienced several flood damages over the last few decades. This includes a preliminary investigation into the risk of coastal flooding and sea-level rise in the case study site.

Chapter 4 presents methodologies that are necessary for the assessment of flexible adaptation options in regard with real options analysis. This chapter focuses on integrating all the key processes from flood risk analysis and real options analysis in order to offer a basic foundation upon which to quantify flexible options/strategies.

Chapter 5 shows the results of assessing a single deferrable adaptation option in a real-option based framework. The flexibility of wait is incorporated into coastal adaptation measures under the uncertainty of sea-level rise and socio-economic development. This chapter, thus, gives an important insight on how the flexibility of wait can reduce the uncertainty of future

climate change or optimise the investment decision. The option value and investment timing of a single deferrable adaptation is of a main concern in this chapter.

Chapter 6 assesses multiple-stage adaptation options with the same framework as conducted for a single deferrable adaptation option in Chapter 5. Thus, each stage of the multiple-stage adaptation is considered as a single deferrable adaptation option in this chapter. For the analysis, we split a single large investment into two- or three- stage investments. Diverse adaptation pathways have been constructed with different investment costs. All the adaptation paths or sequential strategies are assessed in quantitative terms.

Chapter 7 discusses the results of real options analysis applied into both option-to-wait case and option-to-grow case, respectively and draw the implications of real options analysis for applications to other cases.

Chapter 8 concludes with some suggestions of strategical adaptation measures for Lymington, including general lessons from the applications for future research.

To provide the detailed explanations, the thesis includes appendices at the end of this thesis:

- **A.** Analysis of wave effects on coastal flooding
- **B.** Applying Brownian motion into Sea-level rise (SLR)
- **C.** Change in ESWL by MLSR for different SLR scenarios
- **D.** Change in ESWL by Brownian SLR for different SLR scenarios
- **E.** Investment costs to each stage of multiple stage investment
- **F.** Friction coefficient of floodplains in Lymington
- **G.** Results of flood simulations at various loading conditions
- **H.** Flood damages (£) – Extreme Still Water Levels
- **I.** Change in EAD for MSLR and Brownian SLR
- **J.** Change in expected annual benefit (EAB) across sea-level rise for adaptation measures
- **K.** Change in EAB for MSLR under different SLR scenarios
- **L.** NPV distribution of an adaptation option at different investment times
- **M.** Optimisation of investment time and its option value by formulation
- **N.** Effects of discount rates on optimal investment time
- **O.** Effects of future growth rates on optimal investment time
- **P.** Sensitivity test on different factors

Q. Optimal investment time in the stochastic case of sea-level rise by dynamic programming

R. Derivation of formula for optimal investment time in the stochastic cases of climatic variable(s)

S. Quantitative comparisons of adaptation paths by different premium values

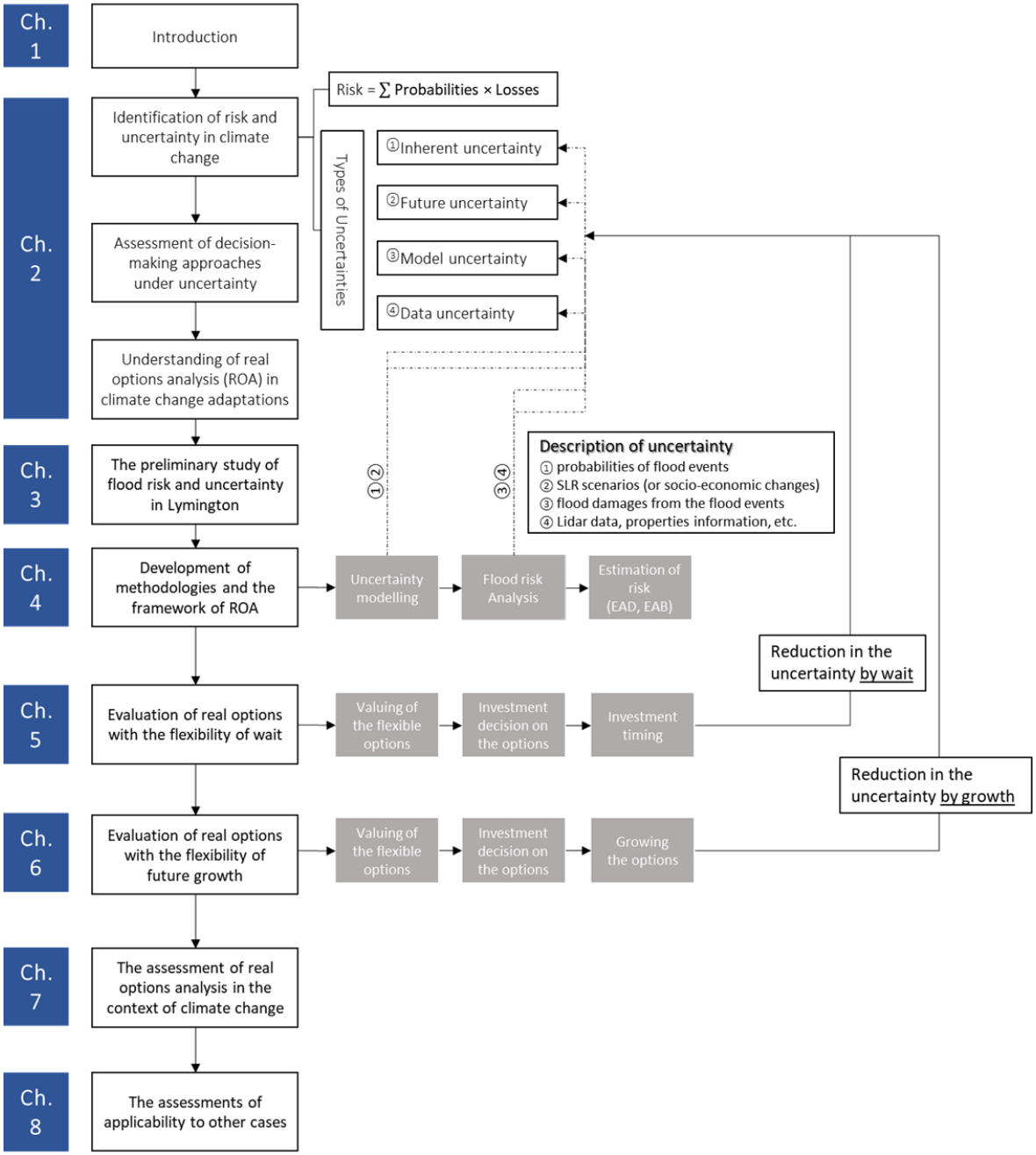

Figure 1.1 Logical flow of the chapters for the thesis

2. Literature review

This literature review chapter includes preliminary studies to make sure the problems and issues are explicitly recognised and addressed. This part focuses on the understanding of uncertainty in climate change as well as the identification of relevant issues in climate change adaptation in order to achieve the goals of the thesis.

This chapter is structured as follows. Firstly, we explore issues on uncertainty and risk around climate change adaptation through relevant literature reviews. This helps identify the natures and types of uncertainty around climate change adaptation as well as define the non-stationary nature of risk of coastal flooding due to climate change or sea-level rise. The next section reviews decision-making tools that are currently used in climate change adaptation. The comparisons of several decision-making tools enable us to understand the characteristics of real options analysis. In the next section, the thesis investigates into the principles and practices of real options analysis with skills and techniques available for real options analysis. Lastly, we review some relevant studies on the use of real options analysis or approach to climate change adaptation issues. This will allow us to know and identify gaps between what is now available and what needs to be improved for real options analysis.

2. 1 Definition and characteristics of uncertainty and risk

There are a number of definitions for uncertainty in human-related issues. Uncertainty is literally defined as ‘the state of being uncertain,' ‘doubt,' ‘unpredictability,' ‘indeterminacy’ or ‘indefiniteness’ (Oxford Dictionary, 2016). In practice, it is used to describe ‘the state of imperfect and/or unknown information in human’s knowledge and action’ ranging from philosophy, through physics, statistics and economics to policies and engineering (Grossi and Kunreuther, 2005). Uncertainty is everywhere there is the imperfection or lack of knowledge on what we pursue. In the perspective of flood risk management, uncertainty is generally defined as ‘the imperfection of our knowledge regarding risk’ (Willows et al., 2003; Hall et al., 2007; Ranger et al., 2013). The uncertainties in FRM may come from the unpredictability of occurrence of natural events (e.g. earthquake), the lack of human’s ability to describe natural or physical systems, unknown future states and limitations on source data for modelling (Willow et al., 2003; Hall and Solomatine, 2008; Tang and Aung, 2008).

There have been a wide variety of research and studies to address uncertainty in and around climate change adaptation (Arnell, 1989, Willows et al., 2003; Ang and Tang, 2006; Ban-Heim, 2006; Hall et al., 2007; Lempert et al., 2007; Hallegatte, 2009; IPCC, 2014; Nicholls et al., 2014). According to the traditional Knightian view (Knight, 1921), the uncertainty was considered as something to be separate from risk. From this perspective, risk was traditionally defined as 'a known character or state with a known probability' while uncertainty was defined 'an unknown risk with an unknown probability' (Knight, 1921). The traditional risk analysis described risk with a known probability that was based on the observations of occurrence and magnitude of the past natural events. On the contrary, the uncertainty was addressed by evaluating the performance of potential strategies or options against individuals' assumed future states (Knight, 1921; Wald, 1949; Savage, 1951).

Currently, regardless of whether risk is known or not, it is defined as the overall possible or probable consequences which have harmful effects on human or natural systems (Willow et al., 2003; Grossi and Kunreuther, 2005; Hall and Solomatine, 2008). Thus, flood risk management and assessment, in quantitative terms, defines risk as the product of the probabilities of occurrence of extreme events and the corresponding damages (Willow et al., 2003; Hall and Solomatine, 2008). On the contrary, uncertainty is now defined as the quality or state of knowledge on risk (Willow et al., 2003). Thus, if our understanding is imprecise, or insufficient, to define natural hazards or events, such a state is defined or termed as 'uncertain'.

The risk and uncertainty are currently treated together in flood risk management because the uncertainty affects both the probability and magnitude of risk (Willow et al., 2003; Hall and Solomatine, 2008; Field et al., 2012). In such an interplay between risk and uncertainty, some important aspects need to be considered for FRM. Firstly, probability distributions are commonly utilised to represent uncertain conditions in engineering or science issues whether they are known or not (Arnell, 1998; Ang and Tang, 2008). It is accepted that the probability distributions of outcomes or predictions are an effective way to communicate uncertainty (Lempert et al., 2007, Lowe et al., 2009; Kunreuther et al., 2013; IPCC, 2014). For example, Intergovernmental Panel on Climate Change (IPCC) represents the confidence of climate change projections with probabilistic ranges (IPCC, 2014; Hinkel et al., 2015). The IPCC report represents a future sea-level rise projection and its uncertainty with a statement that "it is very likely that global mean sea-level rise for the period of 2046 to 2065 (relative to the 1986-2005) will lie between 0.22m and 0.38m for RCP 8.5" (IPCC, 2014). Here, the term

'very likely' means a 90% confidence, while 'likely' means a 66% confidence level (Hinkel et al., 2015). This view or expression of uncertainty is based on a Bayesian probability theory which represents the state of experts' belief or knowledge to uncertain futures or conditions with assumed or well-defined probability (i.e. probability density function, hereafter, termed pdf) – This Bayesian probability is not based on the observation of past events (Ang and Tang, 2005). In this regard, although the uncertainty is an unknown character, the assumed probability for its quantity is assigned to describe the future state. The climate change projections or scenarios developed from IPCC follow Bayesian views in describing the uncertainty of climate change projections (IPCC, 2014). The UKCP projections downscaled from IPCC data also employ the Bayesian probability to express the uncertainty of the projections (Lowe et al., 2009).

Secondly, the risk and uncertainty of climate change occur simultenuously, interacting to each other. For example, let us consider a highly-developed and a non-developed area at the risk of 1-in-200 year coastal flooding, which is a storm surge event with a peak water level of 2.0 mAOD from the present-day perspective. As sea-level rises with time, both areas will be more likely to be innnudated by increased extreme water levels in the future. However, there will be no damage in the non-developed area as there is no valuable assets such as properties, businesses and infrastructure. For explanation, we exclude other asset values such as environment in this exemplary case. Thus, there is no flood risk in the non-developed area.

However, in the highly-developed area, uncertainty has substantial influences on what people value within the area. In this case, not only does the quantity of risk depend on assets within the flooded area, but also it is affected by future sea-level rise which increases the likelihood of coastal flooding. As sea-level rise is uncertain, the risk in the developed area is also uncertain in magnitude and occurrence. This comparison demonstrates how uncertainty and risk interact with each other in association with values and objectives that stakeholders consider within the area of interest (Adger et al., 2009; Hall and Solomatine, 2008; King et al., 2015).

In this regard, a wide variety of definitions of risk and uncertainty appear in literature on flood risk management and climate change adaptation. Generally, in any given year *t*, risk r_t is defined by equation (1) (Hall and Solomatine, 2008).

$$r_t = \int_0^\infty D(\mathbf{X}_t) f(\mathbf{X}_t) d\mathbf{X}_t \tag{1}$$

Where, $D(\mathbf{X}_t)$ is a damage function of $\mathbf{X}_t$, $\mathbf{X}_t$ is a vector of k variables (= (x_1 , … , x_k)) describing possible future states in year t, $f(\mathbf{X}_t)$ is a probability density function:

$\int_0^\infty f(\mathbf{X_t})d\mathbf{X_t} = 1$. It should be noted that a set of future states ($\mathbf{X}_t$) are variables over time so the subscript t is used to denote the year.

In the case of the non-developed area, r_t is zero in equation (1) where there is nothing valuable ($D(\mathbf{X}_t) = 0$). Thus, the uncertainty of the future states $\mathbf{X}_t$ has no effect on the risk in this case. However, if ($D(\mathbf{X}_t) \neq 0$), the uncertainty of the future states $\mathbf{X}_t$ affects the risk. The higher the value of the assets (e.g. properties or commercial buildings) within the area, the higher the damage will be given the future states $\mathbf{X}_t$ in year t. Thus, equation (1) demonstrates that the more highly developed an area is, the more sensitive the risk is to uncertainty.

Due to the characteristics of risk and uncertainty, there are some issues and challenges that need to be addressed in decision-making, in particular, FRM. Firstly, climate change is a long-term event spanning over a century or longer. Thus, uncertainty in climate change is deep and large (Lempert et al., 2003; Groves et al., 2008; Ranger et al., 2010). In terms of sea-level rise, it will occur for multiple centuries (Nicholls et al., 2014; 2018). To adapt our systems and environments to such a long-term change, the centennial or decadal-scale projections of climate change are necessary.

Secondly, the scale and direction of changes in climate conditions (i.e. sea level, rainfall and temperature) are hard or impossible to precisely predict (Hawkins and Sutton 2009; Ranger et al., 2013; Nicholls et al., 2018). Although, in the future, advanced scientific modelling and analyses are expected to improve the accuracy of prediction on future climates, they will inevitably include some level of uncertainty (Stainforth et al., 2007; Pielke et al., 2012; Ranger et al., 2013). Hence, decisions that are influenced by future climate have to be made under wide uncertainty. For instance, Hallegatte et al. (2013) forecast that the 136 largest coastal cities may experience severe flood damages expected to reach US $52 billion/year over the next 50 years due to increase in population, property and its value. In addition, if flood defences are not upgraded, the flood damages at the global scale are expected to increase to US$ 1 trillion or more (Hallegatte et al, 2013; Nicholls et al., 2015). As there is deep uncertainty in sea-level rise, the needs and actions for upgrading the flood defences

upgrades are or will be placed in the context of uncertainty. It is because, the longer the time frame of the decision is, the greater the uncertainty will be.

Thirdly, uncertainty issues are substantial in decision-making processes that evaluate potential strategies and options against risk (Ban-Heim, 2006; Lempert et al., 2007; Hall and Solomatine, 2008; Kunreuther et al., 2013). To address uncertainty within the existing analysis framework such as cost-benefit analysis, risk analysis bounds the range of plausible future scenarios under which potential strategies or options are evaluated according to defined criteria such as economic efficiency, standard of protections, or tolerable risk. Then, it provides the most optimum strategies or options that performs well against the assumed future scenarios (Ban-Heim, 2006; Lempert et al., 2007; Hall and Solomatine, 2008; Kunreuther et al., 2013). The optimum strategies or options chosen by risk analysts may work well for individually defined futures. In other cases, they may perform poorly under unexpected or ignored future states.

The defined future states are subject to how risk analysts have viewed the risk and uncertainty of the futures (Hall and Solomatine, 2008). For example, risk analysts' attitudes towards risk aversion affect an extent to which risk can be tolerated within our system in the worst-case scenario (Lempert et al., 2012). In addition, uncertainty concerns a possibility or probability that such the worst case may or not occur in the future (Hall et al., 2012). Thus, decisions on optimal strategies differ depending on the contexts of flood risk managements and climate change policies (Smit and Pilifosova, 2003; Adger et al., 2009). Apart from that, if socio-economic scenarios are considered together with climate change scenarios, the process of FRM becomes more complicated than excluding socio-economic changes.

Due to various problems identified in FRM, there are increasing calls for comprehensive and integrated approaches to address both uncertainty and risk together (Hall and Solomatine, 2008; EA, 2012). To understand the characteristics of such demands from climate change adaptation, this thesis has reviewed the types and characteristics of uncertainties that frequently appear in climate change adaptation. This helps not only to identify uncertainty issues in FRM, but also set a right direction for real options analysis to address substantial uncertainty issues in climate change adaptation.

2. 2 Types and characteristics of uncertainty and its issues on decision-making

Uncertainty exists in and around climate change issues where the knowledge of the future is not enough to provide complete information or outcomes for involved stakeholders and decision-makers (Willows et al., 2003; Stern, 2007; EA, 2010). Even if climate change predictions or simulations become more accurate and precise in the future than now, the likelihood and intensity of natural hazards will remain uncertain because of imperfection of information and knowledge on the natural hazards (Stern, 2007). Uncertainty in climate change adaptation is defined and classified in many different ways (Willows et al., 2003; Grossi and Kunreuther, 2005; Hall and Solomatine, 2008). The definitions and characters of uncertainty are different depending on where it comes from and how it appears in the process of decision-making (Hall and Solomatine, 2008). Due to the natures and complexities of uncertainty in climate change adaptation, most governments or institutions require the full understanding and explanation of uncertainty in decision-making processes (EA, 2010).

In a broad sense, uncertainty is classified into inherent uncertainty and epistemic uncertainty (Ang and Tang, 2003; Willows et al., 2003; Grossi & Kunreuther, 2005; Hall and Solomatine, 2008). The former type of uncertainty concerns the natural variability of the magnitude and likelihood of environmental disasters (e.g. earthquake or coastal flooding) in the real world whereas the latter type comes from the incomplete human understanding of physical systems, the inaccuracy of data and input parameters, model simulations and any other factors. Therefore, ‘natural variability’ is called ‘aleatory uncertainty’, which cannot be reduced so that it is addressed in probabilistic methods or analyses (Ang and Tang, 2003), whereas ‘epistemic uncertainty’ is referred to as ‘knowledge uncertainty’, which is more detailed into future uncertainty, model uncertainty, and data uncertainty (Willows et al., 2003). Table 2.1 explains the characteristics and examples of uncertainty that emerges in climate change adaptation.

Table 2.1.Types and characteristics of uncertainties in climate change (Source: Willows et al., 2003; Hall and Solomatine, 2008)

Types of Uncertainty	Characteristics	Examples of uncertainty in climate change adaptation
Inherent uncertainty (or natural variability)	Inherent or natural uncertainty defined as uncertainty that exists inherently in natural phenomenon and events regardless of whether our knowledge is perfect or not. Environmental events or extreme climates come under this type of uncertainty. These types of uncertainty are related to the magnitude and likelihood of the natural phenomena (e.g. earthquake, rainfalls, storm surges, etc.). This uncertainty cannot be reduced by advanced analysis and is referred to as 'inherent or aleatory uncertainty' in climate change (Willows et al., 2003; Hall and Solomatine, 2008)	• The magnitude and occurrence of natural events such as water level, waves, tidal/surge, discharge/rainfall, etc.
Data uncertainty	This type of uncertainty is due to limitations on the precision and accuracy of observation, measurements, estimation or data processing. This uncertainty comprises measurement errors, incomplete or insufficient data collection and extrapolation (Willows et al., 2003)	• Size or property of flood defence system • Model grid size • Roughness of floodplain or coastal defence • Representation of buildings and properties in DEM data • Price of buildings and assets
Knowledge uncertainty (or future uncertainty)	This uncertainty is related to the lack of knowledge and evidence on problems that decision-makers may face. Knowledge uncertainty mostly concerns about uncertain futures. Therefore, it is often called 'epistemic or future uncertainty' (Willows et al., 2003; Grossi & Kunreuther, 2005)	• Future land use and properties development • Change in populations and business • Social and urban vulnerability • Change in social discount rate • Change in construction industry/agriculture • Path of greenhouse gas emission scenarios
Model uncertainty	This type of uncertainty reflects our limitations on modelling the real world or physical systems with our insufficient knowledge and techniques. The model uncertainty can be classified as a type of knowledge uncertainty. This uncertainty is due to model choice and structure, input values, parameters and output variables (Willows et al., 2003)	• Climate change projection models • Downscaling from global scale to local scale vice versa • Roughness of floodplain or coastal defence • Statistical uncertainties in estimating extreme events • Flood depth-damage relations • Limitation of simulation programmes • Resolution of model analysis • DEM model

A great deal of efforts towards addressing uncertainty have been made from the improvement of climate change models and projections to the development of decision-making tools (Hall et al., 2012; Haasnoot et al., 2013; Hinkel et al., 2015). Some scientists have made contributions to accurate predictions of future climate scenarios through improved Global Climate Models (GCM) and Regional Climate Models (RCM) (Feyen et al., 2013; Wolf et al., 2015) while others have focused on quantifying uncertainty with a probabilistic range of climate change projects such as rainfall, surface temperature, and sea-level rise (Murphy et al. 2004; Grossi and Kunreuther, 2005; IPCC, 2014). The UK Climate Projection 2009 (hereafter, UKCP 2009) has provided the dataset of climate variables with probabilitic ranges (Lowe et al., 2009; EA, 2010) which have been downscaled from climate change projections at the global scale.

Flood risk management or assessment has also introduced a variety of decision-making tools such as Robust Decision Making (RDM), Multi-Criteria Analysis (MCA), Managed Adaptive Approach in order to provide robust or optimal strategies against the uncertainty of climate change adaptation (Haasnoot et al., 2013; Ranger et al., 2013). Most governments and institutional organizations that address fluvial and coastal flooding recommend the use of appropriate decision-making tools to address uncertainty in climate change adapatation (Willows et al., 2003; EA, 2010; Hallegatte, 2012; OECD, 2016; MLIT, 2016).

However, there are still unsolved issues relating to uncertainty in climate change adaptation. Firstly, climate change (e.g. temperature, rainfall and sea-level rise) at the global or regional scale is occurring over a long-term period (Ranger et al., 2013; Nicholls et al., 2018). According to the IPCC AR5 (Intergovernmental Panel on Climate Change Fifth Assessment Report), the global warming and sea-level rise in 2081-2100 (relative to 1986 to 2005) is predicted to be in the range of 2.6 to 4.8 C° and 0.45 to 0.82 m for RCP 8.5 (Representative Concentration Pathways), respectively (IPCC, 2014). As the estimates of global temperature rise and sea-level rise differ depending on emission scenarios, AR 5 provides separate global temperature rise and sea-level rise scenarios according to emission scenarios (e.g. RCP 2.6, 4.5, 6.0 and 8.5). Moreover, another issue in association with the predictions of climate change is what scale of climate change will happen and whether it will continue in the future (Ranger et al. 2013; Haigh et al., 2014). The future climate scenarios by IPCC AR 5 report show much variation in the possible ranges of sea-level rise projections depending on model

types, scales of simulated areas and emission scenarios as illustrated in Figure 2.1 (IPCC, 2014). In this regard, the climate change projections in AR5 do not fully satisfy the demand of risk analysts or decision-makers involved in climate change adaptation decisions (Hinkel et al., 2015). For example, IPCC AR5 seeks to provide an acceptable prediction of climate change scenario within the defined (likely) range, while risk analysis is more concerned about a high-impact event than a highly-likely event (Nicholls et al., 2014; Hinkel et al., 2015). Also, the IPCC data does not reflect the high-end scenario that needs to be addressed in most risk assessment (King et al., 2015: p. 223).

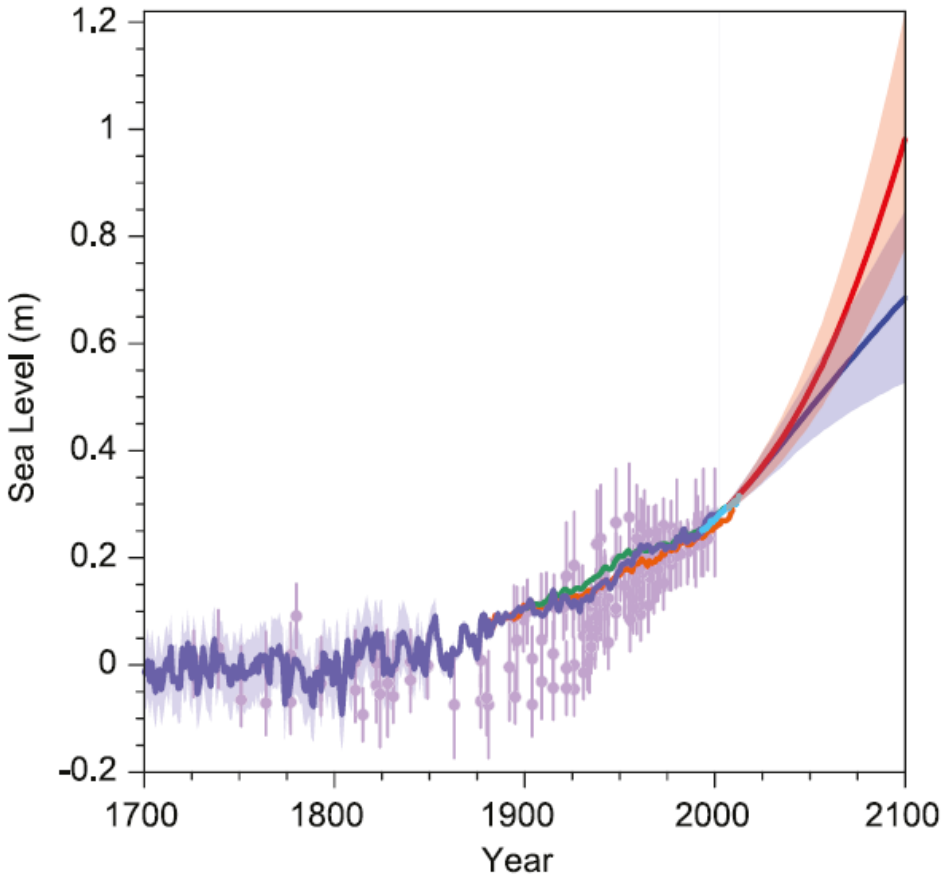

Figure 2.1 Past and future sea-level rise. Proxy data in light purple and tide gauge data in blue, green and orange present the past sea-level rise. Future sea-level projections and 'very likely' ranges (shaded areas) are represented for very high emissions (red, RCP 8.5 scenario) and very low emissions (blue, RCP 2.6 scenario). (Source: IPCC AR5 Fig. 13.27) (Church et al., 2013)

If the uncertainty of future climate is apparent in the process of decision-making, the uncertainty issues are substantial in investment decision (HM Treasury, 2003; Hall, 2007; Gilboa et al., 2009; Ranger et al., 2013). For example, the priority of risk management is on

the aversion of a critical state in which extreme events may cause intolerable damages to human systems or built environments (Ranger et al., 2013). In addition, any casualty due to coastal flood cannot be accepted in societal norms. However, from the perspective of budget holders, or investors, the economic efficiency of climate change adaptation is of main concern (Boardman, 2008; Mendelsohn, 2011). In this respect, incomplete information may lead to the investment being too early or late due to over- or under-estimation of the risk of climate change (Mandelson, 2011). The hasty investments may also result in over-protections or sunk investments whereas the over-delayed investments may result in maladaptation which causes significant costs for recovery due to flood damages.

In this context, the purpose of risk assessment should be aimed to make a balance between the mitigation of flood risk and the economy efficiency of adaptation options under the uncertainty of the future climate change (Nelson et al., 2009; Hall et al., 2012; King et al., 2015; Kim et al., 2018). The choice or preference of options for climate change adaptation is, consequently, subject to the contexts of flood risk management such as the uncertainty of climate change projections, limitations on resource allocations and environmental conditions (Cox and Stephenson 2007; Stern, 2007; Hall and Solomatine, 2008; Hawkins and Sutton 2009; Nelson and Anderies, 2009; Meldelsohn, 2011). In this context, risk analysts or decision-makers are placed in the face of significant challenges in prioritising options or strategies that should meet both the decision criteria of economy efficiency and the standard of protection (Tol, 2003; Hinkel et al., 2015; King et al., 2015: p.45-46). Thus, in some occasions, an investment in climate change adaptation forces decision-makers to trade-off between strategies with the best performance and those with relatively low performance, but less sensitivity, to pursue both the alleviation of flood risk and the economy efficiency of the investment (Hall et al., 2012; Nelson and Anderies, 2009).

2. 3 Decision-making approaches in climate change adaptation

A wide variety of decision-making approaches to address uncertainty are found in climate change adaptation literature. Cost-Benefit analysis (CBA), Robust Decision Making (RDM), Info-Gap theory, Adaptation Pathways (AP) and Real Options Analysis (ROA) are good examples to deal with uncertainty in climate change adaptation (Hall and Solomatine, 2008; Haasnoot et al., 2013; Hallegatte et al., 2012; Ranger et al., 2013; Woodward et al., 2014).

Most approaches are aimed to evaluate and provide an optimal or robust option against uncertainty embedded in the context of climate change adaptation. The decision-making approaches currently used for climate change adaptation are summarised in Table 2.2.

Table 2.2 Summary of decision-making approaches for climate change adaptation

Approaches		Summary	Application to adaptation
Traditional tool	Cost-benefit analysis	Evaluate all costs and benefits of all options and estimate net profits (the overall benefits minus the overall costs)	Worldwide
Decision-making tool under uncertainty	Robust decision making	Define the robustness of options by policy goals, economy efficiency or costs and evaluate the robustness of all candidate options under assumed future states.	Vietnam, UK, US
	Adaptation pathways	Establish a portfolio of sequentially connected adaptation options and decision nodes within possible future scenarios and take investment decisions in response to future states.	Netherlands, South Korea, UK, US
	Real options analysis	Incorporate flexibility (i.e. wait or future growth) in irreversible adaptation options and evaluate the flexible options within possible future states	Bangladeshi, Ethiopia, Mexico UK, US

Each decision-making approach has its advantages and constraints in application. The selection of a decision-making approach relys on the scales and levels of uncertainty and the availability of data (Lempert et al., 1996; Evans et al., 2004; Hall and Solomatine, 2008; EA, 2010; Dittrich et al., 2016). Though uncertainty matters have not been fully resolved by choosing an appropriate decision-making, such decisions should be made upon a comprehensive consideration of all the potential impacts of uncertain factors as well as the primary sources of uncertainty during an economic evaluation. Two critical issues are found in the deision of climate change adaptation: (1) how to define and model uncertainty from changing climate; and (2) how to quantify risk which interacts between the magnitude of natural disasters and the value of human's assets under uncertainty (Hall and Solomatine, 2008; Dawson et al., 2015; RACC, 2015). Thus, uncertainty in climate change adapatation cannot be addressed without considering decisions to be made and assumptions required for such decisions (Hallegatte et al., 2012).

The successful application of any decision-making tool is subject to judgements made by decision-makers in the context of climate change adaptation (Hall and Solomartine, 2008). In this respect, there is no decision-making tool that fully resolves uncertainty issues in climate

change adaptation (Watkiss et al., 2015). It is important to identify the features of decision-making processes in dealing with uncertainty. The following sections have compared decision-making processes commonly and widely used in addressing uncertainty in climate change adaptation. There are also other relevant approaches to deal with uncertainty such as Info-Gap theory, Multi-Criteria Decision Analysis (MCDA), Portfolio Analysis (PA) and so on. However, rather than investigating all approaches available for flood risk analysis, this thesis seeks to extract the salient characteristics of real options analysis in contrast to relevant decision-making processes with a focus on comparison between flexibility and non-flexibility in option evaluation.

2.3.1 Cost-benefit analysis (CBA)

Traditionally, cost-benefit analysis is commonly used to assess options where expected gains and losses can be quantitatively measured in terms of the social preference of the present over the future (Dasgupta and Pearce, 1972; Tol, 2003). In cost-benefit analysis, the expected gains should be greater than the expected losses for an option to be implemented. This simple rule is directly represented with a formulation of net present value in equation (2):

$$Net\ Present\ Value\ (NPV) = V - I = \sum_{i=0}^{L} \frac{B(i)}{(1+r)^i} - \sum_{i=0}^{L} \frac{C(i)}{(1+r)^i} \qquad (2)$$

$$NPV = V - I < 0 \qquad (Not\ invest)$$

$$NPV = V - I > 0 \qquad (invest)$$

Here, *V* is project value, *I* is investment cost, *B(i)* is an expected benefit at year *i*, *C(i)* is an expected cost at year *i*, *L* is the length of project life and *r* is discount rate. Conventionally, cost-benefit analysis under uncertainty follows several steps as outlined below (Hallegatte et al., 2012)

1) Identify potential projects or options for flood risk management
2) Explore the sources of uncertainty and future states
3) Evaluate overall costs and benefits for each project during the period of its life
4) Calculate the present value of all the streams of the costs and benefits
5) Test the sensitivity of net present value to uncertain futures

The results (i.e. Net Present Value, hereafter, termed NPV) from CBA are very sensitive to option parameters (i.e. discount rate and project life) and conditions (i.e. future scenarios) (Hallegatte et al., 2012). In applying cost-benefit analysis in climate change adaptation, one particular issue is related to the representation of the probability of future events or states as it has significant effects on expected benefits from candidate options. The expected benefit is defined as reduction in flood damage due to any adaptation measure (e.g. coastal defence upgrades). Conventionally, the expected benefits under uncertain future states are estimated by averaged values or expected utilities (Dasgupta and Pearce, 1972; Von Neumann and Morgenstern, 2007). The expected benefit under uncertain futures implies the most likely value in a statistical sense.

In this context, some literature has pointed out that the result of the cost-benefit analysis is highly dependent on experts or analysts' belief on the likelihood of possible states of futures (Von Neumann and Morgenstern, 2007; Hallegatte et al., 2012). As CBA is based on the best estimate of climate change scenario, subsequent decisions are highly likely to fail to meet the criteria of cost-benefit rules under a rare or low-probability, but high impact, future (Morgan et al. 1999; HM Treasury 2003; Stern, 2007). Besides, another issue raised in cost-benefit analysis is that all the possible events are statistically averaged (Halleggate et al., 2012; Hinkel et al., 2015, King et al., 2015). Thus, despite the effect of extreme or disastrous event on the real life, its effect may be little in option evaluation.

Many studies in literature suggest that decisions from cost-benefit analysis should be tested against various future states (Morgan et al. 1999; HM Treasury 2003; Tol, 2003; Stern, 2007). Despite such disadvantages, the cost-benefit analysis is a basic approach that most government and institution require for investment decisions (EA, 2010; IPCC, 2014). Therefore, the merit and demerit of cost-benefit analysis should be understood before its application to risk management. The cost-benefit analysis is routinely used with other approaches (e.g. robust decision making) to address uncertainty in climate change adaptation.

2.3.2 Robust Decision making (RDM)

Robust decision making (RDM) pursues the robustness of potential options against all plausible futures rather than an optimal response to a single most-likely future (Lempert et

al., 2007; Hall et al., 2012; Hallegatte et al., 2012). This implies that options immune to variations in the future states are considered to be robust in option choice. This approach invented by Lempert et al. (2007) provides a decision framework in which experts and decision-makers evaluate the performance of candidate options against all the plausible futures. This approach is considered useful when uncertainty is very large or future information is missed (Watkiss et al., 2016).

Robust decision-making can be applied to environmental policies, flood protection measures or any other interventions which may cause the long-term effects on reducing the risk of climate change under uncertainty (Lempert et al., 2006; Lempert and Collins, 2007, Hall et al., 2012; McInerney et al., 2012). Though its procedure differs depending on where it applies, RDM follows four major steps as below.

1) Determine candidate strategies and assume a range of uncertain future states
2) Examine the candidate strategies or options over the range of assumed future states
3) Bound future states in which the candidate options meet target performance established by policy goals, budget constraints, or economy efficiency
4) Assess the robustness of each option within the defined or assumed futures

This analysis takes iterative processes from step 1 to 4 to ensure the comparisons of the performances of all the candidate options under the assumed future states. Thus, depending on criteria based on the performance metric, no regret option or minimax option can be selected to meet the objective of the decision-making process. The performance metric can be cost, benefit, loss or reliability. The robustness for any candidate option x_i for a given set of future states S, is defined in equation (3).

$$\text{Robustness} = R(x_i, S) \tag{3}$$

Here, R is any function representing the robustness metric of a candidate option x_i for a given set of future states $S = \{S_1, S_{2,\ldots,} S_n\}$. The robustness is calculated by transforming the performance metric $f(x_i, S)$ $(= \{f(x_i, S_1), f(x_i, S_2) \ldots\ldots f(x_i, S_n)\})$ to $R(x_i, S)$ over the set of scenarios (Hall et al., 2012; McPhail et al., 2018). Although different robustness metrics (e.g. no regret, minimax, expected utility) can change the definition of the robustness in equation

(3), the principle of RDM pursues to find a robust option that satisfies the target goal of the robustness set by decision-makers under a given set of future states. This assessment process enables stakeholders to engage with decision-making by recognizing the vulnerability of potential policies or options. This approach helps decision-makers to identify the success/failure conditions over a wide variety of futures.

2.3.3 Adaptation pathways approach or adaptive management (AM)

There are numerous terms used to refer to Adaptive Management (AM) or adaptation pathways approach in the literature on climate change adaptation. For instance, pathway flexibility, dynamic adaptive planning, iterative risk management, and managed adaptation are all classified under the adaptation pathways approach (Haasnoot et al., 2013; Ranger et al., 2013).

In adaptation pathway approach, adaptive plans or strategies are implemented sequentially in response to the increasing risk of coastal flooding and, thus, they can be adjusted, or switched to other options as new information emerges (Ranger et al., 2013). The flexibility in this approach can be a structural (e.g. the extension of coastal defence), non-structural measure (e.g. flood warning system, policy) or both (Ranger et al., 2013). The flexibility included in a set of adaptation measures enables the adaptive management to be more robust against risk and uncertainty than traditional approaches without such flexibility. For example, the extension plan of coastal defence for a long-term timescale can be included in the early stage of construction of the coastal defence (Reed et al., 2009; EA, 2010; Haasnoot et al., 2013; Ranger et al., 2013). Once such flexibility for future extension has been included in adaptation options, it will be optionally or selectively used to improve the capacity of coastal defence in response to the future risk of flooding.

The adaptive management defines a route-map including a portfolio of options, decision paths, and nodes under all the possible range of future states or scenarios (Nicholls et al., 2015). All of the options and paths are well connected to each other within the narrative of adaptation strategies against all the possible future states (Ranger et al., 2013). According to the realized climatic variable and future learning about climate change (e.g. sea levels), the sequentially- connected options within adaptation pathways will be taken to cope with the rising risk of coastal flooding over time. The options can be structural (e.g. seawall) or non-structural (e.g. flood warning). Therefore, this strategy is characterised by switching or

adjusting options within a route map in response to the future states. In general, the adaptation pathways approach follows several steps as below (Hasnnoot et al., 2013).

1) Describe the current and future situations of risk and define the objectives of adaptation policies
2) Analyse the vulnerability of floodplains under the plausible future scenarios
3) Identify appropriate options or plans to address the vulnerability
4) Analyse the ensembles of transient climate change scenarios
5) Determine the sequence of adaptation actions to deal with the future scenarios
6) Map out decision paths and thresholds to trigger the sequentially- connected adaptation actions

An important feature of adaptation pathways approach is the identification of climatic (or other) variables to trigger changes to the selected pathway (Haasnoot et al., 2013; Ranger et al., 2013). Adaptation pathways are made up of decision nodes and pre-defined threshold values above which the system or environment will be critically vulnerable to the risk of coastal flooding unless the adaptation measure is implemented (Hallegatte, 2009; Ranger et al., 2013). Thus, the adaptation pathways approach is an iterative, dynamic and heuristic process.

This method has been applied in the Thames Estuary 2100 (TE 2100) project, which is well known to be the first infrastructure project to deal with deep uncertainty in the UK (Reeder et al., 2009; Ranger et al., 2013; Nicholls et al., 2015). A portfolio of options are sequentially planned to cope with sea-level rise from 4 to 6 m so that this strategy covers all the possible or probable futures over the next one to two centuries, including the most extreme case of West Antarctic Ice Sheet (WAIS) collapse. A group of sequential adaptation options planned in pathways are considered to be robust as a whole against the uncertainty of futures, not only because the adaptation pathways approach prepares for all the possible risk of future sea-level rise, but this approach enables stakeholders to avoid the possibility of wrong or irreversible investment. This adaptation pathways concept is vigorously used in a number of cases such as the South-western Delta and Dutch Delta programme (Netherlands) and New York city (US) (Haasnoot et al., 2013). The merits and demerits of the adaptation pathway approach are summarised in Table 2.3.

Table 2.3 The merits and demerits of the adaptation pathways approach (Ranger et al., 2013)

Advantages	Disadvantages
Decision-Centric adaptation planning: This approach maintains flexibility in decision to ensure its planning is adaptable to diverse scenarios, so its approach is scenario-neutral	Possibility of exposure to risk: During the period of delaying an option, losses from the risk may happen
Effectiveness of investment timing: Investment timing can be adjusted when climate change is different from what is expected	Maladaptation: In a case where an initial investment is not possible at the outset, the delay can be considered as maladaptation or may cause higher costs than the investment now, if disastrous flooding occurs
Robustness of decision: Decision is flexible enough to cover all the sources of risk and uncertainty of climate change	The complexity of analysis: This approach is difficult to simplify and apply so that the cost-benefit analysis can be more complicated.

2.3.4 Real options analysis

If there is large uncertainty in investment decisions, waiting, switching, shrinking or growing can be an alternative decision or strategy that analysts or decision-makers can add to the existing options (Dixit and Pindyck, 1994; Park, 2002). These types of options allow our knowledge to increase and potentially reduces uncertainty by allowing more time to be spent on observing how the future unfolds (Hallegatte et al., 2012). These types of decision-making processes are all classified under real options approaches or analyses, which originally emerged from financial options or strategies (Arrow and Fisher, 1974; Dixit and Pindyck, 1994; De Neufville, 2003; Hallegatte et al., 2012; Woodward et al., 2014; Hino and Hall, 2017). A difference between the adaptation pathways approach and the real options analysis is that investment for real options analysis should be irreversible. In real options analysis, flexibility that decision-makers or investors can take under uncertain future states is considered to be an additional option that needs to be assessed in option evaluation (Dixit and Pindyck, 1994). In this respect, the real options analysis is different from standard cost-benefit analysis which cannot include flexibility in option evaluation.

A real option value (ROV) comprises a net present value (NPV) and a real option premium as shown in Figure 2.2 (Park, 2002). The real option premium is attributable to flexibility added

on an option, whereas NPV is a value that investors or option holders will receive when the option is implemented immediately. If the real option value is higher than the net present value (i.e. ROV > NPV), the wait is preferred to the immediate investment. Otherwise, the investment now (i.e. NPV >0) or abandonment (i.e. NPV <0) is a plausible strategy or reasonable decision for option holders to take.

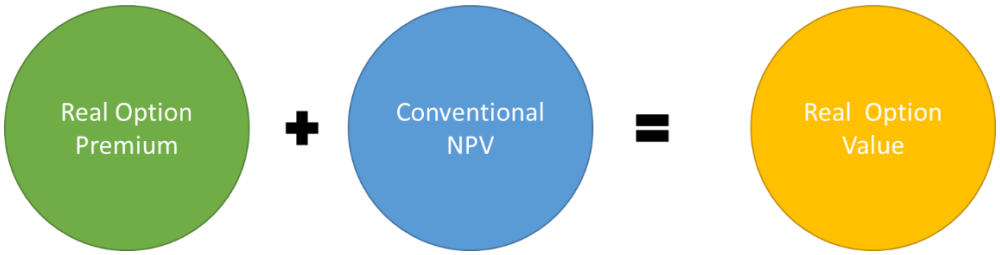

Figure 2.2 Illustration of real option value with real option premium and conventional NPV

Even if NPV of an option is below zero (i.e. the overall benefit is less than the overall cost), the option value may become positive in real options analysis. The real option analysis evaluates a possibility that gains from the investment will be higher in the future than now (Park, 2002). An ability to defer or wait allows investors or decision-makers to learn more about the potential choices via observation. Thus, the decisions including the possibility of future learning will make options more robust against the uncertain futures. Generally, real options analysis follows a few of steps as below.

1) Determine the sequence of options lasting over, at least, two periods of future states
2) Define two or more possible future states regarding climatic variables
3) Allocate the estimates of probabilities to each of the future states
4) Evaluate the net present value (NPV) of each set of options under each future state
5) Aggregate the probability-weighted NPVs from step 4.

Real options approach is applicable where three investment conditions are satisfied: (1) *flexibility*: investors or option holders have an ability to defer an investment with no restriction; (2) *irreversibility*: the investment is irreversible; and (3) *uncertainty*: the future gains may rise or fall depending on the future states (Dixit and Pindyck, 1994). In this regard, real options analysis seems to be similar to adaptation pathways approach because both hold options until more information is available. However, the adpatation pathways approach can take structural or non-structural measures (e.g. flood warning system) to reduce flood risk.

Some measures included in the adaptation pathways may be reversible. In addition, the quantification of flexibility in real options analysis is a key feature to distinct itself from the adaptation pathways apporach. The value of real option enables decision-makers to know whether flexibility incorporated in real options is worthy. In this respect, the real options analysis is also involved with decisions with respect to the investment timing under uncertainty (Dixit and Pindyck, 1994).

To understand the characteristic of real options analysis in climate change adaptation, the methods explained so far are compared according to various criteria considered in decision-making as shown in Table 2.4 and 2.5. However, it should be noted that the choice of decision-making process depends on the objectives of adaptations, the degree of uncertainty and the types of adaptation measures. In the end, the use of real options analysis or approach is subject to the context of climate change adaptation.

Table 2.4 Advantages and disadvantages of decision-making approaches that address uncertainty in climate change adaptation

Methods	Principles and assumptions	Advantages	Disadvantages	References
Cost-Benefit Analysis (CBA)	CBA compares the overall costs and benefits from preferred options during the project life. It is based on expected utility theorem. Thus, the options are evaluated under the most likely scenario rather than the worst or best scenario. All the cash flows are discounted to the present for comparisons of the present and future values of the options.	1. CBA is axiom for investment decisions in economic terms 2. The investment rule is simple (the overall benefits exceed the overall costs) 3. The option is assessed under the most likely future state which is considered as rational 4. The application is not difficult 5. CBA is used with other approaches so that the method of CBA is complementary	1. A selected option is optimal only to a single most-likely future 2. It is difficult to monetise all values in option evaluation. If social values are monetised, its outcome appears to be subjective. 3. The outcome is very sensitive to uncertainty or different futures. 4. No future learning and irreversible decisions 5. The single most-likely future may be also subjective to analysts	Bernoulli (1738), Tol (2003), Von Neumann and Morgenstern (2007), Penning-Rowsell et al. (2014)
Robust Decision Making (RDM)	RDM evaluates the performance of options under various plausible futures. The uncertainty of the future is considered by assuming the various future states. The performance of the adaptation option is traded off with the less sensitivity to the future when the option is selected.	1. The performance of a selected option meets the defined criteria under plausible futures 2. RDM is a systematic approach to ensure the selected options are immune to uncertainty 3. The approach is useful when future uncertainties are poorly characterised 4. The robust option performs well over a wide range of scenario futures	1. It is complicated and expensive to assess options over a number of plausible futures 2. The decision is robust only for futures assumed by decision-makers. 3. Decisions may differ depending on the criteria of the option performance and the views of analysts towards the futures 4. It is difficult to adjust a decision when the unexpected future is realized	Lempert et al.(2007), Hall et al.(2012)
Adaptive Management (AM) or Adaptation Pathways Approach	A sequence of adaptation measures provides a robust strategy as a whole against all the possible future scenarios. The adaptation pathways consist of predetermined multiple interventions, critical thresholds and decision paths to cope with varying future risks.	1. This strategy is, as a whole, robust against all the possible futures 2. It includes future management strategies against the uncertainty of future 3. The strategy is flexible so that it can avoid irreversible or sunken investments 4. Future learning and observation are key elements for this approach 5. It helps implement options at the right time	1. The method of economic appraisal within the framework of AM is less developed 2. Planning adaptive strategies is complex 3. It may lead to maladaptation if thresholds to trigger options are too high 4. The strategy may be highly subject to decision-makers' attitudes towards risk 5. Costs at the outset are high due to future extension	Hallegatte (2009), Haasnoot et al. (2013), Ranger et al.(2013), Nicholls et al. (2015)
Real Options Analysis (ROA)	The core character of ROA is to evaluate flexible options under uncertainty. This approach assumes possible future states to which the probabilities are assigned by experts' judgements. The option may be implemented or not in response to the future state. This flexibility is assessed in the framework of option evaluation.	1. Flexibility (e.g. wait or future extension) is included in investment decisions 2. It is a systematic approach to evaluating options and flexibility under uncertainty 3. It is useful when considering the investment timing or adjustment of investment in stages 4. The value of flexible option is achieved by future learning and actions so that the future actions can be estimated in this framework	1. It is complicated to apply ROA to real engineering issues 2. It is less developed in adaptation issues 3. It is hard to define future states 4. It may lead to maladaptation when an option is delayed to the long distant future 5. ROA requires additional costs for flexibility 6. Flood events may trigger adaptation actions rather than the results of ROA in the real world	Dixit and Pindyck (1994), De Neufville (2003), Woodward et al. (2014), Hino and Hall (2017)

Table 2.5 The assessment of the decision-making approaches according to various aspects in addressing uncertainty

Approaches	Cost-Benefit Analysis	Robust Decision Making	Adaptive Management	Real Options Analysis
Robustness of options against uncertain futures	Very low	High	Very High	High
Understanding of futures	Deterministic with no future learning	Probabilistic with no future learning	Deterministic with future learning	Probabilistic with future learning
Economic efficiency under uncertainty	Low	Medium	Medium	High
The possibility of sunk investment (if expected future are not realized)	The investment may result in over- or under-estimation	The investment may result in over- or under-estimation under different futures. However, such possibility has already been considered in the decision	Only the spending for flexibility may be sunk, but the proper amount of payment on the flexibility needs to be evaluated.	Only the spending for flexibility may be sunken, but the proper amount of spending has already been evaluated in option evaluation
Way to manage the risk of climate change	An option that performs well under a single likely future is selected	Candidate options are assessed under all possible futures, but this method compromises the performance of options	A portfolio of options are made up to cover all the future states and the options will be implement in response to the future states	A set of options are made against predefined futures and the options will be implemented in response to the future states
Attitudes towards flood risk	Neutral	Aversion	Aversion	Neutral
Optimality or robustness of options to future	Optimal only to the most likely future	Robust to a set of assumed futures	Robust to all the possible futures	Robust and optimal to all the possible futures
Quantification of flexibility	No	No	No	Yes
Flexibility of options	No	No	Yes	Yes
Attitudes towards the futures	The most likely future is subject to decision makers views or interests. Selected options are highly likely to be subjective to the worldview of decision-makers.	All the plausible futures are considered by decision-makers. Decisions are also likely to be subject to the agreed views by decision-makers towards the future or risk.	All the possible range of futures are considered as well-defined scenarios by experts for option selection	Experts consider all the possible futures. However, the probabilities of the future states are, though, consequently subject to expert's views.
Decision-making process	Economic evaluation of options in the most-likely future	Iterative process of option evaluations for all the possible futures	Scenario-based and decision centric approach	Evaluation of flexible options under the probability-weighted futures
Implementation timing	Now	At a defined specific time	Depending on the future	Depending on the future
Additional actions after decisions	Nothing	Nothing	Observations and future learning	Observations and future learning

2. 4 Principle and characteristics of Real Options Analysis (ROA)

2.4.1 Natures and types of real options

As aforementioned, flexibility is an essential element of real options analysis (Dobes, 2010). The types of real options can be subsequently defined by how or where to incorporate flexibility in association with options that we consider under uncertainty (Park, 2002; De Neufville, 2003). For instance, how to make our designs or systems more flexible to uncertain future conditions may be of a primary interest to engineering designs or physical systems (De Neufville, 2003). Designing a wider base, or buying adjacent lands for the future upgrade of coastal defences against climate change, is a good example of real options (Dobes, 2010).

This type of real option is classified as real option 'in' system because the flexibility should be planned or designed in options or strategies at the outset (De Neufville, 2003; Wang and De Neufville, 2005; Woodward et al., 2014). This type of adaptation option needs additional cost for flexibility to be maintained in itself (Woodward et al., 2014; Hino and Hall, 2017). On the other hand, stakeholders or decision-makers in financial markets seek to pursue the best benefit from investment under uncertainty (De Neufville, 2003). Their main concerns are on when the investment should be triggered, given, for example, the fluctuation of stock or energy price. They can use flexibility for deferring the investment to the best timing in the future. This type of real option is called real option 'on' system because the flexibility of wait or deferral can be added onto the option without any internal adjustment to the original option (De Neufville, 2003; Wang and De Neufville, 2005). Thus, the analysis of real options 'on' system relates to investment timing under uncertainty.

These different types of flexibilities need to be explored in association with the uncertainty of climate change and, in particular, sea-level rise as the uncertainty of climate change is fundamentally different from that of the price of commodities or stocks. The uncertainties in climate change occur in a longer-term timescale than in financial markets and they are represented by various scenarios, provided by the narratives of the future climates and scientific modelling. The objectives and characteristics of real options analysis are compared between financial markets and physical systems in Table 2.6.

Table 2.6 Comparison of real options analysis between physical (or engineering) systems and financial options (De Neufville, 2003)

Areas	Physical systems	Financial markets
Objective of analysis	Go or not	Return on investment
Accuracy of data	Low	High
What to observe	Future state of physical conditions	Market price of assets or products

Depending on how to include flexibility in options, option holders can create the various forms of real options: (1) invest now (2) wait (3) grow (or shrink) or (4) do nothing (Park, 2002). For example, decision-makers can either defer an option to a date when more information is available, or launch an option at the start (Park, 2012: p.731-737). In some cases, decision-makers are more willing to partly invest in an option at the outset due to limitation to available resources, or constrained budgets, so that such decisions may leave the remaining part for the future decision. How such a flexibility applies to investment decisions depends on how decision-makers or risk-analysts will manage uncertainty and allocate the investment cost over the life of a project (Dixit and Pindyck, 1994; Woodward et al., 2010; Jeuland and Whittington, 2014). The types of real options are arranged in the order of the degree of 'reversibility' and 'adaptability to climate change'. Figures 2.3 and 2.4 show typical examples of real options according to the degree of flexibility/reversibility.

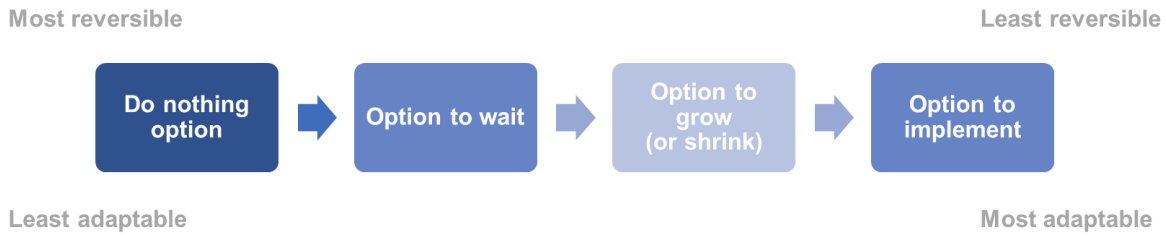

Figure 2.3 Types of real options in order of reversibility

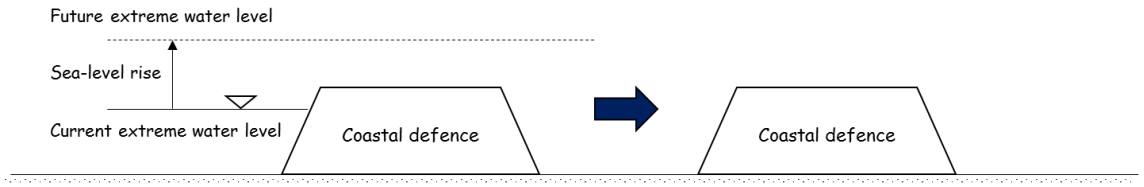

(a) Do-nothing option

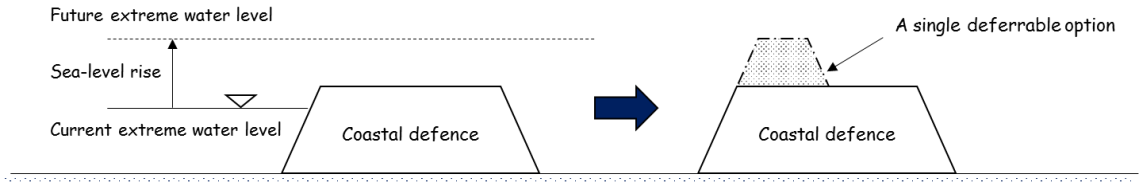

(b) Option to wait

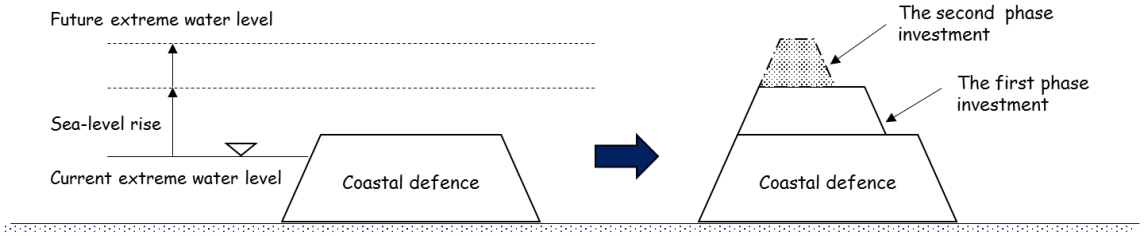

(c) Option to grow

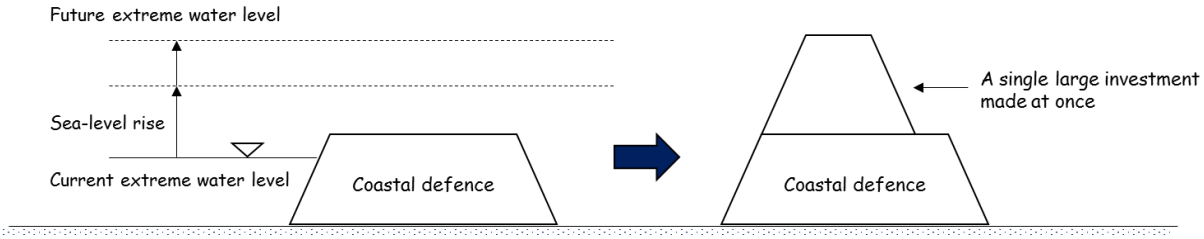

(d) Option to invest now

Figure 2.4 Examples of real options for the case of coastal defences: (a) Do nothing option; (b) Option to wait; (c) Option to grow; and (d) Option to implement – The coastal defences have been upgraded according to sea-level rise - The dash-lined coastal defence is the upgrade scheme whereas the solid-lined coastal defence means the upgraded defence.

The terms of real options differ depending on how to include flexibility in options. The common types of real options are detailed as follows (See Figure 2.4).

(1) Option to do nothing is defined as a baseline scenario to describe the current state of defence condition. It is the least adaptive option to the risk of coastal flooding and climate change among all the possible options. This option incurs no capital cost of

upgrading coastal defence but the cost of maintenance and monitoring. Note that the cost of maintenance and monitoring is all the same with other options. This option can be considered as maladaptation in the growing risk of coastal flooding. However, there is no possibility that the investment is sunk in the future.

(2) Option to wait describes a state that an option is ready to go against the future risk, but it is held until more information is available. This type of option appears similar to 'do nothing option' at the outset. However, it aims to explicitly address the certain level of the future risk. The option to wait is to keep observing and learning about the future in order to take an action timely. This can be a case where the design of upgrading coastal defence has been completed, but the implementation is held due to the future uncertainty. Thus, the 'option to wait' is more adaptable to the future risk of coastal flooding than the 'option to do nothing'. An important issue on an option to wait is investment timing (Dixit and Pindyck, 1994).

(3) Option to grow is sequential or multiple-stage investments in practice (Dixit and Pindyck, 1994). It refers to a state that an initial investment has been made in the first stage, and the remaining parts of the investment are held until more information is available. Subsequently, the option to grow includes a component of option to wait as an additional decision. The implementation of the remaining parts also depends on the future states. If necessary, the rest of the option will be implemented in the future. Otherwise, it will be abandoned (Dixit and Pindyck, 1994).

(4) Option to shrink is similar to 'option to grow'. Both use flexibility to adjust/modify statregies or plans in the future. However, it is designed to enable decision-makers to contract the excessive capacity of an option in the future. For example, decision-makers can develop an airport larger than its required capacity for increasing use in the future. If its capacity to manage the extra number of passegeners or airplanes turns out to be redundant, this additional capacity can be switched to other uses or purposes (i.e. accommodation, business, commercial areas, etc.) (Dobes, 2010). In climate change adaption literature, an excessive investment cannot be found with future shrinkage in mind. However, it is less reversible than the option to grow as a huge

amount of money is excessively spent on the redundunt part of the adaptation. Sometimes, this decision may cause a criticism of over-investment or adaptation.

(5) Option to invest now is the same as a traditional option made on a now-or-never basis. As the option is based upon the most-likely future, this type of decision is deterministic, comparing to other types of real options (Dixit and Pindyck, 1994). Thus, the option to invest now is the most irreversible to the uncertainty of futures unless the most-likely future occurs in the future (ibid). However, this option may be more appropriate than the option to wait, or do nothing, where the flood risk is explicitly high. Most decisions implemented now can be classified under this type of option.

The concept of real options explained can be applied for climate change adapatation to address the risk of future climate change, as well as to avoid sunk investment (Dobes, 2010; Linquiti and Vonortas, 2012; Woodward et al., 2014). Thus, the focus of real options analysis should be on how to better incorporate flexibility into investment decisions and how to quantitatively evaluate real options in the context of the rising risk of coastal flooding. The next section explains the principles and methods of evaluating real options under the uncertainty of future prices or profits.

2.4.2 Basic principles of evaluating real options

The value of flexibility incorporated in real options can be clearly understood by considering a simple case where uncertainty lasts over only two periods. If a price or annual profit is expected either to go up or down after 5 years, investing in 5 years can be a better option to reduce the impact of uncertainty on project values. To assess such flexibility, a price or annual profit is assumed to go up or down in 5 years with its probability of p or q, respectively. This simple case also assumes that change in the price or profit occurs once and, then, becomes constant after 5 years. Figure 2.5 illustrates how the price changes over the two periods.

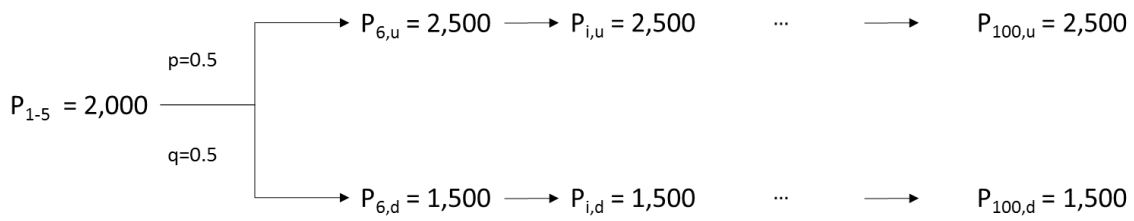

* $P_{1\text{-}5}$ = Price for the first 5 years, $P_{i,u}$, $P_{i,d}$ = Upward or downward price at year *i*, respectively

Figure 2.5 Example of option valuation for change in price over two periods (unit: £ K)

In a standard cost-benefit analysis, net present value (NPV) can be simply evaluated as below. For convenience, the discount rate is assumed to be 10 % during the life of the project. The investment cost is £ 20 million and has to be made at *t*=0.

$$NPV = V_0 - I = \sum_{t=1}^{100} \frac{(P_o)}{(1+r)^t} - I = \sum_{t=1}^{100} \frac{(2{,}000)}{(1.1)^t} - 20{,}000 \quad (4)$$

$$= 19{,}998 - 20{,}000 = -£\,2\ (K)$$

Where, V_0 : present value of the project

I : investment cost

r : discount rate (= 10%)

In real options analysis, the uncertainty on the price (P_1) after 5 years can be considered in the option evaluation. Suppose that option holders withhold the option till $t = T_5$ (= 5 yrs). If the value of P_1 goes up to £ 2.5 million after 5 years, the investment will be made with £20 million spent in year T_5. However, if the value goes down (P_1 = £ 1.5 million), the investment will not be made at year 5 (T_5). In this regard, the option to wait gives a different NPV than when calculated in the standard cost-benefit analysis. In the perspective of a standard cost-benefit analysis, the price P_1 is just the aggregation of the probability-weighted prices (i.e. $P_1 = P_{1,u} \times q_u + P_{1,d} \times q_d$ = £ 2 M). The real option value for the option to wait is computed using the cost-benefit analysis as if the option is deferred to time T_5 as below. The calculation of real option value (ROV) is as below

$$ROV = (q)_u * \left(\sum_{t=6}^{105} \frac{(P_{1,u})}{(1+r)^t} - \frac{I}{(1+r)^5}\right) + (q)_d * \left(\sum_{t=6}^{105} \frac{(P_{1,d})}{(1+r)^t} - \frac{I}{(1+r)^5}\right) \quad (5)$$

$$= 0.5 \times \left(\sum_{t=6}^{105} \frac{(2{,}500)}{(1+0.1)^t} - \frac{20{,}000}{(1+0.1)^5}\right) + 0.5 \times \left(\sum_{t=6}^{105} \frac{(0)}{(1+0.1)^t} - 0_{(no\ invest)}\right)$$

$$= 0.5 \times (15{,}521 - 12{,}418) + 0.5 \times (0) = £1{,}551\ K$$

Where, $(q)_u$: the probability of the price going up

$(q)_d$: the probability of the price going down

$(P_{1,u})$: an upward price from T_5

$(P_{1,d})$: a downward price from T_5

As seen in equation (5), the second term of the option value at the downward price $P_{1,d}$ is zero, because no investor will launch the project in this case. As the investment is not made at this downward value of P_1 = £1.5 (million), there will be no benefit in this case. If the investment is made with the declining value $P_{1,d}$ of £1.5 (million), the NPV in the second term will be -£ 3.15 million ($=NPV = \left(\sum_{t=6}^{100} \frac{(1500)}{(1+0.1)^t} - \frac{20{,}000}{(1+0.1)^5}\right)$). As such flexibility enables us to avoid the undesirable investment at the downward price, the real option value we have obtained here is higher than a standard NPV. This means that an initially worthless option can now be worth investing in the future if there is the possibility of price or profit going up in the future (Dixit and Pindyck, 1994). Therefore, the result of real options analysis suggests that such flexibility needs to be considered in option evaluation.

This example is the simplest case of real options analysis where change in price or annual profit occurs only once over the two periods. In practice, change in price or annual profit occurs in a more complicated way. For example, stocks or energy prices in financial markets, or sea-levels or global warming in physical systems continuously change over time with a large uncertainty. Nevertheless, the two-period uncertainty is a useful example because it gives an insight of how uncertainty affects option values.

With analogy to this simple case, it can be inferred that the real options analysis consists of two parts: (1) how to model changes in uncertain variables; and (2) how to calculate option values when the option is deferred to the future. The former part relates to ‘stochastic process’, which defines uncertain variables that randomly evolve over time in part or fully (Dixit and Pindyck, 1994). Discrete-time random walk (sometimes referred to as Binomial

Lattice), Geometric Brownian motion, Mean-reverting process or Jump process are examples of stochastic processes which describe the random movement of variables over time. The latter part relates to evaluating options including flexibility. As investigated in the two-period case, this thesis estimates option values when the investment is postponed to the future. The ability to defer options allows option holders to see the future prices after 5 years so that they can make more informed decision to avoid the sunken investment. The principle of stochastic processes and option valuations will be further investigated for the application of real options analysis for the case of coastal flooding and sea-level rise.

2. 5 Option evaluation methods for real options

Dynamic programming developed by Bellman (1952) is a commonly used numerical approach in real options analysis. It is a stepwise approach to optimise investment during a planning horizon by comparing 'option to wait' and 'option to invest' at every time step (Dixit and Pindyck, 1994, p. 93). The principle is explicit and straightforward to understand for real options analysis. This approach explicitly gives an investment rule in regard to investment timing. If the value of wait is higher than the value of investment at any time, this implies that the wait is preferred to the investment at the time and the option should be deferred to the next year. Otherwise, it is better to invest in the option at this year. This comparison process continues every time step (= year) during the time horizon. This process starts from the end of the time horizon by a backward induction (Bellman, 1953). The dynamic programming has now become more powerful in evaluating real option value due to advances in computational technologies (Dixit and Pindyck, 1994; Linquiti and Vonortas, 2011; Woodward et al., 2014).

The alternative is contingent claims approach, which is based on a financial theory to construct risk-free assets to hedge the risk of a project or investment against uncertain prices of stocks or commodities (Black and Scholes, 1973; Merton, 1971, 1973). This method is more appropriate to evaluating financial options than physical or engineering issues (Dixit and Pindyck, 1994) because this approach defines a risk-free interest rate for capital assets and their portfolios. Thus, this thesis focuses on the Bellman's approach (dynamic approach) for option evaluations rather than the contingent claims approach. Further information about the evaluation methods can be found in Dixit and Pindyck (1994, P.114-119).

2.5.1 Dynamic programming for two periods (or Binominal lattice approach)

Let P_0 denote an expected profit at the year 0 with the uncertainty of its price going up or down in the next year. The two-period case assumes that, after the expected profit (P) changes between year 0 and year 1, it remains constant in perpetuity, and that the duration of the project tends to infinity. The variation in the expected profit is represented using the probabilities of upward and downward movements of the price as below (Figure 2.6).

$$P_1 \begin{cases} P_{1,u}: (1+u)P_0 \text{ with probability } q \\ P_{1,d}: (1-d)P_0 \text{ with probability } 1-q \end{cases} \tag{6}$$

Here, $P_{1,u,}$ and $P_{1,d}$ are the upward and downward prices at year 1, respectively, u and d are the upward and downward factors of the price, respectively, q and $1-q$ are the probabilities of the price going up and down, respectively and P_0 is the price at year 0.

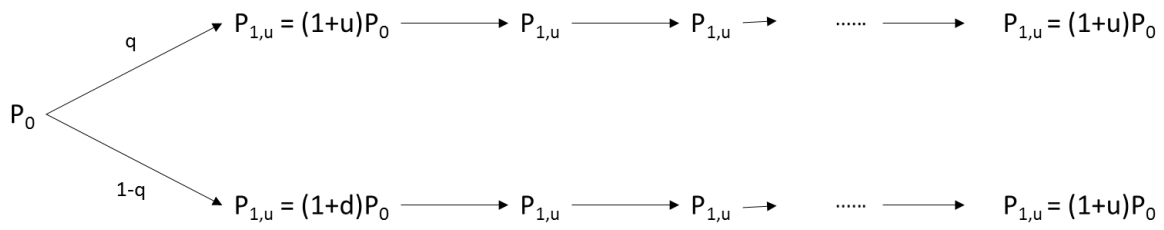

Figure 2.6 Changes in an expected annual profit (P) with the probabilities (q and 1-q) of the upward and downward movement of the profit

If we multiply the project value of upward and downward profits ($P_{1,u,}$ $P_{1,d}$) with the corresponding probabilities, respectively, we can estimate the present value of the project value V_0 using a constant discount rate r as below.

$$V_0 = P_o + q\sum_{i=1}^{\infty}\frac{P_{1,u}}{(1+r)^i} + (1-q)\sum_{i=1}^{\infty}\frac{P_{1,d}}{(1+r)^i}$$

$$V_0 = P_o + q(1+u)P_o\sum_{i=1}^{\infty}\frac{1}{(1+r)^i} + (1-q)(1-d)P_o\sum_{i=1}^{\infty}\frac{1}{(1+r)^i}$$

$$= \frac{[1+r+q(u+d)-d]P_o}{r}$$

If the project value V_0 at year 0 is higher than the investment cost *I*, the investment will be made with the net payoff of $V_0 - I$. Otherwise, the investment needs to be abandoned and subsequently, the net payoff will be zero. Using a max operator, we can represent the net payoff of the project (Ω_0) as follow.

$$\Omega_0 = max[V_0 - I, 0] \tag{7}$$

Then, let us assume that the investment is held for the next year 1. That is, this decision is an option to wait. The present value of the project at the year 1 is

$$V_1 = P_1 + \frac{P_1}{1+r} + \frac{P_1}{(1+r)^2} + \cdots = \frac{P_1(1+r)}{r}$$

In much the same way, the decision at year 1 will be made with the investment cost *I* if the net payoff V_1 is larger than the investment cost *I* (=$V_1 > I$). Otherwise, no investment will occur at year 1. Thus, the expected net payoff at year 1 is represented using a max operator in equation (8)

$$F_1 = Max[V_1 - I, 0] \tag{8}$$

This value F_1 is called a continuation value because the value can exist only when the option is alive till year 1. If the investment is made in year 0, this value will not occur at the next year. From the perspective at the time 0, the expected profit of P_1 is a random variable. Its profit may go up or down by uP_0 or dP_0, respectively. Therefore, F_1 and V_1 are random variables from the perspective at the time 0. Therefore, the expected value of F_1 is expressed as below.

$$E_0[F_1] = q \max\left[(1+u)P_0 \frac{(1+r)}{r} - I, 0\right] + (1-q)\max\left[(1-d)P_0 \frac{(1+r)}{r} - I, 0\right] \tag{9}$$

Equation (9) is referred to as the expectation of a continuation value with the uncertainty of the possible net payoff at the year 1 weighted by the corresponding probabilities. E_0 denotes an expectation from year 0 towards a future option value. Thus, $E_0[F_1]$ implies an expected option value in year 1 from the perspective of year 0. Back to the year 0, we can combine the continuation value (8) with the net payoff (7) from investment at year 0. This is a more general form indicating an optimal investment rule regarding an option to wait for two-time

period case. The equation (10) denotes this value by F_0

$$F_0 = \max\left[V_0 - I, \frac{1}{1+r} E_0[F_1]\right] \quad (10)$$

Here, F_0 is an option value either to wait or to invest at year 0, V_0 is the present value of the investment at year 0, I is the investment cost, r is a discount rate, which is assumed to be constant, and F_1 is an option value at year 1. The discounting factor 1/(1+r) deflates $E_0[F_1]$ to year 0, so that it can be compared to $(V_0 - I)$.

The optimal decision is one that maximises option value (F_0) in equation (10). If the first term is higher than the second term, the option is better to implement with F_0 to be $V_0 - I$. Otherwise, the best option is to wait with F_0 expected to be $1/(1 + \mathrm{r}) \times E_0[\mathrm{F}_1]$. In equation (7), the value Ω_0 only comes up when the option is implemented at year 0. That is, the implementation of the option closes all the decision processes at year 0. For this reason, it is called a termination value, which is also used as a boundary condition in dynamic programming. This is a basic idea of dynamic programming for the simplest case with uncertainty lasting over two periods. This calculation can be extended to more complicated cases such as many-time periods or continuous time.

2.5.2 Dynamic programming for many periods

The binominal lattice approach can be extended to a more general case. Let x_t denote the current value of a state variable at time t – which is a price or profit at time t. From the perspective of time t, x_t is a known variable, but x_{t+1} and x_{t+2} are unknown random variables. Let u_t denote control variable representing the state of a decision on whether to invest now or wait at time t. That is, a control variable, u_t has either 0 for a wait, or 1 for an implementation in application of investment decisions. The state variable x represents a current state or value affecting the operation and expansion of an investment opportunity whereas the control variable u is related to the matter of investors' choice on whether to go or not with the current state given to the investors.

In the many-periods case, the investment decision is determined by the combination of the state variable x and control variable u at time t. Let us suppose a price resulting from a decision at time t is $P_t(x_t, u_t)$. The value of the project at time t can be given by the price and continuation value in a similar way as done in binomial lattice approach for the two-period

case (Dixit and Pindyck, 1994).

$$F_t(x_t) = \max_{u_t}\left\{P_t(x_t, u_t) + \frac{1}{1+r}E_t[F_{t+1}(x_{t+1})]\right\} \quad (11)$$

Here, $F_t(x_t)$ is the expected net present value of an option with state variable x_t at time t, $P_t(x_t, u_t)$ is a price by a state and control variable (x_t, u_t) at time t, r is discount rate between the two periods and $F_{t+1}(x_{t+1})$ is the expected net present value of an option with state variable x_{t+1} at time t+1. As $F_{t+1}(x_{t+1})$ is a random variable from the perspective of time t, it is, thus, written as $E_t[F_{t+1}(x_{t+1})]$, which implies the expected option value of time t+1 from time t. Thus, the expected net present value ($F_t(x_t)$) of an option can be defined by the sum of all the streams of profits and costs during the project life in equation (12) and (13).

$$F_t(x_t) = \sum_{i=t}^{L+t}\frac{P_t}{(1+r)^{i-t}} \qquad (invest\ at\ time\ t) \quad (12)$$

$$F_t(x_t) = \frac{1}{1+r}\,F_{t+1}(x_{t+1}) \qquad (defer\ to\ time\ t+1) \quad (13)$$

This equation (11) is called the 'Bellman's equation' or 'fundamental equation of optimality' (Bellman, 1952; Bellman, 1957; Bellman and Cooke, 1963; Dixit and Pindyck, 1994; Pindyck, 2000). This Bellman's equation provides an explanation of 'Bellman's principle of optimality':

> "*An optimal policy has the property that, whatever the initial action is, the remaining choices constitute an optimal policy with respect to the sub-problem starting at the state that results from the initial actions* (Bellman, 1957)".

This statement is implicitly included in the principle of real options analysis because real option values depend on the remaining choice either to invest, or wait, with the expected project value in the next year given to option holders. If we do not have any flexibility in our options, we will not have any remaining choices that can optimise our already-made decisions against undesirable futures. Thus, according to the Bellman's principle of

optimality, flexibility in options provides an opportunity to optimise sub-problems that may occur in the future. The first term in max operator in equation (11) clearly shows how such flexibility is considered in option evaluation. If the investment is deferred to the end of the time horizon (*T*), the equation will have a termination payoff Ω_T as a boundary value. The Bellman's equation at time *T* is written for time *T-1* as below (Dixit and Pindyck, 1994, p. 101).

$$F_{T-1}(x_{T-1}) = \max_{u_{T-1}} \left\{ \pi(x_{T-1}, u_{T-1}) + \frac{1}{1+r} E_{T-1}[\Omega_T(x_T)] \right\} \quad (14)$$

From the time T, we can work backwards to solve Bellman's equation. This process to calculate the option value becomes more usable due to advances in computational techniques.

2.5.3 Stochastic differential equation for continuous time

The Bellman's equation shown in equation (11) can be expressed as a continuous form in the limit where Δt goes to zero. The rewritten form of Bellman's equation for continuous time is as below (Dixit and Pindyck, 1994, p.105).

$$rF(x,t) = \max_{u} \left\{ P(x,u,t) + \frac{1}{dt} E[dF] \right\} \quad (15)$$

Here, *F(x, t)*: an option value dependent on state variable *x* and control variable *u*

$\frac{1}{dt} E[dF]$: a rate of expectation of dF

r: a discount rate per unit time

$P(x,u,t)$: a price per unit time

On the right side of this equation (15), the expectation of $E[dF(= F_{t+dt} - F_t)]$ depends on the current information on state variable *x* and control variable *u* at time *t* as explained in the case of many periods. That is, the option value F_{t+dt} at time $t+dt$ is determined by the expectation on the future state variable x_{t+dt} whereas the option value F_t at time *t* is determined by the current state variable x_t and control variable u_t. However, as the future state variable x_{t+dt} is

random variable from the point of view at time *t*, $F_{t+dt}$is also a random variable. Thus, the expectation of *dF* should be defined in association with the stochastic process of the state variable *x*.

Ito process is used to represent the change (*dF*) in the value of *F* during *dt* (Cox and Miller, 1965; Merton, 1971; Chow, 1979). It is well known as a convenient method to calculate an investment opportunity or option value (*F*), depending on random variables *x*, by using Taylor series expansions and Brownian motion. This mathematical approach enables solving a differential equation with high order terms in more convenient ways. Generalized Geometric Brownian motion is defined as below by any functions of $a(x,t)$ and $b(x,t)$.

$$dx = a(x,t)dt + b(x,t)dz \tag{16}$$

Here, *x*: state variable such as stock price
$a(x,t), b(x,t)$: any functions of *x* and *t*
dz: a Weiner process ($dz^2 = dt$ for Brownian motion)

Since $(dx)^2$ has a simple form by ignoring the higher order terms which goes faster to 0 than *dt*, we can have an option value (*F*) by using Taylor Series Expansion as below

$$(dx)^2 = a^2(x,t)(dt)^2 + 2\,a(x,t)b(x,t)(dt)^{3/2} + b^2(x,t)dt$$
$$\therefore (dx)^2 = b^2(x,t)dt \tag{17}$$

$$dF = \frac{\partial F}{\partial x}dx + \frac{\partial F}{\partial t}dt + \frac{1}{2}\frac{\partial^2 F}{\partial x^2}(dx)^2 + \frac{1}{6}\frac{\partial^3 F}{\partial x^3}(dx)^3 + \cdots$$

As previously done, if the higher order of terms is ignored, change in option value *dF* is

$$dF = \frac{\partial F}{\partial x}dx + \frac{\partial F}{\partial t}dt + \frac{1}{2}\frac{\partial^2 F}{\partial x^2}(dx)^2 \tag{18}$$

We can gain the expression of Ito's Lemma by combining two equations (17) and (18) for *dx*

$$dF = \left[\frac{\partial F}{\partial t} + a(x,t)\frac{\partial F}{\partial x} + \frac{1}{2}b^2(x,t)\frac{\partial^2 F}{\partial x^2}\right]dt + b(x,t)\frac{\partial F}{\partial x}dt \qquad (19)$$

In equation (15), if we decide to wait at time *t*, there will be no profit ($P_t = 0$) during *dt.* Therefore, Bellman's equation can be expressed as below.

$$rF(x,t) = \frac{1}{dt}E[dF] \qquad (20)$$

By substituting $E[dF]$ by equation (19), we can have

$$rF(x,t) = \frac{\partial F}{\partial t} + a(x,t)\frac{\partial F}{\partial x} + \frac{1}{2}b^2(x,t)\frac{\partial^2 F}{\partial x^2} + b(x,t)\frac{\partial F}{\partial x} \qquad (21)$$

By solving the differential equation (21), we can estimate option value *F* in respect to variable *x* and time *t*. For any variable *x* and time *t*, there are always two possible decisions for the optimal investment as long as an option is alive: continuation (waiting) and termination decision (investing). If x^* is denoted by a critical value that divides space (x,t) into continuation and termination regions, we can estimate option values by various boundary conditions (Dixit and Pindyck p.79, 1994). As sea level is stochastically rising over time (*t*) with uncertainty, the stochastic differential equation (21) can be considered as one of models to describe changes in option value (*F*) of any investment in adaptation options. This will be investigated later in Chapters 4 and 5 in association with the investment timing.

2.5.4 Stochastic differential equation for European options

The previous sections have investigated evaluation methods for real options which can be implemented at any time. This type of option that option holders can exercise at any time is called American-style options in the literature of real options analysis (Park, 2002; Wang and Caflisch, 2009). On the contrary to this, option holders can make a contract to allow options to be exercised at a specific date, which is referred to as maturity (*T*). This type of option is called European-style option in the literature of real options analysis (Cooper, 1999).

The relevant terms regarding European-style option are defined as below.

- Call option (C): a right to buy assets at a specific price at a specific time
- Put option (P): a right to sell assets at a specific price at a specific time
- Strike price (K): a specific price at which option holders can sell or buy the assets
- Maturity (T): a period within which option holders can exercise call or put option

The Black Scholes model is an option evaluation model for financial instruments such as call or put options under the uncertainty of the price of the underlying assets (Black and Scholes, 1973; Cooper, 1999; Park, 2002). This option pricing model is commonly used in evaluating financial options (call or put options) (Park, 2002).

Call or put options have effects on profits that option holders might have at the maturity. They give the option holders a right, but not an obligation, to buy or sell stocks at a strike price (K) (Black and Scholes, 1973). Regardless of the uncertainty of the price of stocks, the option holders can hedge the investment against the risk of the stock price fluctuation by holding put or call options.

A call option with a strike price (K) allows option holders to defer buying stocks whose future price is uncertain from the perspectives of the present. By exercising the call option at the expiration date, the option holders can purchase a certain amount of stocks at the agreed price from the counterpart contractors of the call option, if the price per stock is higher than the strike price. Otherwise, the loss of the option holders is only a payment for the call option. In this way, the option holders can reduce the risk of the investment from the future uncertainty. The characteristics of European-style options (i.e. Black –Scholes model) and American-style options are compared in Table 2.7.

Table 2.7 Comparisons of stochastic differential equations between European-style options and American-style options in real options analysis

Option types	European-style options	American-style options
Governing equation	$\frac{\partial V}{\partial t} + \frac{1}{2}\sigma^2 S^2 \frac{\partial^2 V}{\partial S^2} + \alpha S \frac{\partial V}{\partial S} - rV = 0$ Here, V: the price of a call option at year t S: the price of stock α: the drift parameter of stock price σ: the variance parameter of stock price r: a risk-free interest rate	$\frac{\partial F}{\partial t} + \frac{1}{2}\sigma^2 x^2 \frac{\partial^2 F}{\partial x^2} + \alpha x \frac{\partial F}{\partial x} - rF = 0$ Here, F: the value of an investment deferred to year t *x*: expected annual profit or price from the investment α: the drift parameter of annual benefit σ: the variance parameter of annual benefit r: a discount rate
Hedging method	Call options and observation of stock price	Wait and observation of price or profit during the wait
Uncertainty Modelling	Geometric Brownian motion for stock price ($dS = \alpha S dt + \sigma S dz$)	Geometric Brownian motion for expected annual price or profit ($dx = \alpha x dt + \sigma x dz$)
Result of option analysis	The present price (V) of the call option with strike price at the expiry date	The net present value (NPV) of the investment option at the investment time
The price of option	$C(S_t, t) = N(d_1)S_t - N(d_2)Ke^{-r(T-t)}$ $d_1 = \frac{1}{\sigma\sqrt{T-t}}\left[In\left(\frac{S_t}{K}\right) + \left(r + \frac{\sigma^2}{2}\right)(T-t)\right]$ $d_2 = d_1 - \sigma\sqrt{T-t}$ Here, $C(S_t, t)$: the price of call option at year t S_t: the price of stock at year t N(d): a standard normal cumulative distribution function ($= \frac{1}{\sqrt{2\pi}} \int_{-\infty}^{d} e^{-\frac{z^2}{2}} dz$) T: the maturity of call option, expiry date K: the strike price of call option	$F_t = max\left[F_{ex,t}, F_{w,t}\right]$ $F_{ex,t} = PV_t - I_t$ $F_{w,t} = \frac{1}{(1+r)} \times Max\left[F_{ex,t+1}, F_{w,t+1}\right]$ Here, F_t : the value of option to wait at year $F_{ex,t}$: a termination value when invested at year t $F_{w,t}$: a continuation value when deferred at year t PV_t : project value when invested at year t I_t : investment cost at year t r: discount rate
Investment time	When the call or put option price reaches maximum	When NPV reaches a maximum value
Option evaluation Method	Black-Scholes model (Black and Scholes, 1973)	Dynamic programming (or Bellman's equation) (Dixit and Pindyck, 1994)

The stochastic differential equation for a European style option, or for an American style option, needs to be approached in different ways. The Black-Scholes model can be applied only for European call or put options. Thus, it is not proper to apply this model where climate change adaptation can be implemented at any time. However, as Black-Scholes model is a

formulised approach to estimate the value of a call or put option, the use of Black-Scholes model is very convenient where the strike price (K) of the call or put option is fixed at the expiry date (T). Instead, in order to apply it for climate change adaptation, a call or put option needs to be devised to hedge the investment risk of adaptation measures under the uncertainty of climate change. One study has been found to use Black-Scholes model for the estimation of water cost with or without storage in severe drought (Sturm et al., 2017).

On the other hand, the stochastic differential equation for American style option is applicable where an adaptation measure needs to be implemented at any time under uncertainty. Thus, the approach to American style options is appropriate to the purpose of this thesis.

However, one of critical tasks is that it needs to define stochastic variable (x) by which the option value (F) of an adaptation measure continuously changes. As an example of a stochastic differential equation in Table 2.7, we have defined stochastic variable (x) to be Geometric Brownian motion. However, it is, in practice, difficult to assume that the stochastic variable (x) - that is affected by the severity of coastal flooding or sea-level rise in this thesis – follows Geometric Brownian motion. In addition, it is also hard to directly solve the stochastic differential equation. In this regard, the thesis suggests Bellman's dynamic programming approach to find a maximum option value (F) and a critical variable (x^*) for climate change adaptation. The adjustment of Bellman's dynamic programming approach will be considered later in association with coastal flooding and sea-level rise in the following chapters 4.

2. 6 Real options analysis in climate change adaptation

2.6.1 Issues of real options in association with climate change adaptation

Real options analysis has recently been highlighted in a wide variety of engineering and environmental problems such as coastal flooding, dam planning, water resource and water quality management (De Nefville, 2004; Dobes, 2010; Linquiti and Vonortas, 2012; Jeuland and Whittington, 2014; Woodward et al., 2014). Most of the studies commonly seek to find robust and optimal solutions or strategies against the uncertain futures of climate change. The optimality has been achieved by estimating the performance of candidate adaptation measures, while the robustness has been improved by allowing the selected adaptation measure to be deferred until information becomes more certain.

As reviewed in the previous sections, some issues are identified in application of real options analysis in climate change adaptation. Firstly, real options analysis needs to define the probabilities of prices going up and down in the investment decisions (Refer to Section 2.5.1). Apart from that, a question arises as to what factor (e.g. sea-level rise or flood damage) in climate change adaptation corresponds to prices in financial investment. This question is more substantial when modelling the uncertainty of climate change.

Secondly, uncertainties come from different sources in climate change adaptation. We have investigated the types and characteristics of uncertainties in climate change (Section 2.2). To apply the real-options approach in climate change adaptation, we need to analyse and structure the various types of uncertainties in the framework of real options analysis. This thesis views sea-level rise as a main driver to cause uncertainty issues in investment decisions. In the context of research-setting, a new and integrated framework is needed to enable the incorporation of uncertainty in option evaluations.

Thirdly, IPCC and UKCP 09 data provide sea-level rise projections and probabilistic ranges for each sea-level rise scenario. In each SLR scenario, the projected magnitudes and rates of sea-level rise have large uncertainty, which, thus, is expressed by Bayesian probability to describe the confidence level of the sea-level rise projection. Apart from that, UKCP 09 and IPCC data provides separate sea-level rise scenarios corresponding to different emission scenarios. In this regard, defining the probabilities of future states of sea-level rise needs to be further investigated in association to applying the framework of real options analysis for climate change.

Lastly, most uncertainty sources are attributable to climate change models, data errors and inputs, natural variability and the lack of knowledge on future climates. As all these uncertainties have influence on flood damages, the investment decisions should be made upon the consideration of all the uncertainties. Consequently, this requires an integrated assessment process to connect between uncertain climatic variables and the performances of an adaptation option. This needs a more complicated process in engineering or physical systems than in financial systems because the performance of an adaptation option is monetised for valuation. With these issues in mind, this thesis has investigated the previous studies of real options analysis in climate change adaptation.

2.6.2 The reviews of the previous real options analysis in flood risk management

A recent study has evaluated a set of sequential options that upgrade coastal defences over time in the Thames Estuary under various scenarios of sea-level rise using real options analysis (Woodward et al., 2014). The research shows how flexibility can be incorporated in the design of coastal defence at the outset as well as how the upgrade plan for coastal defence, following real options approach, can be evaluated under a set of plausible futures. The upgrade of the coastal defence was divided into the first and the second phase options over two periods. After implementing the first-phase option, the implementation of the second phase option depends on whether sea-level rise reaches the pre-defined threshold value or not.

This research also estimated the probabilities of two possible cases where the predefined threshold of sea-level is exceeded or not by UKCP 09 data. Each path of sequential options (for example, option A→B or option A→C in Figure 2.7) that will be selected in response to each future state is evaluated by cost-benefit analysis. By aggregating all the NPVs weighted by the corresponding probabilities, it provides an option value of the flexible strategy consisting of a set of the sequential options against the assumed future states.

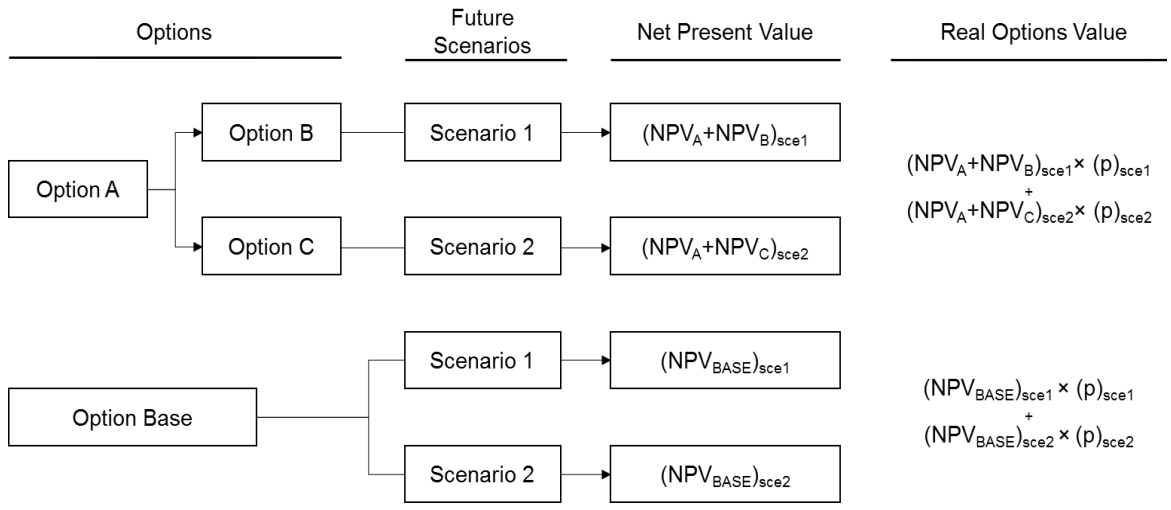

Figure 2.7 Concepts of evaluating real options under possible future scenarios (Here, NPV_i: net present value of option i, $(p)_{sce\ i}$: the probability of scenario i)

The real option value has been compared to the value of a baseline option implemented without flexibility. Most real options analyses in climate change adaptation or flood risk management follow this approach. It is well demonstrated that a set of sequential options,

allowing future growth or adjustment against uncertain futures, are more robust than the conventional option excluding flexibility in economic terms (Linquiti and Vonortas, 2012; Woodward et al., 2014; Hino and Hall, 2017). Even though a set of sequential flexible options are more costly than a conventional (non-flexible) option, the studies show that the net present values of such sequential investments are higher than those of the conventional options (Dobes, 2010; Whitten et al., 2012; Jeuland & Whittington, 2014). It is because the sequential options can not only address the future risk of sea-level rise, but they also allow option holders to avoid the unexpected outcomes of sunk investment by stopping further investment.

The previous approach could have been improved by considering the investment timing of the remaining options. For example, the result of real options analysis by the previous study suggests that the investment in the second phase option should be made later when the defined threshold value during the planning horizon is at least reached. This threshold value enables us to find a specific investment timing by matching the threshold value to sea-level rise in any sea-level rise (SLR) scenarios. This concludes that the investment time differs depending on SLR scenarios.

As shown in Binominal lattice approach (Section 2.5.1), the investment timing can be determined by forcinlgy establishing time steps (e.g. two periods). In this regard, the previous real options approach can be considered as a Binominal approach in which one of two decision paths will be chosen according to the realization of the future. In this case, if sea-level rise exceeds the defined threshold value, the remaining option will be implemented. Otherwise, it will be abandoned. In this circumstance, one problem is explicitly identified in estimating the value of the adaptation option. It is because the option value is significantly affected by investment timing and discount rate (r) (Tol, 2003). Besides, the investment timing also depends on what climate change scenario will materialise in the future. Due to such issues in evaluating the economic values of future options, the fixed investment time and threshold value may constrain the investment decision from real options analysis in its application. Generally, the real options analysis estimates the probabilities of future states at the fixed investment time. However, it should be noted that these estimated probabilities differ depending on how to set the investment timing of an adaptation option on the passage of time.

This issue needs to be further addressed to improve real options analysis in the area of climate change adaptation of which the investment decisions depend on time and climatic

variable (i.e. sea-level rise). In this regard, decision-makers who are willing to use real options analysis in climate change adaptation need to consider some issues as below.

(1) Investment timing

If a decision time is placed in the distant future (e.g. 2050, 2080 or even 2100), the option value from such a decision is significantly discounted. This may be a case where the threshold value for implementing an option is set to be very high. In this case, the investment decision on an adaptation option will be left with no upgrade to the future generation unless sea level reaches such a threshold value.

(2) Uncertainty of SLR scenarios

SLR scenarios by UKCP 09 have the different rates of sea-level rise. Sea level increases more slowly in the Low SLR scenario than in the High SLR scenario. In this regard, sea level is expected to reach the defined threshold value at different years depending on SLR scenarios. If a decision time is planned for one particular or fixed year, it may lead to a different decision in the real world. For example, if the threshold value of sea-level rise is set to be 0.37m in London, such a rise is, thus, expected to reach in 40 or 60 years for the High or Low SLR scenarios, respectively. Thus, if the investment decision whether to go or not is fixed at a particular year, option holders may miss an investment opportunity that they may have by waiting longer. This implies that a threshold value to trigger an investment in real options analysis needs to be addressed with consideration on when it will be reached under various SLR scenarios.

(3) Sea-level rise in the real world

Lastly, if sea level rises at the lower rate in the real world than sea-level rise projections, the option implementation time will occur much later than expected. There will be, thus, no need for action to such an unexpected case because sea-level rise in this scenario is less likely to exceed such a threshold value in the near future. In economic term, it is a more strategical decision that the option holders leave this option for the future generation than they consider now because the option value of the investment in the distant future is very low. On the contrary, there may be an opposite case where sea level rises at a very fast rate (e.g. the H ++ scenario) in the real world. In this case, sea level will exceed the threshold value in the near future, urging decision-makers to implement the adaptation option immediately. Thus, if the sea-level rise follows the H ++ SLR scenario, the pattern of sea-level rise, that is, whether sea-level rise follows H++ SLR or not, needs to be detected in the early stage.

2.6.3 The choice of real options approach in context of climate change adaptation

There are various approaches to analyse real options in physical or engineering systems (Dixit and Pindyck, 1994; De Neufville, 2003). Depending on the characteristics of uncertain variables, the choice of a real options approach differs. Binominal or trinomial lattice approach, stochastic differential equation method, Brownian motion approach, Black-Scholes model and Dynamic programming approach are all categorised as real options approaches. Thus, when taking one of the real options approaches to an area of interest, analysts need to consider what factors are influential on uncertainty and how to model uncertain variables. This process is referred to as uncertainty modelling in the literature of real options analysis (Yang and Blyth, 2007). This section provides the detailed explanations of various approaches used in real options analysis (Table 2.8).

Among all the approaches in Table 2.8, the Binominal Lattice Approach is excluded because sea-level rise does not show downward movement during the period of a SLR projection and it is not changing in a stepwise pattern over time. It is rare to observe the upward or downward movement of sea-level rise at any time in reality.

The Brownian motion approach had been taken into account to describe the uncertainty of sea-level rise. The choice of this approach is reasonable because the behaviour of sea-level rise appears similar to the behaviour of Brownian motion. As seen in UKCP 09, a sea-level rise projection consists of the most likely trajectory (i.e. the 50^{th} percentile) and its uncertain ranges (i.e. the 5^{th} and 95^{th} percentiles). This thesis estimates the drift and variance parameters of Brownian motion by fitting each SLR projection to Brownian motion. In this way, the drift and variance parameters of Brownian motion have been calibrated for the real options analysis. However, there is no evidence that sea-level rise follows Brownian motion. Thus, the use of this method is limited to describing the stochastic case of sea-level rise in this thesis. One of challenges we face in applying real options analysis is how to establish and solve a stochastic differential equation for option evaluations. This is related to assumptions required for establishing a stochastic differential equation for some reasons.

Table 2.8 Types of real options analyses according to uncertainty modelling (Dixit and Pindyck, 1994)

Approaches	Methods	Characteristics	Application to climate change adaptation
Binominal or Trinomial lattice approach	1. Define the probabilities of the upward and downward movements of uncertain variables 2. Set up adaptation options and paths in response to the future states 3. Value all options under each possible future state 4. Aggregate the probability-weighted values of all options	1. It is useful when the uncertain variables can be simply defined by two or three states. 2. This approach may increase the complexity of the analysis by allowing more binominal decisions for many time steps 3. This approach is fit only for discrete time 4. It is hard to define the probabilities of uncertain variables exceeding a certain threshold value in the future	Linquiti and Vonortas (2011), Woodward et al. (2014)
Brownian motion approach	1. Define the property of the stochastic process of uncertain variables (x) adjusted to any type of Brownian motion 2. Set up a relation between option values (F) and uncertain variables (x) 3. Estimate the option values and likely ranges for an adaptation option	1. It is hard to define the parameters of Brownian motion for uncertain variables. 2. Brownian motion is valid when variables are continuous 3. It is difficult to establish a mathematical relation between option values and uncertain variables in physical systems 4. Traditionally, the parameters of Brownian motion are made by experts' judgement towards the future	Abadie et al. (2016)
Black-Scholes model	1. Devise flexibility (call or put option) to be included in a system under uncertainty 2. Determine the conditions of call or put option which are strike price, expiry date and so forth 3. Apply Black-Scholes formulation to estimate the price of the flexibility (call or put option)	1. This approach is fit to European style option which can be exercised only at the expiry date. 2. The price of call or put option is formulised. 3. The solution is valid for continuous time 4. This approach is suitable for investment decisions where strike price can be set such as R&D or patent	Sturm et al.(2017)
Stochastic Differential Equation	1. Define the property of the stochastic process of uncertain variables adjusted to any type of Brownian motion 2. Establish a stochastic differential equation with the parameters of Brownian motion (α, σ) 3. Solve the stochastic differential equation to find a maximum option value and its investment time	1. This approach is valid when uncertain variables are continuous and definable for Brownian motion 2. It is hard to solve a stochastic differential equation 3. It is hard to define a stochastic differential equation for uncertain variables in physical systems	Not found to date
Dynamic Programming Approach	1. Set up Bellman's equation ($rF = E(dF)$) for uncertain variables (Here, r: discount rate, F: option value, $E(dF)$: an expectation of change in F) 2. Define an option value (F) with regard to uncertain variables 3. Compute the option values numerically or analytically	1. This approach is fit for American style option 2. This approach can estimate the option value and investment time either in a numerical or analytical way. 3. As computation techniques develop, this approach is more powerful than ever. 4. The numerical type of dynamic programming can be solved by backward induction method.	Yang and Blyth (2007), Kim et al. (2018)

Firstly, the process of uncertain variables must follow Brownian motion. The uncertain variables involved in a stochastic differential equation meet this requirement. It should be noted that the uncertain variables for the stochastic differential equation are the performance (or economic efficiency) of an adaptation option against the risk of coastal flooding. These variables are represented by expected annual benefits (EABs) from an adaptation option. The description of temporal changes in EAB requires a series of complicated processes (e.g. uncertainty modelling; flood risk analysis for each defence condition; monetisation process). In addition, it would be difficult to argue that changes in EAB follow Brownian motion.

Secondly, the uncertain variables for the stochastic differential equation must be continuous. The expected annual benefit (EAB) from an adaptation cannot be assumed to be continuous in extremely severe SLR scenarios. It is because of the limitations on the capacity of adaptation measures (i.e. coastal defence) against extreme coastal events. Likewise, as climate change adaptation is a more complicated process that requires a detailed understanding of interactions or dynamics between physical systems (i.e. adaptation measures) and climatic systems (i.e. extreme water levels and sea-level rise), the application of real options analysis into climate change needs more attentions than in financial analysis.

Thirdly, solving a stochastic differential equation requires the drift and variance parameter of Brownian motion of uncertain variable(s). As the former two conditions are rarely satisfied in climate change adaptation, it is, therefore, hard to obtain the parameters of Brownian motion of uncertain variables (i.e. EAB). This implies that analytical or mathematical approaches to real options, which demand analysing Brownian motion and stochastic differential equation, are not suitable for climate change adaptation.

In these contexts, this thesis takes a numerical approach to find a maximum option value and its investment time for an adaptation option under the uncertainty of sea-level rise. This approach allows us to avoid not only solving a stochastic differential equation of EAB, but also calculating the drift and variance parameters of Brownian motion of EAB. Instead, we directly solve the Bellman's equation ($rF = E(dF)$, Here, r: discount rate, F: option value and dF: change in option value) in a numerical way. It is of note that a stochastic differential equation for real options analysis is a different form of Bellman's equation with the variables assumed to follow Brownian motion and Ito's Lemma (Dixit and Pindyck, 1994).

This thesis uses a backward induction method based on Bellman's equation to compare a continuation value and a termination value in each year from the end of time horizon. This

method has already been proved by a published paper (Kim et al., 2018). The option values (F) have been directly estimated with the summation of expected annual benefits minus investment costs during the life of the coastal defence (= 100 years) with alternations to investment year. In this regard, this thesis provides a new numerical framework to supplement the previous analytical approaches which have the limitation on the application of real options analysis in climate change adaptation. This thesis improves the previous real option approaches in two ways. Firstly, we allow the investment time to continuously vary and, secondly, we consider a wide range of sea-level rise scenarios from UK climate projections 09 (UKCP 09) per se (Lowe et al., 2009). These scenarios are considered independent of each other and this analysis provides each real option value for each sea-level rise scenario rather than a single averaged value for all the SLR scenarios.

The aim of this thesis is to assess the potential roles of real options analysis in climate change adaptation under the uncertainty of sea-level rise – in this case, defence raising to stop increased coastal flooding from sea-level rise. The coastal area between Lymington and Milford-on-Sea, Hampshire (UK) is selected as a case study area (henceforth referred to as Lymington). This is a good example of a coastal zone with urban areas that has been flooded several times in the past, and is still vulnerable to coastal flooding and sea-level rise in the future (Ruocco et al., 2011; Wadey et al., 2013). While the flood defence has been upgraded for the last 20 years, it is still recognised that a further upgrade is needed in 30 to 60 years (NFDC, 2010). So, upgrading the next phase of adaptation is already an issue. In addition to this, this thesis follows flood risk assessment guidance (EA, 2010) and cost-benefit analysis rule commonly used in UK project appraisals. Thus, this thesis provides us an opportunity to compare the previous decision-making tools with real options analysis and help to identify the potentials of real-options-based approach in climate change adaptation.

2. 7 Summary

This chapter firstly has investigated into the general understanding of risk and uncertainty in climate change. Traditionally, it was well known that risk was a danger or threat with a known probability; while uncertainty was unknown risk with an unknown possibility (Knight, 1921). Now, the risk is understood by the products of the probabilities of occurrence of extreme events and the corresponding damages (Hall and Solomatine, 2008); while the uncertainty is rather qualitatively understood with the recognition of incomplete knowledge

or information on risk (Willow et al., 2003; Hall et al., 2007; Ranger et al., 2013). For this reason, uncertainty and risk are treated together in flood risk assessment or management (Willow et al., 2003; Hall and Solomatine, 2008; Field et al., 2012). In addition, uncertainty and risk interact to each other, leading to increases in the complexity of climate change adaptation and flood risk management (Willows et al., 2003; Adger et al., 2009). This ambiguity between risk and uncertainty makes it difficult to trigger adaptation measures. Also, the long-term timescale and non-stationarity of climate change places climate change adaptation in the face of great challenges (Lempert et al., 2003; Groves et al., 2008; Ranger et al., 2013). As structural adaptation measures in flood risk management incur a significant amount of expenditure, actions to implement the adaptation measures require a full understanding of uncertainty in and around the adaptation measures (EA, 2012; MLTM, 2016).

The types and characteristics of uncertainties that are currently recognised in climate change adaptation are well understood by the previous studies (Willow et al., 2003; Grossi and Kunreuther, 2005; Hall and Solomatine, 2008). However, the methods or skills to represent and reduce the uncertainties from different sources have been developed and applied separately in different sectors such as climate change models (Feyen et al., 2013; Wolf et al., 2015), the predictions of greenhouse gas emissions and sea-level rise (Lowe et al., 2009; Nicholls et al., 2014; IPCC, 2015), socio-economic scenarios, the observations and analyses of climate change patterns (Haigh et al., 2014, Hinkel et al., 2015), decision-making tools (Hall et al., 2012; Haasnoot et al., 2013; Ranger et al., 2013) and the introduction of effective adaptation measures (EA, 2012). It is also understood that, as the various types of uncertainties occur simultaneously in climate change adaptation, the effects of the uncertainties are substantial in decision-making or flood risk management.

In this context, the purpose of this thesis is meaningful as it links the recognised uncertainty issues with a newly introduced decision-making tool. Thus, this thesis views a real-options-based approach, or real options analysis, as an alternative way to fill the gap between climate change adaptations and investment decisions. This thesis can provide some important implications in two aspects.

1) This thesis seeks to views uncertainties in climate change, in particular, sea-level rise and coastal flooding as they are. The uncertainties that are considered to be critical and substantial in coastal flooding are taken into account in the framework of real-

options-based approach without any modification. The results from real options analysis into adaptation options have, thus, excluded the subjective views and judgements on the current understanding of the uncertainties in coastal flooding and sea-level rise.

2) This thesis also recognises that flexible options to be adjusted in response to future states are an effective strategy to reduce uncertainties. However, this research focuses more on the basic principles and operational use of real options analysis for further and more general application to climate change adaptations. The assessment methods of flexible adaptation options are adjusted to fit the context of climate change adaptation, in particular, coastal flooding.

This thesis makes efforts towards integrating physical aspects from climate change and flood risk management and economic aspects from option evaluation. Thus, the development of an analytical framework for the real-options-based approach into Lymington (UK) can provide a practical method to increase the efficiency and effectiveness of adaptation strategies within the limitation on resources (i.e. budgets), time or information. Other previous studies have also addressed these aspects in climate change adaptation sectors such as coastal defence upgrades, dam constructions and crop productions (Jeuland and Whittington, 2012; Linquiti and Vonortas, 2012; Whitten et al., 2012; Woodward et al., 2014; Hino and Hall, 2017). All the studies suggest that flexible options are more efficient than non-flexible options as they enable eliminating the irreversibility of the investment. To supplement the previous studies, this thesis is aimed to develop an overarching framework in which adaptation options, including flexibility of wait, or future growth, are systematically assessed and compared with more focus on reducing the subjective views of decision-makers towards the uncertain futures. All the key processes for flood risk management against coastal flooding and sea-level rise are integrated to address all the relevant uncertainty issues that are considered to be substantial in policy or scientific context of climate change adaptation. The following chapter reviews the present risk of coastal flooding and the past flood events in Lymington. Also, the future risk of coastal flooding, due to sea-level rise, are previewed with adaptation measures considered in shoreline management plan (SMP) in Lymington.

3. Overview of case study area

This chapter overviews a case study area in association with the past flood events. The coastal area between Lymington and Milford-on-Sea, Hampshire (UK) (henceforth, referred to as Lymington) is selected as an experiemental area (Figure 3.1). This is a good example of a coastal zone with urban areas that have been flooded many times in the past, and is still vulnerable to coastal flooding and sea-level rise in the future (Ruocco et al., 2011; Wadey et al., 2013).

Most data and records mentioned in this chapter are obtained from the previous research by Wadey (2103) and Haigh et al. (2011) which investigated the past flood events and the current flood risk in Lymington by the flood simulation model. To understand how susceptible the case study area is to coastal flooding and sea-level rise, this part investigates the previous research and public documents recording the past coastal events. Thus, this chapter provides a basis upon which to analyse the current and future flood risk to Lymington as well as to assess current adaptation measures to protect Lymington from coastal flooding and sea-level rise. Two historical flood events that caused significant damages to Lymington are throughly investigated in this preliminary analysis.

This chapter is structured as follows. Firstly, we explore the case study area in terms of geological, hydrological and environmental conditions. Secondly, we investigate two main past flood events that occurred in Lymington, and, then, review the current and future flood risks of Lymington in association with sea-level rise. Lastly, we will review adaptation measures that are currently planned in Lymington.

3. 1 Hydrological and geological characteristics of the Solent

The Solent is a tidal strait located between the Isle of Wight and the mainland of England. This area is covering 32 km from east to west and 1.5 to 6.5 km from south to north. This area includes Lymington, Portsmouth, Southampton, Isle of Wight and Sesely Bill. Prehistorically, the Solent was a river system before the last ice age. Geological or marine research on the Solent estimates that the river system of the Solent was inundated after the rapid sea-level rise 7000 years ago (Wadey, 2013). After the progressive development and reclamation of Southampton Water and Portsmouth in the 19th and 20th centuries, the current

form and extent of the Solent estuary was shaped **(**Levasseur, 2008**)**. The Solent-Southampton Water Estuary system is the largest estuary on the UK south coast.

The Solent is one of the highest flood risk regions in the UK (Wadey et al., 2013). 24,138 properties in the Solent are estimated to be susceptible to the high risk of coastal flooding due to the combined effects of sea-level rise and storm surge events (NFDC, 2010). The severity and frequency of coastal flooding is the third largest in the UK after London and Hull (Wadey et al., 2013). If sea-level rise of 0.5m is added to a 1-in-200 year coastal flooding, the extent of the inundated areas and properties will increase by 140 to 600 % depending on the combined conditions of storm surges and defence failure (Wadey et al., 2012).

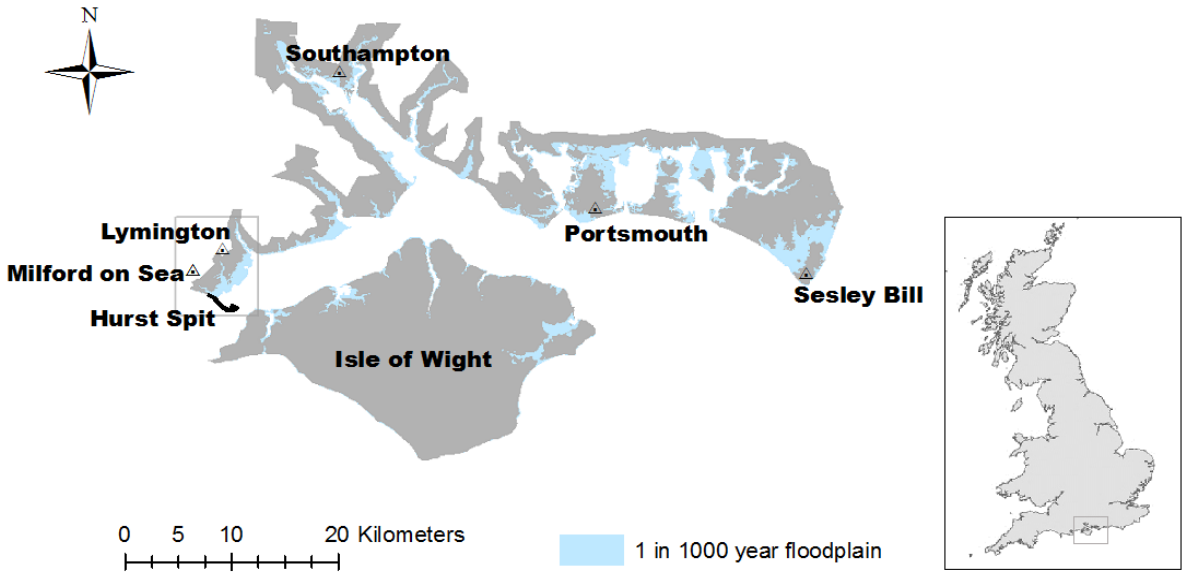

Figure 3.1 Lymington and the wider Solent region on the English channel coast, UK, including the 1-in-1000 coastal floodplain (Wadey et al., 2013).

Isle of Wight shelters much of the Solent area from south-westerly Atlantic waves (Wadey et al., 2013). In addition, a shingle barrier at the west end of the Solent (Hurst Spit) and the associated shoal of the Shingles Bank in Christchurch Bay at the further west (not shown in Figure 3.1) protects the West Solent, including Lymington, from incoming waves from the west (Wadey et al., 2013). Extreme still water events in the Solent are normally developed from low pressure systems moving from Atlantic eastwards over Southern England. On the other hand, small surge events in the Solent are mainly attributable to large North Sea storm

surges transmitted into the English Channel through the Dover strait (Haigh et al., 2011). The Solent region is well known to have a very complicated tidal mechanism in which double high waters occur and are particularly pronounced during large spring tides, and at mid-flood tide, the tide is constant for an hour (Pugh, 1996). Tidal residual, which is a difference between the actual water level and the predicted water level, is mostly observed to be less than 1m with a difference between a 1-in-10 and a 1-in-1000 year water level estimated to be only 0.33m (Haigh et al., 2009; Wadey et al., 2013). Tidal range, which is a difference between the lowest and highest astronomical tides, increases from 2m at Hurst to 5m at Selsey Bill. Typical semi diurnal lunar spring tidal cycles in the Solent are shown in Figure 3.2.

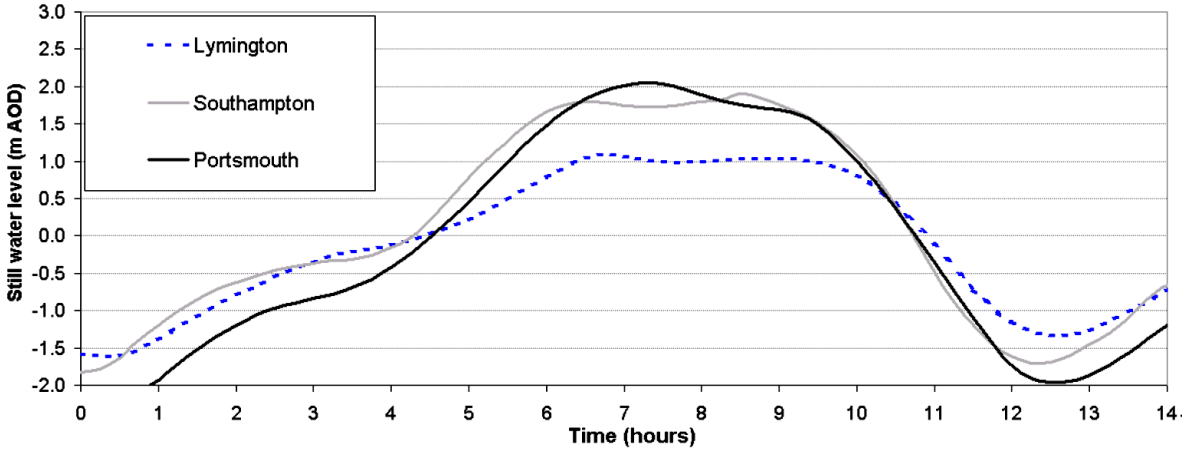

Figure 3.2 Water level time-series: recorded at three locations across the Solent during a typical spring tide from Wadey et al. (2013)

3. 2 Description of Lymington in association with flood risk

Lymington is a coastal town in southern England that has experienced a number of coastal floods over the last century, including 13-17 December 1989, 25 December 1999 and 10 March 2008 (Ruocco et al., 2011; Wadey et al., 2013). The coastal defences have been upgraded several times in response to these floods and currently are at 2.5~3.0m (AOD) elevation, but, as sea levels are rising, the risk of coastal flooding is growing. The Shoreline Management Plan (SMP) in and around Lymington has selected a Hold-the-Line (HTL) policy, which involves the enhancement of the coastal defence to maintain the current coastline against the rising risk of coastal flooding (NFDC, 2010). While the flood defences have been upgraded in the last 20 years, it is recognized that the further upgrade is needed in

30 to 60 years (NFDC, 2010). Therefore, the timing and sequence of the defence upgrade is of importance to Lymington.

Figure 3.3 A case study area of floodplains in Keyhaven, Pennington and Lymington – Flood inundation has been simulated in hatch area.

Most of the site is valuable grazing and marsh designated as a Site of Special Scientific Interest (SSSI). Parts of Lymington and the villages of Keyhaven and Milford-on-Sea are at the risk of coastal flooding.

There is a historic landfill (which is filled with wastes) closer to the shoreline which is significantly threatened by erosion over a century (Beaven et al, 2017). The landfill site was formed between 1962 and 1969 to accommodate a mixture of inert, industrial, commercial and household wastes. This landfill site covers 7.5 (ha) area and the maximum surface height is 4.1 mAOD as shown in Figure 3.4.

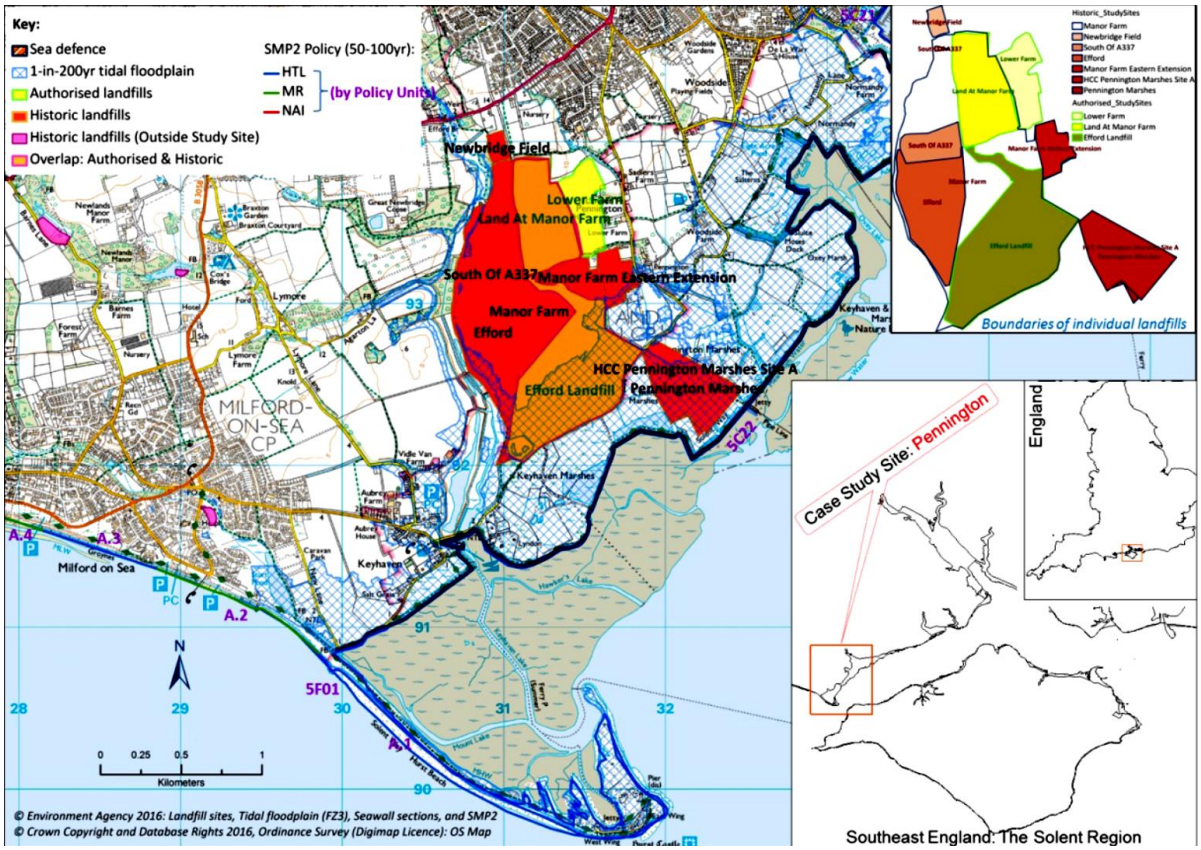

Figure 3.4 Shoreline Management Plans and historic landfill sites in Pennington (Source: Beaven et al., 2017)

The landfill site lies on rural areas which include grassland/coastal marshes and brackish lagoons. Now, it is protected by well-maintained seawall (named Pennington wall), Hurst Spit and saltmarsh. The current shoreline management policy has already been planned as a Hold-The-Line (HTL) for the short, medium and long-term. However, due to sea-level rise, the saltmarsh on the seaward side of the sea-wall is being eroded at the rate of 0.5 to 5 m per year (Beaven et al, 2017). As this saltmarsh provides a service of mitigating the effects of incoming waves on the sea-wall, the loss of saltmarsh is recognised as a threat to the flood-

prone area and the landfill site. The coastal zone at Pennington becomes vulnerable to flooding with the erosion of saltmarsh proceeding. The current Hold-The-Line SMP policy will need the upgrade of coastal defence in the near future if sea levels keep rising.

3.2.1 Current coastal defence conditions in Lymington

As Hurst Spit and Isle of Wight are located before the compartment areas (i.e. Lymington, Keyhaven and Pennington), the wave climates are governed by south-west winds and locally-generated waves (Wadey et al., 2013). Due to Hurst Spit, the effects of the incoming waves are weak with significant wave heights estimated between 0.3m and 0.8m (Halcrow, 1998). In the lee of Hurst Spit, there is earth and grassed embankment which stretches 1km eastwards. This embankment ends at Keyhaven which is protected by a mixture of masonry and concrete sea walls. Keyhaven is an important residential area, which is low-lying and dependant on Hurst Spit and concrete sea defences. The fronting saltmarshes also play a protective role, as a natural defence, in increasing the performance of flood defences and Hurst Spit.

From Keyhaven eastwards, there lies Pennington wall the length of which is approximately 8.1km to Lymington. The front face of the wall is protected by interlocking concrete blocks. This wall protects over 500 ha of land and a nature reservoir at mean high water spring tide (Martin, 1994). The wall had been breached on the 19th December 1989 and, then, was reconstructed with the crest of the coastal defence raised by 0.4 to 0.5m (the highest being raised to 3.0 mAOD at the east end and the lowest raised to 2.45 mAOD at the west end). This coastal defence provides an approximately 1-in-25 year standard of protection (Wadey et al., 2012). The coastal defence near Lymington is made of masonry and concrete wall. This seawall is erected along the coastline to protect the low-lying area where residential and commercial properties, industrial facilities, yacht yards and a railway station are located. Most defence conditions in Lymington are classified under Grade 2 with the residual life estimated to be 31 to 40 years (NFCD, 2010). The current costal defences around the case study area are shown in Figure 3.5.

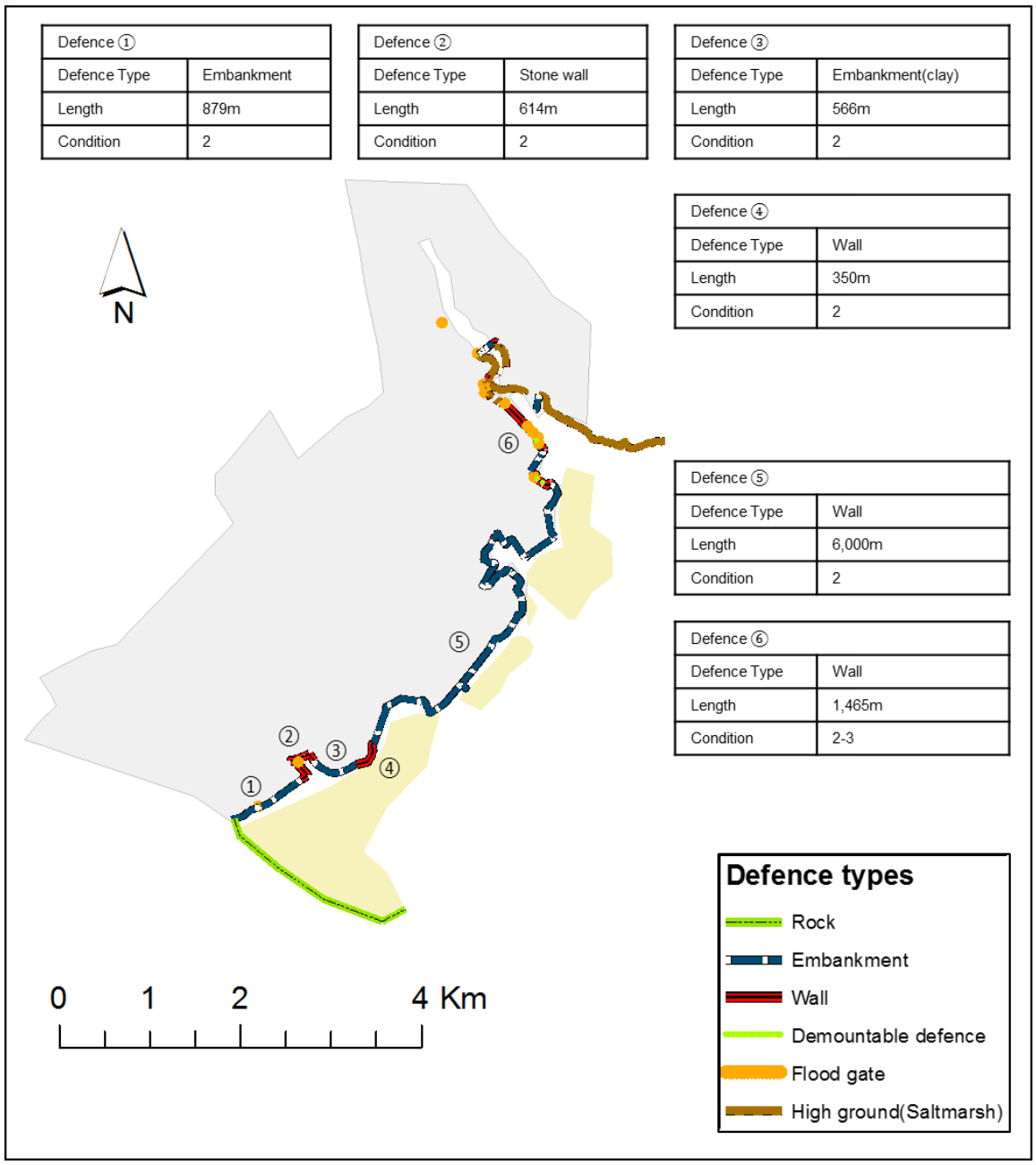

Figure 3.5 Types of the current coastal defences around Lymington (including Pennington and Milford-on-sea) provided by Shoreline Management Plan (NFDC, 2010)

3.2.2 Appraisal of defence conditions for breaching failure

In order to consider breaching failure, the defence conditions have been investigated on the base of the previous research by Wadey (2012). This review also helps construct additional breaching scenarios by finding the weak points of coastal defence along Lymington. To analyse defence failure mechanisms, fragility curves are used to provide the conditional probability of breaching for a given loading. Generating the fragility curves requires site-

specific information such as defence types, defence conditions, slopes and surface protection (Buijs et al., 2007). The previous study also provides useful information on how probable the breaching failure occur over the possible loading conditions (Wadey et al., 2013). The probability of breaching at a 1-in-200 year water level (i.e. 2.41 mAOD) is estimated to be between 0.59 and 0.76 for Pennington sea-wall (including Keyhaven) and between 0.77 and 1 in Lymington sea-wall, respectively. The past breaching events and hydraulically disconnected points (i.e. flood gates) are spotted where the breaching is also very likely to occur in the extreme case of coastal flooding. The coastal defences that are assessed to be at the risk of breaching are shown in Figure 3.6.

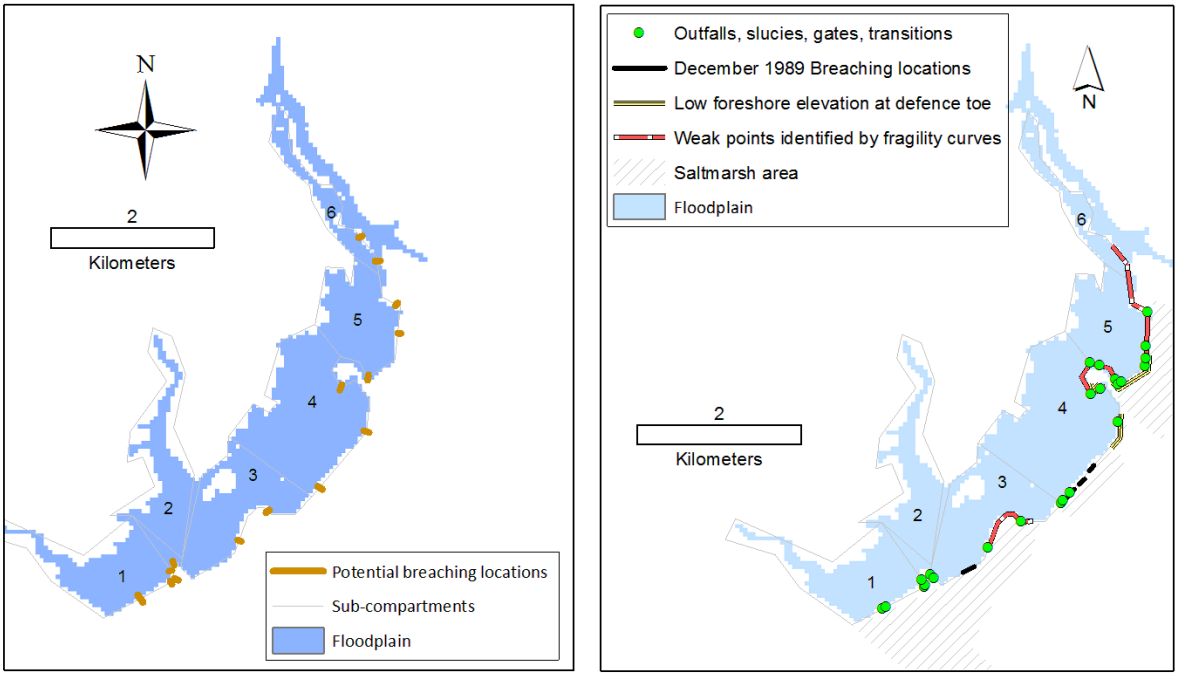

Figure 3.6 (a) Potential locations for the breaching scenario at Lymington; and (b) defence weak points and approximate locations of 17th December 1989 breaches redrawn from the previous analysis by Wadey (2012).

This thesis assumes that, if the coastal defences are managed properly, the performance of the coastal defence will last during the period of the project life. The shoreline management plan also includes maintenance costs for the coastal defence during a century (NFCD, 2010). In this respect, this thesis assumes that the coastal defence will be able to provide a service to protect Lymington over the life of the coastal defence (=100 years). However, the effects of different residual life on real options analysis will be considered for applications to different residual life of coastal defence.

3. 3 Past flood events in the Solent

Coastal flooding has been a common occurrence in the Solent over the last century. Ruocco et al (2011) catalogued flood events in the Solent from 1935 to 2005 and identified 34 flood events in the Solent and 14 flood events at Lymington. This work found that, while sea levels were rising, the incidence of coastal flooding in the Solent was actually declining due to improving flood defences, especially at coastal hotspots. This includes Lymington which has seen significant damages in flood defences in the last 30 years. Subsequent flood events in the Solent are reported by Wadey (2013); Wadey et al. (2013; 2015b); Oszoy et al. (2016) and Haigh et al. (2017). Notable events occurred on 10 March 2008 and in the exceptional season of 2013/14, most notably the 14 February 2014 (or the 'Valentines Storm'). Wadey et al. (2015a) catalogue the storms in the West Solent impacting Yarmouth on the Isle of Wight: with its upgraded flood defences Lymington escaped serious damage compared to earlier storms. Here two extreme flood events which had flood impacts in Lymington are considered in detail to inform the later flood modelling.

3.3.1 The 14th and 17th December 1989 West Solent flood

The 14th to 17th December 1989 flood event is recorded the worst storm surge event in the Solent in the last 50 years (Ruocco et al., 2011; Wadey, 2013). Eight successive high tides exceeded the highest astronomical tide causing widespread flooding, especially in Lymington and Portsmouth. Around Lymington, successive severe flood events occurred on the 14th and 17th December 1989 (the two highest tides). On the 14th December, sea water overflowed and overtopped the coastal defences between Lymington and Milford-on-Sea. On the 17th December, breaching occurred, leading to the rapid inundation of the floodplains behind the breached coastal defence with seawater. A National River Authority report (NRA, 1990) and Wadey (2013) documents the event. On the 17th December there was inundation of 10 properties in Pennington, while overtopping also affected 50 properties in Lymington. The main cause of flooding was exceptional high-speed south-westerly winds combined with high sea levels on both dates. A mean wind speed at the height of the storm on the 17th December was recorded to be 44 knots with gusting 56 knots which could generate strong waves with the height of 1.2-1.3m in Lymington (Wadey et al., 2012). Water levels at Lymington on the 14th and 17th December were 1.92 mAOD and 2.1 mAOD, respectively.

Hurst Spit, which protects the West Solent, especially Milford-on-Sea and Pennington from wave effects, was also breached by the combination of high water level and extreme waves on the 17th December 1989. This breaching allowed sea water to enter into the inter-tidal area, leading to the rapid erosion of the saltmarsh behind the Hurst Spit (Stripling et al., 2008). The barrier has since been reinforced by shingle nourishment and provides significant protection to Milford-on-Sea as well as much of the Solent. This extreme event is understood as a consequence of interactions between various flood sources (e.g. surge events, wind and wave conditions, tides) and the resultant breaching of the coastal defence (Wadey, 2013). Although this flood event had caused such severe damages in Lymington, detailed information about the December 1989 event (e.g. wave conditions and water level time series) is not found. Most of the coastal defence in Lymington has been upgraded and reinforced since the 1989 December event. Thus, the flood simulation based on the December 1989 event may show different inundation patterns from plausible flood risks based on the current defence systems.

Figure 3.7 Erosion and breaching of Hurst Spit after the flood event on 17th December 1989. This photo was taken from the website of Ian West (http://www.southampton.ac.uk/~imw/Hurst-Spit-Historic-Coastal-Events.htm)

3.3.2 The 10th 2008 flood event

This section explains a storm surge event on the 10th March 2008 which is a well-documented extreme flood event in the Solent region. This thesis investigates this event with the previous thesis and paper provided by Wadey (2013) and Haigh et al. (2011), respectively.

On the 8th March 2008, a low depression was developed off Southeast Greenland. As this moved southeast with the central pressure dropping from 975mb to 946mb, it turned to be a typical storm that generated large surges in the English Channel (Wadey et al., 2013; Haigh et al., 2016). The time of the high spring tide predicted for the 10th March coincided with the passage of the storm. This joint event generated a surge of 1m in the central regions of the English Channel. These skew surges exceeding 0.7m were recorded at six stations: Weymouth, Southampton, Portsmouth, Jersey, Cherbourg and Le Havre (Haigh et al., 2011). In the Solent, the storm surge peak and high tide occurred at the same time. Peak water level was observed 12:00 at Lymington, 12:30 at Southampton, 13:00 at Portsmouth and 13:30 at Sesley Bill (Wadey, 2103). Water level time-series at each location are shown in Figure 3.8.

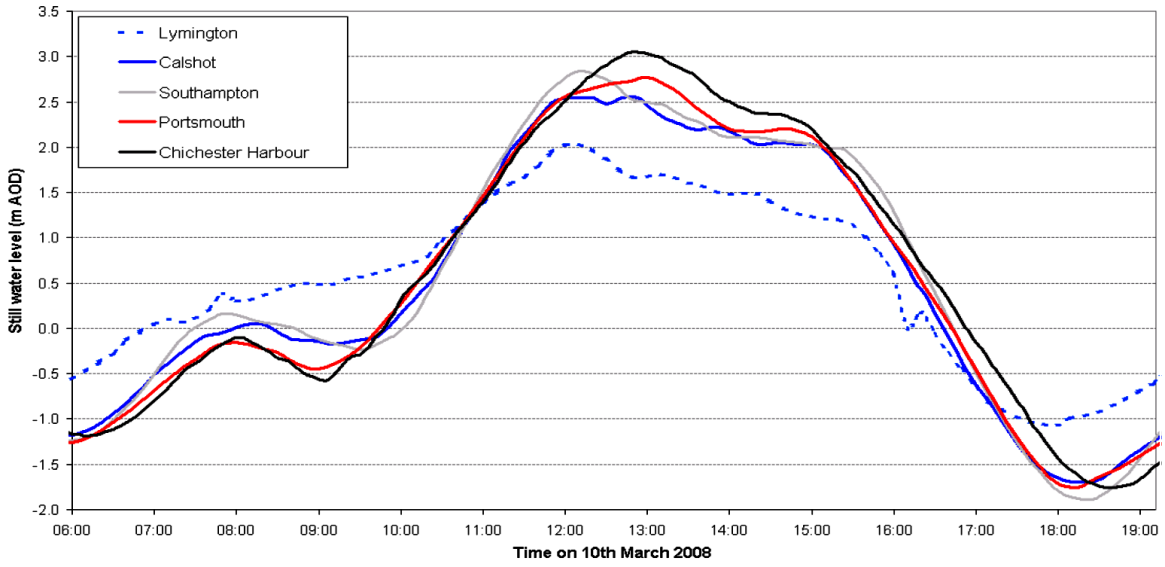

Figure 3.8 Still water level time-series on the Solent areas during the event 2008 (Source: Wadey et al., 2013) – This data is originally taken from Channel Coastal Observatory (CCO)

Flood warning against this daylight event was issued across most of the affected areas (EA, 2010b), allowing people to take preventive actions such as moving possessions or building sandbags (Wadey et al., 2013). Flood damage was relatively minor although more than 30 properties were flooded at Selsey during the 2008 event (EA, 2010b). New defences in

Lymington reduced the impact of overflowing and overtopping on the floodplain. Breaching failure was not reported during the event (Wadey, 2013).

Most defence failure type that occurred during the 2008 event was overflowing which means that water levels exceed the crest level of coastal defence. A peak water level measured at Lymington on the 2008 event was recorded to be 2.04 mAOD according to Coastal Channel Observation (CCO) and 2.17 mAOD according to the Environment Agency, respectively. Figure 3.9 shows the flood extents and depths simulated from the peak water levels of 2.0 mAOD and 2.4 mAOD, respectively.

The wave height (H_s) at Lymington during the event was observed to be 0.91m with the wave period (T_p) of 3.3 sec. This wave height during the 2008 event was less than a 1-in-1 year wave height. Although most flood types during the 2008 event were overflowing in the Solent, overtopping and breaching failure were also observed in Portsmouth and Selsey Bill, respectively (Wadey et al., 2013).

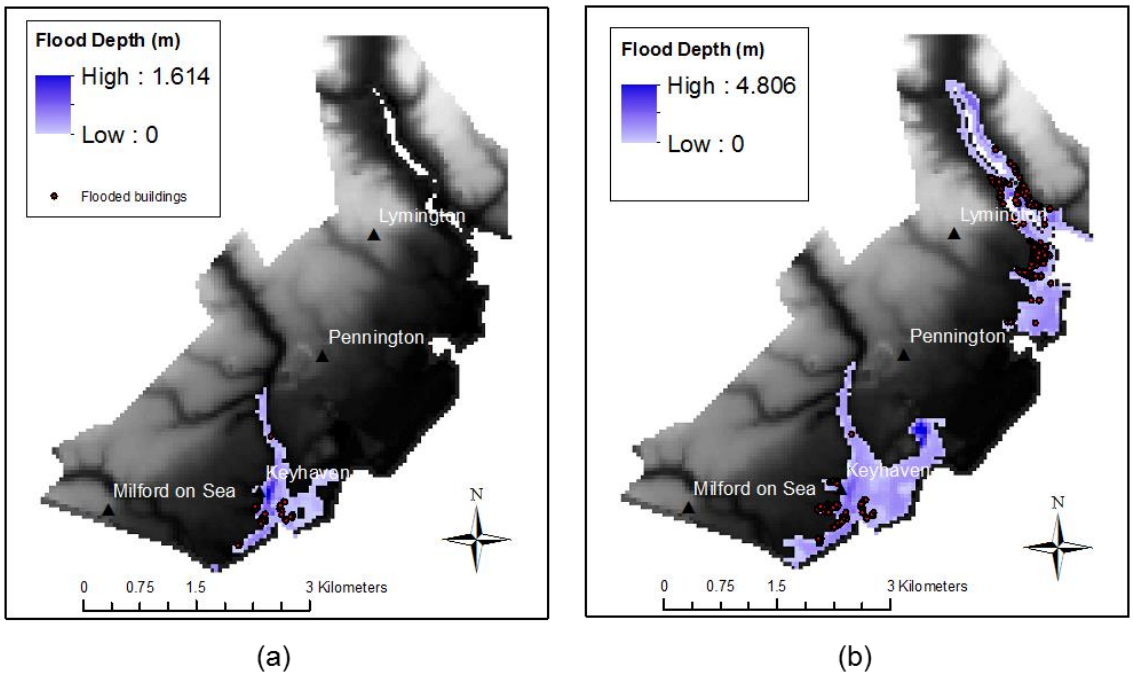

Figure 3.9 Extents of flood damages simulated with the current defence system at the extreme still water level of (a) 2.0 mAOD (water level on the 2008 event) and (b) 2.4 mAOD (approximate 1-in-200 year water level) in Lymington.

Data on climatic conditions and detailed damage information during the 10th March 2008 flood event have been well-documented; although the flood damages on the 2008 flood were relatively minor in Lymington comparing to flood damages on the 1989 flood event. Thus, in

this thesis, the 2008 flood event is assumed to be a typical flood event that may occur again in the future as this flood event occurred in the same defence system with the current defence system. The coastal flood simulations based on the 2008 flood event enable us to know which area in Lymington is still vulnerable to coastal flooding and rising sea levels. Although much flood damage was not reported and recorded during the 2008 flood event, the coastal flooding could cause more severe damages to the floodplain, if there were higher water level due to sea-level rise than it was. The previous research conducted by Wadey (2012) shows the relevance of the extreme water levels during the flood events to flood damages. Table 3.1 summarises the flood damages to Lymington during each flood event with the highest recorded water level. It also shows tidal levels recorded during the flood events at Lymington.

Table 3.1 The highest water levels during the past flood events at Lymington with the brief explanation of the flood damages – This data is taken from Wadey (2013). Tidal levels are from the Channel Coastal Observatory (CCO) and return periods are McMillan et al. (2011).

Water Levels (mAOD)	Date	Relevance / description of event	Source
2.41	1 in 200 return period water level statistically generated by McMillian et al. (2011)		
2.17	10th March 2008	Approx. 1 m storm surge in the Solent. The highest water level since 1992 recorded at Environment Agency tide gauge; although the water level was also recorded 0.13 m less at an alternative gauge nearby (CCO, 2011).	(EA, 2010b)
2.10	17th December 1989	Storm surge of 1.1 m. Overtopping and overflow caused flooding to 50 houses and 10 commercial properties in the town of Lymington, some to a depth of 1.2 m. Submergence of railway line and electrical substations. Breaching and flooding of the rural site, damaging 10 houses and the hinterland marsh environment. Severe erosion of Hurst Spit.	(NRA, 1990)
1.99	24th-25th December 1999	Flooding occurred in Lymington due to the river overtopping upstream of the Toll Bridge on the Lymington side and flowing on to the railway.	(O'Connell, 2000)
1.92	14th December 1989	Wave overtopping on the river estuary and open coast caused flooding in Lymington and the Pennington marshes.	(NRA, 1990)
1.89	1 in 1 return period water level (Approx.)		
1.02	Mean high water spring tides		
0.62	Mean high water neap tides		
0	Ordnance Datum (approximately mean sea level at Newlyn, Cornwall)		
-0.58	Mean low water neap tides		
-1.28	Mean low water spring tides		
-1.98	Chart datum at Lymington		

3. 4 Coastal Flood Risk Management Plans for Lymington

3.4.1 Shoreline Management Plans (SMPs) for Lymington

Shoreline Management Plan (SMP) describes a strategy to manage coastlines against flood and/or erosion (NFDC, 2010). This management plan sets out the next 20, 50 and 100-year policies to assist decision-making on flooding from sea and coastal erosion. Four different shoreline management policies are present in SMP (Nicholls et al., 2013):

- No active intervention – No planned investment in defending against flooding or erosion, whether or not an artificial defence has existed previously.
- Hold the (existing defence) line – A policy to keep the position of the shoreline as it is. Thus, this policy needs to build or maintain the existing defence.
- Managed realignment – Allowing the shoreline to move naturally, but managing the process to direct it in certain areas. This is usually done in low-lying areas, but may occasionally apply to cliffs.
- Advance the line – New defences are built on the seaward side.

To protect Lymington including other near sites from the increasing risk of coastal flooding, the shoreline management plan has been established as the short, mid and long-term policies with the timescales of 0-to-20 years, 20-to-50 years and 50-to-100 years, respectively (NFDC, 2010). All these management options are developed and selected in partnerships between local authorities and Environment Agency. For the Solent, North Solent Shoreline Management Plan has been established to provide a broad assessment of the long-term risks associated with coastal processes as well as to identify and recommend strategic coastal defence policy options for particular length of coast to reduce these risks to people, the developed and natural environments (Nicholls et al., 2013).

The management plan chooses the Hold-the-Line (HTL) policy in the coastal areas of Lymington, which is to keep the current position of the coastline and the standard of protection by upgrading the coastal defences. As this plan is a high-level decision, the detailed scheme of replacement and maintenance is not found in the shoreline management plan. This management plan provides an estimate of the investment cost for the HTL policy. The estimated cost is shown in Table 3.2.

Table 3.2 The cost of the coastal defence replacement and maintenance for the Hold-the-Line policy for Lymington (NFDC, 2010) – The cost in the table indicates expenditures due on each epoch. Thus, it should be discounted by discount factors to indicate the present value (2016).

Location	Timescales	The length of policy unit	Replacement cost (£ M)	Maintenance cost (£ M)	Total (£ M)
Elmer's court to Lymington Yacht Haven	0 to 20 years	2.13km	-	0.4	0.4
	20 to 50 years		8.6	1.0	**9.6**
	50 to 100 years		-	2.1	2.1
Lymington Yacht Haven to Saltgrass lane	0 to 20 years	12.4km	-	1.6	1.6
	20 to 50 years		49.1	5.4	**54.6**
	50 to 100 years		-	12.0	12.1

3.4.2 Flood risk of the Solent in the present and future

The SMP also provides narrative scenarios of coastal flood and erosion risk for each unit area of the floodplain during 21st century (NFCD, 2010). This description shows how coastal flood risks and defence conditions change over time. This scenario expects that the performance and effectiveness of the Hurst Spit will reduce according to the severity and frequency of storm events. These recursively occurring storm events will lower the crest level and width of the spit, leading to increase in the risk of over-washing and breaching of the spit (NFCD, 2010). If the breaching occurs to Hurst Spit, it will create harmful and significant damages to residential, industrial, heritage and agricultural assets (Wadey et al., 2012). In addition to this, sea-level rise will prompt the loss of saltmarsh, reducing the effectiveness of the existing defences (Beaven et al., 2017). Due to the complexity of modelling shoreline behaviour at this site, it seems difficult to predict and quantify the erosion risk.

The existing seawall (i.e. Pennington seawall) lying between Keyhaven and Lymington would deteriorate due to the loss of inter-tidal saltmarshes, which play a role as a natural protection in reducing the effects of the incoming waves. The SMP also predicts that the performance of Pennington wall not fronted by the inter-tidal saltmarshes will end in 2035 through damaging overtopping events and toe scour (NFDC, 2010). If the breaching occurs to the seawall, it will also cause a serious pollution risk to the hinterland. The wide spread inundation may affect the landfill site behind the seawall. SMP report (NFDC, 2010)

estimates that 113 properties are within a 1-in-200 flood risk zone and the potential flood risk in 2105 would affect 180 properties. It is expected that the coastal flooding coupled with sea-level rise would also have an adverse effect on the designated brackish and freshwater habitats and species.

The shoreline management plan for the Solent provides the estimates of the number of properties at the risk of a 1-in-200 year tidal flooding in 2007 and 2115, respectively (NFDC, 2010). The change in the number of the properties at the risk of a 1-in-200 year coastal flooding is also shown in Table 3.3. This change in the number of the properties is attributed to sea-level rise. Unless the coastal defence is upgraded, most area of the Solent will be at the high risk of coastal flooding. According to EA return period water levels guidance (McMillian et al., 2011), the water level with such a return period is estimated to be 2.41 mAOD in Lymington. However, sea-level rise will lead to increase in the frequency of 2.41 mAOD water level and the resultant risk of coastal flooding in the future.

In more detailed analysis, the North Solent Shoreline management plan expects the case study area to be at the higher risk of coastal flooding in the future (Wadey, 2013; Haigh et al., 2014). The number and location of residential and commercial properties at risk from tidal flooding were based on the National Property Dataset (2005) (NFCD, 2010). Figures 3.10 and 3.11 illustrate the point-based locations of the properties at the risk of a 1-in-200 year coastal flooding in Lymington, Pennington and Milford on Sea in 2007 and 2115, respectively.

Table 3.3 The number of properties at the risk of a 1-in-200 year flood in case study area in 2007 and 2115 according to the type of properties – Note that the number of the properties are counted on the current level of developments (source: NFCD (2010))

Councils		The number of properties at risk of a 1 in 200 year event					
		Total		Commercial		Residential	
		2007	2115	2007	2115	2007	2115
Study sites	Lymington Town	126	527	27	51	99	476
	Milford	148	258	14	37	134	221
	Pennington	13	20	7	9	6	11
The sub total		287	805	48	97	239	708

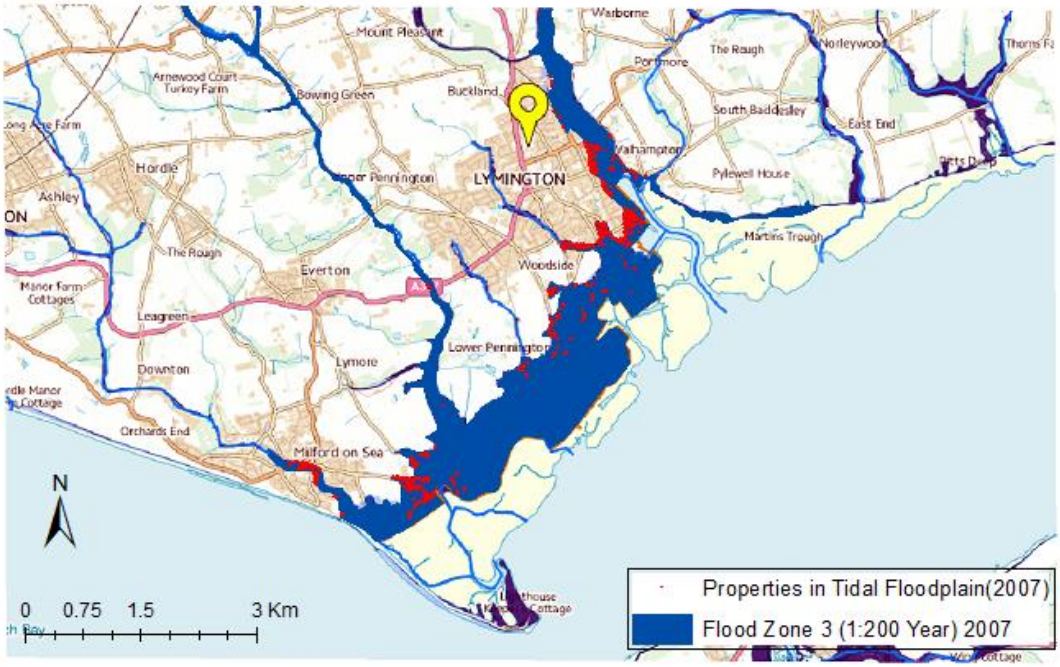

(a)

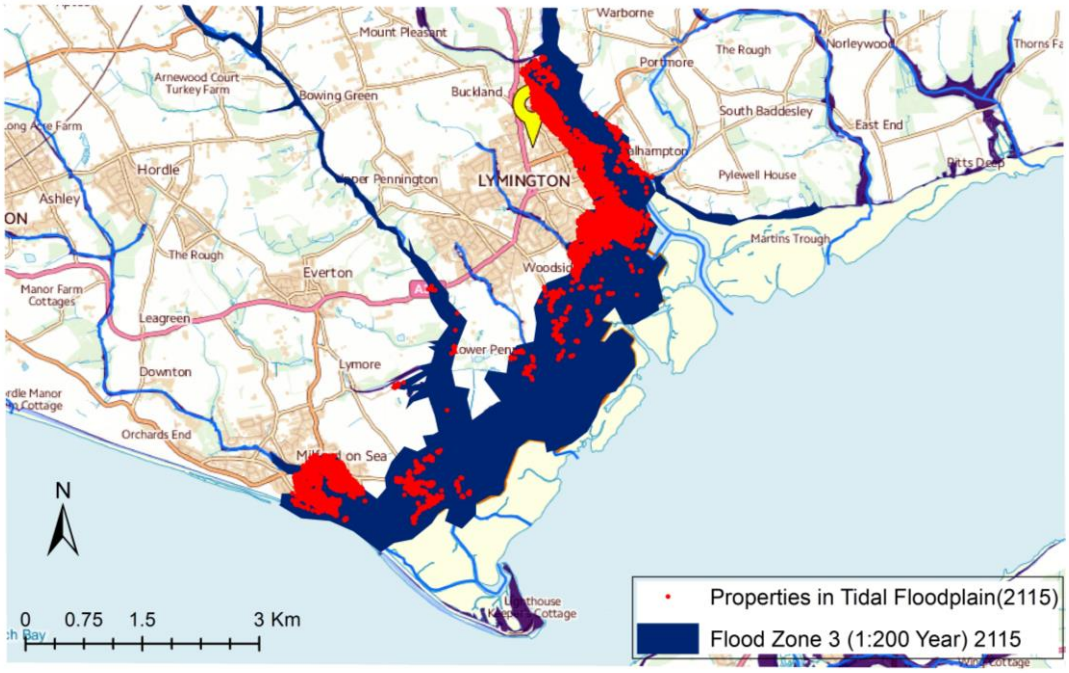

(b)

Figure 3.10 Property locations at the risk of a 1-in-200 year coastal flooding within Lymington (including Pennington and Milford on Sea) with no defence upgrade (a) in 2007 and (b) in 2115 (redrawn from the source data of NFDC (2010))

3. 5 Summary

This preliminary study on the case study area and the past flood events provides an overview of how coastal flooding will affect the flood prone areas in the future. Through the review of characteristics of the coastal flooding on the Solent, some important implications have been drawn from this chapter.

Firstly, the Solent in particular, Lymington is a site to show very complicated hydrodynamics influenced by coastal defence systems and morphology (i.e. saltmarshes). Also, the geological characteristic of Lymington also leads to a site-specifically unique behaviour of coastal flooding. The coastal flooding in Lymington is understood as a consequence of meteorological, astronomical and morphological effects. If the future sea-level rise is combined to the present pattern of coastal flooding, the analysis of flood risk will be more complicated than now.

Secondly, this site may experience the ongoing changes in hydrological conditions due to sea-level rise, even if the current coastal defence systems are well maintained. For example, the loss of saltmarsh due to sea-level rise will lead to the reduction in the performance and effectiveness of the current coastal defence systems. Thus, this may cause the breaching of the current defence system. In addition, as sea levels rise, the risk of coastal flooding in Lymington will grow over time. This will lead to need for understanding of more complicated mechanisms of coastal flooding in Lymington.

Lastly, the lessons from the past flood events enable us to know which area in Lymington is vulnerable to coastal flooding. In the 1989 flood event, breaching due to strong winds and successive flood events within the short period was a main cause to damage floodplains in Lymington and Pennington. On the other hand, the high tides with the storm surges of over 1m had adverse effects on the overall Solent area during the 2008 event. Although the failure modes of the coastal defence and the mechanisms of coastal flooding are different between the 1989 and 2008 flood events, the understanding of two past flood events provide a useful way to identify the vulnerability of the coastal area against rising flood risk in Lymington. Thus, the flood risk has been analysed upon a typical coastal flooding with plausible failure mode of the current coastal defence so that the results of flood simulations in this thesis reflect the characteristics of the 2008 flood event.

This chapter has explored the current defence systems and shoreline management plans that will be implemented to address the future risk of the coastal flooding. In these hydrological

and site-specific contexts, the shoreline management plan at the level of decision-making is very challenging to risk analysts or decision-makers because the uncertainty of climate change and flood simulation makes it difficult to provide economically proper adaptation options for Lymington. In this regard, Lymington is appropriate as a case study area for investigating flood risks in association with the implementation of adaptation measures.

In the following chapter, we will review generic methodologies for analysing flood risks as well as for addressing uncertainty in investment decisions for Lymington.

4. General Methodologic Background

This chapter aims to provide detailed explanation of methods on how to integrate all the climatic data and all the processes for real options analysis. This integration needs some assumptions and simplifications to interpret flood risk and value adaptation options. The estimation of flexible options against uncertainty is central to the real options analysis (Woodward et al., 2014). This enables us to understand how sensitive (or robust) the flexible adaptation options are to the uncertainty of climatic variables. As the comparisons of the adaptation options are generally made in terms of costs and benefits, the option values in this thesis are partly based on the principle of cost-benefit analysis. To investigate the impacts of coastal flooding and sea-level rise on flood plains in Lymington, this research simplifies the mechanisms of coastal flooding and defence failure modes in Lymington by focusing on overflowing and overtopping from storm surges and waves - For comparison, the effect of breaching failure on the result of real options analysis has been investigated later. This integrated analysis enables us to understand how sea-level rise as a major uncertainty increases the risk of coastal flooding in Lymington. This methodology chapter explains the uncertainty modelling of climatic data, flood simulations, the monetisation of flood risk and real options evaluations. Thus, this chapter helps understand the use of the data and methods shown in this thesis.

4. 1 The overview of real options analysis in climate change adaptation

This chapter adjusts the framework of real options analysis used in financial sectors for climate change adaptation in particular, the upgrade of coastal defense. In a broad sense, real options analysis addresses two essential issues: (1) how to define and model uncertainty; and (2) how to evaluate real options including flexibility under the modelled uncertainty (Dixit and Pindyck, 1994; Park, 2002; Yang and Blyth, 2007). For uncertainty modelling, real options analysis needs to consider how uncertainties from various sources such as sea-level rise and extreme still water levels affect option values. On the other hand, the evaluation of real options is relevant to the estimation of the monetary value of their flexibility against the modelled uncertainty. The monetisation of flexibility is a unique feature of real options analysis compared to traditional option evaluations (i.e. cost-benefit analysis) as it quantifies an opportunity to observe and learn the future (Woodward et al., 2104). Thus, the option evaluation is based on the explicit explanation of relationship between uncertain variables and option values.

The procedure of real options analysis in climate change adaptation is structured as follows: (1) collection of data; (2) uncertainty modelling; (3) setting-up of real options; (4) flood risk analysis; (5) estimation of expected annual damage (hereafter, EAD) and expected annual benefit (EAB); and (6) option evaluation. All the processes are designed to estimate the values of real options for the given uncertainty of sea-level rise. Thus, the results enable us to compare the candidates of real options (e.g. deferrable adaptation option or future growth options) in quantitative terms. This thesis also assesses the real options under various socio-economic scenarios by employing different future growth rates in option evaluations. Figure 4.1 illustrates an analytical framework of real options analysis for climate change adaptation.

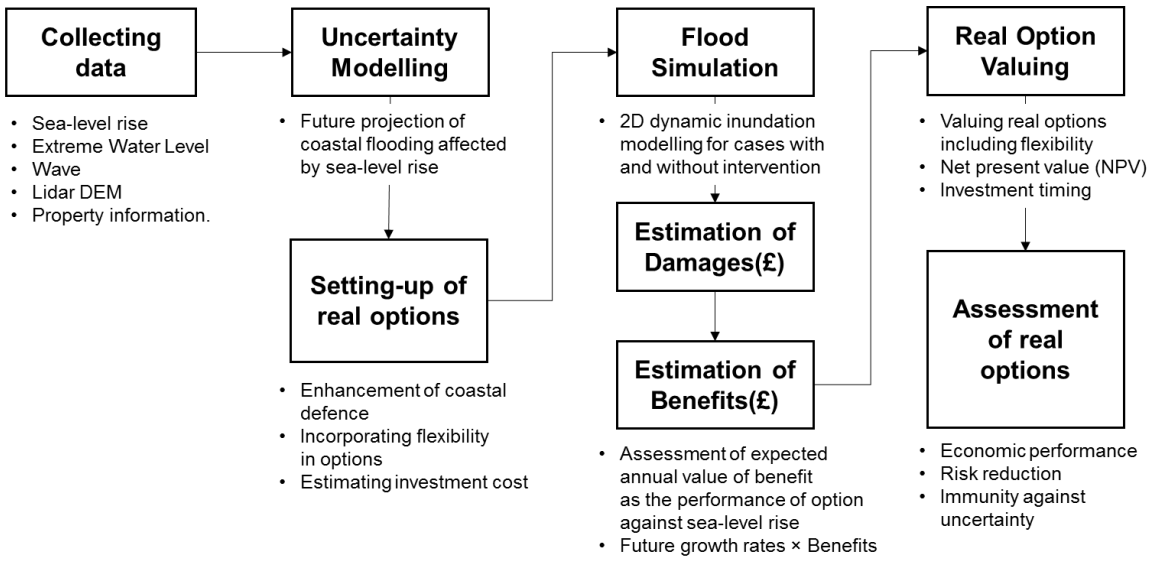

Figure 4.1 Framework of real options analysis for coastal flooding under sea-level rise

The option evaluation process follows guidance and instruction provided by Environment Agency in UK (EA, 2010). Each component of real options analysis adjusted in this thesis is mainly based on Dixit and Pindyck approach (1994) which provides various methods for real option analysis. However, this approach provides only the theoretical background of real options analysis with some examples of its application in ideal cases such as financial investments or idealised projects. As climate change adaptation is a more complicated and uncertainty is surrounded by various factors, it is difficult to apply the approach to coastal flooding without adjustment. All the data in this thesis are provided by UK government and other relevant research. Thus, the method explained in this chapter is considered to be reproductive for any other cases where coastal flooding needs to be managed in the UK

regions. The following chapters explain generic methodologies required for flood risk analysis and real options analysis as listed.

4. 2 Data collection and analysis for uncertainty modelling

This thesis employs extreme still water levels, waves and sea-level rise projections to simulate coastal flooding. Also, all the data are combined to describe the uncertainty of coastal flooding that may occur under sea-level rise. This section gives a detailed account of uncertainty modelling process.

4.2.1 Extreme still water level

Extreme still water level (hereafter, termed ESWL) is a widely used concept as loading conditions for coastal flooding and defense designs (McMillian et al., 2011). The data for ESWL are provided at every point spaced 2km along the whole coastline of the UK (Batstone et al., 2013). The ESWL means the elevation of seawater surface in extreme storm surge events (McMillian et al., 2011). This is a consequence of combination of astronomical tides and meteorologically generated skew surges as shown in Figure 4.2 (McMillian et al., 2011; Haigh et al., 2016). ESWL dataset for every point is expressed with a set of magnitudes and their recurrence periods to represent the uncertainty of extreme sea level events in a statistical way.

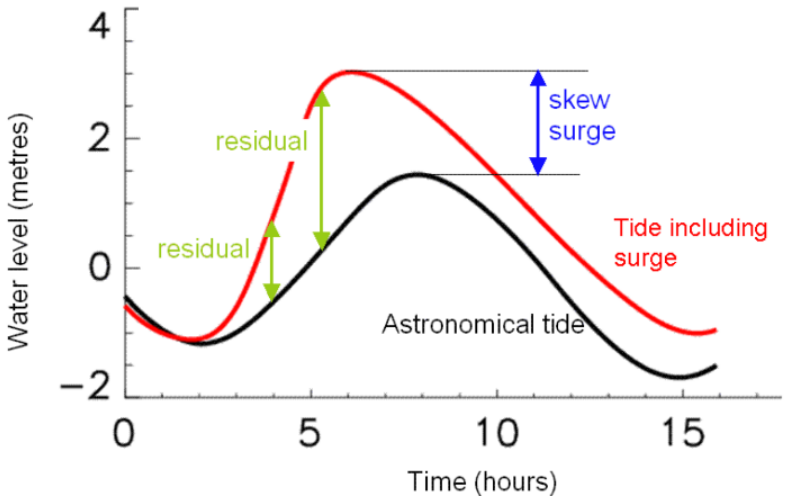

Figure 4.2 Illustration of extreme still water levels (McMillian et al., 2011)

The data points of ESWL are selected in the nearshore area around Lymington (i.e. P1 to P4 in Figure 4.3). The base year of ESWL data is 2008. EA provides these data points by an Arc-GIS shapefile which includes the magnitudes and occurrence periods of storm surge events as attribute data in the corresponding tidal zones (McMillian et al., 2011).

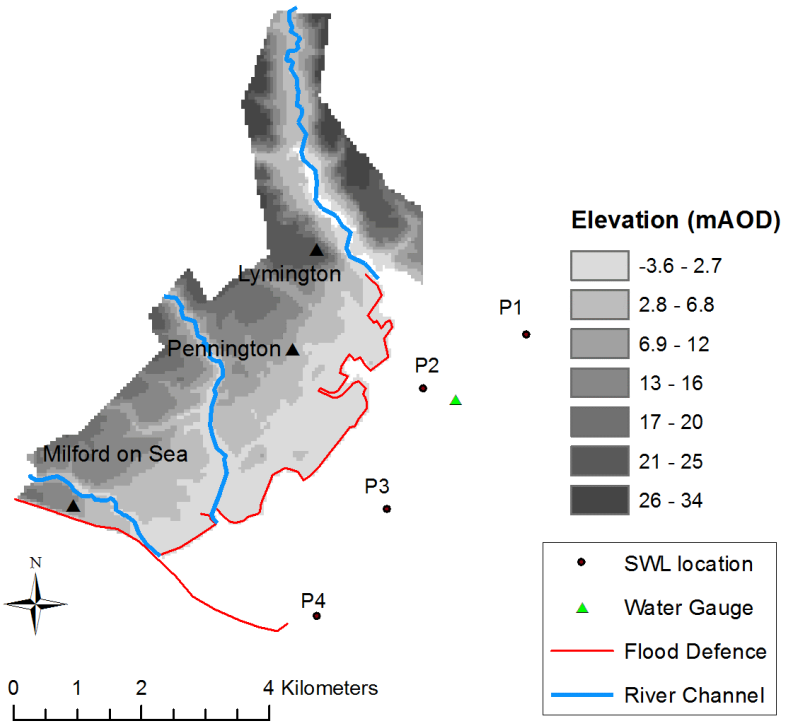

(Unit: Metres, mAOD)

Return Period (Years)	1	10	50	100	200	1000	10000
P1	1.89	2.14	2.30	2.35	2.41	2.54	2.72
P2	1.80	2.06	2.21	2.27	2.33	2.46	2.64
P3	1.71	1.97	2.12	2.18	2.24	2.37	2.55
P4	1.63	1.88	2.03	2.09	2.15	2.28	2.46

Figure 4.3 Locations and attributes of extreme still water levels in Lymington and Milford-on-Sea (McMillian et al., 2011) - The reference of water level throughout this thesis is mAOD (metres above Ordnance Datum, which is approximately mean sea level)

The value of ESWL decreases by 0.08m at every move of point location from P1 to P4 for each return period, or about 0.05m/km. Compared to the rate of sea-level rise (< 2 mm per year) in the Solent (Haigh et al., 2009; 2011), this spatial variation is considered significant in

the flood simulation of a storm surge event. Thus, we assume that the spatially-varying ESWLs with the same return period occur simultaneously at each location.

The choice of a probability distribution for ESWL is required to estimate the likelihood of flooding from extreme sea-level events (Wahl et al., 2017). However, for the convenience of calculation and data fitting, this method adopts exponential distribution as shown in Figure 4.4. The cumulative distribution function $F(x)$ and probability density function $f(x)$ of extreme still water level at P_1 is represented by equations (1) and (2), respectively (Here, x: ESWL).

$$F(x) = 1 - e^{(-10.2701*(x-1.89))} \quad (1)$$

$$f(x) = 10.2701\, e^{(-10.2701*(x-1.89))} \quad (2)$$

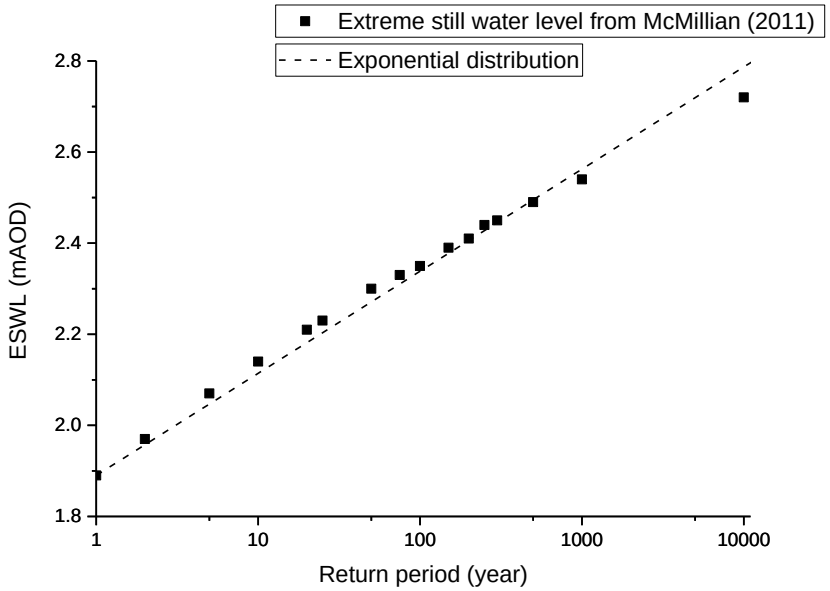

Figure 4.4 Comparison of extreme still water levels by McMillian et al. (2011) with estimates of extreme still water levels obtained by an exponential distribution for Lymington ($R^2 = 0.99$)

The exponential distribution is useful and manageable, when statistically combining sea-level rise and return period extreme still water levels as shown in equations (3) and (4).

$$x_i = x_0 + SLR_i \quad (3)$$

$$E(x_i) = E(x_0) + SLR_i \quad (4)$$

$$Var(x_i) = Var(x_0 + SLR_i) \quad (5)$$

Here, x_0 is a stochastic variate representing return period extreme still water levels at the base year (2008) and SLR_i is deterministic or stochastic variable representing sea-level rise at year i. x_i is the stochastic variate of extreme still water level at year i. $E(x_i)$ is the mean of x_i at year i and $Var(x_i)$ is the variance of x_i at year i. The cumulative distribution function (CDF) and probability density function (PDF) for extreme still water level at the base year of 2008 is drawn in Figure 4.5. The probabilistic representation of ESWL enables the statistical simulation of storm-surge events whose magnitudes and occurrences are uncertain (Willow et al., 2003).

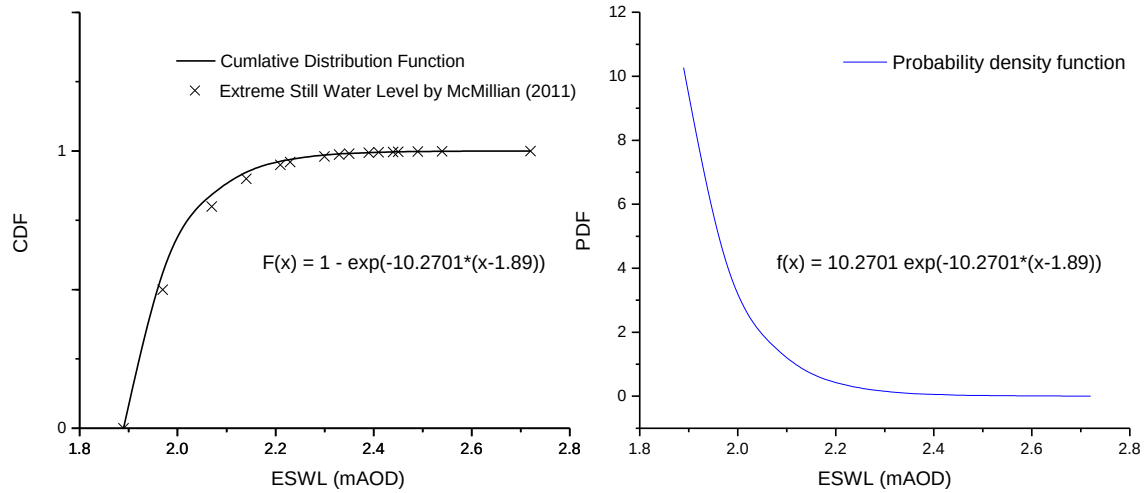

Figure 4.5 (a) Cumulative probability distribution (CDF) and (b) probability density function (PDF) for extreme still water level at Station P1 in the base year of 2008

4.2.2 Waves

The data of ESWL does not consider the effects of waves (McMillian et al., 2011). Waves also increase the likelihood of coastal flooding, although waves may be less influential than storm surges in inundation modelling (Fox, 2009). In addition, the study site is sheltered due to the presence of the Isle of Wight and Hurst Spit. Salt marshes in the foreshore around Lymington and Pennington also mitigate the impact of waves on the floodplains (Cope et al., 2008; Wadey et al. 2013). Thus, wave effects on coastal flooding are considered to be small when comparing to the effects of high still water levels in the case of Lymington. Table 4.1 shows the return periods and magnitudes of waves around Lymington and Milford-on-Sea.

Table 4.1 Wave return periods for the Lymington area from Wadey (2013)

Site	Data range	Return period for significant wave height (m)					10^{th} March 2008	
		1	10	50	100	200	H_s (m)	T_p (s)
Lymington	1991-2002	1.09	1.20	1.28	1.31	1.34	0.91	3.3

Overtopping volume by waves is subject to a freeboard which is a distance between the surface of still water level and the crest of coastal defence. Thus, overtopping rates continuously change over time due to continuous change in the elevation of seawater surface during a storm surge event. The mechanism of seawater overtopping crests is illustrated in Figure 4.6 (Reeve and Burgess, 1993). Overtopping rate is calculated by dividing an overall overtopping volume with its duration. Following the previous study (Dawson et al., 2005), overtopping rate (*l/m/s*) is converted to an equivalent height by using a weir formula. Then, the equivalent height is uniformly added to a time-series of still water level during a flood simulation (HRW, 2003; Wadey et al., 2012). However, if the water level exceeds the crest level of coastal defense, overflowing prevails over overtopping. For this reason, the equivalent height by waves is limited up to 0.2m - which is recommended as a maximum equivalent height of wave overtopping in flood simulation (HRW, 2003; EurOtop, 2016).

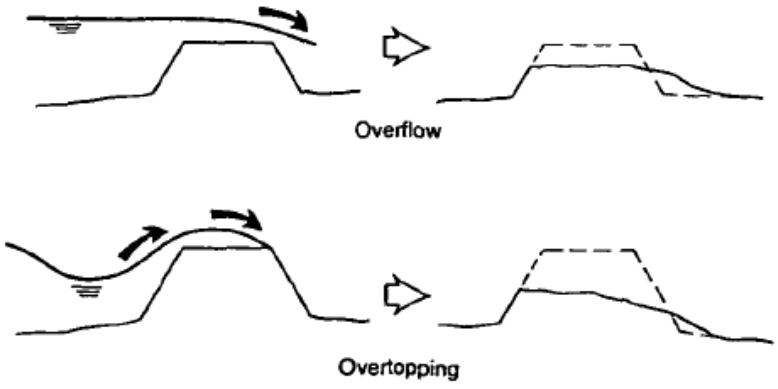

Figure 4.6 Sea wall failure modes (Reeve and Burgess, 1993) - The image is copied from the thesis of Wadey (2013)

A number of studies provide empirical formulas of mean overtopping discharge for various conditions such as types of defence structure, seaward slopes of coastal defence, crest heights and roughness (HRW, 2003; 2004; EurOtop, 2016). This thesis adopts an overtopping

volume formula from Owen (1980) to estimate overtopping discharges over sloping coastal defences which are the most common type of coastal defence in Lymington.

The Owen (1980) formulation explains overtopping volume by using a dimensionless discharge (Q_*) and freeboard (R_*). This formulation also reflects the shape and slope of various coastal defences by empirically determined coefficients (A, B) as shown in equation (6), (7) and (8).

$$Q_* = A \exp(-B \times R_*/r) \quad (6)$$

$$Q_* = Q / (g\, T_m\, H_s) \quad (7)$$

$$R_* = R_c / (T_m\, (g\, H_s)^{0.5}) \quad (8)$$

Here, Q: overtopping discharge rate per unit length of defence

H_s: significant wave height (m) at the toe of structure

T_m : wave period (s) at the toe of structure

R_c : crest freeboard

r : roughness coefficient

A, B: empirical coefficient

R_* : dimensionless freeboard

The mean overtopping rate and the proportion of waves causing overtopping have been estimated in association with the time-series of extreme still water levels (EurOtop, 2016). For the analysis of wave overtopping, this research adopts the standardised time-series of still water levels for Lymington, which were drawn from the most recent coastal flood event of the 10th March 2008 event. The standardised time-series of extreme water levels are shifted up or down by the difference of peak water levels between the 2008 flood event and the simulated flood event. As the still water level time-series provide information on water surface levels on an hourly basis during a cycle of a flood event (about 12 hr), the hourly change in water surface level provides the estimates of crest freeboard (R_c). The procedure to calculate the overtopping discharge follows a standard manual provided by EurOtop (2016). The characteristic of a seawall in the above formulation is defined with constants A and B representing the slope of the coastal structure and the roughness of its surface, respectively (Owen, 1980). Thus, if the slope and roughness of a seawall and its crest freeboard is known, this formulation provides an approximate overtopping discharge for a certain wave height (H_S) and wave period (T_p). There are various types of the coastal defences with different

slopes (1:2 to 1:5) in Lymington. For the analysis of wave overtopping rates, the shape and roughness parameters (A, B) of coastal defence are taken from the most vulnerable section of the Lymington defences. This leads the wave overtopping volumes to be over-estimated in some parts of the coastal defences. However, since difference in overtopping volume due to the defence parameters is relatively small in comparison to the effect of freeboards, this thesis assumes that the choice and simplification of the defence parameters have little effect on flood simulations.

By the calculation of wave overtopping rates for various peak water levels, this thesis has established a relationship between peak water levels and wave overtopping volumes (in height) as shown in Figure 4.7. The numerical relation enables us to deterministically generate wave overtopping volumes for peak water levels which are the highest water levels during the time-series of water levels. The overtopping volumes by waves highly rely on water levels during a flood event. Thus, this thesis assumes the overtopping volumes to be dependent on water levels (i.e. ESWL+SLR). This helps reduce computational time for statistically integrating waves, extreme water levels and sea-level rise. The process to calculate wave overtopping rates is well documented in Appendix A.

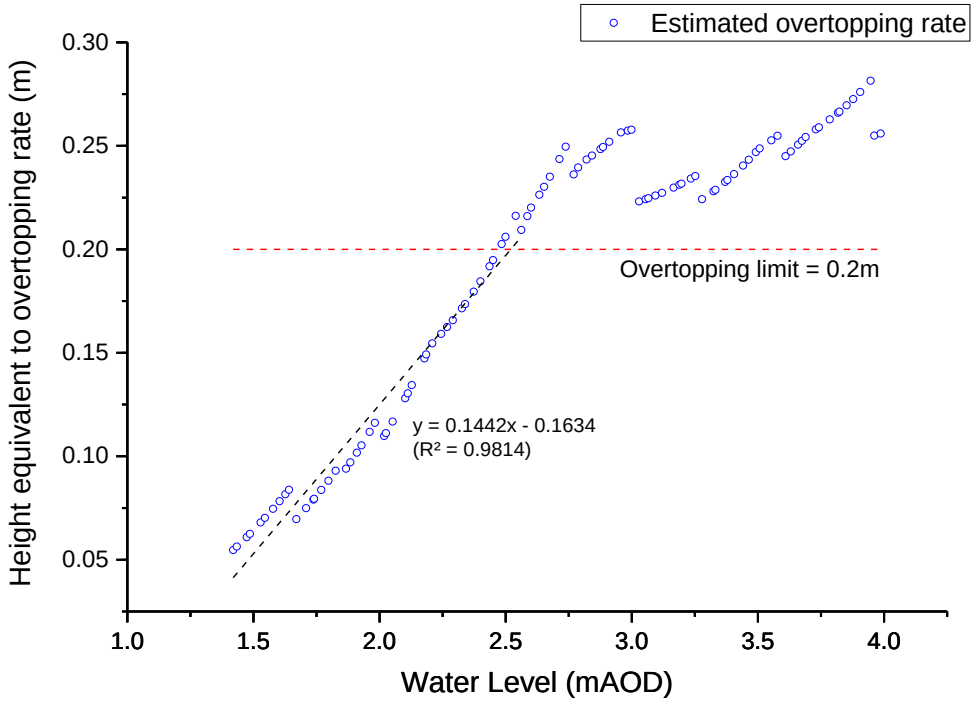

Figure 4.7 A relation between overtopping rates and water levels (= ESWL + SLR) for the wave conditions (H_s =0.91m and T_p =3.3s) in Lymington

4.2.3 Sea-Level Rise Scenarios

A. Characteristics of sea-level rise from UKCP 09

Sea Level Rise (SLR) data are taken from UKCP 09, which provides multiple sea-level rise scenarios (e.g. Low, Medium and High) between 1990 and 2100 (Lowe et al., 2009). The sea-level rise scenarios of UKCP 09 are represented with probabilistic projections consisting of the most likely trajectories and their probabilistic ranges. The relative sea-level rise (RSLR) is adopted for flood risk analysis in the coastal area of Lymington.

The UKCP 09 scenarios consider three sources of uncertainty on the projections of SLR: (1) scenario uncertainty is associated with the emission of greenhouse gases, global warming, aerosols and the responses of earth or ocean systems to global warming; (2) internal climate variability comes from natural variation in atmospheric and oceanic circulations which have influence on climate change model conditions; and (3) modelling uncertainty is attributable to the various sources of climate model inputs and assumptions, modelling errors, and the types of global climate change models (Lowe et al., 2009). UKCP 09 data represent these uncertainties with the sea-level rise trajectory and its probabilistic range for each scenario. Given a set of sea-level rise scenarios, the probabilistic ranges of sea-level rise projections are considered as an effective way to quantify the uncertainty of sea-level rise (Lowe et al., 2009).

There is also a strong need for the most extreme, but very unlikely, scenario for flood risk management (Lowe et al., 2009; Nicholls et al., 2014; Hinkel et al., 2015). This scenario is called an H++ SLR scenario in UKCP 09. For a sensitivity purpose, we have produced an H++ scenario for Lymington by scaling up the central estimate of the High SLR scenario in Lymington with the ratio of the H++ SRL scenario to the High SLR scenario at the global scale suggested by Nicholls et al. (2014). The H++ SLR scenario for Lymington projects sea levels to rise by up to 1.78m on average in 2100.

This thesis also includes the current trajectory of sea-level rise in the analysis. This is the most realistic reflection of sea-level rise based on the observation of the past sea-level rise around Lymington (Haigh et al., 2014). This projection includes the strong memory of sea level due to the role of climate sensitivity which is the response of sea level to greenhouse emissions (Nicholls et al., 2014). The rate of sea-level rise is recorded to be 1.4mm/yr in Southampton gauge which is the nearest point from Lymington with the long-term record on sea levels from 1935 (Haigh et al., 2104). For convenience, the current sea-level rise is

termed to be the Historical trend SLR scenario. All the trajectories of SLR scenarios have been presented in Figure 4.8.

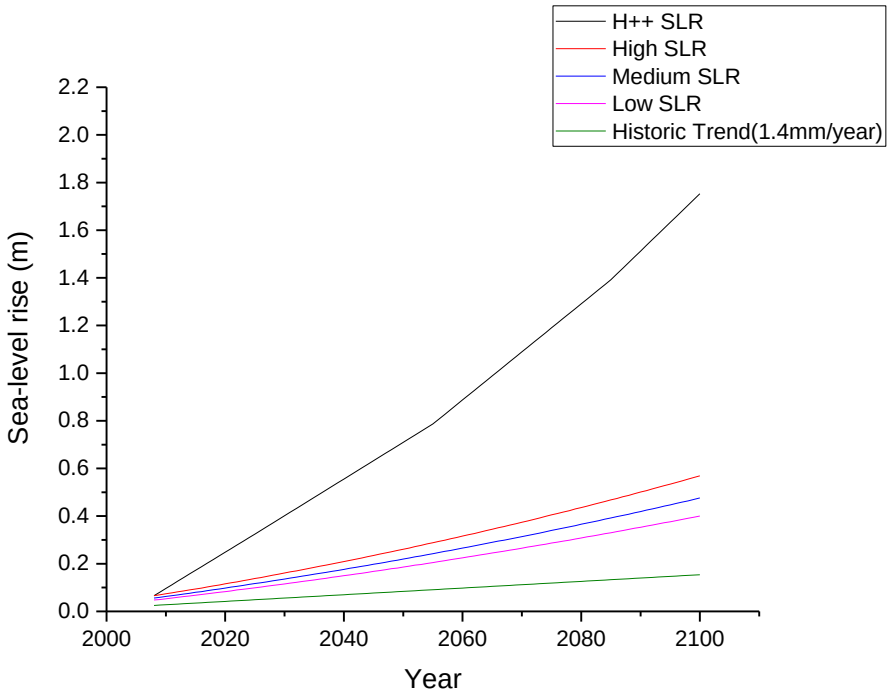

Figure 4.8 Sea-level rise projections from 1990 to 2100 for each SLR scenario in Lymington – The High ++ SLR is made by scaling-technique using the data from Nicholls et al. (2014), High, Medium and Low SLR scenarios have been taken from UKCP 09, and the Historical trend scenario (1.4mm/year) is based on the observations from Haigh et al.(2009).

B. Representation of uncertainty of sea-level rise

This thesis takes two approaches to incorporate the uncertainty of sea-level rise projections into coastal flooding. The first method takes only the central estimates (i.e. the 50^{th} percentile line) of the sea-level rise projections. This is statistically the most likely value during the period of sea-level rise. In this method, this approach just adds mean sea-level rise to the magnitude of climatic variables (i.e. extreme still water levels and waves).

The second method employs Brownian motion to describe the evolving pattern of sea-level rise in UKCP 09. Brownian motion is a simple way to represent a stochastic process with the small number of parameters. This enables us to simulate a realistic description of random changes in uncertain variables (i.e. sea-level rise) over time by calibrating drift (α) and variance (σ) parameters. The usefulness of Brownian motion has already been demonstrated in many other areas such as economics, physics and statistics (Dixit and Pindyck, 1994;

Gersonius et al., 2013; Abadie et al., 2016). This thesis assumes that the Brownian motion is similar to the behaviour of sea-level rise for some reasons. Firstly, sea-level rise is a consequence of physical interactions between the earth and the oceanic systems (Nicholls et al., 2014). The effects of physical and oceanic processes on sea-level rise are likely to continue for a long-term period over and beyond the 21st century. However, the amount of sea-level rise varies, with large uncertainty, depending on oceanic circulations, changes in regional gravity, land lift/subsidence and any other factors for a given emission scenario (Nicholls et al., 2014).

Secondly, IPCC dataset represents each sea-level rise projection with a long-term expectation and its probabilistic range (Lowe et al., 2009; IPCC, 2007, 2014). The normalised probabilistic range of the sea-level rise projection implies that a particular amount of sea-level rise in the real world will be observed within a symmetrical probabilistic range with a certain chance (IPCC, 2014; Hinkel et al., 2015). Thus, one of sea-level rise simulations by Brownian motion emulates such a stochastic property of IPCC or UKCP 09 data because any change in the stochastic process of Brownian motion over a time interval is assumed to follow a normal distribution. In this regard, the Brownian motion is considered to be a proper statistical expression to represent the uncertainty of sea-level rise for IPCC.

The method to calculate the drift and variance parameters for the Brownian motion is detailed in Appendix B. This thesis takes General Brownian motion. For discrete time ($\Delta t = 1$), the General Brownian motion has a discrete form in equation (9).

$$x_{t+1} - x_t = a(x,t)\Delta t + b(x,t)\Delta z \tag{9}$$

$$= a(x,t) + b(x,t)\epsilon$$

$$\therefore\ x_{t+1} = x_t + a(x,t) + b(x,t)\epsilon$$

Here, x_{t+1}, x_t : variables at time t and t+1, respectively

$a(x,t), b(x,t)$: any function of variable x and time t

ϵ : a random variable normally distributed with μ of 0 and σ of 1

The former parameter $a(x,t)$ is computed by fitting the long-term expectation of Brownian motion to the central trend (the 50th percentile) of a sea-level rise projection whereas the latter

parameter $b(x,t)$ is evaluated by fitting the variance of the Brownian motion to the variance of sea-level rise by UKCP 09 at any time *t*. However, it is difficult to find a variance function $b(x,t)$ which represents the uncertainty range of sea-level rise projection of UKCP 09. This is because the width of sea-level rise range in UKCP 09 keeps increasing with time. Thus, this thesis assumes that the variance function $b(x,t)$ at time *t* increases according to the variance (σ_t) of sea-level rise at time *t*, which is the width of the 5th and 95th probabilistic boundaries of sea-level rise divided by 1.645 (Refer to Figure B.2 in Appendix B). Therefore, the formula of the variance parameter is shown in equation (10)

$$b(x,t) = \frac{\sigma_t}{\sqrt{(t-t_0)}} \tag{10}$$

Here, $b(x,t)$: a variance function of variable *x* and time *t*

σ_t: a variance of sea-level rise at time *t* from UKCP 09

t_0: a starting year of sea-level rise projection (i.e. 1990)

The time-series of the General Brownian motion with the stochastic property of UKCP 09 are simulated by a programmed spreadsheet (Refer to B.7 in Appendix B). The result of the General Brownian motion for a sea-level rise projection is shown in Figure 4.9. When the average rate of sea-level rise and its standard deviation during the projected period are estimated by a least square method, the estimated stochastic properties are similar to those of the currently observed sea-level rise at Southampton. For instance, in the High SLR scenario, the rate and standard deviation of time-series of sea-level rise randomly generated from the General Brownian motion are estimated to be 3.3~7.5 mm/year and 0.07~0.19mm/year, respectively. The observed rate and standard deviation of sea-level rise in Southampton gauge is 1.4mm/year and 0.18mm/year, respectively (Haigh et al., 2010).

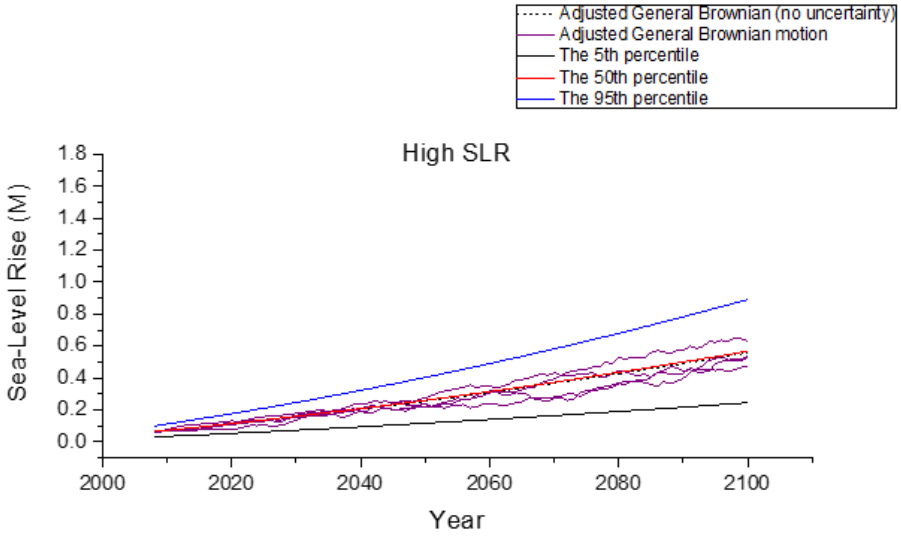

Figure 4.9 Examples of time-series of sea-level rise by General Brownian motion for High SLR scenario

For the validation of Brownian motion, this thesis has estimated the mean and variance of the probability distribution of sea-level rise in 2100. For denotation, the mean and variance in 2100 is termed μ_{2100} and σ_{2100}, respectively. The demonstration has randomly generated 10,000 time-series of sea-level rise by the General Brownian motion and, then, constructed the probability distribution of sea-level rise at 2100 as shown in Figure 4.10. The generated probability distribution by the General Brownian motion shows a normal distribution with a similar mean value with UKCP 09. However, the standard deviation is little smaller than that of UKCP 09.

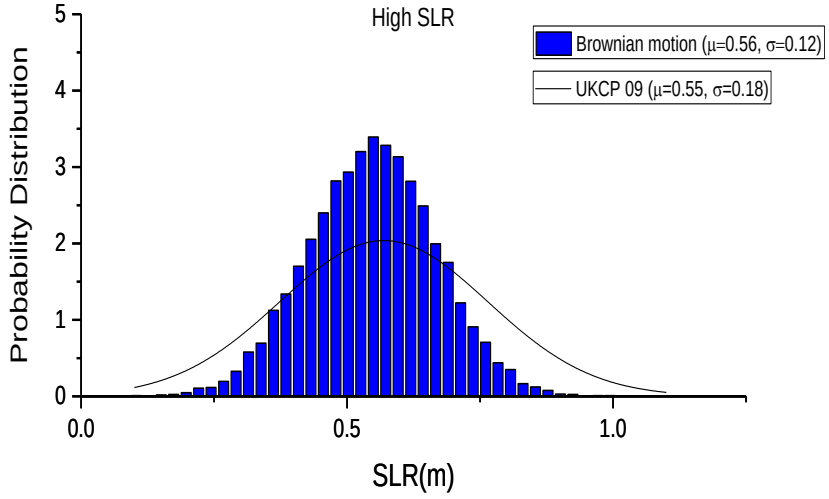

Figure 4.10. Comparison of the probabilistic ranges of stochastic variables of sea-level rise in 2100 by adjusted General Brownian motion and UKCP projection for the High SLR scenario – Note that there is no difference in mean between adjusted GBM and UKCP 09

4. 3 Integration of climatic variables for uncertainty modelling

Sea-level rise increases the risk of coastal flooding (Wahl et al., 2017). It will affect the magnitude and frequency of coastal flood events by shifting up the level of storm surges (Lowe et al., 2009; Ranger et al., 2013; Woodward et al., 2014; Wolf et al., 2015; Haigh et al., 2017). This analysis assumes that sea-level rise is independent of extreme still water level. In fact, the wind stress forcing is distributed over a different level of sea-water so that change in sea level affects the propagation of surges and tides. However, these effects are ignorable in combining sea-level rise and extreme still water level (Lowe et al., 2001). This assumption allows the thesis to simply sum extreme still water levels and sea-level rise. The integration process for storm surge events, sea-level rise and waves is illustrated by flow chart in Figure 4.11. Firstly, this method sums extreme still water levels and sea-level rise in every year during the SLR projection period. Secondly, we estimate overtopping rates in height which are assumed to be dependant only on the water surface levels (i.e. ESWL+SLR). Lastly, the estimated overtopping rate (m) is added to the water surface levels. As ESWL+SLR is stochastic variable, ESWL+SLR+WAVE is also stochastic variable (This thesis, hereafter, terms water levels including overtopping rates ESWL+SLR+WAVE).

This process takes a numerical approach by employing a probability simulation programme based on Monte-Carlo method (@Risk) which is an added-in programme to Microsoft Excel. This combined programme allows for the construction of probability distributions of newly generated variables and the estimation of statistical properties of the variables. @Risk programme helps analyse stochastic variables in a numerical way (Palisade, 2018).

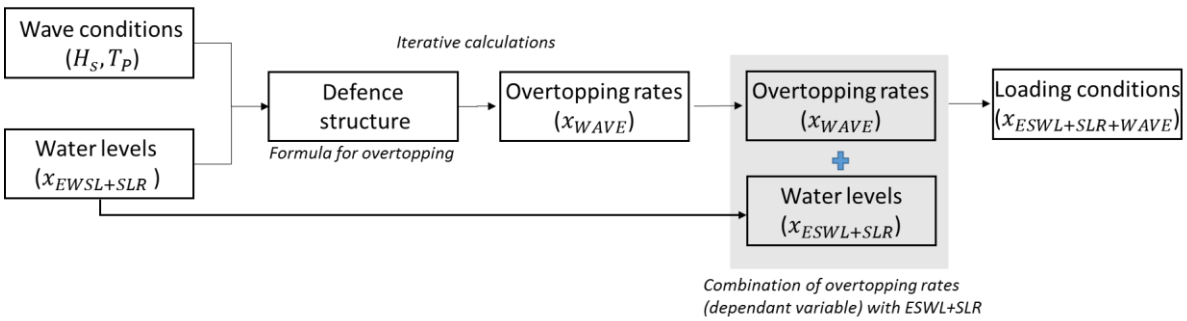

Figure 4.11 A process to construct the probability of wave, still water level and sea-level rise

A. Mean sea-level rise (MSLR)

Firstly, for the integration, we use MSLR for the simulation of coastal flooding. This will provide how the probability of extreme still water levels changes according to each MSLR scenario. The inverse function of Cumulative Distribution Function (CDF) is shown in equation (11). In order to randomly generate the annual maximum values of extreme still water levels for any year, the cumulative probability ($F(x)$) is substituted by an evenly distributed random value (R) between 0 and 1.

$$ESWL = 1.89 - \frac{1}{10.2701} * [\ln(1 - R)] \quad (11)$$

Here, ESWL: Random variable of extreme still water level

R: Random values evenly distributed between 0 and 1

Sea-level rise and extreme still water levels are combined over the period between 2008 and 2100. The random time-series of ESWL are simply superposed on MSLR (= ESWL+MSLR). Thus, sea-level rise shifts up the likely range of ESWL with time.

As wave overtopping rate is highly dependent on the water surface level (i.e. ESWL+SLR), the wave overtopping rate in height is expressed as a function of water surface level by equation (12). This estimated overtopping rate has been added to the corresponding ESWL + SLR. The result is shown for the High MSLR scenario in Figure 4.12.

$$\begin{aligned} WAVE &= 0.1442\ (ESWL + SLR) - 0.1634\ (m) \quad \text{(WAVE} < 0.2\text{)} \\ WAVE &= 0.2\ (m) \quad \text{(WAVE} \geq 0.2\text{)} \end{aligned} \quad (12)$$

The 5th and 95th percentiles every 20 years from 2020 to 2100 are estimated by the sampling process of ESWL+SLR+WAVE using @ Risk programme. Those values for the intermediate years are interpolated by data-fitting. Thus, this thesis provides the trajectories of 5th and 95th percentiles during the 21st century. The stochastic variables of ESWL+MSLR+WAVE are observed within the 5th and 95th percentile range. Note that the chance of the variable of ESWL+MSLR+WAVE being observed within this range is 90% in a statistical sense.

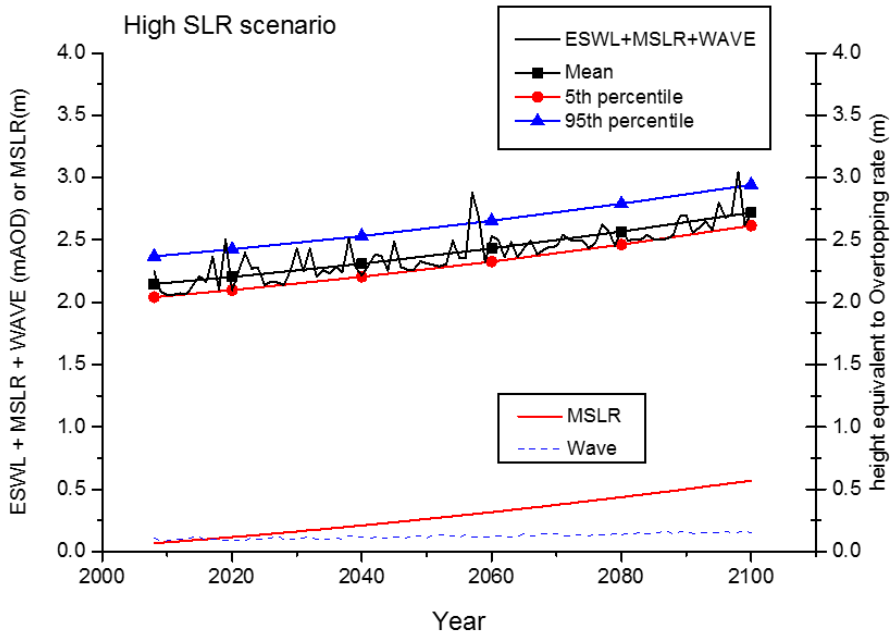

Figure 4.12 The results of uncertainty modelling of ESWL+MSLR+WAVE for the High sea-level rise scenario –The results of ESWL+MSLR+WAVE for other MSLR scenarios are shown in Appendix C.

B. Sea-level rise by General Brownian motion

This thesis has also combined extreme still water levels with random time-series of sea-level rise created by the General Brownian motion for each SLR scenario. The sea-level rise described by the General Brownian motion follows equation (13).

$$x_{t+1} = x_t + \alpha * t + \beta + \sigma_t/\sqrt{t - t_0} * \epsilon \qquad (13)$$

Here, x_{t+1}, x_t : random variable of sea-level rise at time $t + 1$ and t, respectively

t: time in year

t_0: the start year of UKCP 09 projection (=1990)

α, β: constants for a drift function

σ_t : a variance at time t from UKCP 09

ϵ: a normally-distributed random variable (mean = 0 and standard deviation = 1)

The thesis combines sea-level rise, described by General Brownian motion, with extreme still water levels in a numerical way. By summing equation (8) and (13), this process produces the time-series of ESWL over Brownian sea-level rise at any time t in equation (14). For denotation, this thesis terms ESWL over sea-level rise at any time *t* to be $ESWL + SLR_t$

$$ESWL + SLR_{t+1} = \left[1.89 - \frac{1}{10.2701} * \ln(1 - R)\right] + \left[SLR_t + \alpha * (t) + \beta + \sigma_t / \sqrt{t - t_0} * \epsilon\right] \quad (14)$$

Here, $ESWL + SLR_t$: extreme still water level over Brownian sea-level rise at year t
R: a random variable evenly distributed between 0 and 1
SLR_t : sea-level rise at year t by General Brownian motion
α, β: constants for the deterministic motion of General Brownian motion
σ_t: a variance at year *t* from a UKCP 09 probabilistic projection
t : time in year (Here, t_0 = a starting time of the UKCP 09 projection)
ϵ: a normally distributed random variable (mean = 0 and standard deviation = 1)

The equation (14) enables us to simulate the time-series of random values of extreme still water levels plus Brownian sea-level rise. Two random variables (R, ϵ) in equation (14) is independent of each other. By generating a great number (i.e. 10,000 times) of variables of ESWL+SLR_t, we can construct a probability distribution of ESWL+SLR_t numerically. The overtopping rate in height has also been added to the corresponding ESWL+SLR_t by using the wave-water level relation in equation (12). The stochastic properties of ESWL+SLR_t+ WAVE have been measured by @Risk programme with the results represented by the 5th, 50th and 95th percentiles over time. All the central values and the 5th and 95th percentiles of ESWL+SLR+WAVE are plotted during the projection of sea-level rise. The result of ESWL+SLR+WAVE is shown for the High SLR scenario in Figure 4.13. For other SLR scenarios, refer to Appendix D.

As seen in Figure 4.13, the time-series of extreme still water level, sea-level rise and waves (black solid line with dots) lie within the boundary of the 5th and 95th percentile lines. Comparing to the cases of MSLR, the distance between the 5th and 95th percentiles from the General Brownian motion is wider than that from MSLR. This is mainly due to the uncertainty of climate change models in UKCP 09.

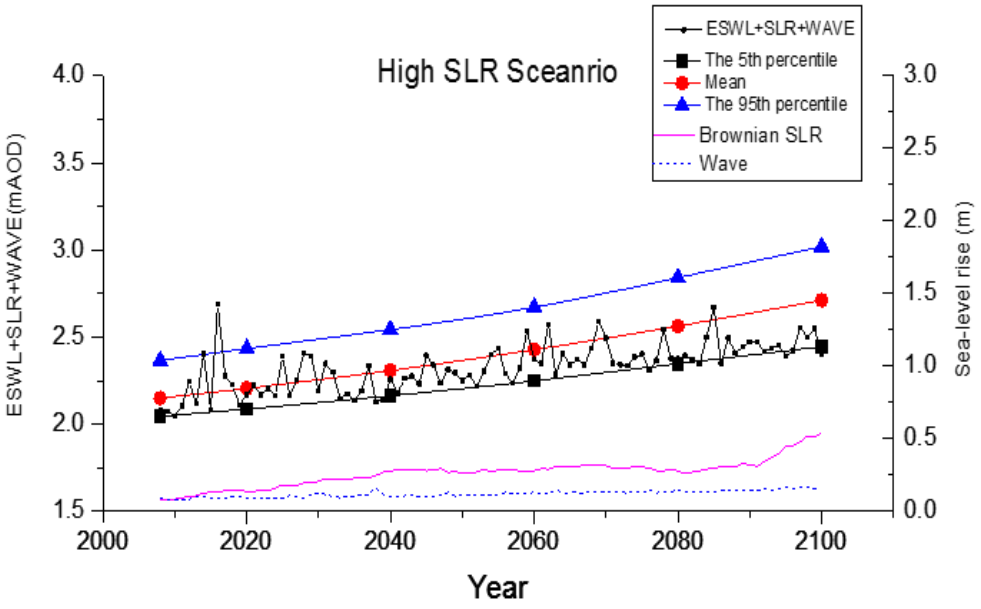

Figure 4.13 The results of uncertainty modelling of ESWL+Brownian SLR+WAVE for the High SLR scenario – Note that SLR and Wave are plotted on y-axis on the right.

C. Implication of results from MSLR and Brownian SLR

These integrated loading conditions of ESWL+SLR+WAVE have important implications for flood risk analysis and option evaluation. Firstly, a numerical approach has been used to produce the probability of combined loading conditions for each year during the 21st century. The probability of the loading condition in any year can be reconstructed by randomly generating a large number of the time-series of ESWL+SLR+WAVE. Thus, this numerical approach enables us to statistically generate flood loading conditions during the 21st century under the non-stationary state.

Secondly, a random variable of ESWL+SLR+WAVE at any given year reflects all the statistical and physical properties as a consequence of combinations of sea-level rise, extreme still water level and waves. Thus, the random variable is considered as a proper tool, at least in this thesis, to communicate uncertainties from all the components of flood loading.

Thirdly, this numerical approach combines different types of uncertainties together. The uncertainty of sea-level rise comes from climate change model outputs and future emissions (Lowe et al., 2009) whereas the uncertainty of extreme still water level is based on internal variability from the long-term observations of extreme water levels (McMillian et al., 2011). Thus, as the different types of uncertainties have been represented by their own probabilities, the combined variables have different probabilities from their own probabilities. This

probabilistic combination helps estimate the probability of coastal flooding for Lymington based on the existing dataset.

Lastly, as seen in Table 4.2, there is little difference in the mean value (μ) between the cases of MSLR and Brownian SLR. On the other hand, the standard deviation (σ) in the case of Brownian SLR is larger than that of MSLR. This implies that the choice of MSLR or Brownian SLR does not have influence on the result of option evaluations because the options are assessed on the averaged values. This will be further investigated in estimating expected annual benefits or damages.

Table 4.2 Comparisons of stochastic properties (μ: mean and σ: standard deviation) of random variables of ESWL+MSLR+WAVE and ESWL+Brownian SLR+WAVE (Unit: mAOD)

SLR	Year	ESWL+MSLR+WAVE		ESWL+ Brownian SLR+WAVE		Remark
		μ	σ	μ	σ	
H++	2008	2.15	0.11			Brownian motion is not defined for H++ SLR
	2020	2.35	0.11			
	2040	2.71	0.11			
	2060	3.07	0.10			
	2080	3.48	0.10			
	2100	3.94	0.10			
High	2008	2.15	0.12	2.15	0.11	
	2020	2.21	0.11	2.21	0.11	
	2040	2.31	0.11	2.31	0.12	
	2060	2.43	0.11	2.43	0.13	
	2080	2.57	0.11	2.56	0.15	
	2100	2.72	0.11	2.71	0.18	
Medium	2008	2.13	0.11	2.14	0.11	
	2020	2.18	0.11	2.19	0.11	
	2040	2.27	0.11	2.28	0.12	
	2060	2.37	0.11	2.38	0.12	
	2080	2.49	0.11	2.50	0.14	
	2100	2.61	0.11	2.63	0.15	
Low	2008	2.13	0.11	2.13	0.11	
	2020	2.17	0.12	2.17	0.11	
	2040	2.24	0.11	2.25	0.12	
	2060	2.33	0.11	2.33	0.12	
	2080	2.42	0.11	2.43	0.13	
	2100	2.53	0.11	2.53	0.14	
Historical Trend	2008	2.10	0.11	2.10	0.11	Brownian motion is based on the observed data at Southampton gauge (1.3±0.18mm/yr)
	2020	2.12	0.11	2.12	0.11	
	2040	2.15	0.11	2.15	0.11	
	2060	2.18	0.11	2.18	0.11	
	2080	2.22	0.11	2.21	0.11	
	2100	2.25	0.11	2.24	0.11	

4. 4 The setting-up of coastal defence in climate change adaptation

4.4.1 Types of real options: Option to wait and to grow

The real options analysis in this thesis is aimed to assess the performance of coastal adaptation options including flexibility under the uncertainty of sea-level rise. There are many other available adaptation options such as flood warning system, flood insurance and regulation of land use that are all plausible against the increasing risk of coastal flooding. However, the characteristic of real options is salient only when the investment is irreversible (Dixit and Pindyck, 1994). Thus, reversible adaptation options such as flood warning and insurance are eliminated in considering real options for coastal adaptation.

This research considers two approaches to raising the crest level of coastal defence. Firstly, the upgrade of coastal defence adopts a single adaptation path in which to raise the crest of coastal defence at once. Once the investment is completed with a large amount of cost, this adaptation option will be irreversible. As reviewed previously, a single irreversible, but deferrable, option is defined as an 'option to wait' (Park, 2002; De Neufville, 2003; Woodward et al., 2013). As long as a choice either to invest, or to defer, is alive, flexibility still remains in the option. An example for an option-to-wait case is conceptually illustrated with a 1-in-200-year ESWL over sea-level rise (Figure 4.14).

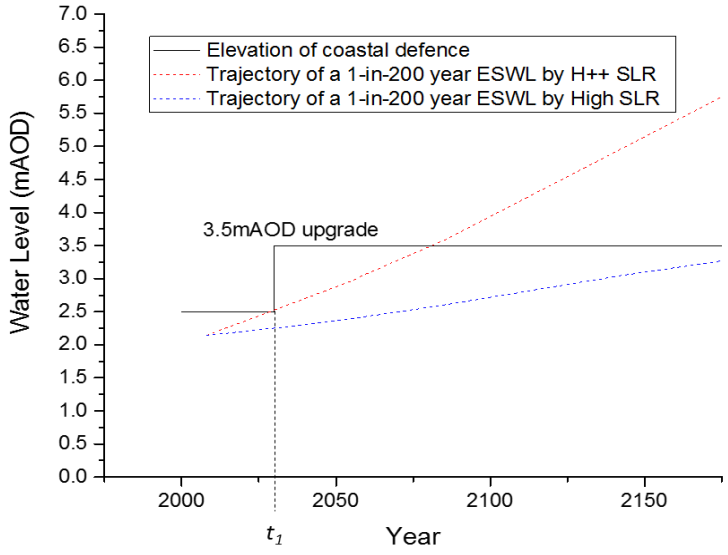

Figure 4.14 Adaptation path for an option to wait (i.e. raising coastal defence up to 3.5 mAOD) against an increasing 1-in-200 year extreme still water level due to sea-level rise in Lymington. Here, t_1 is an investment time for the upgrade of coastal defence.

The first upgrade scheme is to raise all the coastal defence uniformly up to 3.5 mAOD at once. Therefore, the upgraded coastal defence can, at least, protect floodplains in Lymington from coastal flooding equivalent to a peak water level of 3.5 mAOD. Since the peak water level recorded in the 2008 flood event was 2.14 mAOD, the 3.5 mAOD level coastal defence may be considered as an over-adaptation. However, this upgrade plan of raising the coastal defence to 3.5 mAOD sufficiently protects Lymington from coastal flooding during the most period of projected sea-level rise. However, if sea-level rise follows the fastest growing rate in the H++ SLR scenario (i.e. 2.54cm/year), storm surge events are more likely to occur over extremely high tides raised by sea-level rise. This will lead to Lymington being more frequently exposed and vulnerable to coastal flooding. Thus, the coastal defence raised up to 3.5 mAOD may not be enough to protect Lymington in the future under the H++ SLR scenario.

The second approach is to take multiple-stage options or pathways for the upgrade of coastal defence. This enables decision-makers to adjust adaptation options in response to sea-level rise. This thesis considers two or three stages of sequential investments for the coastal defence upgrade. The crest of coastal defence will be raised from current level (approximately 2.5 mAOD) through 3.0 mAOD, or 3.5 mAOD, to 4.0 mAOD in stages. This type of option is referred to as ‘option to grow’ or ‘real options in system’ (Dixit and Pindyck, 1994; Park, 2002; De Nuefville, 2003) because the flexibility of future extension should be incorporated in the coastal defence upgrade system. The concept of ‘option to grow’ is illustrated in Figure 4.15.

As seen in Figure 4.15, the flexibility of future extension enables us to have multiple adaptation paths for the upgrade of the coastal defence. For the case of option-to-grow, the investment decisions on the height of the upgraded coastal defence depend on the rate of sea-level rise in the future. Thus, the second or remaining investment options are also the right but not the obligation in the case of option-to-grow.

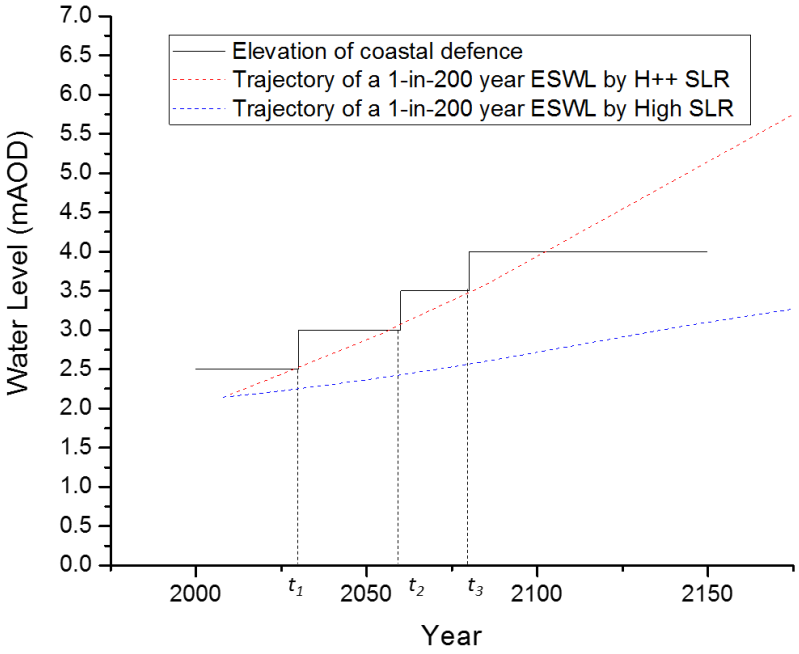

Figure 4.15 The schematization of option to grow for the multiple-stage adaptation of defence upgrade against increasing extreme still water levels due to sea-level rise. Here, t_1, t_2 and t_3 are investment times for the corresponding upgrades of coastal defence, respectively.

For the multiple-stage adaptation options, this thesis considers raising the crest level of the coastal defence up to 3.5 mAOD in two stages. The first stage raises the crest level of the coastal defence up to 3.0 mAOD and the next stage, if necessary, raises the crest level up to 3.5 mAOD in response to sea-level rise. If sea-level rise does not take an extreme path, the first investment will be left without a further upgrade. Another adaptation pathway is to raise the crest level to 4.0 mAOD in two or three stages. This adaptation path incurs a larger investment cost than the previous path up to the 3.5 mAOD because it requires additional measures or plans to meet the high standard of protection such as the wider base area of the coastal defence or the acquisition of the adjacent land. In this upgrade scheme, more flexible and diverse pathways are possible by transforming a single large investment into two- or more- stage sequential investments.

The possible sets of adaptation pathways are conceptualized in Figure 4.16. For simple expressions, this thesis denotes $U_{i\rightarrow j}$ to an adaptation measure of raising the crest of coastal defence from the initial height (i) to the upgraded height (j). For instance, upgrading coastal defence from the current level to 3.5 mAOD is expressed by $U_{c\rightarrow 3.5m}$ (Here, subscript c denotes the current state of the coastal defence). This terminology also represents a set of multiple-stage adaptation paths by putting terms together in a sequential order. For example,

a two-stage defence upgrade from the current level through 3.0 mAOD to 3.5 mAOD are denoted by $U_{c\to 3.0m} * U_{3.0m\to 3.5m}$. Thus, this representation for the single- or multiple- stage adaptation paths is used throughout this thesis.

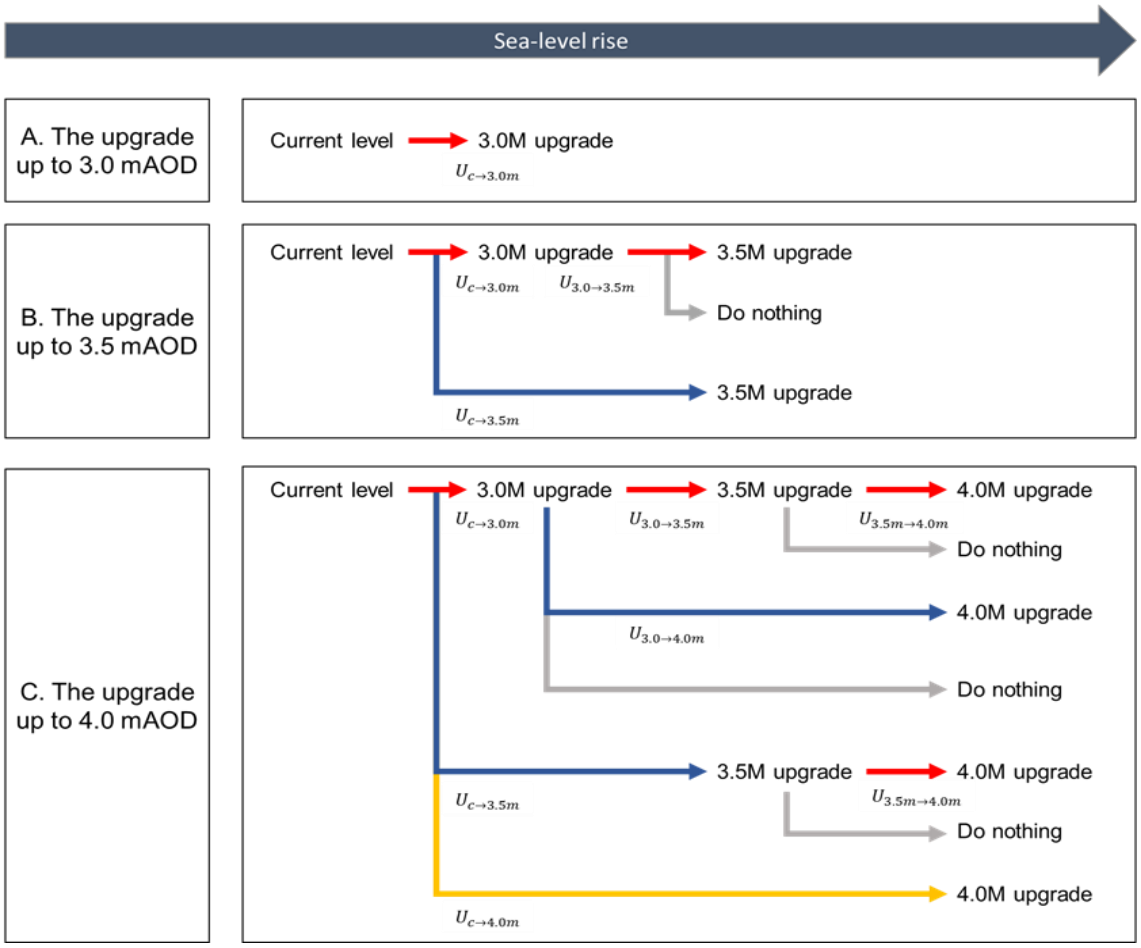

Figure 4.16 Illustration of possible options and pathways for the upgrade of the coastal defence up to (a) 3.5 mAOD and (b) 4.0 mAOD, respectively.

4.4.2 Analysis of investment costs for adaptation paths

The inclusion of the flexibility requires an additional expenditure to be paid in the design of coastal defence (Woodward et al., 2013; 2014). Widening the base of coastal defence for future extension is a good example as explained in Figure 2.4 (De Nufeville, 2003; Dobes, 2010). This study assumes that dividing a single-stage option into two or three phases of sequential options causes additional costs. The increased costs are also considered as variables that affect investment decisions on future extension. The increase in the overall cost

of an adaptation option is defined as a premium cost to be paid for flexibility in this thesis. The premium cost is required for the inclusion of flexibility in coastal defence adaptation. If not, the multiple stage adaptation option at no price of premium costs would be always a better option than the equivalent single-stage adaptation option. Thus, the payment of the premium cost enables decision-makers to have the right, not the obligation, either to upgrade the coastal defence or to drop the option in the future. In this respect, the premium cost conceptually corresponds to the price of a call or put option premium in financial markets.

In practice, the whole life costing is a very complicated process to analyse and identify all the relevant expenditures for the acquisition and use of an asset (EA, 2015). In order to estimate the whole life costs, all the processes from planning through construction to monitoring need to be thoroughly considered. The key element costs for upgrading coastal defence are (1) procurement and design costs; (2) capital construction costs; (3) operation and maintenance costs; (4) monitoring costs; and (5) replacement costs. As the acquisition of infrastructure in general takes many years, the estimated cost of constructing coastal defence varies with time depending on site contexts such as the varied nature of works required, site conditions and the costs, availability and source of materials (EA, 2015). Thus, the investment cost is also uncertain variable. In addition, including an intentional delay in construction work will add complexity to estimating costs due to the variability of the construction costs. In this regard, the premium cost should be practically and theoretically included in the process of transforming a single-stage adaptation option into multiple-stage adaptation options.

This thesis assumes that any flexibility to divide a single investment into multiple sequential investments increases the overall investment cost as shown in equation (15) and (16).

$$I_o = I_{o,1} + I_{o,2} \tag{15}$$

$$I_o + I_{premium} = I_1 + I_2 \tag{16}$$

$$I_1 = I_{o,1} + \frac{1}{2} I_{premium},\ I_2 = I_{o,2} + \frac{1}{2} I_{premium} \tag{17}$$

Here, I_o is the cost of an original option, $I_{o,1}$ and $I_{o,2}$ are the net capital costs of the first- and the second- phase options from the original option, respectively, $I_{premium}$ is an premium cost to be paid for flexibility (i.e. dividing the investment option), and I_1 and I_2 are the investment costs of the first- and the second- phase options, respectively.

The investment cost of an original option which raises the crest of coastal defence from the current level to 3.5 mAOD (i.e. $U_{c \to 3.5m}$) is £ 64 million (NFCD, 2010). Though the cost of

coastal defence upgrade for Lymington is not given with a great accuracy, it provides indicative information on how much resource or budget will be allocated to the planned adaptation measures for coastal areas. Thus, this indicative cost is used as a reference for the coastal adaptation measures in Lymington. The cost has also been compared by using the unit costs of dike heightening (per m rise per km length) in other countries; although the costs are site dependent (Hillen et al., 2010). Table 4.3 outlines the unit costs of coastal defence upgrade in different countries. These data help estimate the cost price of coastal defence upgrade at the level of project planning. The unit cost for Lymington is within the range of the unit cost for rural areas in Netherland. As the economy status and environment of both countries are similar, the estimated cost of coastal adaptation measures in Lymington has been accepted for the analysis.

Table 4.3 The unit costs of dike heightening by 1m per unit length (km) in different countries (unit: million £ / m / km) (Hillen et al., 2010) - The price is in 2009.

	Rural areas	Urban areas	Maintenance cost
Netherlands	3.56-9.57	12.23-19.14	0.09 per year
US (New Orleans)	4.59		
Vietnam	0.62-1.06		0.018 per year
IPCC (1990)	0.92	9.2	
Lymington	6.49*		

* The currency rate (1 € = 0.89 £) in 2019 is applied for calculation.

** The unit cost is calculated by dividing the whole cost (=64.2 M £) with the length of overall coastal defence (=9.87km)

In order to consider different heights of coastal defence upgrade, the cost of defence heightening (I) is assumed to have a linear relation to the raised height (H). This assumption follows the previous studies on relations between coastal defence heightening and estimate of costs for exemplary cases (Eijgenraam, 2006; Hillen et al., 2010; Jonkman et al., 2013). In practice, the costs of coastal adaptations are dependent on local circumstances. With sea-level rise, dike height, required nourishment volumes, base of the dike and required purchase of land linearly increase, whereas dike volume and the expected cost of moving buildings and objects behind exiting defence increase non-linearly (Hillen et al., 2010).

As reviewed previously, Lymington is a small village composed of rural and urban areas. In the rural area, most coastal defence system is made of embankment fronted with interlocking blocks while, in the populated area, the coastal defence is mainly masonry and concrete walls

which are small part of the coastline. Thus, this thesis assumes that the dike height and required purchase of land determine the adaptation costs for Lymington. This assumption allows us to conclude that the cost of defence heightening is proportional with raised defence height as shown in Table 4.4. In order to take into account the uncertainty of costs, this thesis sets out 20%, 30%, 40% and 50% premium cost scenarios. The investment cost for each adaptation path is summarised according to the different premium scenarios in Table 4.4. The calculation process of the investment costs for multiple adaptation options is explained in Appendix E.

Table 4.4 Investment costs for each adaptation path according to premium scenarios

Adaptation paths	Premiums	The 1st stage cost	The 2nd stage cost	The 3rd stage cost	The total investment cost
$U_{c\to3.0m}$	-	£ 32.1 M	-	-	£ 32.1 M
$U_{c\to3.5m}$	-	£ 64.2 M	-	-	£ 64.2 M
$U_{c\to4.0m}$	-	£ 96.3 M	-	-	£ 96.3 M
$U_{c\to3.0m}$ * $U_{3.0m\to3.5m}$	20%	£ 38.52 M	£ 38.52 M	-	£ 77.04 M
	30%	£ 41.73 M	£ 41.73 M	-	£ 83.46 M
	40%	£ 44.94 M	£ 44.94 M	-	£ 89.88 M
	50%	£ 48.16 M	£ 48.16 M	-	£ 96.33 M
$U_{c\to3.0m}$* $U_{3.0m\to4.0m}$	20%	£ 58.14 M	£ 58.14 M	-	£ 116.28 M
	30%	£ 62.98 M	£ 62.98 M	-	£ 125.97 M
	40%	£ 67.83 M	£ 67.83 M	-	£ 135.66 M
	50%	£ 72.68 M	£ 72.68 M	-	£ 145.35 M
$U_{c\to3.5m}$* $U_{3.5m\to4.0m}$	20%	£ 73.89 M	£ 41.79 M	-	£ 116.28 M
	30%	£ 78.74 M	£ 46.63 M	-	£ 125.97 M
	40%	£ 83.58 M	£ 51.48 M	-	£ 135.66 M
	50%	£ 88.42 M	£ 56.32 M	-	£ 145.35 M
$U_{c\to3.0m}$* $U_{3.0m\to3.5m}$* $U_{3.5m\to4.0m}$	20%	£ 58.14 M	£ 34.89 M	£ 34.89 M	£ 127.91 M
	30%	£ 62.98 M	£ 40.94 M	£ 40.94 M	£ 144.86 M
	40%	£ 67.83 M	£ 47.48 M	£ 47.48 M	£ 162.79 M
	50%	£ 72.68 M	£ 54.51 M	£ 54.51 M	£ 181.70 M

4. 5 Flood risk analysis

Flood risk analysis examines how the risk of coastal flooding changes over time under different sea-level rise scenarios with a focus on the relation between climatic variables (e.g. extreme still water level or sea-level rise) and risks, the latter being hereafter represented by expected monetized flood damages or expected annual damages. This analysis defines avoided risk as benefit from an adaptation option, following conventional flood risk assessments and studies (Grossi and Kunrether, 2005; Hall and Solomartine, 2008). The flood risk analysis in this thesis assumes that a certain magnitude of coastal event leads to a certain amount of flood damage. Coastal flooding is the consequence of the combining effects of storm surge events and astronomical tides (McMillian et al., 2011). The extents and damages of coastal flood events associated with the possible magnitude of climatic variables (i.e. ESWL+SLR+WAVE) are estimated, assuming for both the current and upgraded defences each year. Hence, this estimation provides a couple of damage curves and a benefit curve for an intervention measure (i.e. raising the crest level of coastal defence) over all the possible climatic variables. Based on that, we have statistically estimated the expected flood damages for both cases and the expected benefit from the intervention each year. This process has been conducted for each SLR scenario. The procedure is summarized in Figure 4.17.

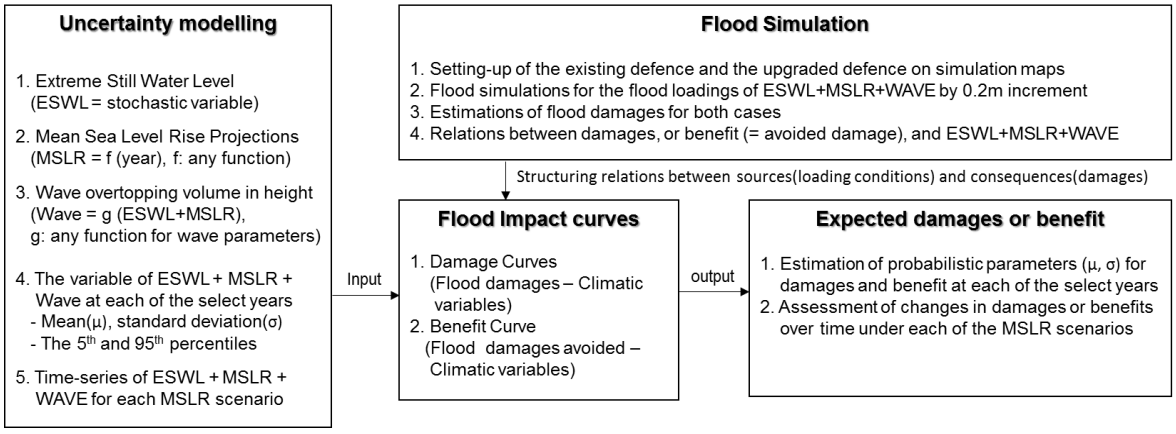

Figure 4.17 The framework of flood risk analysis for evaluating statistically expected monetised damages and benefits in sea-level rise.

4.5.1 Flood Inundation Modelling

A. Overviews of flood inundation modelling

A number of flood inundation simulations (15 times for each defence scenario) have been performed with various climatic variables (i.e. ESWL+MSLR+WAVE). This thesis

considers three different levels to which the coastal defence will be raised from the current level: (i) 3.0 mAOD, (ii) 3.5 mAOD and (iii) 4.0 mAOD. The physically possible flood loadings of ESWL+MSLR+WAVE are discretised in 0.2m increments from 1.2 to 4.0 mAOD. This covers all the range of coastal flood events that may occur due to sea-level rise through the 21st century in Lymington.

A pair of flood risks for the existing defence and the upgraded defence are assessed, assuming overflowing and overtopping defence failures, for the same magnitudes of coastal flood events, respectively. While flood risk analysis investigates hydrological relationships for given coastal defence conditions, the hydrological relationships between climatic variables (ESWL+SLR+ WAVE) and flood damages are assumed to be constant over time. Thus, coastal morpho-dynamics (generally erosion) is not considered within the framework of flood risk analysis established in this thesis. This simplification of flood risk analysis can be found in many other previous studies using a source-pathway-response-receptor (SPRR) concept for flood risk analysis (Evans et al., 2004; Narayan et al., 2012; Wadey et al., 2013).

Flood depths and extents need to be predicted from various combinations of forcing conditions (i.e. meteorological, tidal, and wave conditions) and defence conditions with a topographic given as (x, y, z) coordination. There are various numerical hydrodynamic models which help simulate coastal flooding at such a variety of conditions (Bates et al, 2005; Dawson et al., 2005). This thesis employs LISFLOOD-FP which is a simplified two-dimensional dynamic model using the continuation and momentum equations of free-surface water flow between grid cells (Dawson et al., 2005; De Almeida et al., 2012). As the thesis is aimed to evaluate coastal flood risk at the high levels of decision-making, LISFLOOD-FP is considered as an efficient model for flood simulation.

B. Hydrological setting of coastal defence conditions

Information on the location and height of the coastal defence has been obtained from a 1m resolution DEM data. The LIDAR data were produced by Environment Agency in 2008. The quality check of DEM data has been made in comparison to recent DEM data (in 2015). Little difference in DEM data has been found when comparing the heights of each cell between the DTM data in 2008 and in 2015. Field trips (the 24th of May on 2106 and the 3rd of March on 2017) had been conducted to supplement the defence information from the DEM data and any other documents. Defence types, shapes and materials were also investigated through the field trips.

These defence locations are overlaid on the 1m resolution DEM data – which include object information (e.g. buildings, agricultural lands, rails, roads, etc.) on the ground. The defence heights have been measured at each point spaced along the defence line on the DEM data. GIS software enables us to extract a raster value at every intersection of a defence line and a grid cell. Thus, the defence height data have relatively a high accuracy with RMSE $\pm$ 0.15m. The height for each segment of the coastal defences on the DEM map is determined by choosing an average height. The measured defence heights have been allocated to each segment of the defence lines in a GIS shapefile. These processed data on the coastal defence are included in relatively low-resolution DEM data that will be used for flood simulations.

C. Conditions of flood loadings and floodplains

The 10m and 50m resolution LIDAR data are used for flood simulations, respectively. The comparison of flood depths and damages from different resolution LIDAR sources has been made to investigate the sensitivity of model results to the sizes of grid cells. There is little difference in the model results between 10m and 50m resolution data because the low-lying areas affected by coastal flooding are relatively less populated areas. To simulate inundation from a coastal event associated with a peak water level, a loading condition needs to be defined on boundary cells in DEM data from which seawater inflows into floodplains. The raster cells intersected by the coastal defence lines in DEM data are set to be the boundary cells as shown in Figure 4.18.

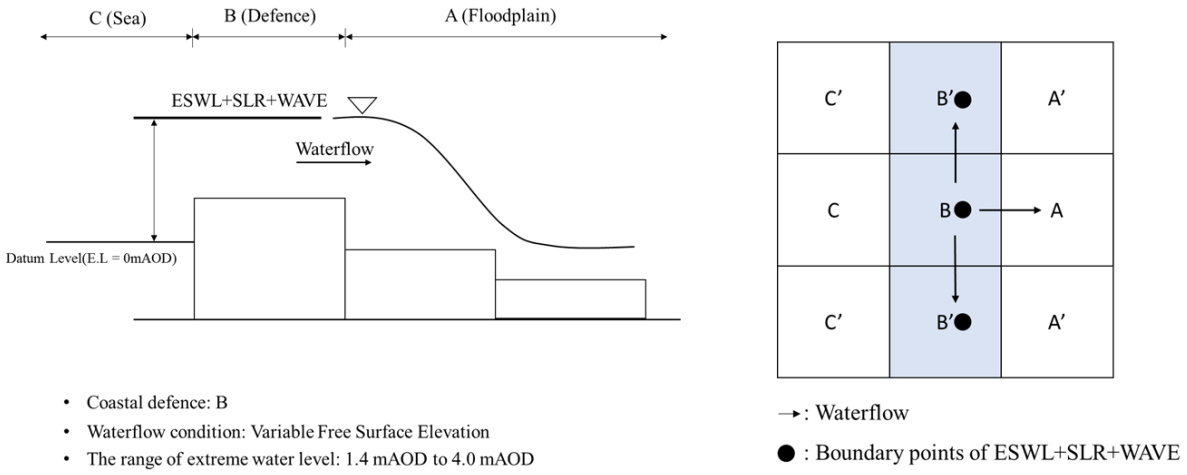

- Coastal defence: B
- Waterflow condition: Variable Free Surface Elevation
- The range of extreme water level: 1.4 mAOD to 4.0 mAOD

Figure 4.18 Boundary conditions for flood loading of ESWL+SLR+WAVE on the coastal defence

A series of time-varying water levels are applied as flood loading conditions on each cell of the coastal defence. This analysis assumes that the time-series of water levels from the 2008

coastal event are a typical sequence of water levels which is the most likely to have an effect on tidal floodplain in Lymington. The water level time-series during a flood event with a specific peak water level have been produced by offsetting the standardised time-series by the difference between the peak water levels of the 2008 event and the considered flood event (Figure 4.19).

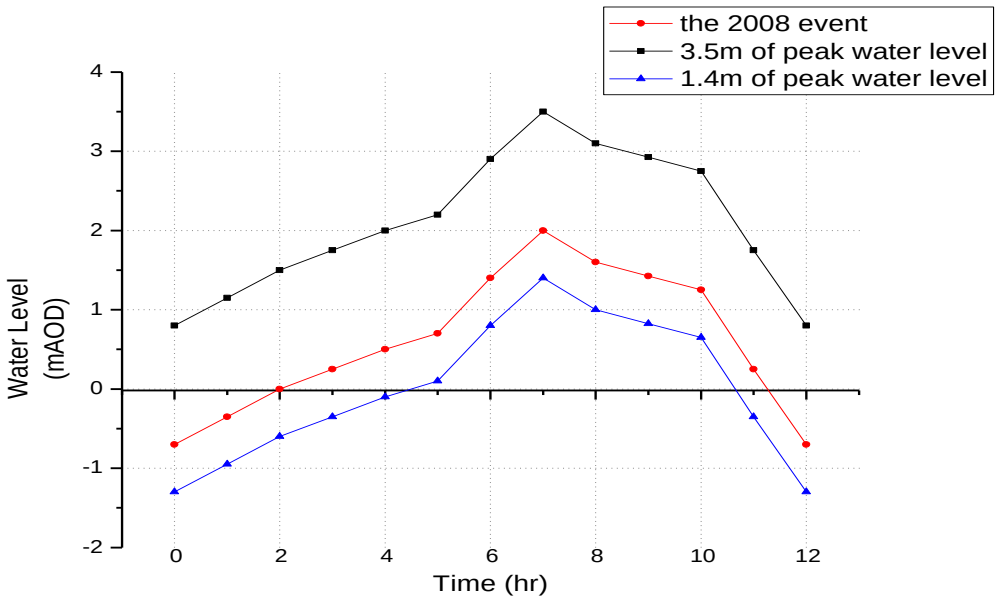

Figure 4.19 The standardised water level time-series on an hourly basis from the 2008 event (peak water level = 2.0 mAOD) and the water level time-series of simulated coastal events associated with peak water levels (e.g. 3.5 and 1.4 mAOD)

The flood inundation also considers spatial variations in peak water levels to simulate a statistically uniform event with the same return period. The magnitude of peak water level for each tidal zone shows a 0.09m increase at each move along data points from P1 to P4. The time-series of water levels within each tidal zone are uniformly applied as a flood loading condition (Figure 4.20). The water level time-series for each tidal zone have been coded as each flood loading condition in flood simulation programme (i.e. LISFLOOD-FP).

A uniform representative *n* value has been used for the 50m resolution DEM data. This value is an averaged *n* value by the estimation of surface roughness for Lymington. The study site is a rural area most of which is covered by pasture and agricultural lands. Residential and commercial areas are located at each side of the entire floodplain. Thus, the flood simulation adopts a uniform value of $n = 0.035$ which is averaged for flood simulations in the 50 m resolution DEM data.

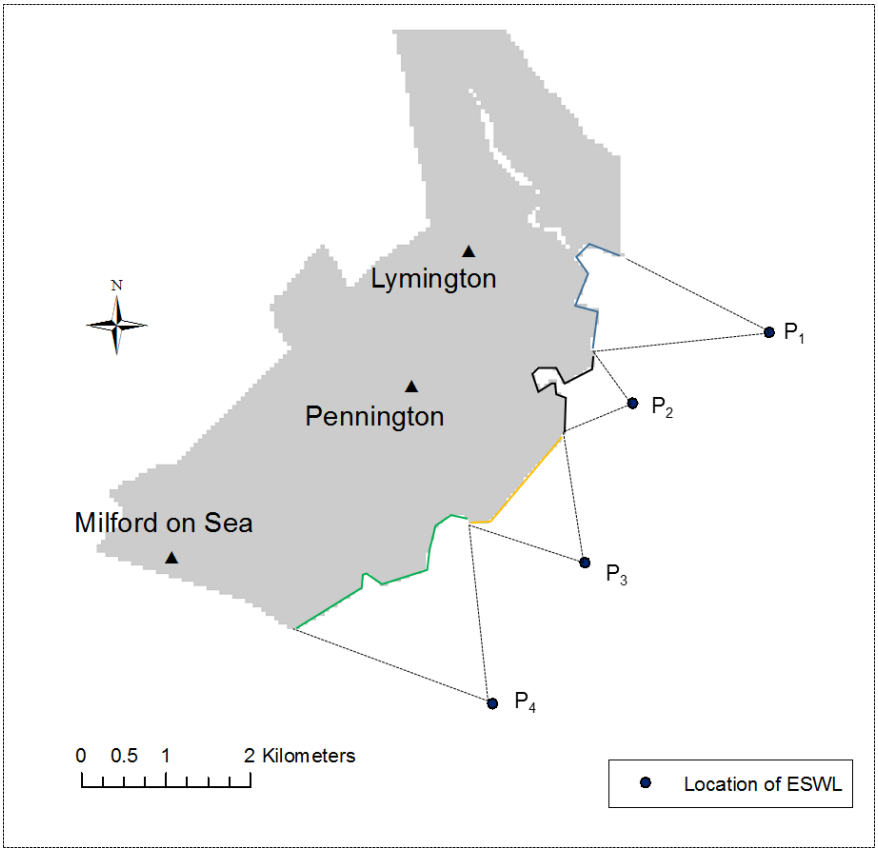

Figure 4.20 The sections of tide zones for flood loadings of extreme still water levels around Lymington

On the contrary, the flood risk analysis in 10m resolution modelling makes the use of spatially-distributed Manning coefficients which are observed on the OS land-use map of Lymington. The floodplain has been divided into sub-regions according to the land use on the OS map. The appropriate *n* values are allocated to each sub-region according to the classification of *n* values provided by the LISFLOOD-FP manual (Bates et al., 2008) as shown in Appendix F.

D. Flood simulations with different flood defences

The flood simulations have been conducted at various flood loading conditions for each defence condition. The examples of overlaying flood extents upon objects from the topography data are shown in Figure 4.21. As a result, LISFLOOD-based flood simulation generates the raster values of maximum flood depths in all the grid cells of DEM for each loading condition and each defence condition. To investigate the stability of model results by LISFLOOD-FP, Q-errors that indicate volume error per unit time (m^3s^{-1}) during a simulation have also been checked after each simulation. The values of Q-error for most simulations have been observed within the acceptable level (e.g. $1\sim2 \times10^{-14}$ to 10^{-11} m^3s^{-1}).

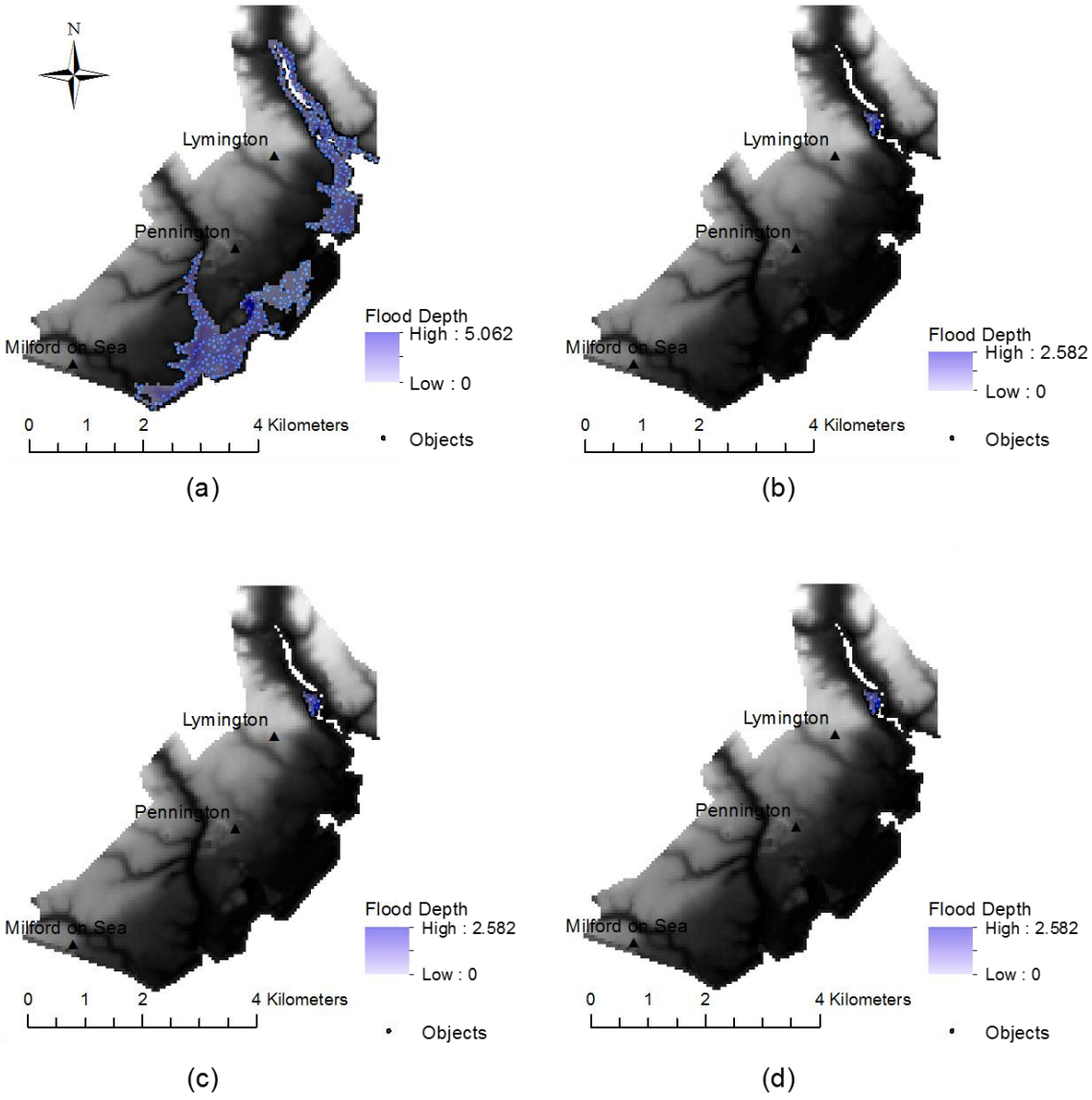

Figure 4.21 Flood extents at a 1-in-200 year coastal flooding associated with a peak water level of 2.41mAOD for (a) the current coastal defence; (b) the 3.0 mAOD upgraded defence; (c) the 3.5 mAOD upgraded defence; and (d) the 4.0 mAOD upgraded defence.

The raster value of flood depth in each cell is overlaid on topography data which contains information on buildings, lands, roads and natural objects from Ordnance Survey (OS, 2015). All the objects in a topography map have been transformed from polygon vectors to point vectors by Arc-GIS programme to ensure all the objects have their own (*x, y*) coordinates in British National coordination system. Arc-GIS helps extract a raster value of flood depth at each object within a flooded area. Table 4.5 and Figure 4.22 show flood damages (i.e. the number of flooded properties) across flood loadings (i.e. ESWL+SLR+WAVE) for each

defence condition. The results of the flood risk analysis into Lymington are attached for different defence conditions in Appendix G.

Table 4.5 The number of inundated properties by various water levels for each defence condition

Water levels (mAOD)	The current defence	3.0 mAOD upgraded defence	3.5 mAOD upgraded defence	4.0 mAOD upgraded defence
1.2	0	0	0	0
1.4	0	0	0	0
1.6	0	0	0	0
1.8	4	0	0	0
2	20	9	9	9
2.2	130	22	22	22
2.4	179	22	22	22
2.6	216	24	24	24
2.8	304	24	24	24
3	416	35	35	35
3.2	508	208	38	38
3.4	631	429	41	41
3.6	715	661	128	44
3.8	797	759	399	73
4	846	846	701	79

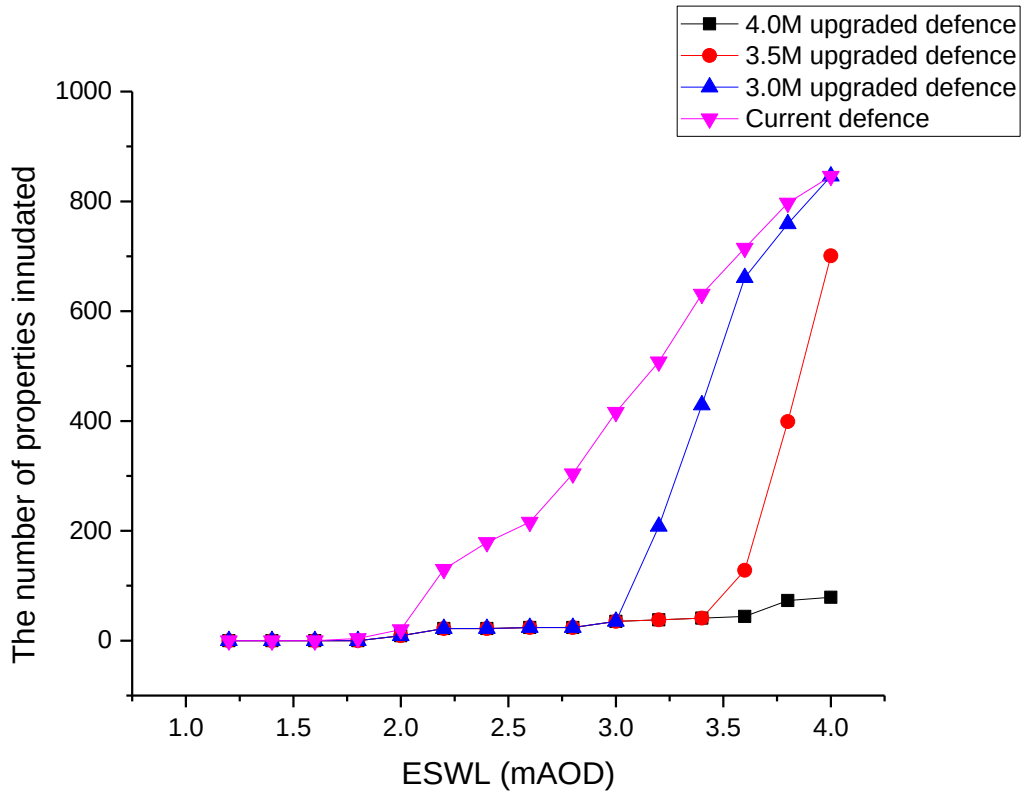

Figure 4.22 The number of properties inundated by peak water levels from 1.2 to 4.0 mAOD according to each defence condition in Lymington

E. Validation of flood simulation models

In general, a model is acknowledged to be validated if its accuracy and prediction proves to be within an acceptable level. The reliability of the results of flood damages by LISFLOOD-FP depends on the quality of input datasets, key topographic features and interference from other flood sources (i.e. compound flooding) (Bate at al., 2005; De Almeida et al., 2012). Inherently, model results have uncertainty due to the lack of our ability to describe physical dynamics or systems in the real world. In this regard, the validation of the model results in this thesis is limited because the flood simulations have been conducted with unprecedented high extreme water levels. For Lymington, the most severe flood water level on record was 2.14 mAOD which had been observed in the 2008 flood event. In addition, the flood damages are simulated with the coastal defences ideally set on DEM. Thus, the predicted flood damages and extents from this thesis inevitably include uncertainty.

In order to test the validity of the model, a fit measure has been used to see an agreement between predicted and observed flood extents (Bates et al., 2005; Gallien et al., 2011). A fit measure is determined by the intersections and unions of observed (E_o) and predicted (E_p) pixels as shown by equation (18). A full agreement gives a value of 1 while no agreement does a value of zero. To see whether the flood simulation model is within an acceptable level (i.e. $F_A > 0.75$), the thesis compares the model results by LISFLOOD-FP with the result by Environment Agency (Refer to Figure 4.23).

$$F_A = \frac{E_0 \cap E_p}{E_o \cup E_p} \tag{18}$$

The flood risk zone 3 which indicates an area at the 1-in-200 risk of coastal flooding is overlaid on DEM dataset for comparison of the simulated results. The flood risk zone 3 by EA covers a larger area than the inundated area simulated with a coastal flooding associated with 2.41 mAOD by this thesis as shown in Figure 4.23.

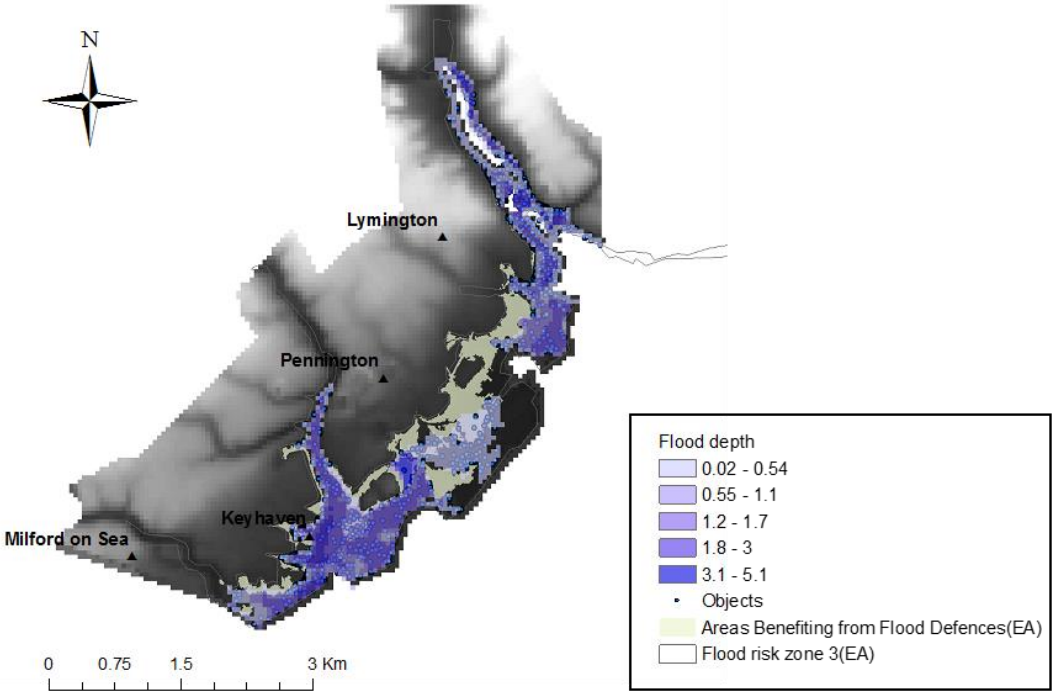

Figure 4.23 Comparison between the EA flood risk zone and the simulated zone in a 1-in-200 year coastal flooding associated with a peak water level of 2.41 mAOD.

This is because the flood risk zone by EA is the estimate of areas at the risk of 1-in-100 year fluvial flooding and 1-in-200 year coastal flooding with the current coastal defence removed in the simulation. As the flood simulation by this thesis has been conducted with the current defence system, the flooded areas by 1-in-200 year coastal flooding becomes smaller than the EA flood risk zone. Nevertheless, when beneficiary zones due to the current coastal defence are removed from the flood risk zone 3, the rest area corresponds with the flooded zone by this thesis with a fit measure of 0.85. Thus, the DEM-based flood simulation model seems to provide the reliable results of flood simulation for Lymington.

The DEM data and boundary flood loading conditions are also validated by comparing the result of the flood simulation with that by Wadey (2012) in the number of inundated properties as shown in Figure 4.24. Wadey (2012) analysed flood damages across various loading conditions ranging from 1.5 mAOD to 3.0 mAOD in different failure modes: (1) full breaching scenario; (2) max wave scenario; and (3) no wave scenario. The flood damage curve by this thesis is compared with that of no wave scenario by Wadey (2012).

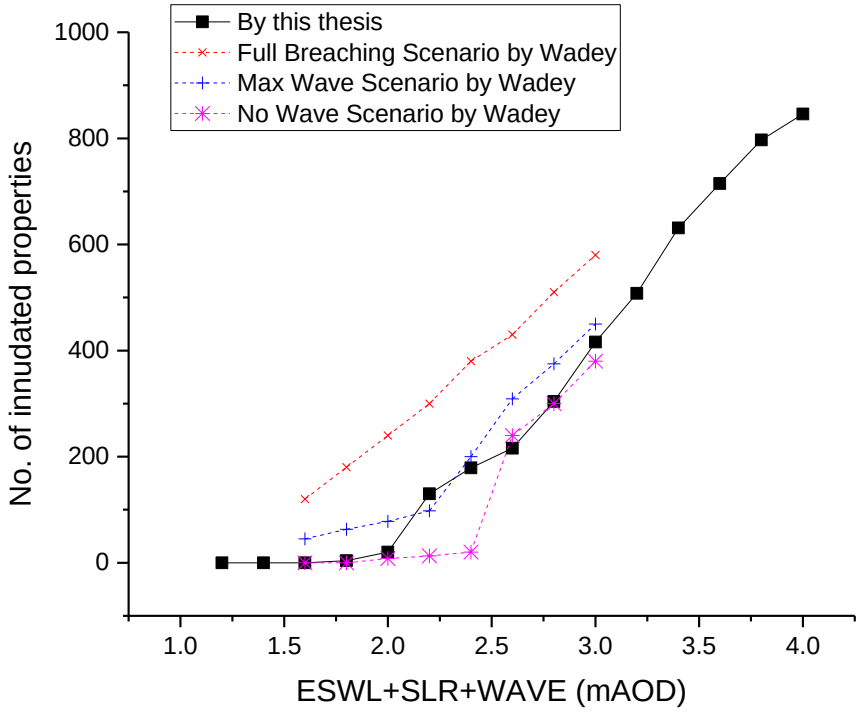

Figure 4.24 Comparisons of the number of inundated properties between the flood simulations by this thesis and the previous research (Wadey et al., 2012)

As seen in Figure 4.24, in a range of ESWL+SLR+ WAVE from 1.6 mAOD to 2.0 mAOD, two flood damage curves show an agreement in the number of inundated properties. However, from 2.0 mAOD to 2.6 mAOD, they show much difference of 120 to 150 in number. This is because this thesis sets defence height in some parts of Lymington equal to 2.0 mAOD. Thus, a significant increase in the number of inundated properties starts to occur from 2.0 mAOD. From 2.6 mAOD afterward, two curves show a fair agreement again.

Overall, the model result shows a fair agreement with that of Wadey et al.(2012); although little difference between both studies is found in a certain range of water levels. However, it should be acknowledged that the model result has a large uncertainty, particular, in the range of high water levels (2.4 to 4.0 mAOD) that Lymington has never experienced but are likely to occur in the future due to sea-level rise. The uncertainty from the flood simulation model is attributable to the imperfection of describing physical or hydrological dynamics for Lymington. Thus, the model uncertainty should be addressed by different approaches such as improving skills and computational techniques. The effect of the uncertainty from the flood simulation model on the results of real options analysis will be investigated with comparisons to the uncertainty of sea-level rise later in chapter 5.

4.5.2 Monetisation process of flood damages

The number of inundated properties and the flood depth of each property have been determined in each flood simulation. Based on property information provided by Ordnance Survey (UK), flood damages for each coastal flood event have been monetised to quantify the risk of the coastal flood event. The monetisation process follows the guideline provided by Environment Agency (2010) and Penning-Rowsell et al. (2010; 2014).

For the estimation of flood risk, this thesis takes several steps to convert flood extents and depths to economic losses. Firstly, the economic loss of each property within a flooded area has been estimated by a flood depth-damage curve for a property provided by Penning-Roswell et al. (2014). Secondly, all the flood damages for the inundated properties are aggregated for each coastal defence condition and for each flood loading. The next step estimates difference in flood damages between the existing and upgraded defence conditions at each flood loading, which is reduction in flood damage by a flood defence upgrade. Lastly, this process has been iterated with 0.2m increments of flood loadings, providing monetised damage and benefit curves across all the flood loadings from 1.2 to 4.0 mAOD.

A. Conversion of flood depth to flood damage in currency

If a property is inundated by a coastal event, the flood event will depreciate the property value with recovery costs incurred. The economic losses also depend on flood depth to which the property is inundated. Multi-Coloured Manual (MCM), which is a commonly used guidance for flood risk analysis in the UK (Penning-Rowsell et al., 2010; 2014), provides a unique relation between damages (£) and flood depths (m) in a property in England and Wales. The MCM defines four types of properties - detached, semi-detached, terraced houses and flat in England and Wales. Since the OS map does not provide specific information on house types, it is not possible to define all the house types of flooded properties at the spatial scale of the flood simulation. This analysis, instead, takes the averaged value of the economic losses from all the types of properties at each flood depth. A relationship between the averaged economic losses and the flood depths is plotted as a single square root curve in Figure 4.25.

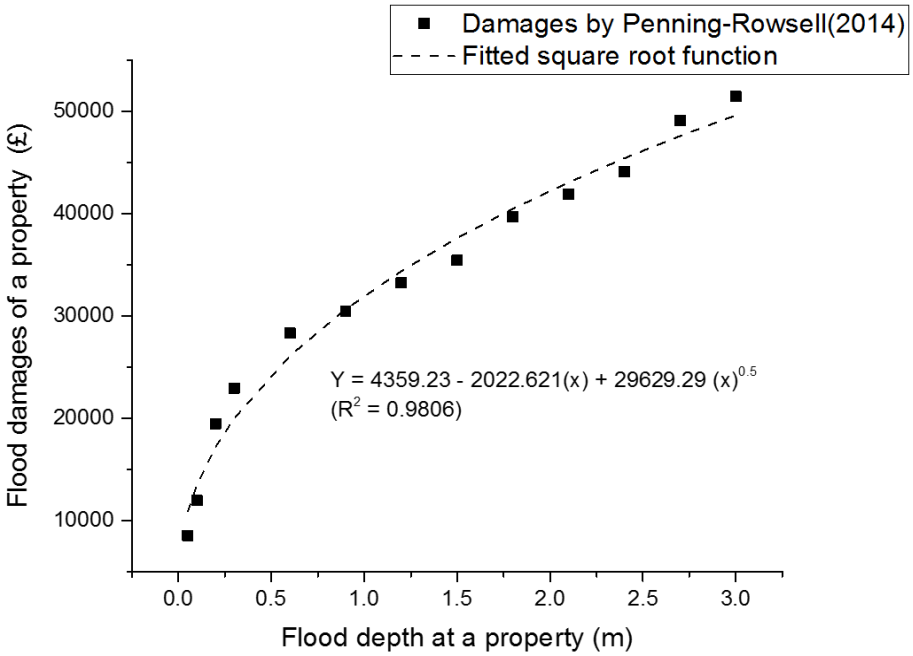

Figure 4.25 Flood damages or economic losses (£) by different flood depths for an inundated property in England and Wales (in 2016 prices)

The economic loss (£) is represented by a square root function of flood depth. This fitted function helps convert a flood depth of each property to a flood damage in currency. All the flood damages of inundated properties are aggregated for each extreme water level discretised with a 0.2m interval. This iterative calculation provides a relation between peak water levels and flood damages for a given coastal defence condition. All the flood damages are monetised in 2016 price. Figure 4.26 show relationships between flood events associated with peak water levels (i.e. ESWL+SLR+WAVE) and flood damages for each defence condition. Each relationship, hereafter called a flood damage curve, represents the response of the floodplain with the current coastal defence or the upgraded coastal defence to various amounts of coastal flooding.

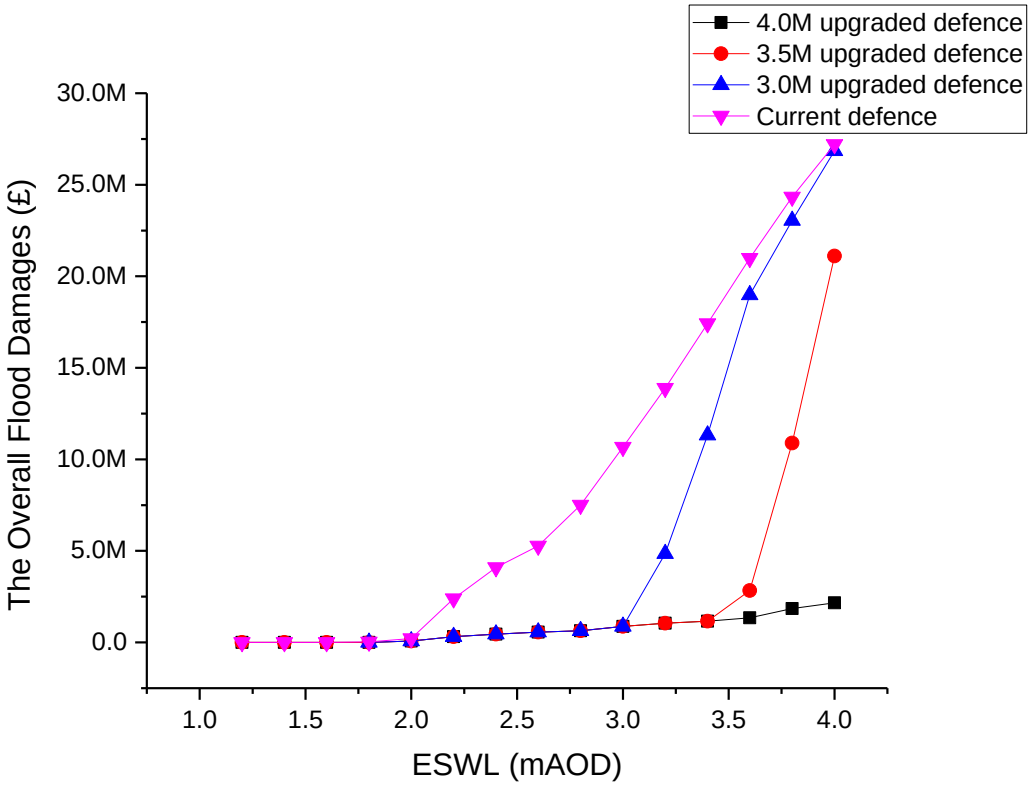

Figure 4.26 The overall flood damages by peak water levels according to different defence conditions in Lymington

B. Flood risk and expected annual damages (EAD)

Flood risk for any year is represented by expected annual damage (EAD) which is a statistical expectation of flood damage per a year in economic terms (Hall and Solomatine, 2008). This is estimated by integrating all the possible flood damages in respect to the corresponding probabilities. The probability distribution of flood damages, or benefits due to an adaptation measure, is assumed to coincide with the probability distribution of the corresponding flood loadings (i.e. ESWL+SLR+WAVE) by the damage- or benefit- flood loading relation, respectively. This enables us to estimate expected annual damages (EAD) and expected annual benefits (EAB) for different defence conditions during the period of sea-level rise.

The flood damages are represented with a function of peak water levels which is made by fitting multiple linear lines to each damage curve (Refer to Appendix H). The multi-linear functions allow us to express each damage curve as a function of peak water levels in different interval ranges at a high accuracy (R^2 = 0.99). Thus, the flood damage for each

defence condition can be represented by a function of peak water levels (i.e. ESWL+SLR+ WAVE) as shown in equation (19).

$$D_d = f_d(x) \quad (19)$$

Here, D_d is a flood damage at a certain magnitude of peak water level under a given defence condition, subscribed by *d* (e.g. the current defence, 3.5m upgrade defence, etc.), f_d is any function defining a relation between peak water levels and flood damages, and x is climatic variable of extreme still water level, sea-level rise and wave (i.e. ESWL+SLR+WAVE). As all the componential variables in climatic variable *x* are random variables, the flood damages represented by equation (19) are also random variables. The function for each defence condition is shown in Appendix H.

The flood damage function ($f_d(x)$) for each defence condition is used to convert the probability distribution of ESWL+SLR+ WAVE into the probability distribution of flood damages at any year. This Monte-Carlo simulation-based approach has been conducted for 2008 (the reference year of the probability of ESWL) and every 20 years from 2020 to 2100 in all the SLR scenarios. This thesis has modelled changes in flood damages by MSLR and the Brownian motion of SLR, respectively, as shown in Figure 4.27. The estimates of mean and standard deviation (μ, σ) of flood damages for the selected years by other SLR scenarios are shown in Appendix I.

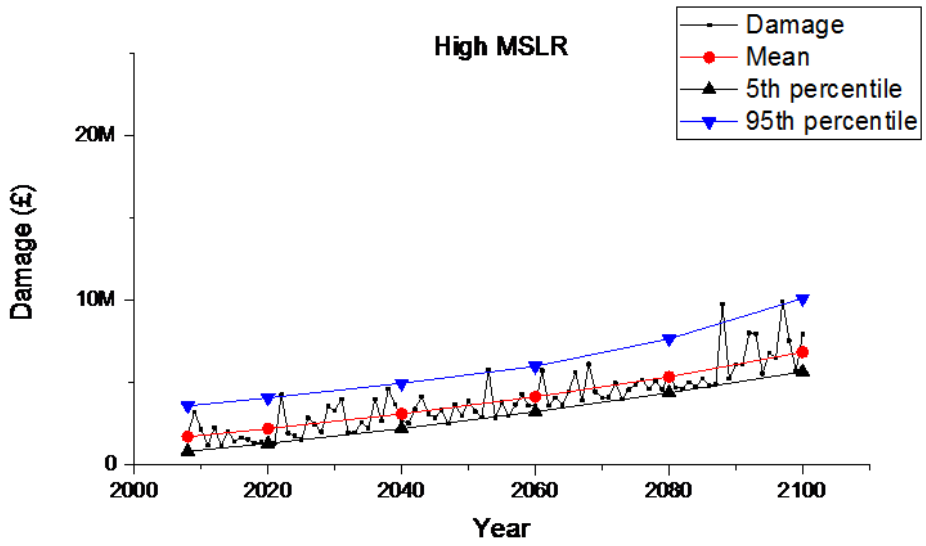

(continue)

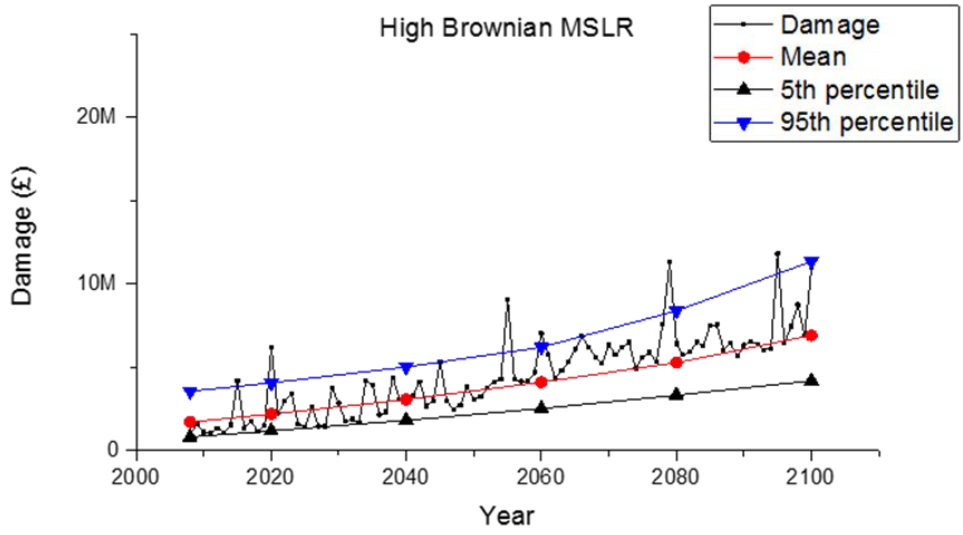

Figure 4.27 Temporal changes in flood damages under the current flood defence (a) in the High MSLR scenario and (b) the High Brownian SLR scenario – Note that the time-series of flood damages are randomly generated annual maxima.

The graphs in Figures 4.27 show the possible risk profiles of coastal flooding during sea-level rise by combining storm surge events, astronomical tides and sea-level rise. These graphs show temporal changes in the mean (red line) and probabilistic range (bounded by blue and black lines) of flood damages under the High SLR scenario by MSLR and Brownian SLR, respectively. This representation of annual flood damages has important implications in addressing flood risk assessment issues.

Firstly, the random time-series of flood damages for the current coastal flood defence have been quantified based on the current projections of future sea-level rise and the extremity of coastal flooding (i.e. extreme still water level and wave). Thus, the annual flood risk (EAD) reflects all the stochastic properties of factors which have effects on flood damage at a given year. Secondly, the mean value of flood damage at a given year implies the most likely value of flood damage at the year. Thus, the mean value of flood damage represents expected annual damage (EAD) in a given year. Lastly, we have also found that there is little difference in EAD between the cases of MSLR and Brownian SLR. This implies that difference in the uncertainty range of sea-level rise projection from UKCP 09 has no effect on the evaluation of flood risks. However, the flood damages from MSLR yield relatively narrower probabilistic ranges than those from the Brownian SLR.

C. Flood reduction and expected annual benefit (EAB)

The selection of a pair of damage curves provides a unique relation as the performance of an adaptation measure to a wide range of flood loadings as shown in Figure 4.28 (See Appendix J for the other adaptation measures)

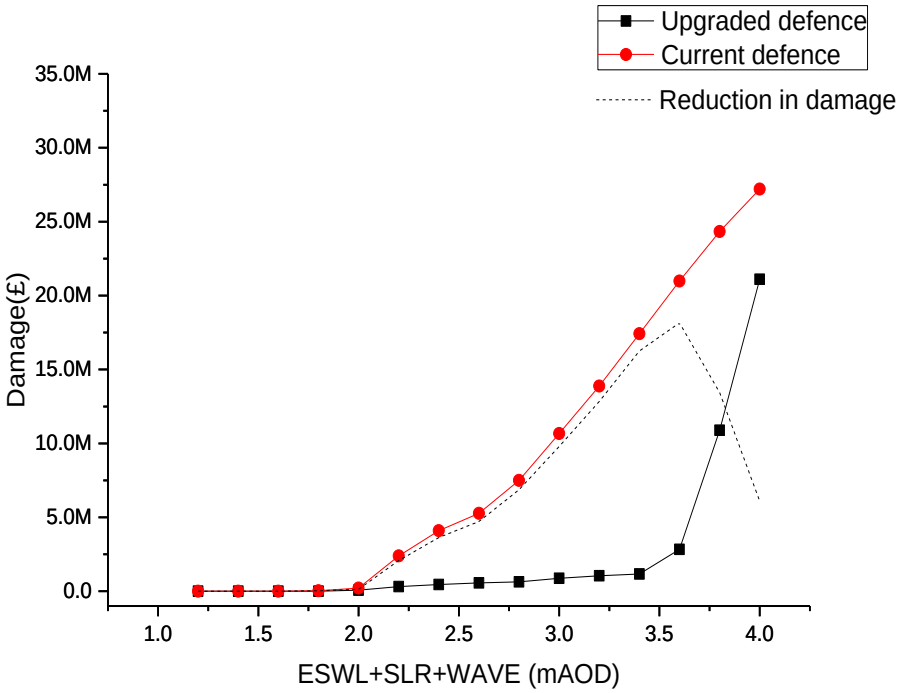

Figure 4.28 Monetised flood damages and reduction in the monetised flood damages (£ in 2016).

The benefit from the upgrade of the coastal defence at any year is also random variable dependant on the loading conditions of ESWL+SLR+WAVE. As seen in Figure 4.28, the benefit from an adaptation option has discontinuity with climatic variable at extremely high water levels. In other words, the flood damage reduction effect declines beyond a certain water level. This is because of the capacity of the adaptation option. In this regard, for the estimation of expected annual benefits (EAB), we also adopt a Monte-Carlo simulation to sample a large number of variables of ESWL+SLR+ WAVE from a predefined probability distribution at a given year into the benefit relation. This helps construct a new probability distribution of benefit values for a given intervention measure (i.e. the upgrade of coastal defence). The examples of change in EAB (i.e. mean) and its probabilistic range (i.e. 5th and 95th percentiles) over time are shown for an adaptation measure ($U_{c\rightarrow 3.5m}$) in the cases of High MSLR and Brownian SLR, respectively (Figure 4.29). The temporal changes in EAB for other adaptation measures by different SLR scenarios are shown in Appendix K.

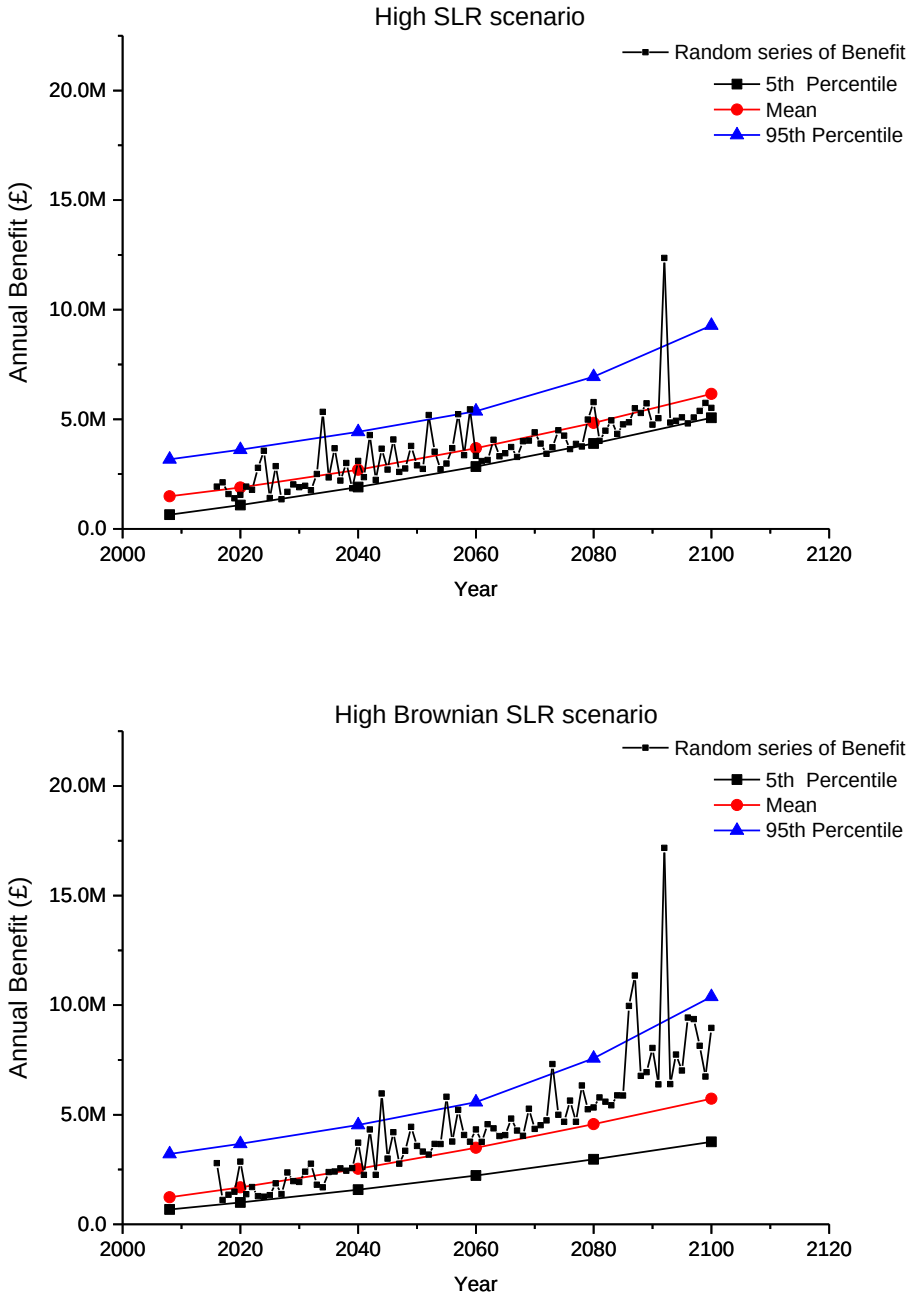

Figure 4.29 Changes in benefit from the upgrade of coastal defence (the current level → 3.5 mAOD) and its probabilistic range under each MSLR scenario

As sea level rises, the benefit from the upgrade of coastal defence increases. As the rising sea level increases the likelihood of flood damages in the floodplain, it leads to increase in the utility of the upgraded coastal defence. The mean values (red line) plotted in Figure 4.29 describe the statistical expectation of benefit values (i.e. EAB) from the present perspective. As the future value is uncertain and random, EAB has to be estimated upon the statistical expectation towards the future. Likewise, a real option decision either to invest, or wait, at

any year should be based on the statistical expectation of the benefit values in the future. If the investment decision is made with the expectation of a high impact, but low probability, event or past flood events which occurred at any year, the decision will always lead to immediate investment in an adaptation option at any occasion.

As shown in Figure 4.29, the trajectories of the 5^{th} and 95^{th} percentiles allow us to visualise how random benefit values occur with a certain probability (i.e. 90%). This illustrates that, although the extreme events out of the 95^{th} percentile line are plausible in Lymington during the 21^{st} century, EAB due to the adaptation measure changes smoothly. This also implies that our statistical estimation of the expected values or expected flood damages that may occur in the future change smoothly under the non-stationarity of climatic variables, even if we observe a disastrous flood event that has a harmful effect on human environments. Thus, the estimation of EAB provides an economically rational basis upon which to assess real options and to make a real option decision.

4. 6 Option evaluation

The real option evaluation is a process that assesses the performance of the upgraded coastal defence including flexibility under various sea-level rise scenarios. This section addresses several aspects in applying real options analysis into flood risk management. Firstly, the real options analysis in this thesis employs a dynamic programming approach (Bellman, 1953) which is designed to numerically compare the values of wait and investment for an adaptation option at all the years. This approach will be adapted to the case of coastal defence adaptation. Secondly, this section considers different boundary conditions at the end of sea-level rise projection from which the option evaluation starts backwardly. Lastly, this part accounts for discount rates and socio-economic development scenarios in regard to real options analysis.

4.6.1 Bellman's Dynamic Programming: continuation and termination values

This thesis takes a Bellman's dynamic programming approach to evaluating real options in climate change adaptation. As long as we can defer an option, a choice, either to invest or to defer, remains alive. Thus, the Bellman's approach assesses two option values at a given time: (1) a continuation value, which is an option value when the option is deferred, and (2) a termination value, which is an option value when the option is implemented. The real option

value in any given year *t* can be defined by equation (20) (Bellman, 1952; Dixit and Pindyck, 1994).

$$F_t = max\left[F_{con,t}, F_{ex,t}\right] \tag{20}$$

Here, $F_{con,t}$ is a continuation value in year *t*, $F_{ex,t}$ is a termination value in year *t* and F_t is an option value in the year *t*, which is the higher one of the two values at the year. If a continuation value ($F_{con,t}$) is higher than a termination value ($F_{ex,t}$) at a given year, it suggests waiting is preferable to implementation and vice versa (Bellman, 1952). The termination value ($F_{ex,t}$) at any year *t* is the net present value of the investment made at year *t*:

$$F_{ex,t} = \sum_{i=t+1}^{L+t} \frac{EAB_i}{(1+r)^i} - \frac{I}{(1+r)^t} \tag{21}$$

Where, EAB_i is the expected annual benefit of a project at year *i*

$$EAB_i = \sum_{m=1}^{M} p_i(x_{m,i}) \times B(x_{m,i}) \tag{22}$$

r is a discount rate, *I* is investment cost, and *L* is the number of project years, p_i is the probability density function at the year *i*, *B* is a benefit function of climatic variable $x_{m,i}$ representing a benefit curve (i.e. reduction in flood damages associated with the *m*th event), $x_{m,i}$ is the *m*-th event of climatic variable (i.e. ESWL+MSLR+WAVE) at year *i*, *M* is the number of discrete events adopted to describe the distribution of probabilty of coastal events.

On the other hand, when the investment is deferred from year *t* to year *t*+1, a continuation value ($F_{con,t+1}$) and a termination value ($F_{ex,t+1}$) at the year *t*+1 are values the option holder can expect from the year *t* by waiting for one year longer. The continuation value at year *t* is the higher one of these two values discounted from year *t*+1 to year *t* in equation (23).

$$F_{con,t} = \frac{1}{(1+r)} \times Max\left[F_{ex,t+1}, F_{con,t+1}\right] \tag{23}$$

This option evaluation process provides two decision criteria. Firstly, the overall benefits (B) during the project life (L) should be higher than the overall costs (C). The second one concerns investment timing for which the termination and continuation values are compared every year. The calculation of the continuation and termination values starts from the end of the period of wait (denoted by *T*) using a backward induction method (Bellman, 1952; Dixit and Pindyck, 1994; Yang and Blyth, 2007). Figure 4.30 illustrates an option evaluation process by the backward induction method.

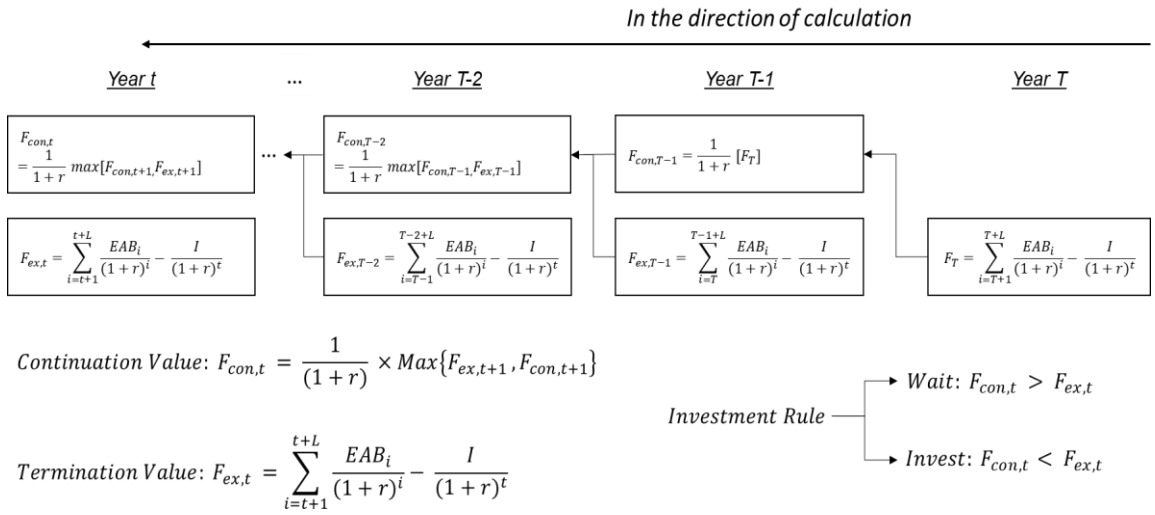

Figure 4.30 The concept and process of real options valuation based on dynamic programming (Bellman, 1952)

4.6.2 Boundary values for option evaluations

The backward induction method requires a boundary value at the end of the time horizon for option evaluation (Dixit and Pindyck, 1994; Yang and Blyth, 2007). The end year is set to be 2100, consistent with the period of the SLR scenario from UKCP 09. The boundary value is an option value when the investment is made at 2100 on the assumption that the investment can be deferred to 2100 by the option holder. To obtain the boundary value for each SLR scenario, the analysis has extrapolated sea-level rise from 2101 to 2200, following the rate of sea-level rise from the last 10-year data from 2090 to 2100. This thesis assumes three post-2100 sea-level rise scenarios for a sensitivity purpose: (1) linearly increasing trend, (2) accelerating trend, or (3) no change as shown in Figure 4.31. The effects of the post-2100 sea-level rise on option values will be investigated later in chapter 5.

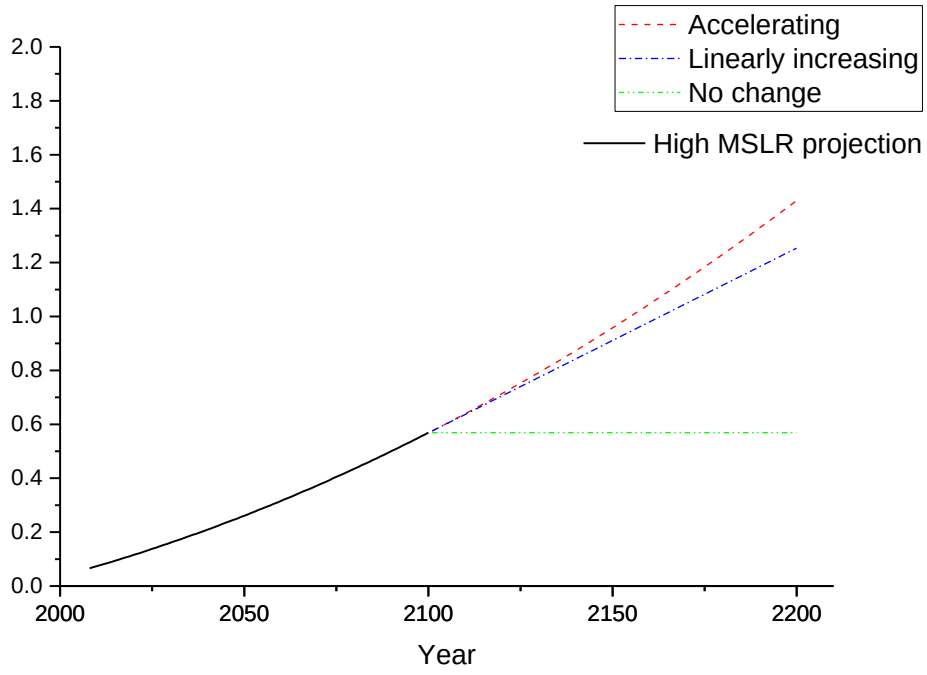

Figure 4.31 Post-2100 SLR projections based on the MSLR projection from 2008 to 2100

4.6.3 Discount rates for option evaluations

A discount rate indicates a social preference of time (Tol, 2003; Hunt and Tailor, 2009). It is a socially-agreed value by compromising the values of the future and the present (ibid.). If the present value is more important than the future value, a high discount rate is chosen for option evaluation. Otherwise, a low discount rate is used. The discount rates differ depending on the economic status of countries and the culture of societies (Adger et al., 2009). South Korea uses 5.5% discount rate, while most European countries including UK use 3.5% discount rate. This research applies the Green Book discount rates for option evaluation which are commonly used in project appraisal in the UK. It is a reasonable choice because Lymington is located in the UK.

The Green Book applies different discount rates depending on the period of time (HM Treasury, 2003). It uses 3.5% for the first 30 years, 3.0 % for the next 45 years and 2.5% afterwards for discount rates. As these discount rates are legally compulsory instruction for project appraisals in the UK and most climate change adaptation needs government funds, this research also uses these rates for option evaluation. However, note that there are various arguments for discount rates in the realm of climate change research (Maddison, 1996; Tol and Yohe, 2006; Stern, 2007; Weitzman, 2007; Mendelsohn, 2011). For instance, Stern

(2007) argues that a low discount rate (e.g. 1.4%) should be used to less discount the harmful effects of greenhouse gas emissions on the future generations and the costs of reductions in the greenhouse gas emissions in the economic analysis of climate change, while others (Tol and Yohe, 2006) argue that such a low discount rate provides the over-estimation of adaptation or mitigation actions. Despite such debates, this thesis seeks to avoid the social debates over the selection of proper discount rates for climate change adaptations. Instead, this thesis adopts standard discount rates (i.e. Green Book discount rates) for option evaluation. For the purpose of sensitivity, this research also investigates the effects of discount rates on the results of real options analysis.

4.6.4 Socio-economic scenarios for option evaluations

As climate change occurs over many decades or centuries, such a long timescale needs to consider changes in socio-economic factors such as property developments and population growth (Dawson et al., 2015). This thesis also takes into account those factors by using future growth rates. To apply the future growth rates in Lymington, this thesis assumes that the number of properties changes at constant rates over time. The socio-economic change scenarios in this thesis adopt (-) 0.5%, 0%, 1% and 2% annual growth (or decline) rates to represent changes in property developments or populations in Lymington. Different future growth rates are related to socio-economic development scenarios of how people in Lymington respond to flood risk and sea-level rise as outlined in Table 4.6.

Table 4.6 Socio-economic development scenarios according to future growth rates

Future growth rates	Socio-economic scenarios	Details
-0.5%	Shrink in the use of coastal area	People are concerned about coastal flooding due to sea-level rise. The floodplains are designated as flood risk zone by EA. They will decide to leave the coastal area vulnerable to coastal flooding. Thus, the number and value of properties in flood risk areas will decline with time
0%	Stay in the current status	People are also worried about coastal flooding due to sea-level rise. However, there is no plan to leave the flood risk area. Property owners still believe that they can endure coastal flooding. Those who are willing to develop properties in coastal area will avoid this flood risk zone for property development. Thus, the number of properties in the floodplain keeps constant.

Future growth rates	Socio-economic scenarios	Details
1%	Moderate development	People are less worried about coastal flooding and sea-level rise. People believe that coastal flooding will be reduced by technologies and adaptation measures. There is still desire to own properties in coastal areas. Development pressures are moderate
2%	Vigorous development	People are very keen to develop properties in coastal areas due to economic status. Despite flood risk and sea-level rise, the value of properties in coastal zone keeps increasing so that the number of properties will increase by new property developments. They believe that adaptation measures will be taken properly to protect their own properties. Thus, the coastal area will be populated in the future.

To understand the effects of socio-economic changes on option values, this thesis multiplies the annual growth factors $(1+\rho)^t$ with EAB_t at year *t* estimated from a non-growth rate scenario (i.e. 0%) (Here, ρ: growth rate, t: distance in time from the base year of 2016). Figure 4.32 shows changes in EAB under different growth rate scenarios. Newly developed properties will be spatially-evenly distributed according to the density of the current properties and populations.

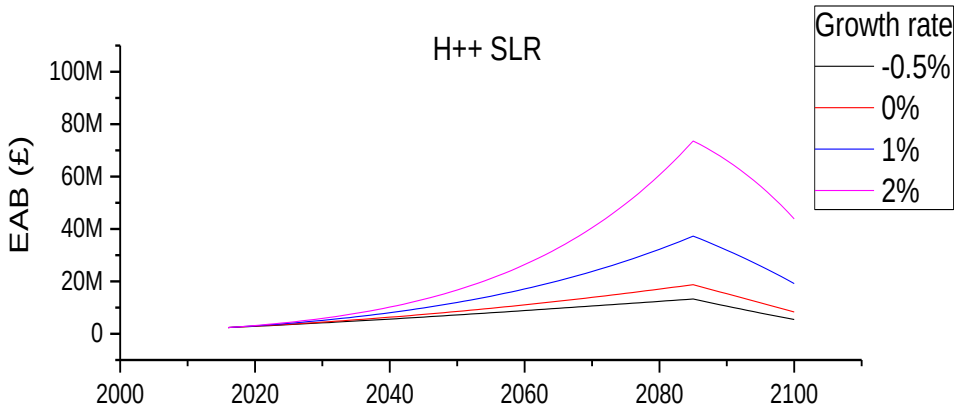

(Continue)

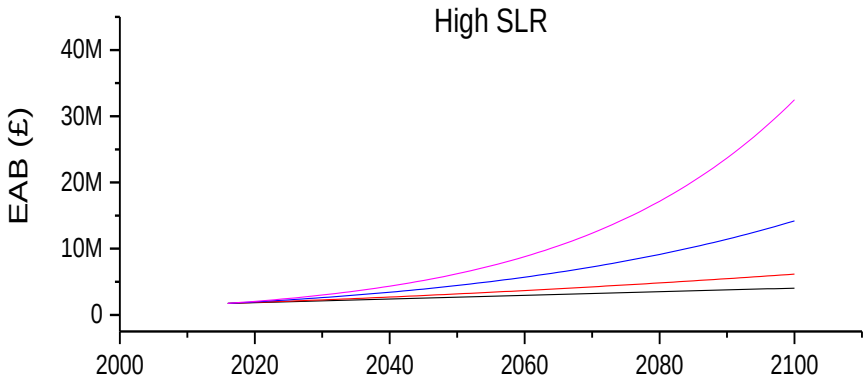

Figure 4.32 Changes in expected annual benefit (EAB) by the different future growth rates and by different SLR scenarios. Note the different scales of y-axis for the H++ SLR scenario - The estimates of EAB decline under the H++ scenario after 2080 due to the capacity of coastal defence against sea-level rise.

4. 7 Summary

This chapter has provided generic methodologies as to loading conditions, uncertainty modelling, coastal flood simulations, monetisation process, risk assessment (i.e. EAD or EAB) and option evaluations. All the processes are integrated to assess monetised flood risk and benefit due to adaptation measures in Lymington and subsequently to evaluate real options including flexibility. The integration of the processes for real options analysis provides a basis upon which to quantify coastal adaptation options including flexibility under the uncertainty of coastal flooding and sea-level rise.

This study has sought to combine all the uncertainties from sea-level rise (SLR), extreme still water level (ESWL) and overtopping rates (WAVE) in statistical ways so that this thesis can produce various flood loading conditions (i.e. ESWL+WAVE+SLR) with their own properties considered in uncertainty modelling. The uncertainty modelling coupled with the probabilistic analysis enables us to estimate how risky coastal flood event is in the present, and will be in the future due to sea-level rise. To do so, the flood damages for each defence condition have been assessed from various loading conditions (ranging from 1.2 mAOD to 4.0 mOAD) with the corresponding probabilities. Subsequently, the risk and uncertainty of coastal flooding coupled with sea-level rise have been reflected on expected annual damage

(EAD) and the economic performance (i.e. EAB) of the upgraded defence under each of the SLR scenarios.

As investigated, the flood risk analysis is strongly based on a relation between climatic variables and flood damages for Lymington. If this relation changes, EAD and EAB will change, leading to different results of option evaluations. Thus, the relation of climatic variables to flood damages needs to be thoroughly investigated to ensure the results of real options analysis are robust in its application. The uncertainties from assumptions the analysis has made may be more influential on the results of real options analysis than the uncertainties of climatic variables per se. In this regard, the sensitivity analysis to various factors will be conducted to validate the results of real options analysis in the next chapter.

In addition, EAD and EAB have been estimated upon the assumption that no breaching failure occurs. If breaching failure is still a possible flood event like the 17th December 1989 event in Lymington, EAD will increase and subsequently the upgrade of coastal defence may give more benefit to Lymington. This aspect needs to be considered in association with real options analysis. This will be also investigated as the component of this research later in chapter 5. Based on the methods explained in this chapter, this thesis will evaluate ‘deferrable adaptation options’ and ‘multiple-stage adaptation options’ for Lymington in chapters 5 and 6, respectively.

5. Results of real options analysis in a deferrable option

5. 1 Overview of real options analysis for a deferrable option

The assessment of a single deferrable option (or option to wait) is concerned on whether it is worth investing now or later (Dixit and Pindyck, 1994; De Neufville, 2003; Wang and De Neufville, 2005). This idea can be extended to climate change adaptation. A single deferrable adaptation option has important implications in decision-making as it enables us to assess investment timing under uncertainty. In this context, the option evaluation of a deferrable adaptation option focuses on investment time with its time to vary. The option evaluation process is summarised in Figure 5.1.

This chapter is structured as follows. Firstly, we provide the option value and investment timing of a deferrable adaption option under each SLR scenario. Secondly, we explore the effects of various factors on option values such as post-2100 SLR scenarios, investment times, sea-level rise at the optimal investment time, discount rates and future growth rates. The sensitivity analysis has also been conducted to see which factor is more influential on the option value and investment time. Additionally, this thesis considers the effect of breaching failure mode on the option value and investment timing. Lastly, this chapter extends the framework of real options analysis to the stochastic case of sea-level rise.

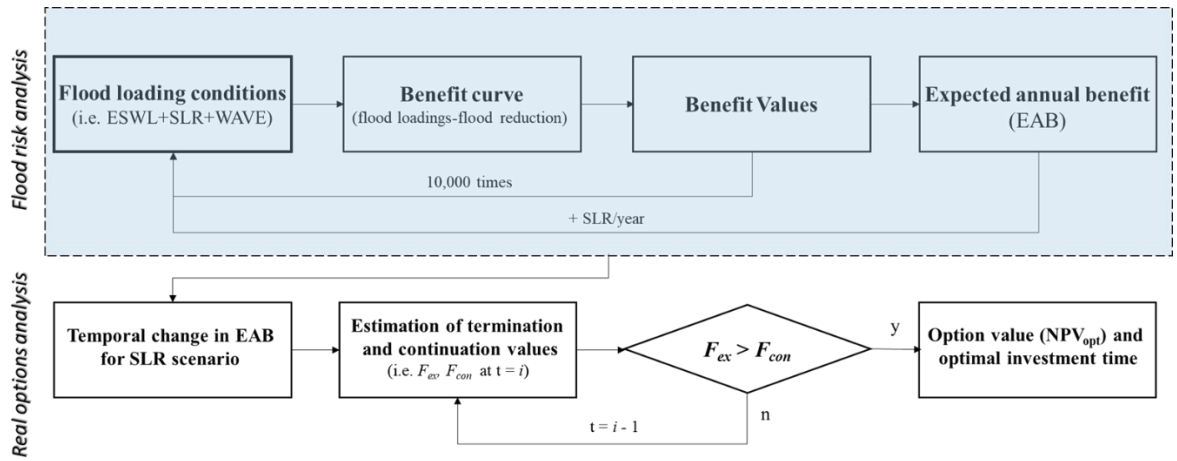

Figure 5.1. The process of option evaluation for a single deferrable adaptation option

5. 2 Results of real option analysis in an option to wait

5.2.1 Effect of SLR scenarios on option values

For the case of option to wait, this thesis first considers the coastal defence upgrade of raising the crest level from approximately 2.5 mAOD to 3.5 mAOD under the uncertainty of future sea-level rise. The height of 1-in-200 year storm surge event is 2.41 mAOD in Lymington. Thus, the current coastal defence system is now capable of protecting Lymington from possible flood events. However, its capacity will not be sufficient due to sea-level rise. Thus, there are concerns of whether the upgrade of coastal defence is necessary for Lymington and when it is implemented in the future. Table 5.1 summarises conditions for option evaluation. The calculation of a continuation and termination value for each year is conducted under each MSLR scenario. The results are shown in Figure 5.2.

Table 5.1 Conditions for real options analysis in Lymington

Investment conditions	Details
Investment cost	£ 64.20 M (Price in 2016)
Discount Rate (HM Treasury)	3.5% (0 – 30 years) 3.0% (31 to 75 years) 2.5% (after 75 years)
Project Life (L)	100 years
Post 2100 Sea Level Rise (average rates from 2090 to 2100) The rates are assumed constant after 2100	H++ MSLR: 24.1 mm/year High MSLR: 6.8 mm/year Medium MSLR: 5.7 mm/year Low MSLR: 4.7 mm/year Historical MSLR: 1.4mm/year

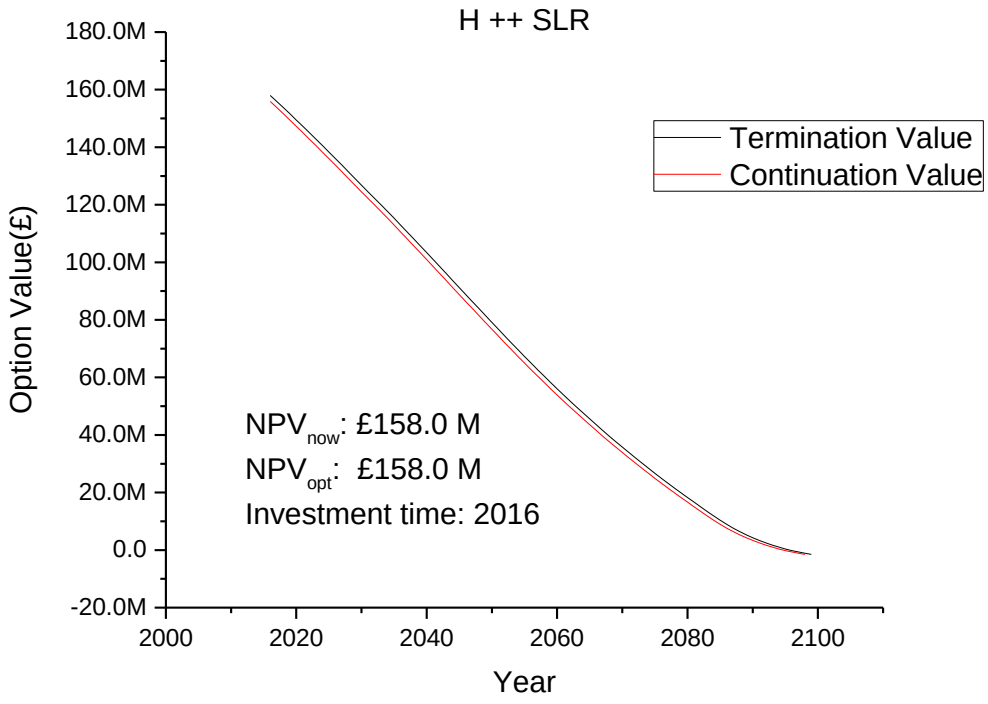
H ++ SLR
Option Value(£)
180.0M
160.0M
140.0M
120.0M
100.0M
80.0M
60.0M
40.0M
20.0M
0.0
-20.0M
2000
2020
2040
2060
2080
2100
Year
Termination Value
Continuation Value
NPV_now: £158.0 M
NPV_opt: £158.0 M
Investment time: 2016

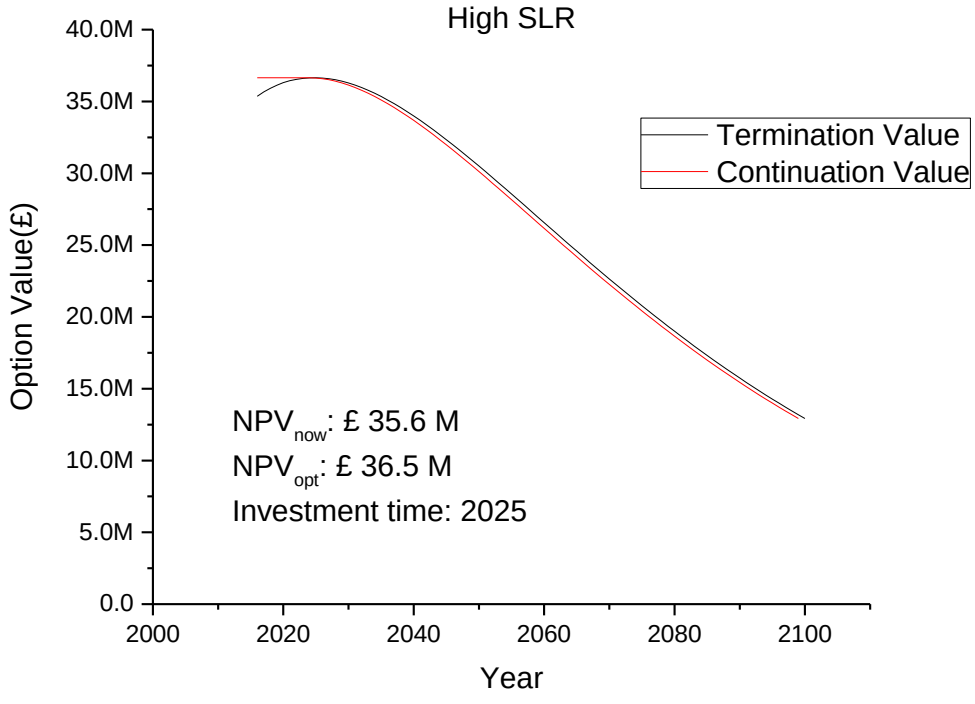
High SLR
Option Value(£)
40.0M
35.0M
30.0M
25.0M
20.0M
15.0M
10.0M
5.0M
0.0
2000
2020
2040
2060
2080
2100
Year
Termination Value
Continuation Value
NPV_now: £ 35.6 M
NPV_opt: £ 36.5 M
Investment time: 2025

(Continue)

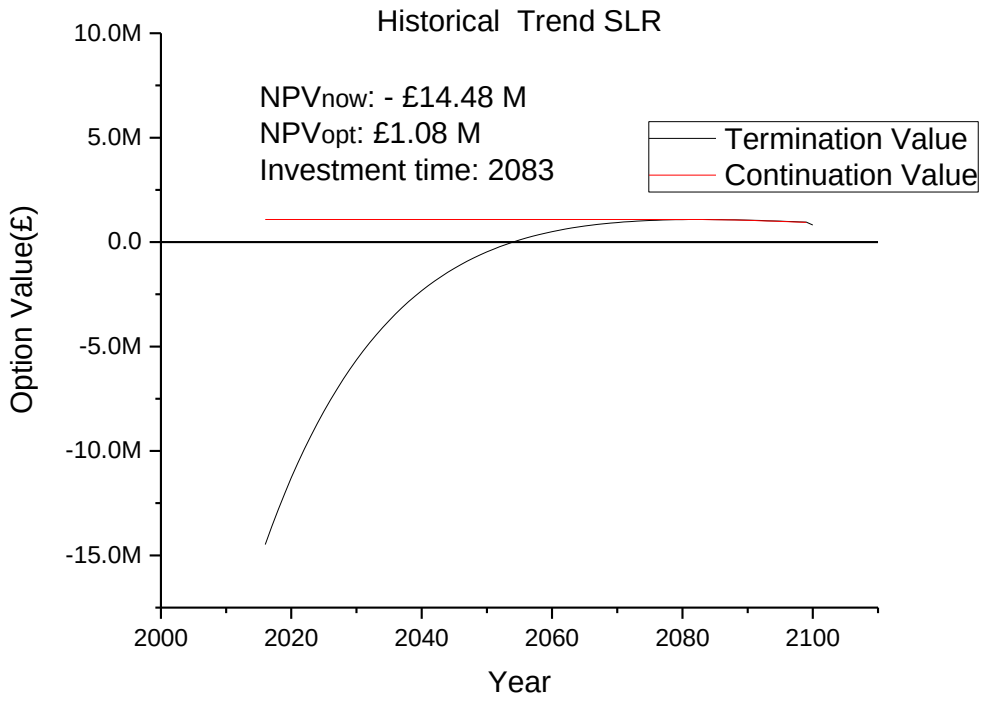

Figure 5.2 Option values by termination value (black line) and continuation value (orange line) for different sea-level rise scenarios – all the option values are present value in 2016. Note the very different scales on the y-axis.

Figure 5.2 shows how the option value for the upgrade of coastal defence changes according to investment time in each MSLR scenario. As shown in Figure 5.1, the termination value (black line) is little smaller than the continuation value (red line) at 2016 for all the MSLR scenarios, except the fastest rise in sea level (the H++ SLR scenario). As we move forwards in time, the termination value exceeds the continuation value at a certain time, indicating the optimum time to invest. By this information, we can determine when the investment should be implemented in order to produce the largest net profit (i.e. the overall benefits minus the overall costs) given a sea-level rise scenario. After the optimum investment time, the option value keeps declining with time so that the deferrable adaptation option becomes less and less efficient in economic term.

Importantly, the more extreme the MSLR scenario is, the earlier the optimum investment time occurs. For rapid sea-level rise, we need to react quickly, while for slow sea-level rise we have more time to act (See Table 5.2). In addition, the difference between the option values of the optimum investment (i.e. NPV_{opt}) and the immediate investment (i.e. NPV_{now}) indicates the value of flexibility that option holders can gain from delaying the adaptation option under a given MSLR scenario. As the Historic trend scenario has the slowest rate of

sea-level rise (i.e. 1.4mm/yr), both option values (i.e. NPV_{now}, NPV_{opt}) are the lowest among all the MSLR scenarios with NPV_{now} estimated to be negative.

Table 5.2 Results of real options analysis by different MSLR scenarios.

Scenarios	H++	High	Medium	Low	Historic trend
Investment cost	£ 64.20 M	£ 64.20 M	£ 64.20 M	£ 64.20 M	£ 64.20 M
Optimal Investment Time	2016 (i.e. now)	2025	2029	2033	2083
NPV_{now}	£ 158.0 M	£ 35.3 M	£ 23.19 M	£ 13.92 M	£ (-) 14.48 M
NPV_{opt}	£ 158.0 M	£ 36.5 M	£ 25.46 M	£ 17.77 M	£ 1.08 M
$\Delta(=NPV_{opt}- NPV_{now})$	0 M	£ 1.2 M	£ 2.27 M	£ 3.85 M	£ 15.56 M

In the H++ MSLR scenario, sea level will rise by 1.75m in 2100. As expected, this scenario gives the highest NPV_{now} and NPV_{opt} and the earliest optimal investment time (2016) among all the MSLR scenarios. This is acceptable because the risk of coastal flooding is very high and fast-growing. In this case, the investment in 2016 already gives a larger option value than delaying the option. Thus, the investment was already optimal in 2016 in the most extreme scenario. (More generally, it is found that, when the rate of sea-level rise exceeds 4.9mm/year, the optimal investment time occurs in 2016).

There are two noteworthy points from the results of this extreme scenario. Firstly, the upgrade of coastal defence up to 3.5 mAOD will become less and less useful with time unless the investment is made. The extremity of coastal flooding due to sea-level rise will have reached the limit of coastal defence capacity in 2080. Thus, the expected annual benefit (EAB) starts to decline (See Figure 4.32) from this time because of the capacity of the upgraded defence. This implies that the coastal defence needs to be raised higher than the current plan (raising up to 3.5 mAOD) if sea-level rise follows the H++ MSLR scenario. Thus, an additional adaptation option or a higher standard-of-protection defence should be considered for the protection of Lymington under the H++ SLR scenario. The real options analysis explicitly shows that the real option values –continuation and termination values – are below zero after 2095 as shown in the H++ SLR scenario (Figure 5.2). This implies there is no use of an adaptation measure with such a low standard of protection after 2095, even if the coastal flooding is very severe due to sea-level rise. Secondly, the option value in the H++ MSLR scenario rapidly declines from £158 million in 2016. Thus, the early detection of

the rate of sea-level rise is a critical task for the optimal investment, if the extreme sea-level rise is occurring.

5.2.2 Implication of optimal investment time in real options analysis

The effect of the optimal investment on option value has been examined under the uncertainty of climatic variable. To do so, the probability distributions of the option value have been constructed in three different cases where the investment is made immediately (2016), at the optimal investment time, and in distant future (e.g. 2060). The probability distributions have been made for each MSLR scenario. For calculations of the option value, we have substituted the variable of EAB_i in the equation of termination value (Refer to equation (21) in Section 4.6.1) by the stochastic variable of B_i, which is obtained from the relation between benefit values and climatic variables (i.e. ESWL+SLR+WAVE) for 3.5 mAOD level coastal defence as shown in equation (1).

$$F_{ex,t} = \sum_{i=t+1}^{L+t} \frac{B_i}{(1+r)^i} - \frac{I}{(1+r)^t} \quad (1)$$

Here, r is a discount rate, I is investment cost, and L is the number of project years (i.e. 100 years), B_i is a benefit value which is a fuction of climatic variable ESWL+MSLR+WAVE at year i, t is invesemtnt year. In the calculation of annual benefits, the option evaluation considers the annual maxima of ESWL+MSLR+ WAVE, following the traditional option evaluation method. The probability distributions of the option values at the different investment years have been constructed by 10,000 runs for High SLR scenario as shown in Figure 5.3. For other SLR scenarios, refer to Appendix L.

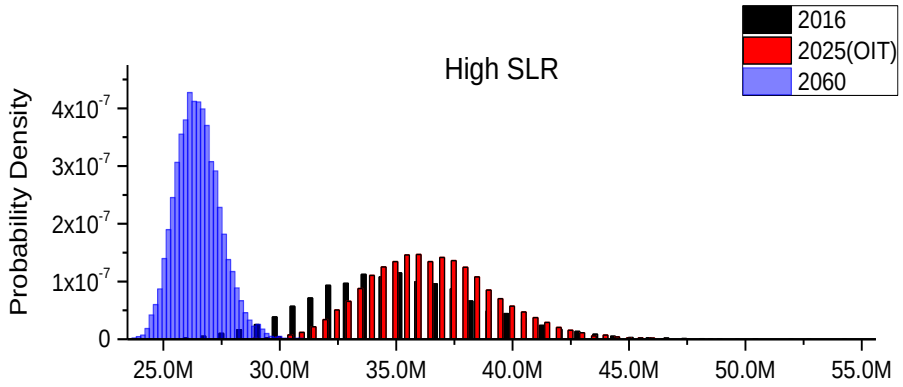

Figure 5.3 NPV distributions at different investment years (i.e. 2016, the optimal investment year and 2060) under 10,000 random time-series of ESWL+SLR+WAVE in High SLR scenario.

As shown in Figure 5.3, the option values from the optimal investment are likely to be higher than those from other investment times. If the investment is made earlier than the optimal investment time, the probabilistic range of option value (black bar) occurs in a lower region with a large variance. If the investment is made later than the optimal time, its range (blue bar) also lies in the lower region, but with a narrower variance. It is because the discount factors $(1+r)^t$ as denominators in equation (1) increase significantly with the investment time so that the probabilistic range of the option values becomes narrower.

For the slowest rate of SLR scenario (Refer to Appendix L), the probabilistic range of NPV_{now} occurs in negative value. Thus, if the investment is made in 2016 in this scenario, the decision is highly likely to be over-investment with 100% statistical confidence. If the current sea-level rise keeps rising with the historic rate, the investment should be deferred until the optimal investment year (i.e. 2083). This probabilistic analysis shows that the investment at the optimal investment time statistically provides the largest option value at a materialised sea-level rise, whatever it will be, under the uncertainty of occurrence and magnitude of coastal flooding.

5.2.3 The effects of boundary values (F_T) on option values

To see the effects of boundary values on the results of real options analysis, this section assesses the adaptation option under three post-2100 SLR scenarios: (1) linearly increasing at rates of the past 10-year sea-level rise; (2) accelerating with the past trajectory of sea-level rise; and (3) being constant at the end of sea-level rise. The patterns and rates of the post-2100 sea-level rise are listed for each of the SLR scenarios in Table 5.3.

Table 5.3 Post-2100 sea-level rise scenarios by the patterns of sea-level rise (linearly-increasing, accelerating or constant) under each of the SLR scenarios

SLR scenario	Post 2100 SLR	Rates of sea-level rise (or sea-level at 2100)	Remark
H++ SLR	L	24.1 (mm/year)	t: time in year
	A	$6 \times 10^{-5}\, t^2 - 0.2324 \times t + 221.04$ (mm)	
	C	1.75 (m)	
	W.C	Sudden increase in sea-level rise up to 4m in 2150	
High SLR	L	6.8 (mm/year)	
	A	$2 \times 10^{-5}\, t^2 - 0.0909\, t + 88.558$ (mm)	
	C	0.569 (m)	

SLR scenario	Post 2100 SLR	Rates of sea-level rise (or sea-level at 2100)	Remark
Medium SLR	L	5.7 (mm/year)	
	A	$7 \times 10^{-06}\, t^2 - 0.0236\, t + 19.255$ (mm)	
	C	0.476 (m)	
Low SLR	L	4.7 (mm/year)	
	A	$6 \times 10^{-6}\, t^2 - 0.0197\, t + 16.107$ (mm)	
	C	0.4 (m)	
Historical Trend SLR	L	1.4 (mm/year)	Sea level linearly increases so an accelerating rate is undefinable
	A	Non-defined*	
	C	0.154 (m)	

* L: the linearly increasing post-2100 SLR scenario, A: the accelerating post-2100 SLR scenario, C: the constant post-2100 SLR scenario, W.C. : West Antarctic Collapse Scenario

The results of option values (i.e. NPV_{now} and NPV_{opt}) and optimal investment times (OIT) are shown for each combination of the SLR scenarios and the post-2100 SLR scenarios in Table 5.4. There is little difference of NPV_{now}, NPV_{opt} and optimal investment time (OIT) between the linear post SLR scenario (L) and the accelerating post SLR scenario (A). This is because there is little difference in the trajectories of sea-level rise between the accelerating scenario and the linearly increasing scenario (See Figure 4.31). Also, as the stream of benefits after 2100 is significanlty reduced by discounting factors $1/(1+r)^i$ (Here, r: discount rate, i: distance in time from the present), the difference in option value and optimal investment time is ignorable in option evaluations.

On the other hand, the constant post sea-level rise scenario (C) gives different results from the linearly increasing scenario (L) and accelerating (A) scenario. From the perspective of risk analysts, the constant post SLR scenario is less severe than the L or A post SLR scenario. However, in the H++ SLR scenario, the constant post SLR scenario provides higher option values of NPV_{now} and NPV_{opt} than any other post SLR scenarios. This is because of the capacity limit of coastal defence to protect Lymington under the H++ SLR scenario. In this regard, the early upgrade of coastal defence, as investigated, is more beneficial than the later upgrade of coastal defence as its utility will rapidly decline under the most extreme SLR scenario. This capacity limit of the coastal defence is reflected on the option value of the adaptation option.

Table 5.4 The option values of the immediate and optimal investments (i.e. NPV_{now} and NPV_{opt}) in the coastal defence by different post MSLR scenarios

SLR scenarios		Investment cost	Investment Time	NPV_{now}	NPV_{opt}	$\Delta(=NPV_{opt}-NPV_{now})$
H++	*L*	£ 64.20 M	2016	£ 158.0 M	£ 158.0 M	0
	A	£ 64.20 M	2016	£ 158.0 M	£ 158.0 M	0
	C	£ 64.20 M	2016	£ 167.5M	£ 167.5M	0
	W.C	£ 64.20 M	2016	£ 160.6M	£ 160.6M	0
High	*L*	£ 64.20 M	2025	£ 35.3 M	£ 36.5 M	£ 1.2 M
	A	£ 64.20 M	2026	£ 35.4 M	£ 36.9 M	£ 1.5M
	C	£ 64.20 M	2020	£ 33.9 M	£ 34.1 M	£ 0.2 M
Medium	*L*	£ 64.20 M	2029	£ 23.19 M	£ 25.46 M	£ 2.27 M
	A	£ 64.20 M	2029	£ 23.2 M	£ 25.6 M	£ 2.4 M
	C	£ 64.20 M	2025	£ 22.5 M	£ 23.9 M	£ 1.4 M
Low	*L*	£ 64.20 M	2033	£ 13.92 M	£ 17.77 M	£ 3.85 M
	A	£ 64.20 M	2034	£ 14.01 M	£ 18.07 M	£ 4.06 M
	C	£ 64.20 M	2031	£ 13.4 M	£ 16.4 M	£ 2.0 M
Historical trend (+1.4mm/yr)	*L*	£ 64.20 M	2083	£ (-) 14.48 M	£ 1.08 M	£ 15.56 M
	C	£ 64.20 M	2083	£ (-)14.64M	£ 0.40 M	£ 15.04 M

As observed in Table 5.4, the C post SLR scenario gives higher option values (£ 167.5 M) than the L or A post SLR scenario in the H++ SLR scenario, while, in other SLR scenarios, the contrary results are observed. Thus, the extremity of post SLR scenario has no effects on increase in the option value and optimal investment time under the most extreme SLR scenario due to the capacity of coastal defence. This argument is more apparent when the West Antarctic Collapse scenario is applied as a post SLR scenario in Figure 5.4. For an illustrative purpose, sea-level rise and the corresponding change in EAB are drawn under the combination of the H++ SLR scenario and the W.C. SLR scenario.

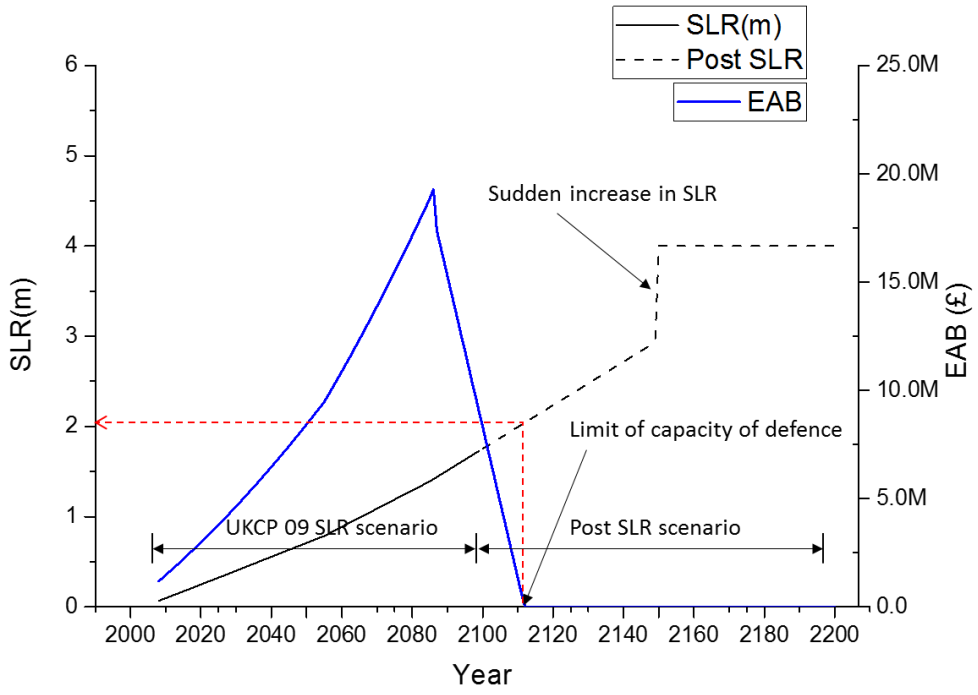

Figure 5.4 UKCP 09 SLR and its post SLR until 2200 and the corresponding change in EAB as the performance of the coastal adaptation ($U_{c\to 3.5m}$) for the H++ SLR scenario.

For the mild SLR scenarios (i.e. High, Medium and Low SLR scenario), the L or A post scenario gives a higher option value than the C post SLR scenario. However, the C post SLR scenario leads to earlier investment than the L or A post SLR scenario. This is because the utility of the adaptation measure will never increase after 2100 in the C post SLR scenario, while the delay of the adaptation measure decreases the option value by discount factors $(1+r)^i$.

In this regard, this thesis adopts the linearly-increasing SLR scenario as the most likely post-2100 SLR scenario, rather than the constant SLR scenario, on an assumption that the future sea-level rise will continue to follow its prior trajectory of sea-level rise with a strong memory. If sea level is constant after 2100, there should be an extreme or unrealistic intervention that overturns the physical processes of earth and ocean systems. To the best of our knowledge, this is not considered as feasible in physical systems. In addition, we have observed little difference in boundary values between the linearly-increasing scenario and the accelerating scenario.

In the Historical trend SLR scenario, the option value of the investment now (i.e. NPV_{now}) is a minus with the optimal investment value (i.e. NPV_{opt}) estimated to be £ 1.08 M and £ 0.41 M for the L and C SLR scenarios, respectively. In this case, the investment is to be made in

the long distant future (i.e. 2083). From the perspective of the present, the returns from the investment at 2083 are very small and highly discounted. Thus, in the mildest SLR scenario, the post SLR scenario has little effect on the option value and optimal investment time.

5.2.4 Absolute sea-level rise at the optimal investment time

A noteworthy finding in this thesis relates to an absolute sea-level rise at optimal investment time for all the MSLR scenarios except the H++ MSLR scenario. MSLR at the optimal investment time is found at 13 to 14 cm relative to 1990 with EAB estimated around £ 2 million for all the MSLR scenarios (Table 5.5). As EAB is dependent on the probability distribution of climatic variables (i.e. ESWL+ SLR+WAVE) at a given year, the certain value of MSLR at the optimal investment time leads to the certain value of EAB. The absolute sea-level rise has important implications for determining the optimal investment time in real options analysis, as it can be used, as a single threshold value, to predict the investment timing for an adaptation option (Figure 5.5). This thesis also proves that the threshold value at the optimal investment is constant regardless of SLR scenarios (Refer to Appendix M). It is determined by the investment cost (I) of an adaptation option and discount rates (r) (= rI). By observing the rate and magnitude of sea-level rise at any time, rather than identifying the ongoing pattern of sea-level rise, we can decide when to implement the upgrade of the coastal defence under the various SLR scenarios.

Table 5.5 MSLR and EAB at optimal investment time in each of the SLR scenarios

MSLR scenarios	Optimal Investment Year	MSLR (cm)	EAB (£ M)
H++	2016	19	1.49
High	2025	14	2.07
Medium	2029	13	2.03
Low	2033	13	1.99
Historical trend	2083	13	2.03
Critical rate (4.9mm/yr)	2016	13	2.00

However, the H++ MSLR scenario shows different patterns in MSLR and EAB at the optimal investment time from other SLR scenarios. The investment time for the H++ MSLR scenario occurs at the earliest time (i.e. 2016) among all the MSLR scenarios since the MSLR and EAB at this time have already been 19cm and £2.33 M, respectively. Even though the optimal investment time and MSLR had been further traced to the past before 2016, the

termination value was already higher than the continuation value. Thus, in the most extreme H++ MSLR scenario, the adaptation option should be implemented immediately. This implies that the investment timing for the adaptation option is less sensitive to sea-level rise in the most extreme scenario. In other words, the adaptation measure of upgrading the coastal defence should be implemented immediately under the extreme SLR scenarios beyond the rate of 4.9mm/year. This view is line with the perspectives of flood risk management. However, as sea-level rise does not yet reach 13cm (relative to 1990) in Lymington, the current trajectory of sea-level rise does not seem to be the H++ MSLR scenario.

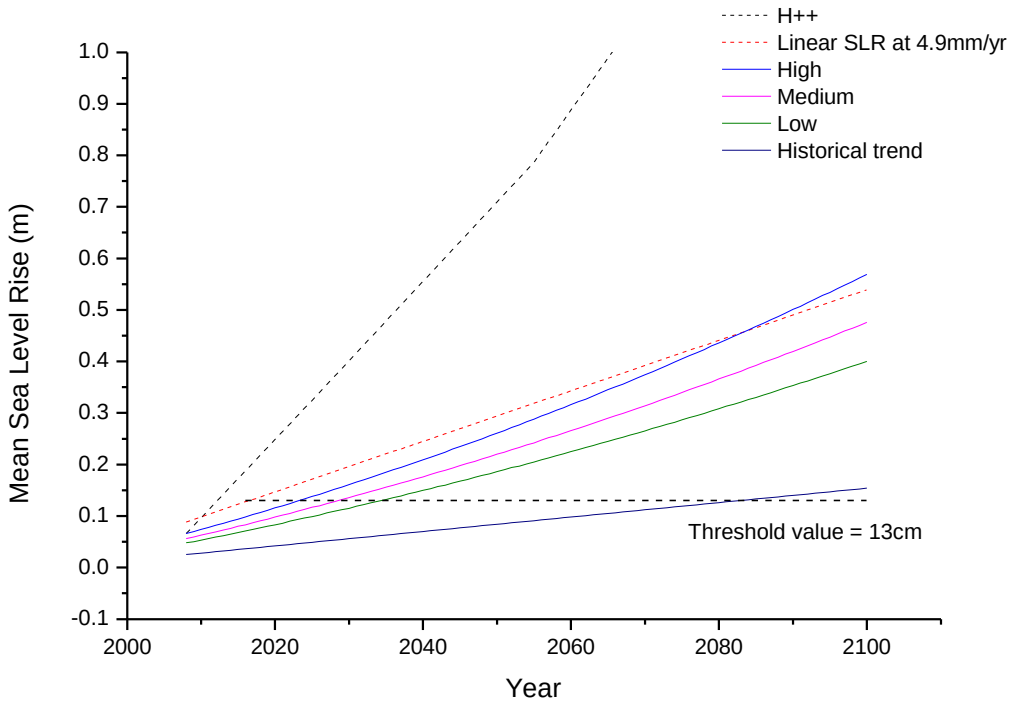

Figure 5.5 The optimal investment time for a threshold value of 13cm across all the MSLR scenarios – The H++ SLR scenario is only plotted within the y-scale. The linearly increasing sea-level rise (4.9mm/yr) is plotted to illustrate the maximum rate of sea-level rise to which the threshold value of 13cm is valid.

5.2.5 Effect of future development on option values

This thesis also extends real options analysis to the cases of socio-economic developments at -0.5%, 1%, and 2% annual growth rates. This represents decline or growth in property stocks and values. The rates of the socio-economic change are assumed to be constant over time. Based on the projections of EAB, the backward induction approach has been applied from

2100 to 2016 for each combination of the growth rate scenarios and the MSLR scenarios. The results are shown in Table 5.6 and Figure 5.6.

Table 5.6 The results of option values and optimal investment times for different future growth rates in each MSLR scenario.

MSLR Scenario	Future growth rate (%)	NPV_{now} (£ M)	NPV_{opt} (£ M)	Optimal Investment Time	MSLR at optimal investment time (cm)	EAB at optimal investment time (£ M)
H++	-0.5%	118.0	118.0	Now	19.0	2.39
	0%	158.0	158.0	Now	19.0	2.39
	1%	278.0	278.0	Now	19.0	2.39
	2%	489.0	489.0	Now	19.0	2.39
High	-0.5%	17.7	18.7	2027	14.7	2.03
	0%	35.3	36.5	2025	13.8	2.07
	1%	93.8	98.1	2029	15.6	2.54
	2%	207.8	245.4	2054	28.3	7.15
Medium	-0.5%	7.7	10.6	2034	15.2	2.02
	0%	23.2	25.5	2029	13.2	2.03
	1%	72.9	76.6	2030	13.6	2.37
	2%	168.7	194.7	2053	23.3	6.11
Low	-0.5%	0.25	5.5	2043	16.0	2.00
	0%	13.9	17.8	2033	12.6	1.98
	1%	57.5	61.9	2030	11.5	2.18
	2%	141.2	158.2	2045	16.8	4.19
Historical trend	-0.5%	-22.35	-1.06	No investment	-	-
	0%	-14.47	1.08	2083	13.0	2.03
	1%	9.96	20.47	2045	7.7	2.08
	2%	55.56	70.16	2044	7.6	2.69

As the positive future growth rates exponentially increase the expected annual benefit (EAB) during the project life, the option values of NPV_{now} and NPV_{opt} increase with the future growth rates as shown in Table 5.6. However, the optimal investment time for the high growth rate (i.e. 1 or 2 % growth rates) occurs later than that for the 0% growth rate in the High, Medium and Low MSLR scenarios. For the proof, the relations between optimal investment times and future growth rates are derived for different SLR scenarios by the formulation in Appendix N. It is because the optimal investment time is a moment for the investment to give the largest option value under a given combination of SLR scenario and future growth scenario. Thus, the result of real options analysis suggests ‘waiting longer’ for a high future growth scenario than for a low future growth rate scenario, as it provides a larger investment opportunity for option holders.

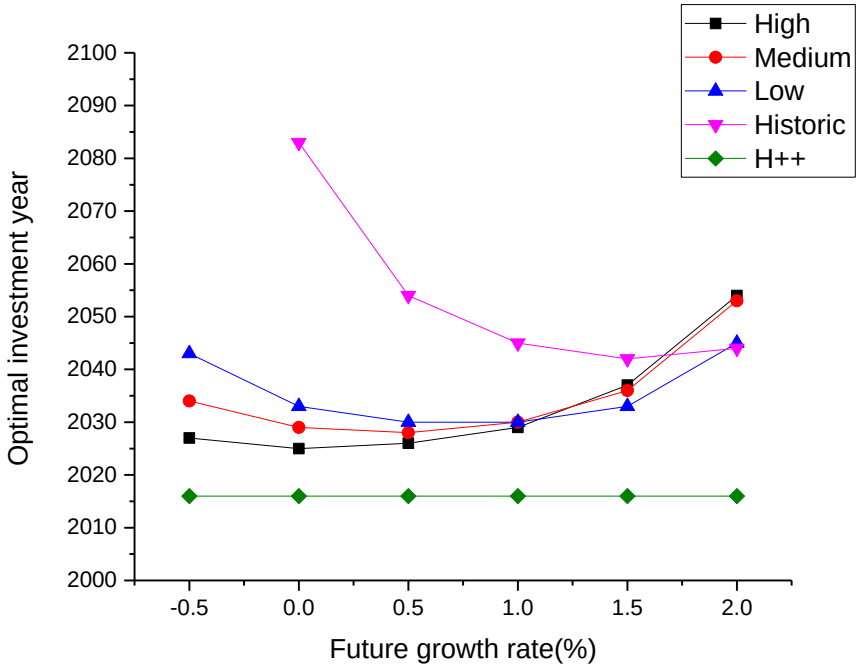

Figure 5.6 Change in optimal investment time by different future growth rates according to SLR scenarios

When evaluating an adaptation option under the various combinations of climate change scenarios and socio-economic scenarios, careful attentions need to be paid to the application of future growth rate scenarios. The option value is greater for scenarios with high growth rates than with low growth rates. If a high growth rate is strongly expected, a decision based on a non-growth rate scenario can be a strategic decision in terms of investment timing because it is likely to lead to relatively early investment in comparison to a decision based on a high future growth rate. Also, the option value will be increased by a realised high future growth rate. In this case, the investment timing is considered as a less important factor than the option value. In other words, even if the investment time is incorrect in high growth rates, the option value will be very high due to the high growth rate, resulting in the investment in an adaptation option.

For example, the selection of a 2% growth rate scenario in High MSLR scenario will lead to Lymington being unprotected until 2054 when sea-level rise reaches 28cm. Instead, if a non-growth rate scenario is taken for investment time, the investment will be made in 2025 with NPV_{2025} (which is termed for the investment at 2025) expected to be at least £ 36.5M in the non-growth scenario. However, if the future growth rate is turned out to be 2% with such a decision (i.e. invest in 2025), the option value of the investment at 2025 (i.e. NPV_{2025}) will reach £ 225M as the 2% future growth rate realises.

However, if both future growth rate and sea-level rise scenario are uncertain, the investment decision needs time to wait for observing a future growth rate. In this regard, climate change scenarios and future growth rate scenarios can be properly combined in order to prompt adaptation actions in a timely manner. As shown in Figure 5.7, the colour map shows optimal investment times by different combinations of the SLR scenarios and future growth rate scenarios, providing additional information on the sequential order of applications of the sea-level rise scenarios and future growth rate scenarios.

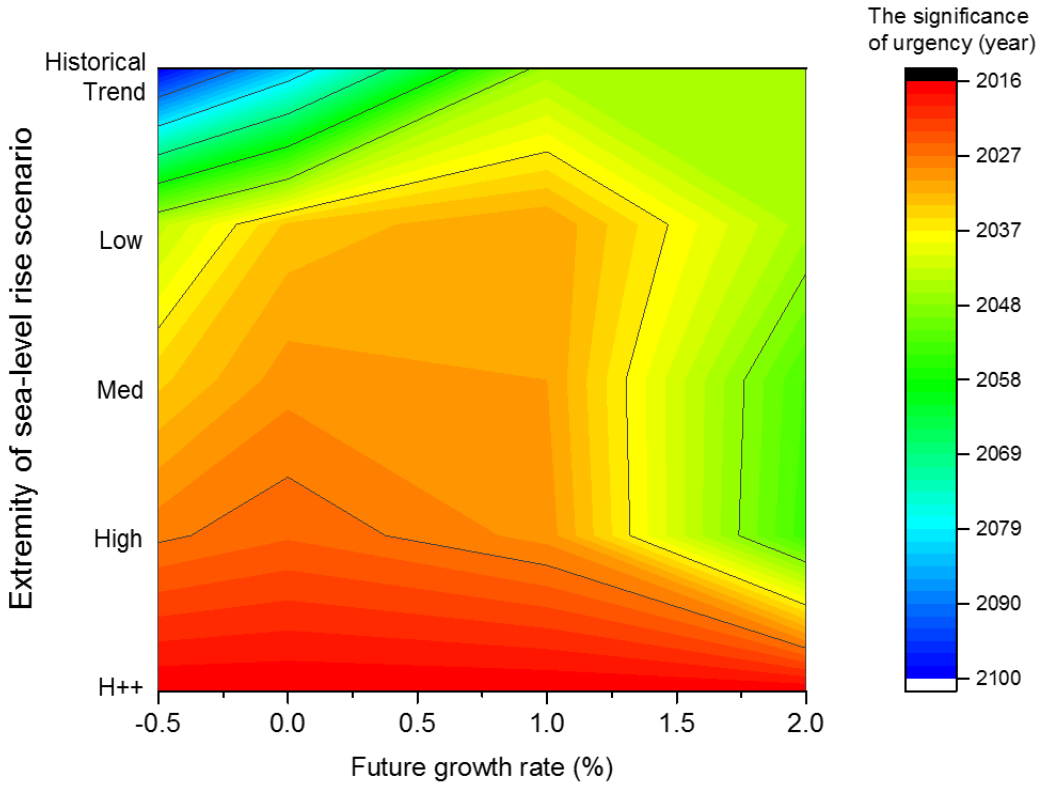

Figure 5.7 The priority of sea-level rise scenarios and future growth rate scenarios in investment time – The colour where the sea-level rise scenario and the growth rate scenario intersect indicates the optimal investment time. Conversely, the scenarios should be addressed in the sequential order of the optimal investment time. Note that the sea-level rise scenarios on the y-axis are equally distanced for the illustrative purpose.

The coloured map indicates the time priority of combinations of sea-level rise scenarios and future growth rate scenarios within the given timescale. For example, the red region indicating optimal investment time between 2016 and 2020 is corresponding to the H++ SLR scenario and (-) 0.5-to-2.0% future growth rate scenarios. This implies that we need to first consider the H++ SLR than any other scenarios in 2016 and 2020. If sea-level rise is

identified to be the H++ SLR scenario during the period, the investment should be made at that time. Otherwise, we need to wait until the next period. Subsequently, the next candidate scenarios in orange or green region will be considered with the next high priority for the investment decision.

By following this process, the real options approach can achieve a maximum option value and optimal investment time by resolving uncertainties from sea-level rise scenarios and socio-economic scenarios with the sequential order. In addition, the milder the SLR scenario is, the more sensitive the optimal investment time is. In the H++ SLR scenario, the optimal investment time is insensitive to the future growth rates, indicating the investment in 2016, while in the Historical Trend SLR scenario, the optimal investment time significantly varies between 2040 and 2100, depending on the future growth rate scenarios.

5.2.6 The effect of discount rates on option values and optimal investment time

This thesis has also estimated optimal investment times across a range of discount rates. Figure 5.8 shows optimal investment times by different discount rates, which are estimated by Bellman's dynamic programming approach. The optimal investment times for different discount rates (i.e. 0.5%, 2.5%, 3%, 3.5% and 4.5%) are marked with dots along the optimal investment time-discount rate relation which is drawn from a formulation in Appendix O.

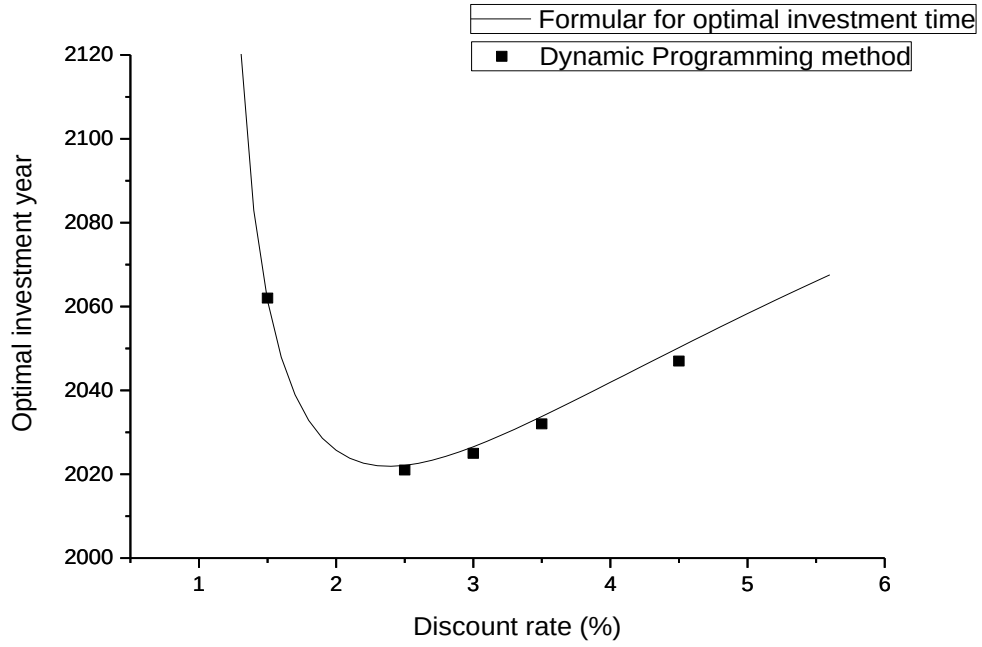

Figure 5.8 Change in optimal investment time according to discount rates for the High SLR scenario by the formulation method (line) and the dynamic programming (square points)

As seen in Figure 5.8, as the discount rate increases in a range from 2.5% to 5.5%, the optimal investment time becomes later. The optimal investment time is the earliest around 2.25%. If the discount rate lowers below 2.25%, the optimal investment time becomes later. This is counterintuitive to the rule of standard cost-benefit analysis as well as the practical use of discount rates. In general, the low discount rate considers the future value to be more important than the present value. This implies that the choice of a low discount rate prompts an immediate investment for the future generation in a common sense. However, the real options analysis gives different results from the cost-benefit analysis. Thus, the optimal investment time is not valid in very low discount rates in practice. In addition, as the option value is less discounted in the low discount rates, the investment will provide large option values in comparison to the investment in the high discount rates. In such a low discount rate, the immediate investment based on cost-benefit analysis can be a more reasonable and efficient decision than the optimal investment based on real options analysis. This pattern is observed in other SLR scenarios (Figure 5.9).

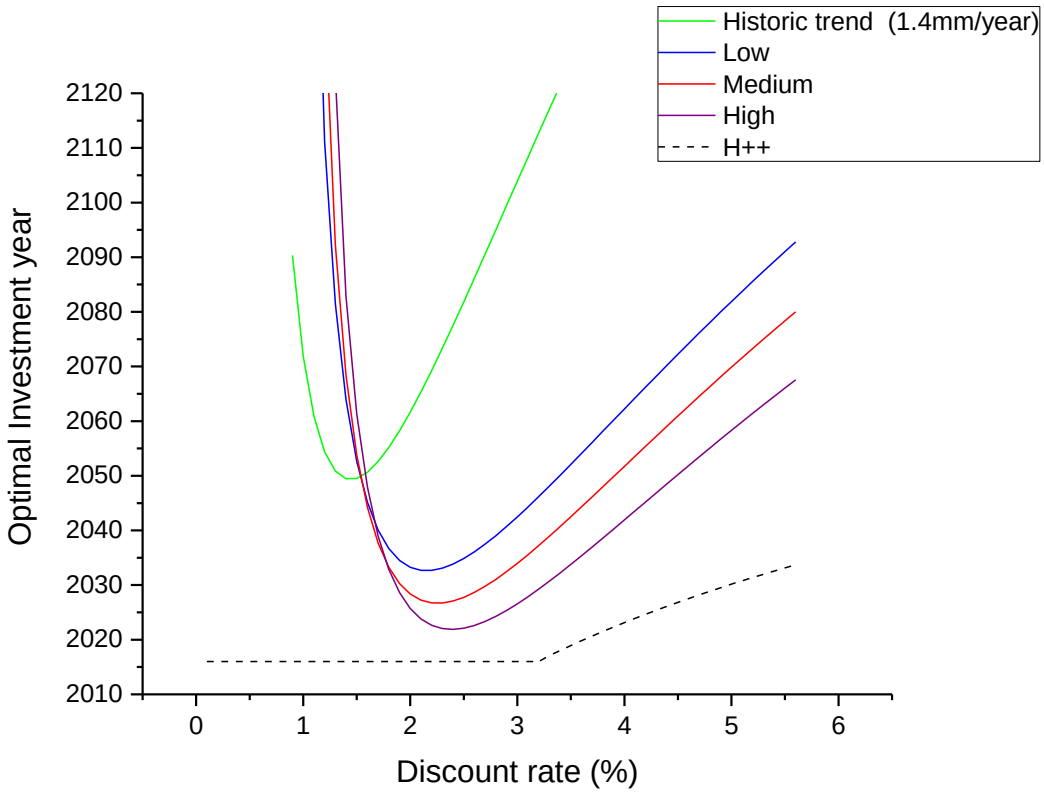

Figure 5.9 Optimal investment times according to different discount rates by the formulation method for each SLR scenario

On the other hand, the optimal investment time in the H ++ SLR scenario has different patterns from other scenarios. In the H++ SLR scenario, the current risk of coastal flooding is very high and the performance of the upgraded coastal defence will rapidly reduce due to the limitation on its capacity under extreme sea-level rise. Most optimal investment time occurs earlier than now (i.e. 2016) even at the low discount rates – although the optimal investment time becomes later than 2016 beyond the discount rate of 3.2%. For the purpose of expression, we simply set the investment years before 2016 to be 2016. The optimal investment time is insensitive to the discount rates in the most extreme SLR scenario (i.e. H++ SLR scenario). Interestingly, it is also found that the Green Book (i.e. 3.5% for the first 30 years, 3.0% for the next 45 years and 2.5% afterwards) discount rate gives earlier optimal investment time (i.e. 2025) than the constant discount rates (e.g. 3.5%).

5.2.7 Effect of the residual life (or longevity) of coastal defence on option evaluation

The previous analysis has applied the real options analysis upon the assumption that the life of coastal defence is constant (= 100 years). Thus, the coastal defence is supposed to be managed properly in order to protect Lymington during the whole life. The coastal adaptation measures in SMP also include maintenance costs in the overall costs. However, the life of coastal defences differs depending on how they are managed or how severely or frequently coastal flood events will occur in the future. Thus, the framework of real options analysis needs to be applied where coastal defences have different life periods. The benefits and costs of the coastal defence change depending on the life of the project. Thus, this thesis has also estimated the option values and optimal investment times of a coastal adaptation measure (i.e. $U_{c\rightarrow 3.5m}$) with its duration to alter. The sensitivity analysis assumes that the life of the coastal defence is increased or decreased by 5%, 10%, 20% or 25%, respectively. The results from the application of real options analysis are shown in Table 5.7. As an exemplary case, the Medium SLR scenario with the rate of 3.3mm/year has been selected for a sensitivity test with other conditions (i.e. investment cost, discount rate, etc.) being constant.

Table 5.7 Results of option values and optimal investment times by different life periods of the coastal adaptation measure at 3.3 mm/year of sea-level rise

Residual life	optimal investment time	NPV_{now}	NPV_{opt}	SLR at OIT (cm)
75	2042	3.19	10.22	17.16
80	2039	6.06	11.71	16.17
90	2033	11.11	14.67	14.19
95	2031	13.33	16.1	13.53
100	**2029**	**15.7**	**17.4**	**12.87**
105	2027	17.22	18.84	12.21
110	2025	18.92	20.12	11.55
120	2022	21.89	22.5	10.56
125	2021	23.18	23.59	10.23

As seen in Table 5.7, the longer the life of the coastal defence is, the earlier the optimal investment time is. It is because, as the residual life increases, the period in which benefits from the coastal adaptation measure will be gained is longer. Thus, the option values of the coastal adaptation measure (i.e. NPV_{now} and NPV_{opt}) increase together with the life of the coastal defence. However, NPV_{now} rises more rapidly than NPV_{opt} as shown in Figure 5.10 - Note that the increased benefits from the distant future are more discounted so that the effects of the benefits from the distant future are smaller than from the near future. This leads to little difference between NPV_{now} and NPV_{opt} in the coastal adaptation measure with a long residual life (Figure 5.10 (a)). This implies that the optimal investment time occurs little earlier for the coastal defence with the long residual life. Thus, the investment needs to be made earlier if the coastal adaptation measure has the longer residual life.

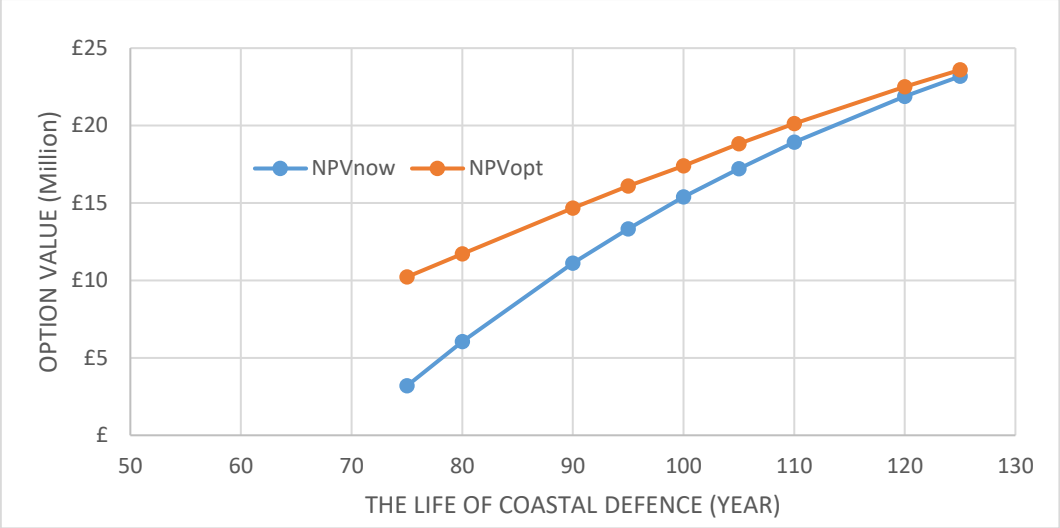

(a)

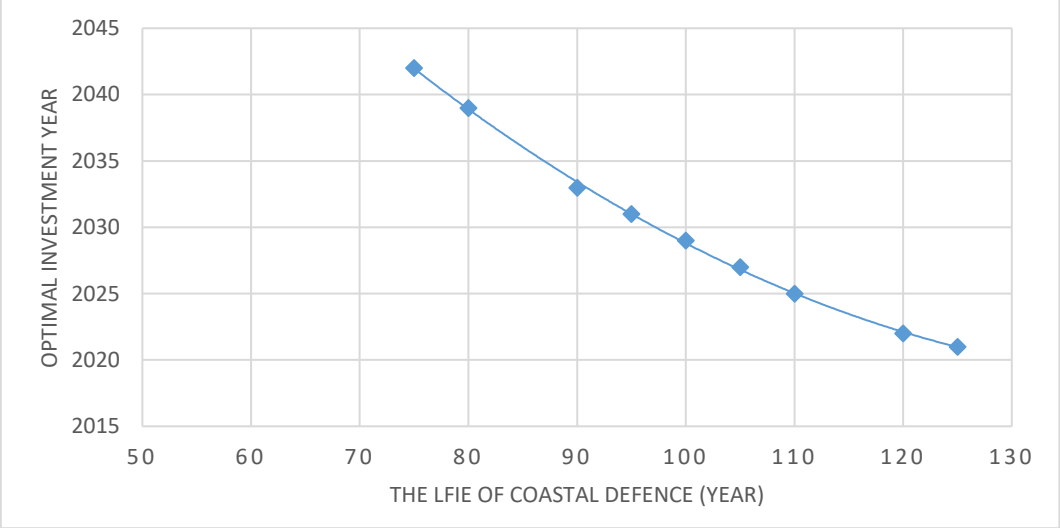

(b)

Figure 5.10 (a) Change in NPV_{now} and NPV_{opt}; and (b) change in optimal investment year by different life periods of coastal adaptation measure at 3.3mm/year of sea-level rise

This analysis has been made on an assumption that the maintenance cost of the coastal adaptation is constant, even though the life of coastal defence extends. In a common sense, prolonging the life of coastal defence requires more costs and resources for management. For a more sophisticated analysis, the increased costs for the extension of the coastal defence life need to be considered by comparing with the increase in option values (NPV_{now} and NPV_{opt}). For instance, increase in the residual life by 10 years leads to increase in NPV_{now} and NPV_{opt} by £ 3.2 M and £ 2.7 M, respectively (Table 5.7). If it increases the maintenance cost by £ 5

M, NPV_{now} and NPV_{opt} are estimated to be £ 16.89 M and £ 18.84 M, respectively, which are little higher than in the case of the 100-year residual life. The optimal investment time is just one year earlier than that of the 100-year-life coastal defence. If the maintenance cost increases significantly for the management, the optimal investment time may be found later, though it increases the residual life of the coastal defence. The effects of the residual life on the option values and optimal investment times need to be considered in association with the maintenance costs.

5.2.8 Effect of SLR projection periods on option evaluation

The IPCC data provide information on SLR projections until 2100 (Lowe et al., 2009). Since real option analysis calculates option values backwardly from the end year of SLR projection, the year of 2100 is set as a start year for the option evaluation. However, the projected period of sea-level rise can differ depending on data types, climate change prediction models or computational techniques. It is plausible that the real options are assessed under different projection periods of sea-level rise. To see the effects of SLR projection periods on option evaluation, this part estimates the option values and optimal investment times of an adaptation option (i.e. $U_{c\rightarrow 3.5m}$) with different SLR projection periods. The results are summarised in Table 5.8.

Table 5.8 Results of real options analysis by different periods of sea-level rise projections

Periods of SLR Projection	Optimal investment time	NPV_{opt}	SLR at OIT (cm)
2075	2029	17.49	12.87
2080	2029	17.49	12.87
2090	2029	17.49	12.87
2095	2029	17.49	12.87
2100	**2029**	**17.49**	**12.87**
2105	2029	17.49	12.87
2110	2029	17.49	12.87
2120	2029	17.49	12.87
2125	2029	17.49	12.87

As shown in Table 5.8, the projected periods of SLR have no effects on option values and optimal investment years. This is because a continuation value and a termination value at

every year have been estimated upon the extrapolated trajectory of the SLR projection. The estimation process has been iteratively conducted in a backward way. Thus, whenever the option evaluation starts, the real options analysis gives the same results of option value and optimal investment time as long as the extrapolated SLR projection never change. It can be concluded that the SLR projection periods have no effect on option evaluation in real options analysis.

5.2.9 Sensitivity analysis of option values and optimal investment times

As investigated previously, the option values and optimal investment times are subject to various factors. As coastal adaptation measures are implemented under various conditions, the option values and optimal investment times have large uncertainty intrinsically. Thus, it is important to understand which factor will play an influential role in real-options-based decisions. The sensitivity analysis of the optimal investment and option value has been conducted with changes made to individual factors such as the rates of sea-level rise, future growth rates, discount rates, investment costs and the life of coastal defence. For sensitivity test, the individual factors have been increased or decreased by 5%, 10%, 20% and 25%. For comparison, a reference condition has been set out with the rate of sea-level rise (=3.3mm/yr), investment cost (= £ 64.2 M), discount rate (=3.5%) and residual life (=100 years). The results are shown in Appendix P. For an illustrative purpose, the variations in optimal investment time, option value and sea-level rise at the optimal time are ranged by 10%- and 20%- changes to each factor in Figure 5.11.

As seen in Figure 5.11, the optimal investment time and option value both are sensitive to all the factors except the project year. In other words, the optimal investment time and option value are determined by various investment conditions. By comparing the variations in the option values and optimal investment times by each factor, some important aspects have been found in applying the real options analysis into climate change adaptation.

(a) Optimal investment year

(b) Option value of optimal investment (NPV_{opt})

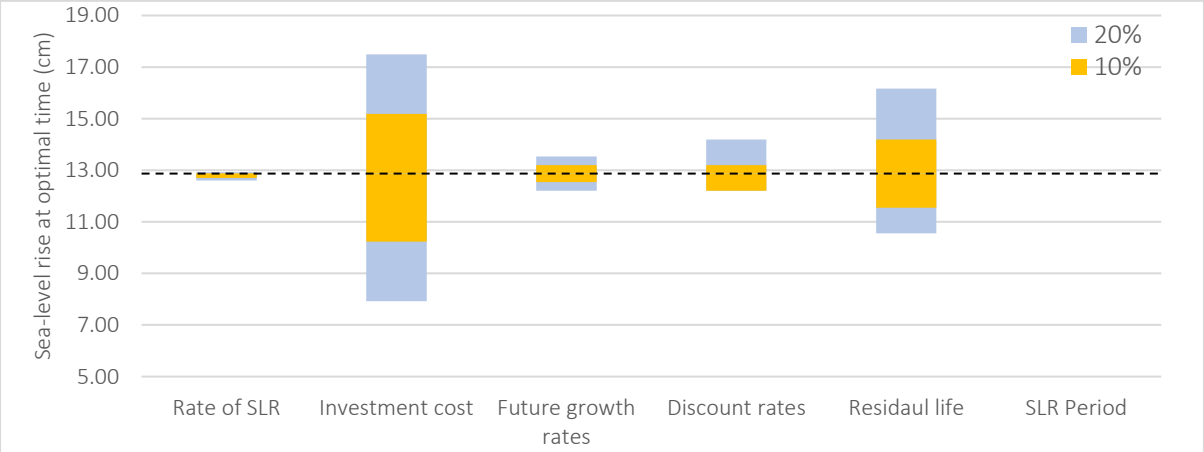

(C) SLR at optimal investment time

Figure 5.11 Variations in optimal investment time, option value and sea-level rise at optimal investment time according to 10%- and 20%- changes to each factor, respectively

Firstly, as investigated in Figures 5.11 (a) and (b), the optimal investment time and option value are most sensitive to the investment cost. The option value is determined by all the benefits minus all the costs. Thus, the investment cost directly affects the option value. In the real-life issues, uncertainty from investment cost can stem from various sources such as the nature of construction work, human's error or mistake, planning, budgeting and economic situations. Thus, when applying the real options analysis, the investment costs need to be tackled with more attention.

Secondly, the option value is also sensitive to the rate of sea-level rise. However, the sea-level rise at optimal investment time is insensitive to the rate of sea-level rise. As reviewed previously, the optimal investment time is when EAB from an adaptation measure is equal to the investment cost times discount rate. Thus, the similar values of sea-level rise at the optimal investment time occur for an adaptation measure, even if the rates of sea-level rise are different. This has also been investigated by deriving the formulas of optimal investment condition in section 5.2.4.

Thirdly, although the optimal investment time is subjected to the future growth rates and discount rates, the sensitivity of the optimal investment time to those factors is less than to other factors. This is because the future growth rates and discount rates increase (or decrease) the option values of NPV_{now} and NPV_{opt} together by multiplication. As the optimal investment time is related to the difference between NPV_{now} and NPV_{opt}, the sensitivity of the optimal investment time due to those factors is small in comparison to that of the option value (NPV_{opt}) - Note that those two factors increase the option values considerably.

In terms of the residual life of coastal defence, it is also influential on real-option-based decisions. As it significantly changes the optimal investment time and option value, this factor can act as uncertainty in investment decisions. As the residual life is related to the management of coastal defence, a way to reduce uncertainty from the residual life is to consider sufficient maintenance cost in coastal adaptation planning. This will ensure the coastal defence performs well until the expected life.

Lastly, as seen in Figure 5.11 (a), (b) and (c), the change in SLR projection period has no influence on the optimal investment time, option value and sea-level rise at the optimal investment time. Thus, this factor does not need to be considered in option evaluation.

5. 3 The effect of breaching failure modes on option evaluation

The previous analysis has been conducted upon the assumption of no-breaching. As reviewed in the past flood events, Lymington had experienced the breaching failure events. Although the coastal defence has been upgraded after the most recent breaching event on 17th December 1989, Lymington still has the possibility of the coastal defence being breached due to extreme coastal flood events and sea-level rise. However, this thesis assesses the possibility of the breaching to be very rare in Lymington due to the proper upgrade of coastal defence. Weak points where the breaching might occur in the future are represented based on the previous research on Lymington by Wadey et al. (2012) in Figure 5.12 (a). As an exemplary case, a possible breaching failure has been simulated with a 1-in-200 year flood event in Figure 5.12 (b). Whether breaching failure occurs or not depends on water levels, defence conditions and waves (Dawson and Hall, 2006; Wadey, 2013). Thus, the occurrence of breaching failure is uncertain and probable.

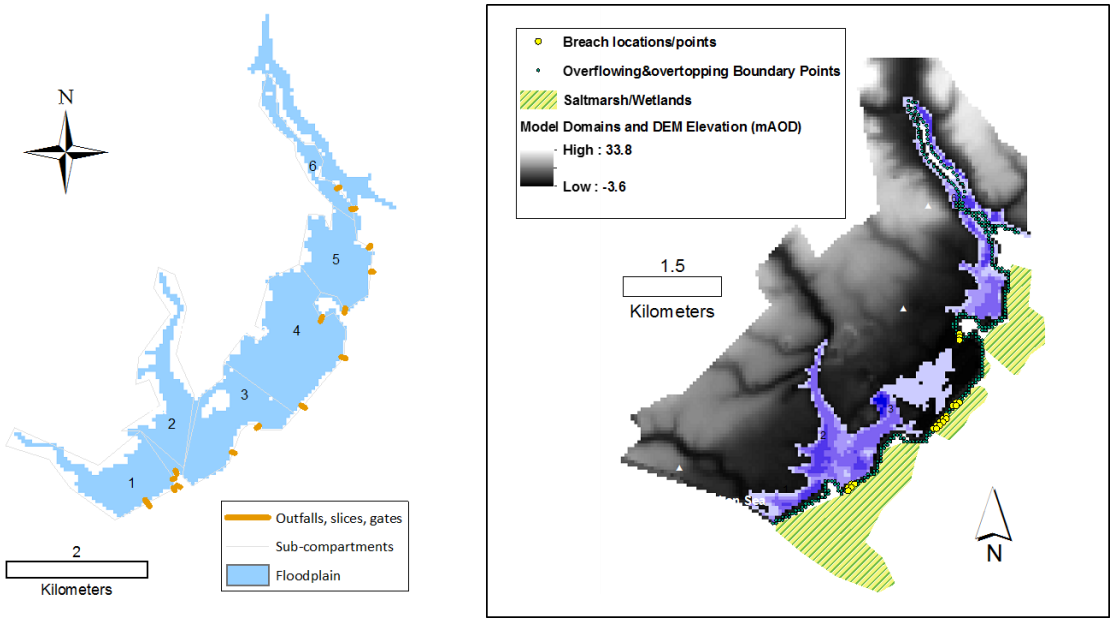

(a) (b)

Figure 5.12 (a) Vulnerable spots of breaching failure within the current coastal defence system (Wadey et al., 2012) (b) Breaching failure simulation against a 1/200 coastal flood event

To examine the effects of breaching failure on real options analysis, this thesis re-establishes the relationship between climatic variables and monetised flood damages as shown in Figure 5.13. The breaching failure is assumed to occur when the water level reaches near the crest level of coastal defence. In a more detail, when the water level exceeds 40cm below the crest

of the coastal defence, the breaching is assumed to occur. This deterministic assumption may lead to the overestimation of flood damages. However, as the purpose of this analysis is to understand the effect of breaching failure on option evaluation, this thesis adopts this assumption for the estimation of flood damages. The sections of the coastal defence at the possible breaching points are forcingly lowered by 1m in DEM data. Flood simulations have been conducted with various water levels (i.e. ESWL+SLR+WAVE) by 0.2m increments.

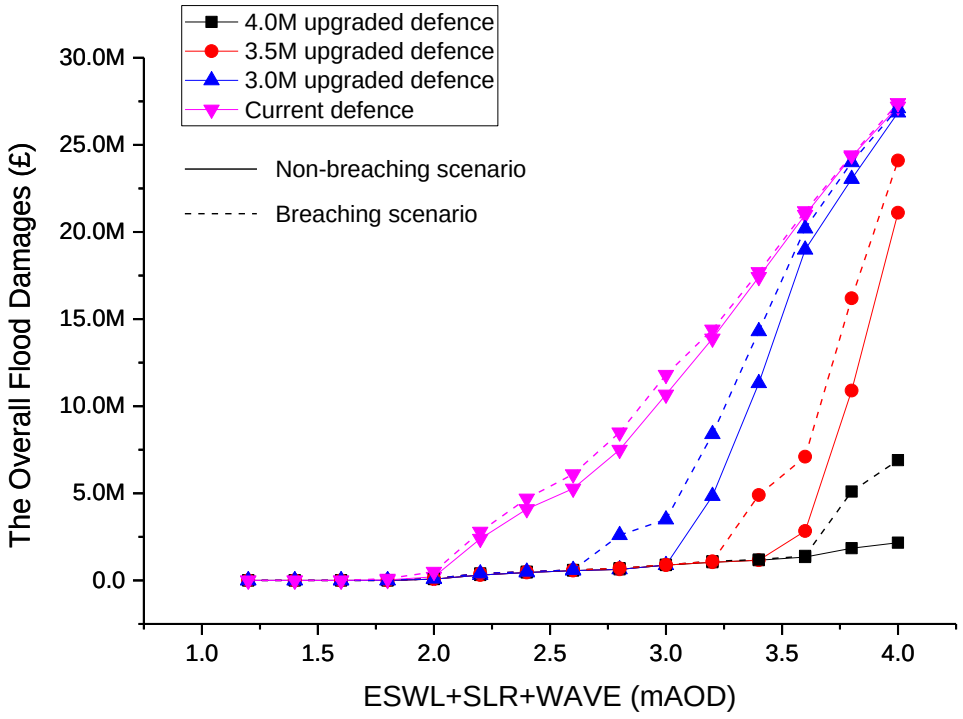

Figure 5.13 Monetised flood damage curves for each defence condition in breaching and non-breaching scenario - which represent relationships between water levels and flood damages.

As illustrated in Figure 5.13, considering the breaching failure in the defence failure scenarios changes flood damage-water level relations over climatic variables. The flood damages by high water levels near the crest of coastal defence are increased as shown in Figure 5.13. This leads to increase in EAD for each coastal defence condition. Subsequently, the EAB from the adaptation measure changes due to the inclusion of the breaching failure mode. Based on the estimation of EAB for an adaptation measure (i.e. $U_{c\rightarrow 3.5m}$), the termination and continuation curves have been drawn in Figure 5.14.

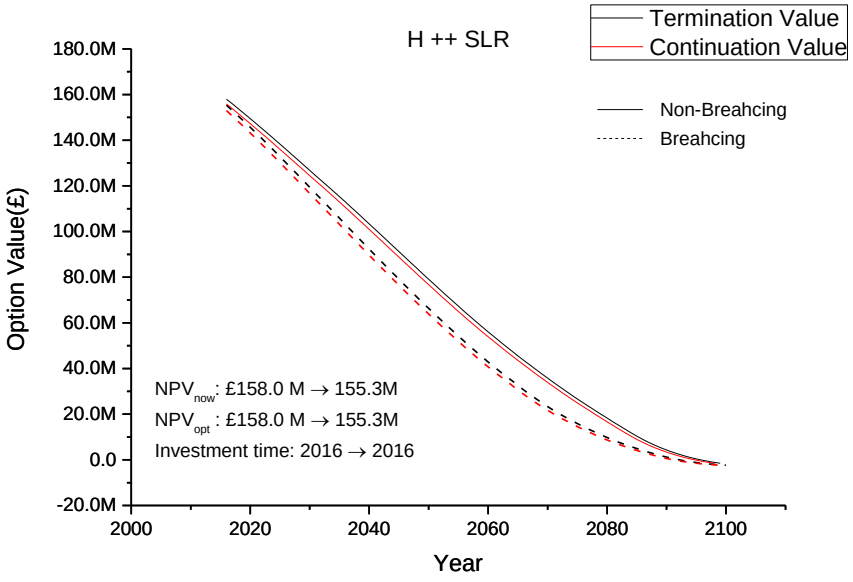

(a)

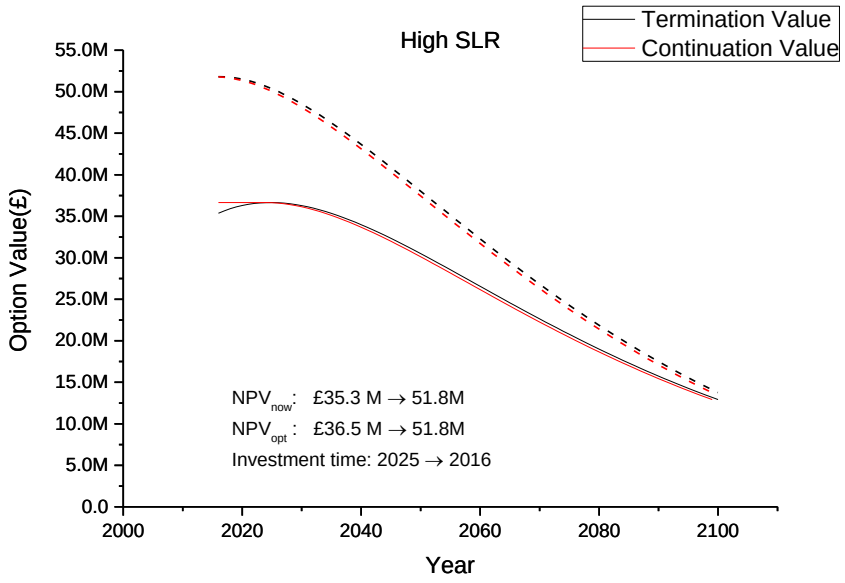

(b)

Figure 5.14 The option values (i.e. NPV_{now} and NPV_{opt}) and optimal investment times in breaching (dash line) and non-breaching scenario (solid line) for (a) H++ SLR scenario and (b) High SLR scenario

As shown in Figure 5.14, the curves of the termination and continuation value have been changed due to the inclusion of the breaching failure. For the H++ SLR scenario, the option value drops as a whole whereas, for the High SLR scenario, the option value increases up. This contradiction is due to the capacity limit of the coastal defence to protect the floodplain against coastal flooding. For instance, in the H++ SLR scenario, extreme flood events with

water levels over 3.5 mAOD can occur frequently. This extremity of coastal flooding is more likely to exceed the capacity limit of the upgraded defence condition. Thus, it may cause breaching more frequently even if the coastal defence has been upgraded. The effect of the adaptation measure (i.e. $U_{c\rightarrow 3.5\mathrm{m}}$) becomes less useful at such an extreme still water level. This leads to the overall decreases in EAB and, subsequently, option values. It implies that the coastal defence needs to be strong enough to withstand the extreme coastal flooding, if sea-level rise follows the H++ SLR scenario. On the other hand, in the High SLR scenario, the upgraded coastal defence can cover the extremity of coastal flood events in which an expected maximum water level is approximately 3.0 mAOD. This height is within the protective capacity of the upgraded coastal defence. Thus, the upgraded coastal defence reduces the risk of breaching failure, leading to increase in the utility of the upgraded coastal defence. Also, the option values of NPV_{now} and NPV_{opt} increase, as a whole, with the early occurrence of the optimal investment time in the High SLR scenario.

As investigated, different defence failure modes need to be considered for the estimation of option values and optimal investment times. However, the dynamics of coastal flooding combined with various defence failure modes are very complicated to describe only with flood damage curves and benefit curves used in this thesis. In addition, as this analysis assumes that the defence breaching at extreme water levels near or above the defence crest occurs with a probability of 1.0, the flood damages obtained here might have been overestimated. In this respect, the results of real options analysis are conditional on the assumption of defence failure modes. Nevertheless, this approach enables us to have an important insight into how to include various defence failure modes in option evaluations and how the flood-damages curves affect the results of real options analysis.

5. 4 Real options analysis in the stochastic case of sea-level rise (Brownian motion)

The previous section has applied real options analysis only in the MSLR scenarios. As done in the case of MSLR, the real option approach can be applied for the stochastic process of sea-level rise (i.e. Brownian sea-level rise). This is a special case made upon an assumption that sea-level rise can be described with Brownian motion (Refer to Section 4.2.3). The dynamic programming approach has been applied to calculate option values for randomly evolving sea-level rise which is generated by General Brownian motion. A great number of

stochastic processes of sea-level rise are possible from the Brownian motion. The Brownian motions of sea-level rise from High SLR scenario are produced for the analysis.

As sea-level rise is stochastic variable, EAB is also stochastic variable dependent on sea-level rise. To estimate EAB from the stochastic process of sea-level rise, this thesis establishes a relationship between EAB and SLR as shown in Figure 5.15, which has been made by estimating each EAB by 0.2m-increment of sea-level rise.

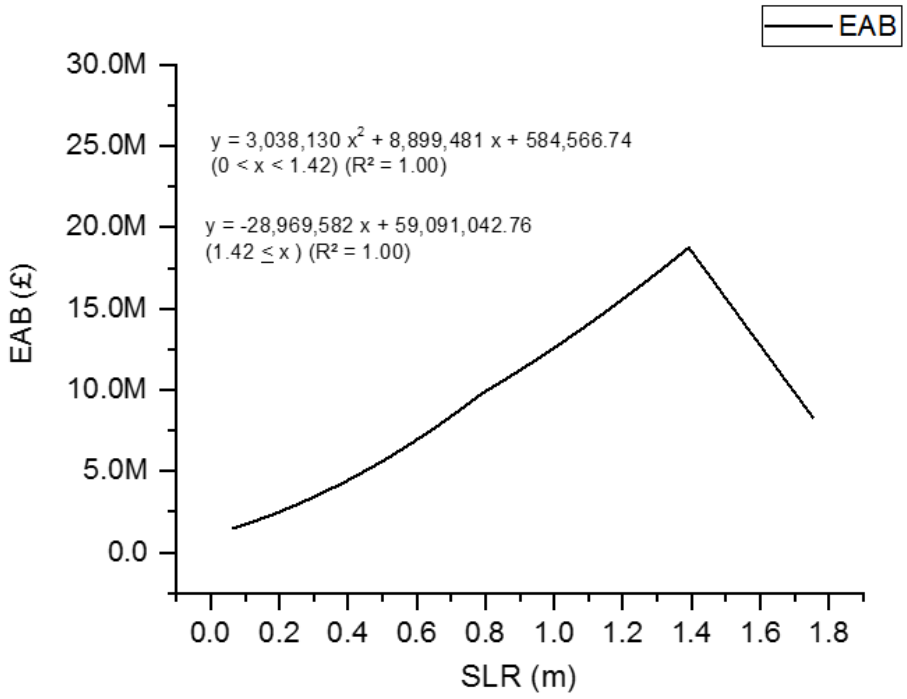

Figure 5.15 Relation between EAB and SLR for the upgrade of coastal defence to 3.5 mAOD

Change in EAB is plotted with the time-series of likely benefit values and their probabilistic ranges (the 5th and 95th percentiles) as shown in Figure 5.16. Thus, the likely flood benefits in Figures 5.16 indicate the performances (i.e. reduction in flood damages) of the coastal adaptation measure against the annual maxima of coastal flood events.

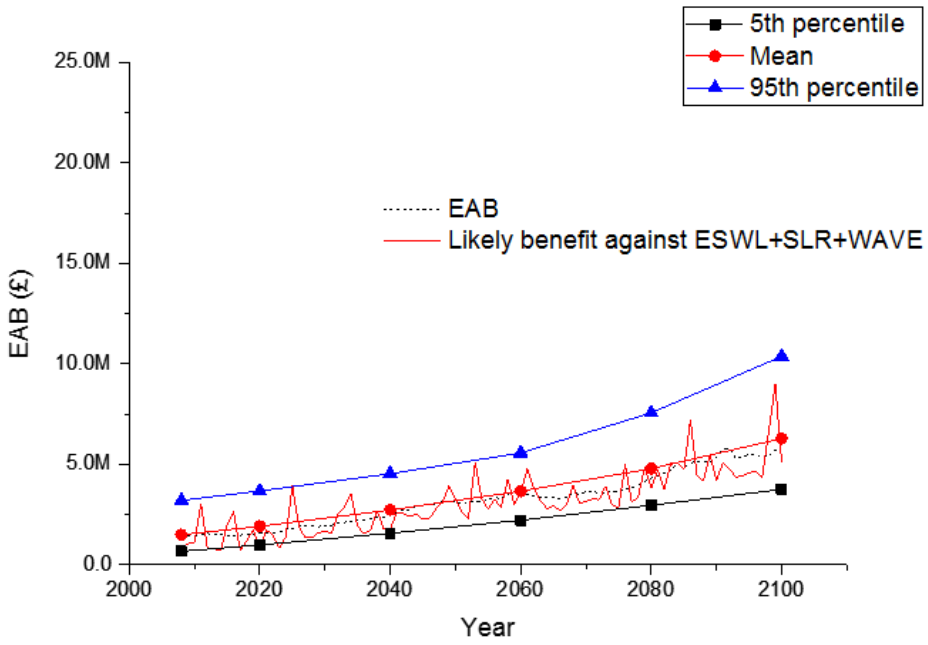

Figure 5.16 Random time-series of EAB (dash line) and likely annual benefits (red solid line) due to the upgraded coastal defence with its probabilistic range for High SLR scenario.

As the evolving patterns of sea-level rise are random, the results of optimal investment time and option values (i.e. NPV_{now} and NPV_{opt}) are also random and uncertain. Figure 5.17 shows changes in sea-level rise and the corresponding option values (i.e. termination and continuation values) for the Brownian motion of sea-level rise and mean sea-level rise, respectively.

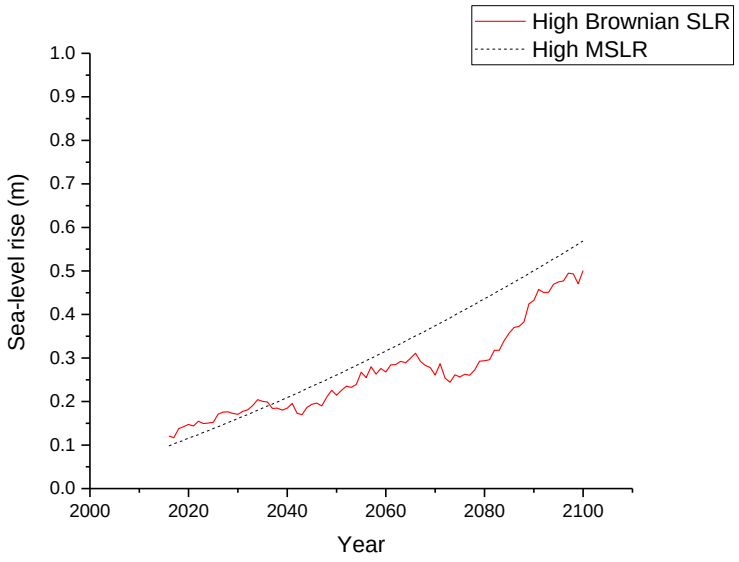

(a)

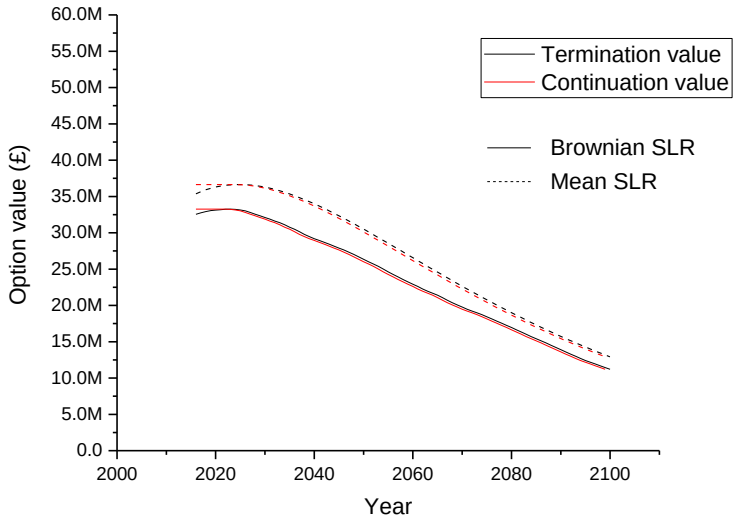

(b)

Figure 5.17 (a) An example of Brownian motion of High SLR with mean sea-level rise (dash); and (b) option values by Brownian SLR (solid lines) and Mean SLR (dash lines) – Other examples are shown in Appendix Q

As seen in Figure 5.17, the option value and optimal investment time vary depending on the increasing patterns of sea-level rise over the 21st century. Sea-level rise starts from 12 (cm) at 2016 and keep increasing to 50 cm until 2100. In this pattern of sea-level rise, the optimal investment time occurs around 2023, which is earlier than the optimal investment time (i.e. 2025) for the High MSLR. However, the values of NPV_{now} and NPV_{opt} are smaller than those of the High MSLR scenario. The results of optimal investment time and option values from other patterns of sea-level rise are included in Appendix Q.

This example shows practical issues regarding the uncertainty of sea-level rise. This uncertainty issue is substantial in investment decisions because the optimal investment time and option value randomly vary according to the pattern of sea-level rise. However, a meaningful finding is that the optimal investment time also occurs when sea-level rise reaches the critical threshold value in most SLR patterns shown in Figure 5.18. In the case of MSLR, this thesis has already proved that the optimal investment time for coastal adaptation measure (i.e. $U_{c\to 3.5m}$) in Lymington is when sea-level rise reaches approximately 13 cm.

When we read the values of sea-level rise at the optimal investment time under all the example cases, most values of sea-level rise are found around this critical threshold value (= 13cm) as shown in Figure 5.18. This has an important implication in climate change adaptation decisions. Even though sea-level rise in the future randomly evolves over time, the

investment decision based on the critical threshold value is likely to provide a maximum option value under a materialised sea-level rise. Thus, however sea-level rise evolves in the future, this critical threshold value enables us to find the optimal investment time in the real world.

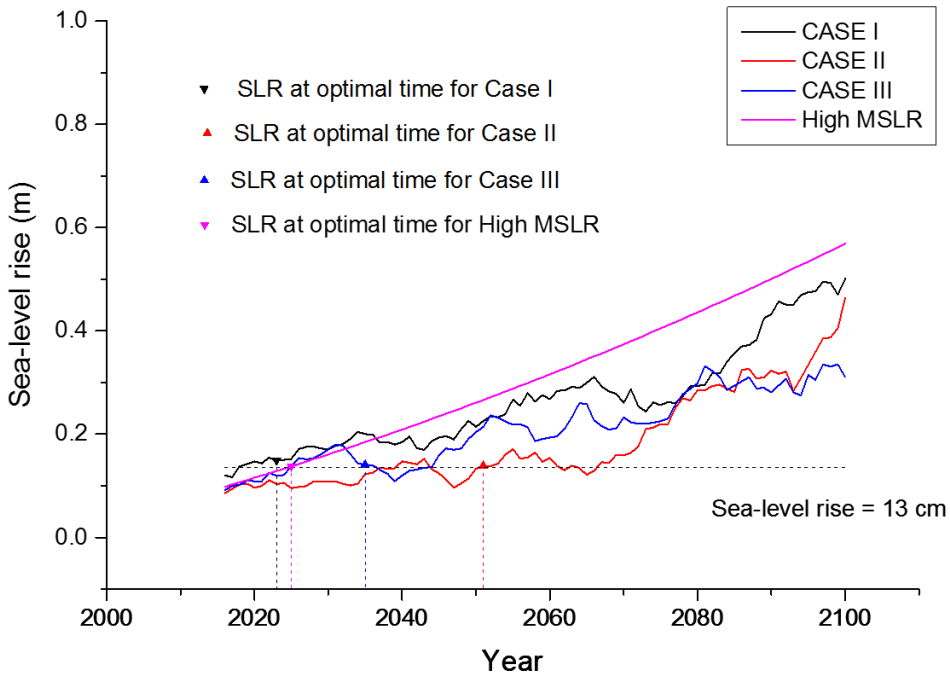

Figure 5.18 Sea-level rise at optimal investment time (indicated by triangles) for each case – years where the vertical dash lines intersect x-axis indicate the optimal investment years for the corresponding sea-level rise patterns. Most values of sea-level rise at the optimal investment times are found near the critical threshold value (13cm).

As seen in Figure 5.18, the values of sea-level rise in Case II and Case III (indicated by red and blue lines) exceed the critical threshold value (i.e. 13cm) before the optimal investment times, drop below it and exceed again. In these cases, the critical threshold value does not seem valid. However, when we observe the termination and continuation values in the Cases II and III (Refer to Appendix Q), the termination value almost reaches the maximum option value when sea-level rise exceeds the critical threshold value. This implies that, if the investment is made at the critical threshold value, the decision is highly likely to provide a maximum option value or, at least, a slightly lower value than its maximum under the given pattern of sea-level rise. To support this argument, this thesis has also derived a formulation to explain a relationship between optimal investment time and critical threshold value in the stochastic case of sea-level rise in Appendix R. The finding of a critical threshold value is very important in investment timing in real-options-based approach because it is a key

indicator to ensure an adaptation option is implemented at the optimal investment time under the uncertainty of sea-level rise. As investigated, this finding is also valid in both cases of deterministic and stochastic SLR scenarios. In this regard, the critical threshold value gives a practical way of how to use the flexibility of wait in climate change adaptation under the uncertainty of magnitudes and patterns of sea-level rise.

5. 5 Summary

This chapter has investigated how a single deferrable adaptation option can be implemented optimally and economically in terms of timing. Through this analysis, it is understood that a decision on whether to invest or wait is closely related to the investment timing. The part of this thesis provides an innovative way to estimate the option values and optimal investment times of a single deferrable adaptation option for all the SLR scenarios in both cases of MSLR and Brownian SLR. The option value increases with time to a maximum (which is a real option value (NPV_{opt}) at optimal investment time) and then decreases again after this time. The analysis suggests that the investment in the upgrade of the coastal defence up to 3.5 mAOD in Lymington needs to be deferred under all the SLR scenarios except the H++ SLR scenario. It has been also demonstrated that the adaptation option implemented at the optimum time statistically has a maximum value with a statistical confidence.

The most important finding for a deferrable adaptation option is that there is an absolute critical value of sea-level rise that indicates the optimal investment time under each SLR scenario. Conversely, the optimal investment time is when sea-level rise reaches this absolute threshold value. For this reason, the real options analysis in climate change adaptation can be supported by an observation process to detect the critical value (in this case, sea-level rise) and optimal investment time. Thus, decision-makers can trigger the adaptation option at the optimal investment time by observing this value in the real world. This chapter suggests that the observation improves the quality of our decisions under the uncertainty of sea-level rise. Also, the absolute sea-level rise enables us to know when the investment should be implemented, even if we do not know the current trajectory of sea-level rise in the real world. Subsequently, the effectiveness of real options approaches will rely on the ability to measure the amount of sea-level rise relative to a base year (i.e. 1990).

In application of real options analysis in climate change adaptation, it should be noted that different future growth rates result in different investment times and option values. They also

change the optimal investment time and the critical value of sea-level rise, except for the H++ SLR scenario. Nevertheless, the framework of real options analysis helps to understand which combination of SLR scenario and future development scenario prompts actions in a timely manner with future learning. This analysis enables us to prioritise SLR scenarios and future growth scenarios in time for the investment to gain a maximum option value during the period of the wait.

This chapter has also investigated the option values and optimal investment times of an adaptation option under the breaching scenario. As seen in Figure 5.13., the inclusion of the breaching failure at higher water levels increases expected annual damages in a statistical sense for all the defence conditions. Thus, the changed relations between climatic variables and flood damages or benefits from adaptation measures have altered the optimal investment times and option values in the framework of real options analysis. This thesis assumes that defence breaching will occur at a certain water level in a deterministic way. As well known, the breaching failure is probable, depending on water levels, waves and defence grades. Thus, how to incorporate the probability of breaching failure in the framework of real options analysis needs to be further investigated. Due to the limitation on PhD research, this part is left for future research.

This chapter has also applied the framework of real options analysis for the stochastic case of sea-level rise (i.e. Brownian motion). As sea-level rise is a random process, the option value and optimal investment time are also random depending on the pattern of sea-level rise. However, it has been demonstrated that the critical threshold value of sea-level rise is still valid, indicating optimal investment time in the stochastic case of sea-level rise.
One of issues in this chapter is that a single deferrable adaptation option does not manage the current risk of coastal flooding in Lymington. If we invested in a significant flood defence upgrade in 2016, we might benefit from the upgraded coastal defence immediately. However, this decision closes the future investment opportunity as the investment is irreversible. This balance should be considered in decision-making process. In this context, one question is ‘do we have to wait after a severe flood damage to Lymington?’. The option to wait or the optimal investment time cannot answer this question. As a possible answer, we can reduce an initial size or investment cost of an adaptation option so that it will bring forwards the optimal investment time within a given timescale. However, in this case, as the flexibility disappears after the early investment, the real-options-based approach is of no use in dealing with future uncertainty.

As a possible alternative strategy, we can take multiple-stage investments or growth options by phasing a single-large investment into multiple-stage investments. This type of option including a future extension can manage the current risk of coastal flooding as well as the future risk by the future extension option kept open within the timescale of the adaptation planning. This type of adaptation option is called ‘option to grow’ as reviewed in the literature chapter. The nature and characteristics of multiple-stage adaptation option are different from those of a single deferrable adaptation option. This option will be addressed in the next chapter.

6. Results of real options analysis in future growth options

6. 1 Overview of future growth options

A single deferrable adaptation option cannot manage the current risk of coastal flooding, if the result of real option analysis suggests waiting for a decade or longer. Such decisions may leave people and areas exposed to the risk of climate change during the period of the wait. One of possible ways to address this issue is to transform a single large investment into two or more sequential investments. This type of adaptation strategy is referred to as adaptive management, adaptation pathways approach, dynamic adaptations, option to grow or future growth option (Hallegatte, 2009; Haasnoot et al., 2013; Ranger et al., 2013). In addition, the future extension provides an opportunity to learn the future, thus, leading to more informed decisions in the future (Ranger et al., 2013). In this context, the multiple-stage adaptation option provides some advantages, allowing us to upgrade the coastal defence in response to sea-level rise in the future. The option value of a multiple-stage adaptation is obtained by estimating each stage option of the multiple-stage adaptation. The process to assess a multiple-stage adaptation is shown in Figure 6.1.

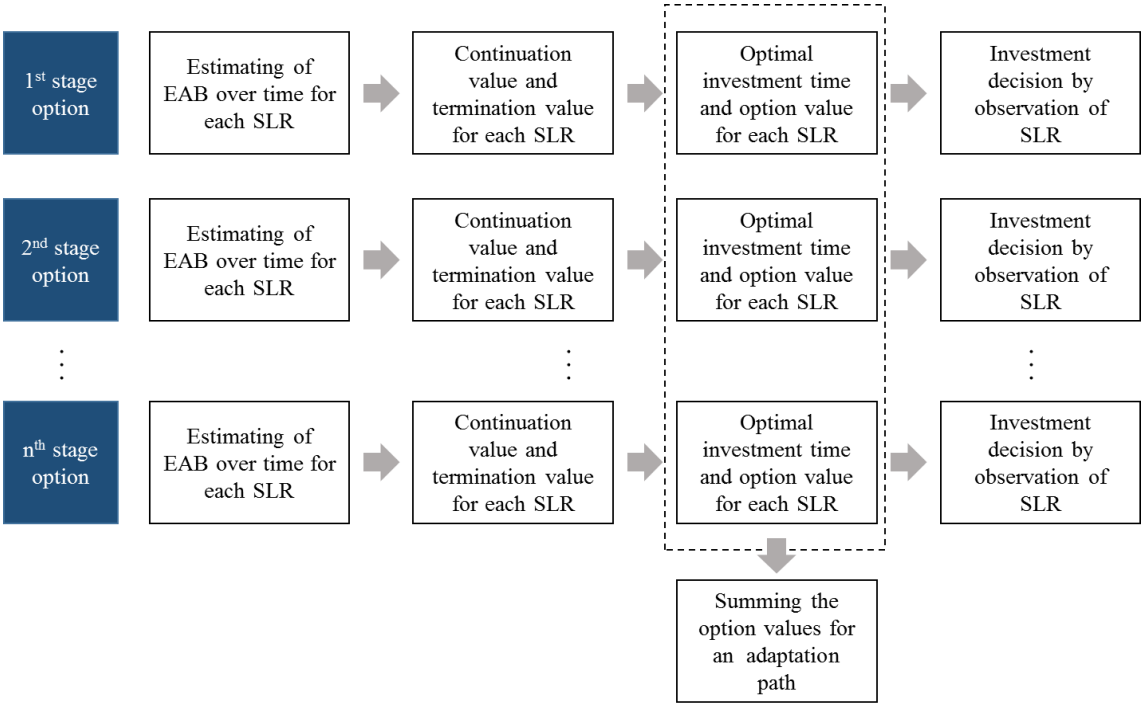

Figure 6.1 The framework of the assessment of multiple-stage adaptation path for option values and optimal investment times

This chapter aims to evaluate the multiple-stage adaptation options under the uncertainty of future climate change and sea-level rise. This chapter is structured as follows. Firstly, this

chapter provides the results of option evaluation for all the adaptation paths by different premium costs in different SLR scenarios. Secondly, the quantitative comparison of all the adaptation paths is conducted to find the most efficient and robust strategy under the uncertainty of SLR scenarios. Lastly, the chapter highlights the result and its implications of the multiple-stage adaptation options in association with real options analysis.

6. 2 The results of option evaluation for multiple-stage adaptation options

6.2.1 Single-stage adaptation paths

For the baseline scenarios of the coastal adaptation measures, this thesis has assessed single-stage adaptation options with the different crest levels of the coastal defence. As the investment in such adaptation options is made at once, there is no additional or premium cost for the single-stage adaptation options. Each of the adaptation options has different option values (i.e. NPV_{opt}, NPV_{now}) and optimal investment times according to SLR scenarios. The results are shown in Table 6.1.

Table 6.1 Option values (i.e. NPV_{now} and NPV_{opt}) of investment now and at the optimal investment time by different MSLR scenarios for each single-stage adaptation option – Note that, if NPV_{now} is maximum, NPV_{opt} is NPV_{now}.

Adaptation paths	SLR scenarios	Investment cost	NPV_{now}	NPV_{opt}	Investment time	SLR at the optimal time
$U_{c\rightarrow 3.0m}$	H++	£ 32.1M	£ 124.8 M	£ 124.8 M	Now (i.e. 2016)	19 cm
	High		£ 67.2 M	£ 67.2 M	Now (i.e. 2016)	10 cm
	Medium		£ 54.9 M	£ 54.9 M	Now (i.e. 2016)	8 cm
	Low		£ 45.7 M	£ 45.7 M	Now (i.e. 2016)	7 cm
	Historic		£ 17.3 M	£ 17.3 M	Now (i.e. 2016)	4 cm
$U_{c\rightarrow 3.5m}$	H++	£ 64.2M	£ 158.0 M	£ 158.0 M	Now (i.e. 2016)	19 cm
	High		£ 35.3 M	£ 36.5 M	2025	14 cm
	Medium		£ 23.2 M	£ 25.5 M	2029	13 cm
	Low		£ 13.9 M	£ 17.7 M	2033	13 cm
	Historic		£ (-) 14.5 M	£ 1.08 M	2083	13 cm
$U_{c\rightarrow 4.0m}$	H++	£ 96.3M	£ 175.4 M	£ 175.4 M	Now (i.e. 2016)	19 cm
	High		£ 3.26 M	£ 20.6 M	2048	25 cm
	Medium		£ (-) 8.98 M	£ 12.4 M	2056	25 cm
	Low		£ (-) 18.2 M	£ 7.2 M	2066	25 cm
	Historic		£ (-) 46.6 M	£ (-) 0.84 M	No investment	-

6.2.2 Two-stage adaptation paths

The option values of two-stage adaptations have been estimated under different SLR scenarios. At first, we have divided the single-stage adaptation up to 3.5 mAOD or 4.0 mAOD into two-stage adaptations, respectively. The possible two-stage adaptation paths for the upgrade of the coastal defence are denoted by

- Coastal defence upgrade up to 3.5 mAOD: $U_{c\to 3.0m} * U_{3.0m\to 3.5m}$
- Coastal defence upgrade up to 4.0 mAOD: $U_{c\to 3.0m} * U_{3.0m\to 4.0m}$ or $U_{c\to 3.5m} * U_{3.5m\to 4.0m}$

If a single-stage investment is divided into two sequential investments, it causes an additional cost (defined as a premium cost) for including flexibility in the two-stage investments. Thus, this thesis assumes that the premium cost is added to the cost of the two-stage adaptations with the variation of the premium cost from 20% to 50% of the overall investment cost (i.e. I_{premuim} = percentage × $I_{\text{overall cost}}$).

(1) $\boldsymbol{U_{c\to 3.0m} * U_{3.0m\to 3.5m}}$

When the coastal defence is raised to 3.0 mAOD, the optimal investment time occurs now (i.e. 2016) for all the SLR scenarios because the initial investment cost in the first stage is the least among all the adaptation options. However, for the Historical trend scenario, the upgrade of the crest level to 3.0 mAOD needs to be awaited until 2025, 2033 and 2042 for 30%, 40% and 50% premium cost scenarios, respectively.

For the H++ SLR scenario, the occurrence of extreme storm surges over 3.0 mAOD is expected to become more frequent from 2050 onwards. As sea-level rise is around 1.75m at the end of the 21st century in this scenario, the further upgrade will be needed to protect Lymington in the future.

On the contrary, for other mild SLR scenarios, storm surge events over 3.0 mAOD will rarely occur during the 21st century. Thus, over 3.0 mAOD level coastal defence is considered as redundancy based on the current analysis. In the High SLR scenario, sea-level rise is expected to be around 0.5m in 2100. In this scenario, the implementation of the second adaptation option will be needed at the end of 21st century (i.e. 2100). In other milder SLR scenarios than the High SLR scenario, the second adaptation option is not needed. The option values and the optimal investment times of the second adaptation option ($U_{3.0m\to 3.5m}$) have also been estimated in response to the realisation of different SLR scenarios. The results of option evaluations are shown in Table 6.2.

Table 6.2 Option values (NPV_{opt}) and optimal investment times (OIT) by different premium costs in different SLR scenarios for the adaptation path of $U_{c\to 3.0m} * U_{3.0m\to 3.5m}$.

SLR scenario	Premium scenario	The first phase adaptation ($U_{c\to 3.0m}$)			The second phase adaptation ($U_{3.0m\to 3.5m}$)			The overall adaptations ($U_{c\to 3.0m} * U_{3.0m\to 3.5m}$)	
		$I+I_{prem}$ (£ M)	NPV_{OPT} (£ M)	OIT	$I+I_{prem}$ (£ M)	NPV_{OPT} (£ M)	OIT	$I+I_{prem}$ (£ M)	NPV_{OPT} (£ M)
H++	20%	38.52	118.4	Now	38.52	38.2	2048	77.04	156.6
	30%	41.73	115.3	Now	41.73	37.6	2049	83.46	152.9
	40%	44.94	112.0	Now	44.94	36.6	2051	89.88	148.6
	50%	48.16	108.8	Now	48.16	35.7	2052	96.33	144.5
High	20%	38.52	60.6	Now	38.52	0.92	2100	77.04	61.52
	30%	41.73	57.4	Now	41.73	0.81	2100	83.46	58.21
	40%	44.94	54.32	Now	44.94	0.64	2100	89.88	54.96
	50%	48.16	50.9	Now	48.16	0.46	2100	96.33	51.36
Medium	20%	38.52	48.5	Now	38.52(0)	-1.0 (0)	-	38.52	48.5
	30%	41.73	45.4	Now	41.73(0)	-1.1 (0)	-	41.73	45.4
	40%	44.94	42.2	Now	44.94(0)	-1.3 (0)	-	44.94	42.2
	50%	48.16	38.9	Now	48.16(0)	-1.5 (0)	-	48.16	38.9
Low	20%	38.52	39.3	Now	38.52(0)	-1.6 (0)	-	38.52	39.3
	30%	41.73	36.2	Now	41.73(0)	-1.7 (0)	-	41.73	36.2
	40%	44.94	32.9	Now	44.94(0)	-1.9 (0)	-	44.94	32.9
	50%	48.16	29.6	Now	48.16(0)	-2.0 (0)	-	48.16	29.6
Historical Trend	20%	38.52	10.9	Now	38.52(0)	-2.1 (0)	-	38.52	10.9
	30%	41.73	8.3	2025	41.73(0)	-2.3 (0)	-	41.73	8.3
	40%	44.94	6.1	2033	44.94(0)	-2.4 (0)	-	44.94	6.1
	50%	48.16	4.6	2042	48.16(0)	-2.6 (0)	-	48.16	4.6

* In the second phase, if NPV_{opt} is estimated to be negative, there is no need to invest in the second phase upgrade. Thus, the investment cost and NPV_{opt} is represented to be zero.

- For the H++ SLR scenario, the first and second adaptation options will be implemented with the optimal investment time of 2016 and 2048 to 2052, respectively. The investment costs for the first and second adaptations will be spent at the corresponding investment years. In the end, the option value of the adaptation path $U_{c\to 3.0m} * U_{3.0m\to 3.5m}$ is expected to reach £ 156 M to 144 M, depending on premium costs, with the overall investment cost to be £ 77 M to 96 M in the H++ SLR scenario.
- In the High SLR scenario, the first and second adaptation will be also implemented with the investment time of 2016 and 2100. However, the investment time of the second adaptation option is so far from the present that the option value from the second adaptation option is very small ranging from £ 0.46 M to 0.92 M. The overall investment cost spent in the High SLR scenario is the same with the overall cost in the

H++ SLR scenario. However, the overall option value is much lower than in the H++ SLR scenario, while it is higher than in other milder SLR scenarios.

- In the Medium, Low and Historical trend SLR scenarios, the first adaptation option is implemented whereas the second adaptation option will not be done. The overall investment cost is estimated to be £ 38.52 M to 48.16 M, which is much lower than the investment cost in the High and H++ SLR scenario.

The faster sea levels rise, the higher the overall option value of the adaptation option will be. In addition, as the premium cost increases, the overall option value decreases. The overall investment costs and option values for different SLR scenarios have been assessed in the last columns of Table 6.2.

(2) $U_{c\rightarrow 3.5m} * U_{3.5m\rightarrow 4.0m}$

The two-stage upgrade of the coastal defence up to 3.5 mAOD cannot protect Lymington from extreme water levels above 3.5 mAOD. The coastal defence upgrade up to 4.0 mAOD level may be needed if the most extreme coastal flood event is expected to occur (i.e. the H++ SLR scenario). The adaptation path with the start of 3.5 mAOD level upgrade in the first stage may be more efficient in the H++ SLR scenario than an adaptation path starting 3.0 mAOD level coastal defence in the first stage. Although this option appears to be similar to the single-stage adaptation up to 3.5 mAOD level ($U_{c\rightarrow 3.5m}$) at the outset, the investment cost for $U_{c\rightarrow 3.5m} * U_{3.5m\rightarrow 4.0m}$ is higher due to the premium cost for flexibility or future extension, than the single-stage adaptation (i.e. $U_{c\rightarrow 3.5m}$). Table 6.3 shows the results of $U_{c\rightarrow 3.5m} * U_{3.5m\rightarrow 4.0m}$ by different premium costs ($I_{premium}$) in different SLR scenarios.

- For H++ SLR scenario, the first and second adaptation option will be implemented with the investment time of 2016 and 2068 to 2077, respectively. As the overall investment cost increases due to increase in the overall size of the coastal defence, the investment time of the second adaptation occurs later than that in $U_{c\rightarrow 3.0m} * U_{3.0m\rightarrow 3.5m}$.
- In High, Medium and Low SLR scenarios, the first adaptation option will be implemented with the different investment time depending on the SLR scenarios and premium costs. However, the second adaptation option will not be implemented in the future. This is a case where the investment cost is too high for the first stage investment to proceed.

- No investment will be made in the Historical trend SLR scenario.

Overall, the optimal investment time in this adaptation path is later than the adaptation path of $U_{c\rightarrow 3.0m} * U_{3.0m\rightarrow 3.5m}$. In addition, the option value is much lower than the former adaptation path in all the SLR scenarios except the H++ SLR scenario.

Table 6.3 Option values (NPV_{opt}) and optimal investment times (OIT) by different premium values in different SLR scenarios for the adaptation path of $U_{c\rightarrow 3.5m} * U_{3.5m\rightarrow 4.0m}$

SLR scenario	Premium scenario	The first phase adaptation ($U_{c\rightarrow 3.5m}$)			The second phase adaptation ($U_{3.5m\rightarrow 4.0m}$)			The overall adaptations ($U_{c\rightarrow 3.5m} * U_{3.5m\rightarrow 4.0m}$)	
		$I+I_{prem}$ (£ M)	NPV_{OPT} (£ M)	OIT	$I+I_{prem}$ (£ M)	NPV_{OPT} (£ M)	OIT	$I+I_{prem}$ (£ M)	NPV_{OPT} (£ M)
H++	20%	73.89	146.5	Now	41.79	13.89	2068	116.28	160.39
	30%	78.74	143.5	Now	46.63	13.62	2071	125.97	157.12
	40%	83.58	138.6	Now	51.48	12.82	2074	135.66	151.42
	50%	88.42	133.8	Now	56.32	12.31	2077	145.35	146.11
High	20%	73.89	30.4	2032	41.79(0)	-2.32(0)	-	73.89	30.4
	30%	78.74	27.8	2036	46.63(0)	-2.59(0)	-	78.74	27.8
	40%	83.58	25.5	2039	51.48(0)	-2.86(0)	-	83.58	25.5
	50%	88.42	23.5	2043	56.32(0)	-3.13(0)	-	88.42	23.5
Medium	20%	73.89	20.1	2038	41.79(0)	-2.32(0)	-	73.89	20.1
	30%	78.74	18	2042	46.63(0)	-2.59(0)	-	78.74	18
	40%	83.58	16.2	2046	51.48(0)	-2.86(0)	-	83.58	16.2
	50%	88.42	14.6	2050	56.32(0)	-3.13(0)	-	88.42	14.6
Low	20%	73.89	13.3	2044	41.79(0)	-2.32(0)	-	73.89	13.3
	30%	78.74	11.5	2049	46.63(0)	-2.59(0)	-	78.74	11.5
	40%	83.58	10.1	2054	51.48(0)	-2.86(0)	-	83.58	10.1
	50%	88.42	8.9	2058	56.32(0)	-3.13(0)	-	88.42	8.9
Historical Trend	20%	73.89(0)	-1.6(0)	-	41.79(0)	-2.32(0)	-	0	0
	30%	78.74(0)	-1.9(0)	-	46.63(0)	-2.59(0)	-	0	0
	40%	83.58(0)	-2.1(0)	-	51.48(0)	-2.86(0)	-	0	0
	50%	88.42(0)	-2.4(0)	-	56.32(0)	-3.13(0)	-	0	0

(3) $U_{c\rightarrow 3.0m} * U_{3.0m\rightarrow 4.0m}$

The previous two-stage upgrades have evenly distributed a premium cost into each stage of the adaptation path. When considering a higher standard-of-protection coastal defence in the final stage, the distribution rule for investment and premium cost needs to be modified to allocate more costs in the first stage than in the later stage. For example, the first-stage upgrade in an adaptation path which is designed to be raised up to 4.0 mAOD in all the stages should cost more than the first upgrade in an adaption path raised up to 3.5 mAOD. This implies that the part of construction work (e.g. strengthening the base) for the future

extension should be conducted in the first stage. Therefore, the cost of the first-stage upgrade up to 3.0 mAOD has been estimated with in mind the future extension up to 4.0 mAOD. Firstly, we have evenly divided the overall investment cost (i.e. $I + I_{premium}$) for $U_{c\to 3.0m} * U_{3.0m\to 4.0m}$ into the first and the second stage. After the first upgrade of the coastal defence is made up to 3.0 mAOD, we can upgrade the coastal defence from 3.0 mAOD to 4.0 mAOD in response to sea-level rise. Table 6.4 shows the option values of $U_{c\to 3.0m} * U_{3.0\to 4.0m}$ under different SLR scenarios and premium cost scenarios.

Table 6.4 Option values (NPV_{opt}) and optimal investment times (OIT) by different premium values in different SLR scenarios for the adaptation path of $U_{c\to 3.0m} * U_{3.0m\to 4.0m}$.

SLR scenario	Premium scenario	The first phase adaptation ($U_{c\to 3.0m}$)			The second phase adaptation ($U_{3.0m\to 4.0m}$)			The overall adaptations ($U_{c\to 3.0m} * U_{3.0m\to 4.0m}$)	
		$I+I_{prem}$ (£ M)	NPV_{OPT} (£ M)	OIT	$I+I_{prem}$ (£ M)	NPV_{OPT} (£ M)	OIT	$I+I_{prem}$ (£ M)	NPV_{OPT} (£ M)
H++	20%	58.14	99.11	Now	58.14	54.97	2050	116.28	154.08
	30%	62.98	94.27	Now	62.98	53.49	2051	125.97	147.76
	40%	67.83	89.42	Now	67.83	52.04	2052	135.66	141.46
	50%	72.68	84.57	Now	72.68	50.63	2052	145.35	135.20
High	20%	58.14	41.43	2019	58.14(0)	-0.17(0)	-	58.14	41.43
	30%	62.98	37.70	2023	62.98(0)	-0.41(0)	-	62.98	37.70
	40%	67.83	33.91	2028	67.83(0)	-0.71(0)	-	67.83	33.91
	50%	72.68	30.86	2031	72.68(0)	-0.97(0)	-	72.68	30.86
Medium	20%	58.14	29.77	2022	58.14(0)	-2.10(0)	-	58.14	29.77
	30%	62.98	26.48	2027	62.98(0)	-2.34(0)	-	62.98	26.48
	40%	67.83	23.19	2032	67.83(0)	-2.64(0)	-	67.83	23.19
	50%	72.68	20.64	2037	72.68(0)	-2.91(0)	-	72.68	20.64
Low	20%	58.14	21.49	2027	58.14(0)	-2.69(0)	-	58.14	21.49
	30%	62.98	18.66	2032	62.98(0)	-2.94(0)	-	62.98	18.66
	40%	67.83	15.86	2037	67.83(0)	-3.23(0)	-	67.83	15.86
	50%	72.68	13.70	2042	72.68(0)	-3.50(0)	-	72.68	13.70
Historical Trend	20%	58.14	1.89	2067	58.14(0)	-3.23(0)	-	58.14	1.89
	30%	62.98	1.26	2018	62.98(0)	-3.48(0)	-	62.98	1.26
	40%	67.83	0.77	2092	67.83(0)	-3.77(0)	-	67.83	0.77
	50%	72.68	0.47	2100	72.68(0)	-4.04(0)	-	72.68	0.47

- In the H++ SLR scenario, the first and second adaptation option will be implemented with the investment time of 2016 and 2050 to 2052, respectively. The overall investment cost is expected to be £ 116 M to 145 M with the overall option value of the adaptation path to be £ 154 M to 135 M, respectively.

- In the High to Low and Historical Trend SLR scenarios, the first adaptation option will be implemented while the second adaptation option will not be done. The overall investment cost will be spent on the first stage adaptation option in these scenarios. The investment time of the first adaptation option is sensitive to the premium values and SLR scenarios.

6.2.3 Three-stage adaptation ($U_{c\rightarrow 3.0m} * U_{3.0m\rightarrow 3.5m} * U_{3.5m\rightarrow 4.0m}$)

The three-stage adaptation option gives more flexible paths that decision-makers can take in response to sea-level rise. This adaptation path is also more robust against the risk and uncertainty of coastal flooding than the previous two-stage adaptation paths. However, the three-stage adaptation option requires more premium cost than the two-stage adaptation option due to the increase in flexibility. In the three-stage adaptation path, the distribution rule of the investment cost can be applied simply by dividing the second-stage adaptation ($U_{3.0\rightarrow 4.0m}$) into two-stage adaptations ($U_{3.0\rightarrow 3.5m} * U_{3.5\rightarrow 4.0m}$). Thus, the three-stage adaptation path can be made by paying more premium cost for the second adaptation option ($U_{3.0\rightarrow 4.0m}$) of $U_{c\rightarrow 3.0m} * U_{3.0\rightarrow 4.0m}$ in the future. The result of option values for the three-stage adaptation according to SLR scenarios are shown in Table 6.5.

- The option value and optimal investment time of the first adaptation ($U_{c\rightarrow 3.0m}$) are the same with those of the first adaptation in $U_{c\rightarrow 3.0m} * U_{3.0\rightarrow 4.0m}$ for all the SLR scenarios.
- In the H++ SLR scenario, all the adaptation options are to be implemented with the investment time of 2016, 2045 to 2055 and 2069 to 2081 for the first, second and third adaptation option, respectively. The overall investment cost is the highest among all the adaptation paths.
- In the High SLR scenario, the first and second adaptation option will be implemented while the third option will be left without investment. The overall option value is expected to reach £ 42 M to 30 M with the overall cost to be £ 93 M to 127 M.
- In the Medium to Low and Historical Trend SLR scenarios, only the first stage adaptation option will be implemented with the overall investment cost ranging from £ 58.14 M to 72.68 M. The overall option value varies depending on the premium costs and SLR scenarios.

Table 6.5 Option values (NPV_{opt}) and optimal times (OIT) by different premium values in different SLR scenarios for the adaptation path of $U_{c\to 3.0m} * U_{3.0m\to 3.5m} * U_{3.5m\to 4.0m}$

SLR scenario	Pre-mium	The first phase adaptation ($U_{c\to 3.0m}$)			The second phase adaptation ($U_{3.0m\to 3.5m}$)			The third phase adaptation ($U_{3.5m\to 4.0m}$)			The overall adaptations	
		$I + I_{prem}$ (£ M)	NPV_{OPT} (£ M)	OIT	$I + I_{prem}$ (£ M)	NPV_{OPT} (£ M)	OIT	$I + I_{prem}$ (£ M)	NPV_{OPT} (£ M)	OIT	$I + I_{prem}$ (£ M)	NPV_{OPT} (£ M)
H++	20%	58.14	99.11	Now	34.89	39.54	2045	34.89	14.29	2069	127.91	152.94
	30%	62.98	94.27	Now	40.94	37.48	2049	40.94	13.99	2080	144.86	145.74
	40%	67.83	89.42	Now	47.48	35.51	2053	47.48	13.27	2080	162.79	138.2
	50%	72.68	84.57	Now	54.51	33.63	2055	54.51	12.80	2081	181.70	131
High	20%	58.14	41.43	2019	34.89	1.13	2100	0	0	-	93.03	42.56
	30%	62.98	37.70	2023	40.94	0.79	2100	0	0	-	103.92	38.49
	40%	67.83	33.91	2028	47.48	0.43	2100	0	0	-	115.31	34.34
	50%	72.68	30.86	2031	54.51	0.04	2100	0	0	-	127.19	30.9
Medium	20%	58.14	29.77	2022	0	0	-	0	0	-	58.14	29.77
	30%	62.98	26.48	2027	0	0	-	0	0	-	62.98	26.48
	40%	67.83	23.19	2032	0	0	-	0	0	-	67.83	23.19
	50%	72.68	20.64	2037	0	0	-	0	0	-	72.68	20.64
Low	20%	58.14	21.49	2027	0	0	-	0	0	-	58.14	21.49
	30%	62.98	18.66	2032	0	0	-	0	0	-	62.98	18.66
	40%	67.83	15.86	2037	0	0	-	0	0	-	67.83	15.86
	50%	72.68	13.70	2042	0	0	-	0	0	-	72.68	13.70
Histori-cal Trend	20%	58.14	1.89	2067	0	0	-	0	0	-	58.14	1.89
	30%	62.98	1.26	2088	0	0	-	0	0	-	62.98	1.26
	40%	67.83	0.77	2092	0	0	-	0	0	-	67.83	0.77
	50%	72.68	0.47	2100	0	0	-	0	0	-	72.68	0.47

6. 3 Quantitative comparisons of the adaptation pathways

The previous section has estimated the option values of the multiple stage adaptation options under all the SLR scenarios by using the framework of real options analysis. The quantified option values of the adaptation paths imply the economic efficiencies or performances of the adaptation options under uncertainty. Two types of flexibilities have been incorporated in the adaptation paths: (1) an ability to defer – option holders can defer an adaptation option to the future; and (2) an ability to split an adaptation option – option holders can take multiple-stage adaptations by dividing an adaptation option into a set of sequential adaptations. Thus, in the former case, the economic efficiency of the adaptation options can be improved by investment timing, while, in the latter case, the economic efficiency of the adaptation options can be increased by incorporating flexibility in the design of the coastal defence upgrade. In this context, the focus of this chapter is on which adaptation path will give us more benefit

under uncertain futures. This question leads us to consider how to transform a single-stage investment into multiple-stage investments in an economically efficient way. Table 6.6 shows the option values of all the adaptation paths considered in the previous section. For comparison, the option values of each adaptation path are plotted across premium costs under each of the SLR scenarios as shown in Figure 6.2. For other SLR scenarios, refer to Appendix S.

Table 6.6 Real option values for each adaptation pathway in a stage, or in two or three stages by different sea-level rise scenarios and premium costs

SLR scenarios	Premium	Adaptation pathways						
		$U_{c\to 3.0m}$	$U_{c\to 3.5m}$	$U_{c\to 3.0m} * U_{3.0m\to 3.5m}$	$U_{c\to 4.0m}$	$U_{c\to 3.5m} * U_{3.5m\to 4.0m}$	$U_{c\to 3.0m} * U_{3.0m\to 4.0m}$	$U_{c\to 3.0m} * U_{3.0m\to 3.5m} * U_{3.5m\to 4.0m}$
H++	20%	**124.8**	158.0	156.6	**175.4**	160.39	154.08	152.94
	30%			152.9		157.12	147.76	145.74
	40%			148.6		151.42	141.46	138.2
	50%			144.5		146.11	135.2	131
High	20%	**67.2**	36.5	61.52	**20.6**	30.4	41.43	42.56
	30%			58.21		27.8	37.70	38.49
	40%			54.96		25.5	33.91	34.34
	50%			51.36		23.5	30.86	30.9
Medium	20%	**54.9**	25.46	48.5	**12.4**	20.1	29.77	29.77
	30%			45.4		18	26.48	26.48
	40%			42.2		16.2	23.19	23.19
	50%			38.9		14.6	20.64	20.64
Low	20%	**45.7**	17.77	39.3	**7.2**	13.3	21.49	21.49
	30%			36.2		11.5	18.66	18.66
	40%			32.9		10.1	15.86	15.86
	50%			29.6		8.9	13.70	13.70
Historic Trend	20%	**17.3**	1.08	10.9	**-0.84**	0	1.89	1.89
	30%			8.3		0	1.26	1.26
	40%			6.1		0	0.77	0.77
	50%			4.6		0	0.47	0.47

* The highest and lowest option values (NPV_{opt}) in each SLR scenario have been written in black and red bold, respectively.

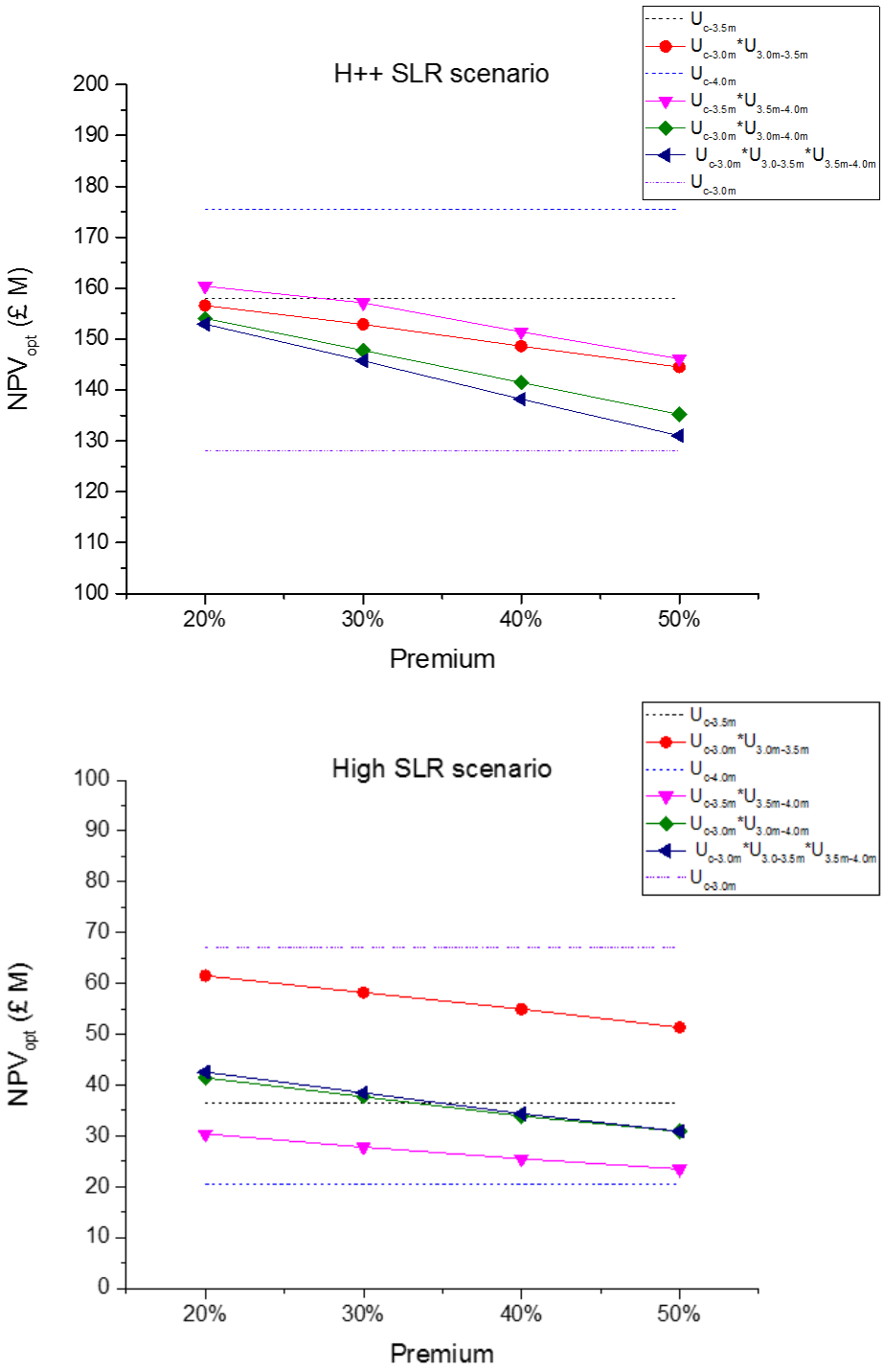

Figure 6.2 Option values (i.e. NPV_{opt}) for each of the adaptation pathways across the premium costs by different SLR scenarios – For other SLR scenarios, refer to Appendix S

For the most extreme SLR scenario (i.e. H++ SLR scenario), the single-stage adaptation path such as $U_{c\to4.0m}$ or $U_{c\to3.5m}$ shows much higher economic efficiency than the multiple-stage adaptation paths. The adaptation paths of $U_{c\to4.0m}$ and $U_{c\to3.5m}$ show the first and second highest option values under the H++ SLR scenario, respectively. When assessing the two-

stage adaptation path of $U_{c\to3.0m} * U_{3.0m\to3.5m}$, $U_{c\to3.0m} * U_{3.0m\to4.0m}$ or $U_{c\to3.5m} * U_{3.5m\to4.0m}$ under the H++ SLR scenario, the adaptation path with the first upgrade of 3.5 mAOD level shows a higher option value than those with the first upgrade of 3.0 mAOD level. As the risk of coastal flooding is very high and sea-level is fast-growing at the rate of 2.54cm/year in the H++ SLR scenario, the real options analysis suggests that the high standard-of-protection coastal defence is economically more efficient for reduction in flood risk. In this scenario, the adaptation paths including $U_{c\to3.0m}$ in the first stage show relatively low economic efficiency than any other adaptation paths because this adaptation option cannot provide sufficient protection for Lymington against the fast-growing risk of coastal flooding under the H++ SLR scenario.

In the High SLR scenario, the economy efficiency of the adaptation pathways shows different patterns from that in the H++ SLR scenario. The largest single-stage investment ($U_{c\to4.0m}$) show the lowest option value whereas the smallest single-stage investment ($U_{c\to3.0m}$) shows the highest option value. In the High SLR scenario, on the whole, the adaptation paths including the first upgrade of $U_{c\to3.0m}$ show higher option values than otherwise. As the High SLR scenario is mild comparing to the H++ SLR scenario, the high standard-of-protection coastal defence is excessive for reducing flood risk in Lymington. Thus, the second-stage adaptation of $U_{3.0m\to3.5m}$ or $U_{3.0m\to4.0m}$ will remain unimplemented as redundancy in the High SLR scenario. The two-stage adaptation path of $U_{c\to3.0m} * U_{3.0m\to3.5m}$ shows the second highest option value in economic efficiency in the High SLR scenario. Thus, unless the worst scenario is expected in the future, the adaptation option of $U_{c\to3.0m}$ or $U_{c\to3.0m} * U_{3.0m\to3.5m}$ is likely to provide the highest option value. The same patterns are also observed in other mild SLR scenarios (i.e. the Medium to Low and Historical trend SLR scenarios).

In addressing the uncertainty of sea-level rise, the adaptation path of $U_{c\to3.0m} * U_{3.0m\to3.5m}$ can be a more robust strategy than $U_{c\to3.0m}$ because $U_{c\to3.0m}$ is very sensitive to the uncertainty of SLR scenarios in terms of economy efficiency. Thus, $U_{c\to3.0m} * U_{3.0m\to3.5m}$ protects floodplains in Lymington more efficiently than $U_{c\to3.0m}$ in most SLR scenarios. In addition, the economy efficiency of the coastal adaptation up to 4.0 mAOD (i.e. $U_{c\to3.0m} * U_{3.0m\to4.0m}$ or $U_{c\to3.0m} * U_{3.0m\to3.5m} * U_{3.5m\to4.0m}$) is lower than that of $U_{c\to3.0m} * U_{3.0m\to3.5m}$ in the High SLR scenario. The coastal defence upgrades above the elevation of 3.0 mAOD are likely to be an over-adaptation in the High SLR scenario.

The high premium cost increases the overall investment cost of the multiple-stage adaptation paths, thus, leading to lowering the economic efficiency of the multiple-stage adaptations. As shown in Figure 6.2, the adaptation pathways of $U_{c\to3.0m} * U_{3.0m\to4.0m}$ and $U_{c\to3.0m} * U_{3.0m\to3.5m} * U_{3.5m\to4.0m}$ are less efficient options in any occasions than the adaptation path of $U_{c\to3.0m} * U_{3.0m\to3.5m}$. This is because high standard-of-protection adaptation paths including a low standard-of-protection adaptation, as a component, lead to incurring the unnecessary large premium cost in the first stage. In addition, the second or third stage upgrade in the high standard-of-protection adaptation paths will not be implemented under the mild SLR scenarios. Thus, such adaptation paths should be rejected in investment decisions under both H++ SLR and High SLR scenarios.

Through the quantification of all the multiple-stage adaptation paths, this chapter could find some important findings that are intuitively or qualitatively understood in the application of multiple-stage adaptation into climate change adaptation. The single-stage investment with the highest standard-of-protection (i.e. $U_{c\to4.0m}$) is the most efficient strategy in the most extreme SLR scenario (i.e. the H++ SLR scenario). However, this adaptation path shows the lowest performance in other SLR scenarios, which means that such a large single-stage investment is very sensitive to the uncertainty of SLR scenarios with its investment efficiency significantly varying according to the SLR scenarios. On the contrary, the smallest single-stage investment (i.e. $U_{c\to3.0m}$) shows the lowest performance in the H++ SLR scenario, while it shows the highest option value in the High SLR scenario. Thus, this option is also sensitive to the uncertainty of SLR scenarios. In this regard, the single-stage adaptation is considered as a less efficient option under the uncertainty of SLR scenarios than the multiple-stage adaptation because the multiple-stage adaptation options allow us to have a choice either to invest in, or to abandon the remaining option after investing in the first-stage option.

6. 4 Summary

This chapter provides a new practical way to quantify multiple-stage adaptation options (or paths) including flexibility by using the framework of real options analysis. The same analytical framework used in the option-to-wait case has been applied to each stage of the multiple-stage adaptation paths. Thus, this analysis provides the option value and optimal investment time of each stage adaptation option under various SLR scenarios. The overall option value of an adaptation path could be obtained just by summing all the option values

from each component of the adaptation path. This option value is a maximum that option holders can achieve by using the flexibility of wait and future growth. The optimal investment can be made by implementing each stage adaptation at each critical threshold value of sea-level rise as done in a single deferrable adaptation option. In this context, a multiple-stage adaptation option or adaptation path is considered as a sequential composite made of many deferrable adaptation options.

As the multiple-stage adaptation has more choices than the single-stage adaptation, this type of adaptation option can make a balance between flood risk and economic efficiency under the uncertainty of sea-level rise. However, as the number of adaptation stages and subsequent premium costs may reduce the economy efficiency of the overall adaptation pathway, the quantitative comparison of adaptation pathways needs to be made to achieve not only robustness but also efficiency against the uncertainty of sea-level rise. This thesis made seven plausible pathways by dividing single-stage adaptation paths into two- or three- stage adaptations with the crest level of the coastal defence to be raised by 0.5 m or 1 m. Through the comparison of the plausible pathways for Lymington, this chapter can discover important findings or suggestions for choosing an economically efficient adaptation path under the uncertainty of sea-level rise.

Firstly, multiple-stage investments are likely to provide larger option values than single-stage investments. It is because the sequential investments provide an opportunity to adjust plans or investment decisions in unexpected or undesirable situations. In this context, if the High SLR scenario is strongly expected, however, with more extreme SLR scenario in mind, choosing a multiple-stage investment is more efficient strategy than a single-stage large investment. This investment decision also enables us to change the adaptation plan in the future in response to sea-level rise.

Secondly, the size and cost of the first stage adaptation play a critical role in increasing the economic efficiency of the adaptation path. Diverse adaptation measures with different sizes and costs in the first stage should be compared with the combination of various possible adaptation pathways in quantitative terms. This comparison makes us understand what adaptation measure should be taken in the first stage. This analysis concludes that the adaptation path of $U_{c\rightarrow 3.0m}$ in the first stage increases the economic efficiency of the overall adaptation pathways and reduces the flood risk of coastal flooding in the early stage for Lymington.

Lastly, it should be noted that, if the premium cost is very high, multiple-stage adaptation paths can be less efficient than single-stage adaptations. Explicitly, many-stage adaptations have the higher degree of flexibility, than one- or two- stage adaptations. However, transforming a single-stage option into multiple-stage options increases the overall cost due to the premium cost. Thus, taking the first-stage adaptation option with a high investment cost may defer the investment time further than it is due. In this respect, if the current risk of coastal flooding is considered to be high, we have to make an effort towards reducing the size of the first-stage adaptation in order to avoid maladaptation or over-investment at the outset.

The quantitative assessment shows us how to economically design or include flexibility in adaptation options under the uncertainty of sea-level rise. By doing this, we can make robust, flexible and efficient adaptation plans lasting for the short- and long- term period. In this context, this chapter has important implications as it helps compare flexible adaptation options under the uncertainty of sea-level rise. This comparison also helps find answers regarding issues raised in a single deferrable adaptation. This aspect will be addressed in discussion chapter.

7. Discussion

The aim of this research is to develop and assess an integrated method for the evaluation of flexible/adaptive strategies that will be implemented in response to the realisation of climate change. This method has been applied to the representative case study area – Lymington on the Solent (UK) - which is or will be susceptible to coastal flooding and sea-level rise. The method used in this thesis can be distinguished from the previous studies by some aspects : (1) using the integrated method of flood risk analysis and real options analysis for flexible adaptation options; (2) allowing the investment time to continuously vary during the period of sea-level rise; (3) evaluating single deferrable adaptation options and multiple-stage adaptation options in the same framework; (4) quantifying different types of adaption options under the deterministic and stochastic cases of sea-level rise, respectively; and (5) incorporating the uncertainties of UKCP 09 SLR projections per se into the framework of real options analysis so as to exclude subjective views towards the future sea-level rise.

This chapter is aimed to discuss the characteristics and implications of the real-options-based approach in a broader context of flood risk management and climate change adaptation. This chapter is structured as follows. Section 7.1 analyses the characteristics of the real option method with potential issues in applications. Section 7.2 provides key findings from the real options analysis into Lymington. Section 7.3 discusses identified issues through the application of real options analysis. Section 7.4 investigates the effects of the assumptions on the results of real options analysis. Lastly, this thesis will reconsider the potentials of real options analysis for the applications to general cases, in comparison to other relevant studies.

7. 1 Reconsideration of the methodology of real options analysis

The core characteristic of real option analysis is to quantify the option value and investment timing of an adaptation option under assumed sea-level rise scenarios (Woodward et al., 2014; Kim et al., 2018). Figure 7.1 summarises the workflow of real-options-based approach used in this thesis. This analysis process aids investment decisions in regard to flexibility under uncertainty with the quantified option values and optimal investment time. For a multiple-stage adaptation option, this evaluation process is repeated for each phase adaptation.

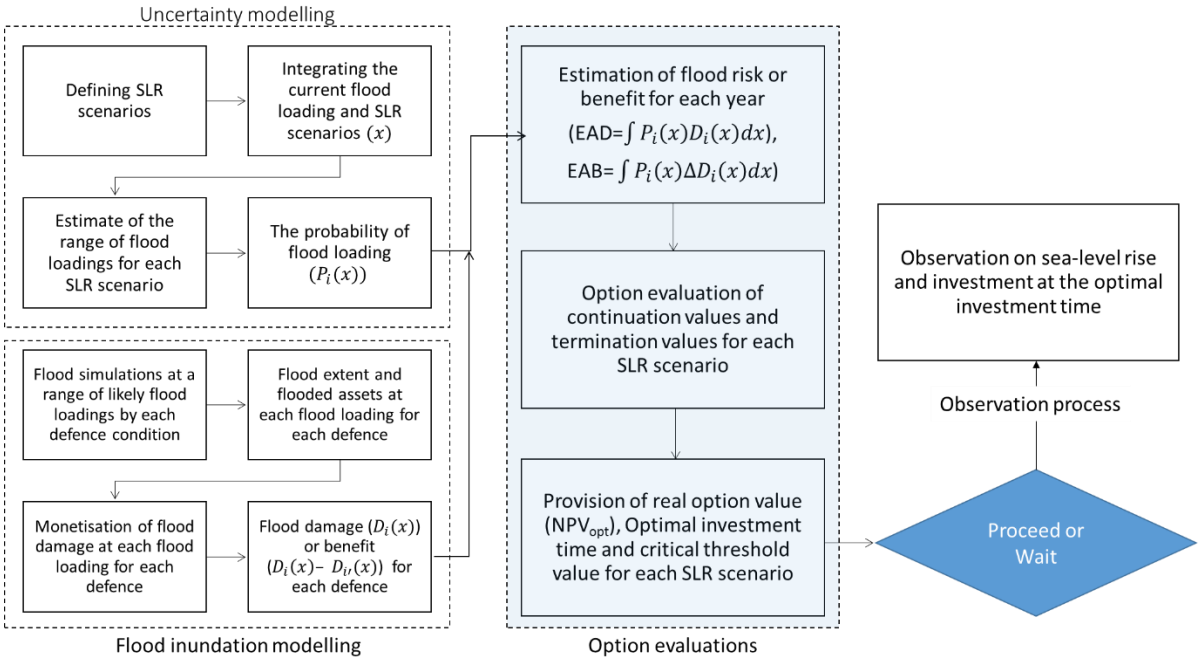

Figure 7.1 Integrated methodology to assess flexible adaptation options under the uncertainty of coastal flooding and sea-level rise. In a multiple-stage adaptation option, the processes are repeated for each phase adaptation option.

For the applications of real options analysis in other climatic events, some important assumptions in the process of real options analysis need to be reconsidered in a broad sense.

Firstly, this thesis assumes that sea-level rise will shift up the probability distribution of return period water levels (i.e. ESWL). Thus, the changed, or newly generated, probability of occurrence of extreme still water levels in a given year is conditional on sea-level rise. All the flood events or damages associated with ESWL+SLR (or Brownian SLR)+WAVE are generated with these conditional probabilities. As the flood dynamics in Lymington are more complicated than represented in this thesis, this probability can be applied only in the modelled conditions in this thesis. If we consider other cases or more complicated flood dynamics, ways to describe the probability of flood loadings should be reconsidered. Nevertheless, this probabilistic analysis enables us to approximate the probability of future flood events affected by sea-level rise. Thus, whether the probability represents real flood events in the future needs to be further investigated with the observation of coastal flood events.

Secondly, this analysis is strongly based on one-to-one correspondence between climatic variables and benefits, or damage values. In fact, a more complicated coastal flood event can be plausible, for example, compound flooding coupled with fluvial flooding or breaching. As

reviewed, the breaching failure mode changes the flood damage and benefit curves in Lymington, leading to changes in the option value and optimal investment time. In addition to this, hydrological and morphological conditions vary over time due to the loss of salt marsh by sea-level rise. All these aspects will change the relationship between climatic variables and flood damages, or benefits from an adaptation measure. Thus, all the factors that may change the relation between climatic variables and flood damages act as uncertainty in real options analysis. In this regard, the flood damage curve is a simplified representation of flood dynamics against the modelled flood loadings. Nevertheless, the relation provides a basis on which this analysis converts the probability of flood loadings into the probability of flood damages or benefits for a defence condition.

Thirdly, the monetisation of flood damages is an essential process to measure the performance of an adaptation option in a monetary term. This process inherently has large uncertainty in its estimation because it is impossible to monetise all the individual flood damages at a great accuracy. Thus, the estimate of a monetised flood damage from the flood damage curve needs to be compared to the real losses from a coastal flooding in Lymington. Due to the lack of data on the monetised flood damages, this validation process could not be conducted in this thesis. To apply real options analysis into other areas or countries, a way to monetise flood damages needs to be prepared prior to flood risk management.

Fourthly, a decision either to invest or defer is made on the expectation of the future values (i.e. EAB) in real options analysis. In the point of a general view, a disastrous flood event in our memory may prompt an adaptation investment rather than the intangible value (i.e. EAB). This thesis also agrees with this general view. However, we strongly argue, at least, in option evaluation that investment decision in an adaptation option should be based on the statistical estimation of flood damages in the future. If not, the investment will go at any occasion. This aspect needs to be discussed in a wider context including other option evaluation approaches (e.g. cost-benefit analysis).

The analysis has adopted a numerical approach to estimate EAB from an adaptation measure. A benefit curve across water levels (i.e. ESWL+SLR+WAVE) for an upgraded coastal defence condition cannot be defined in continuous forms (due to the capacity limit of coastal defence) so that the integral of the benefit curve in respect to climatic variables seems to be implausible. Thus, estimating EAB based on the conditional probability has been aided by Monte-Carlo simulation approach.

To find a maximum option value over investment time, this thesis also employs the dynamic programming approach which compares a continuation and termination value for every year backwardly from the end of time horizon. This method seems to perform well in climate change adaptation where the option values (i.e. NPV_{now} and NPV_{opt}) and EAB of an adaptation option cannot be defined in an analytical or mathematical form. The dynamic programming approach enables us to avoid solving a stochastic differential equation of option value (i.e. NPV_{opt}) in respect to EAB. A programmed Excel spreadsheet has been devised to find the option values and optimal investment time of an adaptation option under various conditions (e.g. cost, discount rate, extreme still water levels) in both deterministic and stochastic cases of sea-level rise.

As climate change occurs in a long-term timescale and its change is very slow, it is very difficult to match the current trajectory of sea-level rise to one of the SLR scenarios provided by UKCP 09 for optimal investment. In fact, the current trajectory of sea-level rise (i.e. 1.8 mm/yr) seems to be far from the UKCP 09 SLR projections. Thus, a focus after the analysis should be on the observation of sea-level rise. Though an absolute sea-level rise also helps us to find the optimal investment time by identifying it, some practical issues are found in the application of the absolute sea-level rise. It is sensitive to investment cost, discount rates, future growth rates and other investment conditions. Thus, the critical threshold value also has uncertainty in itself.

This thesis also finds the optimal investment time upon the assumption of instantaneous construction. As construction work or adaptation measures take many years or decades to complete, the optimal investment seems to be difficult to make in practice. Thus, these limitations need to be further considered for general applications to other cases in climate change.

7. 2 Key findings from application of real options analysis in Lymington

Through the analysis, the thesis has discovered meaningful findings in addressing investment decisions under uncertainty in climate change adaptation as below.

- ✓ The case of single deferrable adaptation options
  - There is a maximum option value (i.e. NPV_{opt}) for an adaptation option, which can be achieved by investing at the optimal investment time

- The maximum option value and optimal investment time of an adaptation option are dependant on investment conditions (e.g. investment costs, discount rates, future growth rates) and environmental conditions (e.g. the rates of sea-level rise, hydrological features of floodplains and defence failure conditions)
- There is an absolute sea-level rise for an adaptation option which constantly occurs at the optimal investment time regardless of the rates of sea-level rise
- An absolute sea-level rise can be used as an indicative value to trigger the adaptation option under the uncertainty of sea-level rise
- The absolute sea-level rise is dependent on the investment cost (I) of an adaptation option and discount rate (r) so that, if the investment cost or discount rate changes, the absolute sea-level rise changes
- The absolute sea-level rise is related to the expected annual benefit (EAB) of an adaptation option at the optimal investment time
- At the optimal investment time, EAB of an adaptation option is the investment cost (I) of the adaptation option times the discount rate (r) (i.e. $EAB = rI$)
- In the most extreme SLR (i.e. the H++ SLR scenario), the investment time is now (i.e. 2016) so that the investment should be made immediately for Lymington
- In the H++ SLR scenario, sea-level rise at the investment time is 19cm. However, as the current sea-level rise in Lymington is 5cm, this scenario does not seem to be the current trajectory of sea-level rise from the present perspective
- The boundary value in real options analysis is defined to be an option value when the investment would be made at the end year of the project period
- The option value of an adaptation option is also affected by the boundary value from which the option value is calculated year-by-year in a backward way
- The more severe the post 2100 SLR scenario is, the higher the boundary value will be. This will lead to increase in the option value of an adaptation option
- There seems to be the limit of the boundary value for an adaptation option due to the capacity limit of coastal defence to protect floodplain against the extremity of coastal flooding
- For Lymington, the investment decision in the adaptation ($U_{c\rightarrow 3.5m}$) should be deferred until sea-level rise relative to 1990 reaches 13 to 14 cm
- The absolute sea-level rise of 13 to 14 cm is valid for the rate of sea-level rise less than 4.9 mm/year

- The optimal investment is likely to provide the highest option value even under the uncertainty of occurrence and magnitude of coastal flooding in a statistical sense
- The future growth rates exponentially increase the option values of adaptation options
- The high future growth rates do not bring forwards the optimal investment time
- The discount rate exponentially decreases the option values of adaptation options while the low discount rate brings forwards the optimal investment time
- There is a critical discount rate which makes the optimal investment time occur at the earliest time for an adaptation option - For Lymington, the critical discount rate is approximately 2 to 2.5 (%)
- If the discount rate is below the critical discount rate, it defers the optimal investment time
- The option value and optimal investment time of an adaptation option is the most sensitive to the investment cost among all the factors
- The periods of sea-level rise projections have no effects on change in option value and optimal investment time
- The long residual life of coastal defence leads to increase in option value with optimal investment time being earlier than the short life of coastal defence
- The inclusion of breaching failure as a possible defence failure mechanism increases EAD or EAB so that the option value of an adaptation option will rise on the whole with the investment time becoming earlier than otherwise
- All the findings observed in the case of mean sea-level rise are also valid in the case of stochastic sea-level rise (i.e. Brownian motion)

✓ The case of multiple-stage adaptation options

- Diverse adaptation paths can be made by dividing a single stage adaptation into sequential investments or multiple-stage investments
- The incorporation of flexibility in multiple-stage adaptation options increases the overall investment cost; although the flexibility increases the investment cost – the increase in the cost is defined as a premium cost
- The conversion of a single-stage adaptation to multiple-stage adaptations may increase or decrease the option value – it depends on the types of the multiple-stage adaptations and the rates of sea-level rise

- The maximum option value of a multiple-stage adaptation can be achieved by implementing each component of the multiple-stage adaptation at each optimal time
- The option value (NPV_{opt}) of the multiple-stage adaptation option differs according to SLR scenarios
- The more extreme sea-level rise is, the higher the option value is for all the adaptation paths.
- When ranking all the possible adaptation paths in terms of option value, multiple stage adaptation options are less sensitive to SLR scenarios than single-stage adaptation options
- The ranking of the adaptation paths in option value (i.e. NPV_{opt}) changes depending on SLR scenarios
- In the H++ SLR scenario, a single-large investment provides the largest option value while a single-small investment does the smallest option value
- In the Historical Trend SLR scenario, a single-small investment gives the largest option value while a single-large investment does the smallest option value
- The multiple-stage adaptation path of $U_{c\rightarrow 3.0m} * U_{3.0\rightarrow 3.5m}$ gives the second largest option value in the High to Low and Historical Trend SLR scenarios and the third largest option value in the H++ SLR scenario – This path seems to be relatively insensitive to the uncertainty of SLR scenarios in comparison to other paths
- The investment cost, or size, of the first-stage adaptation plays a critical role in increasing the economy efficiency of the multiple-stage adaptation option

As reviewed from the application into Lymington case, the real options analysis helps understand the characteristics of flexibility included in adaptation options under the uncertainty of sea-level rise. Through the analysis, we can improve the quality of investment decisions in regard to the use of flexibility with additional information on option values and investment timing. These findings seem to have important implications in addressing uncertainty in investment decisions.

7. 3 Issues and limitations in the application of real options analysis

This thesis could identify some practical issues that need to be further discussed before the application into other cases. This section discusses some important issues in the broad context of real options analysis and climate change adaptation.

(1) Conditional probability of coastal flood event

Firstly, the likelihood of occurrence of coastal flooding at any year is conditional on the combination of sea-level rise and return period water levels. As sea-level rise increases the risk of coastal flooding, the occurrence and magnitude of extreme still water levels have been combined with sea-level rise for flood risk analysis. Thus, EAD or EAB is also conditional on how to combine the probability from extreme still water level with sea-level rise. This leads to a question on whether a newly generated probability represents the true probability of coastal flood events in the future. Extreme water level return periods have been made by a long-term observation; although they have been processed by probabilistic assumptions. Thus, there seems to be no way to validate that this conditional probability represents a real probability of occurrence and magnitude of coastal flood events in the future. The issue on the conditional probability of climatic events may be raised in application of this approach to other cases such as fluvial flooding, agriculture, heatwave and droughts. Those willing to use the framework of real options analysis needs to consider how climate change or global warming affects the probability of climatic events such as rainfall, drought duration, heatwave during the climate change. The non-stationarity of climatic events in climate change adaptation is well-known and substantial issues in the realm of climate change. Thus, the validation process of the conditional probability will be necessary to make this framework applicable to other climate change issues. Nevertheless, the generation of conditional probability gives us a way to quantitatively assess flood risks due to sea-level rise without any adjustment to the statistical properties of coastal events (i.e. extreme still water levels).

(2) Uncertainty in description of flood dynamics in Lymington

The flood simulations have been conducted across various flood loadings (i.e. ESWL+SLR+ WAVE) so that we could have a relation between flood loadings and flood damages. As investigated, the relation is a unique response of floodplain with coastal defence to flood loadings, which is represented by the number of inundated properties or monetary losses from flood damages. This thesis has used LISFLOOD-FP for flood simulation with overflowing and overtopping considered as main defence failure mechanisms. The more complicated defence failure modes are possible such as fluvial flooding, breaching or human's mistake on flood management. Those possible flood events may increase the risk of coastal flooding, although the probability of the occurrence is small. Thus, the inclusion of all the possible

flood events with their own probability in flood risk analysis is impossible due to the lack of our ability to describe physical systems. Although advanced technologies may increase the accuracy of flood simulations, the result of the simulation will remain with the uncertainty. Thus, there is uncertainty in each flood damage curve for coastal defence condition.

The uncertainty in flood damage curves also has influence on the results of real options analysis. As shown in Figure 7.2, if the flood damages are over-estimated across climatic variables, the flood risk of EAD will increase with the probability distribution of flood damage shifted rightwards (Curve B). Otherwise, the flood risk will decrease with the probability distribution moved leftwards (Curve C). The flood simulation has effects on flood risk in this way so that this may lead to the different results of option values and optimal investment times.

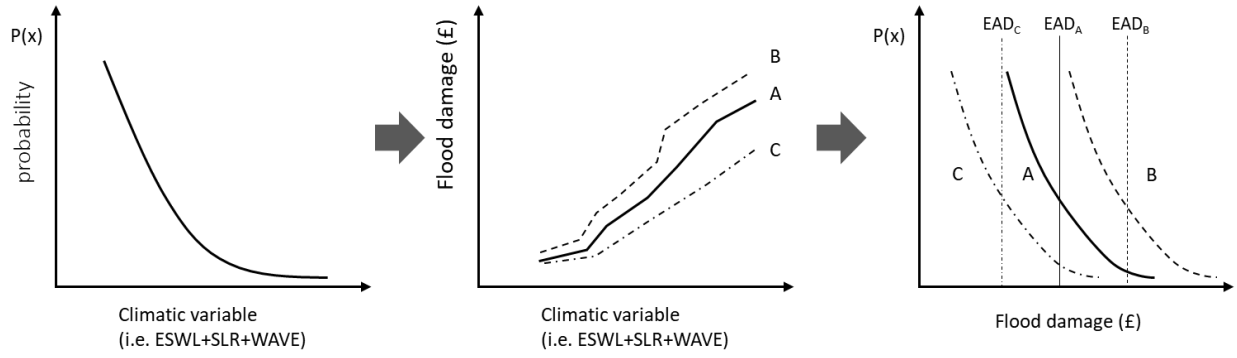

Figure 7.2 Effects of flood damage curves on flood risk or EAD (expected annual damage)

In general, increase in flood risk leads to increase in the utility or effectiveness of adaptation measures because the adaptation measures reduce the flood risk immediately with the investment time becoming earlier than the state of low flood risk. When considering the breaching scenario in Lymington – this case is similar to change in the flood damage curve from A to B (Figure 7.2), the optimal investment is brought forwards from 2029 to 2016 with the option value increased by £ 15 M. From the example, we could understand how the flood damage curve affects the results of real options analysis.

Though we could make more efforts towards increasing the accuracy of flood simulation, this thesis has conducted option evaluations upon the idealised or simplified flood mechanisms. It is because the investment decision on adaptation options is assumed to be made at the level of planning in this thesis. In addition, due to the limitation on the Ph.D. research, it was difficult to allocate much of time and resource on conducting the high accuracy of flood simulations.

Despite those limitations, the flood damage curve for the current defence condition in this thesis relatively agrees well with that from the previous study (Wadey et al., 2012). Thus, the results of flood simulations have been used for the process of real options analysis that is the estimation of EAD or EAB and option evaluations.

(3) The residual life of coastal adaptation

As reviewed, the longevity or residual life of coastal defence also has influence on the option value and optimal investment time of an adaptation option. Generally, the longer the residual life is, the higher the option value will be. This has been observed through the sensitivity analysis. The long life of a coastal adaptation will lead to the optimal investment time being earlier than the short life of a coastal adaptation. The residual life is closely related to the condition of coastal defence. If the coastal defence is well managed with a lot of maintenance cost spent during its life, the residual life will be longer than otherwise. For a sensitivity analysis, this thesis estimates the investment time and option value of an adaptation option with alternations to the residual life of the adaptation. It is found that the option value and optimal investment time is also sensitive to the residual life after the investment cost.

This estimation has been made on an assumption that the benefits will be zero after the life of coastal defence. This is an ideal case because, in reality, flood defence will work after the residual life. However, its performance will become lower. Thus, rather than making the assumption of no benefit from the coastal defence after the residual life, re-estimating the benefit values upon the changed flood-damage curve can provide a more realistic result of real options analysis. This may lead to a less decreased option value and less delayed investment time than assessed. This analysis has simplified an issue on the life of coastal adaptation by applying such an assumption.

(4) Discount rates

Generally, discount rate represents the preference of the present value over the future value in option evaluation (Mandelson et al., 2012). The high discount rate discounts the future cash flows significantly while the low discount rate discounts the future values a little. The discount rate has effects on the option value and optimal investment time of an adaptation option. Thus, the low discount rate gives a high option value while the high rate does a low

option value. The discount rate is a socially agreed value determined by the perceptions and attitudes of societies towards the future. The choice of a discount rate in climate change adaptation depends on the context of societies, cultures or risk aversion (Adger et al., 2009). Although the low discount rate increases the option value of an adaptation option with the optimal investment time advanced, the discount rate below 2 to 2.5% delays the optimal investment time. Therefore, the real options analysis is invalid in such a low discount rate. Although this feature of the optimal investment time has been found in a low discount rate, the critical discount rate differs depending on investment cost and the rate of sea-level rise. For example, the critical discount rate is around 1.5% in the Historical Trend scenario. Thus, the lower discount rate than 2% increases the option value of an adaptation option and advances the optimal investment time to 2050. An effective range of discount rate for the optimal investment time needs to be investigated by applying real options analysis for various discount rates. Nonetheless, the low discount rate gives much a larger option value than the high discount rate. For example, although the optimal investment time is 2062 at 1.5% discount rate in the High SLR scenario, the option values of NPV_{opt} and NPV_{now} is £ 123 M and £ 116 M, respectively. On the other hand, the option value (NPV_{opt}) and optimal investment time at 2.5% discount rate is £ 52 M and 2021, respectively. Thus, as the option value is very high at such a low discount rate, the optimal investment time is less important in investment decision at a very low discount rate than a high discount rate. This implies that, if a very low discount rate is expected in option evaluation, the investment now can be a reasonable decision in an economic term.

(5) Uncertainty of investment timing

From the sensitivity analysis, we could understand that the option value and optimal investment time of an adaptation option is sensitive to investment conditions (e.g. investment cost, discount rates, future growth rates), climatic conditions (e.g. the rate of sea-level rise) and hydrological conditions (e.g. the features of floodplain with coastal defence). The option value and optimal investment time of an adaptation option differs depending on such conditions. As the real options analysis provides more specific information regarding the investment timing, the uncertainties from various sources may be of concern in investment decisions. In other studies, this issue was not found because the investment time was fixed on the passage of time. They estimate the probabilities of climatic variables (e.g. sea-level rise) exceeding a predefined value or not at the determined investment time – this is a main

difference between this thesis and other studies in real options analysis. As the reason to use the flexibility of wait in real options analysis is to maximise the option value of an adaptation option, the investment timing is an important issue in implementing a flexible adaptation option at optimal investment time in the real world.

Though there are various SLR scenarios predicted from UKCP 09, we will see only one true sea-level rise trajectory in the real world, whether or not the true trajectory of sea-level rise is within scenario ranges. In this regard, the identification of the real trajectory of sea-level rise before the optimal investment time is a very challenging task to decision-makers or risk analysts. For example, if the current sea-level rise is the H++ SLR scenario, the optimal investment time is now (to say, 2016). This implies that we should or can say with a 100 % confidence that the current trajectory of sea-level rise is the H++ SLR scenario. It is not plausible to say that the current sea-level rise follows the H++ SLR scenario as there is still large uncertainty unsolved in climate change projections (Haigh et al., 2014). In this context, the implementation of adaptation options based on the real options analysis does not seem to be plausible in the near future because the long-term observation of sea-level rise is required for distinguishing the ongoing pattern of sea-level rise. Even though we have 8 to 15 years for the investment decision under the High-to-Low SLR scenarios, there will still be uncertainty on our observations of sea-level rise.

Despites the uncertainty of investment timing, an absolute sea-level rise enables us to implement an adaptation option at the optimal investment time. This indicative value, at least, helps resolve the uncertainty of investment timing by converting the identification process of optimal investment time into observing the absolute sea-level rise. This is a special case based on the combination of extreme still water level and sea-level rise. In order to apply the real-options-based approach to other cases (e.g. fluvial flooding), this issue needs to be considered in association with how the probability of climatic variables will be modelled and how to identify the optimal investment time in the real world.

(6) Construction lead time

If we have to consider the lead time of construction work for the upgrade of coastal defences, determining the investment timing will be more complicated than in this study (as shown in Figure 7.3). This also affects option values as the stream of benefits occurs right after the construction work is completed. If the completion of the construction work is delayed beyond

the optimal investment time, the option value from the delayed construction will be lower than NPV_{opt} from the on-time construction. Thus, if we are concerned about the economic efficiency of investment in climate change adaptation, the construction work needs to be completed within a targeted year.

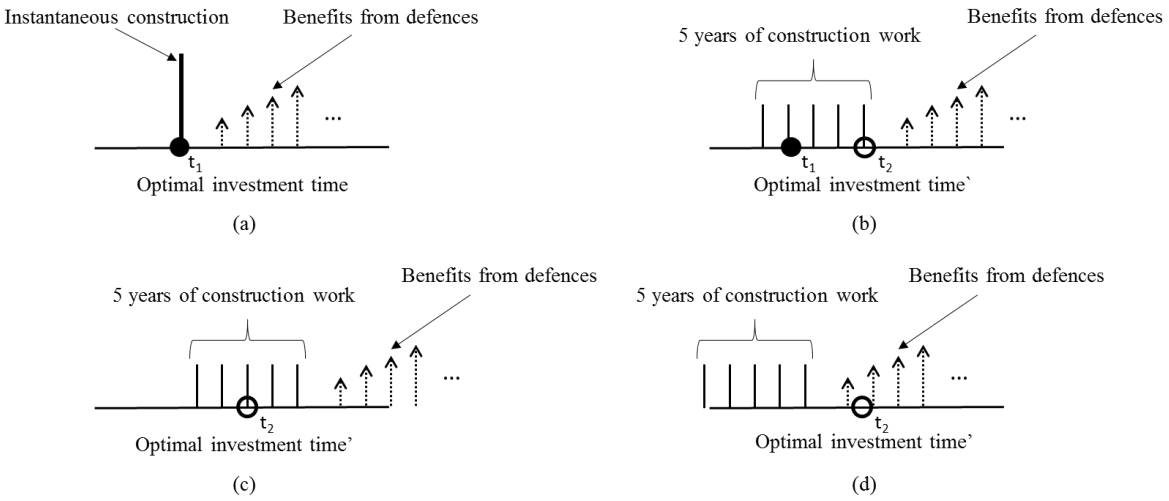

Figure 7.3. Illustration of investment costs (vertical solid lines) and benefits (vertical dot lines) in association with optimal investment times (t_1 and t_2) for (a) instant construction; (b) 5-year construction on time; (c) delayed start of construction; and (d) early start of construction – Note that the length of vertical lines implies the amount of currency.

The thesis assumes that construction work be completed instantaneously. Other previous studies assume that the construction work is ideally completed (instantly or within the planned period) (Linquiti and Vonortos, 2012; Woodward et al., 2014; Hino and Hall, 2017). In practice, this assumption can be an important issue as the construction time changes option values by delaying the period of cash flows or spreading investment costs over different time period.

In Figure 7.3, case (a) shows an ideal case of completing construction work instantaneously. Thus, the construction work is assumed to be completed at the optimal investment time (t_1). This thesis takes this ideal case for the analysis. Case (b) shows that the construction work is undertaken during 5 years and it is completed at the optimal investment time (t_2). As the investment cost is spread over 5 years, the present value of the overall distributed investment costs is higher than the present value of the instant investment cost due to discount factors

$(1+r)^t$. This will delay the optimal investment time due to increased investment costs. Case (c) shows an example of a delayed construction work that is completed within the planned period of 5 years. In this case, the optimal investment time is the same with that of case (b) as the investment cost never change. As the option value is maximum at the optimal investment time, the option value will be reduced little due to the delay of the investment time. Case (d) shows a case of early start of 5-year period construction. Similarly, we will have a reduced option value due to the premature investment. The optimal investment time and option values for different construction periods and different investment times are conceptually illustrated in Figure 7.4.

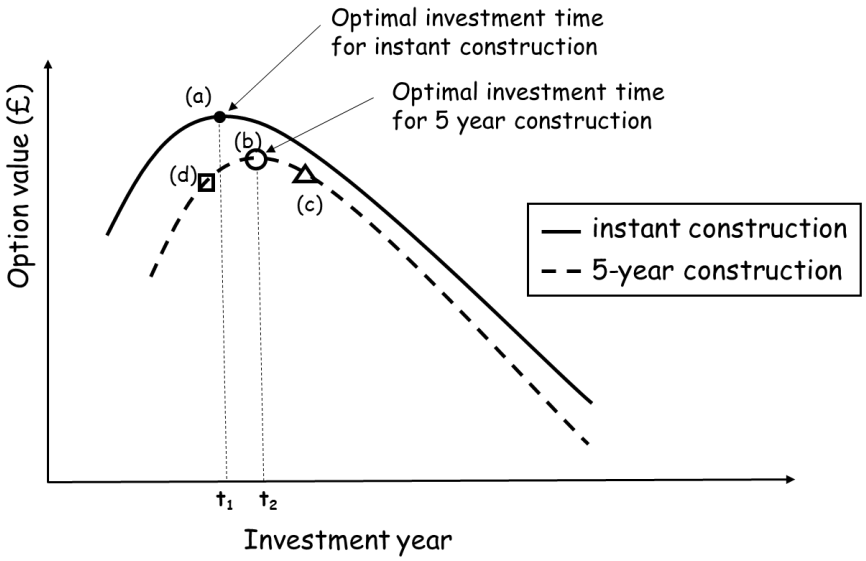

Figure 7.4 Option values and optimal investment times of an adaptation option for different construction work periods and for different investment times - (a), (b), (c) and (d) indicate the option values corresponding to the cases (a), (b), (c) and (d) in Figure 7.3, respectively.

As reviewed, the long lead time of construction work can also act as uncertainty for option evaluation. For example, the lead time of construction work for upgrading the Thames Barrier is expected to be 20 or 30 years (Ranger et al., 2013). Thus, the construction time can be a practical issue for large infrastructure. In this context, we suggest continuous observations on the ongoing pattern of sea-level rise during the construction work as well as the investigation of construction processes and costs during the overall period. Observing the rate and amount of sea-level rise at any decision time enables us to find when the construction work starts or how to manage the construction process to finish it on time.

(7) Real options analysis in the context of severe flood damages

In association with the investment timing, another issue arises as to how sensible it is to base an investment decision on optimal investment timing in context of coastal flooding. Although deferring a decision is a good strategy to avoid uncertainty, such a decision will ironically leave people and areas exposed to the growing risks of climate change during the period of a wait. The deferability of an investment provides an opportunity to observe the future so that we can make more informed decision with newly emerging information on sea-level rise or socio-economic development. However, if we experience a severe flood damage, the public need for taking an adaptation measure will increase.

In such a case, the best strategy is to implement an adaptation option immediately. This will reduce the risk of coastal flooding in Lymington right away. Thus, an immediate investment decision will be hold to decision-makers or policy-makers at the top level in charge of coastal adaptation. A recommendation from this thesis is that, if severe coastal flooding occurs in Lymington, the investment in adaptation option should be made right away to prevent such coastal flooding from occurring again. After the investment now is decided from a top decision level, a focus of adaptation should be on how to upgrade the coastal defence (e.g. single- or multiple- stage, large size or small size of coastal defence, the number of stages and the height to which the coastal defence is raised). If we take a decision criterion as 'no regret' or 'precautionary principle', the immediate investment with large size of coastal defence can be a good strategy to protect Lymington from the rising risk of coastal flooding. However, it will be economically less feasible from the perspective of budget managers. On the contrary, if the budget is limited, the least amount of recovery or upgrade will be a favourable strategy that may be less favourable to risk analysts or the public.

For Lymington, the result of real options analysis suggests that the most economically efficient strategy is two-stage adaptation of $U_{\mathrm{c}\rightarrow 3.0\mathrm{m}} * U_{3.0\rightarrow 3.5m}$. This option keeps flexibility alive to address the uncertainty of sea-level rise. This adaptation path reduces the investment cost at the outset as well as the immediate upgrade of coastal defence can cope with the impending risk of climate change. This also prevents the unnecessary investment from being wasted if an unexpected future scenario occurs. In this regard, the real options analysis used in this thesis is rather an economy-efficiency based approach to provide an opportunity to maximise the option value of an adaptation option, given the uncertainty of sea-level rise.

7. 4 Implications and application of real options analysis in climate change adaptation

This section discusses the validity and applicability of real options analysis in addressing the risk and uncertainty of coastal flooding in a broad context. The real options analysis is assessed in terms of economy efficiency, flood risk and uncertainty, respectively. Thus, this section shows the potential roles of real options analysis in climate change adaptation and flood risk management.

7.4.1 Economic efficiency of flexible adaptation options

As investigated, flexible options give more benefit than non-flexible options (Dobes, 2010; Wood ward et al., 2014; Hino and Hall, 2017). The flexible options including deferability or extendibility enable us to have a choice to invest or to defer in response to a realised future state. As real option values (i.e. NPV_{opt} and NPV_{now}) are variables depending on climatic conditions (i.e. sea-level rise) and investment conditions (i.e. investment cost), a statement 'an adaptation option is more efficient than others' is relative. Thus, the choice of a flexible adaptation option in terms of economic efficiency should be based on the quantitative comparisons of all the candidate options under all the possible future states. As aforementioned, this quantification process is a key of real options analysis to improve the quality of investment decisions under uncertainty (Woodward et al., 2014).

In this context, we suggest that there should be a distinction between controllable conditions and uncontrollable conditions for option evaluations. For instance, investment costs, the size of coastal defence, the number of stages of adaptation path and investment timing are all considered as controllable conditions, whereas sea-level rise, socio-economic factors and the magnitude and occurrence of coastal flooding are considered as uncontrollable. Therefore, an efficient investment decision from the perspective of the real-options based approach is one made by optimising all the controllable conditions against uncontrollable conditions. In doing so, we can inform the optimal investment decision under uncertainty. The possible investment decisions in real-options-based approach are outlined according to the values and quantitative relations of NPV_{now} and NPV_{opt} in Tables 7.1 and 7.2.

Table 7.1 Possible adaptation decisions of a single deferrable adaptation option including flexibility according to the option values of an adaptation option

Option values (NPV_{now}, NPV_{opt})	Quantitative comparisons	Investment decisions	Remark
$NPV_{now} > 0$, $NPV_{opt} > 0$	$NPV_{now} \geq NPV_{opt}$	Invest now	This decision closes flexibility at early stage so that this path cannot cope with the future uncertainty
	$NPV_{now} < NPV_{opt}$	Wait → invest later	This decision keeps flexibility alive as long as the option is deferred, but this decision cannot cope with the current flood risk
$NPV_{now} < 0$, $NPV_{opt} > 0$	$NPV_{now} < NPV_{opt}$	Wait → invest later	This adaptation is likely to be taken in a very distant future. Thus, the investment cost has to be reduced or the multiple-stage adaptation needs to be taken
$NPV_{now} < 0$, $NPV_{opt} < 0$	-	Abandon	Investment will not be made. This adaptation option should be abandoned or adjusted

Table 7.2 Possible adaptation decisions of multiple-stage adaptation options including flexibility according to the option values of an adaptation option

The first phase adaptation		The second phase adaptation		Investment decision*	Remark
Option values (NPV_{now}, NPV_{opt})	Quantitative comparisons	Option values (NPV_{now}, NPV_{opt})	Quantitative comparisons		
$NPV_{now} > 0$, $NPV_{opt} > 0$	$NPV_{now} \geq NPV_{opt}$	$NPV_{now} > 0$, $NPV_{opt} > 0$ $NPV_{now} > 0$, $NPV_{opt} > 0$ $NPV_{now} < 0$, $NPV_{opt} > 0$ $NPV_{now} < 0$, $NPV_{opt} < 0$	$NPV_{now} \geq NPV_{opt}$ $NPV_{now} < NPV_{opt}$ $NPV_{now} < NPV_{opt}$	Not existent** (In)-(W)-(In) (In)-(W)-(In) (In)-(A)	Take this path if the adaptation is to be taken immediately
$NPV_{now} > 0$, $NPV_{opt} > 0$	$NPV_{now} < NPV_{opt}$	$NPV_{now} > 0$, $NPV_{opt} > 0$ $NPV_{now} > 0$, $NPV_{opt} > 0$ $NPV_{now} < 0$, $NPV_{opt} > 0$ $NPV_{now} < 0$, $NPV_{opt} < 0$	$NPV_{now} \geq NPV_{opt}$ $NPV_{now} < NPV_{opt}$ $NPV_{now} < NPV_{opt}$	Not existent (W)-(In)-(W)-(In) (W)-(In)-(W)-(In) (W)- (In)-(A)	Recommenda-ble as long as the investment time is not far from the present
$NPV_{now} < 0$, $NPV_{opt} > 0$	$NPV_{now} < NPV_{opt}$	$NPV_{now} > 0$, $NPV_{opt} > 0$ $NPV_{now} > 0$, $NPV_{opt} > 0$ $NPV_{now} < 0$, $NPV_{opt} > 0$ $NPV_{now} < 0$, $NPV_{opt} < 0$	$NPV_{now} \geq NPV_{opt}$ $NPV_{now} < NPV_{opt}$ $NPV_{now} < NPV_{opt}$	Not existent*** Not existent (W)-(In)-(W)-(In) (W)- (In)-(A)	Not recommenda-ble as it is not economically feasible
$NPV_{now} < 0$, $NPV_{opt} < 0$		$NPV_{now} > 0$, $NPV_{opt} > 0$ $NPV_{now} > 0$, $NPV_{opt} > 0$ $NPV_{now} < 0$, $NPV_{opt} > 0$ $NPV_{now} < 0$, $NPV_{opt} < 0$	$NPV_{now} \geq NPV_{opt}$ $NPV_{now} < NPV_{opt}$ $NPV_{now} < NPV_{opt}$	Not existent Not existent Not existent (A)	Do not take this path due to inefficiency

* (W) – Wait, (In) – Invest and (A) – Abandon

** Practically, if the first and second phase adaptation is to be invested in now, there is no need for multiple-stage adaptation

*** There is no case where the first stage option is not feasible whereas the second option is feasible

In the end, the investment decision will follow one of the possible decisions outlined in Table 7.1 and 7.2. For a single deferrable adaptation option, four investment decisions are made available to decision-makers according to the option values of NPV_{now} and NPV_{opt}. The

characteristics of investment decisions (i.e. invest now, wait and abandon) are summarised in the last column of Table 7.1. Although these types of investment decisions can maximise the option value of the adaptation under a realised condition, one decision closes others. Thus, it is difficult to address both uncertainty and risk from coastal flooding together. If the focus of an adaptation is on addressing uncertainty, it cannot deal with the current risk of coastal flooding. On the contrary, if the focus of an adaptation is on addressing the current risk, it cannot address the uncertainty of coastal flooding. Thus, in an option-to-wait case, one decision is exclusive of others.

In two-stage adaptation options, nine investment decisions are possible to decision-makers. It is of note that the number of possible decisions is made available by dividing a single-stage adaptation into two-stage adaptations. Thus, the design of adaptation paths and investment costs need to be adjusted to satisfy the optimal conditions in the first or second row in Table 7.2. For example, the size and investment cost of coastal defence in the first phase can be of a main concern to option holders who want to launch the project with a small amount of money. By adjusting such investment conditions, the option holders also increase the economy efficiency of an adaptation strategy under uncertain conditions. The design or plan of an adaptation path by human's intuition that meets the optimal condition seems to be very difficult. Thus, the quantitative assessment of the possible adaptation options should be conducted under various conditions. For comparison, the changes in option value for each adaptation option are shown across SLR scenarios by 20% and 50% premium scenarios, respectively (Figure 7.5).

As shown in Figure 7.5, the adaptation curves represent how the option value (NPV_{opt}) of each adaptation path changes according to SLR scenarios. Also, these curves show the ranking of adaptation paths across SLR scenarios in option value. As shown in Figure 7.5, the orders of the adaptation paths in terms of option value never change between the Historical Trend and the High SLR scenarios whereas the ranking of the adaptation paths changes between the High and the H++ SLR scenarios. Consequently, the lowest-ranked adaptation path (i.e. $U_{c\rightarrow 4.0m}$) in the mild SLR scenarios becomes the highest-ranked adaptation path in the most extreme SLR scenario vice versa. As aforementioned, these types of adaptation paths should be rejected from the perspective of real options analysis due to the high sensitivity to uncertainty of SLR scenarios.

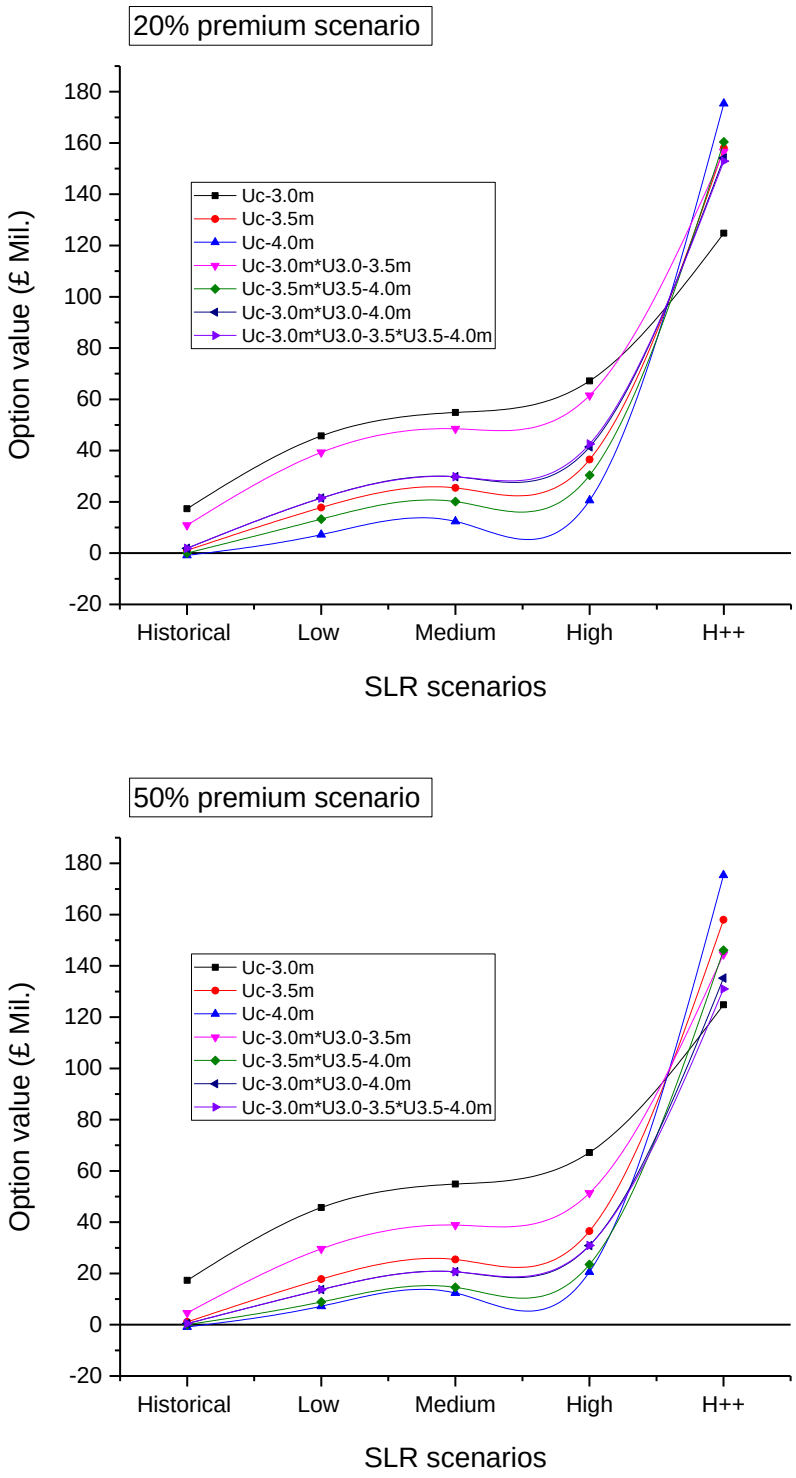

Figure 7.5 Change in the option value of each adaptation path across SLR scenarios by different premium scenarios – Note that the SLR scenarios on the x-axis are equally distanced for the illustrative purpose

As investigated, the adaptation path of $U_{c\rightarrow 3.0m} * U_{3.0\rightarrow 3.5m}$ is the least sensitive to SLR scenarios so that this adaptation path is highly ranked across all the SLR scenarios. This

adaptation path gives relatively high option values across all the SLR scenarios in comparison to other adaptation paths. As the premium value increases, the option values of the multiple-stage adaptation options drop, on the whole, by the increased investment cost. On the contrary, the option values of the single-stage adaptation options stay constant regardless of the premium costs. This leads to change in the ranking of the adaptation paths. Nevertheless, the adaptation path of $U_{c\rightarrow 3.0m} * U_{3.0\rightarrow 3.5m}$ is still ranked the second highest in the mild SLR scenarios (i.e. the Historic and High SLR scenarios) and the third highest in the H++ SLR scenario, respectively.

As reviewed so far, these adaptation curves can be used for a more complicated case to quantitatively compare various adaptation paths in terms of economic efficiency. As the priority of the adaptation paths is relative depending on climatic and investment conditions, these adaptation curves allow us to have an insight into which path is robust against the uncertainty of future climate change.

7.4.2 Risk of coastal flooding in Lymington

If decision-makers take a single-large investment now, a reduction in the risk of coastal flooding takes place immediately after the investment. In terms of risk reduction, the best option for Lymington is to upgrade coastal defences without any delay. It will reduce the flood risk immediately with certainty. However, the real-options-based approach suggests that the adaptation measure that upgrades the coastal defence up to 3.5 mAOD for Lymington needs to be deferred until sea-level rise reaches 13 to 14 cm. Thus, the floodplain behind the coastal defence will be left protected below some optimum during wait or until the coastal defence is upgraded. The temporal changes in the risk of coastal flooding are represented under each SLR scenario for the current coastal defence as shown in Figure 7.6.

As seen in Figure 7.6, if there is no upgrade of the coastal defence, flood risk, represented by EAD, will increase over time due to sea-level rise. For the H++ SLR scenario, the likely annual damages or expected annual damages (EAD, indicated by mean value in Figure 7.6) rise up to £ 30 M/yr in 2100. As EAD significantly increases in the most extreme SLR scenario, Lymington needs flood defence upgrade immediately if this scenario is true.

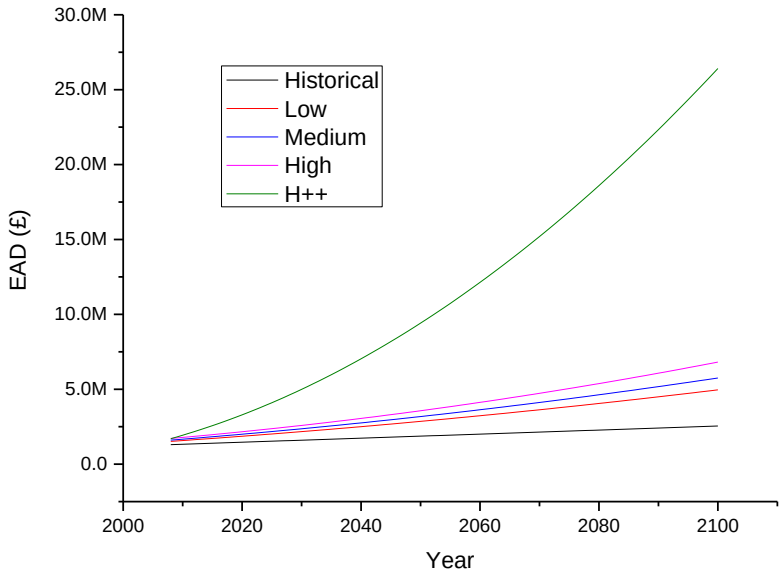

Figure 7.6 Flood risk (EAD) indicated by expected annual damages (£/yr) in Lymington under all the SLR scenarios

If option holders take a single adaptation option $(U_{c\rightarrow 3.5m})$ for protection, the increasing rate of the flood risk in Lymington will differ before and after the investment. For example, once the investment is made at the optimal investment time, the flood risk suddenly drops at the time and, then, keeps constant or slowly-increasing again with sea-level rise. However, during the wait, as shown in Figure 7.7, Lymington will be poorly protected with EAD growing to approximately 2.0 M/yr.

On the other hand, if the option holders take two-stage adaptations ($U_{c\rightarrow 3.0m} * U_{3.0m\rightarrow 3.5m}$), the first-stage adaptation will be taken immediately and the second-stage adaptation will be implemented at the second optimal investment time. The flood risk will be managed by the flexible adaptation path ($U_{c\rightarrow 3.0m} * U_{3.0m\rightarrow 3.5m}$) under £ 0.8 M/yr over the whole period of sea-level rise for the High SLR scenario while, for the H++ SLR scenario, the flood risk will be managed under £ 1.4 M/yr until 2080. The temporal change in flood risk in the case of $U_{c\rightarrow 3.5m}$ is also shown for the H++ and High SLR scenarios in Figure 7.7, respectively. If the current flood risk in Lymington is considered to be significant in the present perspective, the multiple-stage adaptation can be an effective strategy to cope with the current risk of coastal flooding in Lymington. This decision leads to investment now in the first stage adaptation for all the SLR scenarios with flood risk significantly reduced in the early stage.

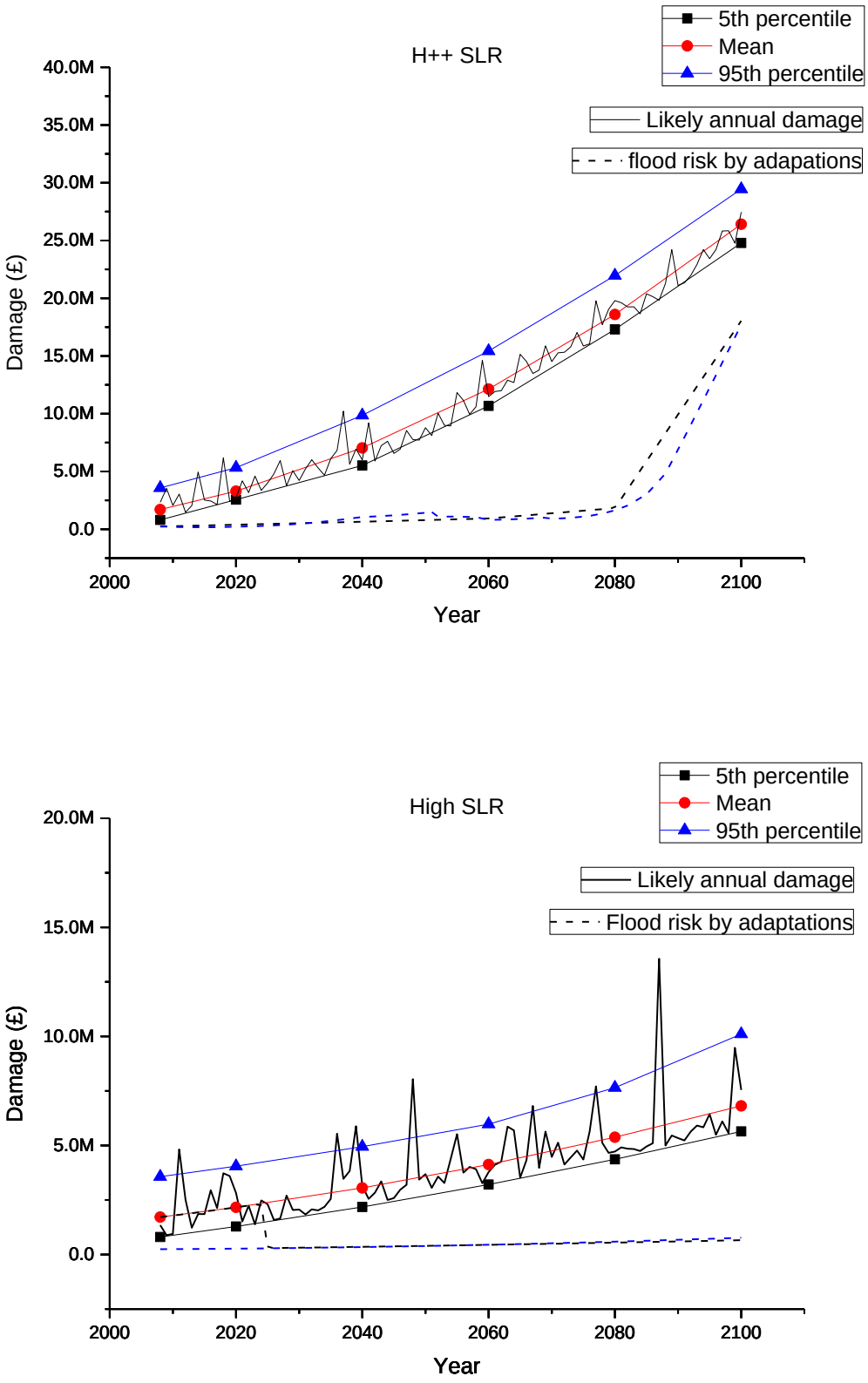

Figure 7.7 Changes in flood risk by different adaptation measures of $U_{c\rightarrow 3.5m}$ (black dash line) and $U_{c\rightarrow 3.0m} * U_{3.0m\rightarrow 3.5m}$ (blue dash line) in the H++ and High SLR scenarios

7.4.3 Uncertainty of sea-level rise and coastal flooding in Lymington

The real-options-based approach provides a set of adaptation paths that are plausible for Lymington. As the risk of coastal flooding increases due to sea-level rise with time, Lymington will choose one of possible adaptation paths in response to sea-level rise. That will be a picture that we can imagine from the perspective of real options analysis.

There are two types of uncertainties identified in the UKCP 09 SLR scenarios. Firstly, one comes from how sea-level rise responses to given emission scenarios (Lowe et al., 2009). This uncertainty is called as climate sensitivity (Nicholls et al., 2014). To deal with this type of uncertainty, UKCP 09 or IPCC data provides the uncertainty range of sea-level rise or other climate variables. Another type of uncertainty relates to greenhouse gas emissions, economic growth, populations or advances in energy technologies (IPCC, 2014; Nicholls et al., 2018). This type of uncertainty is termed 'future uncertainty or epistemic uncertainty' in climate change and flood risk management (Grossi and Kunreuther, 2005). To communicate two different types of uncertainties from sea-level rise, UKCP 09 provides a set of SLR scenarios with probabilistic ranges according to greenhouse gas emissions in the future.

To comply with UKCP 09 data system, this thesis evaluates adaptation options under various SLR scenarios in the case of mean sea-level rise (MSLR) and Brownian sea-level rise, respectively. In both cases, this thesis has found that the optimal investment time is when the climatic variables of sea-level rise reach a threshold value which is constant across the SLR scenarios less than 4.9 mm/yr.

If we take an adaptation path of $U_{c\to 3.0m} * U_{3.0m\to 3.5m}$ which is the most efficient and robust adaptation path among all the paths, the first adaptation measure will be implemented now and the second measure be taken at sea-level rise of 68cm relative to 1990 for 20% premium scenario - Note that the investment rule differs depending on the premium scenarios. By this investment rule, the real-options-based approach provides the largest option value by a sub-optimal decision (i.e. invest in the second-phase adaptation at the optimal time) and can manage the flood risk under a certain level under any given SLR scenario.

However, from the point of the present views, it is still uncertain about what scenario will occur in the future. Thus, the time to learn the future is needed to reduce the uncertainty of SLR scenarios. As discussed in Section 7.2.1, the adaptation path of $U_{c\to 3.0m}$ is sensitive to SLR scenarios because the choice of this strategy (i.e. invest now in $U_{c\to 3.0m}$) does not give any time to learn the future and adjust the decision. In this regard, this option cannot address

the future uncertainty at all. On the contrary, the multiple-stage adaptation (e.g. $U_{c\rightarrow 3.0m} * U_{3.0m\rightarrow 3.5m}$) gives a chance to see the future. It is because the right to invest in the second-stage adaptation allows us to have the time to adjust our decision. In this way, the uncertainty from the future can be resolved by including flexibility in adaptation options. Thus, the real options analysis is an approach to optimise the economic efficiency of an adaptation option under given uncertainty by using flexibility. This implies that, if our investment decision has been made based on real options analysis, it gives us an opportunity to improve our knowledge on the future by optimising all the available resources and choices we can have by flexibility.

7. 5 Comparisons of the real-options-based approach to other studies

If flexibility for an adaptation option is given to decision-makers, it is the right, but not the obligation, to upgrade the adaptation option in the future (Dixit and Pindyck, 1994; Park, 2002; Nefuville, 2003; Linquiti and Vonortas, 2012; Woodward et al., 2014). These types of options incorporate flexibility in the design and planning of infrastructure at the outset (Woodward et al., 2014) or allows decision-makers to defer the investment to the future. The former flexibility (i.e. future growth) is fundamentally different from the latter one (i.e. wait) (Park, 2002; Nefuville, 2003; Kim et al., 2018).

A lot of studies on real options analysis suggest that an adjustable adaptation option in the future is a more robust strategy under the uncertainty of climate change than a non-adjustable adaptation option (Dobes, 2010; Linquiti and Vonortas, 2012; Woodward et at., 2014; Hino and Hall, 2017). This thesis is also in line with the argument from the previous studies. This thesis suggests that the multiple-stage adaptations are more efficient and robust against uncertainty than the single-stage adaptation options. In addition, the proper choice of a multiple-stage adaptation manages flood risk under the optimal level.

Most studies argue that the growth option has some advantages in comparison to a non-growth adaptation option (Dobes, 2010; Linquiti and Vonortas, 2012; Woodward et at., 2014; Hino and Hall, 2017). Firstly, it provides a high degree of freedom in making investment decisions under uncertain future states (Dixit and Pindiyck, 1994). After the first stage option is implemented, the next stage investment will remain flexible for the future extension. Secondly, a multiple-stage adaptation reduces the initial investment cost so that it can facilitate an initial action with a relatively low cost. By reducing the initial size and cost of

the first stage option, we can more efficiently manage the urgent risk of coastal flooding. Lastly, a multiple-stage option enables us to adjust it in response to the future states (Linquiti and Vonortas, 2012). After the investment in a costly infrastructure has been completed, it would be difficult to adjust its capacity and size in response to unexpected conditions (e.g. sea-level rise, socio-economic statues, etc.).

However, this type of adaptation option also requires an additional expenditure to incorporate flexibility (i.e. future extension) into the design or planning (Dobes, 2010; Woodward et al., 2014). For example, the design of extendable coastal defence may require a wider area of land and/or stronger foundations than coastal defence without future extension (Dobes, 2010). Thus, the inclusion of flexibility into an originally static option leads to an increase in the overall costs at the first stage and the subsequent stages. Previous research has also assessed adjustable adaptation options that include the flexibility of future extension in comparison to a baseline adaptation option (without flexibility) in terms of net present value (Linquiti and Vonortas, 2012; Woodward et al., 2014). Linquiti and Vonortas (2012) showed that the adjustable option in the case of Dar-es-Salaam (Bangladeshi) is 5 to 20 times more efficient in net present value than the non-adjustable option under the uncertainty of sea-level rise.

Despite such advantages of the flexible adaptation options, some important issues are found in the previous studies on real options analysis. Firstly, the previous studies assume binominal or trinomial future states in which their main concern is on whether climatic variables exceed a predefined threshold or not. Consequently, the final investment decisions differ depending on the assumed future states. The multiple-stage adaptation options have been assessed by aggregating all the option values weighted by the probabilities of occurrence of the corresponding future states (Linquiti and Vonortas, 2012; Woodward et al., 2014). The result also includes uncertainty associated with the future states (i.e. sea-level rise) in option evaluations. Secondly, the option value differs by investment time. Considering a fixed triggering event for the adaptation option, under a fast rate of sea-level rise, the investment time will be earlier than under a slow rate of sea-level rise. Thus, the value of a remaining adaptation option depends on the rate of sea-level rise or a realised sea-level rise scenario. The previous studies need to include an explicit explanation on the link between threshold values of triggering events for the remaining adaption and the corresponding timing. Lastly, the evaluation of adaptation options is based on the current knowledge and judgement on the future. In addition, as the probabilities of future states are

defined by the analysts or experts' current views, the values of the adaptation options seem to be, to some extent, subjective to their attitudes towards the uncertainty of the futures (e.g. climate change or socio-economic status).

It is expected that uncertainty in future states is reduced with time. The effect of wait on option value has been quantified separately under individual sea-level rise scenarios by Kim et al. (2018). The core character of the paper is to eliminate the subjective views towards the future. This assessment framework provides the unique option value of an adaptation option under each sea-level rise scenario – whether it is multiple-stage or single-stage adaptation option (Kim et al., 2018). In this regard, we, here, focus on assessing the economic efficiency of multiple-stage adaptation options under each of the sea-level rise scenarios provided by the currently available UKCP 09 data (UK climate projection 09) (Lowe et al., 2009). Additionally, this research allows the investment time to vary, following the previous research (Kim et al., 2018). Therefore, the framework of option evaluation used in this thesis seems to be more systematic and objective than the previous analysis. This thesis seeks to exclude such aspects in option evaluations by taking sea-level rise scenarios per se individually. Thus, there is no need to estimate the possibility or probability of the future states (i.e. sea-level rise scenarios) from the current perspectives.

7. 6 Lessons from the application of the real options analysis

The potential roles of real options analysis have been assessed in the contexts of coastal flooding and sea-level rise. Although the developed framework of the real options analysis has been applied only in coastal flooding and sea-level rise, we could identify the possibility of this method for application to other climate change adaptation issues. To see whether the real options analysis is applicable to other climate change issues, this section has highlighted some key lessons as follows.

Firstly, all the possible range of flood damages should be estimated against flood loadings. As investigated, the real options analysis requires a correspondent relation between monetised flood damages and flood loadings for option evaluation. This is assumed to be a unique response of hydrological systems or sites to climatic stimuli such as extreme flood water levels. As flood risk in any year is defined as the integration of all the flood damages times the corresponding probabilities, the probabilities of coastal flood events need to be assigned to the corresponding flood damages. As this analysis assumes that the hydrological

conditions are constant over time, it plays a critical role in linking monetised flood damages and the probabilities of the corresponding flood damages. Thus, this assumption allows us to evaluate flood risk, represented by EAD, in any year and, consequently, benefits (i.e. EABs) from an adaptation option.

This assumption can be extended to other cases of coastal flooding as well as other climate change issues such as fluvial flooding, storms, heatwaves and droughts. To apply this approach to other climate issues, the correspondence between flood loadings and flood damages should be defined prior to option evaluation. This correspondence can be made by iterative flood simulations at various flood loadings within all the possible range or by a model to describe the relation of climatic variables to climate induced damages on a specific site. For example, flood damages (D) – the amounts of precipitation (P), agricultural damages (D) - droughts (Q) or temperature (T) can be an example of climate damage models to describe such relations.

Secondly, the uncertainty of climatic variables should be explicitly defined to quantify the effects of the uncertainty on the performance of an adaptation option. For the comparison of all the adaptation options or pathways, the performance of all the adaption options should be quantified in one metric (in this thesis, economic efficiency). In the case of coastal flooding, this thesis considers three different types of uncertainties in flood loading: (1) one is the natural variability (also referred to as inherent uncertainty) of extreme still water levels; (2) the other is future uncertainty from sea-level rise scenarios; and (3) another is climate sensitivity (or model uncertainty) from an ensemble of climate change models. All the uncertainties have been integrated so that the changes in the probability distribution of extreme still water levels can be modelled in association with sea-level rise. In this way, the uncertainty of climatic events can be modelled to describe changes in the probability distribution of climatic events over time. This concept of uncertainty modelling can be applied to describe the non-stationarity of other climatic variables such as rainfalls, heatwaves, droughts, temperatures and so forth. However, ways to model the uncertainty of climatic variables need to be adjusted according to the characteristic and representation of climatic variables from available dataset (e.g. IPCC projection)

Lastly, an observation process to detect the implementation time of an adaptation option should be defined for application to other climate change adaptation issues. As discussed, the observation is a critical process to ensure the real-options-based approach achieves a maximum option value. This thesis considers sea-level rise as a main driver to change the

statistical properties of climatic events. This thesis has found that the absolute sea-level rise is an important indicator to trigger an adaptation option at the right time. For other climatic variables, the real-options-based approach needs to consider different triggering rules and observation methods to determine the optimal investment time of an adaptation option. For example, in the case of fluvial flooding, how to set up a critical amount of rainfall to implement an adaptation option and how to detect change in the amount of rainfall can be an important question for application of real options analysis. These aspects need to be addressed for future research.

8. Conclusion

The method to evaluate flexible options or strategies has been developed and applied for the case study area of Lymington, UK. In recognition of the large uncertainty, the flexible strategies to adjust adaptation measures in response to sea-level rise are considered as an efficient and robust way to improve investment decisions. In this context, the real options analysis helps to identify an optimal investment decision and quantify adaptation options in a systematic way.

The risk and uncertainty of coastal flooding in Lymington has been considered in previous studies (Haigh et al., 2004; Wadey, 2013; Wadey et al., 2013). However, the effect of adaptation measures to reduce the flood risk are less understood than the causes and consequences of flood damages due to coastal flooding and sea-level rise. This study firstly focuses on the possible adaptation measures to reduce the risk of coastal flooding and the uncertainty of sea-level rise for Lymington. The application of real options analysis in the case study site has been undertaken to draw the potentials and limitations of the real-options-based approach. For application to other sites, the key benefits and limitations need to be considered in a broad context to ensure this thesis could have meaningful insights and practices for climate change adaptation policies or flood risk managements.

8. 1 Applicability of real options analysis in a broader context

The integrated methodology, comprised of a series of processes of uncertainty modelling, flood simulations and option evaluations, enables us to estimate flexible strategies under the uncertainty of sea-level rise. Through the results of real options analysis for both single-stage adaptations and multiple-stage adaptations, we can make more informed decisions for some reasons.

Firstly, the real-options-based approach enables us to know when the adaptation option needs to be implemented under the given rate of sea-level rise with an absolute sea-level rise. Thus, if the investment condition meets a decision criterion ($NPV_{opt} > 0$), an adaptation option will be autonomously implemented at the optimal investment time whatever the rate of sea-level rise is. This is how the real-options-based approach achieves a maximum option value under a given condition. As a multiple-stage adaptation path is made up of two or more single-stage adaptations, this investment rule for single-stage adaptation options is also valid for each stage of the multiple-stage adaptation.

Secondly, the option value of an adaptation option has a large uncertainty due to uncertainties from various sources such as hydrological conditions, future growth rates, the lack of data, the limit of an ability to describe flood dynamics, discount rates, mistakes on cost estimation and so on. This implies that various types of uncertainties from different sources may have substantial effects on the option value and optimal investment time. In terms of the optimal investment time, the uncertainty issue can be resolved by observing the absolute sea-level rise during the wait. In terms of the option value, the uncertainty issue may lead to a wrong investment decision because the option value significantly varies depending on the accuracy of the analysis and data. This may be attributable to the inaccuracy of our interpretation and understanding of coastal flooding such as physical features and statistical properties.

Nevertheless, this thesis has demonstrated that flexibility gives us an opportunity to exploit all the available resources or measures (e.g. investment cost, investment timing and the number of adaptation stages, the size of an adaptation measure) for the optimality of an adaptation. Through this quantification process, we can have the relative order or priority of the possible adaptation paths in option value. This enables us to make a statement that one option is better than others in a certain situation. This approach has seen the ranking of the adaptation paths remain constant across sea-level rise scenarios. This is because the biases from different uncertainties have the same directional effects on the option values of various adaptations. Thus, the biases on the data and simulations can be eliminated or resolved by relative comparisons of candidate adaptations.

Lastly, the multiple-stage options and single-stage adaptations are compared in the same metric in this thesis. Both options are flexible. Thus, how to use the flexibility differs, depending on the rates of sea-level rise and other factors. This approach, at least, provides instructions and methods on how to use such flexibilities incorporated in adaptation options. The option value by the optimal investment is a maximum value we can achieve by the investment rule or instruction. In this regard, the focus of the real options analysis needs to be on how to incorporate flexibilities into adaptation options rather than on how to use the flexibility already included in adaptation option. This thesis has created various adaptation paths by raising the current coastal defence by 0.5 m or 1 m in two or three stages. Although these adaptation paths are arbitrarily made to create experimental conditions for real options analysis, the systematic assessment of all the possible paths allows us to know which path is the most efficient and robust against the uncertainty of sea-level rise.

Despite the advantages, the real options analysis is a very intensive work that requires a great amount of computational resources, time and data process. For example, all the available adaptation paths are seven and SLR scenarios are five in this thesis. Thus, the number of calculations is at least 35 times for all the SLR scenarios and the adaptation paths. In addition, as four premium scenarios are considered in calculations, 48 additional calculations (73 calculations in total) are needed to calculate the option values of all the adaptation options under all the conditions. Thus, the efforts towards reducing the amount of work need to be made for more general applications, if the purpose of the real options analysis in the context of risk management is to make an investment decision at the high level of decision-making.

The arguments above are based on the assumption that the adaptation options are implemented when sea-level rise reaches the critical threshold value or absolute sea-level rise for the corresponding adaptation measure. The optimal condition made by the critical sea-level rise is theoretically based on the relation between EAB and sea-level rise. However, in other cases, it may be difficult or impossible to draw such a relation between EAB and uncertain climatic variables such as rainfall, heatwave and drought. In addition, a way to estimate EAB from an adaptation measure across different climatic variables is a challenging task. As investigated, the estimation of EAB requires the analysis of probabilities of climatic variables and the corresponding climate-induced damages. This may be a critical limitation on the application of the real options analysis into other cases. Thus, the relationship between climatic variables and EAB for an adaptation option should be defined in order to apply this approach to other cases.

8. 2 Implications of the results of real options analysis in climate change adaptation

1) Answer to question 1: Option values in investment decisions

The real option value (NPV_{opt}) estimated for each adaptation option or pathway indicates the present value of a maximum reward that can be achieved by using flexibility under a given future sea-level rise (Kim et al., 2018). Subsequently, the option value derived from real option analysis reflects the effect of flexibility in itself. By estimating and comparing the option values from an immediate investment and an optimal investment, it could be understood whether an adaption option is worth proceeding or waiting to the later date under

any given SLR scenario. In addition, single-stage investments (for option to wait) and multiple-stage investments (for option to grow) are assessed within the same analytical framework. This comparison enables us to analyse which strategy is more efficient against 'do nothing' option: a single investment or sequential investments under the uncertainty of sea-level rise.

Although this real-options-based approach compares the economy efficiencies of adaptation options against the risk of coastal flooding, the option values also indicate how quickly we have to act against the rising risk of coastal flooding or how to split an adaptation option into sequential multiple adaptations. In this regard, the option value is an index that enables us to select the most efficient flexible option or strategy under the uncertainty of climate change.

2) Answer to question 2: The optimisation of flexibility

The second question concerns how we can exercise the adaptation options in association with the outcomes of real options analysis. The answer to this question, thus, focuses on how to implement the adaptation options under the uncertainty of climate change or sea-level rise. As reviewed, the real-options-based decisions differ depending on the option values of NPV_{opt} and NPV_{now} and the optimal investment time of an adaptation option. As the option values and optimal investment time depend on the rate of sea-level rise and future growth rates, if the controllable factors are constant, adaptation actions will be taken in response to these uncontrollable factors observed during the wait. This implies that the success of real options analysis relies on the observation and detection of the patterns of sea-level rise. As long as the flexibility is alive, the observation is an important task for the success of real options analysis.

The flexibility can be used in different ways. As mentioned, the flexibility of a wait is in regard to investment timing. Thus, this type of flexibility can be used without any restriction if we can have an ability to defer an adaptation option. However, splitting an adaptation option into pieces of adaptation options is a different type of flexibility from that of wait. This type of flexibility incurs additional costs and is irreversible if the first phase of investment is made or planned. The use of such a flexibility requires a more detailed analysis to maximise the economy efficiency of an adaptation option.

This flexibility is related to the split and merge of adaptation options under the uncertainty of climatic variables. The best strategy can be found by comparing all the candidates multiple-

stage adaptations against all the possible future states. In this way, the best adaptation strategy can be chosen by trading the best performance with the less sensitivity.

By the result of real options analysis (i.e. option values), the adaptation option can be implemented, deferred, split, reduced, increased or abandoned. In this way, we can optimise a given adaptation option under any of SLR scenarios. Thus, the optimisation of flexible strategies, whether they are single stage options or multiple stage options, can be achieved by the quantitative comparison of all the possible adaptation options under all the possible future states.

3) Answer to question 3: Reduction in uncertainty by flexibility

Uncertainty comes from everywhere there is the lack of understanding and knowledge on what people pursue. This research considers two sources of uncertainties from the future; (1) sea-level rise and; (2) socio-economic developments. As we are not prophets, we cannot know what future will occur. Instead, climate change scientists have created various narratives to describe the possible future states regarding sea-level rise and socio-economic developments. Strictly, the uncertainties cannot be fully resolved by the current knowledge and understanding, as long as the future is still unknown. Since the uncertainty is defined as the imperfection of our knowledge, reduction in uncertainty implies increase in our knowledge or understanding. Thus, it is difficult to define the state of imperfection of our knowledge on future climate change in a quantitative way.

However, as flexibility has been added to, or included in, adaptation options, we have an ability to adjust adaptation options in response to the future states of sea-level rise and socio-economic changes. This is literally how flexible adaptation options or strategies address uncertainty. More correctly, rather than uncertainty has been reduced by flexibility or real options analysis, the real options analysis shows us a way to optimise investment decisions by flexibility under the imperfection of our knowledge on the future. If we have more information about the future, and more advanced technologies for climate change predictions, we can make more informed decisions. In this regard, the question “Has the uncertainty been reduced by flexible strategies” can be answered only in qualitative terms.

In this context, the characteristics of real options analysis are salient in that it quantifies flexible adaptation strategies under various future scenarios. The adaptation options including flexibilities have been assessed in terms of economic efficiency (that is, option value). These assessed values, at least, enable us to know which adaptation path is the most efficient among

all the possible pathways. Thus, the quantification of flexible strategies helps to improve the quality of investment decision on the flexible strategies in addressing the uncertainty of the futures.

8. 3 Directions for future research

This thesis could extend this method to other areas. However, due to the limitations on Ph.D. study, we applied these approaches only to the case study area of Lymington. Nevertheless, the study of Lymington provides the detailed understanding of the principle and mechanisms of the real-option-based approach in addressing the uncertainty of climate change with flexibility. Through the case study, some aspects and lessons that need to be further researched are identified as follows.

1) Changes in hydrological relations

The real options analysis is based on a constant hydrological relation between climatic variables (i.e. sea-level rise), or flood loadings (i.e. ESWL+SLR+WAVE), and flood damages. As well known, sea-level rise also has influence on morphology in coastal areas (Hanson et al., 2015). As a result, the hydrological relation will change over time. This change will also lead to change in the results of real options analysis as the expected annual damage will change with time. In this regard, the hydrological relation needs to be investigated periodically, while waiting for the investment. In addition, the updated information or data will increase the accuracy of describing the hydrological relations between climatic variables and flood damages.

Thus, the information and data such as topography, demography and socio-economic status need to be updated regularly to investigate the validity of the results of the real options analysis in the future. It was difficult to predict or simulate the morphological change in floodplains or saltmarsh before coastal defence in this thesis due to the limitation on techniques and data. The future research into the effect of morphological changes on real options analysis will help understand how to implement adaptation options under the uncertainty of morphological changes.

2) Investment cost of construction

The investment cost of an adaptation option is the most influential factor on the option value and optimal investment time. Thus, if the investment cost changes, the result of real options analysis will provide different option values and optimal investment time. It will lead to change in the priorities or efficiencies of the adaptation options or paths. The estimation of a capital cost for construction requires a site-specific information (EA, 2012). The construction cost varies according to the types of adaptation, environmental conditions (e.g. extreme water levels and coastlines), working conditions (e.g. accessibility to construction sites) and the availability of materials (EA, 2016). Thus, it was difficult to provide an accurate estimate of construction cost at the level of decision-making or academic research. For more convenient applications, it would be helpful to establish a relation between defence heights and construction costs on an ad hoc basis.

3) Probabilistic analysis of different defence failure mode

This thesis has simplified flood mechanisms or dynamics in Lymington by considering overtopping (i.e. waves) and overflowing (i.e. high tides and storm surges) as main defence failure modes. In reality, more complicated failure modes such as breaching or compound flooding combined with fluvial flooding are physically plausible in Lymington. To consider the effects of breaching failure on option evaluation, this thesis assumes that the breaching failure occurs at high water levels near or above the crest level of coastal defence. As well known, the occurrence of the breaching failure is probable, depending on water levels, waves and defence conditions (Dawson and Hall, 2006). It would be a more realistic approach that the breaching failure mode is incorporated into option evaluation in a probabilistic way. For example, the expected annual damage for the breaching failure can be included by estimating the annual probability of occurrence of the breaching (p) and the corresponding flood damage (D) (= p×D). Methods to incorporate the breaching failure in this real options analysis need to be further investigated. In addition, a heavy rain from the upstream of the river Lymington, coupled with a high tide on the river estuary, may cause more severe flooding. Thus, a way to include more complicated cases of flood events needs to be developed for future research.

4) Accuracy of data and modelling

There are various uncertainties coming from each process of real options analysis: (1) uncertainty modelling; (2) flood simulations; (3) monetisation processes and (4) estimation of EAD and EAB. Thus, the inaccuracy or error of data and modelling in each process has an influence on the final results of real options analysis. It would be more helpful to investigate how the uncertainty in each process affects the option value and optimal investment time of an adaptation option. This validation process enables us to understand which process we have to be more cautious on. This also helps know whether a bias or uncertainty in data or modelling can be removed in the option evaluation process as the option evaluation of an adaptation option is conducted upon the difference between flood damages before and after the adaptation measure. The model and data uncertainty in real options analysis may be less influential than other type of uncertainty (i.e. future uncertainty and natural variability). In this regard, the sensitivity of the results of the real options analysis to the accuracy of models and data needs to be examined for future research.

5) Representation of SLR scenarios

This thesis has represented the SLR projections and probabilistic ranges of UKCP 09 with Brownian motion. Since the theory and principles of real option evaluation had been founded on Brownian motion (Dixit and Pindyck, 1994), this thesis has firstly focused on applying Brownian motion to represent the stochastic motion of sea-level rise. A way to describe sea-level rise needs to be further researched for more realistic representation in term of physical aspects or dynamics. For example, if the variance parameter (σ) of Brownian motion is over 2 to 3%, its representation shows an unrealistic behaviour such as 40 cm drops in sea levels or negative sea-level rise. In this regard, this thesis has adjusted Brownian motion by adopting a varying variance parameter according to the probability range of sea-level rise for each SLR scenario.

The Brownian motion using a varying variance parameter shows physically more realistic behaviours of sea-level rise than simply using a constant variance parameter; although its probability range of sea-level rise does fit less to the uncertainty range of sea-level rise from UKCP 09 than that from the constant variance parameter. Thus, the way to estimate variance parameter for more accurate representation of SLR projections needs to be further investigated for a comprehensive representation of sea-level rise in the real world.

As a result of real options analysis into Brownian motion, this thesis has understood that the option value of an adaptation option is affected by the central estimation of SLR projection. This is because the option value is estimated upon the statistically averaged value of sea-level rise or EAD. Thus, the uncertainty range has no effect on option evaluation. This implies that SLR projections need to be more diverse with the uncertainty range being narrower for option evaluation. This enables us to assess option values under more diverse SLR scenarios. How to represent the uncertainty of sea-level rise also needs to be considered for future research.

9. References

ABADIE, L. M., SAINZ DE MURIETA, E. and GALARRAGA, I. 2016. Climate Risk Assessment under Uncertainty: An Application to Main European Coastal Cities. *Frontiers in Marine Science,* 3.

ABP. 2010. Associated British Ports Southampton - Tide Tables 2010, Association of British Port

ADGER, W. N., DESSAI, S., GOULDEN, M., HULME, M., LORENZONI, I., NELSON, D. R., NAESS, L. O., WOLF, J. and WREFORD, A. 2009. Are there social limits to adaptation to climate change? *Climatic change,* 93**,** 335-354.

ANG, A. and TANG, W. H. 2008. *Probability Concepts in Engineering: Emphasis on Applications to Civil & Environmental Engineering*, Wiley.

ARNELL, N. W. 1989. Expected annual damages and uncertainties in flood frequency estimation. *Journal of Water Resources Planning and Management,* 115**,** 94-107.

ARROW, K. J. and FISHER, A. C. 1974. Environmental preservation, uncertainty, and irreversibility. *Classic papers in natural resource economics.* Springer.

BARR, N. A. 1998. *The economics of the welfare state*, Stanford university press.

BATES, P., FEWTRELL, T., TRIGG, M. and NEAL, J. 2008. LISFLOOD-FP user manual and technical note, code release 4.3. 6. *University of Bristol*.

BATES, P. D., DAWSON, R. J., HALL, J. W., HORRITT, M. S., NICHOLLS, R. J., WICKS, J. and HASSAN, M. A. A. M. 2005. Simplified two-dimensional numerical modelling of coastal flooding and example applications. *Coastal Engineering,* 52**,** 793-810.

BEAVEN, R., STRINGFELLOW, A., NICHOLLS, R., HAIGH, I., KEBEDE, A. and WATTS, J. 2017. The impact of coastal landfills on shoreline management plans.

BELLMAN, R. 1952. On the Theory of Dynamic Programming. *Proceedings of the National Academy of Sciences of the United States of America,* 38**,** 716-719.

BELLMAN, R. E. and COOKE, K. L. 1963. Differential-difference equations. *CA: RAND Corporation*.

BELLMANN, R. 1957. Dynamic programming princeton university press. *Princeton, NJ*.

BEN-HAIM, Y. 2006. *Info-gap decision theory: decisions under severe uncertainty*, Academic Press.

BERNOULLI, D. 1738," Specimen Theoriae Novae de Mensure Sortis,". *Cementer Academia Scientiarum Imperalis Petropolitanae***,** 175-192.

BIRKMANN, J., LICKER, R., OPPENHEIMER, M., CAMPOS, M., WARREN, R., LUBER, G., O'NEILL, B. C. and TAKAHASHI, K. 2014. Cross-chapter box on a selection of the hazards, key vulnerabilities, key risks, and emergent risks identified in the WGII contribution to the fifth assessment report. *In:* FIELD, C. B., BARROS, V. R., DOKKEN, D. J., MACH, K. J., MASTRANDREA, M. D., BILIR, T. E., CHATTERJEE, M., EBI, K. L., ESTRADA, Y. O., GENOVA, R. C., GIRMA, B., KISSEL, E. S., LEVY, A. N., MACCRACKEN, S., MASTRANDREA, P. R. and WHITE, L. L. (eds.) *Climate Change 2014: Impacts, Adaptation, and Vulnerability. Part A: Global and Sectoral Aspects. Contribution of Working Group II to the Fifth*

Assessment Report of the Intergovernmental Panel of Climate Change. Cambridge, United Kingdom and New York, NY, USA: Cambridge University Press.

BLACK, F. and SCHOLES, M. 1973. The pricing of options and corporate liabilities. *The journal of political economy***,** 637-654.

BOARDMAN, A. E., GREENBERG, D. H., VINING, A. R. and WEIMER, D. L. 2017. *Cost-benefit analysis: concepts and practice*, Cambridge University Press.

BOSELLO, F., NICHOLLS, R., RICHARDS, J., ROSON, R. and TOL, R. J. 2012. Economic impacts of climate change in Europe: sea-level rise. *Climatic Change,* 112**,** 63-81.

BOYD, P. W., SUNDBY, S. and PÖRTNER, H. O. 2014. Cross-chapter box on net primary production in the ocean. *In:* FIELD, C. B., BARROS, V. R., DOKKEN, D. J., MACH, K. J., MASTRANDREA, M. D., BILIR, T. E., CHATTERJEE, M., EBI, K. L., ESTRADA, Y. O., GENOVA, R. C., GIRMA, B., KISSEL, E. S., LEVY, A. N., MACCRACKEN, S., MASTRANDREA, P. R. and WHITE, L. L. (eds.) *Climate Change 2014: Impacts, Adaptation, and Vulnerability. Part A: Global and Sectoral Aspects. Contribution of Working Group II to the Fifth Assessment Report of the Intergovernmental Panel of Climate Change.* Cambridge, United Kingdom and New York, NY, USA: Cambridge University Press.

BREKELMANS, R., HERTOG, D. D., ROOS, K. and EIJGENRAAM, C. 2012. Safe Dike Heights at Minimal Costs: The Nonhomogeneous Case. *Operations Research,* 60**,** 1342-1355.

BUIJS, F., SIMM, J., WALLIS, M. and SAYERS, P. 2007. Performance and reliability of flood and coastal defences. *Defra and Environment Agency, London, UK*.

CCO 2012. Channel Coastal Observatory - Strategic Regional Coastal Monitoring Programmes. *Data available at: www.channelcoast.org*.

CHURCH, J. A., MONSELESAN, D., GREGORY, J. M. and MARZEION, B. 2013. Evaluating the ability of process based models to project sea-level change. *Environmental Research Letters,* 8**,** 014051.

COMMISION, E. 2018. EU Flood Directives. Published by EU commision. Available: http://ec.europa.eu/environment/water/flood_risk/implem.htm [Accessed 1st June, 2018].

COOPER, N. Testing techniques for estimating implied RNDs from the prices of European-style options. Proceedings of the BIS workshop on implied PDFs, Bank of International Settlements, Basel, 1999.

COPE, S. N., BRADBURY, A. P. and GORCZYNSKA, M. 2008. SOLENT DYNAMIC COAST PROJECT. Published by New Forest District Council/Channel Coastal Observatory. Available: http://www.newforest.gov.uk/nssmp/CHttpHandler.ashx?id=8058&p=0 [Accessed 17th September, 2018].

COPELAND, T. 2003. *Real Options, Revised Edition: A Practitioner's Guide*, Texere Publishing Ltd.

COX, D. R. and MILLER, H. D. 1977. *The theory of stochastic processes*, CRC Press.

COX, P. and STEPHENSON, D. 2007. A changing climate for prediction. *Science,* 317**,** 207-208.

DASGUPTA, A. K. and PEARCE, D. W. 1972. *Cost-benefit analysis: theory and practice*, Macmillan International Higher Education.

DAWSON, R. and HALL, J. Adaptive importance sampling for risk analysis of complex infrastructure systems. Proceedings of the Royal Society of London A: Mathematical, Physical and Engineering Sciences, 2006. The Royal Society, 3343-3362.

DAWSON, R. J., HALL, J., BATES, P. and NICHOLLS, R. 2005. Quantified analysis of the probability of flooding in the Thames Estuary under imaginable worst-case sea level rise scenarios. *Water resources development,* 21**,** 577-591.

DAWSON, R. J., NICHOLLS, R. J. and DAY , S. A. 2015. The Challenge for Coastal Management During the Third Millennium. *In:* NICHOLLS, J. R., DAWSON, J. R. and DAY, A. S. (eds.) *Broad Scale Coastal Simulation: New Techniques to Understand and Manage Shorelines in the Third Millennium.* Dordrecht: Springer Netherlands.

DE ALMEIDA, G. A. M., BATES, P., FREER, J. E. and SOUVIGNET, M. 2012. Improving the stability of a simple formulation of the shallow water equations for 2-D flood modeling. *Water Resources Research,* 48**,** W05528.

DECONTO, R. M. and POLLARD, D. 2016. Contribution of Antarctica to past and future sea-level rise. *Nature,* 531**,** 591.

DESSAI, S., HULME, M., LEMPERT, R. and PIELKE JR, R. 2009. Climate prediction: a limit to adaptation. *Adapting to climate change: thresholds, values, governance***,** 64-78.

DITTRICH, R., WREFORD, A. and MORAN, D. 2016. A survey of decision-making approaches for climate change adaptation: Are robust methods the way forward? *Ecological Economics,* 122**,** 79-89.

DIXIT, A. K. and PINDYCK, R. S. 1994. *Investment under uncertainty,* Princeton, Princeton university press.

DOBES, L. 2010. Notes on applying 'real options' to climate change adaptation measures, with examples from Vietnam. *Crawford School of Ecconomics and Government, Centre for Climate Economics & Policy. Australian National University, Canberra*.

EA. 2010a. Flood and Coastal Erosion Risk Management appraisal guidance: FCERM-AG. Published by Environmental Agency. Available: https://assets.publishing.service.gov.uk/government/uploads/system/uploads/attachment_data/file/481768/LIT_4909.pdf [Accessed June 1, 2016].

EA. 2010b. Solent & South Downs Area Report 10 March tidal flooding event, Hampshire & Isle of Wight. A report of events, consequences and conclusions. Version 2 Jan 2010.

EA. 2015. Cost estimation for coastal protection –summary of evidence, Environment Agency Report –SC080039/R7

EIJGENRAAM, C., KIND, J., BAK, C., BREKELMANS, R., DEN HERTOG, D., DUITS, M., ROOS, K., VERMEER, P. and KUIJKEN, W. 2014. Economically efficient standards to protect the Netherlands against flooding. *Interfaces,* 44**,** 7-21.

EIJGENRAAM, C. J. 2006. Optimal safety standards for dike-ring areas. *Discussion paper nr. 62, ISBN 90-5833-267-5*.

EVANS, E. 2004. *Foresight: Future Flooding. Scientific Summary,* Department of Trade and Industry, US.

FEWTRELL, T., BATES, P. D., HORRITT, M. and HUNTER, N. 2008. Evaluating the effect of scale in flood inundation modelling in urban environments. *Hydrological Processes: An International Journal,* 22**,** 5107-5118.

FEYEN, L., DANKERS, R., BÓDIS, K., SALAMON, P. and BARREDO, J. 2012. Fluvial flood risk in Europe in present and future climates. *Climatic Change,* 112**,** 47-62.

FIELD, C. B., BARROS, V., STOCKER, T. F. and DAHE, Q. 2012. *Managing the risks of extreme events and disasters to advance climate change adaptation: special report of the intergovernmental panel on climate change,* Cambridge University Press.

GERSONIUS, B., ASHLEY, R., PATHIRANA, A. and ZEVENBERGEN, C. 2013. Climate change uncertainty: building flexibility into water and flood risk infrastructure. *Climatic change,* 116**,** 411-423.

GILBOA, I., POSTLEWAITE, A. and SCHMEIDLER, D. 2009. Is it always rational to satisfy Savage's axioms? *Economics and Philosophy,* 25**,** 285-296.

GOULDBY, B., KINGSTON, G., WILLS, M., VAN GELDER, P., BUIJIS, F. and KORTENHAUS, A. 2008. Flood defence reliability calculator: RELIABLE User Manual. *Floodsite Report***,** 08.

GROSSI, P. and KUNREUTHER, H. 2005. *Catastrophe modeling: a new approach to managing risk,* Springer Science & Business Media.

GROVES, D. G., LEMPERT, R. J., KNOPMAN, D. and BERRY, S. H. 2008. *Preparing for an uncertain future climate in the Inland Empire,* Rand Corporation.

HAASNOOT, M., KWAKKEL, J. H., WALKER, W. E. and TER MAAT, J. 2013. Dynamic adaptive policy pathways: a method for crafting robust decisions for a deeply uncertain world. *Global Environmental Change,* 23**,** 485-498.

HAIGH, I., NICHOLLS, R. and WELLS, N. 2011. Rising sea levels in the English Channel 1900 to 2100. *Proceedings of the ICE-Maritime Engineering,* 164**,** 81-92.

HAIGH, I. D., OZSOY, O., WADEY, M. P., NICHOLLS, R. J., GALLOP, S. L., WAHL, T. and BROWN, J. M. 2017. An improved database of coastal flooding in the United Kingdom from 1915 to 2016. *Scientific Data,* 4**,** 170100.

HAIGH, I. D., WADEY, M. P., WAHL, T., OZSOY, O., NICHOLLS, R. J., BROWN, J. M., HORSBURGH, K. and GOULDBY, B. 2016. Spatial and temporal analysis of extreme sea level and storm surge events around the coastline of the UK. *Scientific Data,* 3**,** 160107.

HAIGH, I. D., WAHL, T., ROHLING, E. J., PRICE, R. M., PATTIARATCHI, C. B., CALAFAT, F. M. and DANGENDORF, S. 2014. Timescales for detecting a significant acceleration in sea level rise. *Nat Commun,* 5.

HALCROW. 1998. Western Solent and Southampton Water shoreline management plan Volume 2, Management strategy Halcrow Group Ltd

HALL, J. 2007. Probabilistic climate scenarios may misrepresent uncertainty and lead to bad adaptation decisions. *Hydrological Processes,* 21**,** 1127-1129.

HALL, J., BROWN, S., NICHOLLS, R. J., PIDGEON, N. F. and WATSON, R. T. 2012. Proportionate adaptation. *Nature Clim. Change,* 2**,** 833-834.

HALL, J. and SOLOMATINE, D. 2008. A framework for uncertainty analysis in flood risk management decisions. *International Journal of River Basin Management,* 6**,** 85-98.

HALL, J. W., DAWSON, R., SAYERS, P., ROSU, C., CHATTERTON, J. and DEAKIN, R. A methodology for national-scale flood risk assessment. Proceedings of the Institution of Civil Engineers-Water Maritime and Engineering, 2003. London: Published for the Institution of Civil Engineers by Thomas Telford Ltd., c2000-c2003., 235-248.

HALL, J. W., DAWSON, R. J. and WU, X. Z. 2015. Analysing Flood and Erosion Risks and Coastal Management Strategies on the Norfolk Coast. *Broad Scale Coastal Simulation.* Springer.

HALL, J. W., LEMPERT, R. J., KELLER, K., HACKBARTH, A., MIJERE, C. and MCINERNEY, D. J. 2012. Robust Climate Policies Under Uncertainty: A Comparison of Robust Decision Making and Info-Gap Methods. *Risk Analysis,* 32**,** 1657-1672.

HALLEGATTE, S. 2009. Strategies to adapt to an uncertain climate change. *Global Environmental Change,* 19**,** 240-247.

HALLEGATTE, S. S., ANKUR LEMPERT, ROBERT BROWN, CASEY GILL, STUART 2012. *Investment Decision Making under Deep Uncertainty - Application to Climate Change*.

HANSON, S., FRENCH, J., SPENCER, T., BROWN, I., NICHOLLS, R. J., SUTHERLAND, W. J. and BALSON, P. 2015. Evaluating broadscale morphological change in the coastal zone using a logic-based behavioural systems approach. *Broad Scale Coastal Simulation.* Springer.

HANSON, S., NICHOLLS, R., RANGER, N., HALLEGATTE, S., CORFEE-MORLOT, J., HERWEIJER, C. and CHATEAU, J. 2011. A global ranking of port cities with high exposure to climate extremes. *Climatic change,* 104**,** 89-111.

HAWKINS, E. and SUTTON, R. 2009. The potential to narrow uncertainty in regional climate predictions. *Bulletin of the American Meteorological Society,* 90**,** 1095-1108.

HILLEN, M. M., JONKMAN, S. N., KANNING, W., KOK, M., GELDENHUYS, M. and STIVE, M. 2010. Coastal defence cost estimates: Case study of the Netherlands, New Orleans and Vietnam. *Communications on Hydraulic and Geotechnical Engineering, No. 2010-01*.

HINKEL, J., JAEGER, C., NICHOLLS, R. J., LOWE, J., RENN, O. and PEIJUN, S. 2015. Sea-level rise scenarios and coastal risk management. *Nature Clim. Change,* 5**,** 188-190.

Hino, M. and Hall, J.W., 2017. Real options analysis of adaptation to changing flood risk: Structural and nonstructural measures. ASCE-ASME Journal of Risk and Uncertainty in Engineering Systems, Part A: Civil Engineering, 3(3), p.04017005.

HM TREASURY. 2003. Appraisal and evaluation in central government. *The green book. London* [Online]. Published by Her Majesty's Stationary Office. Available: https://www.gov.uk/government/uploads/system/uploads/attachment_data/file/220541/green_book_complete.pdf [Accessed June 1, 2016].

HRW. 2003. Risk Assessment for Flood and Coastal Defence for Strategic Planning: High Level Method - Technical Report, Environment Agency Report Number W5B-030/TR1, HR Wallingford Report SR603

HRW. 2004. National Flood Risk Assessment 2004: Supported by the RASP HLM plus: Methodology, HR Wallingford Report SR659

HUNT, A. and TAYLOR, T. 2009. Values and cost—benefit analysis: economic efficiency criteria in adaptation. *Adapting to Climate Change: Thresholds, Values, Governance***,** 197.

IPCC 2014. Summary for Policymakers. *In:* FIELD, C. B., BARROS, V. R., DOKKEN, D. J., MACH, K. J., MASTRANDREA, M. D., BILIR, T. E., CHATTERJEE, M., EBI, K. L., ESTRADA, Y. O., GENOVA, R. C., GIRMA, B., KISSEL, E. S., LEVY, A. N., MACCRACKEN, S., MASTRANDREA, P. R. and WHITE, L. L. (eds.) *Climate Change 2014: Impacts, Adaptation, and Vulnerability. Part A: Global and Sectoral Aspects. Contribution of Working Group II to the Fifth Assessment Report of the Intergovernmental Panel on Climate Change.* Cambridge, United Kingdom, and New York, NY, USA: Cambridge University Press.

JEULAND, M. and WHITTINGTON, D. 2014. Water resources planning under climate change: Assessing the robustness of real options for the Blue Nile. *Water Resources Research,* 50**,** 2086-2107.

JOHNSON, C., PENNING-ROWSELL, E. and TAPSELL, S. 2007. Aspiration and reality: flood policy, economic damages and the appraisal process. *Area,* 39**,** 214-223.

JONKMAN, S. N., HILLEN, M. M., NICHOLLS, R. J., KANNING, W. and VAN LEDDEN, M. 2013. Costs of adapting coastal defences to sea-level rise—new estimates and their implications. *Journal of Coastal Research,* 29**,** 1212-1226.

JORGENSON, D. W. 1963. Capital theory and investment behavior. *The American Economic Review,* 53**,** 247-259.

KARLIN, S. and TAYLOR, H. E. 1981. *A second course in stochastic processes*, Elsevier.

KEBEDE, A. S. 2009. Assessing Potential Risks of Impacts of Climate Change on Coastal Landfill Sites: A Case Study of Pennington Landfill Site-Hampshire, United Kingdom.

KELLER, K., TOL, R. S., TOTH, F. L. and YOHE, G. W. 2008. Abrupt climate change near the poles. *Climatic Change,* 91**,** 1-4.

KIM, M. J., NICHOLLS, R. J., PRESTON, J. M. and DE ALMEIDA, G. A. M. 2018. An assessment of the optimum timing of coastal flood adaptation given sea-level rise using real options analysis. *Journal of Flood Risk Management,* 0**,** e12494.

KIM, M. J., NICHOLLS, J. R., PRESTON, M. J. and DE ALMEIDA, A. G. 450 p. Adaptation Futures 2016 : 4th international climate change adaptation conference, Rotterdam, The Netherlands 10-13 May 2016 : practices and solutions : science abstracts. 2016 [S.l.]. PROVIA [etc.].

KING, D., SCHRAG, D., DADI, Z., YE, Q. and GHOSH, A. 2015. Climate Change: A risk assessment Project Report, Centre for Science and Policy

KNIGHT, F. H. 1921. The meaning of risk and uncertainty. *Frank H., Knight. Risk, Uncertainty, and Profit. Boston: Houghton Mifflin Co***,** 210-235.

KOPP, R. E., DECONTO, R. M., BADER, D. A., HAY, C. C., HORTON, R. M., KULP, S., OPPENHEIMER, M., POLLARD, D. and STRAUSS, B. H. 2017. Evolving understanding of Antarctic ice-sheet physics and ambiguity in probabilistic sea-level projections. *Earth's Future,* 5**,** 1217-1233.

LEMPERT, R. J. 2003. *Shaping the next one hundred years: new methods for quantitative, long-term policy analysis*, Rand Corporation.

LEMPERT, R. J. and COLLINS, M. T. 2007. Managing the risk of uncertain threshold responses: comparison of robust, optimum, and precautionary approaches. *Risk analysis,* 27**,** 1009-1026.

LEMPERT, R. J., GROVES, D. G., POPPER, S. W. and BANKES, S. C. 2006. A general, analytic method for generating robust strategies and narrative scenarios. *Management science,* 52**,** 514-528.

LEVASSEUR, A. 2008. *Observations and modelling of the variability of the Solent-Southampton Water estuarine system.* University of Southampton.

LINQUITI, P. and VONORTAS, N. 2012. The value of flexibility in adapting to climate change: a real options analysis of investments in coastal defense. *Climate Change Economics,* 3**,** 1250008.

LOWE, A. J., GREGORY, M. J. and FLATHER, A. R. 2001. Changes in the occurrence of storm surges around the United Kingdom under a future climate scenario using a dynamic storm surge model driven by the Hadley Centre climate models. *Climate Dynamics,* 18**,** 179-188.

LOWE, J., HOWARD, T., PARDAENS, A., TINKER, J., HOLT, J., WAKELIN, S., MILNE, G., LEAKE, J., WOLF, J. and HORSBURGH, K. 2009. UK Climate Projections science report: Marine and coastal projections. Published by Met Office Hadely Centre. Available: http://ukclimateprojections.metoffice.gov.uk/media.jsp?mediaid=87906&filetype=pdf [Accessed July 1, 2017].

MADDISON, D. 1996. A cost benefit analysis of slowing climate change. *Energy and Environment Regulation.* Springer.

MARTIN, D. 1994. The Impact of Conservation Issues on a Sea-Defence Scheme at Pennington. *Water and Environment Journal,* 8**,** 567-575.

MCCARTHY, J. J., CANZIANI, O. F., LEARY, N. A., DOKKEN, D. J. and WHITE, K. S. 2001. *Climate change 2001: impacts, adaptation, and vulnerability: contribution of Working Group II to the third assessment report of the Intergovernmental Panel on Climate Change*, Cambridge University Press.

MCDONALD, R. and SIEGEL, D. 1986. The Value of Waiting to Invest. *The Quarterly Journal of Economics,* 101**,** 707-727.

MCINERNEY, D., LEMPERT, R. and KELLER, K. 2012. What are robust strategies in the face of uncertain climate threshold responses? *Climatic change,* 112**,** 547-568.

MCMILLAN, A., BATSTONE, C., WORTH, D., TAWN, J., HORSBURGH, K. and LAWLESS, M. 2011. Coastal flood boundary conditions for UK mainland and islands. Project SC060064/TR2: Design sea levels.

MCPHAIL, C., MAIER, H., KWAKKEL, J., GIULIANI, M., CASTELLETTI, A. and WESTRA, S. 2018. Robustness Metrics: How Are They Calculated, When Should They Be Used and Why Do They Give Different Results? *Earth's Future,* 6**,** 169-191.

MENDELSOHN, R. 2011. Economic estimates of the damages caused by climate change. *John S. Dryzek, Richard B. Norgaard und David Schlosberg: Oxford Handbook of Climate Change and Society. Oxford, UK, New York: Oxford University Press (Oxford Handbooks)***,** 177-189.

MLIT. 2016. A study on the economic analysis in flood control project, Ministry of Land, Infrastructure and Transport

MONGIN, P. 1997. Expected utility theory. *Handbook of economic methodology***,** 342-350.

MORGAN, M. G., KANDLIKAR, M., RISBEY, J. and DOWLATABADI, H. 1999. Why conventional tools for policy analysis are often inadequate for problems of global change. *Climatic Change,* 41**,** 271-281.

MURPHY, J., SEXTON, D., JENKINS, G., BOORMAN, P., BOOTH, B., BROWN, K., CLARK, R., COLLINS, M., HARRIS, G. and KENDON, E. 2009. UKCP09 Climate change projections. *Met Office Hadley Centre, Exeter*.

NARAYAN, S., HANSON, S., NICHOLLS, R., CLARKE, D., WILLEMS, P., NTEGEKA, V. and MONBALIU, J. 2012. A holistic model for coastal flooding using system diagrams and the Source–Pathway–Receptor (SPR) concept. *Natural Hazards and Earth System Science,* 12**,** 1431-1439.

NELSON, D. R. and ANDERIES, J. M. 2009. Hidden costs and disparate uncertainties: trade-offs in approaches to climate policy. *Adapting to climate change: Thresholds, values, governance***,** 212.

NEUFVILLE, R. 2003. Real options: dealing with uncertainty in systems planning and design. *Integrated Assessment,* 4**,** 26-34.

NEW FOREST DISTRICT COUNCIL. 2010a. North Solent shoreline management plan. Appendix H Economic Appraisal and Sensitivity Testing. Published by New Forest District Council (UK). Available: http://www.northsolentsmp.co.uk/ [Accessed June 1, 2016].

NEW FOREST DISTRICT COUNCIL. 2010b. North Solent shoreline management plan: Appendix F Initial Policy Appraisal and Scenario Development. Published by http://www.northsolentsmp.co.uk/ [Accessed June 1, 2016].

NICHOLLS, R. J., BROWN, S., GOODWIN, P., WAHL, T., LOWE, J., SOLAN, M., GODBOLD, J. A., HAIGH, I. D., LINCKE, D., HINKEL, J., WOLFF, C. and MERKENS, J.-L. 2018. Stabilization of global temperature at 1.5°C and 2.0°C: implications for coastal areas. *Philosophical Transactions of the Royal Society A: Mathematical, Physical and Engineering Sciences,* 376.

NICHOLLS, R. J., HANSON, S. E., LOWE, J. A., WARRICK, R. A., LU, X. and LONG, A. J. 2014. Sea-level scenarios for evaluating coastal impacts. *Wiley Interdisciplinary Reviews: Climate Change,* 5**,** 129-150.

NICHOLLS, R. J. and LOWE, J. A. 2004. Benefits of mitigation of climate change for coastal areas. *Global Environmental Change,* 14**,** 229-244.

NICHOLLS, R. J., REEDER, T., BROWN, S. and HAIGH, I. D. 2015. The risks of sea-level rise for coastal cities. Climate Change: A Risk Assessment. Published by Centre for

Science and Policy. Available: http://www.csap.cam.ac.uk/media/uploads/files/1/climate-change--a-risk-assessment-v11.pdf.

NICHOLLS, R. J., TOWNEND, I. H., BRADBURY, A. P., RAMSBOTTOM, D. and DAY, S. A. 2013. Planning for long-term coastal change: Experiences from England and Wales. *Ocean Engineering,* 71**,** 3-16.

NRA. 1990. Lymington/Pennington flood investigation – interim report, National Rivers Authority Southern Region

O'BRIEN, K. 2009. Do values subjectively define the limits to climate change adaptation? *Adapting to climate change: Thresholds, values, governance***,** 164-180.

OECD. 2016. *Financial Management of Flood Risk.* Available: https://www.oecd-ilibrary.org/content/publication/9789264257689-en ['Accessed' June 1, 2018]

ORESKES, N., STAINFORTH, D. A. and SMITH, L. A. 2010. Adaptation to global warming: do climate models tell us what we need to know? *Philosophy of Science,* 77**,** 1012-1028.

OS. 2001. Ordnance Survey Land-Form PROFILE™ User guide. v4.0 – 5/2001© Crown copyright. Published by www.ordnancesurvey.co.uk [Accessed 1st June 2015].

OWEN, M. W. 1980. Design of seawalls allowing for wave overtopping, HR Wallingford Report EX 924

OXFORD DICTIONARY 2016. The Oxford Dictionary of New Words: A popular guide to words in the news.

OZSOY, O., HAIGH, I. D., WADEY, M. P., NICHOLLS, R. J. and WELLS, N. C. 2016. High-frequency sea level variations and implications for coastal flooding: A case study of the Solent, UK. *Continental Shelf Research,* 122**,** 1-13.

PALISADE. 2018. @Risk for risk anlaysis. Published by Palisade Corporation. Available: https://www.palisade.com/risk/default.asp.

PARK, C. S. 2002. *Contemporary engineering economics*, Prentice Hall Upper Saddle River, NJ.

PENNING-ROWSELL, E., BRITAIN, G. and BRITAIN, G. 2005. *The benefits of flood and coastal risk management: a handbook of assessment techniques*, Middlesex university press London.

PENNING-ROWSELL, E., JOHNSON, C., TUNSTALL, S., TAPSELL, S., MORRIS, J., CHATTERTON, J. and GREEN, C. 2010. The benefits of flood and coastal risk management: a handbook of assessment techniques, Middlesex University Press

PENNING-ROWSELL, E., PRIEST, S., PARKER, D., MORRIS, J., TUNSTALL, S., VIAVATTENE, C., CHATTERTON, J. and OWEN, D. 2014. *Flood and coastal erosion risk management: a manual for economic appraisal,* London, Routledge.

PIELKE, R. A., WILBY, R., NIYOGI, D., HOSSAIN, F., DAIRUKU, K., ADEGOKE, J., KALLOS, G., SEASTEDT, T. and SUDING, K. 2012. Dealing with Complexity and Extreme Events Using a Bottom-Up, Resource-Based Vulnerability Perspective. *Extreme Events and Natural Hazards: The Complexity Perspective***,** 345-359.

PINDYCK, R. S. 2000. Irreversibilities and the timing of environmental policy. *Resource and Energy Economics,* 22**,** 233-259.

PRIME, T., BROWN, J. M. and PLATER, A. J. 2015. Physical and economic impacts of sea-level rise and low probability flooding events on coastal communities. *PLoS One,* 10**,** e0117030.

PUGH, D. T. 1996. *Tides, surges and mean sea-level (reprinted with corrections)*, John Wiley & Sons Ltd.

RANGER, N., MILLNER, A., DIETZ, S., FANKHAUSER, S., LOPEZ, A. and RUTA, G. 2010. Adaptation in the UK: a decision making process. *Environment Agency,* 9.

RANGER, N., REEDER, T. and LOWE, J. 2013. Addressing 'deep' uncertainty over long-term climate in major infrastructure projects: four innovations of the Thames Estuary 2100 Project. *EURO Journal on Decision Processes,* 1**,** 233-262.

REEDER, T., WICKS, J., LOVELL, L. and TARRANT, O. 2009. Protecting London from tidal flooding: limits to engineering adaptation. *Adapting to climate change: thresholds, values, governance***,** 54.

REEVE, D. and BURGESS, K. 1993. A method for the assesment of coastal flood risk. *IMA Journal of Management Mathematics,* 5**,** 197-209.

REHAN, B. M. and HALL, J. W. Uncertainty and sensitivity analysis of flood risk management decisions based on stationary and nonstationary model choices. E3S Web of Conferences, 2016. EDP Sciences, 20003.

ROSENZWEIG, C. and SERIES, N. S. 2010. *Climate Change Adaptation in New York City*, Blackwell Pub. on behalf of the New York Academy of Sciences.

RUOCCO, A. C., NICHOLLS, R. J., HAIGH, I. D. and WADEY, M. P. 2011. Reconstructing coastal flood occurrence combining sea level and media sources: a case study of the Solent, UK since 1935. *Natural hazards,* 59**,** 1773-1796.

SAVAGE, L. J. 1951. The Theory of Statistical Decision. *Journal of the American Statistical Association,* 46**,** 55-67.

SCHNEIDER, S. H. and MOSS, R. 1999. Uncertainties in the IPCC TAR: Recommendations to lead authors for more consistent assessment and reporting. *Unpublished document*.

SCHRAG, D. 2015. GLOBAL SEA-LEVEL RISE. *Centre for Science Policy*, University of Cambridge.

SLIJKHUIS, K., VAN GELDER, P. and VRIJLING, J. 1997. Optimal dike height under statistical-construction-and damage uncertainty. *Structural Safety and Reliability,* 7**,** 1137-1140.

SMIT, B. and PILIFOSOVA, O. 2003. Adaptation to climate change in the context of sustainable development and equity. *Sustainable Development,* 8**,** 9.

SOLOMON, S., QIN, D., MANNING, M., AVERYT, K. and MARQUIS, M. 2007. *Climate change 2007-the physical science basis: Working group I contribution to the fourth assessment report of the IPCC*, Cambridge university press.

STAINFORTH, D. A., ALLEN, M. R., TREDGER, E. R. and SMITH, L. A. 2007. Confidence, uncertainty and decision-support relevance in climate predictions. *Philosophical Transactions of the Royal Society of London A: Mathematical, Physical and Engineering Sciences,* 365**,** 2145-2161.

STERN, N. 2007. *The economics of climate change: the Stern review*, cambridge University press.

STEVENS, A., CLARKE, D., NICHOLLS, R. and WADEY, M. 2015. Estimating the long-term historic evolution of exposure to flooding of coastal populations. *Natural Hazards and Earth System Sciences Discussions,* 3**,** 1681-1715.

STURM, M., GOLDSTEIN, M. A., HUNTINGTON, H. and DOUGLAS, T. A. 2017. Using an option pricing approach to evaluate strategic decisions in a rapidly changing climate: Black–Scholes and climate change. *Climatic Change,* 140**,** 437-449.

TOL, R. J. 2003. Is the Uncertainty about Climate Change too Large for Expected Cost-Benefit Analysis? *Climatic Change,* 56**,** 265-289.

TOL, R. S. and YOHE, G. W. 2006. A review of the Stern Review. *WORLD ECONOMICS-HENLEY ON THAMES-,* 7**,** 233.

TRUONG, C. and TRÜCK, S. 2016. It's not now or never: Implications of investment timing and risk aversion on climate adaptation to extreme events. *European Journal of Operational Research,* 253**,** 856-868.

USWRC. 1983. Economic and Environmental Principles and Guidelines for Water and Related Land Resources: Implementation Studies, Water Resources Council

VAN DANTZIG, D. 1956. Economic decision problems for flood prevention. *Econometrica: Journal of the Econometric Society***,** 276-287.

VAN DER POL, T., GABBERT, S., WEIKARD, H.-P., VAN IERLAND, E. and HENDRIX, E. 2016. A Minimax Regret Analysis of Flood Risk Management Strategies Under Climate Change Uncertainty and Emerging Information. *Environmental and Resource Economics***,** 1-23.

VON NEUMANN, J. and MORGENSTERN, O. 2007. *Theory of games and economic behavior*, Princeton university press.

WADEY, M. 2013. *An Analysis of Defence Failures and Coastal Flood Events: a Case Study of the Solent.* Ph.D., University of Southampton.

WADEY, M., BROWN, J., HAIGH, I., DOLPHIN, T. and WISSE, P. 2015. Assessment and comparison of extreme sea levels and waves during the 2013/14 storm season in two UK coastal regions. *Natural Hazards and Earth System Science,* 15**,** 2209-2225.

WADEY, M. P., COPE, S. N., NICHOLLS, R. J., MCHUGH, K., GREWCOCK, G. and MASON, T. 2015. Coastal flood analysis and visualisation for a small town. *Ocean & Coastal Management,* 116**,** 237-247.

WADEY, M. P., NICHOLLS, R. J. and HAIGH, I. 2013. Understanding a coastal flood event: the 10th March 2008 storm surge event in the Solent, UK. *Natural Hazards,* 67**,** 829-854.

WADEY, M. P., NICHOLLS, R. J. and HUTTON, C. 2012. Coastal flooding in the Solent: an integrated analysis of defences and inundation. *Water,* 4**,** 430-459.

WAHL, T., HAIGH, I. D., NICHOLLS, R. J., ARNS, A., DANGENDORF, S., HINKEL, J. and SLANGEN, A. B. 2017. Understanding extreme sea levels for broad-scale coastal impact and adaptation analysis. *Nature communications,* 8**,** 16075.

WALD, A. 1949. Note on the consistency of the maximum likelihood estimate. *The Annals of Mathematical Statistics,* 20**,** 595-601.

WANG, T. and DE NEUFVILLE, R. 2006. 8.1.3 Identification of Real Options "in" Projects. *INCOSE International Symposium,* 16**,** 1124-1133.

WANG, Y. and CAFLISCH, R. 2009. Pricing and hedging American-style options: a simple simulation-based approach.

WEITZMAN, M. L. 2007. A review of the Stern Review on the economics of climate change. *Journal of economic literature,* 45**,** 703-724.

WHITTEN, S. M., HERTZLER, G. and STRUNZ, S. 2012. How real options and ecological resilience thinking can assist in environmental risk management. *Journal of Risk Research,* 15**,** 331-346.

WILBY, R. L., NICHOLLS, R. J., WARREN, R., WHEATER, H. S., CLARKE, D. and DAWSON, R. J. Keeping nuclear and other coastal sites safe from climate change. Proceedings of the ICE-Civil Engineering, 2011. Thomas Telford, 129-136.

WILLOWS, R., REYNARD, N., MEADOWCROFT, I. and CONNELL, R. 2003. *Climate adaptation: Risk, uncertainty and decision-making. UKCIP Technical Report,* UK Climate Impacts Programme.

WOLF, J., LOWE, J. and HOWARD, T. 2015. Climate Downscaling: Local Mean Sea Level, Surge and Wave Modelling. *In:* NICHOLLS, R. J., DAWSON, R. J. and DAY, S. A. (eds.) *Broad Scale Coastal Simulation: New Techniques to Understand and Manage Shorelines in the Third Millennium.* Dordrecht: Springer Netherlands.

WOODWARD, M., GOULDBY, B., KAPELAN, Z., KHU, S.-T. and TOWNEND, I. 2010. The use of real options in optimum flood risk management decision making. *1st European IAHR Congress, Edinburgh, UK.*

WOODWARD, M., GOULDBY, B., KAPELAN, Z., KHU, S. T. and TOWNEND, I. 2011. Real Options in flood risk management decision making. *Journal of Flood Risk Management,* 4**,** 339-349.

WOODWARD, M., KAPELAN, Z. and GOULDBY, B. 2014. Adaptive Flood Risk Management Under Climate Change Uncertainty Using Real Options and Optimization. *Risk Analysis,* 34**,** 75-92.

YANG, M. and BLYTH, W. 2007. Modeling investment risks and uncertainties with real options approach. *International Energy Agency*.

APPENDICES

Appendix A. Analysis of wave effects on coastal flooding

Waves also affect an inundation process to facilitate inflow towards floodplains during coastal flooding. This type of defence failure by waves is referred to as overtopping in inundation modelling (Owen, 1980; EurOtop, 2016). For a more realistic generation of coastal flooding, the effects of waves need to be considered in inundation modelling. They may cause the breaching of coastal defence. There have also been many studies on breaching failure in flood risk analysis (Hall et al., 2003, Dawson et al., 2005, Gouldby et al., 2008). The breaching failure occurs by the combination of defence conditions and loading conditions during coastal flooding. Once overtopping or overflowing is replaced by breaching, a significant volume of seawater enters floodplains. The probabilistic approach has been developed to express the relative probabilities of breaching failure according to waves (W) and water elevation (H_s) (Dawson and Hall, 2006). However, as the waves coupled with water levels during a flood event are the main cause of the breaching failure, the breaching failure is conditional on waves, extreme still water levels and sea-level rise. It seems difficult to combine the probability of breaching failure with the probability of sea-level rise and extreme still water level.

This appendix is aimed to quantify the effects of waves on inundation with a focus on integrating wave effects with extreme still water levels and sea-level rise. As ESWL and SLR are given in height in this thesis, the volumes of overtopping by waves are converted to be equivalent heights by using a weir formula (Dawson et al. 2005). The estimation of overtopping volumes by waves follows several steps: (1) estimate overtopping volume over the crest of coastal defence; (2) calculate the rate of overtopping during a flood event by dividing the overall overtopping volume by its period; (3) convert the overtopping rate into equivalent height by a weir formula; and (4) add the equivalent height to the corresponding water level (i.e. ESWL+SLR). The following sections explain each process of integrating overtopping effects, extreme still water levels and sea-level rise.

A. 1. Mean overtopping discharge rate

To predict the impacts of waves on floodplains behind the coastal defences, we have calculated the mean overtopping discharge rate (q) by using an Owen's formulas (1), (2) and (3).

$$Q_* = A \exp(-B \times R_*/r) \quad (1)$$

$$Q_* = Q / (g\, T_p\, H_s) \quad (2)$$

$$R_* = R_c / (T_p\, (g\, H_s)^{0.5}) \quad (3)$$

Here, Q : overtopping discharge per the unit length of defence

H_s: significant wave height (m) at the toe of the structure

T_p: wave period (sec) at the toe of the structure

R_c: crest freeboard (= a distance from water surface to the crest of coastal defence)

r : roughness coefficient

A, B: empirically determined coefficient

The mean overtopping discharge rate is defined as the volume of overtopping seawater per unit time per unit width of coastal defence ($m^3/s/m$). The mean overtopping rate depends on wave parameters (H_s, T_m), the elevation of seawater level, the crest height and slope of coastal defences as shown in equation (1) (Owen, 1980). Since it is also affected by the crest freeboard (R_c = crest level –water level), the time-series of water levels during a flood event are also needed for calculations of wave overtopping. The mean discharge overtopping rate during a tidal cycle (= 12.43 hr) has been derived using Owen's formula in Figure A. 1. Table A. 1 shows the parameter values of the wave formulation for the defence conditions, which are taken from the weakest points of the coastal defence around Lymington.

Table A. 1 Parameter values of defence conditions for overtopping calculation

Parameters of Owen's formulation	Values	Remark
Crest height (H_c) of defence	2.5m (AOD)	The lowest height of crest defence
Roughness (n)	0.95	Stone blocks
A	0.0094	Seawall with the slope of 1:2
B	21.6	

This overtopping calculation has been made by using the time-series of still water level and the wave height and period (H_s=0.91m and T_p =3.3s) during the 10th March 2008 flood event, which is a well-documented flood event that occurred in Lymington (Refer to Section 3.2.2).

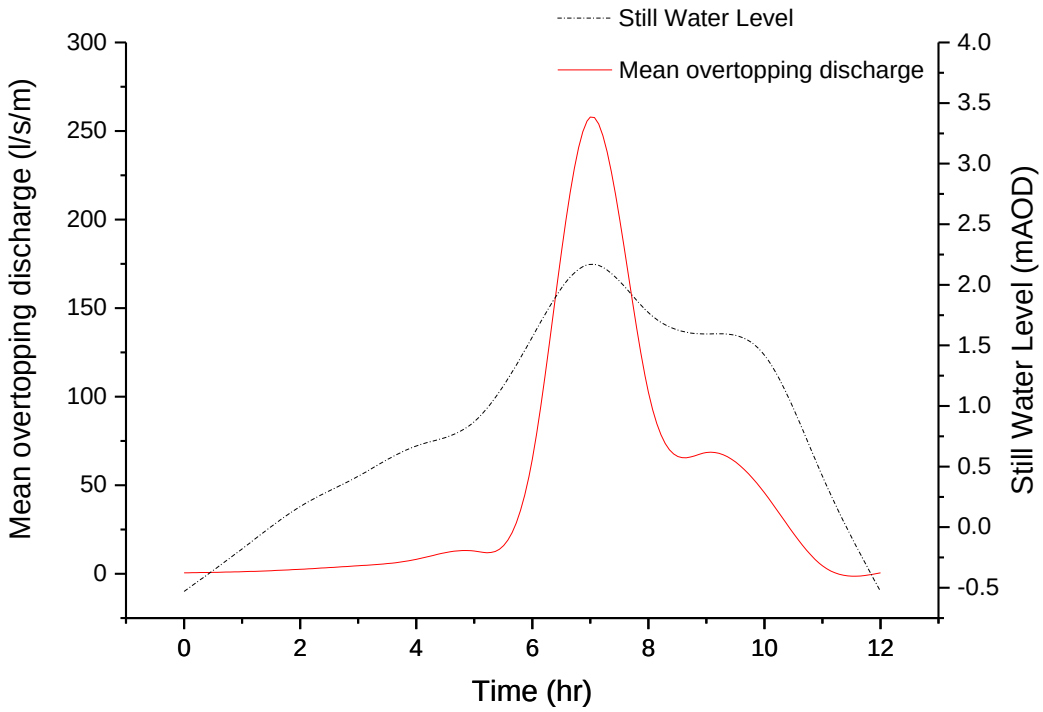

Figure A. 1 Change in mean overtopping discharge rate, corresponding to the time-series of still water level (the 10th March 2008) – calculated with H_s = 0.91 (m) and T_p = 3.3 (sec)

The mean overtopping discharge calculation in Figure A. 1 does not consider the proportion of the overtopping waves to the whole incoming waves. Therefore, the estimated overtopping discharge rates are more than an actual discharge rate. These should be modified by applying the percentage of the overtopping waves to the incident waves (Wadey, 2013). There are many studies that explain the run-up mechanism of wave overtopping in coastal flooding

literature (EurOtop, 2016). This research chose an empirical formula for sloping seawall structures that describes the proportion of overtopping by using dimensionless mean overtopping discharge (Q_*) in equation (2) (HRW, 2003). As the formula represents the proportion of overtopping in relation to dimensionless overtopping discharge (Q_*), it gives a proper approximation of an actual overtopping percentage according to the waves, still water levels and defence conditions. The equations according to the values of Q_* are shown in equations (4), (5) and (6).

$$\frac{N_{ow}}{N_w} = 55.41{Q_*}^{0.634} \quad \text{for } 0 < Q_* < 0.0008 \tag{4}$$

$$\frac{N_{ow}}{N_w} = 2.502{Q_*}^{0.199} \quad \text{for } 0.0008 \leq Q_* < 0.01 \tag{5}$$

$$N_{ow} = N_w \quad \text{for } Q_* \geq 0.01 \tag{6}$$

Here, N_{ow}: The number of waves overtopping

N_w : The total number of waves in sequence

Q_* : The dimensionless overtopping discharge $(= Q/(T_p g H_s))$

Based on the above formulations, the actual overtopping discharge rates have been re-estimated as shown in Figure A. 2.

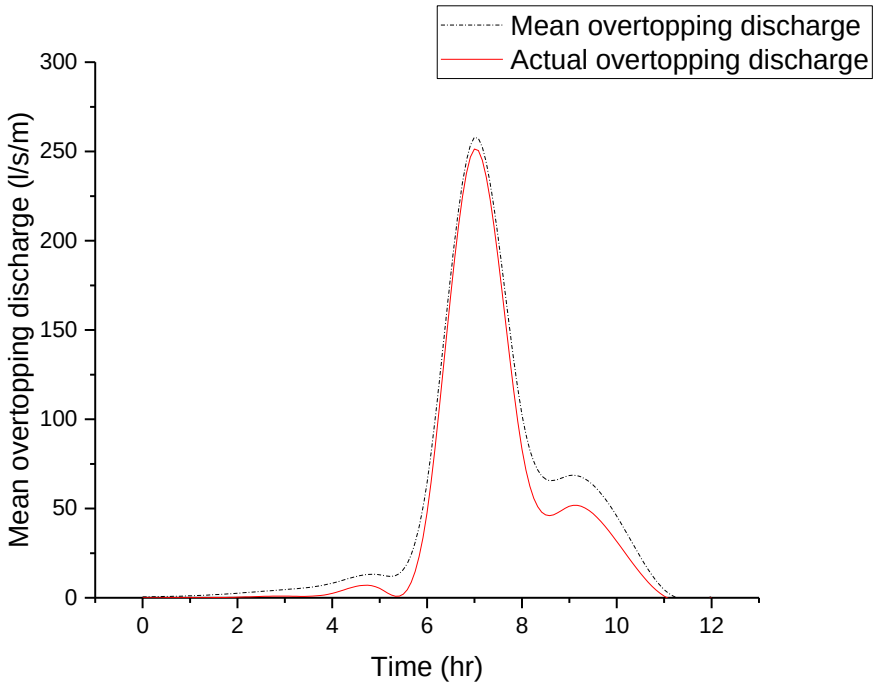

Figure A. 2 Actual rates of wave overtopping during the 2008 event in Lymington

A. 2. Calculation of total volume of overtopping

To consider temporal changes in overtopping rate against varying still water level, this part examines how the overall volume of wave overtopping changes according to peak extreme still water levels under given wave conditions (H_s and T_p). Note that the peak still water level is the highest water level during a storm surge event - In simulating a flood event, this thesis uses a peak water level by which the time-series of still water level during the flood event are generated for a realistic coastal flooding. The relations between peak water levels and overtopping volumes are deterministically established for each of wave heights as shown in Figure A. 3.

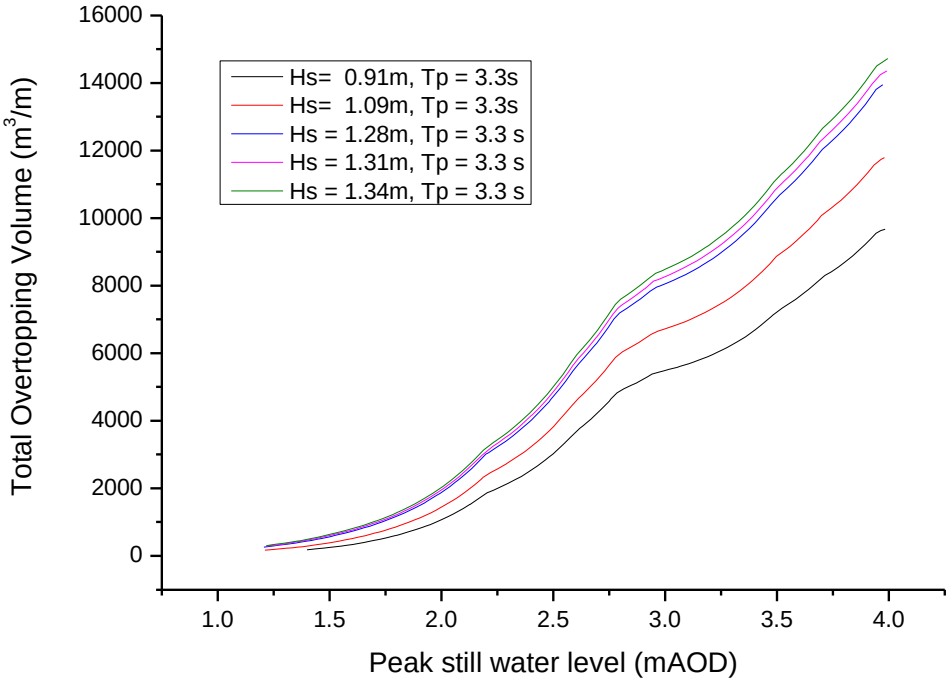

Figure A. 3 Total overtopping volumes for peak extreme still water levels for different wave conditions (H_s = 0.91, 1.09, 1.28, 1.31 and 1,34m and T_p = 3.3s (constant)).

The estimated volume is the overall amount of wave overtopping during a storm surge event for each wave condition. However, in flood simulation, still water level is continuously varying during a storm surge event. The actual overtopping volume at any given time is subject to water level at the time. That is, when water level is much lower than the crest level of coastal defence, the overtopping is unlikely to occur in floodplains behind the coastal defence. However, if water level is higher than the crest level of coastal defence, overflowing prevails over overtopping in flood inundation mechanism. This case is called a negative crest

freeboard (= still water level ≥ crest level) (EurOtop, 2016). In this case, the crest freeboard (R_c) is assumed to be zero in the equation (3) so that the overtopping discharge rate is considered to be constant during overflowing (EurOtop, 2016).

Thus, the overall overtopping volume is allocated to represent the joint effects of overtopping and overflowing during a storm surge event. Generally, if overtopping discharge rates exceed 20 (l/s/m), overtopping causes adverse or intolerable impacts on floodplains behind overtopped coastal defence (HRW, 2003; Wadey et al., 2013). By equating the threshold value of overtopping rate to be 20 (*l/s/m*), this thesis can determine the duration of an overtopping event. The overtopping volume is, then, divided by the duration bounded by the threshold overtopping rate of 20 (l/s/m). The average volume per unit time has been obtained for an overtopping event as shown in Figure A. 4

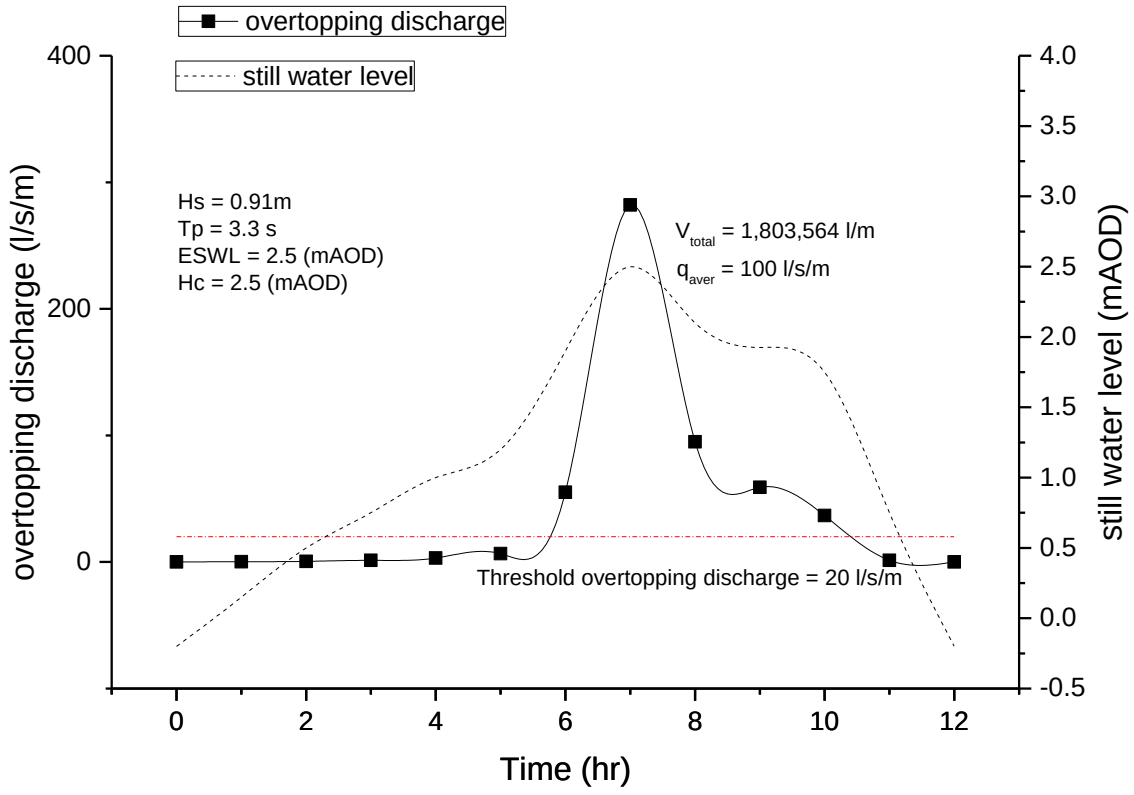

Figure A. 4 Calculation of an overtopping discharge volume (V_{total}) and its average (q_{aver}) for wave (H_s = 1.31m, T_p = 3.3s) and peak still water level (ESWL = 2.5 mAOD) against the coastal defence (H_c = 2.5 mAOD).

To make overtopping discharge have the same dimension with overflowing discharge in flood simulation, the average overtopping discharge (q_{aver}) is converted to the equivalent height above the crest of coastal defence using a weir formula provided by EurOtop (2016).

$$q = 0.51*\sqrt{g*h^3} \quad (7)$$

Here, q: an overtopping discharge

h: height over the crest of weir

This formula enables the calculation of an equivalent height for overtopping volume as shown in Figure A. 5. This data on the equivalent height of the overtopping volume is uniformly added to water level time-series during a flood event in inundation simulation. This combination provides an approximate estimation of wave effects on inundation simulation by shifting up the water level of a coastal flood event (i.e. ESWL+SLR). However, applying the equivalent height on the time-series of extreme still water level may lead to the overestimation of flood inundation because overflowing at high water levels is dominant over overtopping. For this reason, the equivalent height of overtopping is limited to 0.2m, which is recommended as the maximum limit to the effect of overtopping discharge (HRW, 2003; 2004) in Figure A. 5.

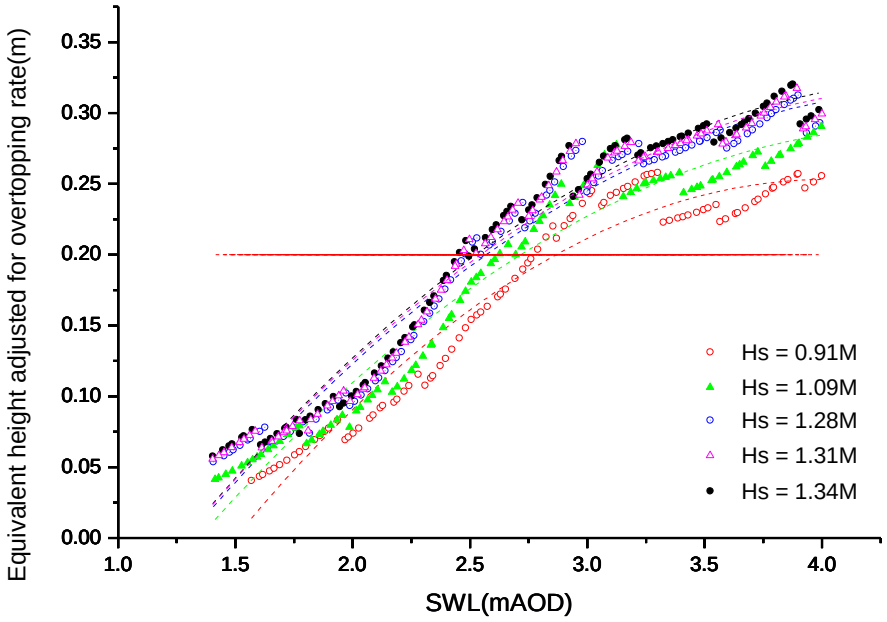

Figure A. 5 Equivalent heights of discharge rates during overtopping events according to peak still water levels for each of the wave heights (H_s = 0.91, 1.09, 1.28, 1.31 and 1.34 m and T_s = 3.3s) - Here, the defence height is 2.5 mAOD.

A. 3. Statistical test on wave, extreme still water level and sea-level rise

The previous part has investigated how overtopping rates change according to seawater conditions such as water levels and wave heights. As still water levels and wave heights are both stochastic variates, overtopping rates are also random variables as a result of combination of extreme still water levels and wave heights. Thus, the overtopping rate has its own probability distribution. The joint probability method based on Monte-Carlo simulation programme allows this analysis to combine the probabilities of waves and extreme still water levels for generating the probability distribution of overtopping rates. However, due to sea-level rise in a long-term period, the joint probability of waves and extreme still water levels keeps changing with time. The statistical integration of waves and extreme still water levels is, thus, a very challenging task in the uncertainty modelling process.

The first issue is a non-stationarity of the probability distribution of extreme still water levels due to sea-level rise. Thus, the joint probability of waves and extreme still water levels will change due to sea-level rise. Strictly, this analysis needs to construct the joint probabilities of waves and extreme still water levels with the effects of sea-level rise reflected on the probabilities.

The second issue is a high dependence between overtopping rates and extreme still water levels. Even if the probability of overtopping rate is defined by the joint probability method at any time, the occurrence of overtopping events relies more on extreme still water levels than waves. Therefore, the probability of waves seems to be less influential than the probability of extreme still water levels in calculation of the probability of overtopping rates.

In these contexts, this thesis simply adopts a fixed wave parameter in order to avoid a very complicated calculation of overtopping rates. The wave parameter has been taken from the 2008 flood event which is considered as a typical flood event for the current defence system in Lymington. To compare the effects of waves and extreme still water levels on overtopping rates, this thesis investigates the joint probability distributions of overtopping rates from waves and extreme still water levels. This research, first, takes the return period wave data between 1990 and 2002 for Lymington from the previous research (Kebede, 2009; Wadey et al., 2013). The Weibull distribution is selected as the best-fit probability distribution to the wave dataset by assessing the relative quality of candidate probability distributions (e.g.

Weibull, Exponential, Gumbul distributions, etc.). Figure A. 6 shows the wave dataset and the fitted Weibull distribution.

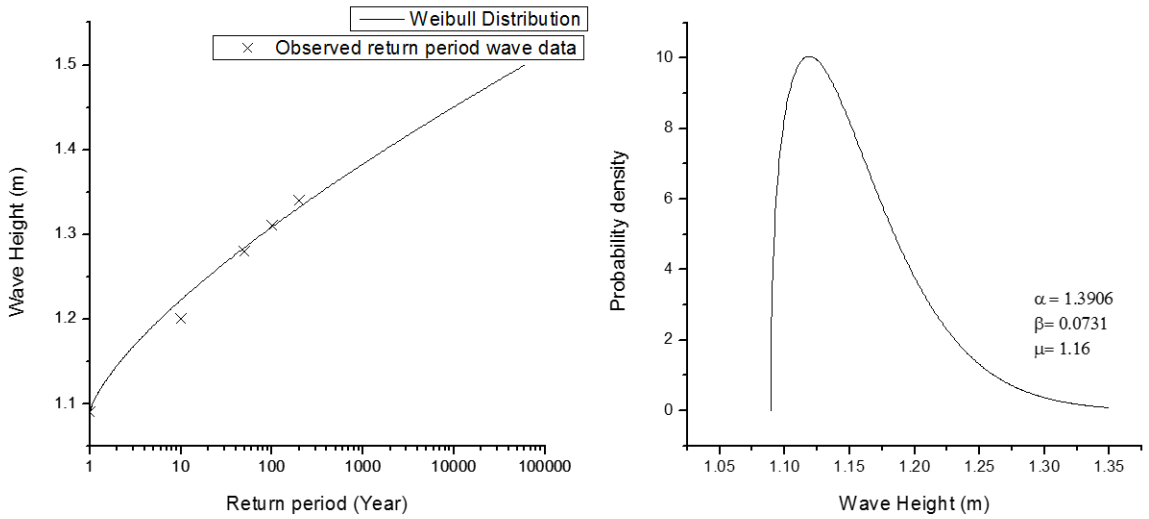

(a) (b)

Figure A. 6 Wave data and probability distribution: (a) Weibull distribution fitting to wave data and (b) Weibull distribution of wave for Lymington

The probability distribution of waves is combined with the probability of extreme still water levels of the base year (2008) for Lymington. By sampling 10,000 data on waves and extreme still water levels from each probability distribution, this probability analysis has constructed the joint probability of the overtopping rates in equivalent height. For comparisons, the probability distribution of overtopping rates is made for each of the wave heights (Figure A.7). The calculation of overtopping rates is based upon the Owen's formulation (1980) (See the previous analysis in Section B. 1) for the coastal defence with a defence height of 2.5m (AOD) and a slope of 1:2 which is the parameter of the weakest coastal defence in Lymington. This calculation process is conducted by a probabilistic analysis programme (@Risk) using sampling method. This programme is also designed to enable the programmed calculations of overtopping rates with stochastic variables of waves and extreme still water levels iteratively. For the generation of the joint probability distributions, the extreme still water levels are taken from the exponential distribution defined in Section 4.2.1.

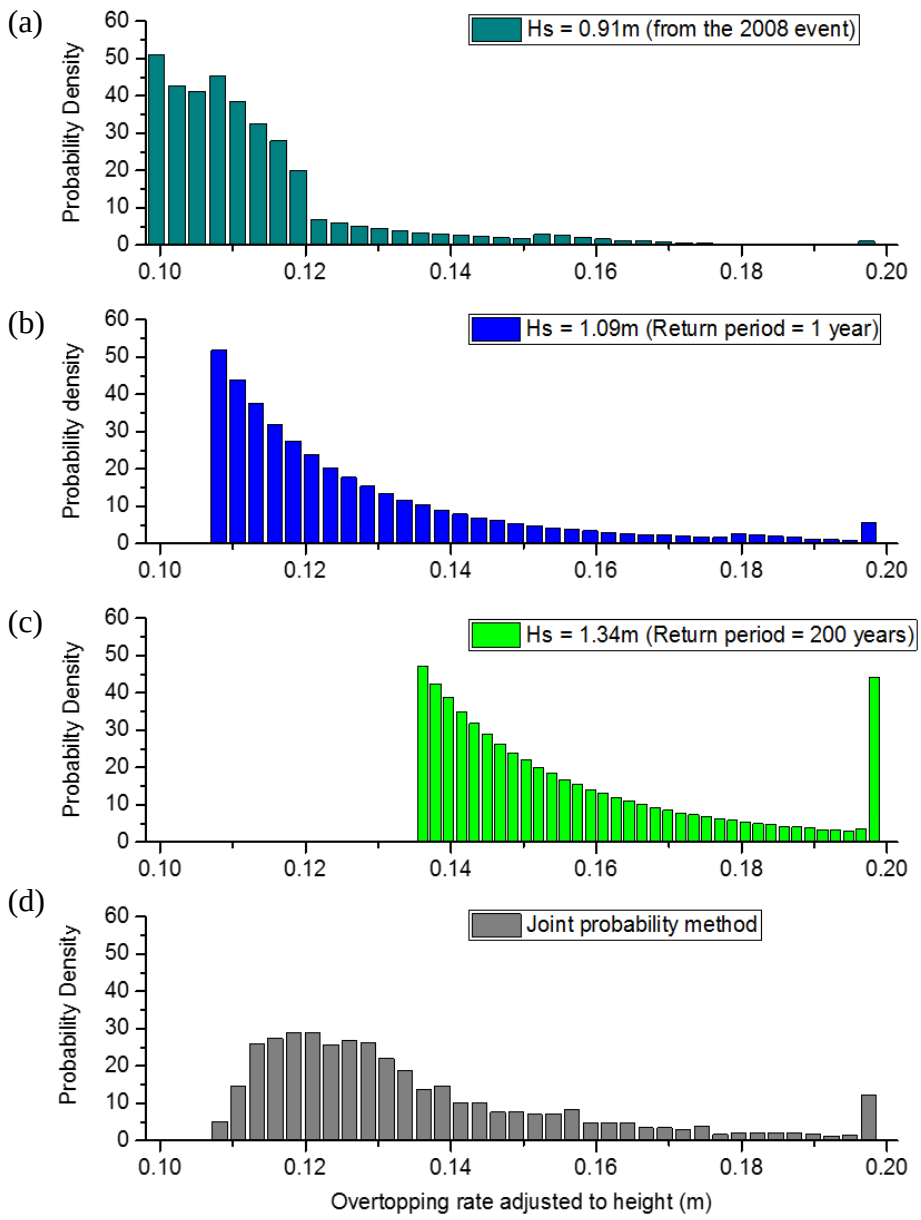

Figure A. 7 (a), (b) and (c) Probability distributions of overtopping rates by the exponential distribution of extreme still water levels (ESWL) and 0.31m of sea-level rise for different wave heights (the wave period is the same with 3.3s) – The probability distribution (d) is made by the joint probability method of waves distribution (Weibull) and ESWL distribution (Exponential).

As shown in Figure A. 7 (a), (b) and (c), the different wave heights lead to different ranges and probabilities of overtopping rates. The joint probability method (Figure A. 7 (d)) gives a well-defined probability distribution of overtopping rates based on the probabilistic characteristics of waves and extreme still water levels. However, this newly produced

probability distribution keeps changing due to sea-level rise. Thus, the joint probability of overtopping rate is transient. In addition, the overtopping rates from this joint probability need to be combined with the corresponding extreme still water level in order to represent the overall effects of overtopping and overflowing in flood risk analysis. The former is mainly due to waves whereas the latter is due to extreme still water level and sea-level rise. If we combine overtopping rates with extreme still water levels independently, this would give a biased result. It is because the overtopping rates are highly dependent on extreme still water levels and sea-level rise. The statistical correlation of two random variables of overtopping rates and extreme still water levels seems to be a very challenging task beyond the limit of this thesis. In addition, the effects of waves on flood simulation are much less than the effects of storm surges. Thus, this research has generated the probability distributions of overtopping rates in respect to the constant wave parameters of H_s and T_p taken from the 2008 flood event. This approach seems to be reasonable when comparing the dependence of overtopping rates on waves with that on extreme still water levels as shown in Figure A.8.

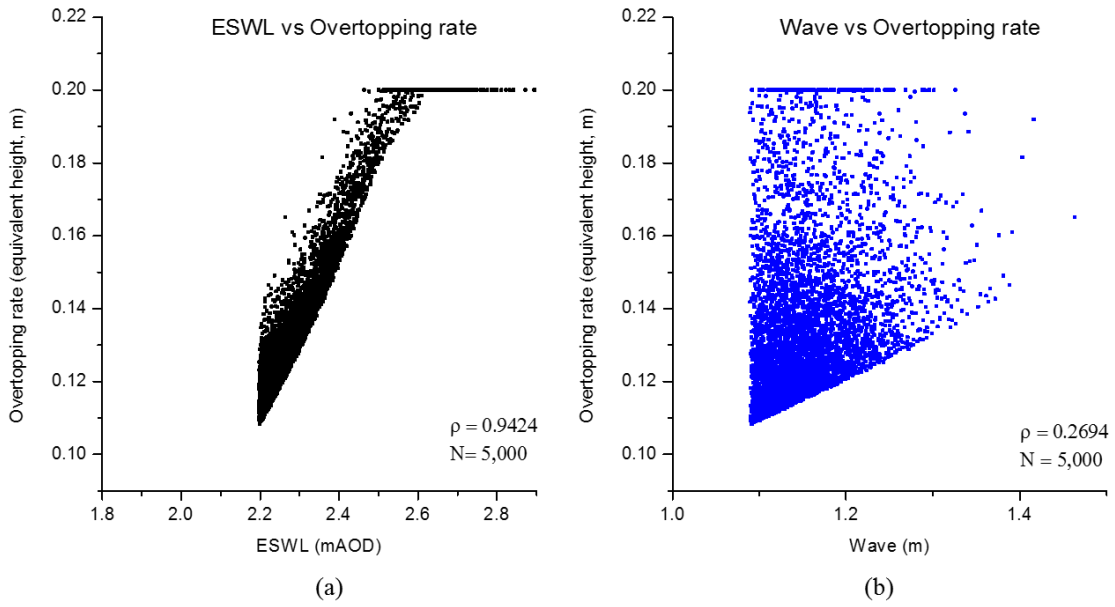

Figure A. 8 The degree of correlation (ρ) of overtopping rates with extreme still water levels (a) and with waves (b) (Here, N is the number of scatters)

In 5,000 calculations of overtopping rates with the random variables of wave and ESWL, the overtopping rates show much higher correlation with ESWLs than waves. The significance between extreme still water levels and overtopping rates is found with a correlation factor estimated at (ρ = 0.9424) as shown in Figure A. 8 (a). However, the correlation between waves and overtopping rates (ρ = 0.2694) is much less significant than that of ESWL as

shown in Figure A. 8 (b); although waves are a main driver to trigger the overtopping failure of coastal defence.

Choosing a wave parameter value (H_s and T_p) affects the possible range of overtopping rates (See x-axis of the graphs in Figure A. 7). As seen in Figure A. 7, the probabilistic range of wave overtopping rate for *Hs* =1.09m (the return period of the wave is 1 year) exactly matches with the width of overtopping rates made by the joint probability method. Taking the low wave heights (e.g. H_s=1.09 or 0.91m) is able to cover the full range of overtopping rates while taking the high wave heights (H_s=1.34m) is unable to the full range of overtopping rates. Thus, the wave parameter (H_s = 0.91m and T_p = 3.3s) is taken from the 10th March 2008 event in Lymington. This wave parameter provides the full range of overtopping rates for inundation modelling in comparison to other wave parameters.

The equivalent heights of the overtopping rates are simply added on the peak still water levels plus sea-level rise for the loading conditions of coastal flooding. As the wave condition (H_s = 0.91m and T_p = 3.3s) is fixed, this provides a deterministic relation between overtopping rates and water levels as shown in Figure A. 9.

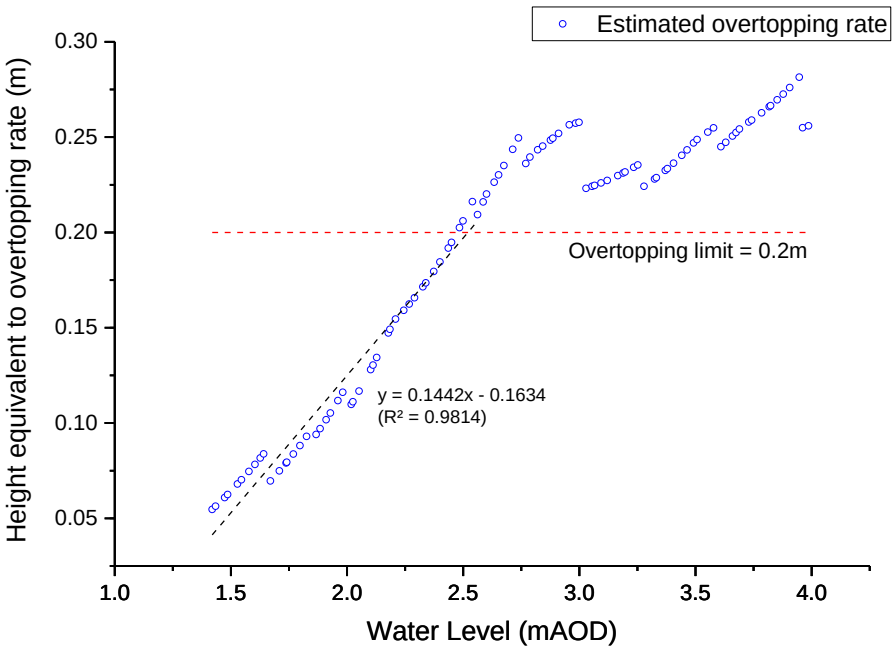

Figure A. 9 A relation between overtopping rates and water levels (= ESWL+ SLR) for the wave conditions (H_s =0.91m and T_p =3.3s)

Appendix B. Applying Brownian motion into Sea-level rise (SLR)

From the perspective of the expected utility theorem (Daniel Bernouli, 1738), option values, based on central values, are the results of statistical expectation regarding the uncertain outcomes of flood damages in the future. Thus, choosing a central estimate of MSLR for option evaluations can be considered as a reasonable approach. Nevertheless, it should be noted that this approach cannot address the low-probability, but high-impact, events in the perspective of risk managements.

To tackle this problem in the mean value of sea-level rise or flood damage, this thesis employs Brownian motion to describe all the possible range of sea-level rise in a statistical way. However, it requires a parametrization process to represent the deterministic and random motion of uncertain variables with drift and variance parameters (α, σ), respectively. This appendix focuses on adjusting the Brownian motion for sea-level rise projections. We apply each type of the Brownian motion for sea-level rise projections: (1) Simple Brownian motion, (2) Geometric Brownian motion and (3) General Brownian motion and, then, choose the most suitable motion to sea-level rise projections by UKCP 09. These continuous stochastic processes describe the motion of uncertain variable in different ways.

B. 1. Simple Brownian motion (SBM)

The drift parameter of Simple Brownian motion, which describes the long-term trend of sea-level rise, can be easily obtained by setting variance parameter to be zero (i.e. the state of no uncertainty) in its expression. That is, the Simple Brownian motion (hereafter, referred to as SBM) with no uncertainty is

$$dx = \alpha\, dt \qquad (1)$$
$$\therefore\ x\text{-}x_0 = \alpha(t\text{-}t_0)$$

Here, α is a drift parameter, x_0 is sea-level rise at year t_0, x is sea-level rise at year *t*. By fitting equation (1) into MSLR, we can have a drift parameter for each sea-level rise projection. The Brownian motion with no uncertainty for each sea-level rise scenario is plotted with mean sea-level rise in Figure B. 1 (R^2 = 0.99).

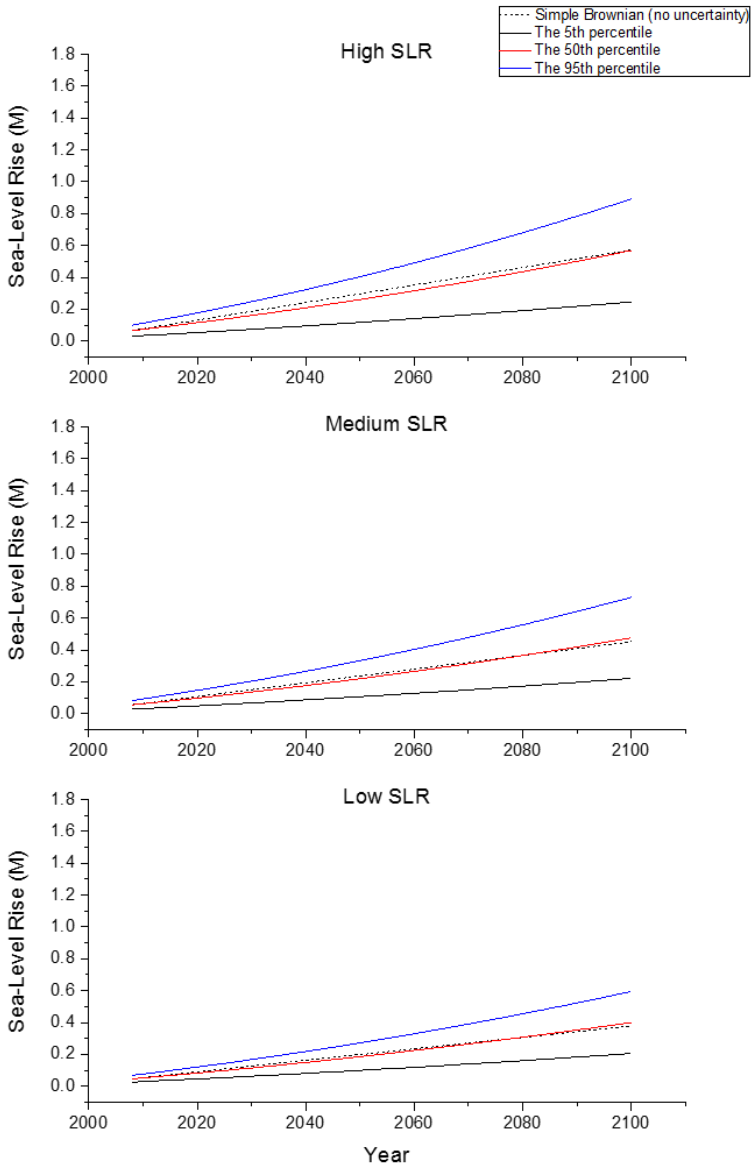

Figure B. 1 Simple Brownian motion (SBM) with no uncertainty for each SLR scenario

The uncertainty of a sea-level rise projection at any given time has been represented by a percentile range at the corresponding time in UKCP 09 data while the variance parameter (σ) of SBM is obtained from the variance (σ_t) of sea-level rise (from UKCP 09) at time *t*. It is of note that, while the variance (σ) of Brownian motion indicates change in the stochastic process over a time interval, the variance (σ_t) of sea-level rise at time *t* indicates the uncertainty range of any variable being observed at time *t*. For SBM, the variance parameter (σ) has a relation with the variance (σ_t) of variable (x_t) at time *t* as below.

$$\mathrm{Var}[x_t] = [\sigma_t]^2 = \sigma^2(t\text{-}t_0)^2 \qquad (2)$$

$$\therefore \quad \sigma = \sqrt{\frac{\sigma_t}{t\text{-}t_0}}$$

Here, $Var[x_t]$: a variance of variable x_t at time t

σ_t: a standard deviation of variable x_t at time t

t_0: a start year of Simple Brownian Motion (SBM)

To estimate the variance parameter of SBM, this analysis selects the variance of sea-level rise at 2100 for each SLR scenario. The standard deviation (σ_t) of sea-level rise at 2100 can be calculated from the width of a 90%-confidence level which is bounded by the 5th and 95th percentile of sea-level rise projection (UKCP 09) at 2100 as shown in Figure B. 2.

As the standard deviation (σ_{2100}) at year 2100 for each SLR projection is known, we can have the variance parameter (σ) of Simple Brownian motion for all the SLR scenarios by equation (2).

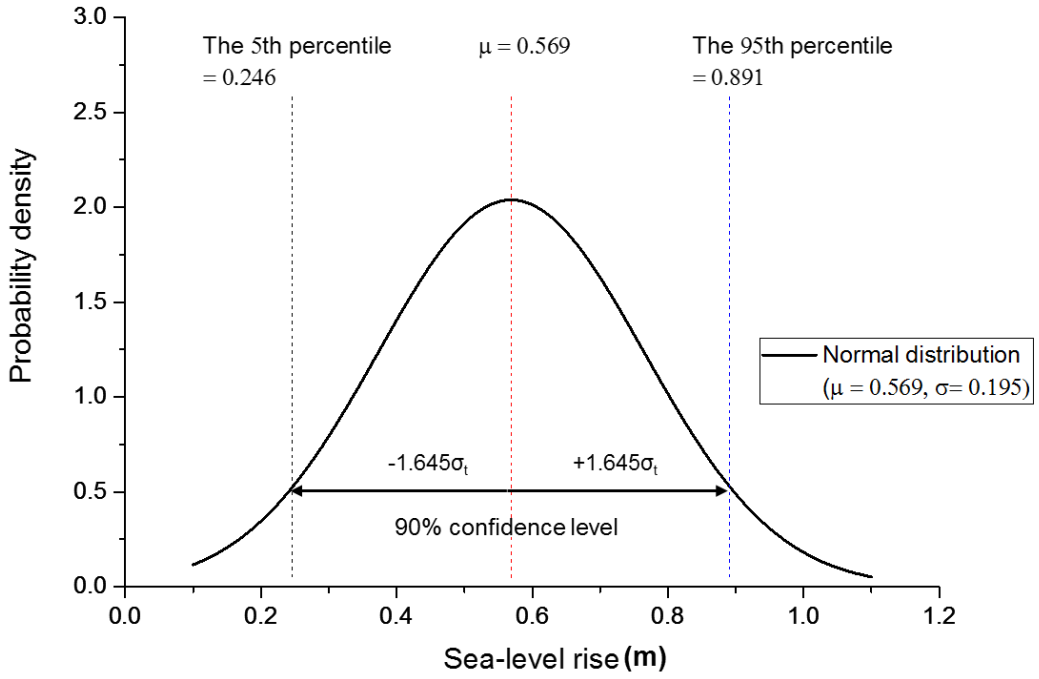

Figure B. 2 Mean (μ), standard deviation (σ_t) and percentiles of sea-level rise at 2100 for high SLR projection from UKCP 09 (Lowe et al., 2009).

Table B. 1 Drift (α) and variance (σ) parameters for each SLR by SBM (unit: m/year)

SLR scenario	Drift parameter (α)	Variance parameter (σ)
High	0.0055	0.0187
Medium	0.0043	0.0147
Low	0.0036	0.0115
Historic trend	0.0013	0.00018*

* The variance parameter is obtained from the observed sea-level rise data at Southampton gauge since 1935 (Haigh et al., 2010)

As the drift and variance parameters (α, σ) are known, the Simple Brownian motions for all the SLR projections can be represented using these parameters. This thesis generates random time-series of sea-level rise for discrete time (Δt =1 year) in a numerical way. The Simple Brownian motion can be expressed for discrete time ($\Delta t = 1$ yr) as below.

$$x_{t+1}\text{-}x_t = \alpha + \sigma\epsilon \tag{3}$$

Here, x_{t+1}, x_t : stochastic variables of sea-level rise at year t+1 and year t

ϵ: a random variable normally distributed with $\mu = 0$ and $\sigma = 1$

The generation of a random variable (ϵ) in equation (3) uses a random value generator provided by Microsoft Excel. The random value generator of the Excel programme returns an evenly-distributed random real number between 0 and 1 at every run. Then, the randomly generated values have been input into an inverse function of normal distribution with the mean of 0 and the standard deviation of 1. This coordinated function enables the equation (3) to randomly generate the time-series of values of sea-level rise on a yearly basis during the period from 2008 to 2100. The four examples of sea-level rise following the Simple Brownian motion are shown for each of the SRL projections in Figure B. 3. Most random series generated by the Simple Brownian motion occur within the 5th and 95th range of sea-level rise projections. As seen in the High to Low SLR scenarios, some of the Brownian motions fall out of the boundaries of the sea-level rise projections. This is statistically possible because the 5th and 95th percentile ranges of the sea-level rise projection just indicate a 90%-confidence interval in which nine of ten simulations of SBM are observed

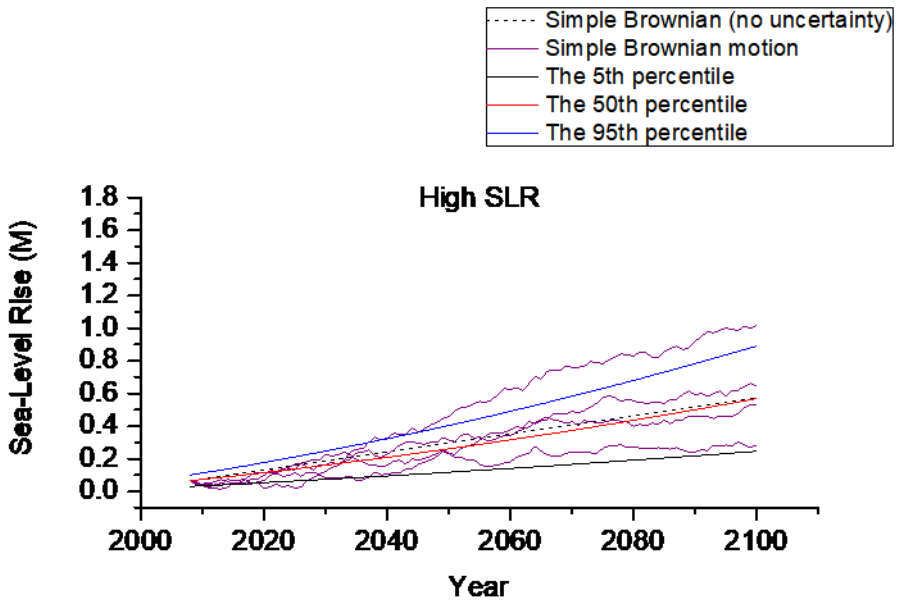
Simple Brownian (no uncertainty)
Simple Brownian motion
The 5th percentile
The 50th percentile
The 95th percentile
High SLR
Sea-Level Rise (M)
1.8
1.6
1.4
1.2
1.0
0.8
0.6
0.4
0.2
0.0
2000
2020
2040
2060
2080
2100
Year

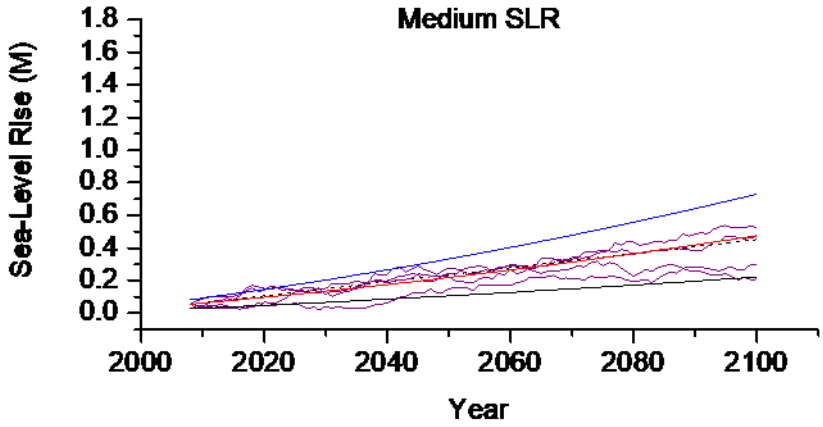
Medium SLR
Sea-Level Rise (M)
1.8
1.6
1.4
1.2
1.0
0.8
0.6
0.4
0.2
0.0
2000
2020
2040
2060
2080
2100
Year

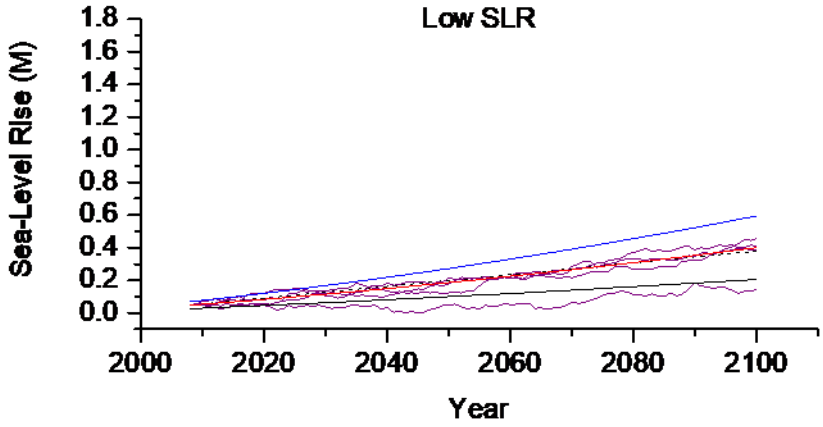
Low SLR
Sea-Level Rise (M)
1.8
1.6
1.4
1.2
1.0
0.8
0.6
0.4
0.2
0.0
2000
2020
2040
2060
2080
2100
Year

(Continue)

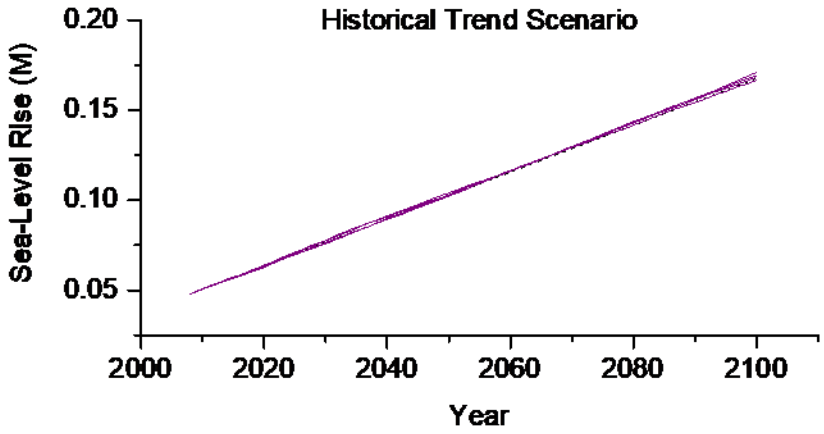

Figure B. 3 Examples of sea-level rise following Simple Brownian motion for each SLR scenario – The Historical trend scenario is made of the current rate of sea-level rise (1.3mm/yr) at Southampton. The variance of sea-lever rise rate (σ = 0.00018mm/yr) is used for the variance parameter(σ) of SBM

The advantage of using the Simple Brownian motion is the convenience of calculation for drift (α) and variance (σ) parameters. Also, the long-term variation of SBM agrees relatively well with the mean variation of sea-level rise projection by the UKCP 09. However, SBM makes sea-level rise occurs in negative regions as shown in the Low SLR scenario in Figure B. 3. In addition, roughly 40 cm falls are observed in Simple Brownian motion of sea-level rise under the H++ SLR scenario. This is not physically plausible during the 21st century. This type of Brownian motion is not appropriate to express the realistic nature of sea-level rise from the perspective of our current observation and scientific understanding.

B. 2. Geometric Brownian motion

Geometric Brownian motion (GBM) of variable *x* is a special case of simple Brownian motion in respect to the logarithm of variable *x*. Thus, the expression and parametrization process of Geometric Brownian motion are the same with those of the Simple Brownian motion with respect to $\ln(x)$. The expression of the Geometric Brownian motion (hereafter, called GBM) is written for a continuous time (*t*) in equation (4).

$$dx = \alpha x\, dt + \sigma x\, dz \quad (4)$$

Here, α: drift parameter of GBM

σ: variance parameter of GBM

dz: a Weiner process ($\Delta z = \epsilon\sqrt{\Delta t}$)

If there is no uncertainty in GBM, equation (4) can be adjusted to be equations (5) and (6).

$$dx = \alpha x\, dt \quad (5)$$

$$\therefore\ x = x_0 e^{\alpha(t-t_0)} \quad \text{or} \quad \alpha = \frac{1}{(t-t_0)} \ln\left(\frac{x}{x_0}\right) \quad (6)$$

Here, x_0: sea-level rise at year t_0

x : sea-level rise at year t

Equation (6) enables us to find a drift parameter (α) of Geometric Brownian motion (GBM) which describes an exponentially increasing pattern of sea-level rise with no uncertainty. The drift parameter (α) of GBM can be obtained by substituting into equation (6) the values of sea-level rise at the base year (2008) and the end year (2100) for a sea-level rise projection, respectively. The GBM with no uncertainty is plotted for each of the sea-level rise scenarios in Figure B. 4 which can be expressed by an exponential function of time ($x = x_0 e^{\alpha(t-t_0)}$).

The variance of x_t at a given year t is given by equation (7) (Dixit and Pyndick, 1994)

$$\text{Var}[x] = \sigma_t^2 = {x_0}^2 e^{2\alpha(t-t_0)}\left(e^{\sigma^2(t-t_0)}-1\right) \quad (7)$$

Here, Var[x]: the variance of variable x at a given year t

σ_t: the standard deviation of variable x at a given year t

x, x_0: variables at a given year t and a start year t_0, respectively

t_0: the start year of Geometric Brownian motion

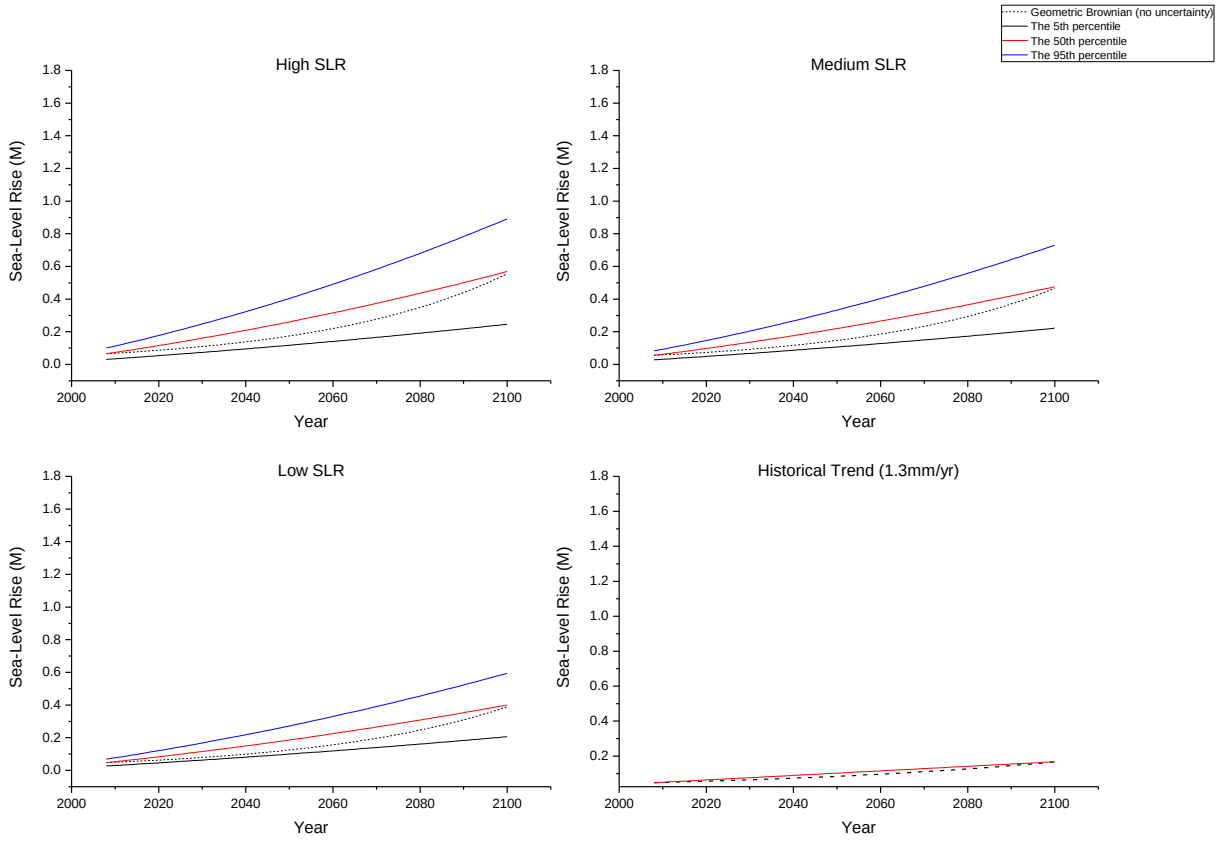

Figure B. 4 Drift parameters of Geometric Brownian motion (σ=0) for each SLR scenario

By equations (6) and (7), we can find the drift and variance parameters of Geometric Brownian motion for each of the SLR scenarios. Table B. 2 shows the results of its calculations.

Table B. 2 Drift (α) and variance (σ) parameters following GBM for each SLR

SLR scenario	Drift parameter (α)	Variance Parameter (σ)
High	0.0234	0.0348
Medium	0.0233	0.0330
Low	0.0230	0.0301
Historical Trend	0.0136	0.00018*

* The variance parameter for the Historical trend SLR is taken from the variance parameter of SBM

If the drift and variance parameters of each SLR scenario are substituted for the discrete-time expression of Geometric Brownian motion in equation (8), it can also generate the annual random time-series of sea-level rise as shown in Figure B. 5 .

$$x_t = (1 + \alpha)x_{t-1} + \sigma\epsilon x_{t-1} \quad (8)$$

Here, x_{t+1}, x_t : the stochastic variables of sea-level rise at year t+1 and year t

ϵ: normally distributed random variable ($\mu = 0$ and $\sigma = 1$)

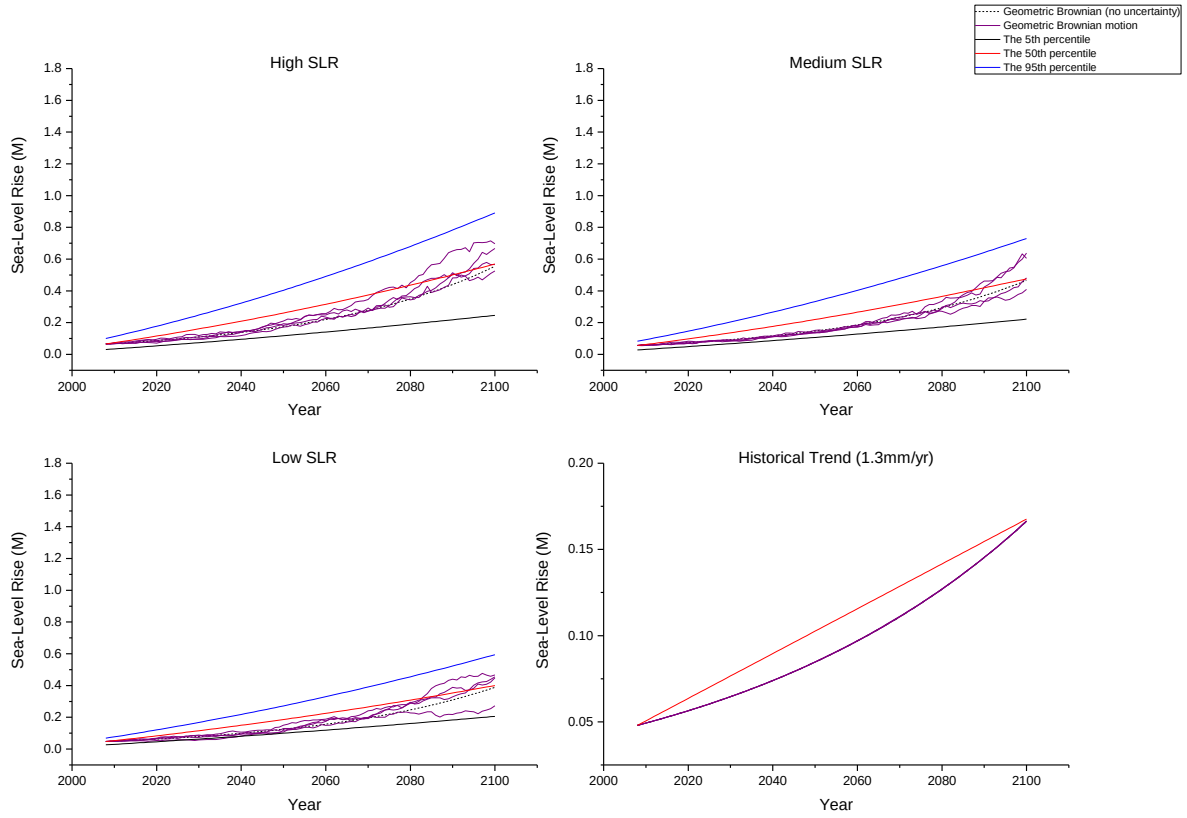

Figure B. 5 Examples of sea-level rise following Geometric Brownian motion (GBM) for each SLR scenario – Note a different y-axis scale in Historical Trend scenario.

However, when applying Geometric Brownian motion to the sea-level rise projections, the exponential function ($x_t = x_0 e^{\alpha(t-t_0)}$) of Geometric Brownian motion does not agree as well with the long-term trend of a sea-level rise projection as the Simple Brownian motion does. The representation of sea-level rise with GBM shows a significant disagreement with the sea-level rise projection of the UKCP 09 in central estimate. Therefore, we conclude that Geometric Brownian motion (GBM) is not appropriate for representing the sea-level rise projections of the UKCP 09. However, one of the advantages in the use of GBM is that its stochastic process does not occur in the negative region as well as the stochastic variables of sea-level rise shows continuously upward trends. Therefore, GBM can be considered as a useful approach to represent climate change projections if sea-level rise is positive or keeps increasing.

B. 3. General Brownian motion

General Brownian motion defines the deterministic and stochastic motion of variable x by any functions $a(x,t)$ and $b(x,t)$, respectively. The mathematical expression of General Brownian motion can be written in equation (9).

$$dx = a(x,t)dt + b(x,t)dz \tag{9}$$

Here, $a(x,t), b(x,t)$: any function of variable *x* and time *t*

dz*:* Wiener process

The advantage of General Brownian motion is that it can take any function $a(x,t)$ or $b(x,t)$ to represent the behaviour of stochastic variable x. Therefore, it fits well with the central value of a sea-level rise projection provided by UKCP 09. If there is no uncertainty in General Brownian motion, General Brownian motion can be written as equation (10).

$$dx = a(x,t)dt \tag{10}$$

From this equation, we can understand that the function $a(x,t)$ of Generalize Brownian motion is the first derivation of variable x with respect to time t, if there is no uncertainty in variable *x*. This thesis has derived a drift function $a(x,t)$ from each sea-level rise scenario whose variation of the central estimate is a quadratic function of time *t* (Lowe et al., 2009). The General Brownian motion with no uncertainty is plotted for each of the SLR scenarios in Figure B. 6.

The function of $b(x,t)$ governs the stochastic motion of variables *x* in General Brownian motion. In most of real options analysis in financial sectors, this function is determined by analysts' experiences and observation about the past records or data.

However, if we take $b(x,t)$ from the past scientific data or observations, its representation appears to be sea-level rise with no uncertainty. For example, if $b(x,t)$ is set to be ± 0.18mm/year for General Brownian motion, the time-series of sea-level rise with such a variance parameter appears along the MSLR of UKCP 09 as shown in Historical Trend scenario in Figure B. 6.

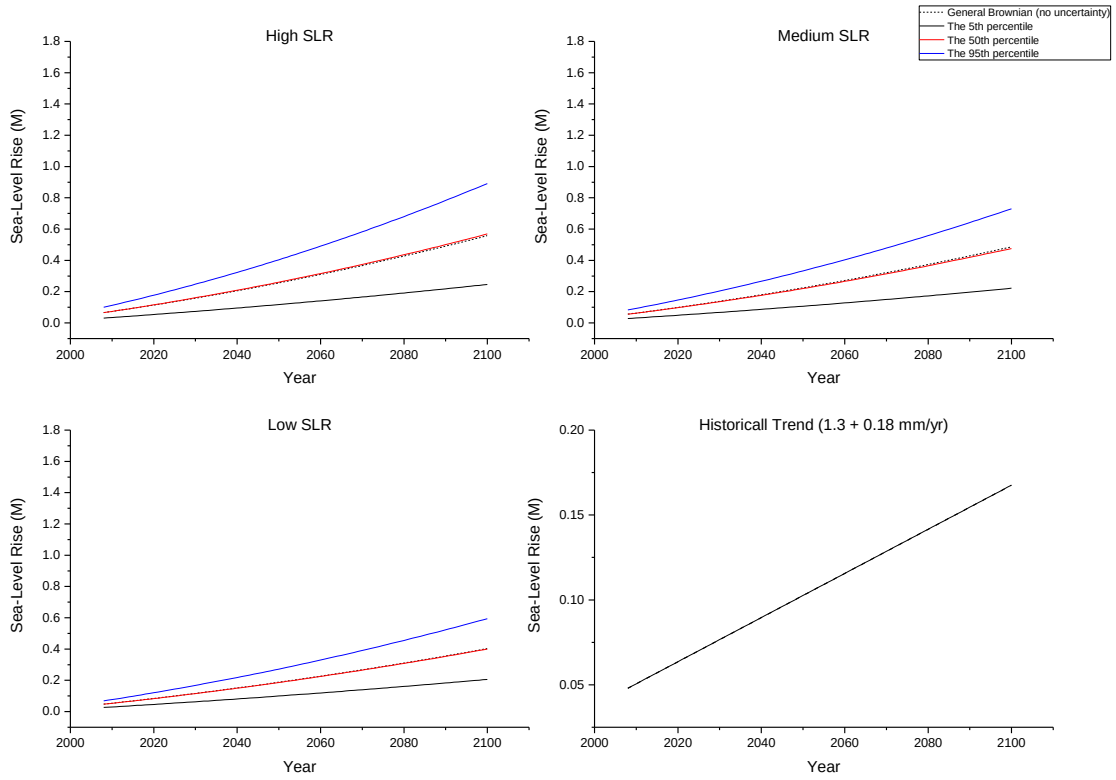

Figure B. 6 General Brownian motion with no uncertainty (σ=0) for each SLR scenario

For the description of uncertainty range of UKCP 09, we have also substituted $b(x,t)$ with a variance parameter from Simple Brownian motion for each sea-level rise projection. General Brownian motion with such a variance makes the time-series of sea-level rise fit within the uncertainty range of UKCP 09. Thus, the probability distribution of sea-level rise by General Brownian motion in 2100 fits well with the probability distribution of UKCP 09 in 2100.

However, this type of General Brownian motion also shows the physically implausible behaviours of sea-level rise (e.g. large drops in sea-level rise or sea-level rise below zero) during the projection period as revealed in Simple Brownian motion. It is because a variance parameter (σ) taken from the uncertainty of sea-level rise at 2100 is too high to describe the uncertainty range of sea-level rise in an early time period of UKCP 09 projection. It is of note that the variance (σ_t) or uncertainty range of sea-level rise in UKCP 09 is small in the early stage of the projection and increases with time. In Simple Brownian motion, the variance parameter (σ) is estimated by dividing the variance (σ_T) of sea-level rise at the end of the projection (i.e. 2100) by a square root of the time distance between the start year and the end year of sea-level rise projection ($= \sqrt{T\text{-}t_0}$, Here, T: the end year of the projection, t_0 : the start year of the projection). Thus, General Brownian motion using the variance parameter from

Simple Brownian motion gives much fluctuation in sea-level rise in the early stage of the time period.

To resolve this issue on the use of variance from Simple Brownian motion, we have modified General Brownian Motion by using a time-varying variance parameter. For denotation, we term this type of General Brownian motion 'adjusted General Brownian motion'. As the variance (σ_t) of sea-level rise at time *t* is known by UKCP 09, a variance from every year during the period of sea-level rise can be obtained for each SLR scenario. As the variance parameter of Simple Brownian motion is calculated, the time-varying variance function $b(x, t)$ at time *t* for adjusted General Brownian motion has been obtained by dividing the variance (σ_t) at time *t* by the square root of time distance from the starting time (t_0) to the time *t*. It is of note that UKCP 09 projection starts from 1990 with uncertainty increasing from zero. In this regard, this thesis assumes that the variance function $b(x, t)$ of the adjusted General Brownian motion at time *t* is proportionate to the variance (σ_t) of sea-level rise at time *t*. The function $b(x, t)$ is written in equation (11).

$$b(x, t) = \frac{\sigma_t}{\sqrt{(t\text{-}t_0)}} \tag{11}$$

Here, $b(x, t)$: The variance function of variable *x* and time *t* for adjusted General Brownian motion

σ_t: The variance of sea-level rise at time t from UKCP 09

t_0: The starting time of sea-level rise projection (i.e. 1990)

For discrete time ($\Delta t = 1$), the equation (9) has a discrete form in equation (12) as below.

$$\begin{aligned} x_{t+1}\text{-}x_t &= a(x, t)\Delta t + b(x, t)\Delta z \\ &= a(x, t) + b(x, t)\epsilon \\ \therefore\ x_{t+1} &= x_t + a(x, t) + b(x, t)\epsilon \end{aligned} \tag{12}$$

Here, x_{t+1}, x_t : variables at time *t* and *t+1*, respectively

ϵ : a random variable normally distributed with μ of 0 and σ of 1

Table B. 3 Drift functions $(a(x,t))$ and variance functions $(b(x,t))$ of General Brownian motion for each SLR – The variance parameters are taken from Table B. 1

SLR scenario	Drift function $(a(x,t))$	Variance function $(b(x,t))^*$
High	0.000032 *t* - 0.06204	0.0001 *t* - 0.2913
Medium	0.000027 *t* - 0.04996	0.0001 *t* - 0.2297
Low	0.000021 *t* - 0.03969	0.00009 *t* - 0.1744
Historical Trend	0.0013	0.00018

* The variance parameter of Brownian motion at time t is the variance of sea-level rise at time *t* from UKCP 09 divided by $\sqrt{t\text{-}t_0}$ (t_0 = 1990) – This time-varying variance parameter is fitted to a linear function with time.

The time-series of adjusted General Brownian motion with the stochastic properties of UKCP 09 can be simulated by a programmed Excel spreadsheet (Figure B. 6).

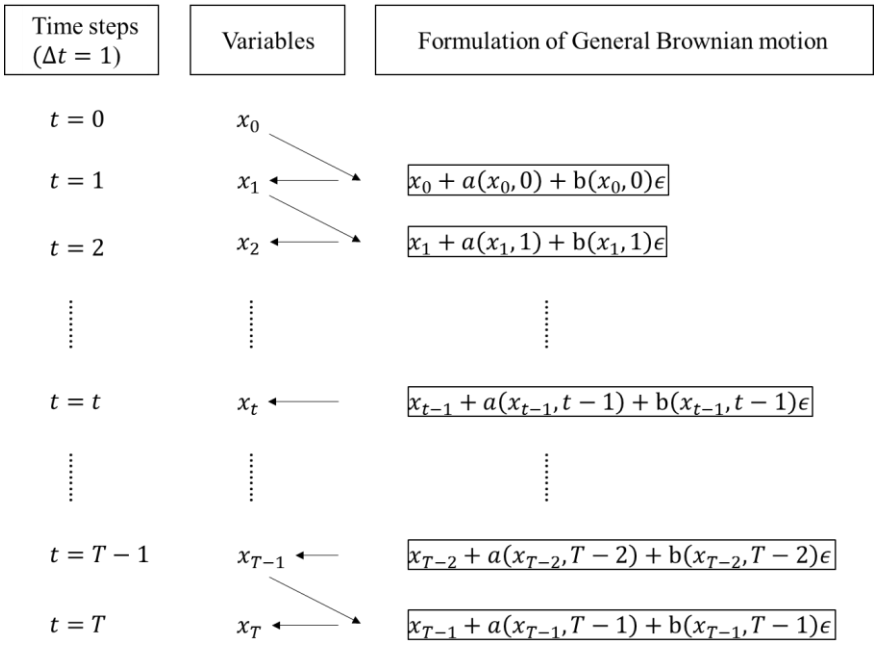

Figure B. 7 The process of computing the variables of adjusted General Brownian motion

Four examples of time-series of sea-level rise randomly generated by adjusted General Brownian motion are shown for each sea-level rise scenario in Figure B. 8. This illustration shows more realistic behaviour of sea-level rise which occurs within the statistical boundaries comprised of the 5th and 9th percentiles. As the variance parameter for adjusted General Brownian motion reflects temporal changes in variance in UKCP 09, significant drops in sea-level rise that appear in Simple Brownian motion are not observed during the simulation of adjusted General Brownian motion.

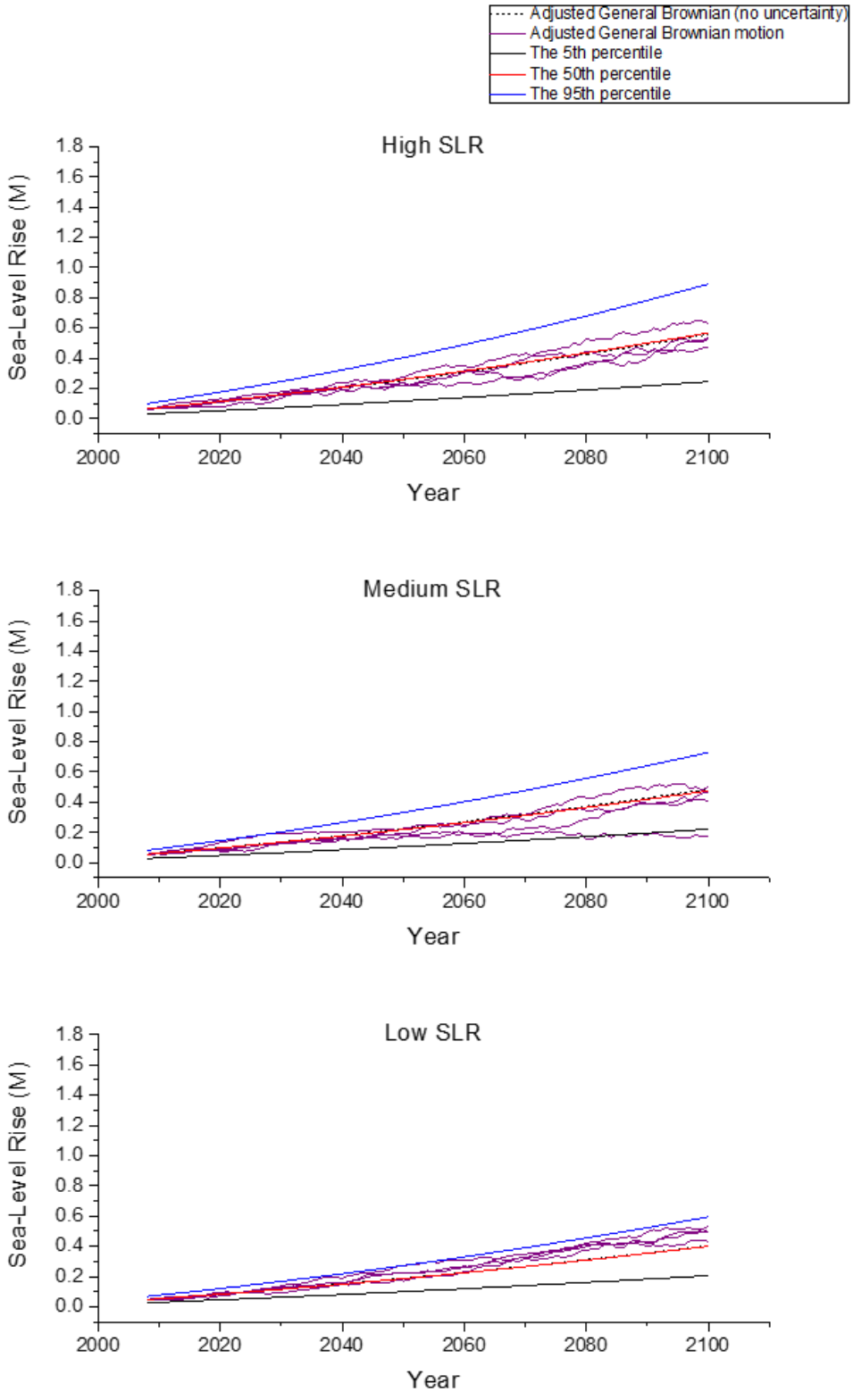

Figure B. 8 Examples of time-series of sea-level rise by adjusted General Brownian motion for each sea-level rise scenario

To see the effects of variance parameter on the patterns of Brownian motion, we have also produced the time-series of General Brownian motions by using different variance

parameters from the historical trend of Southampton and Simple Brownian motion, respectively (Figure B. 9).

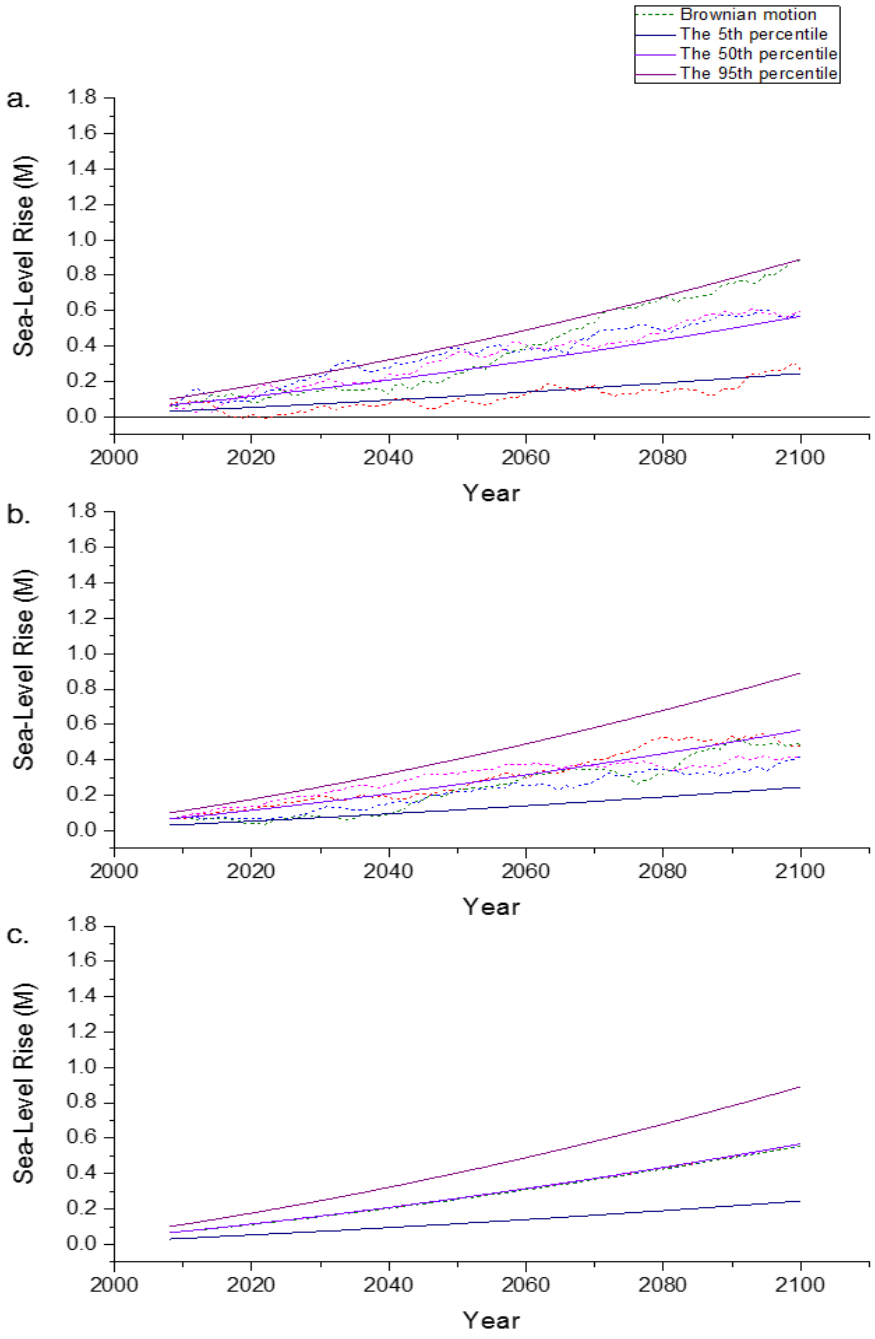

Figure B. 9 General Brownian motions for High SLR scenario using (a) a constant variance parameter taken from Simple Brownian motion (σ=0.0181 m/year); (b) a time-varying variance parameter; and (c) a variance parameter (σ=0.00018 m/year) from the observation of sea-level rise at Southampton gauge (Haigh et al., 2010).

General Brownian motion using the time-varying variance parameter provides more realistic generation of sea-level rise than any others. However, it does not give a full description of the

stochastic properties of uncertainty of UKCP 09. The uncertainty range of the adjusted General Brownian motion is narrower than that of UKCP 09 per se. Nevertheless, the adjusted General Brownian motion produces physically more plausible behaviours of sea-level rise than General Brownian motion using a constant variance parameter from Simple Brownian motion. Large falls in sea-levels are not observed during the simulation. In addition, when the rate and its standard deviation of annual time-series of sea-level rise are estimated by a least square method, these estimates are similar to those of the observed data on sea-level rise at Southampton. For instance, in the High SLR scenario, the rate and standard deviation of time-series of sea-level rise from the adjusted General Brownian motion are estimated to be 3.3~7.5 mm/year and 0.07~0.19 mm/year, respectively. Note that the rate and standard deviation of sea-level rise from 1935 to the present is estimated to 1.3mm/year and 0.18mm/year, respectively (Haigh et al., 2010). Thus, this thesis takes the adjusted General Brownian motion for the description of uncertainty of sea-level rise projection from UKCP 09. To validate the adjusted General Brownian motion, this thesis has measured the properties of the probability distribution of sea-level rise at 2100. We have randomly generated 10,000 time-series of sea-level rise by adjusted General Brownian motion and, then, produced the probabilistic range (i.e. probability distribution) of sea-level rise at 2100 as shown in Figure B.10.

The estimated stochastic properties of sea-level rise generated by the adjusted General Brownian motion have been compared to the mean and variance of sea-level rise projection by UKCP 09 at 2100. Although the probabilistic ranges of sea-level rise from the adjusted General Brownian motion is little narrower than those from the SLR projections of UKCP 09, the probability distributions numerically generated from the adjusted General Brownian motion agree well with those from the SLR projections of UKCP 09 in shape and width. Also, the mean of sea-level rise from the adjusted General Brownian motion is closely approximate to the mean of sea-level rise from UKCP 09 in 2100 (See Figure B. 10). By using the adjusted General Brownian motion, we can numerically generate the random time-series of sea-level rise following sea-level rise projection from UKCP 09. This also enables us to construct the probability distribution of sea-level rise at any year during the sea-level rise projection so that we can numerically convolve the probability distribution of sea-level rise and different types of probability distribution of any other variables (e.g. extreme still water level).

In addition, the mean of the General Brownian motion is well-matched with the mean of the SLR projection during the period of the projection. Thus, this thesis employs adjusted General Brownian motion approach to describe the long-term change and uncertainty of sea-level rise.

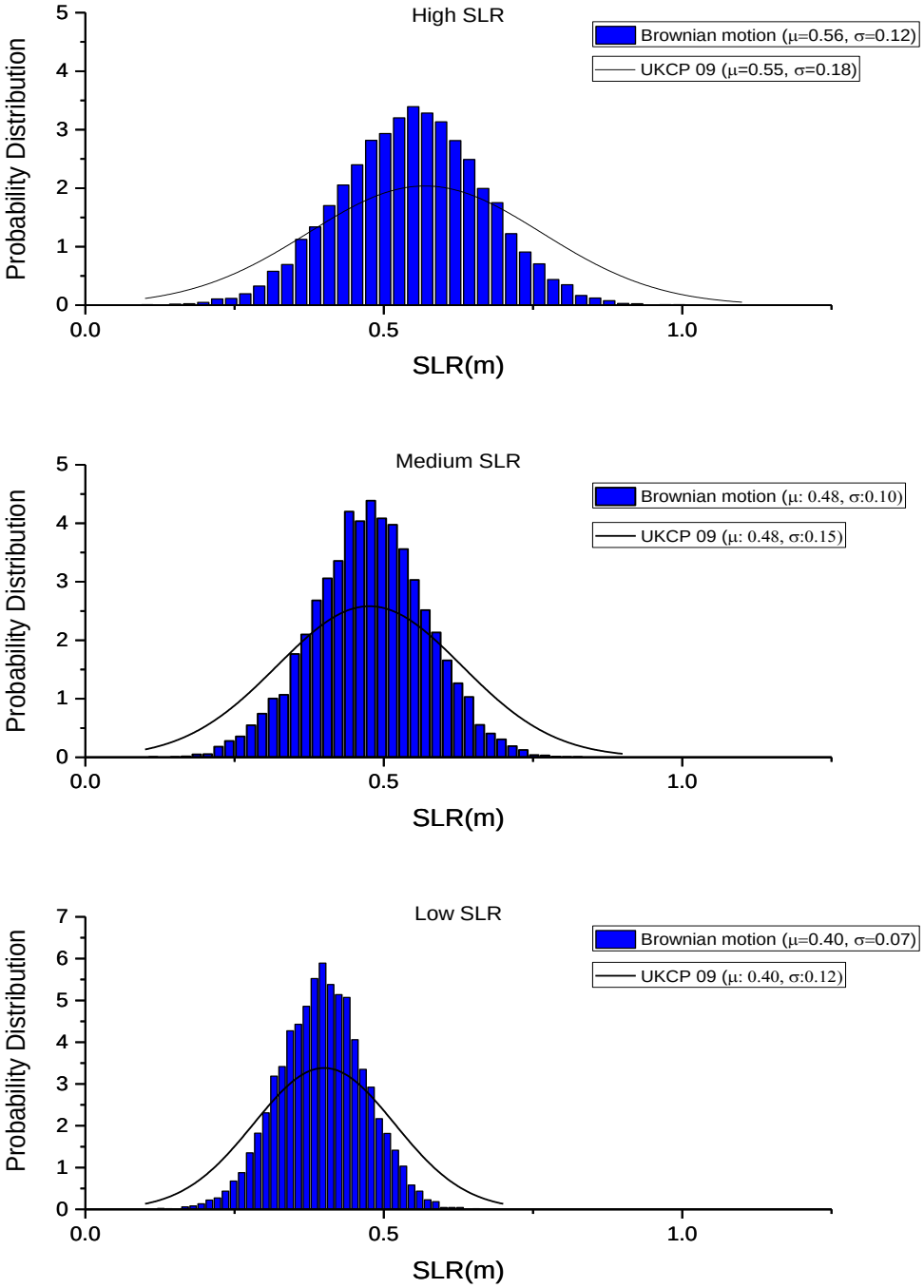

Figure B. 10 Comparison of the probabilistic ranges of sea-level rise by adjusted General Brownian motion and UKCP projection in 2100 for all the SLR scenario – Note that there is no difference in mean between adjusted GBM and UKCP 09

B. 4. Implication of Brownian motion in uncertainty modelling

The Brownian motion approach provides the time-series of the stochastic variables of sea-level rise over time. The random value of sea-level rise at a given year is a result of the random and deterministic motions of Brownian motion. In this regard, the stochastic process of the Brownian motion defines the probability of variable *x* being observed at any given time *t*. Let us denote $\emptyset(x_0, t_0; x, t)$ to the probability of variable *x* being observed at any time *t*, which is the same with the probability density function of variable $x(t)$ at time *t*. Here, x_0 is the value of variable *x* at time t_0, which is a start time of the Brownian motion. The probability density function of variable *x* at time *t* following Brownian motion can be defined by a stochastic differential equation, called Kolmogorov equation (Cox and Miller, 1965; Karlin and Taylor, 1981) as follow.

$$\frac{1}{2}\, b(x,t)^2 \frac{\partial^2}{\partial x^2} \emptyset(x_0, t_0; x, t) - a(x,t) \frac{\partial}{\partial x}\, \emptyset(x_0, t_0; x, t) = \frac{\partial}{\partial t}\, \emptyset(x_0, t_0; x, t) \qquad (13)$$

Here, $\emptyset(x_0, t_0; x, t)$: the probability density of variable x at time t with value x_0 at time t_0

$a(x,t)$: any function for the drift part of General Brownian motion

$b(x,t)$: any function for the variance part of General Brownian motion

By solving the equation, we can estimate the probability of the occurrence of variable $x(t)$ following the General Brownian motion. As seen in the equation (13), it seems to be very hard to find a probability density function of variable *x* at time t. For option evaluation, we also have to define the probability of sea-level rise at any time as flood risk is related to the probability of coastal events. Furthermore, when the probability of sea-level rise is combined to the probability of other variables, the estimation of flood risk is, in practice, impossible to undertake in such a non-stationary state of sea-level rise.

However, due to the advance of computational techniques, we can simulate as many random processes of variables as they are needed to construct and estimate the properties of the probability distribution – This is how a Monte-Carlo simulation works in predicting the probability distribution of unknown variables. Thus, this numerical technique enables us to find the statistical properties (i.e. mean or standard deviation) of newly generated variables without solving the stochastic differential equation.

Appendix C. Change in ESWL by MLSR for different SLR scenarios

This appendix shows the effects of sea-level rise on coastal flooding represented by water levels quantitatively. As sea-level increases with time, the expectation of extreme water levels including waves combined with sea-level rise grows at different rates according to SLR scenarios. The time-series of ESWL+SLR+WAVE and their probabilistic ranges are plotted for each SLR scenario in the cases of MSLR.

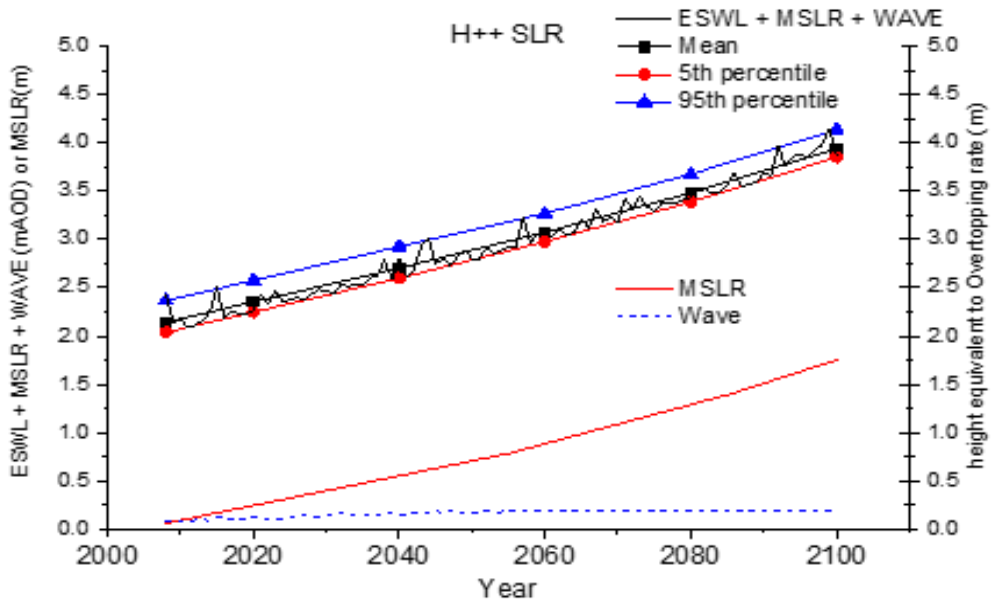

(a) H++ MSLR

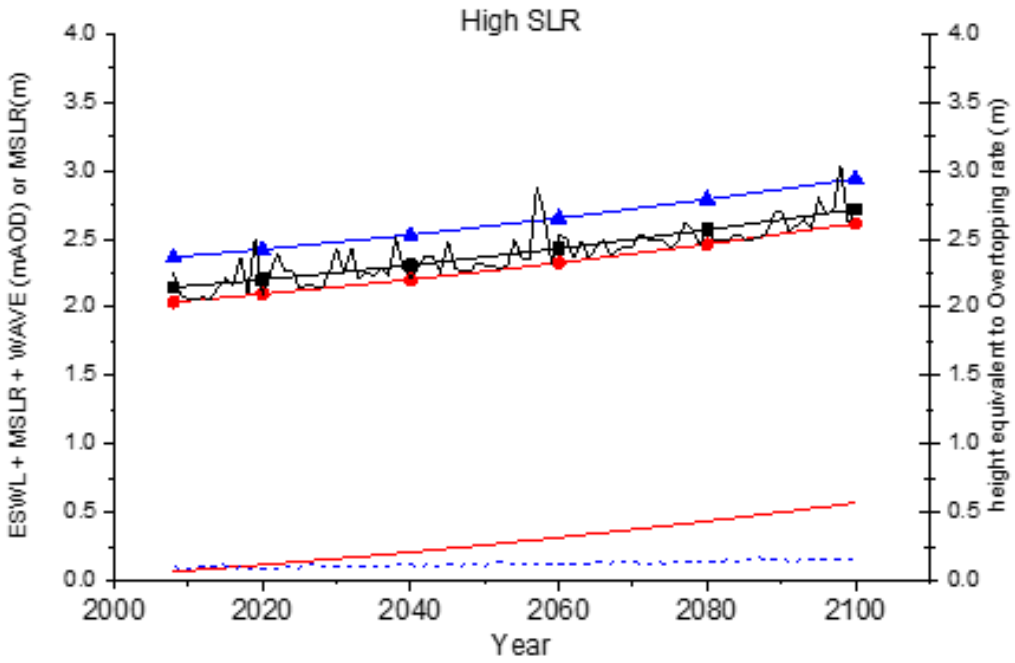

(b) High MSLR

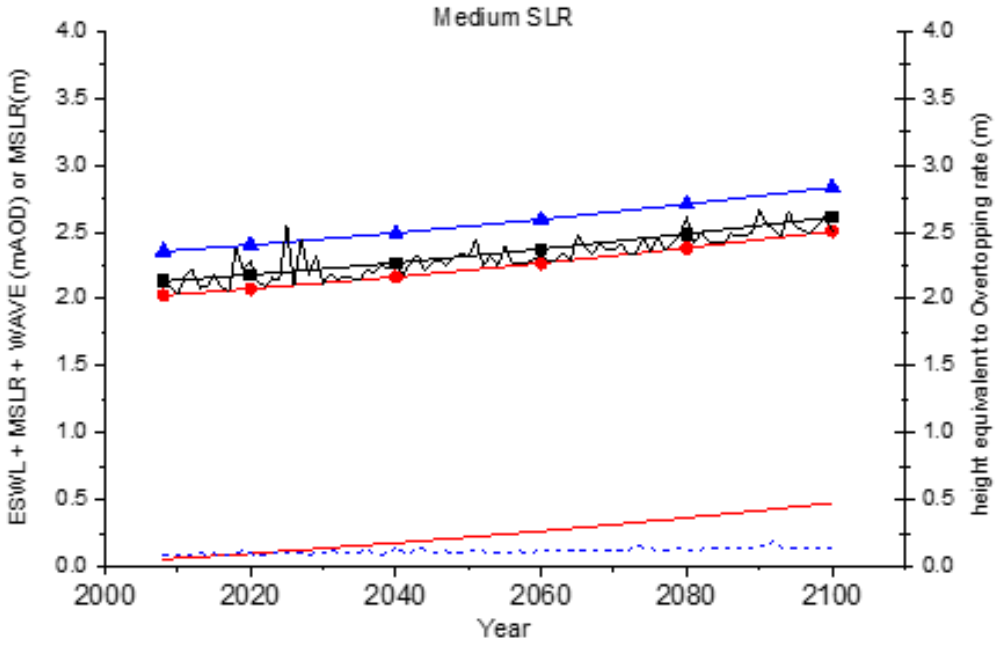

(c) Medium MSLR

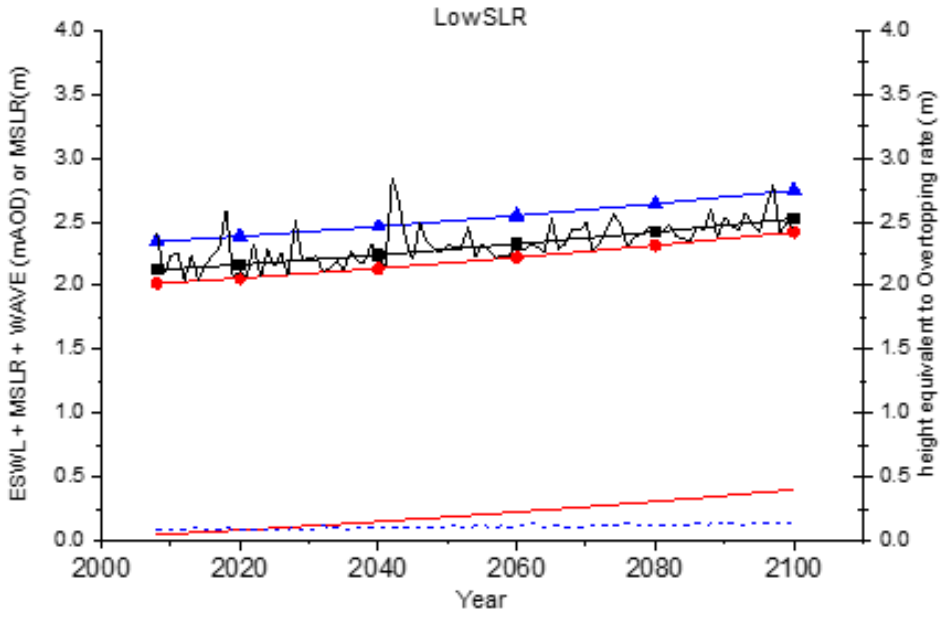

(d) Low MSLR

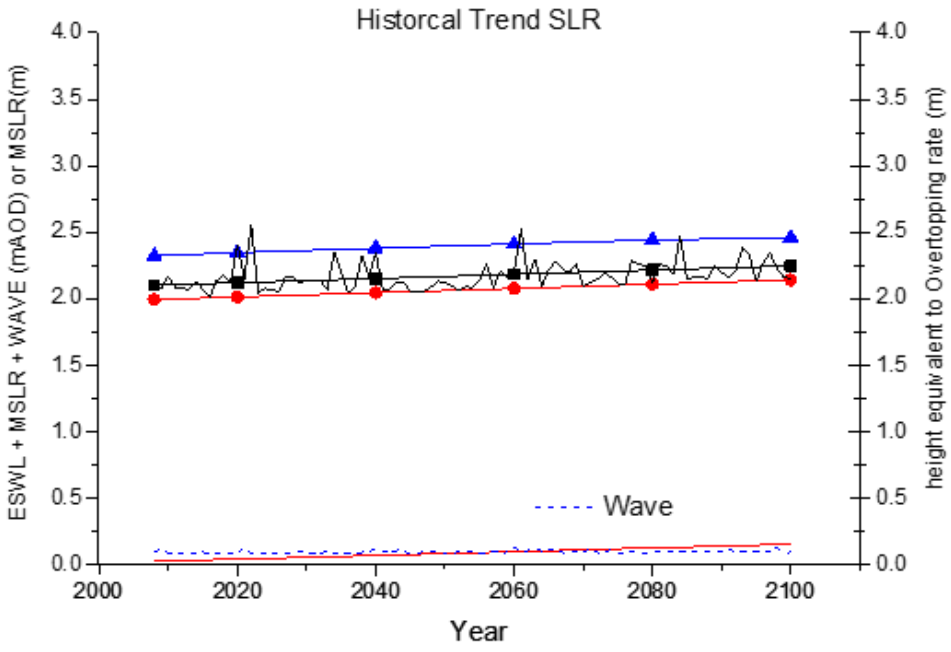

(e) Historical Trend SLR

Figure C. 1 The results of uncertainty modelling of ESWL+MSLR+WAVE for each of the sea-level rise projections

Appendix D. Change in ESWL by Brownian SLR for different SLR scenarios

The time-series of ESWL+SLR+WAVE and their probabilistic ranges are plotted for each SLR scenario in the cases of Brownian SLR in Figure D. 1.

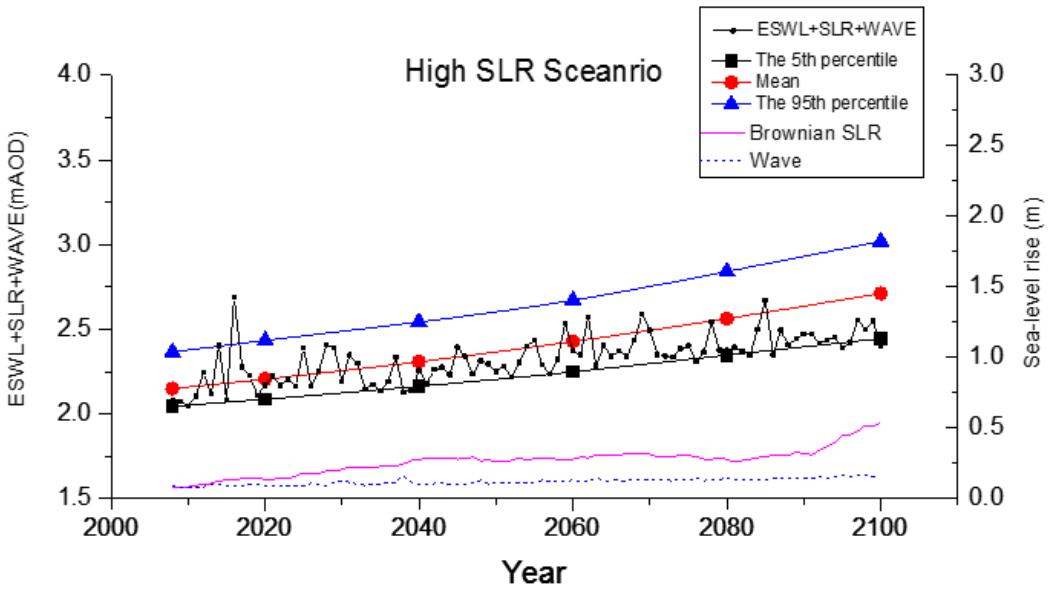

(a) High SLR scenario

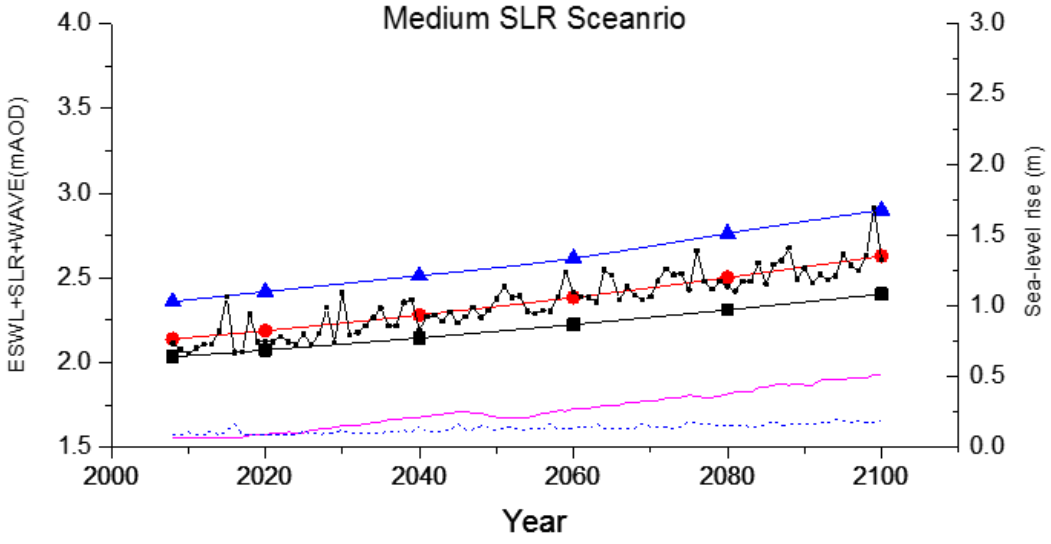

(b) Medium SLR scenario

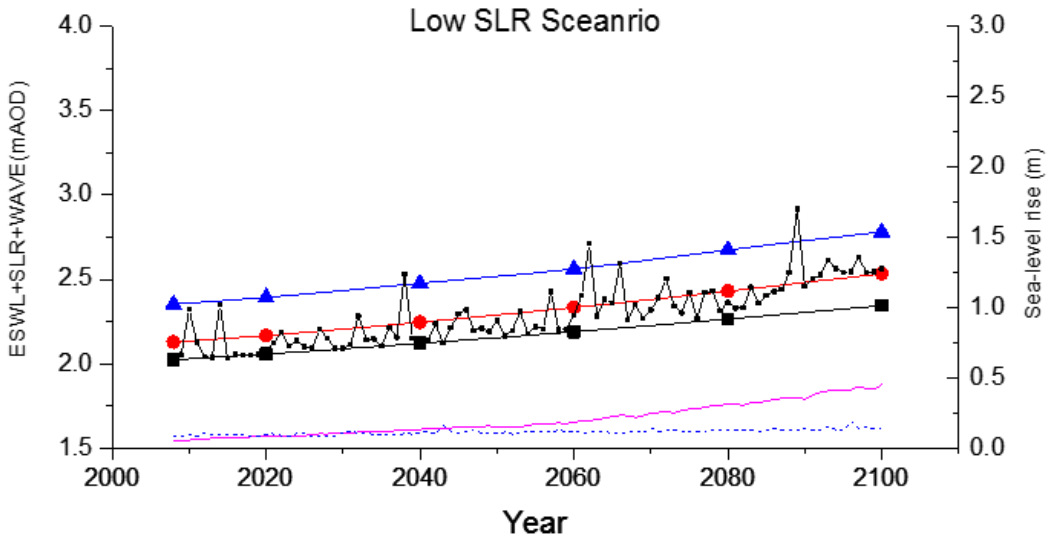

(c) Low SLR scenario

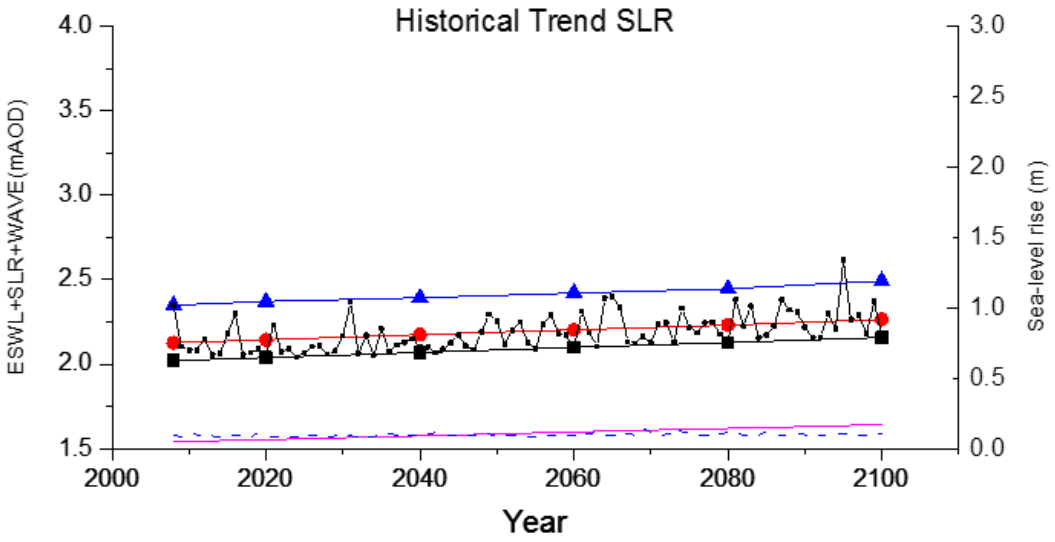

(d) Historical Trend SLR scenario

Figure D. 1 The results of uncertainty modelling of ESWL+Brownian SLR+WAVE for each of the sea-level rise projections – Note that SLR and wave are plotted on y-axis on the right.

The means and standard deviations of ESWL+SLR+WAVE for the selected years are shown for each SLR scenario in both cases of MSLR and Brownian SLR in Table 4.5.

Table D. 1 Comparisons of mean (μ) and standard deviation (σ) of random variables (ESWL+MSLR+WAVE and ESWL+Brownian SLR+WAVE) (Unit: mAOD)

SLR	Year	ESWL+MSLR+WAVE		ESWL+ Brownian SLR+WAVE		Remark
		μ	σ	μ	σ	
H++	2008	2.15	0.11			Brownian motion is not defined for H++ SLR
	2020	2.35	0.11			
	2040	2.71	0.11			
	2060	3.07	0.10			
	2080	3.48	0.10			
	2100	3.94	0.10			
High	2008	2.15	0.12	2.15	0.11	
	2020	2.21	0.11	2.21	0.11	
	2040	2.31	0.11	2.31	0.12	
	2060	2.43	0.11	2.43	0.13	
	2080	2.57	0.11	2.56	0.15	
	2100	2.72	0.11	2.71	0.18	
Medium	2008	2.13	0.11	2.14	0.11	
	2020	2.18	0.11	2.19	0.11	
	2040	2.27	0.11	2.28	0.12	
	2060	2.37	0.11	2.38	0.12	
	2080	2.49	0.11	2.50	0.14	
	2100	2.61	0.11	2.63	0.15	
Low	2008	2.13	0.11	2.13	0.11	
	2020	2.17	0.12	2.17	0.11	
	2040	2.24	0.11	2.25	0.12	
	2060	2.33	0.11	2.33	0.12	
	2080	2.42	0.11	2.43	0.13	
	2100	2.53	0.11	2.53	0.14	
Historical Trend	2008	2.10	0.11	2.10	0.11	Brownian motion is based on the observed data at Southampton gauge (1.3±0.18mm/yr)
	2020	2.12	0.11	2.12	0.11	
	2040	2.15	0.11	2.15	0.11	
	2060	2.18	0.11	2.18	0.11	
	2080	2.22	0.11	2.21	0.11	
	2100	2.25	0.11	2.24	0.11	

Appendix E. Investment costs to each stage of multiple stage investment

Since this analysis evaluates a set of adaptation measures within each adaptation pathway, the investment cost for the upgrade of the coastal defence should be defined for option evaluations under each sea-level rise scenario. As aforementioned, dividing one single option into two parts of sequential options needs additional costs in order to maintain flexibility in the adaptation options. Thus, the increases in cost due to the incorporation of flexibility in engineering or physical options need to be considered as variables that affect investment decisions in the real options analysis of future growth options. This thesis assumes that the overall cost of sequential investments is higher than the cost of the equivalent single investment made at once. If any additional expenditure does not occur to maintain flexibility, option holders or options analysts must choose multiple stage investments to address uncertainty in investment decisions. This is not realistic and possible in practice to the best of our knowledge. In climate change adaptation, these additional expenditures for flexibility are attributable to the increased amount of construction work, mobility or additional enabling costs (e.g. approval). Thus, the increase in the overall cost is defined as a premium to be paid for future extension or flexibility, which conceptually corresponds to a call or put option premium (Dixit and Pindyck, 1994; Park, 2002).

This thesis assumes 20%, 30%, 40% and 50% premium scenarios for the analysis of the option to grow by multiplying an original investment cost (*I*) by the premium rates. That is, when a single large investment is divided into two sequential investments, the division increases the investment cost of each stage as much as the premium as expressed in equation (1).

$$I_o + I_{premium} = I_{1,o} + I_{2,o} \quad (1)$$

Here, I_o is an investment cost for an original option, $I_{premium}$ is an option premium to be paid for flexibility, and $I_{1,o}, I_{2,o}$ is the first and second stage investment costs, respectively.

The analysis of the costs during the project life involves the identification and scoping-out of all the relevant cash flows relating to the acquisition and use of assets for building coastal defences (EA, 2015). The key components of costs considered during the life of coastal defences are as follows: (1) procurements and design costs; (2) capital construction costs; (3) operation and maintenance costs; (4) monitoring costs; and (5) replacement and

decommissioning costs (ibid). As the estimation of a capital cost for construction needs a site-specific information on defence types, environmental conditions (e.g. water levels and coast line), working conditions (e.g. accessibility to construction sites) and the availability of materials, it is difficult to provide an accurate estimate of coastal defence cost in the early stage of projects (EA, 2015). Environment Agency (EA) in the UK provides the indicative costs of coastal defence available for very early stage projects or natural level assessments as shown in Table E.1.

Table E. 1 Indicative costs associated with the cost of coastal defences (EA, 2015)

Options	**Capital cost**	**Maintenance cost**	**Indicative cost (£/m)**
Beach recharge and breakwater	High	Medium	–
Beach recharge and groynes	High	Medium	–
Rock armour	High	Low	–
Impermeable revetments and seawalls	High	Low	2,000–5,000
Timber revetments	Medium	Medium	20–500
Rock revetments	High	Low	1,000–3,000
Groynes	Medium	Medium	10,000 to 100,000 per structure
Nearshore breakwaters	Medium	Low	400–1,000
Artificial rock dune protection	Medium	Low	200–600
Gabion revetments	Medium	Medium	50–500
Beach nourishment	Medium	Medium	50–2,000
Shingle recycling/ re-profiling	Low	Low	10–200

The costs for a single large investment have been taken from the North Solent Shoreline management (NFCD, 2010). This plan estimated the investment cost for the replacement of coastal defence (i.e. Impermeable revetments and seawalls) at £ 64.2 million, which includes a maintenance cost over the life of the project (100 years). The upgrade of coastal defence is planned to be implemented 30 to 60 years later. To estimate the cost of dike heightening in each stage, this thesis uses Van dantzig model (1956) which assumes that the cost of defence heightening (I) has a linear relation with the raised height (H). This model provides a simple representation of relationship between the cost of dike heightening and the increase in dike height in equation (2) (Slijkhuis et al., 1997)

$$I = I_m + I^{'}*(H-H_0) \quad (2)$$

Here, I_m is mobilisation cost, $I^{'}$ is a unit cost per the meter of dike heightening, and H, H_0 is the raised level and the initial level of the defence crest, respectively. The lowest crest level of coastal defence is measured at 2.5 mAOD in Lymington. Thus, H_0 is set to be 2.5 mAOD

in this model. A mobilisation cost (I_m) is assumed to be approximately 10% of the total capital cost, following the EA guidance (EA, 2015). As the capital cost is proportional to increase in the height of the coastal defence by the model, the capital cost and total cost for different levels of coastal defence are assessed as shown in Table E. 2.

Table E. 2 Estimate of indicative costs for the coastal defence upgrade by different sizes of heightening for a single-stage investment option

Upgrade options	Total costs (*I*)	Mobilisation costs (I_0)	Capital cost $I'*(H-H_0)$	Remark
$U_{c\rightarrow 3.5m}$	£ 64.2 M	£ 5.83 M	£ 58.4 M	$I_0 = 10\% \times I'*(H-H_0)$
$U_{c\rightarrow 3.0m}$	£ 32.1 M	£ 2.92 M	£ 29.2 M	
$U_{c\rightarrow 4.0m}$	£ 96.3 M	£ 8.76 M	£ 87.6 M	

This thesis adds premium values for flexibility on the estimated indicative cost of the upgraded coastal defence (Table E. 2) when the single-stage upgrade is transformed into the two- or more- stage upgrade. For example, if the coastal defence is upgraded to 3.5 mAOD level in two stages, this two-stage upgrade incurs premium costs which are calculated by multiplying the premium rates and the original investment cost (e.g. £ 64.2 M). The estimated premium cost is evenly distributed to each stage of the investment. This rule applies thoroughly for the evaluation of the premium cost. The estimated investment costs of each stage for different premium scenarios are shown for 3.5 mAOD and 4.0 mAOD level defence upgrade in Table E. 3 and E. 4.

Table E. 3 Indicative costs for the upgrade of coastal defence up to 3.5 mAOD by different premium scenarios

A. $U_{c\rightarrow 3.0m}*U_{3.0m\rightarrow 3.5m}$

Adaptation paths	Premium scenarios (1)	Original investment cost (2)	Premium cost (3)=(2)×(1)	Investment cost (4)=(2)+(3)	Cost for the 1st upgrade (5)=1/2×(4)	Cost for the 2nd upgrade (6)=1/2×(4)
$U_{c\rightarrow 3.5m}$	0%	£ 64.2 M	0	£ 64.20 M	-	-
$U_{c\rightarrow 3.0m}*$ $U_{3.0m\rightarrow 3.5m}$	20%		£ 9.63 M	£ 77.04 M	**£ 38.52 M**	**£ 38.52 M**
	30%		£ 14.45 M	£ 83.46 M	**£ 41.73 M**	**£ 41.73 M**
	40%		£ 19.26 M	£ 89.88 M	**£ 44.94 M**	**£ 44.94 M**
	50%		£ 24.25 M	£ 96.33 M	**£ 48.16 M**	**£ 48.16 M**

Table E. 4 Indicative costs for the upgrade of the coastal defence up to 4.0 mAOD for different premium scenarios

A. $U_{c\rightarrow 3.0m}$*$U_{3.0m\rightarrow 4.0m}$

Adaptation paths	Premium scenarios (1)	Original investment cost (2)	Premium cost (3)=(2)×(1)	Investment cost (4)=(2)+(3)	Cost for the 1st upgrade (5)=1/2×(4)	Cost for the 2nd upgrade (6)=1/2×(4)
$U_{c\rightarrow 4.0m}$	0%	£ 96.3 M	0	£ 96.6 M	-	-
$U_{c\rightarrow 3.0m}$* $U_{3.0m\rightarrow 4.0m}$	20%		£ 19.38 M	£ 116.28 M	**£ 58.14 M**	**£ 58.14 M**
	30%		£ 29.07 M	£ 125.97 M	**£ 62.98 M**	**£ 62.98 M**
	40%		£ 38.76 M	£ 135.66 M	**£ 67.83 M**	**£ 67.83 M**
	50%		£ 48.45 M	£ 145.35 M	**£ 72.68 M**	**£ 72.68 M**

B. $U_{3.0m\rightarrow 3.5m}$*$U_{3.5m\rightarrow 4.0m}$

Adaptation paths	Premium scenario (1)	Cost for $U_{3.0m\rightarrow 4.0m}$ (2)*	Premium cost (3)=(2)×(1)	Investment cost (4)=(2)+(3)	Cost for the 1st upgrade (5)=1/2×(4)	Cost for the 2nd upgrade (6)=1/2×(4)
$U_{3.0m\rightarrow 3.5m}$* $U_{3.5m\rightarrow 4.0m}$	20%	£ 58.14 M	£ 11.63 M	£ 69.77 M	**£ 34.89 M**	**£ 34.89 M**
	30%	£ 62.98 M	£ 18.90 M	£ 81.87 M	**£ 40.94 M**	**£ 40.94 M**
	40%	£ 67.83 M	£ 27.13 M	£ 94.96 M	**£ 47.48 M**	**£ 47.48 M**
	50%	£ 72.68 M	£ 36.34 M	£ 109.02 M	**£ 54.51 M**	**£ 54.51 M**

* Costs in column (2) comes from the estimated costs of column (6) in the case A ($U_{c\rightarrow 3.0m}$*$U_{3.0m\rightarrow 4.0m}$)

C. $U_{C\rightarrow 3.0m}$*$U_{3.0m\rightarrow 3.5m}$*$U_{3.5m\rightarrow 4.0m}$

Adaptation paths	Premium scenario (1)	Investment cost (2)=(4)+(5)+(6)	Premium cost (3)	The cost for the 1st upgrade (4)*	The cost for the 2nd upgrade (5)**	The cost for the 3rd upgrade (6)**
$U_{c\rightarrow 4.0m}$	0%	£ 96.6 M	-	-	-	
$U_{c\rightarrow 3.0m}$* $U_{3.0m\rightarrow 3.5m}$* $U_{3.5m\rightarrow 4.0m}$	20%	£ 127.91 M	£ 31.31 M	**£ 58.14 M**	**£ 34.89 M**	**£ 34.89 M**
	30%	£ 144.86 M	£ 48.26 M	**£ 62.98 M**	**£ 40.94 M**	**£ 40.94 M**
	40%	£ 162.79 M	£ 66.19 M	**£ 67.83 M**	**£ 47.48 M**	**£ 47.48 M**
	50%	£ 181.70 M	£ 85.1 M	**£ 72.68 M**	**£ 54.51 M**	**£ 54.51 M**

* Costs in column (4) are taken from costs in column (5) of $U_{c\rightarrow 3.0m}$* $U_{3.0m\rightarrow 4.0m}$

** Costs in columns (5) and (6) are taken from columns (5) and (6) in $U_{3.0m\rightarrow 3.5m}$*$U_{3.5m\rightarrow 4.0m}$, respectively.

Appendix F. Friction coefficient of floodplains in Lymington

Table F. 1 Typical n values used in flood risk analysis for the description of surface roughness (Data source: Wadey (2013))

Model	**Class description**	**Friction values (Manning's *n*)**
50 m resolution model	Composite value for Solent floodplains	0.035
10 m resolution model	Asphalt and concrete	0.012
	Grass (gardens, recreational areas, parks etc)	0.035
	Thick grass / marshland vegetation	0.040
	Water bodies	0.010
	Buildings	1.000

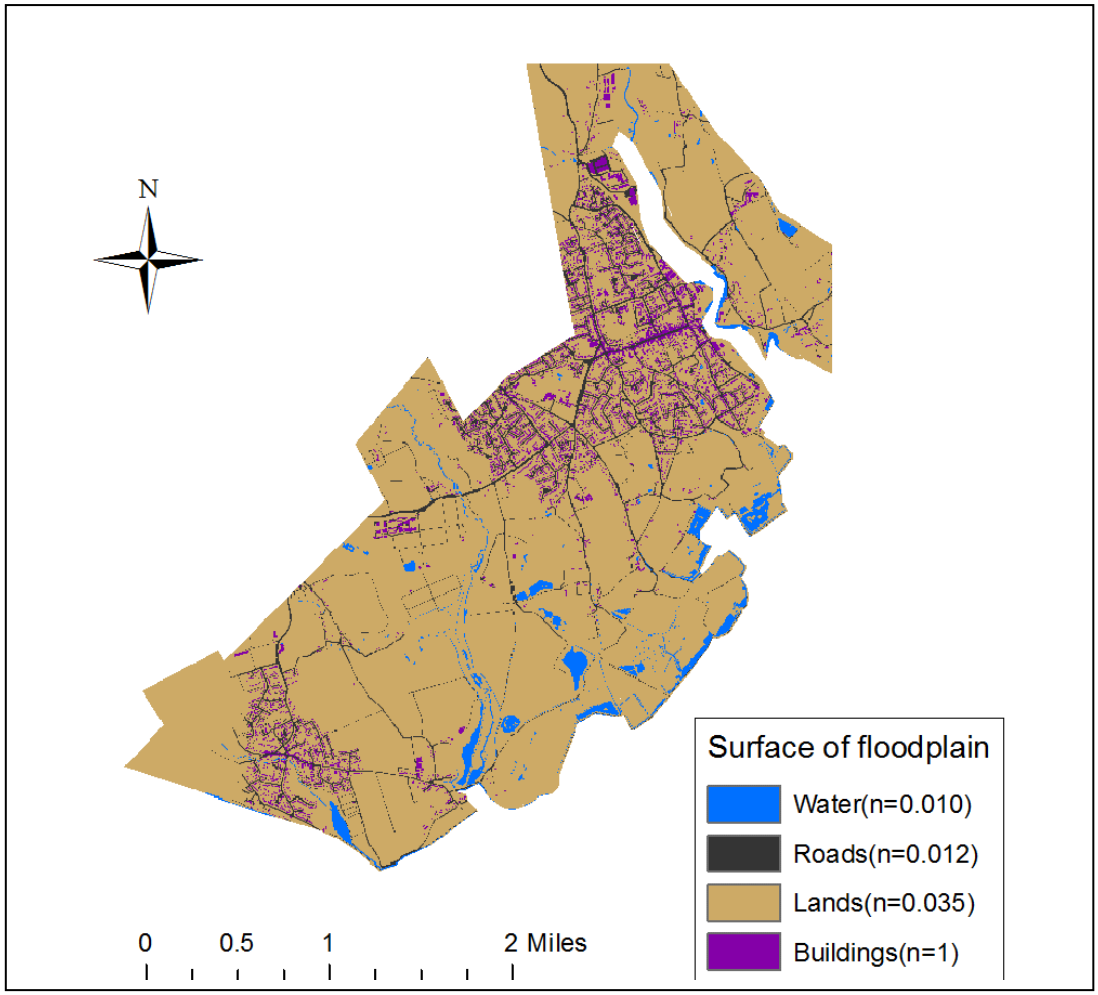

Figure F. 1 *n* values for floodplain surface in Lymington by 10×10m grid cells

Appendix G. Results of flood simulations at various loading conditions

Figure G.1 illustrates the example of a set of flood maps produced from flood simulations at various flood loadings of ESWL+SLR+WAVE under different defence conditions.

A. 50m resolution data

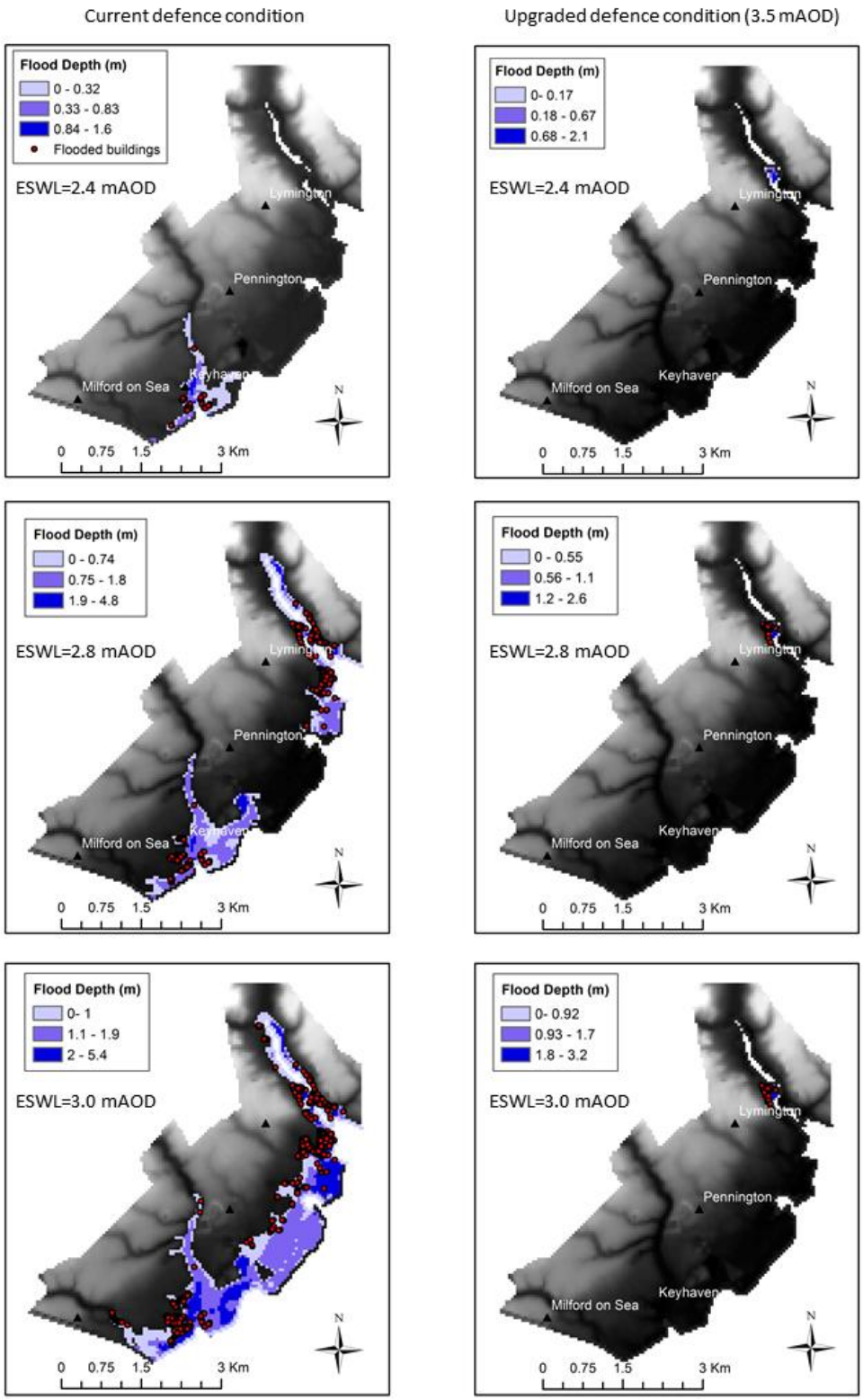

Current defence condition

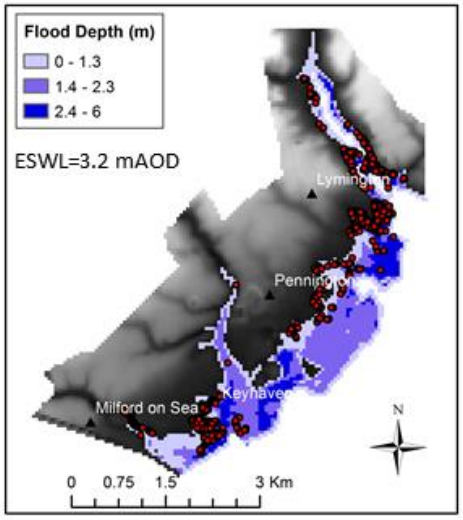

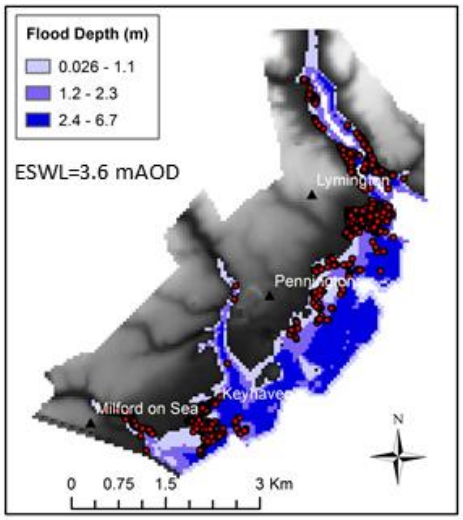

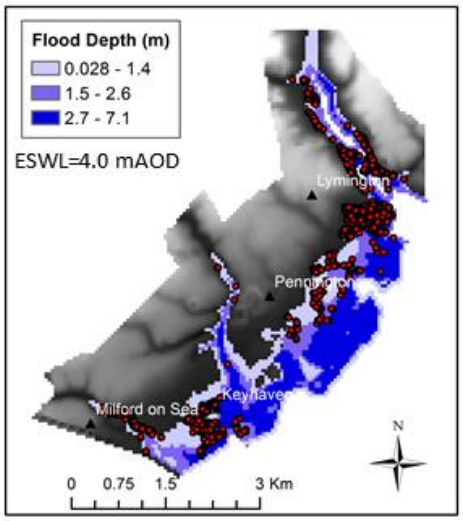

Upgraded defence condition (3.5 mAOD)

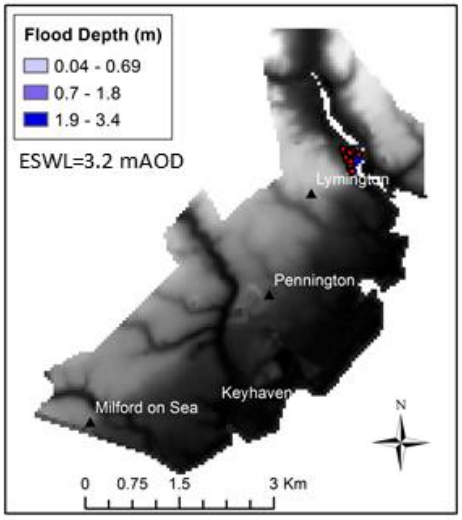

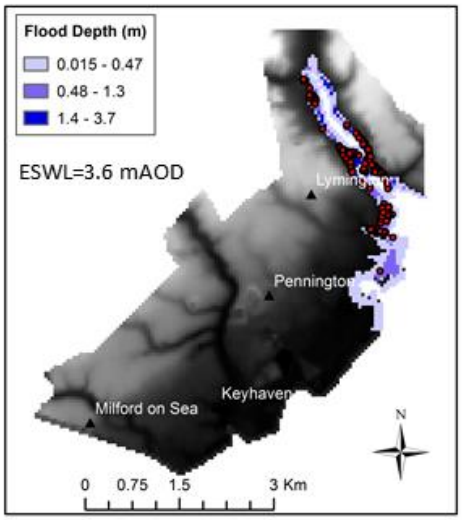

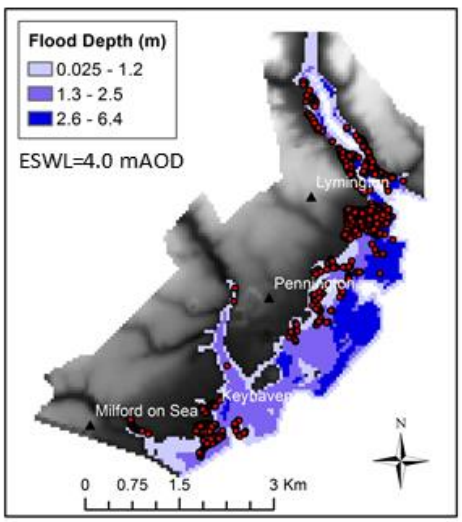

B. 10m resolution data

Current defence condition

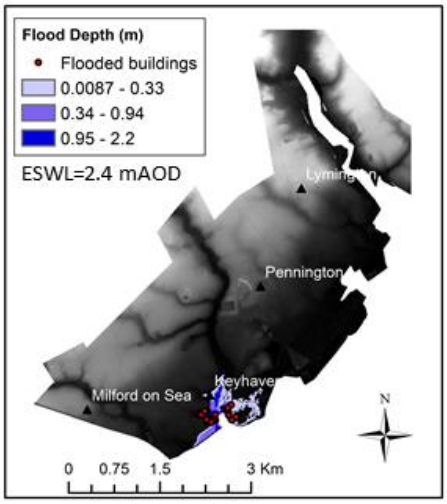

Upgraded defence condition (3.5 mAOD)

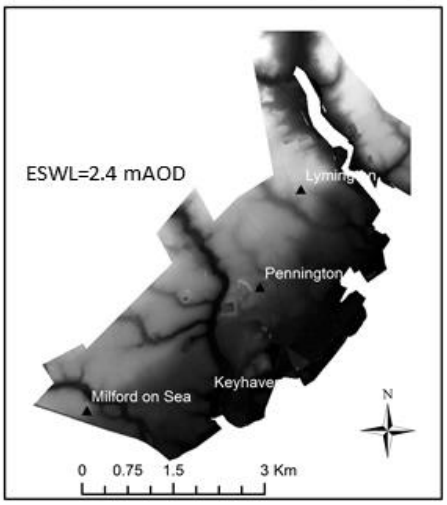

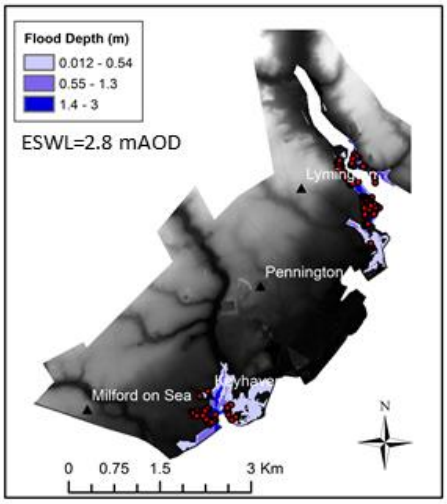

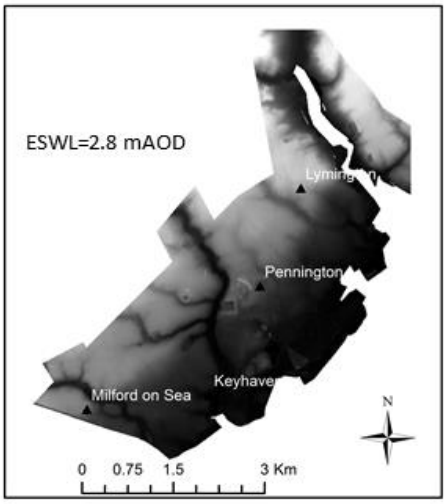

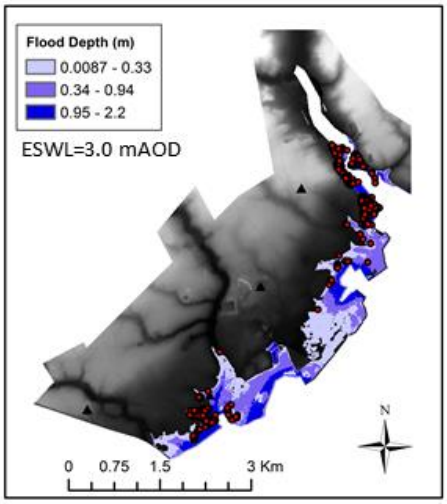

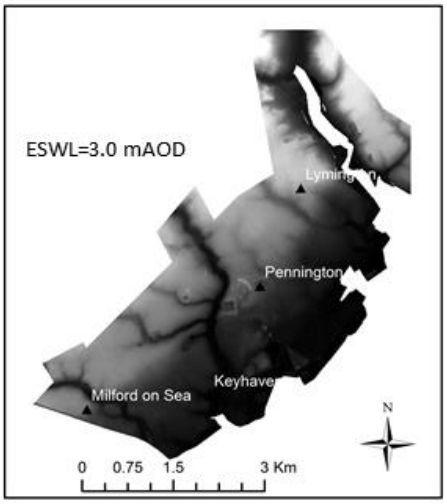

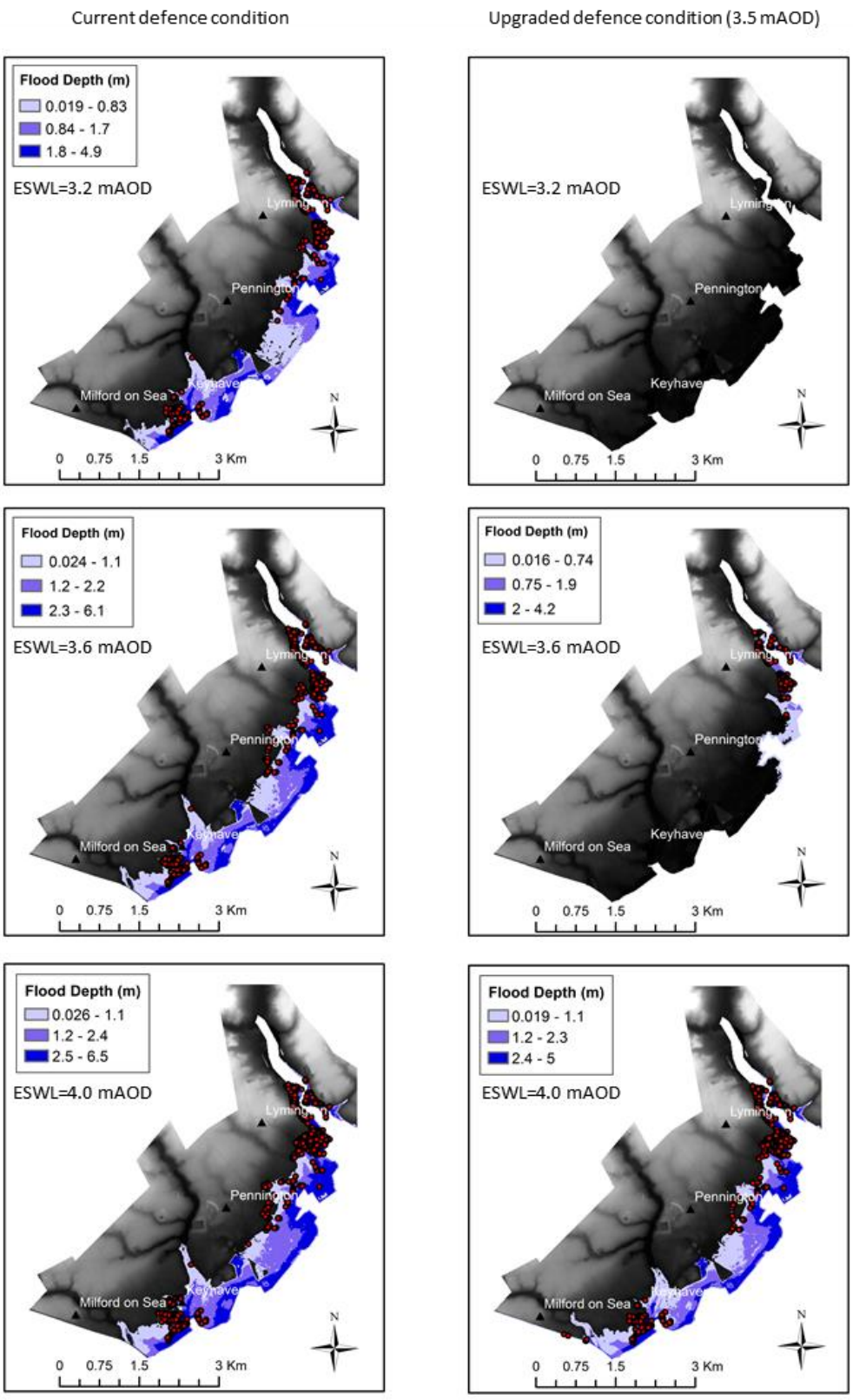

Figure G. 1 Results of flood simulations at various flood loadings of ESWL for the current defence condition and the upgraded defence condition (3.5 mAOD) in 50m and 10m resolution data.

Figure G. 2 shows the result of flood simulations at various flood loading for the upgraded coastal defence up to 3.0 mAOD in 50m and 10m resolution LADAR data, respectively.

A. 50m resolution data

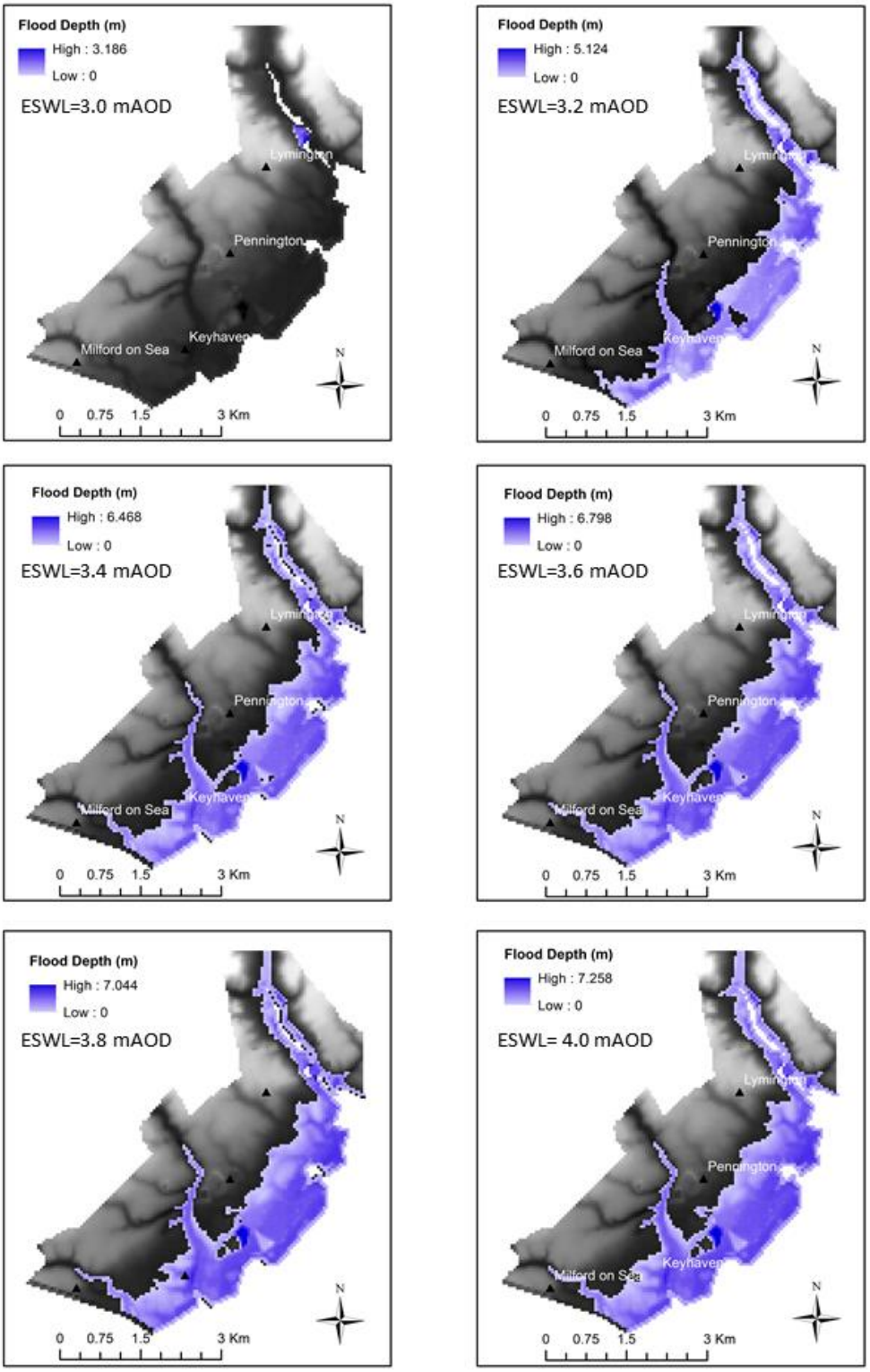

B. 10m resolution data

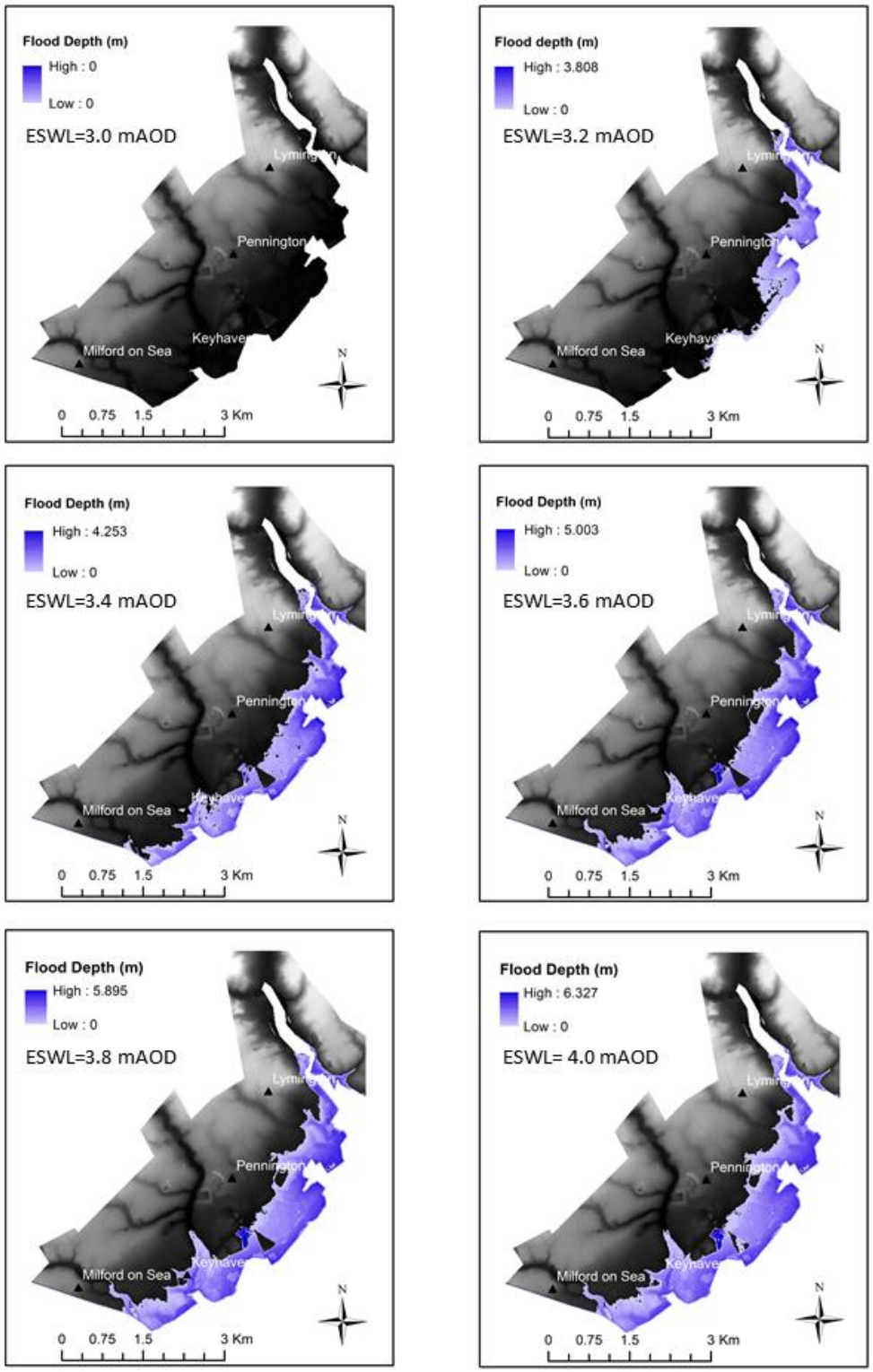

Figure G. 2 Result of flood simulations at various flood loadings for the upgraded coastal defence up to 3.0 mAOD in 10m and 50m resolution data

Table G. 1 and Figure G. 3 show flood damages (i.e. the number of flooded properties) across flood loadings (i.e. ESWL+SLR+WAVE) for each defence condition.

Table G. 1 The number of inundated properties by water levels according to defence conditions

Water levels (mAOD)	The current defence	3.0mAOD upgraded defence	3.5mAOD upgraded defence	4mAOD upgraded defence
1.2	0	0	0	0
1.4	0	0	0	0
1.6	0	0	0	0
1.8	4	0	0	0
2	20	9	9	9
2.2	130	22	22	22
2.4	179	22	22	22
2.6	216	24	24	24
2.8	304	24	24	24
3	416	35	35	35
3.2	508	208	38	38
3.4	631	429	41	41
3.6	715	661	128	44
3.8	797	759	399	73
4	846	846	701	79

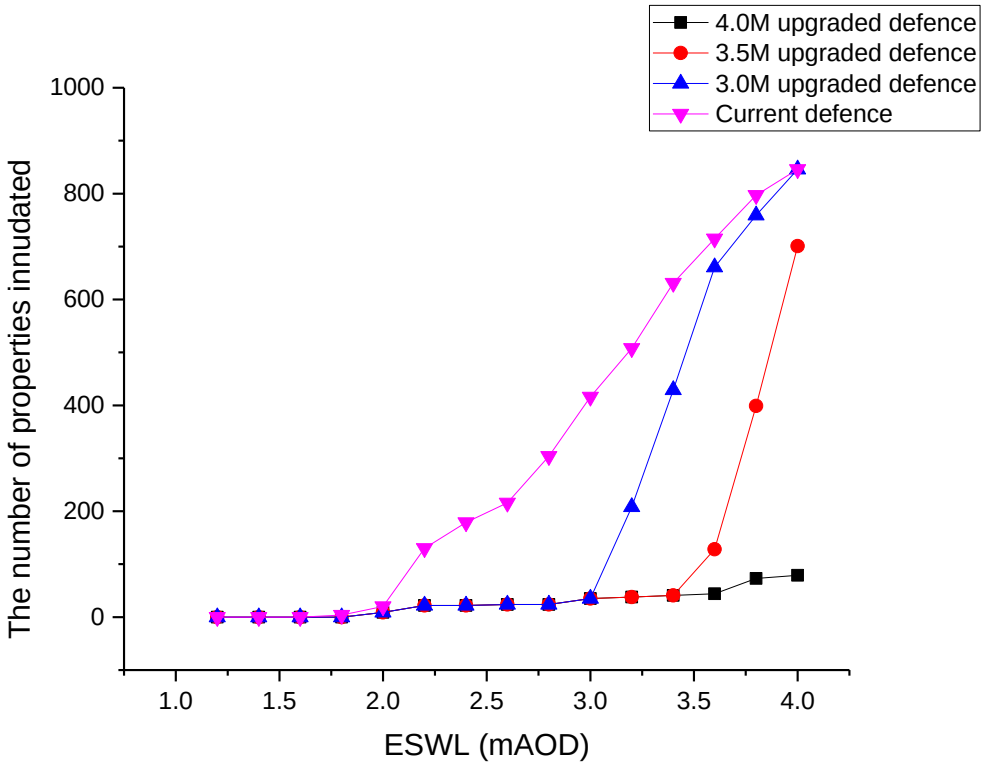

Figure G. 3 The number of properties inundated by peak water levels (or extreme still water levels) according to each defence condition in Lymington

Appendix H. Flood damages (£) – Extreme Still Water Levels

The flood damages are interpolated within all the range of peak water levels by fitting multiple linear lines to the damage curves. The multi-linear interpolations allow us to express each damage curve as a function of peak water levels at high accuracy (R^2 = 0.99). Thus, the flood damage for each defence condition is represented as a function of peak water levels (i.e. ESWL+SLR+WAVE) as shown in equation (1).

$$D_d = f_d(x) \quad (1)$$

Here, D_d is a flood damage at a certain magnitude of peak water level under a given defence condition, subscribed by *d* (e.g. the current defence, 3.5m upgrade defence, etc.), f_d is any function defining a relation between peak water levels and flood damages, and x is a climatic variable of extreme still water level, sea-level rise and wave (i.e. ESWL+SLR+WAVE). As all the components of a peak water level are random variables, the flood damage represented by equation (1) is also random variable. The multiple linear function is used to convert the probability distribution of ESWL+SLR+ WAVE to the probability distribution of flood damage at any year by Monte-Carlo simulation.

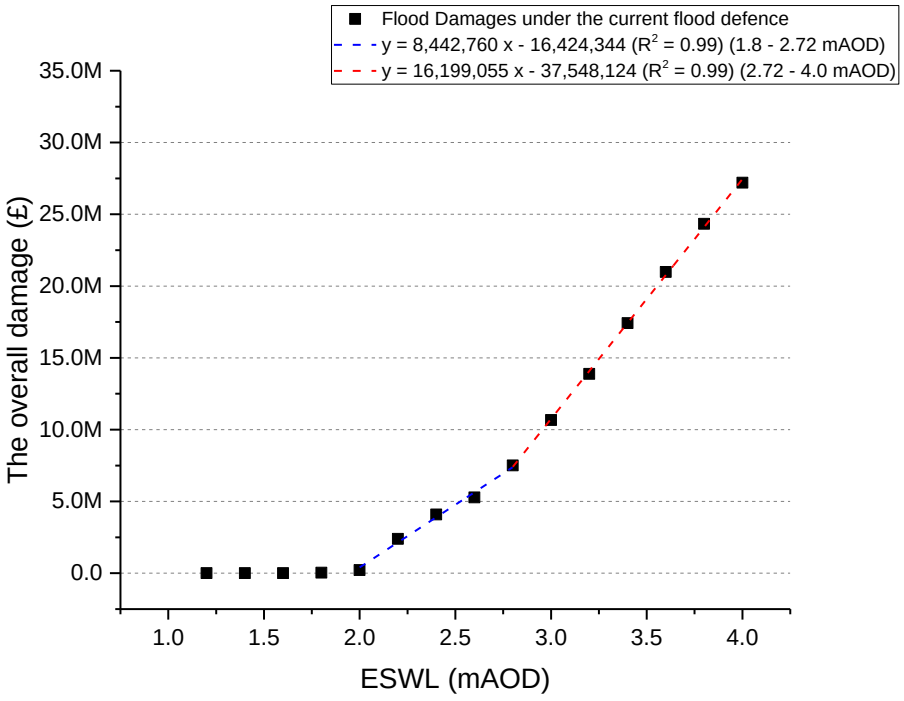

(a) Current coastal defence

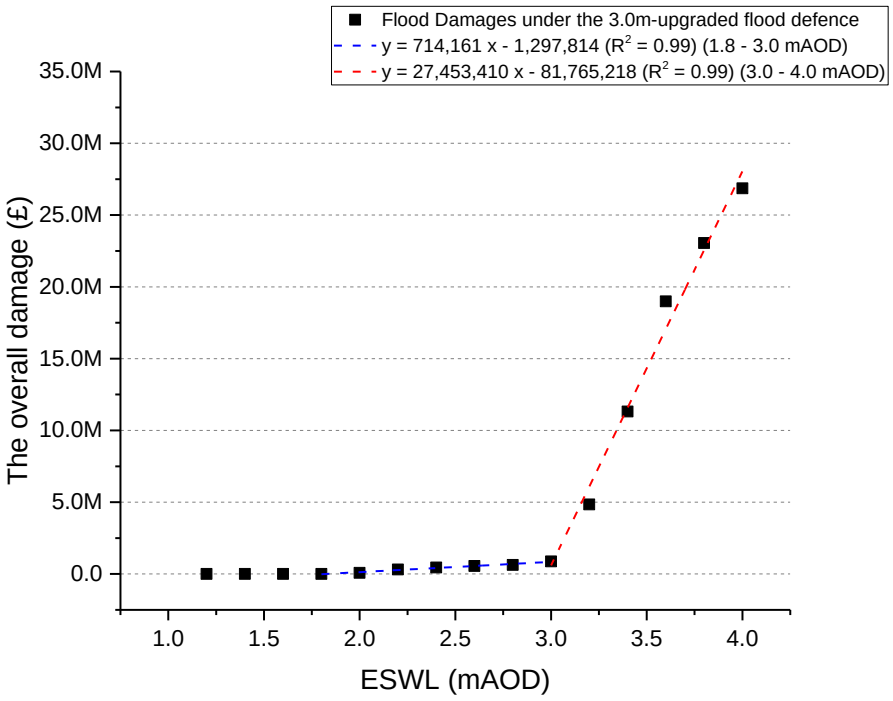

(b) Upgraded coastal defence up to 3.0 mAOD

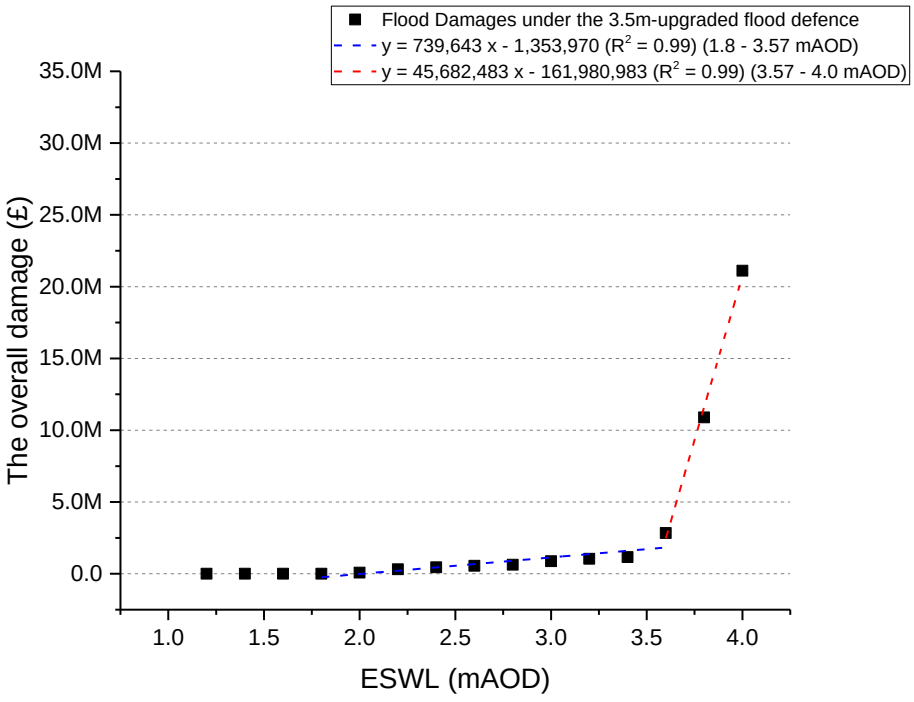

(c) Upgraded coastal defence up to 3.5 mAOD

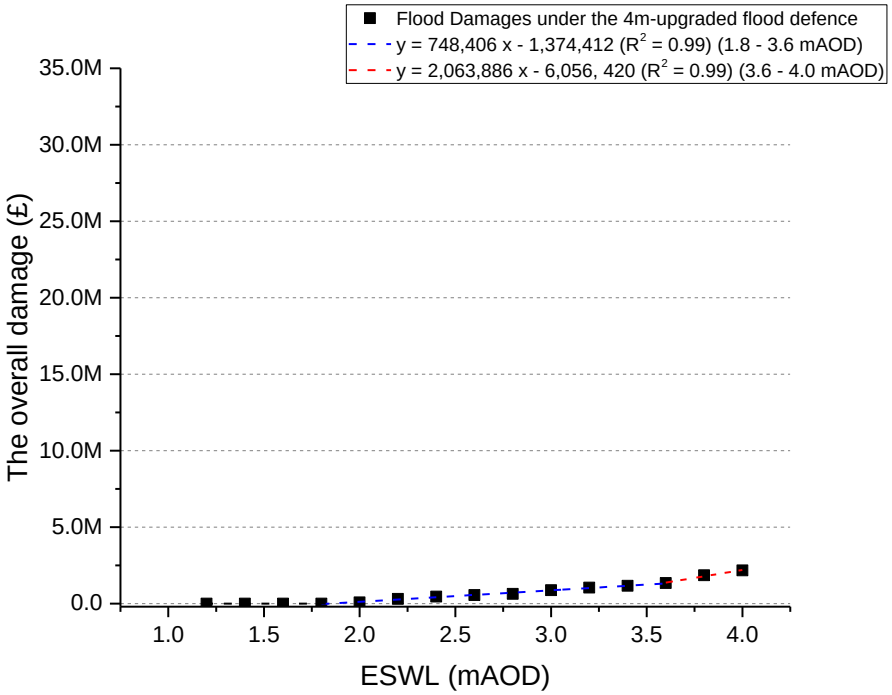

(d) Upgraded coastal defence up to 4.0 mAOD

Figure H. 1 Linear fitting to each of the damage curves (y = f(x), where x is a peak water level as a loading condition)

Appendix I. Change in EAD for MSLR and Brownian SLR

This appendix shows changes in flood damages by MSLR and the Brownian motion of SLR, respectively. Both results are shown in Table I. 1 and Figures I. 1 and I. 2.

Table I. 1 Changes in mean (μ) and standard deviation (σ) of flood damages (Unit: Million £) for the current defence condition by MSLR and Brownian SLR, respectively – The mean of flood damages implies expected annual damages (EAD) under the current defence condition.

SLR	Year	By MSLR		By Brownian SLR		Remark
		μ(EAD)	σ	μ(EAD)	σ	
H++	2008	1.7	1.0			Brownian motion is not defined for H++ SLR scenario
	2020	3.5	1.0			
	2040	6.7	1.5			
	2060	12.3	1.6			
	2080	18.8	1.6			
	2100	26.3	1.6			
High	2008	1.7	1.0	1.7	0.9	
	2020	2.2	1.0	2.2	1.0	
	2040	3.1	1.0	3.1	1.1	
	2060	4.1	1.1	4.1	1.3	
	2080	5.3	1.2	5.3	1.6	
	2100	6.8	1.6	6.9	2.2	
Medium	2008	1.6	1.0	1.6	1.0	
	2020	2.	1.0	2.1	1.0	
	2040	2.8	1.0	2.8	1.0	
	2060	3.6	1.0	3.7	1.2	
	2080	4.6	1.1	4.8	1.4	
	2100	5.8	1.3	6.0	1.8	
Low	2008	1.5	1.0	1.5	0.9	
	2020	1.9	1.0	1.9	1.0	
	2040	2.5	1.0	2.5	1.0	
	2060	3.2	1.0	3.3	1.1	
	2080	4.1	1.1	4.1	1.2	
	2100	5.0	1.2	5.0	1.4	
Historical Trend	2008	1.3	0.9	1.3	0.9	Brownian motion is based on the observed data at Southampton gauge (1.3±0.18mm/yr)
	2020	1.5	1.0	1.5	1.0	
	2040	1.7	1.0	1.7	1.0	
	2060	2.0	1.0	2.0	1.0	
	2080	2.3	1.0	2.2	1.0	
	2100	2.5	1.0	2.5	1.0	

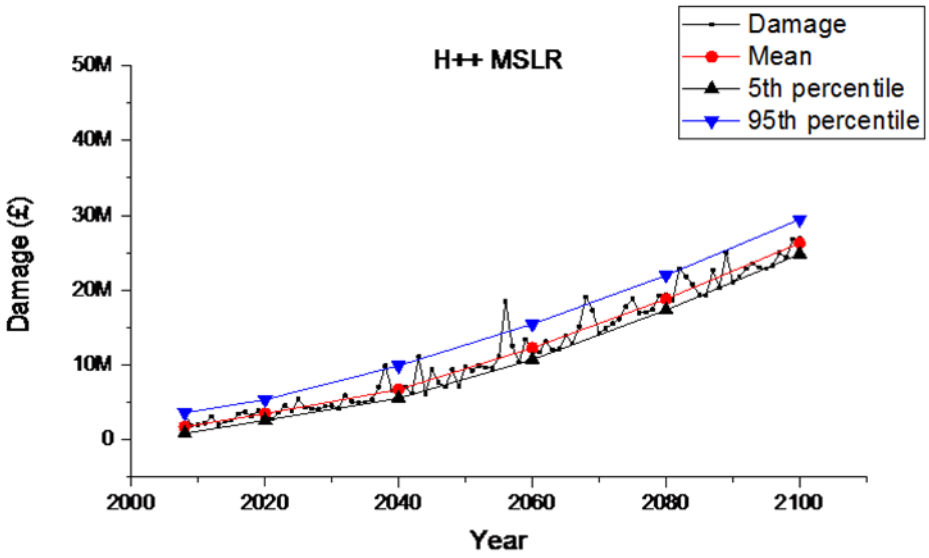
H++ MSLR
Damage
Mean
5th percentile
95th percentile
Damage (£)
50M
40M
30M
20M
10M
0
2000
2020
2040
2060
2080
2100
Year

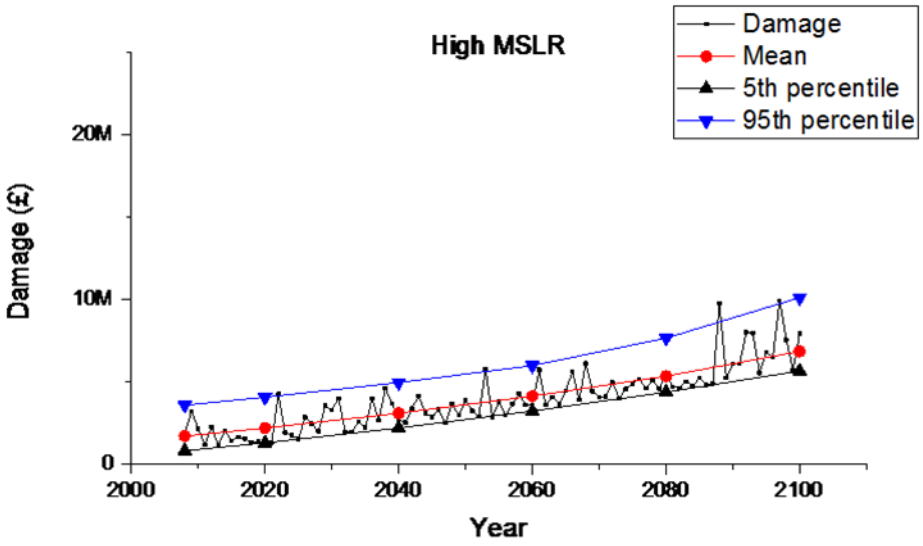
High MSLR
Damage
Mean
5th percentile
95th percentile
Damage (£)
20M
10M
0
2000
2020
2040
2060
2080
2100
Year

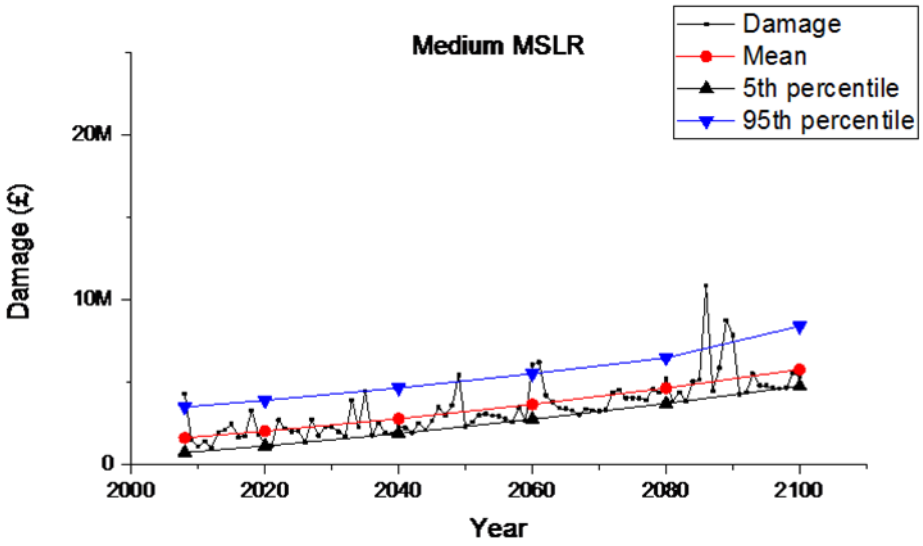
Medium MSLR
Damage
Mean
5th percentile
95th percentile
Damage (£)
20M
10M
0
2000
2020
2040
2060
2080
2100
Year

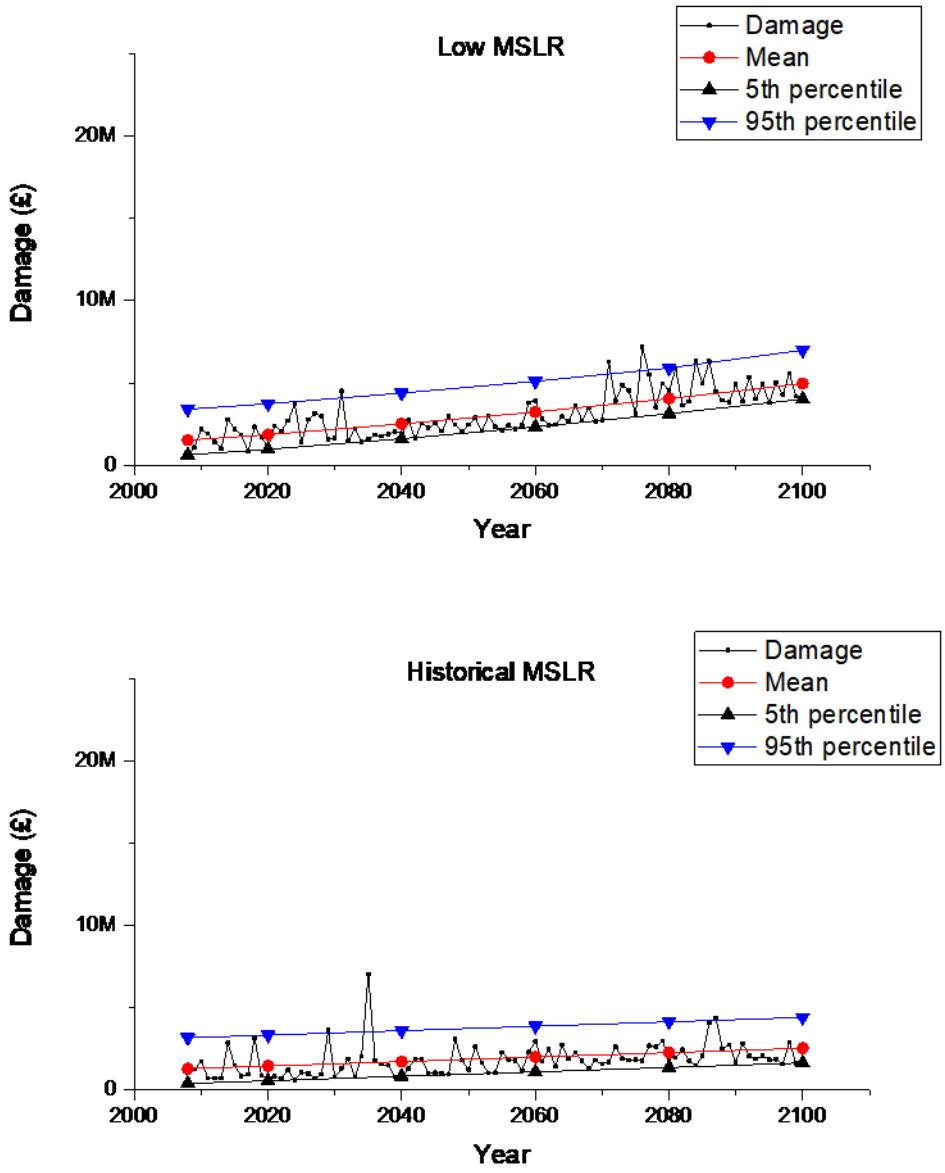

Figure I. 1 Temporal changes in flood damages under the current flood defence by different MSLR scenarios – Note that the time-series of flood damages are annual maxima

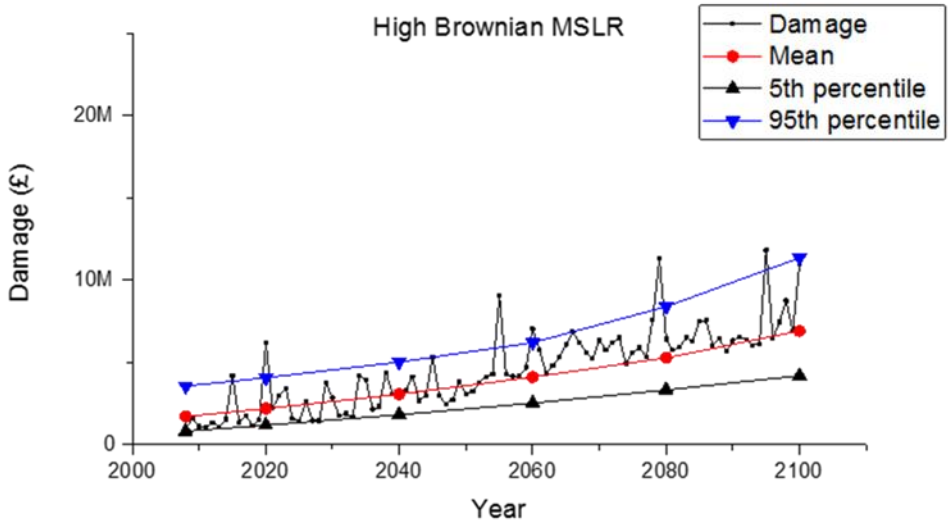
High Brownian MSLR
Damage
Mean
5th percentile
95th percentile
Damage (£)
20M
10M
0
2000
2020
2040
2060
2080
2100
Year

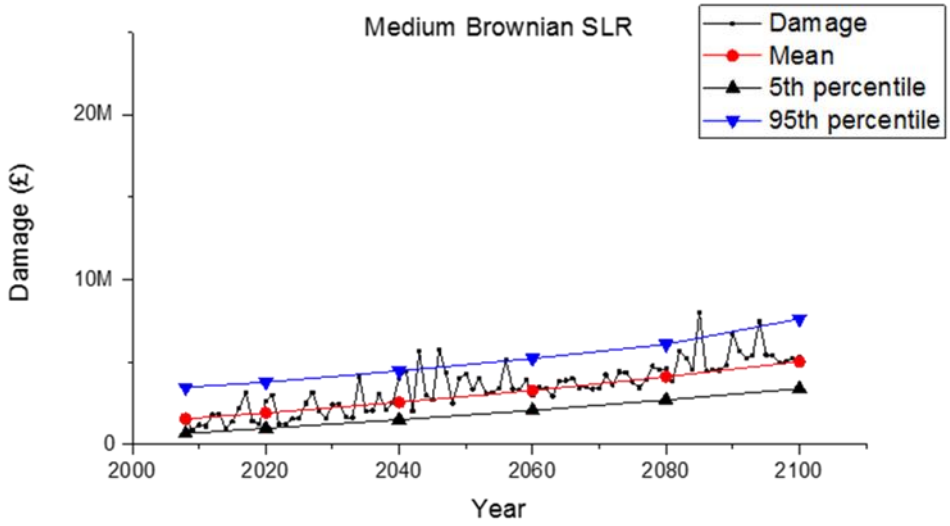
Medium Brownian SLR
Damage
Mean
5th percentile
95th percentile
Damage (£)
20M
10M
0
2000
2020
2040
2060
2080
2100
Year

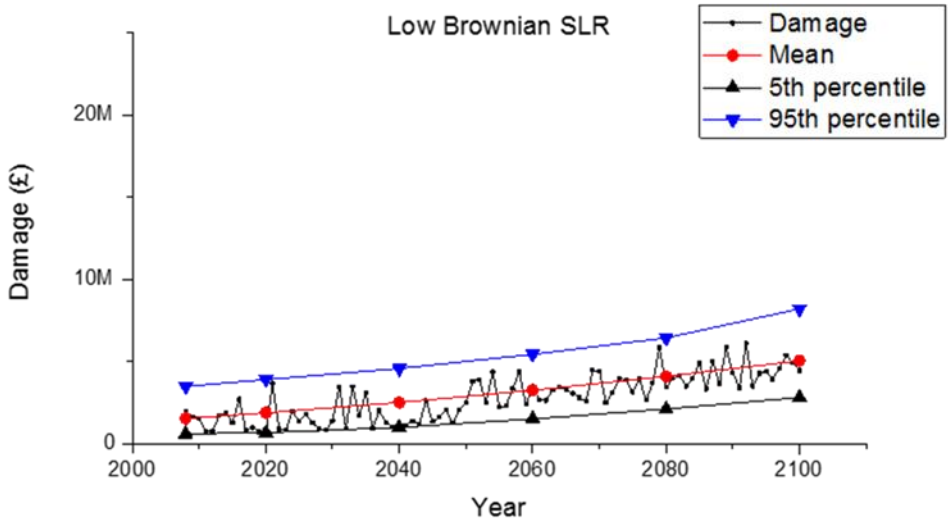
Low Brownian SLR
Damage
Mean
5th percentile
95th percentile
Damage (£)
20M
10M
0
2000
2020
2040
2060
2080
2100
Year

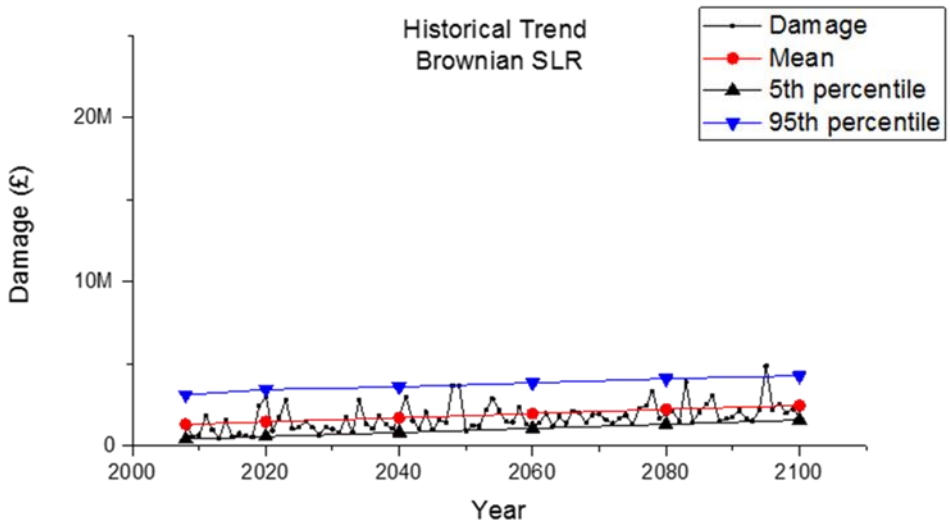

Figure I. 2 Temporal changes in flood damages under the current flood defence by different Brownian SLR scenarios – Note that the time-series of flood damages are annual maxima

Appendix J. Change in expected annual benefit (EAB) across sea-level rise for adaptation measures

Sea-level rise leads to increase in expected annual flood damages (EAD). This thesis has estimated EADs across the possible range of sea-level rise for the current defence condition and the upgraded defence conditions, respectively, as shown in Figure J. 1.

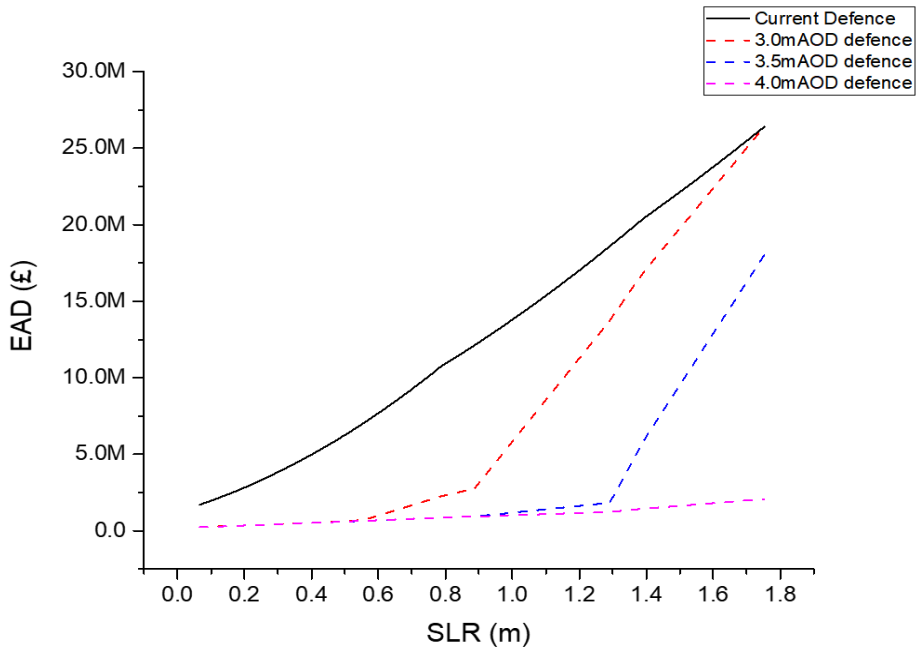

Figure J. 1 Changes in expected annual damage (£) across sea-level rise by different coastal defence conditions in Lymington – The expected flood damages are estimated by flood simulations with various sea-level rise for different defence conditions

As seen in Figure J. 1, the expected flood damages can be reduced by upgrading the coastal defence. As a reduction in expected annual damage (EAD) is expected annual benefit (EAB) due to the upgrade of the coastal defence, EAB at a given year depends on sea-level rise at the corresponding year and the upgrade of the coastal defence. For each of the adaptation measures, change in EAB is plotted across sea-level rise as shown in Figure J. 2. Note that EAB is the performance of the upgraded coastal defence versus the previous coastal defence against sea-level rise and coastal flooding. Therefore, the relations between EAB and SLR for $U_{3.0m \rightarrow 3.5m}$, $U_{3.0m \rightarrow 4.0m}$ and $U_{3.5m \rightarrow 4.0m}$ are made by estimating the performance of the upgraded defence condition versus the previous stage of defence condition.

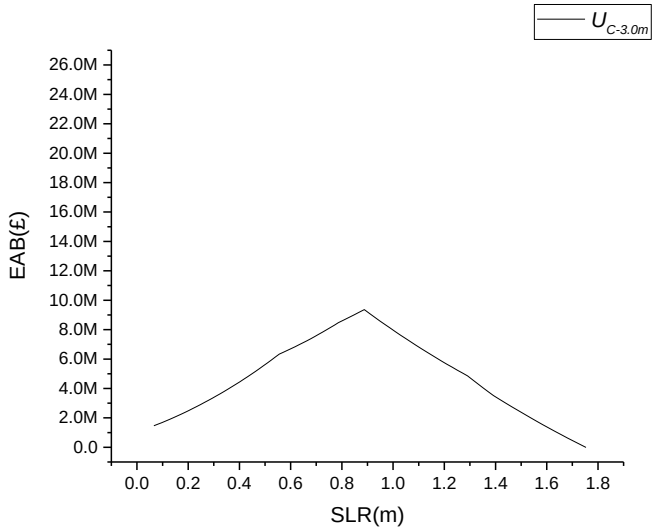
$U_{C\text{-}3.0m}$
EAB(£)
26.0M
24.0M
22.0M
20.0M
18.0M
16.0M
14.0M
12.0M
10.0M
8.0M
6.0M
4.0M
2.0M
0.0
0.0 0.2 0.4 0.6 0.8 1.0 1.2 1.4 1.6 1.8
SLR(m)

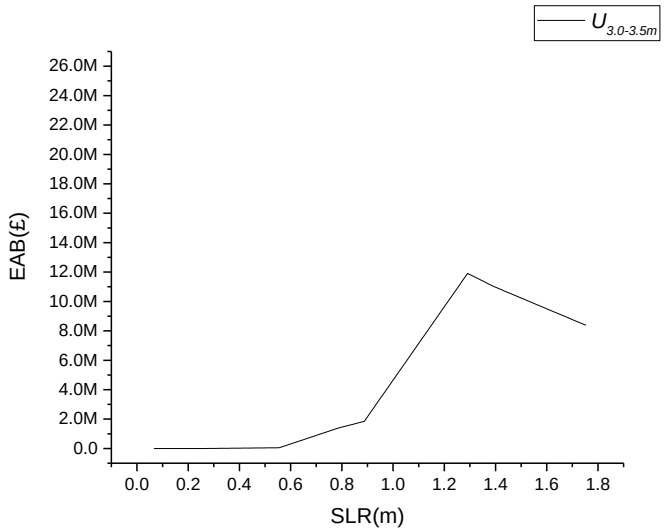
$U_{3.0\text{-}3.5m}$
EAB(£)
26.0M
24.0M
22.0M
20.0M
18.0M
16.0M
14.0M
12.0M
10.0M
8.0M
6.0M
4.0M
2.0M
0.0
0.0 0.2 0.4 0.6 0.8 1.0 1.2 1.4 1.6 1.8
SLR(m)

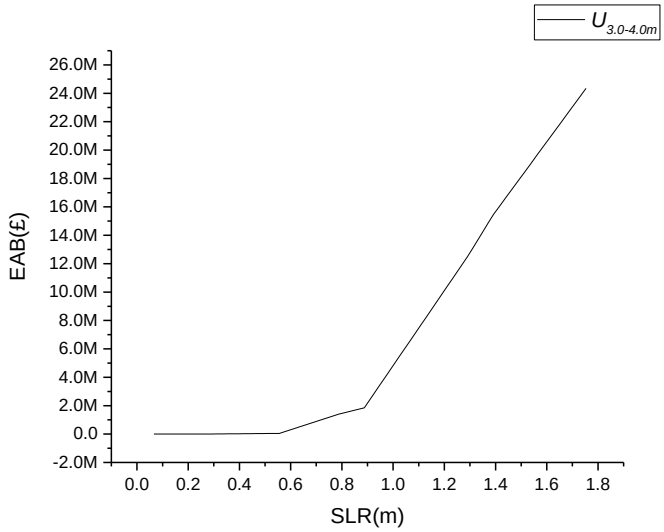
$U_{3.0\text{-}4.0m}$
EAB(£)
26.0M
24.0M
22.0M
20.0M
18.0M
16.0M
14.0M
12.0M
10.0M
8.0M
6.0M
4.0M
2.0M
0.0
-2.0M
0.0 0.2 0.4 0.6 0.8 1.0 1.2 1.4 1.6 1.8
SLR(m)

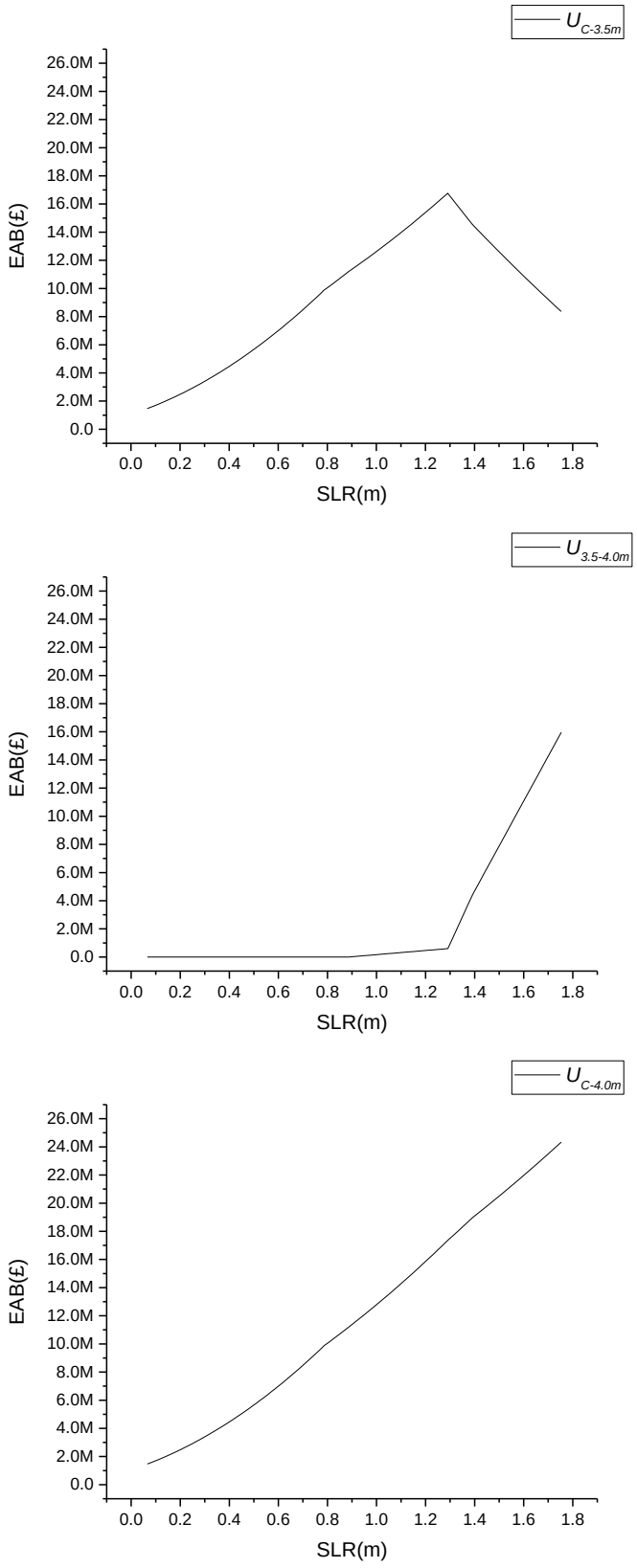

Figure J. 2 Changes in EAB (£) across sea-level rise for each of the adaptation measures – For denotation, an adaptation measure of raising the coastal defence from an initial level (*i*) to an upgraded level (*j*) is denoted by $U_{i\text{-}j}$

Appendix K. Change in EAB for MSLR under different SLR scenarios

This appendix shows temporal changes in the means and variances of the benefits for all the years during 21st century. In order to reduce the amount of work, the means and probabilistic ranges of the benefit values have been estimated for 2008 and every 20 years from 2020 to 2100 under each SLR scenario by @Risk programme. The random time-series of benefit values for an adaptation measure ($U_{c\rightarrow 3.5m}$), as an example, have been generated with their own probabilistic ranges during the period of sea-level rise as shown in Figure K. 1.

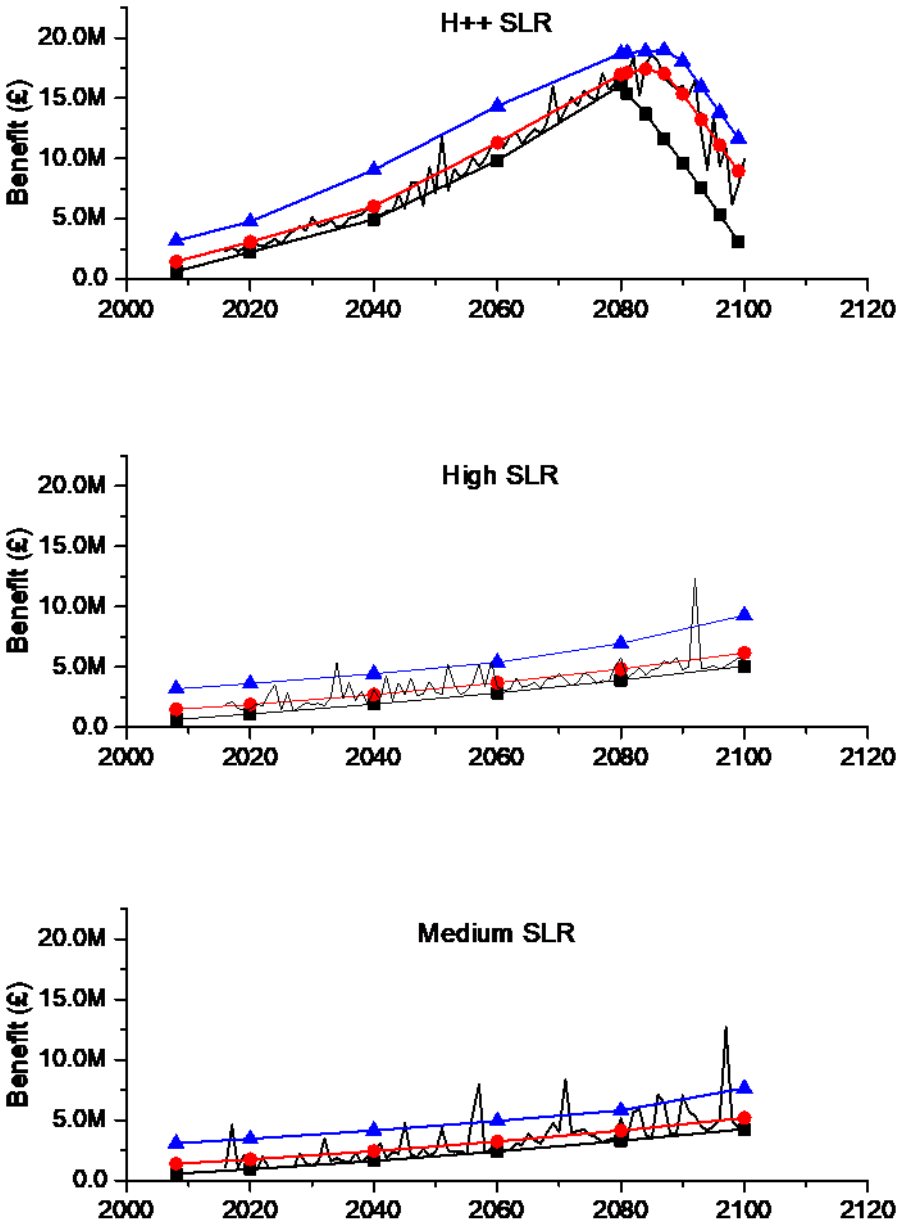

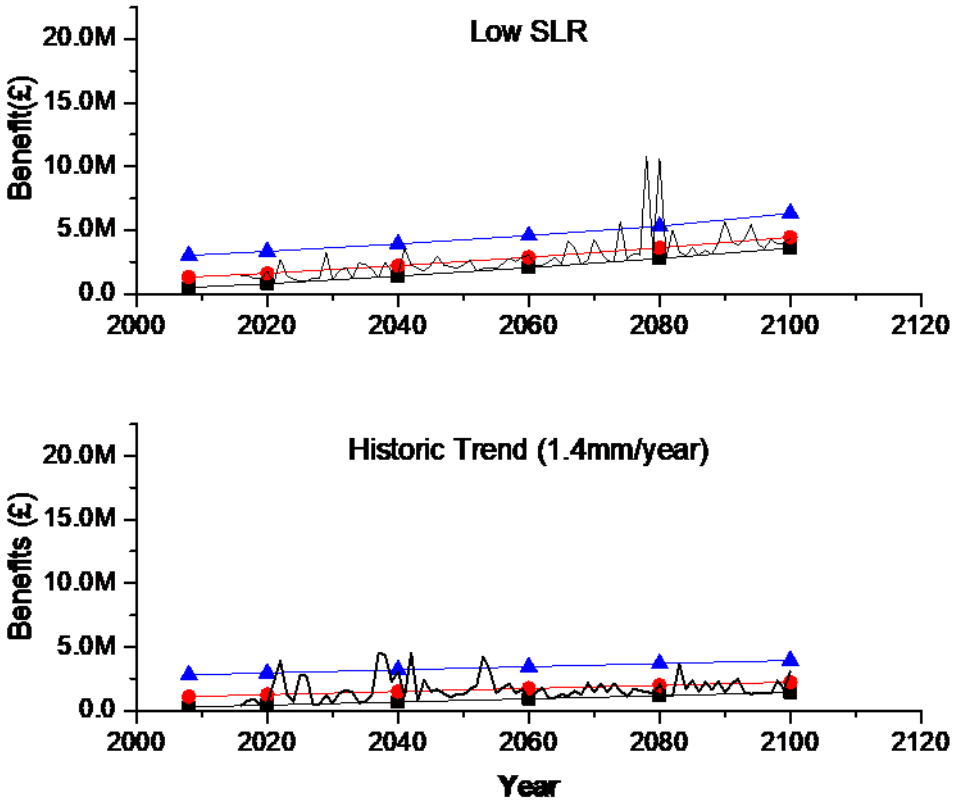

Figure K. 1 Time-series of benefit values due to the upgrade of coastal defences (i.e. $U_{c\rightarrow 3.5m}$) with mean and its probabilistic ranges (the 5th and 95th percentiles) under each of the SLR scenarios

Temporal changes in EAB can be also estimated over time according to MSLR scenarios by using the relations between EAB and sea-level rise. The temporal changes in EAB have been made by correlating EAB curves (Figure J. 2) to MSLR projections. As the rates of sea-level rise differ according to MSLR scenarios, the patterns and rates of change in the EAB differ depending on MSLR scenarios. For example, in the H++ SLR scenario, EAB is the fastest-growing but declining after a certain amount of sea-level rise. This study considers five SLR scenarios and six adaptation measures or paths so that we can make 30 different cases of changes in EAB over time as the responses of each adaptation measure to sea-level rise over time (Figure K. 2). For each adaptation path, temporal changes in EAB are drawn by different SLR scenarios as below.

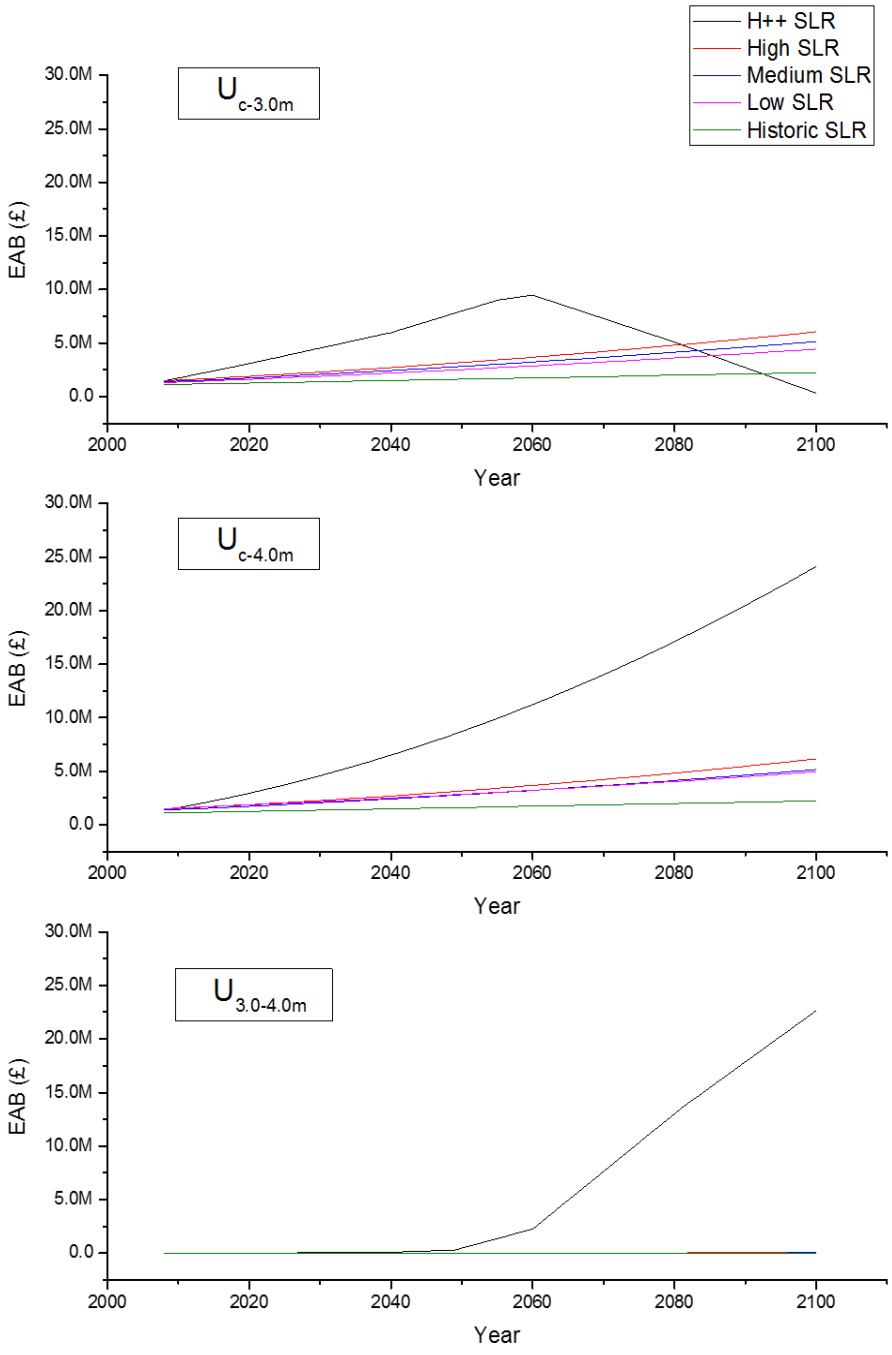
H++ SLR
High SLR
Medium SLR
Low SLR
Historic SLR
U c-3.0m
U c-4.0m
U 3.0-4.0m
EAB (£)
30.0M
25.0M
20.0M
15.0M
10.0M
5.0M
0.0
2000
2020
2040
2060
2080
2100
Year

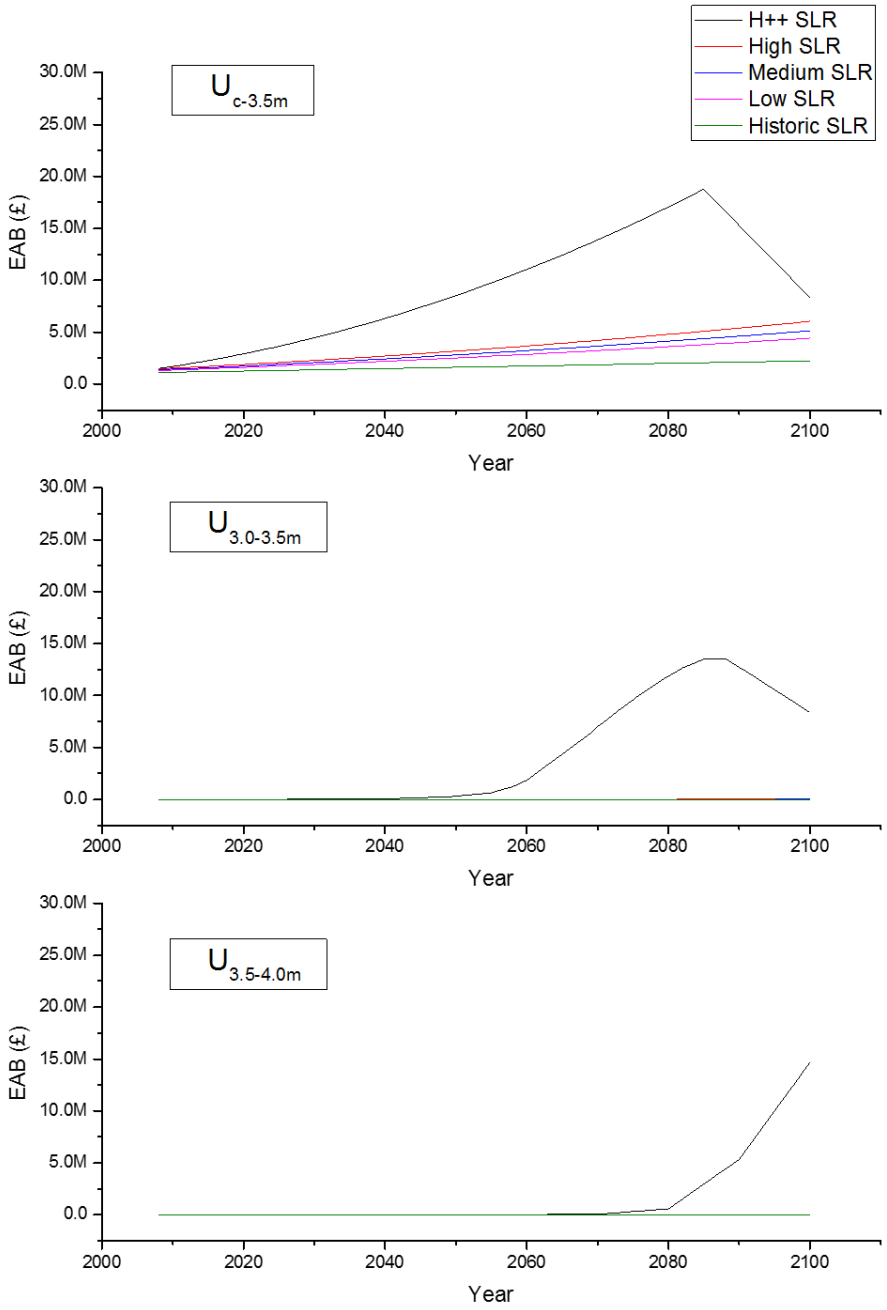

Figure K. 2 Changes in EAB over time for each of the adaptation measures under each sea-level rise scenario for Lymington.

Appendix L. NPV distribution of an adaptation option at different investment times

For sensitivity purposes, the probabilistic ranges of option values have been constructed in cases where the investment is made now (2016), at the optimal investment time, and in the distant future (e.g. 2060) for each of MSLR scenarios. For the calculations, we have substituted the variable of EAB_i in the equation of termination value by the stochastic variable of B_i, which is obtained from the random variable of ESWL+ MSLR+WAVE by the relation between the benefits and the climatic variables for the upgrade of the coastal defence to 3.5mAOD level.

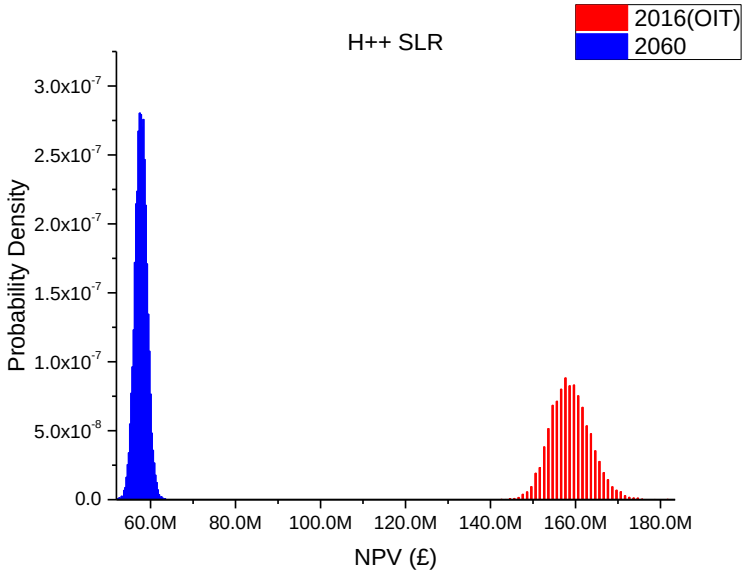

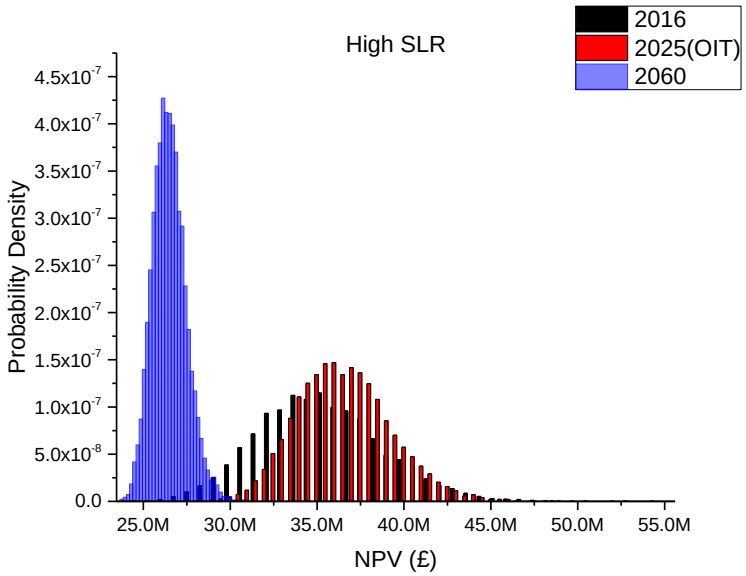

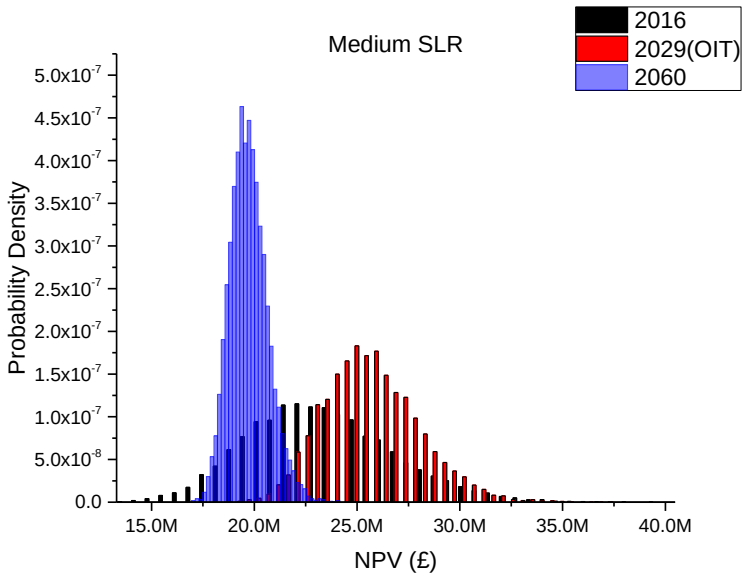
Medium SLR
2016
2029(OIT)
2060
Probability Density
5.0x10-7
4.5x10-7
4.0x10-7
3.5x10-7
3.0x10-7
2.5x10-7
2.0x10-7
1.5x10-7
1.0x10-7
5.0x10-8
0.0
15.0M
20.0M
25.0M
30.0M
35.0M
40.0M
NPV (£)

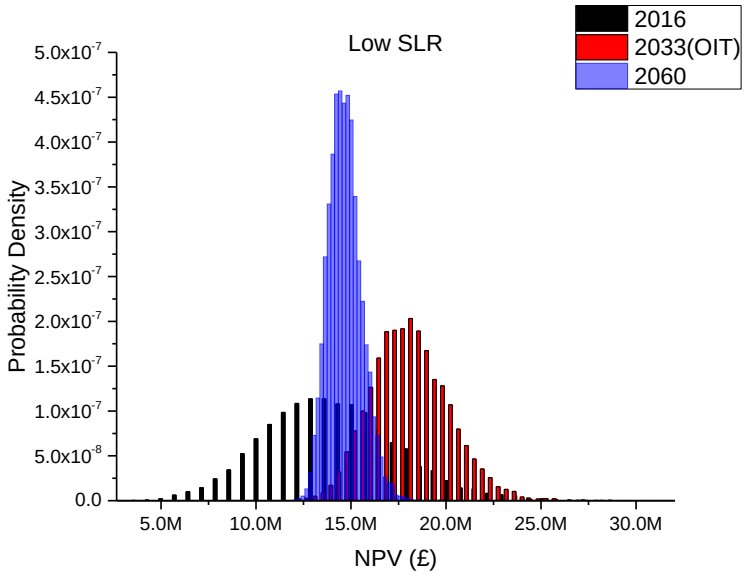
Low SLR
2016
2033(OIT)
2060
Probability Density
5.0x10-7
4.5x10-7
4.0x10-7
3.5x10-7
3.0x10-7
2.5x10-7
2.0x10-7
1.5x10-7
1.0x10-7
5.0x10-8
0.0
5.0M
10.0M
15.0M
20.0M
25.0M
30.0M
NPV (£)

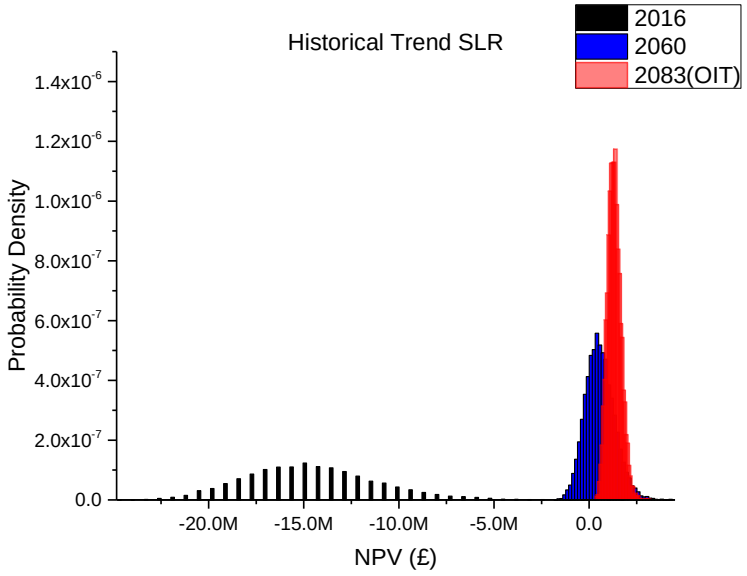

Figure L. 1 NPV distributions at optimal investment time (OIT) and different investment years (i.e. 2016 and 2060) under 10,000 random time-series of ESWL+SLR+WAVE in each of the SLR scenarios. Note the different x and y axis scales

Appendix M. Optimisation of investment time and its option value by formulation

M. 1. Introduction

This appendix is aimed to elucidate the relation between the critical threshold value (i.e. sea-level rise) and the optimal investment time as investigated in section 5.2.4. The real option value grows to a maximum when the option is deferred until the optimal investment time. Though all the optimal investment times differ depending on SLR scenarios and future growth rate scenarios, sea-level rise observed at the different optimal investment times are similar to each other for all the SLR scenarios.

To understand the relation between the maximum option value and the optimal investment time, this appendix derives a formula for the optimal investment time. This formula provides an alternative method to find the optimal investment time of a deferrable adaptation option. In addition, this derivation shows the uniqueness of the critical threshold value for an adaptation option even under the uncertainty of sea-level rise. Thus, this appendix is aimed to support the findings and observations in the option-to-wait case.

Some studies are found, which have sought to formulise the optimal investment time in respect to uncertain variables (Jorgenson, 1963; McDonald and Siegal, 1982). The previous formulations were derived by solving a stochastic differential equation for a deferrable investment option. The 'McDonald and Siegal model' and 'Jorgenson model' defines investment rules to ensure the option value of a deferrable investment option becomes maximum with regard to uncertain annual profits or project values. However, both models are only applicable to ideal cases where uncertain stochastic variables (e.g. the price of stocks or commodities) have simple and mathematical relations with option values (i.e. the net present value (NPV_i) of the investment at year *i* in this thesis). In climate change adaptation, it seems hard to correlate climatic variables (i.e. sea-level rise) with option values (NPV_i) by both models.

Apart from the previous models, this appendix demonstrates that climatic variables at the optimal investment times (or years) are similar to each other. As reviewed in section 5.4.4, this critical threshold value helps identify the optimal investment time of a deferrable option. Thus, a key to making an optimal investment in adaptation decision is to observe whether the relevant climatic variable reaches the critical threshold value. In this context, this appendix

focuses on the derivation of a formula for optimal investment time in a case where sea level continuously rises.

This appendix is structured as follows. Firstly, we review the previous models for optimal investment time and, then, the next section derives formulation for optimal investment time in the deterministic case of sea-level rise - The formula will be also derived in the stochastic case of sea-level rise later in Appendix R.

M. 2. The previous models for optimal investment time

1) McDonald and Siegel Model

This model assumes a project value *V*, which is the sum of total profits during the life of a project (*L*), follows Geometric Brownian motion as below.

$$dV = \alpha V dt + \sigma V dz \tag{1}$$

Here, V is a project value, α is a drift parameter for the deterministic motion of the project value, σ is a variance parameter for the random motion of the project value and *dz* is a Weiner process. If the investment cost of the project is *I*, this model defines an option value (*F*), which is the net of the overall profits minus the cost as below.

$$F(V) = E[\,(V_T - I)e^{-rT}] \tag{2}$$

Here, E denotes the statistical expectation of option values (*F*), V_T is the project value for the investment made at time *T*, *T* is any time in the future, r is discount rate per unit time. In this model, the optimal investment time is when the option value F(V) becomes a maximum in equation (2). McDonald and Siegal (1982) modelled the optimal investment time in a deterministic case and a stochastic case, respectively.

A. Deterministic case (no certainty: σ=0)

In a deterministic case ($\sigma = 0$ in equation (1)), the project value at time *T* is written as below.

$$V(T) = V_0 e^{\alpha T}, \text{ where } V_0 = V(0) \tag{3}$$

Therefore, the option value at any time *T* is written by equation (4)

$$F(V) = (Ve^{\alpha T} - I)e^{-rT} \tag{4}$$

To maximize $F(V)$ in equation (5) with respect to *T*, the first derivative of $F(V)$ with respect to T should be zero.

$$\frac{dF(V)}{dT} = -(r-\alpha)Ve^{-(r-\alpha)T} + rIe^{-rT} = 0$$

$$\therefore \quad T^* = \frac{1}{\alpha}\log\left[\frac{rI}{(r-\alpha)V}\right] \qquad (T^* \geq 0) \tag{5}$$

If T^* is set to be zero, which means the investment now, the project value V^* to satisfy this condition is

$$V^* = \frac{r}{r-\alpha} I \tag{6}$$

Therefore, if $V \geq V^*$, one should invest in the project immediately. This formulation clearly shows a relation between the critical project value (V^*) and the discount rate (r), or the investment cost (I).

B. Stochastic case (σ >0)

In a stochastic case, the derivation of a formulation for a maximum option value is more complicated than in a deterministic case. In this case, the investment timing can be found by solving a stochastic differential equation in equation (7). This stochastic equation can be derived by Ito's Lemma and Geometric Brownian motion as reviewed in section 2.4 (Dixit and Pindyck, 1994).

$$\frac{1}{2}\,\sigma^2 V^2 \frac{\partial^2 F}{\partial V^2} + \alpha V \frac{\partial F}{\partial V} - rF = 0 \tag{7}$$

Here, F(V) is an option value, which is the project value (*V*) minus the investment cost (*I*) in equation (2), α is a drift parameter of the project value (V), σ is a variance parameter of the project value (V) and *r* is constant discount rate.

To maximize F(V) with respect to V, F(V) meets the following boundary conditions for critical value V^*

$$F(0) = 0 \tag{8}$$

$$F(V^*) = V^* - I \tag{9}$$

$$F'(V^*) = 1 \tag{10}$$

For solving the stochastic differential equation (7) subject to the boundary conditions in equations (8), (9) and (10), this model has assumed that F(V) has the form of

$$F(V) = A * V^{\beta} \tag{11}$$

Here, A and β are constants that are determined by the boundary conditions. The critical value V^* at which F (V) *(*= $F(V) = E[\,(V_T - I)e^{-rT}]$ *)* is maximized can be obtained as below

$$V^* = \frac{\beta}{\beta - 1} I \tag{12}$$

Constant A is obtained by equation (11) and (12) and boundary condition (9)

$$A = \frac{V^* - I}{(V^*)^{\beta}} \tag{13}$$

By inserting equation (11) into equation (7) and rearranging, this model can have a relation for β that satisfies the equation (7).

$$\frac{1}{2}\sigma^2\beta(\beta\text{-}1) + \alpha^*\beta\text{-}r = 0 \tag{14}$$

Therefore, β is a root of the quadratic equation (14)

$$\beta_1 = \frac{1}{2} - \frac{\alpha}{\sigma^2} + \sqrt{\left[\frac{\alpha}{\sigma^2} - \frac{1}{2}\right]^2 + \frac{2r}{\sigma}} \quad > 0 \tag{15}$$

By the equations (12) - (15), this model can find the critical value V^* at which the investment is optimal. The investment rule for any time can be obtained by comparing the critical value V^* with project value V at time. Therefore, the investment rule or optimal investment time is a condition satisficing to an equation as below.

$$V > V^* = \frac{\beta}{\beta\text{-}1} I \tag{16}$$

Therefore, according to equation (16), the cost-benefit analysis rule (V - I > 0) is not correct in the case where an option can be deferred to the future. (Dixit and Pindyck, 1994). To maximize an investment opportunity by waiting or deferring, a project value (V) should be higher than $\beta/(\beta\text{-}1) \times I$

If $\sigma \to \infty$ in equation (15), $\beta = 1$ and $V^* \to \infty$ in equation (16). This implies that we have to wait until the project value (V) goes to infinity (∞). This leads to no investment. However, if there is no uncertainty, that is, a deterministic case ($\sigma = 0$),

$$\beta = {}^{r}/_{\alpha} \text{ and } V^* = \frac{r}{r\text{-}\alpha} I \qquad (\alpha > 0) \tag{17}$$

$$\beta = \infty \text{ and } V^* = I \qquad (\alpha \leq 0) \tag{18}$$

McDonald and Siegal model provides a method of estimating a critical project value (V^*) for the deterministic and stochastic cases of uncertain variable, respectively. If the project value (V) is above the critical value(V^*), this model suggests that the investment should be implemented at that time. Otherwise, it indicates that the investment should be deferred until

the project value (V) reaches the critical threshold value (V^*). This model demonstrates how to find the optimal investment time by the critical project value (V^*).

However, one of the problems in application of this model to climate change adaptation is how to estimate the project value (V) in practice. It is because the project value (V) is the sum of future profits or benefits during the life of a project. As the uncertainty of sea-level rise is large and the project life (*L*) of climate change adaptation is many decades or longer, the estimated project value (V) for climate change adaptation will include a large uncertainty in itself. Thus, this model does not seem to be appropriate for finding optimal investment time in climate change adaptation.

2) Jorgenson model

The Jorgenson model provides a method to find a critical profit value (π_t^*) at which any investment produces the largest overall profit during the life of a project. This model assumes that a project is a factory that infinitely produces a profit flow (π_t). Here, this model assumes that the profit flow (π_t) is a stochastic process following Geometric Brownian motion as shown in equation (19).

$$d\pi_t = \alpha\pi_t dt + \sigma\pi_t dz \tag{19}$$

Here, π_t is a profit flow at any time *t,* α is a drift parameter representing the deterministic motion of the profit flow, σ is a variance parameter for the random motion of the profit flow, *dz* is a Weiner process. By using the statistical expectation of the profit flow, the value (V_t) of the project implemented at time *t* can be represented in an integral form in equation (20).

$$V_t = E[\int_t^{\infty} \pi_s e^{-r(s-t)} ds] = \frac{\pi_t}{r-\alpha} \tag{20}$$

Here, E denotes statistical expectation, π_s is a profit at year *s* after investment at year *t*. By substituting equation (20) for V_t in equation (16) from Siegal and McDonald model, a critical profit π_t^* can be obtained in equation (21)

$$\pi_t > \pi_t^* = \frac{\beta}{\beta-1}(r-\alpha)I \tag{21}$$

By rearranging the equation (12) for $\frac{\beta}{\beta\text{-}1}$ (r-α) , we have

$$\frac{\beta}{\beta\text{-}1}\,(\text{r-}\alpha) = \left(\text{r} + \frac{1}{2}\,\sigma^2\beta\right) \tag{22}$$

Thus, the critical profit π_t^* can be written as

$$\pi_t^* = \left(\text{r} + \frac{1}{2}\,\sigma^2\beta_1\right)\text{I} > \text{r I} \tag{23}$$

Here, rI is called the Jorgensonian user cost of capital (Jorgenson, 1963). This indicates that a project with investment cost I should be made when an annual profit at any year exceeds $\left(\text{r} + \frac{1}{2}\,\sigma^2\beta_1\right)\text{I}$. In a special case where there is no uncertainty, the Jorgenson investment rule also shows that the option holders need to wait until $\pi_t = \text{rI}$. However, if there is uncertainty ($\sigma \neq 0$), the option holders should wait longer due to an additional term $\frac{1}{2}\,\sigma^2\beta_1$ than with no uncertainty.

$$\pi_t > \left(\text{r} + \frac{1}{2}\,\sigma^2\beta_1\right)\text{I} \qquad \text{(with uncertainty)} \tag{24}$$

$$\pi_t > \text{r I} \qquad \text{(with no uncertainty)} \tag{25}$$

The Jorgensen Model provides a critical profit π_t^* to maximise the option value (F(V)) under the uncertainty of future profits. Although the investment rule is similar to that of the McDonald and Siegal model (1983), the Jorgenson model (1963) seems more suitable to tackling climate change adaptation. This model uses an annual profit (π_t) to determine the implementation time of any investment. Thus, there is no need to evaluate the project value (V_t) during the life of the project. As this thesis evaluates the option value of a deferrable option with expected annual benefit (EAB), the Jorgenson model provides more meaningful implications for this thesis than McDonald and Siegal model. However, the Jorgenson model has been developed upon the assumption that the future profits (π_t) are produced infinitely. Therefore, some limitations still exist in the application of the Jorgenson model for climate change adaptation.

M. 3. Derivation of formulas for optimal investment time

This part demonstrates a relation between optimal investment time and critical threshold value for an adaptation option. The formulation is firstly derived in the deterministic case where sea-level rise follows MSLR scenario. The derivation starts to differentiate an equation of a termination value ($F_{ex,t}$) with respect to investment time (t). Note that the termination value ($F_{ex,t}$) is the option value of a deferrable option when the investment is made at time t. In the stochastic case of sea-level rise following General Brownian motion, we adopt dynamic programming for the derivation of the formulation of a critical threshold value for an adaptation option with investment cost (I).

The termination value from an investment at any given year t can be obtained as shown in equation (26).

$$\mathrm{F_{ex,t}} = \sum_{\mathrm{i=t+1}}^{\mathrm{L+t}} \frac{\mathrm{EAB_i}}{(1+\mathrm{r})^{\mathrm{i}}} - \frac{\mathrm{I}}{(1+\mathrm{r})^{\mathrm{t}}} \tag{26}$$

Here, EAB_i is the expected annual benefit of a project at any year i after the investment at year t, r is discount rate, I is investment cost, and L is the life of the project in climate change adaptation.

In order to differentiate the equation (26) with respect to investment time t, this analysis transforms the formulation into an integral form with respect to investment time (t). Thus, the investment time (t) is continuous in this derivation. The time-discrete formula of the termination value is set to be a continuous form as shown in equation (27). EAB is assumed to be a continuous function of time ($\mathrm{f} = \mathrm{EAB(t)}$) in this analysis. Therefore, the continuous form of $\mathrm{F_{ex,t}}$ at any investment time (t) can be written as below.

$$\mathrm{F_{ex,t}} = \int_{\mathrm{t+1}}^{\mathrm{t+L}} \mathrm{EAB(i)}*\mathrm{e^{-ri}di} - \mathrm{I}*\mathrm{e^{-rt}} \tag{27}$$

Here, r is discount rate per time, $\mathrm{EAB(i)}$ is the rate of benefit in currency at any time i, t is investment time. If $F_{ex,t}$ in equation (27) becomes a maximum at any investment time t`, the time $t$` is optimal investment time by definition. The derivative of $\mathrm{F_{ex,t}}$ ($= \mathrm{d(F_{ex,t})/dt}$) can be derived by directly differentiating the equation (27) by using Leibniz's theorem as below.

$$\frac{d}{dt}(F_{ex,t}) = EAB(t+L)*e^{-r(t+L)} \times \frac{d(t+L)}{dt} - EAB(t+1)*e^{-r(t+1)} \times \frac{d(t+1)}{dt}$$
$$- \int_{t+1}^{t+L} \frac{\partial}{\partial t}\left(\frac{EAB(i)}{e^{ri}}\right)di + I*r*e^{-rt}$$
$$= \frac{EAB(t+L)}{e^{r(t+L)}} - \frac{EAB(t+1)}{e^{r(t+1)}} + I*r*e^{-rt} \quad (28)$$

As $d(F_{ex,t})/dt = 0$ at the optimal investment time (t'), this derivation will have equation (29) for the optimal investment time. As $e^{-r} \approx 1/(1+r)$ and $e^{-rL} \approx 1/(1+r)^L$, the equation can be rewritten as below

$$\frac{EAB(t'+1)}{(1+r)} - \frac{EAB(t'+L)}{(1+r)^L} = r \times I \quad (29)$$

As you can see equation (29), the first term on the left side is the expectation of benefit the first year after the investment and the second term is the expectation of benefit the L^{th} year after the investment. Both values are discounted to the optimal investment year (*t'*) by discount factors $1/(1+r)$ and $1/(1+r)^L$, respectively. On the left side, the term denotes investment cost (*I*) times discount rate (*r*). Therefore, if the investment cost and discount rate are known for an adaptation option, the optimal investment time (*t'*) satisfies the equation (29). The first term is EAB for the first year after the investment discounted by $1/(1+r)$ while the second term is EAB for the L^{th} year after the investment discounted by $1/(1+r)^L$. However, $(1+r)^L$ is very large if the project year is 100 years. Thus, the second term becomes ignorable compared to the first term. The equation (29) can be rewritten by ignoring the second term on the left-hand side. Thus, we can have equation (30) as below.

$$\frac{EAB(t'+1)}{(1+r)} = r \times I \quad (30)$$

If the discount rate *r* and the investment cost *I* is known, the formulation enables us to evaluate the critical value of *EAB* for the optimal investment time. Let EAB_c denote the critical threshold value of *EAB* for the optimal investment time (*t'*) at which the investment provides a maximum NPV during the project life. Equation (30) can be written as below.

$$EAB_c = (1+r)*r \times I \quad (31)$$

Equation (31) implies that we can determine the optimal investment time by observing whether EAB reaches the critical threshold value (EAB_c). As EAB is projected over time in relation to SLR scenarios, this formulation enables us to find when the optimal investment time occurs by matching EAB_c with the projected EAB in climate change scenario. This equation also suggests that the optimal investment time (t') can be determined independently of climate change scenarios, if we can ignore the second term ($= \mathrm{EAB}(t' + L)/(1 + r)^L$).

This finding is identified in the case study of Lymington where the upgrade of coastal defence is planned with the investment cost of £ 64.2 million. Although the Green Book approach takes different discount rates according to the time periods (3.5% for the first 30 years, 3.0% for the next 45 years and 2.5% afterwards), the values of sea-level rise at the optimal investment time for all the SLR scenarios are found around 13cm in the analysis under the non-future growth scenario. This formulation explicitly shows why the critical threshold value (SLR_c) for the optimal investment time are highly dependent on investment cost (I) and discount rate (r). For the demonstration, *EABs* in the first year and the 100th year after the investment, the optimal investment time and its sea-level rise for each SLR scenario are summarized in Table M. 1.

Table M. 1 Comparison of the investment cost (I) times discount rate (r) with the values from the formulation for each SLR scenario

Scenario	Investment year (t')	Sea-level rise at year t'	$r*I$ (1)	EAB $(t'+1)$	EAB $(t'+L)$	$\frac{EAB(t'+1)}{(1+r)} - \frac{EAB(t'+L)}{(1+r)^L}$ (2)	(1) – (2)
High	2025	13.8cm	£2.21M	£2.11M	£8.79M	£1.76 M	£ 0.45 M[1)]
Medium	2029	13.2cm	£2.21M	£2.07M	£7.06M	£1.77 M	£ 0.44 M
Low	2033	12.6cm	£2.21M	£2.01M	£5.72M	£1.75 M	£ 0.46 M
H++	2016	19cm[3)]	£2.21M	£2.39M	0	£2.30 M	(-) £ 0.09 M[2)]

1) In backward induction method, the value (1) and (2) are not exactly matched with each other because the function EAB is not continuous of time. In addition, the discount rates provided by the Green Book (HM Treasury, UK) are applied differently depending on the time periods of the project year. If we apply a constant discount rate over the time periods, the value (2) is exactly matched with the value (1). Nevertheless, this result explicitly shows that the optimal investment time is approximately when the expectation of EAB at year i+1 reaches the value of $I \times r$.

2) In the H++ scenario, the expectation of benefit value at the end of the project year (2116) is zero because the upgraded coastal defence cannot protect the floodplains from extreme still water level above 3.5 mAOD that are highly expected to occur at 2116. Thus, EAB cannot be defined as a continuous function of time in the H++ SLR scenario.

3) In the H++ scenario, sea-level rise relative to 1990 already exceeded the critical threshold value. Therefore, sea-level rise at the optimal investment time is much higher in this extreme scenario than any other scenarios.

However, if EAB at the end year of the project life is large in equation (29), the critical threshold value (EAB_c) is also affected by EAB at the end year of the project life - This has

already been discovered in option evaluations for high growth rate scenarios (Refer to Section 5.2.5). Therefore, when EAB from the investment is expected to be considerably high, the formulation shows different patterns regarding the optimal investment time.

Nevertheless, the derived formula explicitly explains why the values of sea-level rise and EAB at the optimal investment time are similar to each other, respectively, independently of SLR scenarios. In this regard, this formula has an important implication in finding an optimal investment time under large uncertainty as it allows us to convert a time-dependent investment decision to an observation-based investment decision for the optimal investment. In other words, the identification of the optimal investment time in the real world only requires the values of expected annual benefit (EAB) in the first year and the end year of the project-life, which will be updated by further observations on sea-level rise and advanced technologies in the future.

If we can predict the future value of EAB at year $t' + L$ based on the accurate projection of sea-level rise, the equation (29) will allows us to estimate the critical threshold value of EAB_c – As EAB is dependent on the climatic variable of sea-level rise, the critical expected annual benefit (EAB_c) also provides the critical sea-level rise (SLR_c) at which the investment option should be implemented. By rearranging, the equation (29) can have a more general formulation for the optimal investment time as below.

$$EAB_t < EAB_c \qquad \text{(wait)} \tag{32}$$

$$EAB_t > EAB_c \qquad \text{(invest)} \tag{33}$$

$$EAB_c = (1 + r)[r \times I + \frac{EAB_P(t + L)}{(1 + r)^L}] \tag{34}$$

Here, EAB_t is the observed EAB at any year *t* subject to sea-level rise, EAB_c is the critical threshold value of *EAB,* EAB_p is the predicted EAB at year $t + L$, L is the life of a project or the life of the upgraded coastal defence, I is investment cost, r is discount rate – Note that, if a project living for *L* years is invested in at year *t,* the project lasts until the *t*+*L* year.

It should be of note that EAB at the end year of the project life is relatively small for all the SLR scenarios except the H ++ SLR scenario because its value is significantly discounted by the discount factor of $1/(1 + r)^L$. In this case, the equation (34) has a simpler form as below.

$$EAB_c = (1 + r)[r \times I] \tag{35}$$

Thus, the climatic variables of sea-level rise (SLR_c) or expected annual benefit (EAB_c) at the optimal investment time are similar to each other.

M. 4. Comparisons of the formulations for the optimal investment time

It is demonstrated that the climatic variable of sea-level rise at the optimal investment time has a unique value; although the optimal investment time differs depending on SLR scenarios. For the detailed understanding, this section compares the derived formula with Jorgenson model in Table M. 2.

The Jorgenson model and climate change adaptation model also take similar forms as shown in Table M. 2. However, Jorgenson model assumes that the annual profits after the investment are produced in an infinite time while the formula in this thesis takes into account the expected annual benefits during the life of a project. Thus, the derived formulation is more appropriate for climate change adaptation than Jorgenson model.

Table M. 2. Comparison between Jorgenson model (1963) and formulation by Kim et al. (2018)

Comparisons	**Jorgenson model (1963)**	**Formula for the optimal investment time by Kim et al. (2018)**
Investment condition	A factory with an infinite life	Raising the crest of coastal defence with the project life of L
Profits	Annual profit flow (π)	Expected annual benefit (EAB)
Project life (L)	∞ (Infinity)	The life of a project (L)
Uncertainty	Annual profit flow (π)	Sea-level rise or EAB
Brownian motion	Geometric Brownian motion $d\pi_t = \alpha\pi_t dt + \sigma\pi_t dz$ α: drift parameter σ: variance parameter	Adjusted General Brownian motion $dx = a(x,t)dt + b(x,t)dz$ $a(x,t)$: any function for drift $b(x,t)$: any function for variance
The focus of analysis	Finding the investment timing with the highest option value	Finding the investment timing with the highest NPV
Investment rule	Invest when $\pi = \pi^*$	Invest when $EAB = EAB_c$ or $SLR = SLR_c$
Formulae for the optimal investment time	No uncertainty (σ=0) $\pi^* = rI$ Uncertainty (σ≠0) $\pi^* = \left(r + \frac{1}{2}*\sigma^2\beta\right)I$ Here, *r*: discount rate *I*: investment cost β: constant (See equation 15)	No uncertainty (σ=0) $EAB_c = (1+r)(rI + \frac{EAB(i+L)}{(1+r)^L})$ Uncertainty (σ≠0) $EAB_c = rI + \frac{EAB(i+L)}{(1+r)^L}$ Here, *r*: discount rate *I*: investment cost L: project life

Appendix N. Effects of discount rates on optimal investment time

This appendix explores the effect of discount rates on the optimal investment time. The analysis applies the formulation approach to an ideal case where EAB is assumed to be an exponential function of time. Thus, the expected annual benefit is defined for this analysis as below.

$$\mathrm{EAB} = \mathrm{A}e^{\mathrm{Bt}} \tag{1}$$

Here, A and B are any constant. For the convenience of calculations, the formulation for the optimal investment time can be presented in exponential forms by using discount factor of e^{-rt} instead of $1/(1+r)^t$

$$\mathrm{EAB}(i+1)*e^{-r}\text{-}\mathrm{EAB}(i+L)*e^{-rL} = rI \tag{2}$$

This analysis focuses on validating the derived formulations (2) for a deterministic case of sea-level rise (i.e. MSLR) with a focus on the effects of discount rates (r) on optimal investment time (*i*).

If we substitute the equation (1) for the equation (2), the optimal investment time (*i*) should satisfy equation (3). This analysis assumes that the investment cost is constant over time.

$$\mathrm{A}e^{\mathrm{B}(i+1)}*e^{-r}\text{-}\mathrm{A}e^{\mathrm{B}(i+L)}*e^{-rL} = rI \tag{3}$$

By rearranging the equation (3) for the term of the optimal investment time *i,* the optimal investment time *i* is obtained by

$$i = \frac{1}{B}\log_e\left[\frac{rI_i}{A\,(e^{B-r}\text{-}e^{(B-r)L})}\right] \tag{4}$$

This analysis obtains constants A and B by fitting the exponential function (Eq. (1)) to each EAB projection based on the corresponding MSLR scenario as shown in Figure N. 1. Among the MSLR scenarios, this analysis adopts the High MSLR scenario for demonstration.

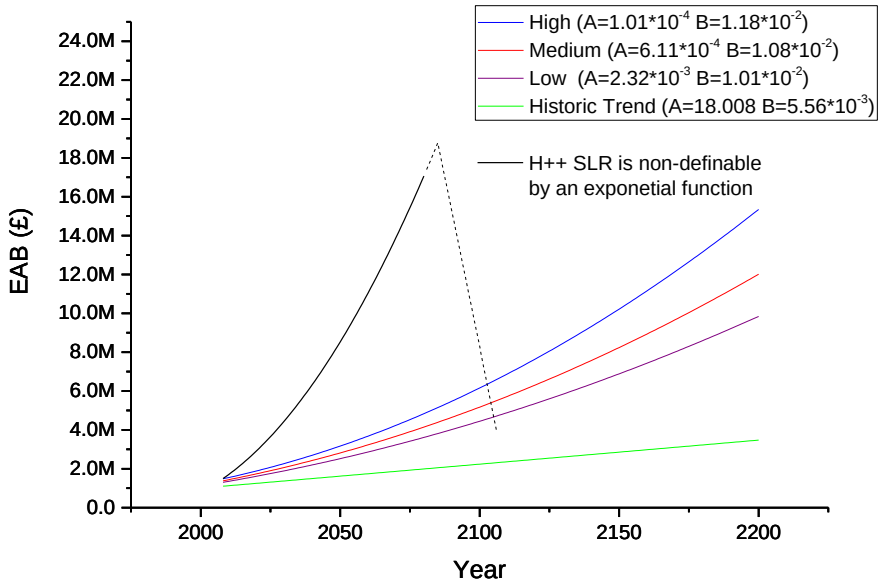

Figure N. 1 Fitted exponential curves of EAB for each MSLR scenario from 2008 to 2200 ($EAB = A \times e^{Bt}$, t in year)

As in the case of Lymington, the investment cost (I) is set to be £ 64.2 million and the life of the project is 100 years. Thus, by subbing the investment cost and the constants A and B into the equation (4), we can have a relation between optimal investment time (i) and discount rate (r) for the High SLR scenario in equation (5).

$$i = \frac{1}{0.01178} \log_e \left[\frac{rI}{0.000101 \left(e^{0.01178 \cdot r} - e^{(0.01178 - r)100} \right)} \right] \qquad (5)$$

This analysis has derived a curve of optimal investment time across the range of discount rate by equation (5). The optimal investment times by different discount rates (i.e. 0.5%, 2.5%, 3%, 3.5% and 4.5%) are dotted along the concave curve, which have been obtained by dynamic programming approaches as shown in Figure N. 2. A set of images in Figure N. 3 show change in optimal investment times by different discount rates.

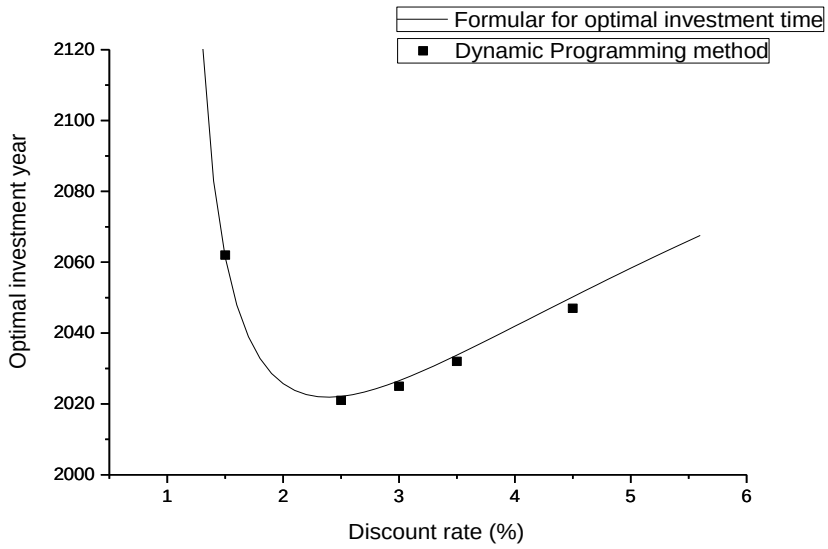

Figure N. 2 Change in optimal investment time according to discount rates for the High SLR scenario by the formulation method (line) and the dynamic programming (square points)

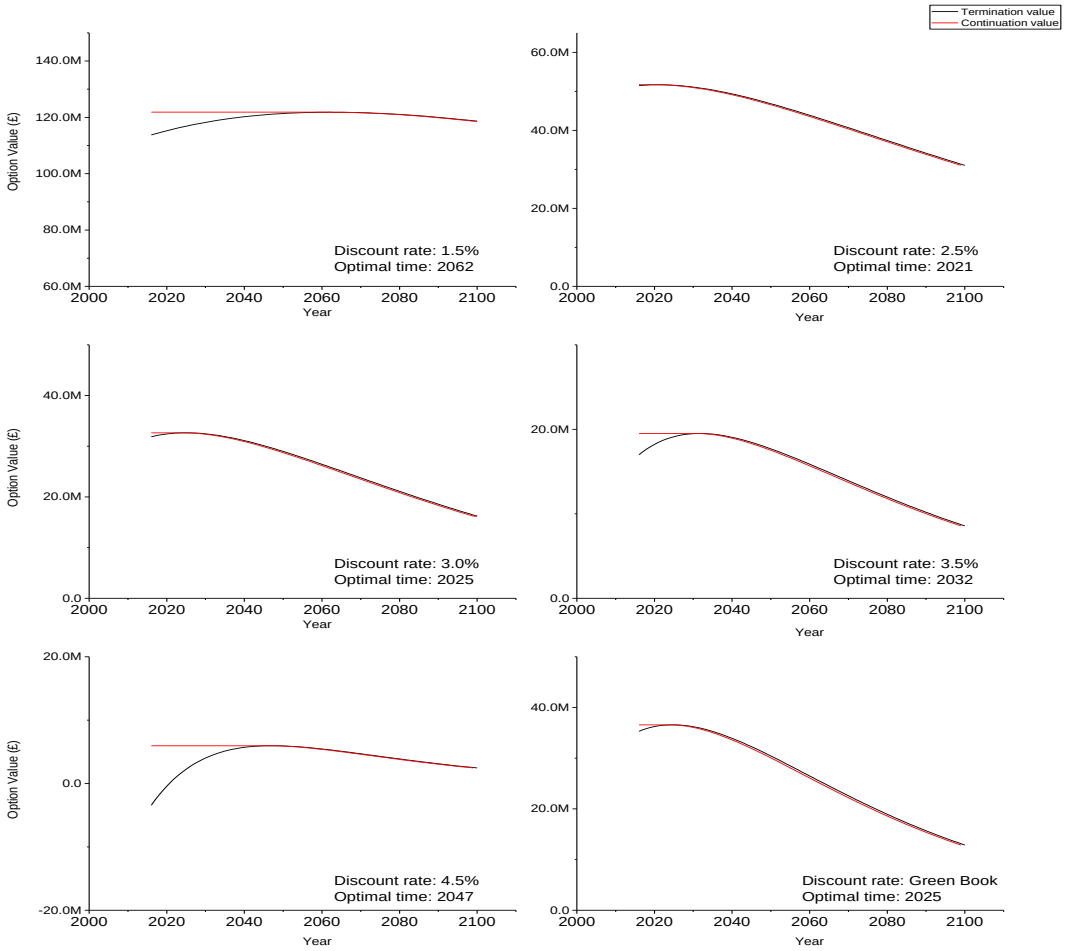

Figure N. 3 Option values and optimal investment times according to different discount rates by a backward induction method for the High SLR scenario – Note different y-scales.

As seen in Figures N. 2 and N. 3, in terms of the optimal investment time, the low discount rates do not lead to the investment being made immediately. If the discount rate is too low below a certain level (i.e. 2.25%), the optimal investment time occurs in the far distant future. As the discount rate is a factor that weighs the present value versus the future value over time (Mandelson, 2012), such an extremely low discount rate, which means the preference of the future value over the present value, leads to the optimal investment time occurring in the far-distant future. For the High SLR scenario, the optimal investment time at a 2.5% discount rate occurs in the earliest time (i.e. 2021) as shown in Figures N. 2 and N. 3.

Green Book discount rate leads to an early optimal investment time (i.e. 2025) in comparison to constant discount rates (e.g. 3.5% or 3.0%). The effects of discount rates on the optimal investment time are shown for other SLR scenarios (Figure N. 4).

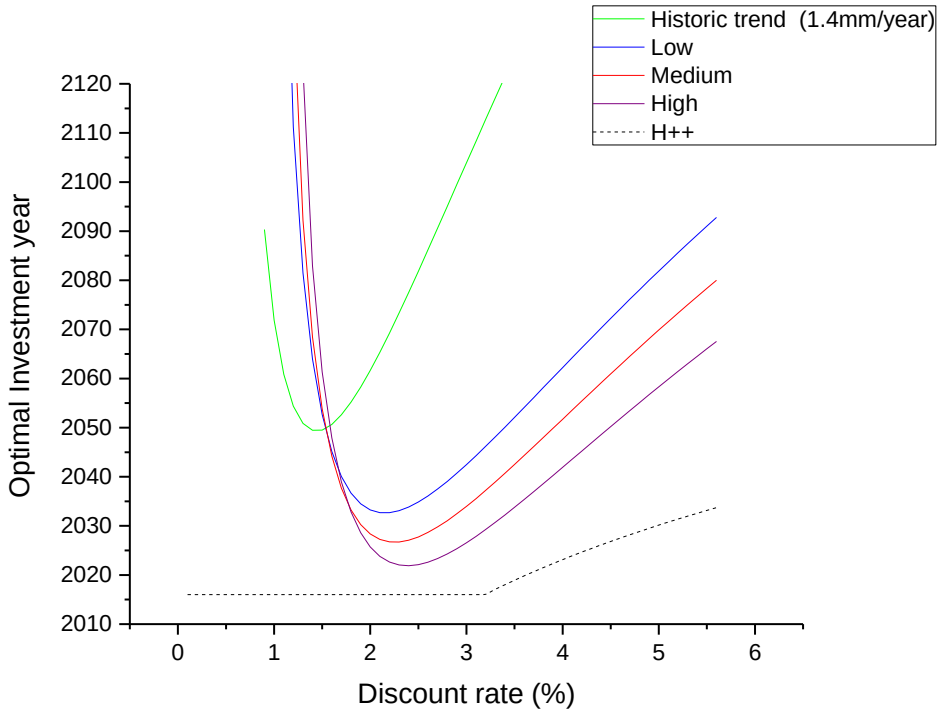

Figure N. 4 Optimal investment times according to different discount rates by the formulation method for each SLR scenario

The curves in Figure N. 4 show relations between the discount rates and the optimal investment times for all the SLR scenarios. These curves except the H++ SLR scenario have concave shapes each of which has the lowest point of optimal investment time at a certain discount rate. As investigated in Section 5.4, it differs depending on SLR scenarios. As the discount rate increases beyond a certain value, the optimal investment time becomes far

distant from the present for all the SLR scenario (except the H++ SLR scenario). This pattern is expectable as the high discount rate implies that the future value is less important than the present value in option evaluation. Thus, the investment is deferred to the far distant future in such a high discount rate.

On the contrary, if the discount rate is too low, the optimal investment time becomes later as the discount rate lowers. In an extremely low discount rate (e.g. 1.5% or 1%), the optimal investment time occurs in the far distant future as shown in Figure N. 4. This is counterintuitive to the perspective of a standard cost-benefit analysis. In general, option evaluations with a low discount rate consider the future value to be more important than the present value. Thus, the choice of a low discount rate generally triggers an investment option immediately. However, real option analysis gives different results contrary to a standard cost-benefit analysis. It is because the investment in the far distant future gives much higher investment opportunity than in the near future in an extremely low discount rate. Despite that, it should be noted that the low discount rate exponentially increases the option values of NPV_{now} and NPV_{opt} simultaneously as shown in Figure N. 3. Thus, the optimal investment timing can be considered as less prior to the option value in such a low discount rate. That is, in a such low discount rate, the investment decision should be made whether or not NPV_{now} is higher than NPV_{opt}.

The optimal investment time in the H ++ SLR scenario shows a different pattern with other SLR scenarios. In the H++ SLR scenario, the current risk of coastal flooding is very high and the performance of the upgraded coastal defence may be lower in the long-distant future (i.e. around 2080) due to the limitations on its capacity under extreme sea-level rise. Thus, most optimal investment time appears earlier than now (i.e. 2016) even at low discount rates. For a simple expression, we set the optimal investment times before 2016 to be 2016. This is shown by dashed line in Figure N. 4.

These curves from the formulation approach provide complementary information that enables decision-makers to see the effects of discount rates on optimal investment times. However, this formulation is only applicable to a constant discount rate over time. For time-varying discount rates such as Green Book discount rates, dynamic programming method or backward induction method is useful in finding optimal investment time for a deferrable option. Nevertheless, the formulation approach is useful as it allows us to find optimal investment time regardless of the uncertainty of SLR scenarios.

Appendix O. Effects of future growth rates on optimal investment time

The formulation approach can also assess optimal investment times in cases where the socio-economic status of floodplains change over time. Climate change adaptation that occurs in a long-term timescale needs to consider socio-economic development scenarios (Stern, 2007; IPCC, 2014; King et al., 2015). This appendix investigates the effects of socio-economic changes on optimal investment time by the formulation approach.

Let ρ denote annual future growth rate. The expected annual benefit (EAB_t) in any year t will increase in proportion to an annual growth factor of $(1 + \rho)^{t-t_0}$ (Here, t_0 is a base year). EAB under a future growth rate scenario (ρ) can be rewritten by multiplying annual growth factor $(1 + \rho)^{t-t_0}$ with EAB in equation (1). For the convenience of derivation, we use an exponential function ($e^{\rho(t-t_0)}$) for the annual growth factor instead of $(1 + \rho)^{t-t_0}$.

$$EAB_t = Ae^{Bt}e^{\rho(t-t_0)} \quad (1)$$

Here, A and B are constants, t is time in year, t_0 is a base year (=2016) and ρ is constant annual future growth rate. By substituting equation (1) for equation (2) in Appendix N, this derivation can have an equation for optimal investment time under future growth rate (ρ) in equation (3).

$$\therefore\ i = \frac{1}{B+\rho}\log_e\left(\frac{rI}{A(e^{(B+\rho-r)-\rho t_0}-e^{(B+\rho-r)L-\rho t_0}}\right) \quad (2)$$

The equation (3) shows a relation between the optimal investment time *(i)* and the growth rate of future development (ρ), or discount rates (r). In the case of the non-growth rate (ρ =0), the equation (3) is equal to the equation (3) in Appendix N. To understand the effects of future growth rates on optimal investment times, we have drawn the curve of optimal investment time across a range of future growth rate with the discount rate fixed at 3% for the High SLR scenario (Figure O. 1). The optimal investment time plotted by the formulation approach is fairly well matched with the results from the dynamic programming of which the results are drawn from Figure O. 2.

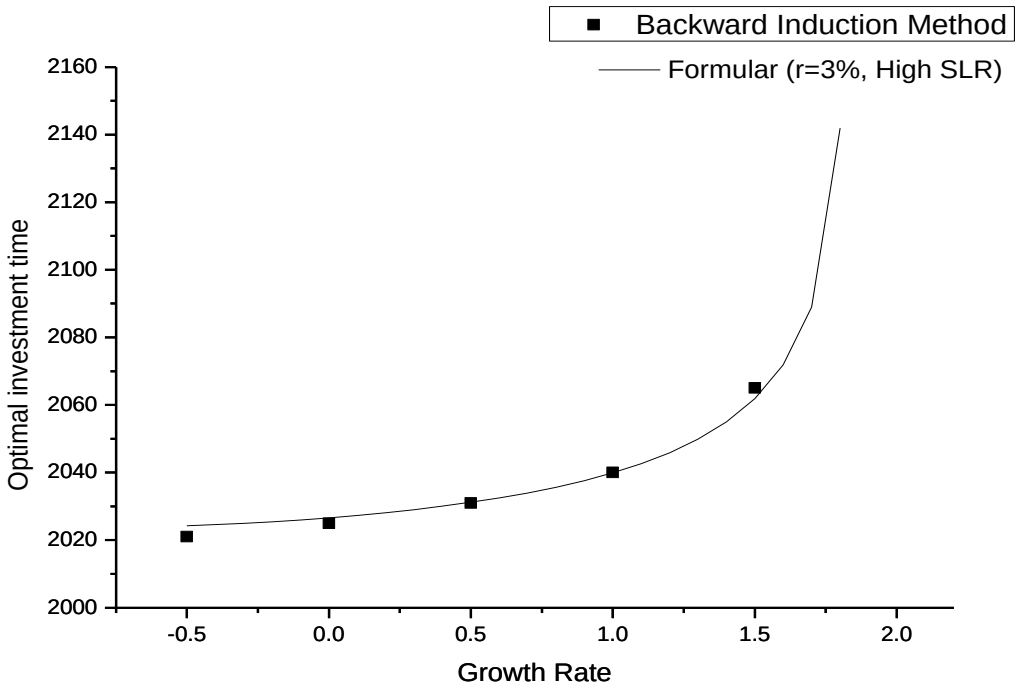

Figure O. 1 Optimal investment times by different future growth rates for a 3% discount rate in the High SLR scenario by formulation approach (solid line) and backward induction method (dots), respectively.

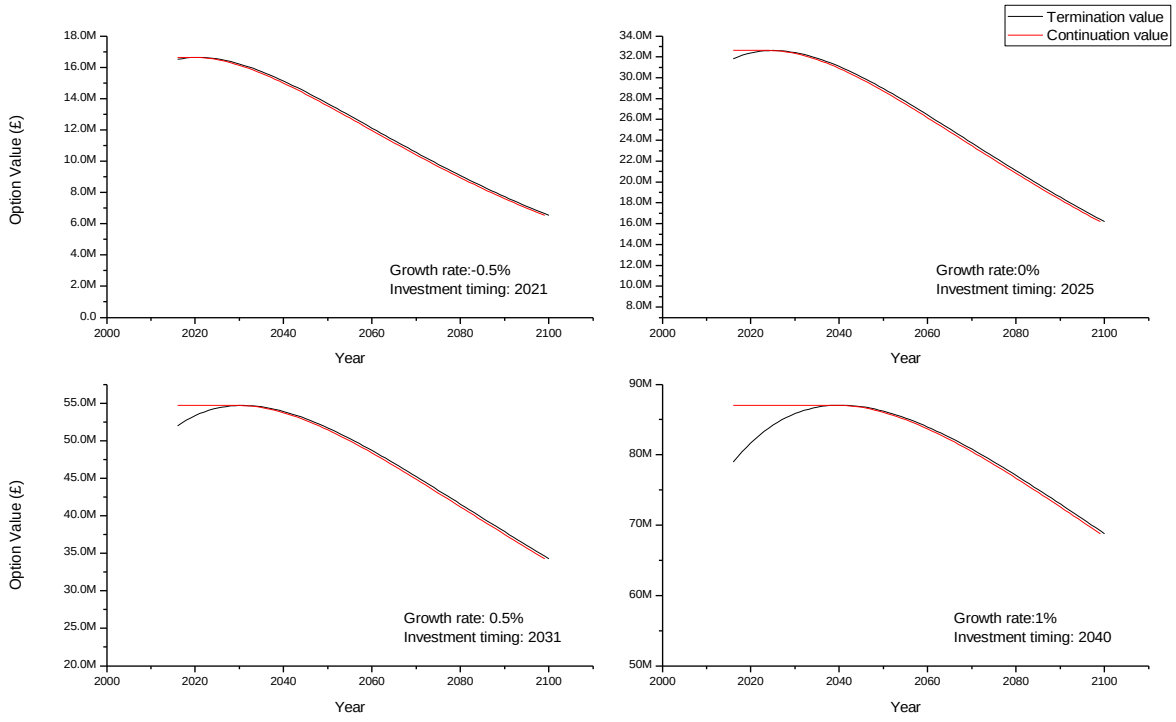

(continue)

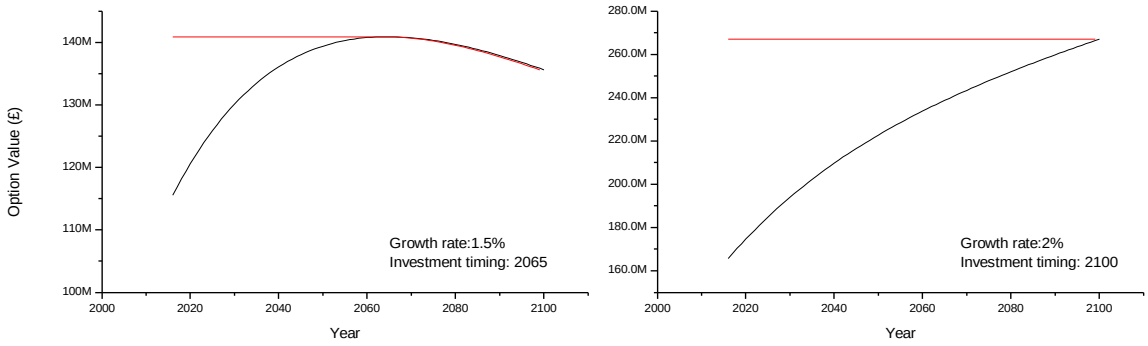

Figure O. 2 Option values and optimal investment times by different growth rates for the High SLR scenario with the discount rate of 3% by the backward induction. Note different y-axis scales.

As seen in Figures O. 1 and O. 2, the high future growth rate makes the optimal investment time occur later than the low growth rate. This case has also been observed in the calculation of real option values by the dynamic programming. Note that the increase in future growth rate leads to significant increases in termination and continuation values simultaneously. However, it leads to the delay of the optimal investment time due to the expectation of highly increasing future values. It is because real options analysis is an approach to evaluate the investment opportunity of flexible options under uncertainty. Thus, this result implies that, the higher the future growth rate is, the higher the investment opportunity in the future will be. Note that, at high growth rates, the investment timing is considered to be a less important aspect than the investment decision of go or not. This is because the future growth rates increase the overall option values exponentially.

In the same way as done with the 3% discount rate, the relationships between the optimal investment times and the future growth rates have been drawn for different discount rates (e.g. 2.5%, 3%, 3.5% and 4.5%) for each SLR scenario in Figure O. 3.

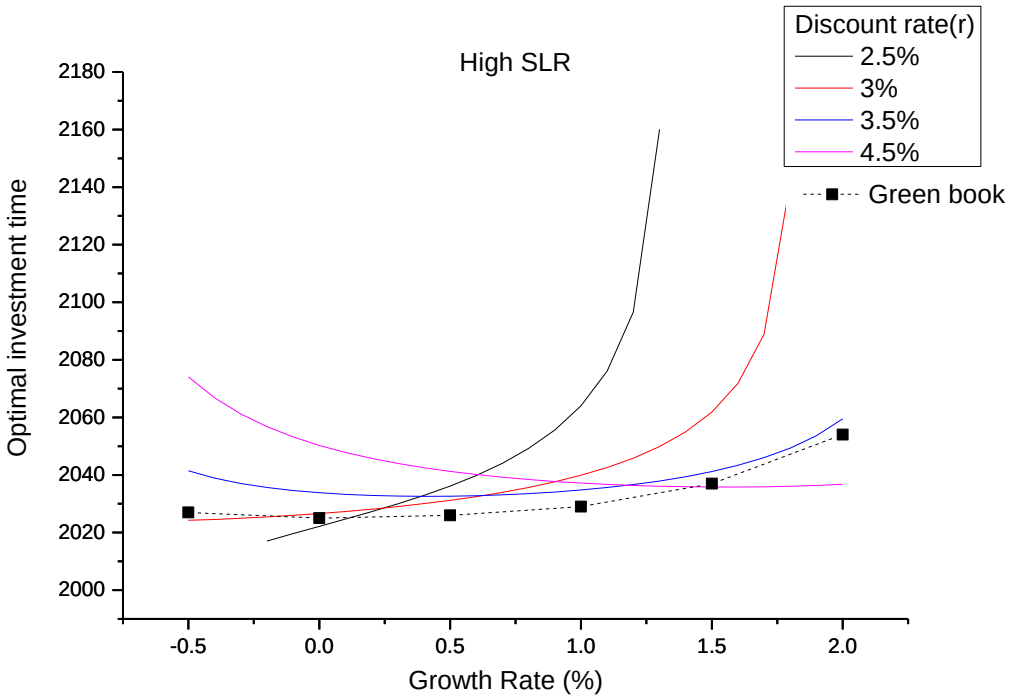

(a) High SLR scenario

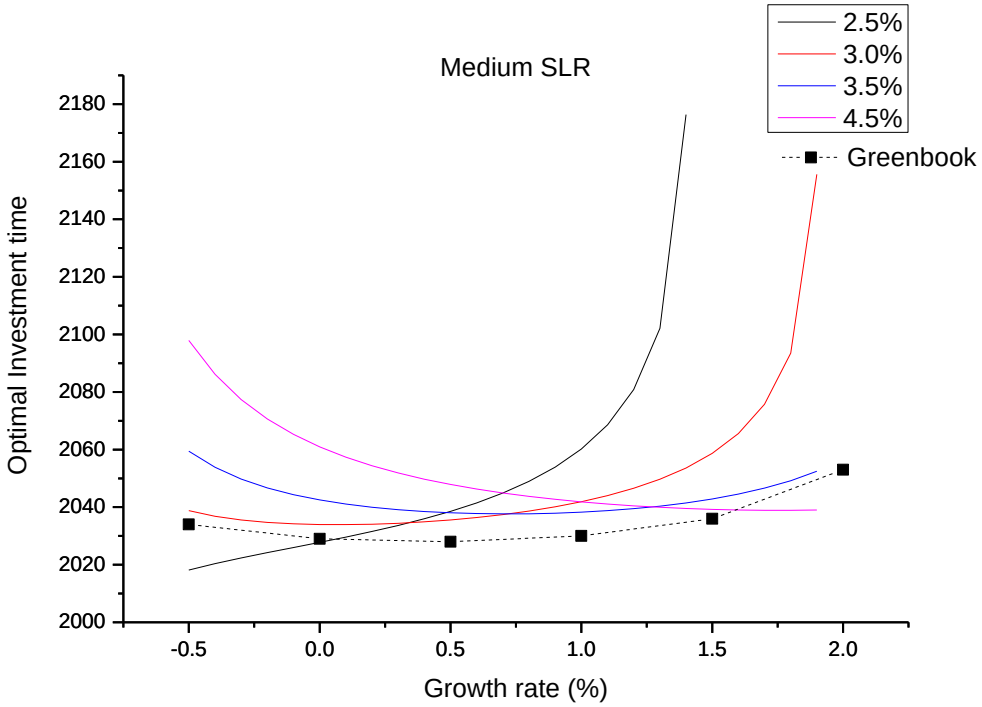

(b) Medium SLR scenario

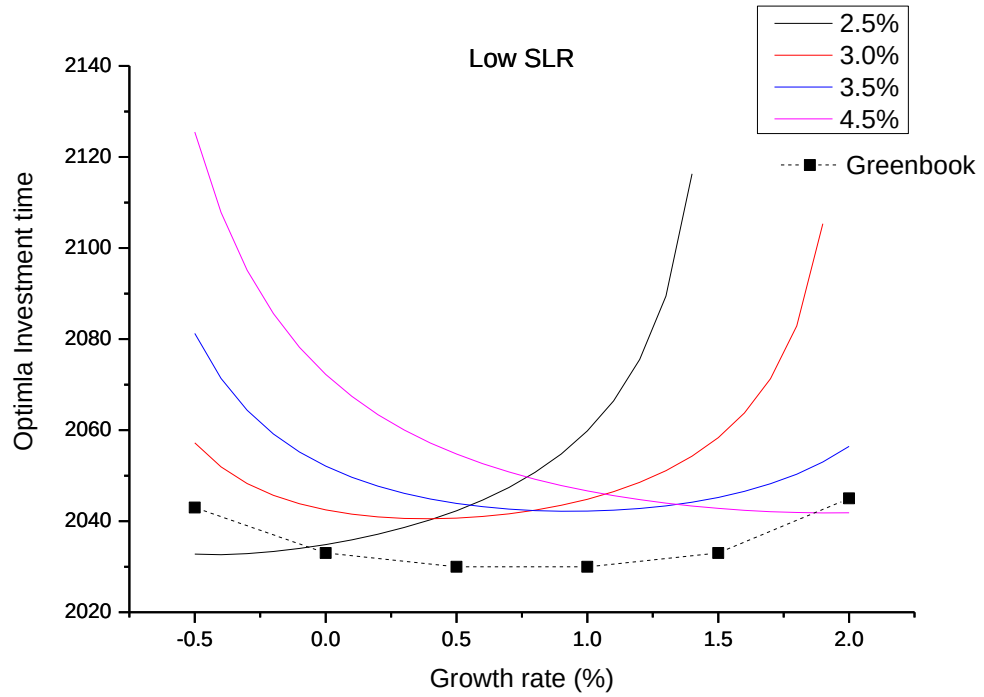

(c) Low SLR scenario

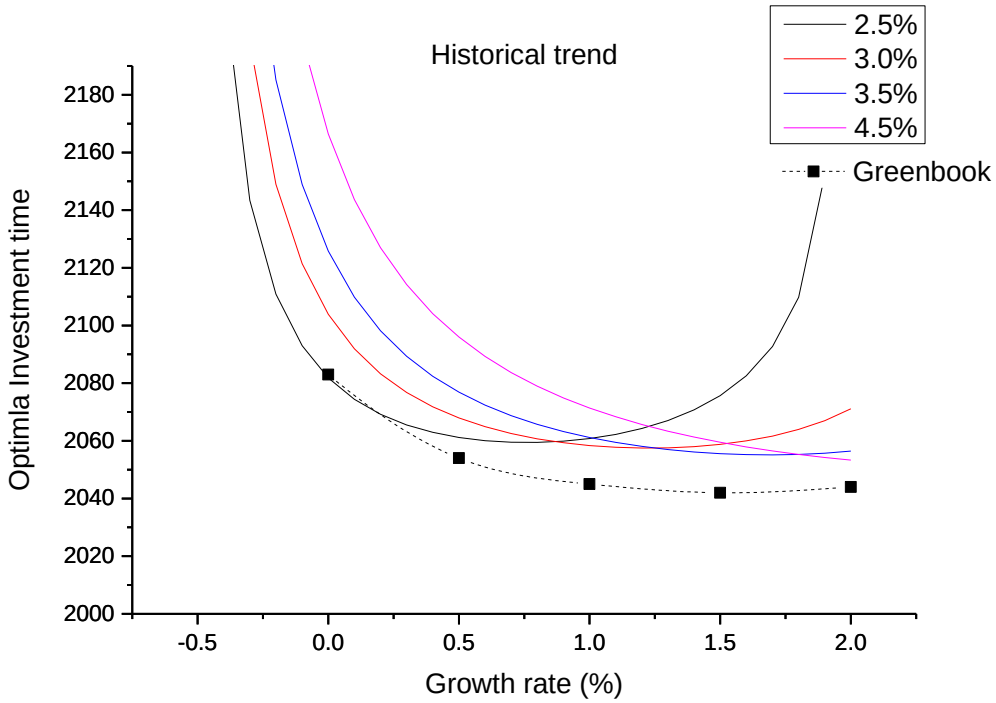

(d) Historical trend SLR scenario

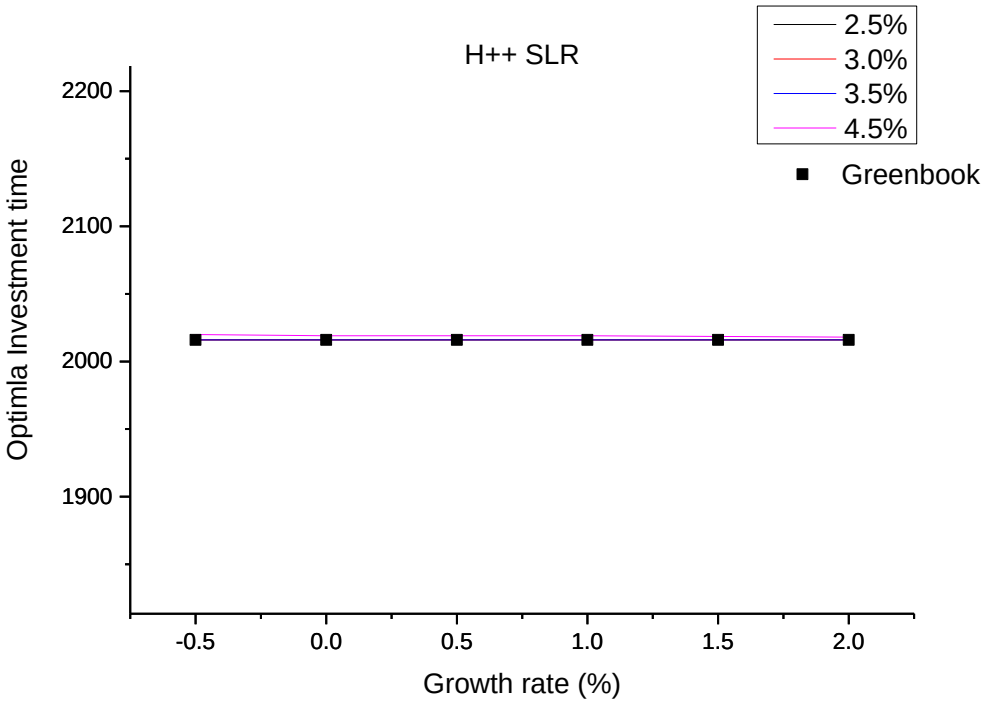

(e) H++ SLR scenario

Figure O. 3 Optimal investment times according to the different growth rates by different discount rates in each SLR scenario – Note the different y-axis scales

(1) High to Low SLR scenarios

As seen in Figure O. 3 (a), (b) and (c), when the discount rate is 2.5%, the optimal investment times for most MSLR scenarios except the H++ SLR scenario show rapidly increasing trends with future growth rates. If the discount rate is higher than 2.5%, the increasing trend of optimal investment times with future growth rates diminishes. If the discount rate is higher than 3.0%, the curve becomes, to some extent, flat over future growth rates. At 3.5% discount rate, the optimal investment time, thus, becomes less sensitive to future growth rates for High, Medium and Low MSLR scenarios. If the discount rate becomes higher than 3.5%, the optimal investment time shows declining trends as future growth rates increase. Thus, the curves at the high discount rate (4.5%) show different trends from those at the low discount rate (2.5%). This is because, the effects of future growth rates on optimal investment time are offset by the effects of discount rates. Therefore, the optimal investment times of adaptation options are subject to both future growth rates and discount rates.

(2) Historic Trend SLR scenario

As shown in the Historic Trend SLR scenario (Figure O. 3 (d)) – 1.4 mm/yr, the relation between the optimal investment times and the future growth rates shows a different pattern from those observed in the previous MSLR scenarios. Note that this is the mildest scenario so that the optimal investment time occurs the latest among all the MSLR scenarios. In this scenario, the optimal investment time occurs in 2083 by 0% future growth rate and Green Book discount rate. Contrary to the High to Low SLR scenarios, the high future growth rates make the optimal investment time come early in the Historic Trend SLR scenario for most discount rates except 2.5% as shown in Figure O. 3 (d). As the high future growth rates increase EAB in the Historic Trend SLR scenario, the increase in future growth rate brings forwards the optimal investment time from 2083. However, in the 2.5% discount rate, the optimal investment time tends to become distant from the present as the future growth rate increases. This is because, while such a low discount rate decreases all the streams of EAB, the high future growth rate increases all the streams of EAB over the period of a project life.

(3) H++ SLR scenario

The H++ MSLR scenario shows a completely different trajectory of optimal investment time from the previous MSLR scenarios as shown in Figure O. 3 (e). This is the most severe and fastest-growing sea-level rise scenario for Lymington. Thus, as the expected annual benefit (EAB) has already increased beyond the critical value of EAB_c, the investment now gives the larger option value than any other types of investments made later. In addition, in the most extreme SLR scenario, the optimal investment time occurs before 2016 across all the discount rates and the future growth rates. However, since the change in EAB cannot be defined by a continuous function due to the capacity limit of coastal defence against sea-level rise under the H++ SLR scenario, we had to estimate the optimal investment times by dynamic programming in this scenario.

(4) Green Book discount rate

Interestingly, most optimal investment times from the Green Book discount rate occur at the earliest stage for most of the future growth rates. The trajectories of the optimal investment times from the Green Book discount rate are flat over or less sensitive to future growth rates than those from other discount rates. Thus, this characteristics of time-varying discount rates (i.e. Green Book discount rate) in regard to investment timing need to be noted for real options analysis.

Appendix P. Sensitivity test of the optimal investment time on different factors

This appendix shows the result of sensitivity tests on optimal investment times and option values by different factors

(1) Rates of sea-level rise

Factors	Percentage (%)	Rates of SLR	Optimal investment time	ROV	SLR at OIT	Remark
Rate of SLR	-25%	2.5	2042	8.16	12.9	
	-20%	2.6	2039	9.79	12.9	
	-10%	3.0	2033	13.40	12.8	
	-5%	3.1	2031	15.40	12.9	
	0%	3.3	2029	17.40	12.9	Ref
	5%	3.5	2027	19.67	12.8	
	10%	3.6	2025	21.93	12.7	
	20%	4.0	2022	26.69	12.6	
	25%	4.1	2021	29.19	12.8	

(2) Investment costs

	Percentage (%)	Investment Costs	Optimal investment time	ROV	SLR at OIT	Remark
Investment cost	-25%	48.2	2010	31.41	6.6	
	-20%	51.4	2014	28.13	7.9	
	-10%	57.8	2021	22.20	10.2	
	-5%	61.0	2025	19.70	11.6	
	0%	64.2	2029	17.40	12.9	Ref
	5%	67.4	2032	15.54	13.9	
	10%	70.6	2036	13.82	15.2	
	20%	77.0	2043	10.94	17.5	
	25%	80.3	2046	9.75	18.5	

(3) Future growth rates

	Percentage (%)	Growth Factor(1+ρ)	Optimal investment time	ROV	SLR at OIT	Remark
Future growth rates	-25%	0.9975	2032	10.65	13.86	
	-20%	0.998	2031	11.92	13.53	
	-10%	0.999	2030	14.61	13.2	
	-5%	0.9995	2029	16.03	12.87	
	0%	1	2029	17.49	12.87	Ref
	5%	1.0005	2028	19.02	12.54	
	10%	1.001	2028	20.59	12.54	
	20%	1.002	2027	23.91	12.21	
	25%	1.0025	2027	25.66	12.21	

(4) Discount rates

	Percentage (%)	Discount rates (%)	Optimal investment time	ROV	SLR at OIT	Remark
Discount rates	-25%	2.63%	2035	23.80	14.9	
	-20%	2.80%	2033	22.31	14.2	
	-10%	3.15%	2030	19.71	13.2	
	-5%	3.33%	2030	18.56	13.2	
	0%	3.50%	2029	17.49	12.9	Ref
	5%	3.68%	2028	16.50	12.5	
	10%	3.85%	2027	15.56	12.2	
	20%	4.20%	2027	13.84	12.2	
	25%	4.38%	2026	13.06	11.9	

(5) Residual life

	Percentage (%)	Residual life	Optimal investment time	ROV	SLR at OIT	Remark
Residual life	-25%	75	2042	10.22	17.2	
	-20%	80	2039	11.71	16.2	
	-10%	90	2033	14.67	14.2	
	-5%	95	2031	16.10	13.5	
	0%	100	2029	17.40	12.9	Ref
	5%	105	2027	18.84	12.2	
	10%	110	2025	20.12	11.6	
	20%	120	2022	22.50	10.6	
	25%	125	2021	23.59	10.2	

(6) Period of SLR projection

	Percentage (%)	Projected Periods	Optimal investment time	ROV	SLR at OIT	Remark
Period of SLR projection	-25%	2075	2029	17.49	12.9	
	-20%	2080	2029	17.49	12.9	
	-10%	2090	2029	17.49	12.9	
	-5%	2095	2029	17.49	12.9	
	0%	2100	2029	17.49	12.9	Ref
	5%	2105	2029	17.49	12.9	
	10%	2110	2029	17.49	12.9	
	20%	2120	2029	17.49	12.9	
	25%	2125	2029	17.49	12.9	

Appendix Q. Optimal investment time in the stochastic case of sea-level rise by dynamic programming

This appendix provides an illustration of optimal investment time and option value for the stochastic case of sea-level rise. As done in the case of the deterministic sea-level rise, the dynamic programming approach has been applied for examples of randomly evolving sea-level rise. As the evolving patterns of sea-level rise are random, the optimal investment times and option values (i.e. NPV_{now} and NPV_{opt}) are also random values. Figure Q. 1. shows the evolving patterns of sea-level rise and the subsequent changes in option values (i.e. termination and continuation values) as exemplary cases.

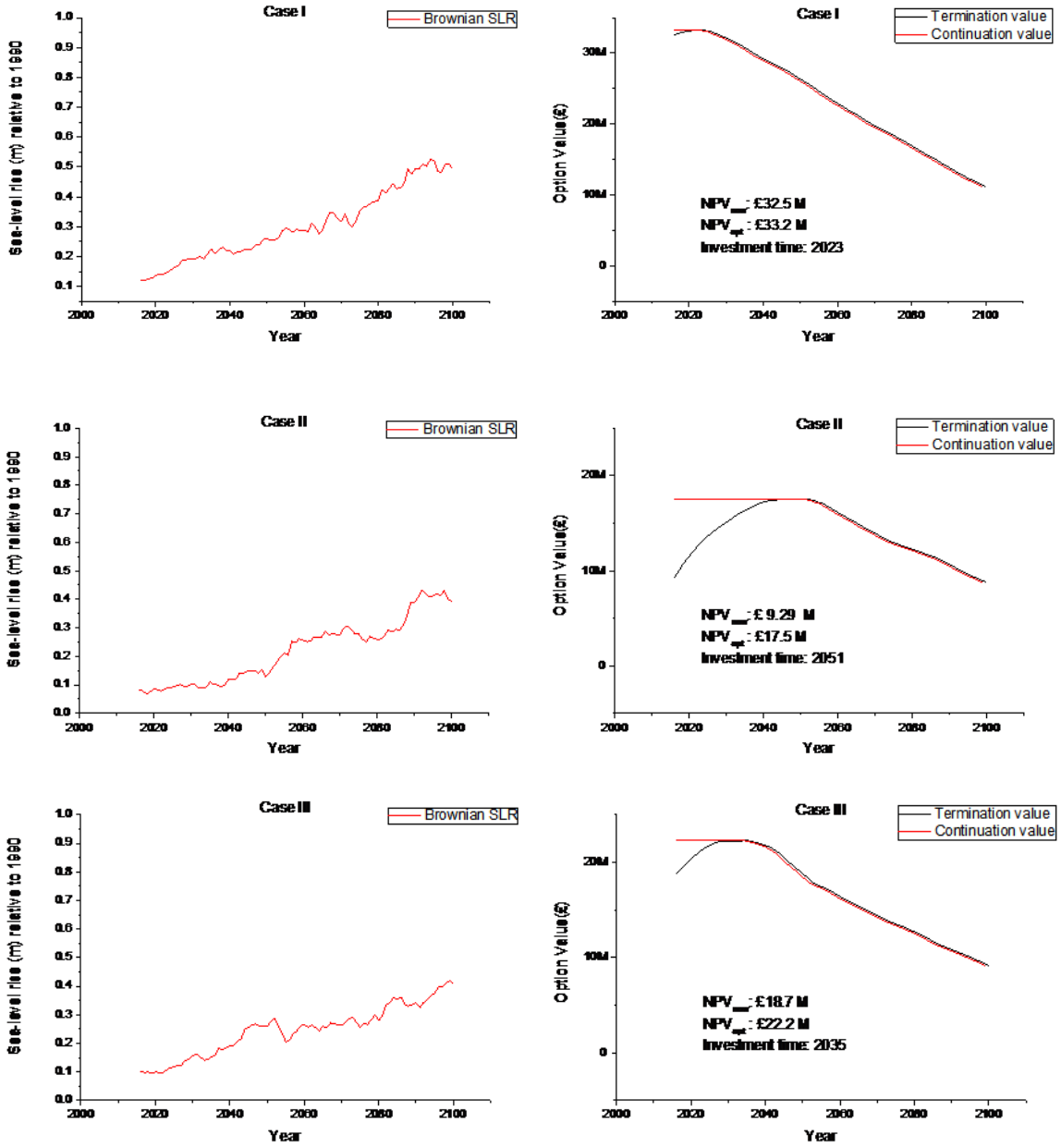

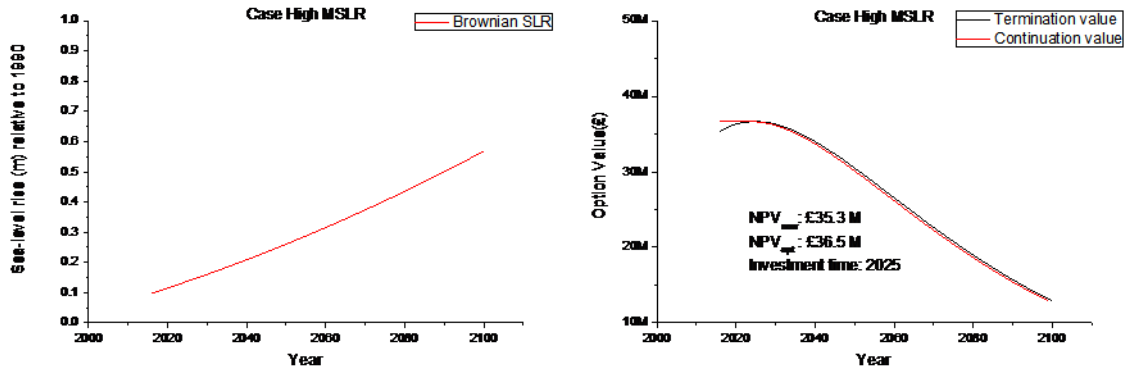

Figure Q. 1 Examples of (a) the Brownian motion (or mean) of the High SLR scenarios (left) and (b) option value indicated by continuation and termination values (top right) – Note that all the Brownian motions of sea-level rise are made from the High SLR scenario.

As seen in Figure Q. 1, the option values and optimal investment times considerably vary depending on the patterns of sea-level rise over the 21st century. For the case I, sea-level rise starts from 12 (cm) at 2016 and keep increasing to 50 cm until 2100. In this pattern of sea-level rise, the optimal investment time occurs around 2023, which is earlier than the optimal investment time (i.e. 2025) for the High MSLR. However, the values of NPV_{now} and NPV_{opt} are smaller than those of the High MSLR scenario. This implies that the higher option value does not lead to the earlier investment time in the stochastic case of sea-level rise.

For the case II, sea level slowly increases until 2040 but it starts to increase rapidly after that. In this pattern of sea-level rise, the termination value (black line in the right image in the case II) increases rapidly and it exceeds the continuation value around 2051, which is the optimal investment time in the case II. In this pattern of sea-level rise, NPV_{now} and NPV_{opt} are much lower with their values being £ 9.29 M and £ 17.5 M, respectively, than the values in the High MSRL. Thus, the investment time occurs at the latest year among the example cases.

In the case III, sea level increases continuously, however, at lower rate than the rate of the High MSLR over the whole period of sea-level rise projection. The optimal investment time occurs in 2035. This pattern of sea-level rise is similar to the Low MSLR scenario rather than the High MSLR scenario.

These examples show real and practical issues regarding the uncertainty of sea-level rise that decision-makers may face in adaptation decisions. This uncertainty issue is substantial in investment decisions because the optimal investment time and option value vary in random ways as they depend on the pattern of sea-level rise. However, a meaningful finding is that the optimal investment time has occurred when sea-level rise reaches a critical threshold

value in most sea-level rise patterns shown in the case I, II and III. In cases of MSLR, this thesis has already found that the optimal investment time is when sea-level rise reaches approximately 13 cm.

When we read the values of sea-level rise at each of the optimal investment times under all the example cases, most values are found around this critical threshold value (= 13cm) as shown in Figure Q. 2. This implies that, even though sea-level rise in the future randomly evolves over time, an investment decision based on the observation of the critical threshold value is likely to provide a maximum option value under given environmental conditions (i.e. sea-level rise).

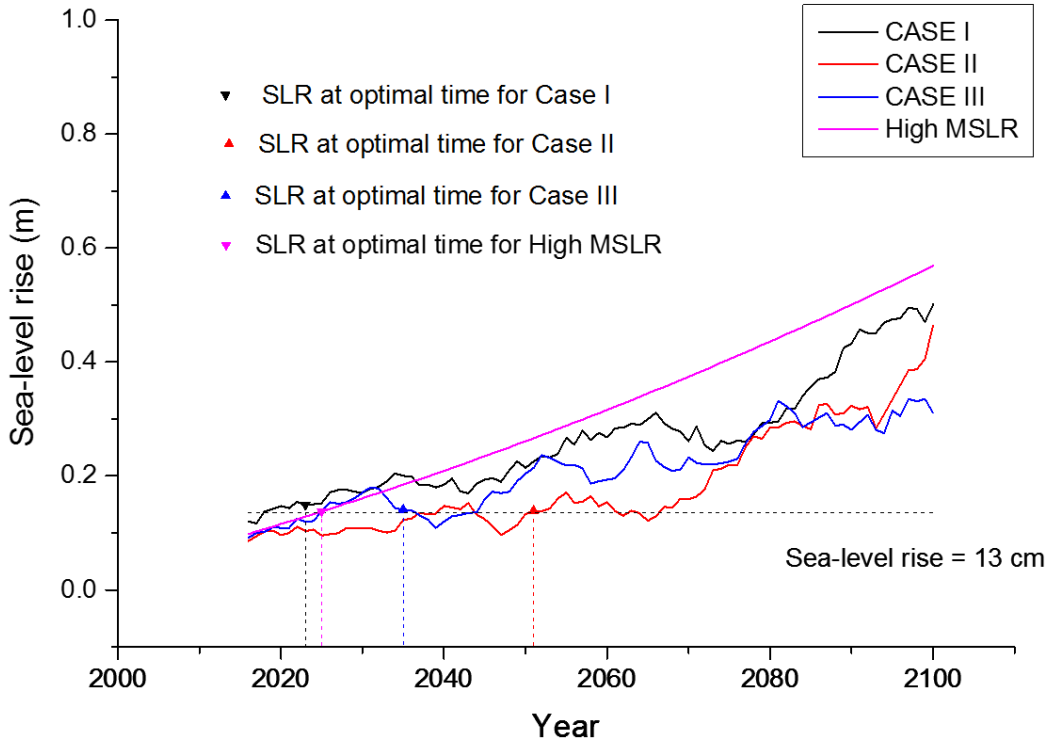

Figure Q. 2 Sea-level rise at optimal investment time (indicated by triangles) for each of the cases – the year at which each of the vertical lines intersects x-axis indicates the optimal investment year for the corresponding sea-level rise patterns. Most values of sea-level rise at the optimal investment times are found near the critical threshold value (13cm).

As seen in Figure Q. 2, the values of sea-level rise in case II and case III (indicated by red and blue lines) exceed the critical threshold value (i.e. 13cm) before the optimal investment times, drop below it and exceed again. When we observe termination and continuation values at the corresponding times in the cases II and III in Figure Q. 2, the termination value almost reaches the continuation value after sea-level rise exceeds the critical threshold value. This

implies that the investment at the critical threshold value is likely to provide a maximum option value under the given sea-level rise.

Appendix R. Derivation of formula for optimal investment time in the stochastic cases of climatic variable(s)

This appendix derives the formulation of the optimal investment time for the stochastic case of sea-level rise. The derivation of a formula for the optimal investment time is conducted by dynamic programming approach introduced by Bellman (1953). This section considers one case where sea-level rise follows General Brownian motion as reviewed in Chapter 5.4. As the rate and magnitude of sea-level rise in the future is uncertain, our decision will be based on whether sea-level rise (SLR) exceeds a certain critical threshold value (that is, $SLR > SLR_c$). That is, this derivation assumes that investment to go, or not, at any year *t* depends on whether sea-level rise (*SLR*) exceeds this critical value (SLR_c) or not. The option value of the investment option (i.e. termination or continuation value) at any given year t is random variable as sea-level rise is stochastic variable(s). To find a maximum option value of a deferrable option in the stochastic case of sea-level rise, the option evaluation process (or dynamic approach) compares a continuation and a termination value for each year from the end year of the SLR projection in a backward way as in equations (1) and (2).

$$F_{ex,t} = PV_t\text{-}I \qquad (SLR_t > SLR_c) \tag{1}$$

$$F_{con,t} = \frac{1}{(1+r)} \times \max\{F_{ex,t+1}, F_{con,t+1}\} \qquad (SLR_t < SLR_c) \tag{2}$$

Here, $F_{ex,t}$ and $F_{con,t}$ are a termination and a continuation value at year t, respectively. PV_t is a project value which is the sum of the overall benefits after the investment at year *t*, I is investment cost, r is discount rate, SLR_t is the stochastic variable of sea-level rise at year t, SLR_c is a critical threshold value at which to trigger the option.

As shown in equations (1) and (2), if the option is deferred at year *t*, we can expect to have one of the option values (i.e. a termination or a continuation value) from the next year (= *t*+1). Thus, the equation (2) discounts the expected option value at year *t*+1 by discount factor 1/(1+*r*). Let us assume that we can estimate the probability of sea-level rise exceeding the critical threshold value at any given year *t* in an analytical or numerical way. Let us denote p_t or q_t to the probability of SLR exceeding the critical threshold value (SLR_c) or not at year t, respectively. Therefore, the expected option value (F_t) at any given year *t* is as follow.

$$F_t = p_t{*}F_{ex,t} + q_t{*}F_{con,t}$$

$$= p_t{*}F_{ex,t} + q_t{*}\frac{1}{(1+r)} \times \max\{F_{ex,t+1}, F_{con,t+1}\} \quad (3)$$

To obtain the option value F_t at year *t*, equation (3) requires a termination value ($F_{ex,t}$) and a continuation value ($F_{con,t}$) with the corresponding probabilities of p_t and q_t, respectively. As real options analysis starts calculation from the end year of the time horizon (denoted by year T), it should determine an option value (F_T) at year *T* as a boundary value. This derivation assumes that sea-level rise (SLR_T) at year T is higher than the critical threshold value (SLR_C) and sea level keeps increasing after year *T*. This assumption also leads to the investment being implemented at the year *T*. Otherwise, there will be no need for the investment in year *T*. This derivation also assumes that expected annual benefit (EAB) is dependent on sea-level rise. Thus, the expected annual benefit is a function of sea-level rise ($EAB = f(SLR)$) in the same as in the deterministic case. As we assume that SLR is random variable following General Brownian motion, EAB is also random variable. The boundary condition of the option value (F_T) at year T can be written as below.

$$F_T = \sum_{i=T+1}^{L+T} \frac{EAB_i}{(1+r)^{i-T}} - I \qquad (SLR_T > SLR_c) \quad (4)$$

Here, F_T is the boundary option value at year T, L is the life of the project, EAB_i is an expected annual benefit at year i (subject to sea-level rise at year *i*) after the investment, r is discount rate and I is investment cost. As we define the boundary value of F_T at year T, we can also calculate the option value at year T-1 by substituting the boundary value (F_T) for the continuation value at year T-1 as shown in equation (5).

$$F_{T-1} = p_{T-1}{*}F_{ex,T-1} + q_{T-1}{*}F_{con,T-1} \quad (5)$$

Here, F_{T-1} is an option value at year T-1, p_{T-1} and q_{T-1} are the probabilities of SLR_{T-1} being greater and SLR_{T-1} being less than SLR_c, respectively, $F_{ex,T-1}$ is a termination value at year T-1, and $F_{con,T-1}$ is a continuation value at year T-1. The termination value ($F_{ex,T-1}$) and continuation value ($F_{con,T-1}$) in equation (5) represent option values when the investment is made and when the investment is deferred at year T-1, respectively. Thus, the termination and continuation value can be written as below, respectively.

$$F_{ex,T-1} = \sum_{i=T}^{T+L-1} \frac{EAB_i}{(1+r)^{i-T+1}} - I \qquad (SLR > SLR_c) \qquad (6)$$

$$F_{con,T-1} = \frac{1}{(1+r)} \times F_T \qquad (SLR < SLR_c) \qquad (7)$$

As aforementioned, EAB_i is a random variable dependent on sea-level rise (*SLR*). Thus, $F_{ex,T-1}$ and $F_{con,T-1}$ are all random variables. By substituting equations (6), (7) and (4) for equation (5), we can have the option value (F_{T-1}) at the year T-1 as shown in equation (8).

$$\begin{aligned} F_{T-1} &= p_{T-1} * F_{ex,T-1} + q_{T-1} * F_{con,T-1} \\ &= p_{T-1} * \left(\sum_{i=T}^{T+L-1} \frac{EAB_i}{(1+r)^{i-T+1}} - I \right) + q_{T-1} * \frac{1}{(1+r)} \times \left(\sum_{i=T+1}^{L+T} \frac{EAB_i}{(1+r)^{i-T}} - I \right) \\ &= p_{T-1} * \left(\frac{EAB_T}{(1+r)} + \frac{EAB_{T+1}}{(1+r)^2} + \frac{EAB_{T+2}}{(1+r)^3} \ldots + \frac{EAB_{T+L-1}}{(1+r)^L} - I \right) \\ &\quad + q_{T-1} * \frac{1}{(1+r)} \times \left(\frac{EAB_{T+1}}{(1+r)} + \frac{EAB_{T+2}}{(1+r)^2} + \cdots \frac{EAB_{T+L-1}}{(1+r)^{L-1}} + \frac{EAB_{T+L}}{(1+r)^L} - I \right) \end{aligned}$$

Since $p_{t-1} + q_{t-1} = 1$, we can rearrange the above equation for the term of $p_{t-1} + q_{t-1}$.

$$\begin{aligned} F_{T-1} = {} & p_{T-1} * \frac{EAB_T}{(1+r)} + (p_{T-1} + q_{T-1}) \left[\frac{EAB_{T+1}}{(1+r)^2} + \frac{EAB_{T+2}}{(1+r)^3} \ldots + \frac{EAB_{T+L-1}}{(1+r)^L} + \frac{EAB_{T+L}}{(1+r)^{L+1}} \right] \\ & - p_{T-1} * \frac{EAB_{T+L}}{(1+r)^L} - p_{T-1} * I + p_{T-1} * \frac{I}{(1+r)} - (p_{T-1} + q_{T-1}) * \frac{I}{(1+r)} \\ & = p_{T-1} * \left[\frac{EAB_T}{(1+r)} - \frac{EAB_{T+L}}{(1+r)^L} - \frac{r}{(1+r)} * I \right] + \frac{1}{(1+r)} * F_T \end{aligned} \qquad (8)$$

The equation (8) represents the option value at year T-1, derived by Bellman's dynamic programming. This equation has important implications for option evaluations. Firstly, this equation has been rearranged in terms of p_{T-1} and F_T. Thus, the option value at year T-1 is affected by the probability (p_{T-1}) of sea-level rise (*SLR*) exceeding the critical threshold value (SLR_c) at year T-1 and the expectation of the option value in the next year T. Here, p_{T-1} can be estimated upon the statistical analysis of sea-level rise or experts' judgement about the future sea-level rise. In this regard, the probability (p_{T-1}) is also uncertain in the current perspectives. However, our knowledge to the probability (p_{T-1}) will become more certain in

year T-1 because we will know whether the sea-level rise (SLR) exceeds the critical threshold value (SLR_C) at the year T-1 by observation. Thus, this probability should be either 1 or 0 when option holders arrive at the year T-1.

Secondly, F_T is a boundary value estimated upon the assumption that sea-level rise (*SLR*) exceeds the critical threshold value of sea-level rise (SLR_c) at year T. This fact gives another implication for the real options evaluation. If the investment is not made at year T - SLR is less than SLR_c, this also means that the investment should not be made in the preceding year T-1. In a common sense, it is unrealistic that option holders invest in an option in any given year (T-1) and, then, they withdraw it in the next year (T). This case violates the irreversibility of the investment in the principle of real options. Therefore, the equation (8) is valid only when there is a belief or confidence that sea level rise (SLR) exceeds the critical threshold value (SLR_c) in the boundary year T. If not, the equation should set the probability of p_{T-1} to be zero, thus, leading to the option value at year T-1 becoming $1/((1+r)) \times F_T$. In the same way, we can have the option value at year T-2.

$$F_{T-2} = p_{T-2}{*}F_{ex,T-2} + q_{T-2}{*}F_{con,T-2}$$
$$= p_{T-2}{*}\left[\frac{EAB_{T-1}}{(1+r)} - \frac{EAB_{T+L-1}}{(1+r)^{L+1}} - \frac{r}{(1+r)}{*}I\right] + \frac{1}{(1+r)}{*}F_{T-1} \quad (9)$$

We can extend this equation to a more general case for evaluation of a deferrable option including two choices of implementation or deferral at any given year t. Thus, for any given year t, the option value F_t is

$$F_t = p_t{*}F_{ex,t} + q_t{*}F_{con,t}$$
$$= p_t{*}\left[\frac{EAB_{t+1}}{(1+r)} - \frac{EAB_{t+L}}{(1+r)^{L+1}} - \frac{r}{(1+r)}{*}I\right] + \frac{1}{(1+r)}{*}F_{t+1} \quad (10)$$

The equation can be rewritten for two cases of *SLR* exceeding SLR_c or not, respectively.

$$F_{ex,t} = \left[\frac{EAB_{t+1}}{(1+r)} - \frac{EAB_{t+L}}{(1+r)^{L+1}} - \frac{r}{(1+r)} * I\right] + \frac{1}{(1+r)} * F_{t+1} \qquad (SLR > SLR_c, p_t = 1) \qquad (11)$$

$$F_{con,t} = \frac{1}{(1+r)} * F_{t+1} \qquad (SLR < SLR_c, p_t = 0) \qquad (12)$$

The equations (11) and (12) represent the termination and continuation value at year *t* for an investment option with an ability to defer. Note that the variables of sea-level rise (*SLR*) and expected annual benefit (*EAB*) are random values. Thus, the option value (F_t) at year *t* is also random variable. The randomness of the option value has already been observed in the chapter 5.4. As the investment should be made when SLR is higher than SLR_c, we can set equal the equations (11) and (12). In addition, as the optimal investment time is when a termination value ($F_{ex,t}$) starts to exceed a continuation value ($F_{con,t}$), let $F_{ex,t}$ equal to $F_{con,t}$ at year *t*. In this case, we should invest in the option, following the investment rule (i.e. $F_{ex,t} > F_{con,t}$) by Bellman's equation. Therefore, when the option is closed, we can have

$$F_{ex,t} = F_{con,t} \quad \text{for any investment time t} \qquad (13)$$

By substituting $F_{ex,t}$ and $F_{con,t}$ for equation (13), we can derive a formulation of an optimal investment time for the random variable of sea-level rise. Note that the investment should be made by the investment rule when $F_{ex,t} \geq F_{con,t}$ or $SLR \geq SLR_c$

$$EAB_{t+1} - \frac{EAB_{t+L}}{(1+r)^L} = r*I \quad \text{when } SLR = SLR_c \qquad (14)$$

This is a formulation for the optimal investment time of a deferrable option with investment cost of I and discount rate r for the stochastic variable of sea-level rise. This formulation enables us to make an investment decision on timing.

As the expected annual benefit is a function of sea-level rise ($EAB = f(SLR)$), SLR_c can be calculated by a critical value of EAB_c estimated by the equation (14), if other variables (i.e. investment cost and discount rates) are known and fixed. However, EAB_{t+L} is a random

variable subject to sea-level rise at year $t + L$. Therefore, SLR_c also varies depending on a random value of EAB_{t+L}. However, if the life of a project is long enough to make the second term go to zero, EAB_{t+1} is only dependant on the investment cost and discount rate ($EAB_{t+1} = rI$) that are known variables over the time period of the project life. Thus, the critical threshold value (SLR_c) can be estimated by equation (14). This formulation based on real options approach or dynamic programming has an important implication for resolving uncertainty in climate change adaptation as this has been derived from the stochastic case of sea-level rise.

In this context, the critical threshold value of SLR_c or EAB_c is a unique value for a deferrable option, which is less sensitive to SLR scenarios than optimal investment times and option values which vary significantly according to sea-level rise scenarios. This formulation for the stochastic case of sea-level rise has a similar form to that for the deterministic case of sea-level rise. However, for the deterministic case, the first term on the left side is discounted by a discounting factor 1/(1+r). As the discount rate (r) is small, the difference between deterministic and stochastic equations are considered small. However, although we take different approaches to derive both formulations for optimal investment time, the derived formulations lead to the same result.

$$\frac{EAB_{t+1}}{(1+r)} - \frac{EAB_{t+L}}{(1+r)^L} = r \times I \qquad \text{(Deterministic case)} \qquad (15)$$

$$EAB_{t+1} - \frac{EAB_{t+L}}{(1+r)^L} = r \times I \qquad \text{(Stochastic case)} \qquad (16)$$

Appendix S. Quantitative comparisons of adaptation paths by different premium values in economy efficiency

This appendix shows changes in the option value of the adaptation paths across premium values in each SLR scenario. This comparison shows the priority or ranking of the possible adaptation paths in economy efficiency.

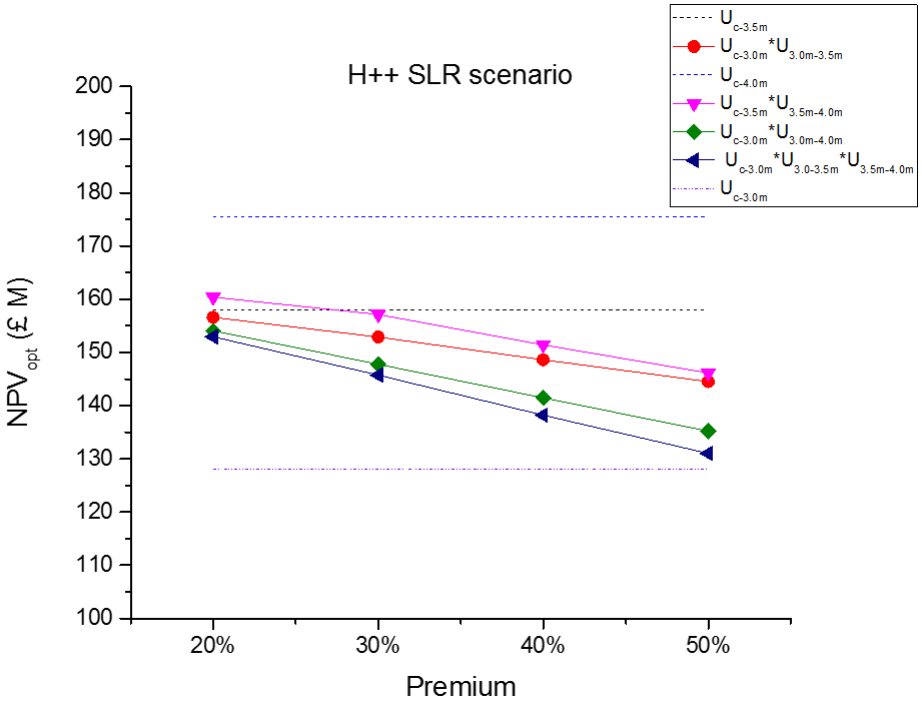

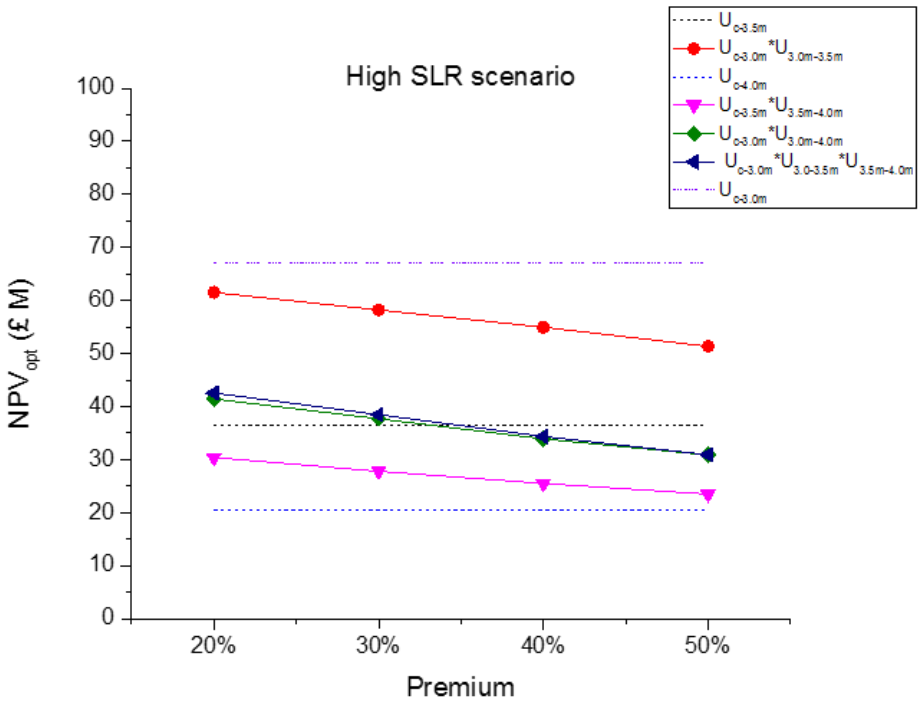

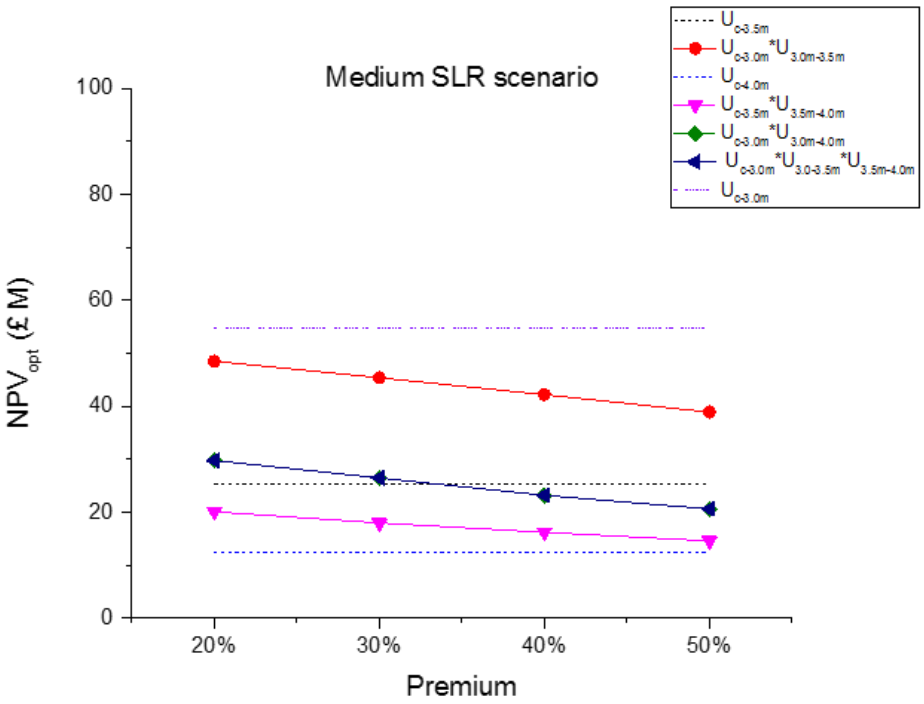
Medium SLR scenario
$U_{c\text{-}3.5m}$
$U_{c\text{-}3.0m}$*$U_{3.0m\text{-}3.5m}$
$U_{c\text{-}4.0m}$
$U_{c\text{-}3.5m}$*$U_{3.5m\text{-}4.0m}$
$U_{c\text{-}3.0m}$*$U_{3.0m\text{-}4.0m}$
$U_{c\text{-}3.0m}$*$U_{3.0\text{-}3.5m}$*$U_{3.5m\text{-}4.0m}$
$U_{c\text{-}3.0m}$
NPV_{opt} (£ M)
100
80
60
40
20
0
20%
30%
40%
50%
Premium

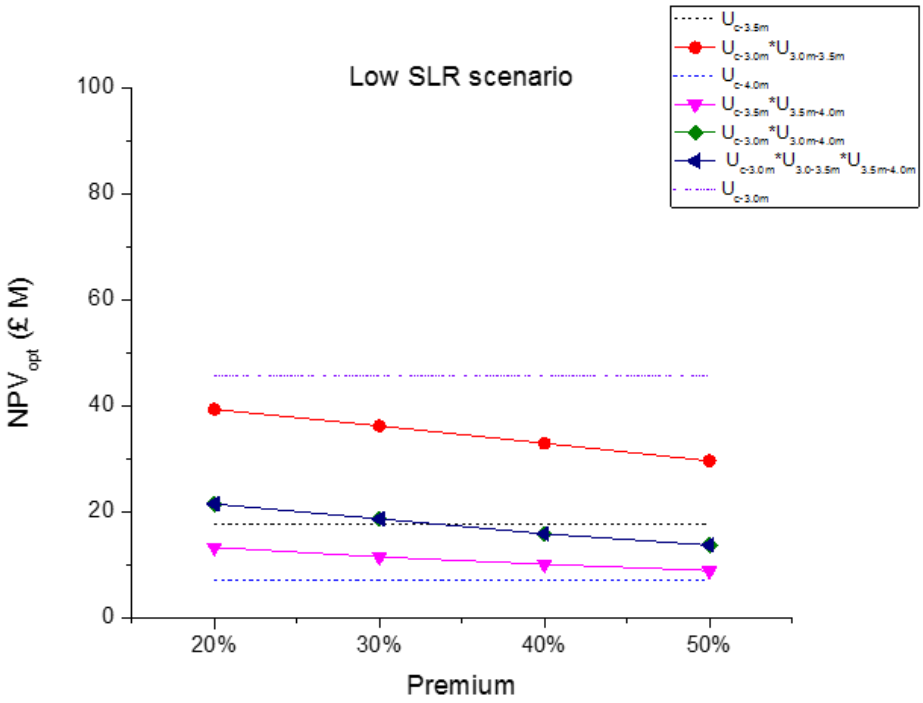
Low SLR scenario
$U_{c\text{-}3.5m}$
$U_{c\text{-}3.0m}$*$U_{3.0m\text{-}3.5m}$
$U_{c\text{-}4.0m}$
$U_{c\text{-}3.5m}$*$U_{3.5m\text{-}4.0m}$
$U_{c\text{-}3.0m}$*$U_{3.0m\text{-}4.0m}$
$U_{c\text{-}3.0m}$*$U_{3.0\text{-}3.5m}$*$U_{3.5m\text{-}4.0m}$
$U_{c\text{-}3.0m}$
NPV_{opt} (£ M)
100
80
60
40
20
0
20%
30%
40%
50%
Premium

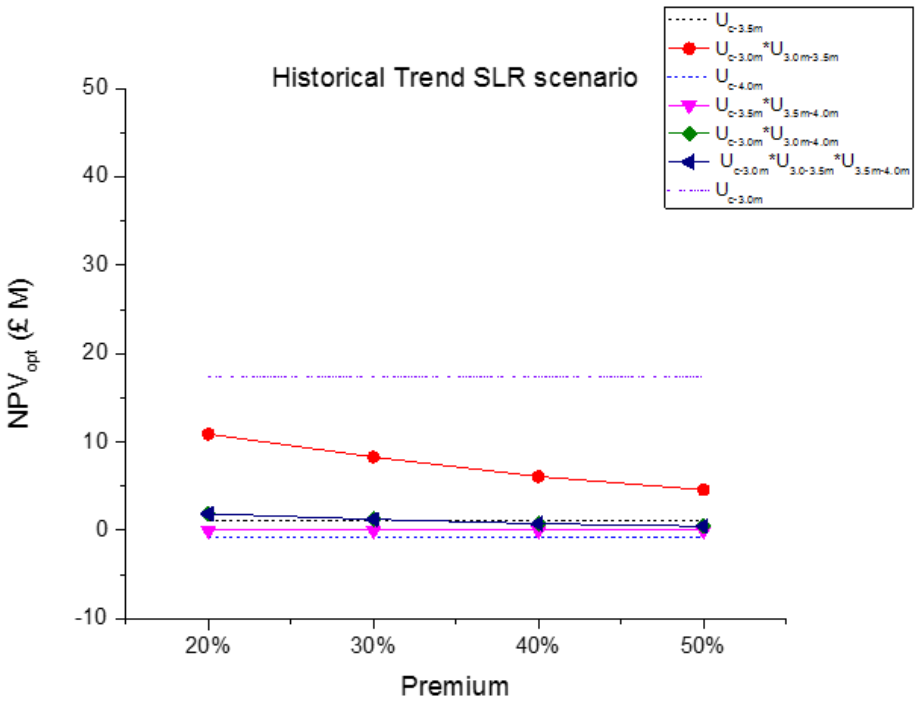
Historical Trend SLR scenario
$U_{c\text{-}3.5m}$
$U_{c\text{-}3.0m}*U_{3.0m\text{-}3.5m}$
$U_{c\text{-}4.0m}$
$U_{c\text{-}3.5m}*U_{3.5m\text{-}4.0m}$
$U_{c\text{-}3.0m}*U_{3.0m\text{-}4.0m}$
$U_{c\text{-}3.0m}*U_{3.0\text{-}3.5m}*U_{3.5m\text{-}4.0m}$
$U_{c\text{-}3.0m}$
NPV_{opt} (£ M)
50
40
30
20
10
0
-10
20%
30%
40%
50%
Premium